Chemistry–A European Journal
Research Article
doi.org/10.1002/chem.202301650
Chemistry Europe
European Chemical Societies Publishing
www.chemeurj.org

Hot Paper

Photochemical [2+2] Cycloaddition of Alkynyl Boronates

Oleksandr S. Liashuk,[a, b, c] Oleksandr O. Grygorenko,[a, c] Yulian M. Volovenko,[a] and Jérôme Waser*[b]

A photochemical [2+2] cycloaddition of alkynyl boronates and maleimides is reported. The developed protocol provided 35–70% yield of maleimide-derived cyclobutenyl boronates and demonstrated wide compatibility with various functional groups. The synthetic utility of the prepared building blocks was demonstrated for a range of transformations, including Suzuki cross-coupling, catalytic or metal-hydride reduction, oxidation, and cycloaddition reactions. With aryl-substituted alkynyl boronates, the products of double [2+2] cycloaddition were obtained predominantly. Using the developed protocol, a cyclobutene-derived analogue of Thalidomide was prepared in one step. Mechanistic studies supported the participation of the triplet-excited state maleimides and ground state alkynyl boronates in the key step of the process.

Introduction

Organoboron compounds are one of the most recognized reagents of modern organic synthesis.[1] After the development of efficient Suzuki-Miyaura cross-coupling protocols, compounds bearing C_{sp^2}-B bonds (i.e., (het)aryl or akenyl boronates) rapidly become highly desirable targets for synthetic organic chemists. Traditionally, these compounds have been prepared via hydroboration,[2] Miyaura borylation,[3] metalation-borylation,[4] boron-Wittig olefination,[5,6] and other methods.[7–10] One of the recent trends in the field of organoboron reagents and the corresponding C–C-bond-forming reactions is related to shift from aromatic compounds towards saturated and partially saturated ring systems[11,12] complying with lead-likeness concepts in drug discovery.[13–15] In particular, cycloalkenyl boronic derivatives or their heterocyclic analogs have found applications in the synthesis of marketed and investigational drugs.[12,16] To date, an increasing interest to all-carbon four membered ring scaffold has emerged due to their abundance in natural compounds[17,18] and unique properties in terms of possible applications for bioisosteric replacements,[19] structural rigidity,[20] chemical stability, and functionalization potential.[18,21,22]

Cyclobutane-derived boronates and their preparation are broadly described in the literature.[23–42] On the contrary, the synthesis of cyclobutene-derived boronates and their applications are very scarce. Thus, lithiation of iodo- (**1a**)[43] or bromocyclobutene (**1b**)[44,45] and subsequent treatment with trialkoxy borates resulted in ionic boronate **2a**,[43] or in neopentyl-protected boronate **2b** after transesterification,[44,45] respectively (Scheme 1, *A*). The same strategy was used to prepare the simplest cyclobutene derivative **2c**, albeit with moderate overall yield.[42] Miyaura-type alkenyl triflate borylation was used for the preparation of boronates **3a** and **3b** (Scheme 1, *B*).[19] In addition, formation of the cyclobutenyl boronate core was observed as a side product in the reaction of boronate **4a** with Fischer carbene complex **5** (Scheme 1, *C*).[46,47] Surprisingly, the construction of the four-membered ring through photoinduced or transition metal-catalyzed [2+2] cycloaddition[48–50] commonly used in the cyclobutane series[51–53] has been virtually unexplored for the boronate-bearing substrates. A unique example of such a transformation is the reaction of cyclopropylethynyl boronate **4b** with ethylene in the presence of a Co(I)-based catalyst, leading to disubstituted cyclobutene **6** (Scheme 1, *D*).[54]

Based on this lack of precedence and our previous experience on photocycloaddition of alkenylboronates,[37] alongside with other reports of this transformation,[24] we decided to develop a photomediated [2+2] cycloaddition of diversely substituted alkynyl boronates and alkenes as a promising approach for the synthesis of polysubstituted cyclobutenyl boronates. Considering the well-established activity of maleimides in photochemical [2+2] cycloaddition reactions,[36,37] we choose them as the alkene partner for this study. Herein, we describe the scope of this transformation and its tolerance to various functional groups (including unprotected amino, hydroxy, and carboxylic groups), as well as the scalability of the developed protocol. An effect of the substituent at the β-atom of the alkynyl boronate on the reaction outcome, as well as a speculative mechanistic pathway are also discussed.

---

[a] O. S. Liashuk, Prof. Dr. O. O. Grygorenko, Prof. Dr. Y. M. Volovenko
Chemical Faculty
Taras Shevchenko National University of Kyïv
Kyiv, Volodymyrska Street 60, 01601, Kyïv (Ukraine)

[b] O. S. Liashuk, Prof. Dr. J. Waser
Laboratory of Catalysis and Organic Synthesis
Institut des Sciences et Ingénierie Chimique
Ecole Polytechnique Fédérale de Lausanne
1015, Lausanne (Switzerland)
E-mail: jerome.waser@epfl.ch
Homepage: http://www.epfl.ch/labs/lcso/

[c] O. S. Liashuk, Prof. Dr. O. O. Grygorenko
Enamine Ltd.
Kyiv, Winston Churchill Street 78, 02094, Kyïv (Ukraine)
Homepage: www.enamine.net

Supporting information for this article is available on the WWW under https://doi.org/10.1002/chem.202301650

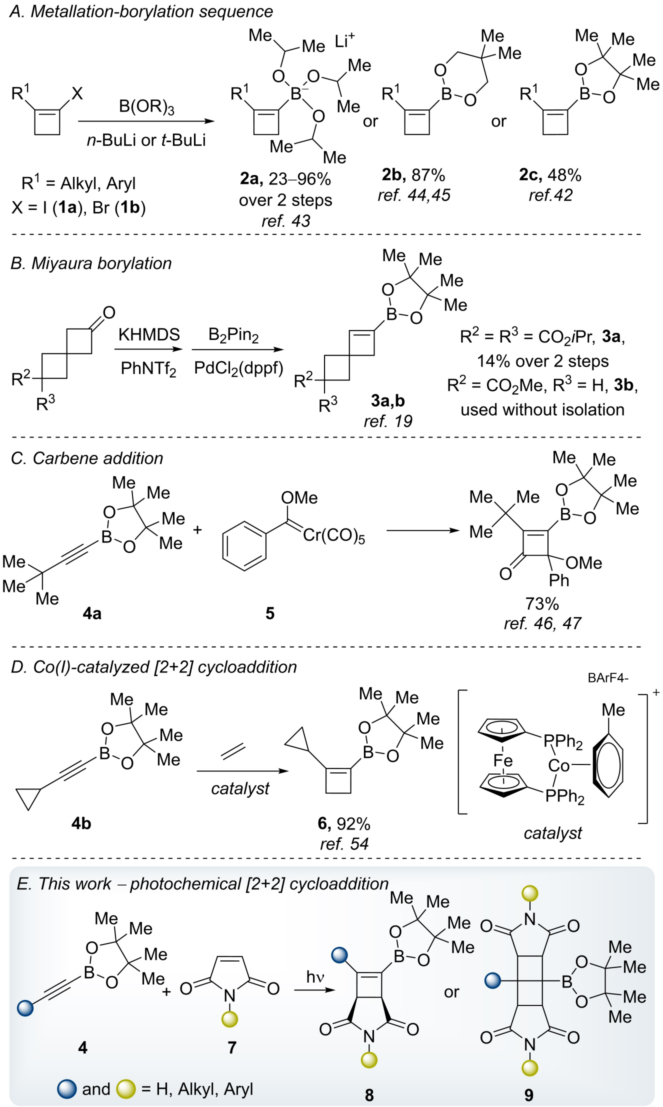

Scheme 1. (*A–C*) Previously reported synthesis of cyclobuteneboronates. (*D*) Single reported example of [2+2] cycloaddition of alkynyl boronates. (*E*) Photochemical [2+2] cycloaddition studied in this work.

Table 1. Screening of reaction conditions for the synthesis of cyclobutene-derived boronate **8a**.

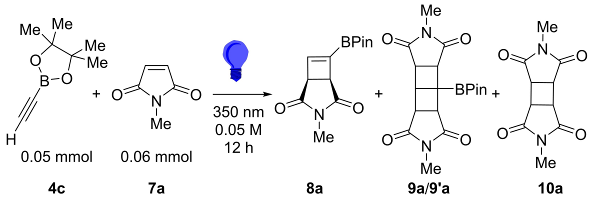

Entry	Solvent	Additive[a]	**8a**:**9a**:**10a**[b]	Conversion of **4c**, %
1	CH_3CN	BP (10%)	24:16:13	53
2	CH_3CN	TX (10%)	28:15:16	54
3	CH_2Cl_2	TX (10%)	41:17:14	100
4[c]	CH_2Cl_2	TX (10%)	78:6:14	31
5	*n*-hexane	TX (10%)	85:1:11	100
6[d]	CH_2Cl_2	$Ir(dFppy)_3$ (5%)	90:0:5	100

[a] BP = benzophenone, TX = thioxanthone. [b] The ratio was determined from ^{1}H NMR spectra using 1,3,5-trimethoxybenzene as the standard. [c] 3 equiv. of alkyne were used. [d] 440 nm irradiation wavelength.

Results and Discussion

Synthesis: We started our study with the model reaction of parent alkynyl boronate **4c** with *N*-methyl maleimide **7a** (Table 1). Initially, we investigated conditions used for analogous transformation of alkenyl boronates (1:1 molar ratio of the reagents, benzophenone as the photosensitizer, MeCN as the solvent, irradiation in a Rayonet® reactor ($\lambda_{max} = 350$ nm), rt, 24 h) (Entry 1).[37,55] In that case, a mixture of the desired cyclobutene **8a** (24% NMR yield), double cycloaddition product **9a** (16% NMR yield), and maleimide dimer **10a** (13% NMR yield) alongside with considerable amounts of starting alkyne **4c** (20% of the starting amount) was obtained. Thioxanthone led to a similar result (Entry 2), but the product purification was simplified, as benzophenone was difficult to separate from the reaction product. In contrary, changing the solvent to CH_2Cl_2 improved the yield (to 41%, Entry 3). Finally, increasing the amount of alkynylboronate **4c** to three-fold excess (Entry 4) or using *n*-hexane as a reaction solvent (Entry 5) the desired product **8a** was obtained in 78 and 85% yield, with only 14 and 11% of side product **10a**, respectively. The observed selectivity enhancement could be rationalized by the poor solubility of cyclobutene **8a** in *n*-hexane, preventing the second cycloaddition to happen. In addition, we have checked the utility of visible light photocatalysts as promotors of the reaction. Using $Ir(dFppy)_3$ and 440 nm irradiation the desired product **8a** was obtained in 90% NMR yield with minimum amounts of byproduct **9a** and full conversion of maleimide **7a** (Entry 6). However, further experiments (Table S14 in Supporting Information) revealed slow conversion rate under visible light irradiation and enhanced instability of the alkynyl boronates **4a** in the presence of metal-based catalysts, so we turn our attention back to the UV – promoted cycloaddition.

With the optimized conditions in hands, we examined the scope of the method (Scheme 2). To our delight, the developed protocol was effective for a wide series of substituted maleimides, including unsubstituted (**7b**), *N*-alkyl- (**7a,c**) and *N*-arylmaleimides (**7d,e**) to give cyclobutenes **8b**, **8a,c** and **8d,e**. Notably, a *N*-aryl substituent at the maleimide slowed down the reaction, which is in agreement with the previous studies on the [2+2] cycloaddition of maleimides.[37,56,57] Moreover, the reaction was successful in the presence of an ester group (**8f**) or *N*-Boc protected amine (**8g**) and tolerated a free alcohol (**8h**), a carboxylic acid (**8i**), or a protonated amine (**8j**).

The scope of alkynyl components of the reaction was further explored using synthetically valuable *N*-benzyl maleimide **7c** as the model substrate. In this case, the reaction proceeded smoothly with alkyl- (**4d,a**), cycloalkyl- (**4b**) and TMS-substituted (**4e**) alkynyl boronates to give products **8ca–cd**. In addition, the reaction tolerated halogen (**8ce**) and nitrile (**8cf**) groups and also worked for protected propargylic

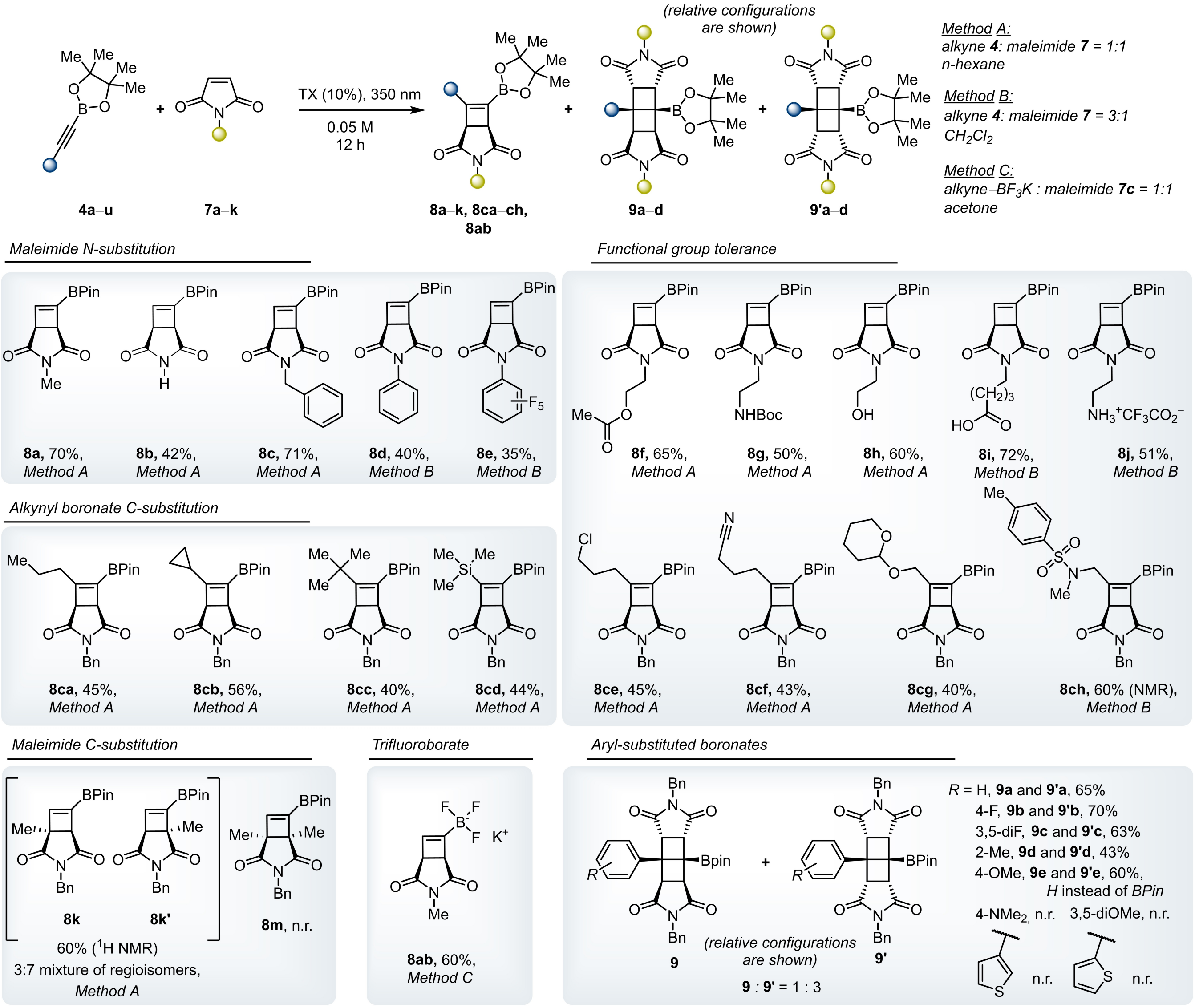

Scheme 2. Scope of the photochemical [2+2] cycloaddition (relative configurations are shown, all compounds are racemic mixtures of *cis*-substituted cyclobutenes). The yields indicated are for the pure boronate isolated after recrystallization.

hydroxy- (**4h**) and amino-substituted (**4i**) boronates to give products **8cg** and **8ch**. The reaction of *N*-benzyl maleimide with enyne-derived boronate **4k**, as well as O-TMS-protected boronate **4l** resulted in complex mixtures of products (see Table S9 of Supporting Information).

In the case of C-substituted maleimides, the reaction of methyl-substituted derivative **7k** resulted in an inseparable mixture of cyclobutenylboronates **8k** and **8k**′, while 1,2-dimethyl-substituted counterpart **7l** did not react at all (for more experiments with mono and di-C-substituted maleimides see Table S15 in Supporting Information). The reaction was not limited to boronate esters: thus, cyclobutenyl trifluoroborate **8ab** could be prepared from potassium ethynyl trifluoroborate using slightly modified conditions (see Tables S6–8 of Supporting Information for more details). The scalability of the developed protocol was demonstrated for boronate **8c**, which gave the target product in 66% yield on a 10 mmol scale.

Unlike their alkyl-substituted counterparts, the reaction of aryl-substituted alkynylboronates **4m–u** with *N*-benzyl maleimide **7c** resulted in double cycloaddition products **9a–e** and **9′a–e** exclusively. Variation of the reaction conditions (i.e., reagent ratio, solvent, photosensitizer) did not affect the reaction outcome (see Table S11 of Supporting Information). Furthermore, the efficiency of the cycloaddition and the side reactions observed (i.e., deboronation or decomposition of the starting materials) depended strongly on the nature of the (het)aryl moiety. Thus, electron-withdrawing substituents at the aryl moiety favored formation of the boron-containing adducts **9a–d** and **9′a–d**, whereas electron-rich substrates typically underwent protodeboration or decomposition under the reaction conditions. It should be noted that the second cycloaddition step occurred in a diastereoselective manner and gave ca. 1:3 mixture of *exo-endo* and *exo-exo* diastereomers **9a–e** and **9′a–e**, respectively, which were easily separated by normal phase column chromatography. The stereochemistry of the pure diastereomers was confirmed by 2D NMR experiments.

To demonstrate the synthetic utility of the obtained cycloadducts, several transformations were performed. Firstly, the Suzuki reaction of boronate **8c** with *p*-tolyl bromide under relatively mild conditions gave cyclobutene **11a** in 60% yield (Scheme 3). The coupling could be also done in a one-pot manner with non-purified crude [2+2] adducts **8c**, **8m**, **8cg**, and **8ch** to give products **11a**–**d** in 30–51% overall yield (see the Supporting Information for more details). Catalytic hydrogenation of **8c** yielded pure *endo*-isomer **12** that had been already obtained by [2+2] cycloaddition of alkenyl boronates as a minor product but was never isolated in pure form (Scheme 4).[37]

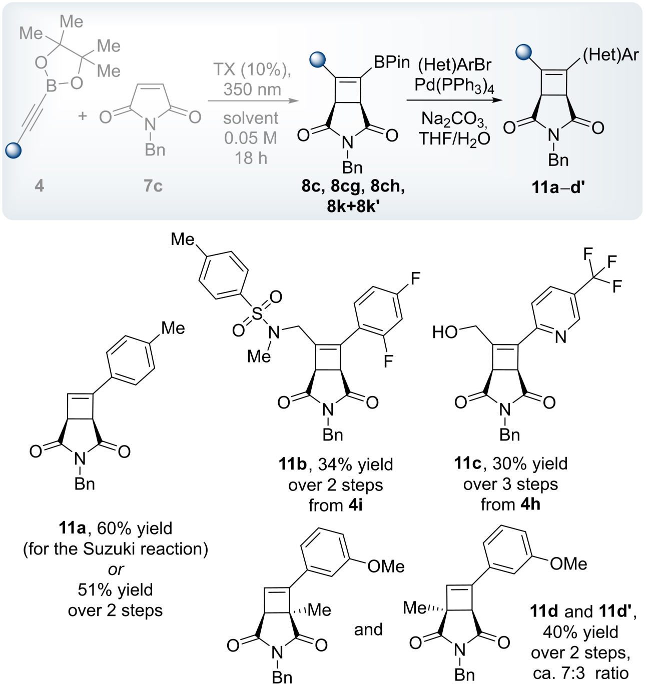

Scheme 3. Suzuki reaction of the synthesized cyclobutene boronates.

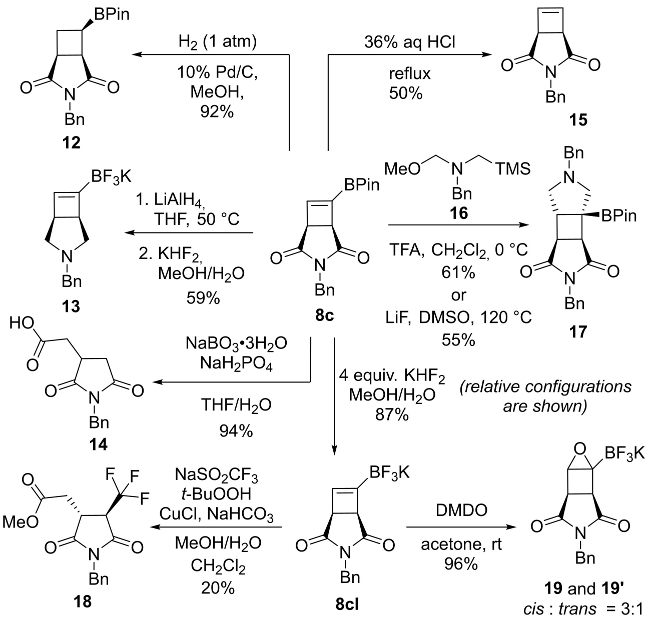

Scheme 4. Other transformations of compound **8c**.

Reduction of the amide groups in **8c** with $LiAlH_4$ followed by treatment with KHF_2 resulted in unsaturated bicyclic boronate **13** in 59% yield. Oxidation with sodium perborate gave cyclobutene ring opening product **14** in almost quantitative yield. Refluxing overnight in concentrated hydrochloric acid generated protodeborylated product **15** in 50% yield. [3+2] cycloaddition of bicyclic adduct **8c** with azomethine yilde precursor **16** resulted in product **17** in 55–61% yield using either TFA-[58] or LiF-promoted[59] ylide generation. Treatment of either pure or non-purified boronate **8c** with KHF_2 provided trifluoroborate **8cl** in 87 and 71% yield (over two steps), respectively.[6] The reaction of the obtained trifluoroborate **8cl** with Langlois reagent[60,61] gave product **18** resulting from cyclobutene ring opening in 20% yield (along with **14** and its methyl ester as the main by-products). At the same time, addition of a freshly prepared dimethyl dioxirane (DMDO) solution[62] to **8cl** resulted in a partially saturated "Dewar furan" analogue **19**[63] containing a tricyclic system of fused three-, four, and five-membered rings (ca. 3:1 diastereomeric mixture) in excellent 96% yield.

Physicochemical and structural properties: To further demonstrate the synthetic utility of the developed approach, a boronate-containing cyclobutene analogue of Thalidomide (compound **8n**, mixture of diastereomers with ca. 1:1 *dr*) was prepared (Figure 1, *A*, *D*). Thalidomide was first introduced as a sedative drug and became infamous due to teratogenic effects.[64] Later, it was approved as an anticancer agent and recently found wide application in design of proteolysis-targeting chimeras (PROTACs).[65] Calculated physicochemical properties[66] of Thalidomide, as well as its cyclobutene- and cyclobutane isosteric analogs showed that the latter replacements should result in a considerable increase of the compound's hydrophilicity and aqueous solubility (Figure 1, *B*). To compare spatial geometry of the discussed bicyclic derivatives, they were analyzed using an exit vector plotting (EVP) tool.[67,68] This approach is based on the simulation of the substituents attached to the scaffold as exit vectors (Figure 1, *C*); four geometric parameters (distance r between the starting points of the vectors, as well as angles ϕ_1, ϕ_2, and θ) are then introduced to describe their relative spatial orientation. Based on the X-ray diffraction studies of compound **8c**,[69] as well as Thalidomide and saturated bicyclo[3.2.0]heptane-2,4-dione derivative **21**,[70] it was found that the 3,6-disubstituted azabicyclo[3.2.0]hept-6-ene-2,4-dione scaffold and its hydrogenated counterpart (with *endo* configuration, as in compound **12**) have somewhat smaller size compared to both Thalidomide derivatives (r=3.21/3.33 Å vs 3.66/4.62 Å), with much better fit for the 4-substituted representative. The angular parameters φ_1/φ_2 and θ also demonstrate reasonable similarity of the bicyclic cyclobutene- and cyclobutane-derived scaffold studied to 4-substituted Thalidomide, with the largest deviations being found for the φ_2 angle values (−20° and 23°, respectively). These results show that the prepared compounds can be considered as sp^3-

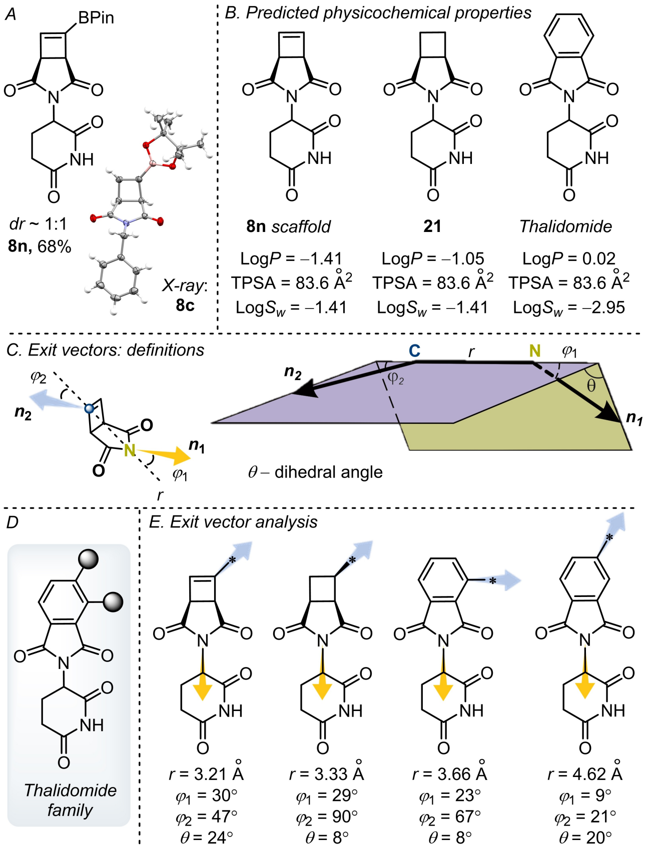

Figure 1. Thalidomide and its cyclobutane-containing analogues **8 n** and **21** (*A*, *D*): predicted physicochemical properties (Log*P*, total polar surface area (TPSA), aqueous solubility (S_w)) (*B*) and exit vector analysis (*C*, *E*).

enriched isosteres of 2,4-disubstituted phthalimide moiety of Thalidomide and other related molecules.

Mechanistic studies: To propose a possible reaction mechanism, we performed several additional experiments. Initially, we checked the reaction of *N*-benzylmaleimide **7 c** with three boronates **4 c**, **4 f**, and **4 m** in the presence of triplet and radical quenchers (Ni(acac)$_2$, oxygen, and TEMPO). In all cases, a significant drop in the reaction yield was observed (to 0–47 % depending on the substrate), which is in accordance with triplet-triplet energy transfer (EnT) process and can be considered as a support for radical species participation in the reaction pathway. Next, we tested the same transformation in the presence of several metal-based photocatalysts. The results were in a good agreement with triplet energies of the corresponding catalysts and not with their redox potentials, which made a single-electron transfer (SET) mechanistic pathway less probable (See Table S14 and Figure S4 in the Supporting Information). Additional UV-Vis measurements showed neither formation of ground state electron donor-acceptor (EDA) complexes nor exciplexes (see Figures S8 and S9 in the Supporting Information), which in combination with the previous data suggests that the cycloaddition proceeds via the triplet-triplet EnT from the catalyst to the substrates.[56,57,71–73]

N-Alkyl maleimides are known to have a non-zero triplet state quantum yield, which allows them to be directly excited upon irradiation with UVB and to participate in photocycloaddition reactions.[53,64,67] Indeed, a control experiment showed significant conversion of the starting materials into the cycloaddition product **8c** (46 %) in the absence of the photosensitizer. Finally, using a Kessil lamp (440 nm) instead of the 350 nm lamp and thioxanthone as the photosensitizer, cyclobutene **8c** was obtained in 63 % yield. At this wavelength, no product was observed in absence of thioxanthone (see Table S14 in the Supporting Information). Therefore, the studied cycloaddition starts both via the direct excitation of the maleimide and the triplet-triplet EnT from the photosensitizer to maleimide at 350 nm, whereas only the photosensitizer pathway is active at 440 nm. From the synthetic point of view, performing the reaction at 350 nm led to higher yields and shorter reaction times.

The next step in the mechanistic pathway is the reaction of the triplet excited state of maleimide and the ground state of alkyne with possible formation of 1,4-biradical intermediates **22 c** and **22′ c** (Scheme 5). A TEMPO adduct with one of these radicals was observed by LCMS during radical quenching experiments. It is known from the literature data that α-boryl radicals are significantly more stable as compared to their non-borylated counterparts;[74] therefore, predominant formation of intermediate **22 c** can be anticipated. Reactions of alkynyl boronates **4c**, **4 b**, and **4 m** with *C*-substituted maleimides **7 k** and **7 m** demonstrated that the attack occurred predominantly at the unsubstituted carbon atom, which could be attributed to both steric effect and/or additional stabilization of the corresponding radical intermediates by the methyl substituent (see Table S14 in the Supporting Information for more details).

Finally, we assume that the different reactivity of aryl-substituted alkynyl boronates in the photochemical [2+2] cycloaddition with maleimides could be rationalized by a lowered LUMO energy of the double bond in the corresponding cyclobutene intermediate due to additional conjugation with aromatic substituent[75] or stabilization of the corresponding 1,4-biradical intermediates **23′** due to the formation of benzylic radical species, resulting in an efficient second cycloaddition in this class of substrates.[76]

Based on the aforementioned results, we proposed a plausible mechanism of the observed transformations which is summarized in Scheme 6. Firstly, a triplet state of maleimide **7** is formed via triplet-triplet EnT process from the excited-state photosensitizer to maleimide **7**. A direct excitation of substrate **7** is also possible, but less efficient. Next, triplet-state maleimide ^{3}**[7]*** reacts with alkynyl boronate **4** with formation of 1,4-biradical intermediate **22**. The latter intermediate undergoes intersystem crossing (ISC) and radical recombination giving

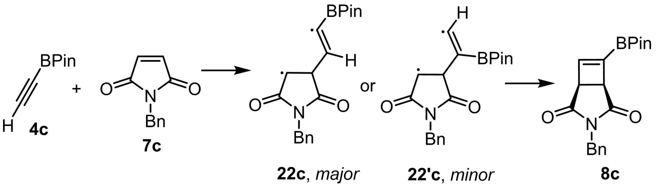

Scheme 5. Formation of 1,4-biradical intermediates **22 c** and **22′ c**.

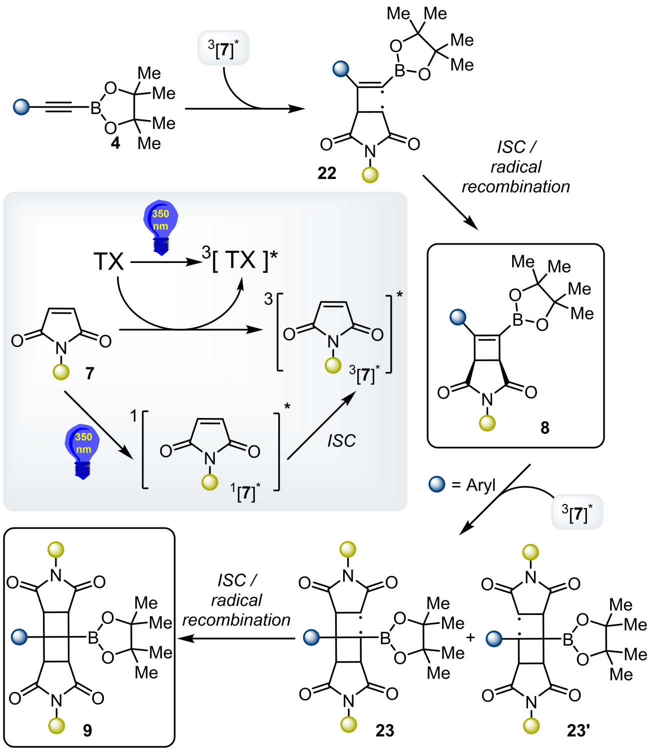

Scheme 6. Plausible reaction mechanism (ISC – intersystem crossing).

cyclobutene boronate **8**. In the case of aryl-substituted alkynyl boronates, product **8** reacts with excited-state maleimide ^{3}[**7**]* in an analogous manner via 1,4-biradical intermediate **23** and/or **23**′ to give double cycloaddition product **9**.

Conclusions

The photochemical [2+2] cycloaddition of the parent and alkyl-substituted alkynyl boronates is a very efficient synthetic approach to access cyclobutene-derived boronates, which was demonstrated for the reactions with various maleimides. The method shows excellent compatibility with numerous functional groups and is amenable for scale-up (up to 10 mmol in a single run). The nature of the substituents directly attached to the reaction centers affects strongly the reaction outcome. Thus, *C*-substitution of the maleimide component precludes initial reaction at this center, and the 3,4-disubstituted maleimide derivative does not react at all. Meanwhile, switching to electron-poor aryl-substituted alkynyl boronates results in a diastereoselective (*dr*~3:1) double cycloaddition providing the corresponding tetracyclic derivatives, whereas electron-rich counterparts undergo decomposition and/or polymerization upon the reaction conditions. Mechanistic experiments demonstrate that the [2+2] cycloaddition proceeds through initial excitation of the maleimide component for both alkyl- or aryl-substituted alkynyl boronates, either through the triplet-triplet energy transfer from the photosensitizer or directly.

The bicyclic cyclobutene-derived boronates obtained can undergo typical reactions of alkenyl boronates, including Suzuki reaction (also in one-pot two-step version), catalytic and hydride reduction, epoxidation, and transformation into trifluoroborates. The utility of the method was demonstrated by the preparation of a cyclobutene-derived analog of Talidomide, an anticancer drug that recently gained much attention in design of PROTACs. Analysis of predicted physicochemical and structural properties of these derivatives revealed potential of the azabicyclo[3.2.0]hept-6-ene-2,4-dione scaffold for isosteric replacements in medicinal chemistry.

Experimental section

Synthesis of cyclobutenyl boronate 8 c

A suspension of maleimide **7 c** (18.7 mg, 0.100 mmol, 1 equiv.), alkynyl boronate **4 c** (15.2 mg, 0.100 mmol, 1 equiv.), and thioxanthone (2.1 mg, 0.010 mmol, 0.1 equiv.) in *n*-hexane (2 mL) was placed into a glass tube, closed with rubber septum and degassed by three vacuum pumping-nitrogen purge cycles. The resulting solution was irradiated in a Rayonet® reactor (λ_{max} = 350 nm) placed at a 3 cm distance from the vessel (see Photos S1 and S2 for the experimental setup) at rt for 12 h. The precipitate (maleimide dimer **10 b**) was filtered off, and the filtrate was evaporated in vacuo. The crude material was dissolved in minimal amounts of pentane (1–2 mL) and stored in refrigerator for 24 h. The precipitate was decanted, washed with cold pentane (3×1 mL) and dried under air to give product **8 c** (23.6 mg, 0.0710 mmol, 71 % yield) as white amorphous solid.

^{1}H NMR (400 MHz, $CDCl_3$) δ 7.33–7.19 (m, 5H, Ar*H*), 6.99 (d, *J* = 0.8 Hz, 1H, C*H*), 4.54 (s, 2H, C*H*$_2$), 3.88–3.57 (m, 2H, 2xC*H*), 1.20 (s, 12H, C*H*$_3$). ^{13}C NMR (101 MHz, $CDCl_3$) δ 174.2, 173.8, 152.4, 135.9, 128.6, 127.8, 84.4, 48.5, 47.6, 42.2, 24.8, 24.6 (carbon signals of phenyl ring are not fully resolved). IR (ν_{max}, cm^{-1}) 2979 (w), 2930 (w), 1768 (w), 1704 (s), 1601 (w), 1386 (m), 1340 (s), 1163 (m), 1140 (m), 853 (m). HRMS (ESI/QTOF) m/z: [M+Na]$^+$ Calcd for $C_{19}H_{22}BNNaO_4^+$ 362.1534; Found 362.1541.

The authors have cited additional references within the Supporting Information.[77–99] Raw NMR data is available free of charge from zenodo.org: https://doi.org/10.5281/zenodo.8099632.

Acknowledgements

This work is supported by EPFL and Enamine Ltd. O.S.L. and O.O.G. received additional funding from Ministry of Education and science of Ukraine (grants No. 0121U100387 (21BF037-01M) and 0122U001962 (22BF037-02)) and Enamine Ltd. We thank Dr. F. F. Tirani from ISIC at EPFL for X-ray diffraction studies, Dr. Oleksandr V. Hryshchuk for helpful insights, Prof. Andrey A. Tolmachev for his encouragement and support, and all the brave people of Ukraine for making this manuscript possible. Open Access funding provided by École Polytechnique Fédérale de Lausanne.

Conflict of Interests

The authors declare no conflict of interest.

Data Availability Statement

The data that support the findings of this study are available in the supplementary material of this article.

Keywords: Boronates · Cycloaddition · Cyclobutene · Maleimide · Photochemistry

[1] J. W. B. Fyfe, A. J. B. Watson, *Chem* **2017**, *3*, 31–55.
[2] R. Barbeyron, E. Benedetti, J. Cossy, J.-J. Vasseur, S. Arseniyadis, M. Smietana, *Tetrahedron* **2014**, *70*, 8431–8452.
[3] T. Ishiyama, N. Miyaura, *Chem. Rec.* **2004**, *3*, 271–280.
[4] M. Oberli, S. Buchwald, *Org. Lett.* **2012**, *14*, 4606–4609.
[5] A. B. Cuenca, E. Fernández, *Chem. Soc. Rev.* **2021**, *50*, 72–86.
[6] M. Kovalenko, D. Yarmoliuk, D. Serhiichuk, D. Chernenko, V. Smyrnov, A. Breslavskyi, O. Hryshchuk, I. Kleban, Y. Rassukana, A. Tymtsunik, A. Tolmachev, Y. Kuchkovska, O. Grygorenko, *Eur. J. Org. Chem.* **2019**, 5624–5635.
[7] M. Christmann, S. Bräse, *Asymmetric Synthesis: The Essentials*, Wiley-VCH, **2007**.
[8] J. Carreras, A. Caballero, P. J. Pérez, *Chem. Asian J.* **2019**, *14*, 329–343.
[9] D. M. Volochnyuk, A. O. Gorlova, O. O. Grygorenko, *Chem. Eur. J.* **2021**, *27*, 15277–15326.
[10] O. O. Grygorenko, V. S. Moskvina, I. Kleban, O. V. Hryshchyk, *Tetrahedron* **2022**, *104*, 132605.
[11] F. Lovering, J. Bikker, C. Humblet, *J. Med. Chem.* **2009**, *52*, 6752–6756.
[12] P. Campbell, C. Jamieson, I. Simpson, A. Watson, *Chem. Commun.* **2018**, *54*, 46–49.
[13] A. R. Hanby, N. S. Troelsen, T. J. Osberger, S. L. Kidd, K. T. Mortensen, D. R. Spring, *Chem. Commun.* **2020**, *56*, 2280–2283.
[14] W. Wei, S. Cherukupalli, L. Jing, X. Liu, P. Zhan, *Drug Discovery Today* **2020**, *25*, 1839–1845.
[15] S. Stotani, C. Lorenz, M. Winkler, F. Medda, E. Picazo, R. Ortega Martinez, A. Karawajczyk, J. Sanchez-Quesada, F. Giordanetto, *ACS Comb. Sci.* **2016**, *18*, 330–336.
[16] F. Pettersson, H. Pontén, N. Waters, S. Waters, C. Sonesson, *J. Med. Chem.* **2010**, *53*, 2510–2520.
[17] J. Li, K. Gao, M. Bian, H. Ding, *Org. Chem. Front.* **2020**, *7*, 136–154.
[18] A. Misale, S. Niyomchon, N. Maulide, *Acc. Chem. Res.* **2016**, *49*, 2444–2458.
[19] J. J. Swidorski, S. Jenkins, U. Hanumegowda, D. D. Parker, B. R. Beno, T. Protack, A. Ng, A. Gupta, Y. Shanmugam, I. B. Dicker, M. Krystal, N. A. Meanwell, A. Regueiro-Ren, *Bioorg. Med. Chem. Lett.* **2021**, *36*, 127823.
[20] C. Nowikow, R. Fuerst, M. Kauderer, C. Dank, W. Schmid, M. Hajduch, J. Rehulka, S. Gurska, O. Mokshyna, P. Polishchuk, I. Zupkó, P. Dzubak, U. Rinner, *Bioorg. Med. Chem.* **2019**, *27*, 115032.
[21] J. Shearer, J. L. Castro, A. D. G. Lawson, M. MacCoss, R. D. Taylor, *J. Med. Chem.* **2022**, *65*, 8699–8712.
[22] M. R. van der Kolk, M. A. C. H. Janssen, F. P. J. T. Rutjes, D. Blanco-Ania, *ChemMedChem* **2022**, *17*, e202200020.
[23] H.-W. Man, W. C. Hiscox, D. S. Matteson, *Org. Lett.* **1999**, *1*, 379–382.
[24] S. C. Coote, T. Bach, *J. Am. Chem. Soc.* **2013**, *135*, 14948–14951.
[25] K. Hong, X. Liu, J. P. Morken, *J. Am. Chem. Soc.* **2014**, *136*, 10581–10584.
[26] R. Murakami, K. Tsunoda, T. Iwai, M. Sawamura, *Chem. Eur. J.* **2014**, *20*, 13127–13131.
[27] S. Plunkett, K. J. Flanagan, B. Twamley, M. O. Senge, *Organometallics* **2015**, *34*, 1408–1414.
[28] S. Kumar Bose, S. Brand, H. Oluwatola Omoregie, M. Haehnel, J. Maier, G. Bringmann, T. B. Marder, *ACS Catal.* **2016**, *6*, 8332–8335.
[29] J. He, H. Jiang, R. Takise, R.-Y. Zhu, G. Chen, H.-X. Dai, T. G. M. Dhar, J. Shi, H. Zhang, P. T. W. Cheng, J.-Q. Yu, *Angew. Chem. Int. Ed.* **2016**, *55*, 785–789.
[30] M. Guisán-Ceinos, A. Parra, V. Martín-Heras, M. Tortosa, *Angew. Chem. Int. Ed.* **2016**, *55*, 6969–6972.
[31] J. He, Q. Shao, Q. Wu, J.-Q. Yu, *J. Am. Chem. Soc.* **2017**, *139*, 3344–3347.
[32] D. Hu, L. Wang, P. Li, *Org. Lett.* **2017**, *19*, 2770–2773.
[33] A. Fawcett, J. Pradeilles, Y. Wang, T. Mutsuga, E. L. Myers, V. K. Aggarwal, *Science* **2017**, *357*, 283–286.
[34] C. Li, J. Wang, L. M. Barton, S. Yu, M. Tian, D. S. Peters, M. Kumar, A. W. Yu, K. A. Johnson, A. K. Chatterjee, M. Yan, P. S. Baran, *Science* **2017**, *356*, 7355.
[35] H. A. Clement, M. Boghi, R. M. McDonald, L. Bernier, J. W. Coe, W. Farrell, C. J. Helal, M. R. Reese, N. W. Sach, J. C. Lee, D. G. Hall, *Angew. Chem. Int. Ed.* **2019**, *58*, 18405–18409.
[36] Y. A. Skalenko, T. V. Druzhenko, A. V. Denisenko, M. V. Samoilenko, O. P. Dacenko, S. A. Trofymchuk, O. O. Grygorenko, A. A. Tolmachev, P. K. Mykhailiuk, *J. Org. Chem.* **2018**, *83*, 6275–6289.
[37] O. P. Demchuk, O. V. Hryshchuk, B. V. Vashchenko, A. V. Kozytskiy, A. V. Tymtsunik, I. V. Komarov, O. O. Grygorenko, *J. Org. Chem.* **2020**, *85*, 5927–5940.
[38] L. Nóvoa, L. Trulli, I. Fernández, A. Parra, M. Tortosa, *Org. Lett.* **2021**, *23*, 7434–7438.
[39] S. O. Scholz, J. B. Kidd, L. Capaldo, N. E. Flikweert, R. M. Littlefield, T. P. Yoon, *Org. Lett.* **2021**, *23*, 3496–3501.
[40] J. Michalland, N. Casaretto, S. Z. Zard, *Angew. Chem. Int. Ed.* **2022**, *61*, e202113333.
[41] Y. Liu, D. Ni, B. G. Stevenson, V. Tripathy, S. E. Braley, K. Raghavachari, J. R. Swierk, M. K. Brown, *Angew. Chem. Int. Ed.* **2022**, *61*, e202200725.
[42] Y. Liu, D. Ni, K. Brown, *J. Am. Chem. Soc.* **2022**, *144*, 18790–18796.
[43] A. N. Baumann, M. Eisold, A. Music, D. Didier, *Synthesis* **2018**, *50*, 3149–3160.
[44] P. Polák, T. Tobrman, *Eur. J. Org. Chem.* **2019**, 957–968.
[45] T. Edlová, H. Dvořáková, V. Eigner, T. Tobrman, *J. Org. Chem.* **2021**, *86*, 5820–5831.
[46] M. W. Davies, J. P. A. Harrity, C. N. Johnson, *Chem. Commun.* **1999**, 2107–2108.
[47] M. W. Davies, C. N. Johnson, J. P. A. Harrity, *J. Org. Chem.* **2001**, *66*, 3525–3532.
[48] Y. Xu, M. L. Conner, M. K. Brown, *Angew. Chem. Int. Ed.* **2015**, *54*, 11918–11928.
[49] D. Didier, F. Reiners, *Chem. Rec.* **2021**, *21*, 1144–1160.
[50] M. M. Parsutkar, V. V. Pagar, T. V. RajanBabu, *J. Am. Chem. Soc.* **2019**, *141*, 15367–15377.
[51] S. Poplata, A. Tröster, Y.-Q. Zou, T. Bach, *Chem. Rev.* **2016**, *116*, 9748–9815.
[52] D. Sarkar, N. Bera, S. Ghosh, *Eur. J. Org. Chem.* **2020**, *2020*, 1310–1326.
[53] P. Yang, Q. Jia, S. Song, X. Huang, *Nat. Prod. Rep.* **2023**, DOI: 10.1039/D2NP00034B.
[54] M. E. Farmer, L. E. Ehehalt, T. P. Pabst, M. T. Tudge, P. J. Chirik, *Organometallics* **2021**, *40*, 3599–3607.
[55] In the original paper, Sylvania Ecologic F25T8/350BL RG2 25 W fluorescent lamps ($\lambda_{max} = 366$ mm) were used.
[56] I. Triandafillidi, N. F. Nikitas, P. L. Gkizis, N. Spiliopoulou, C. G. Kokotos, *ChemSusChem* **2022**, *15*, e202102441.
[57] S. Ha, Y. Lee, Y. Kwak, A. Mishra, E. Yu, B. Ryou, C.-M. Park, *Nat. Commun.* **2020**, *11*, 2509.
[58] V. I. Savych, V. L. Mykhalchuk, P. V. Melnychuk, A. O. Isakov, T. Savchuk, V. M. Timoshenko, S. A. Siry, S. O. Pavlenko, D. V. Kovalenko, O. V. Hryshchuk, V. A. Reznik, B. A. Chalyk, V. S. Yarmolchuk, E. B. Rusanov, P. K. Mykhailiuk, *J. Org. Chem.* **2021**, *86*, 13289–13309.
[59] O. S. Liashuk, I. A. Ryzhov, O. V. Hryshchuk, B. V. Vashchenko, P. V. Melnychuk, Y. M. Volovenko, O. O. Grygorenko, *Chem. Eur. J.* **2022**, *28*, e202202117.
[60] S. R. Dubbaka, M. Salla, R. Bolisetti, S. Nizalapur, *RSC Adv.* **2014**, *4*, 6496–6499.
[61] M. Presset, D. Oehlrich, F. Rombouts, G. A. Molander, *J. Org. Chem.* **2013**, *78*, 12837–12843.
[62] G. A. Molander, M. Ribagorda, *J. Am. Chem. Soc.* **2003**, *125*, 11148–11149.
[63] I. G. Pitt, R. A. Russell, R. N. Warrener, *J. Am. Chem. Soc.* **2002**, *107*, 7176–7178.
[64] N. Vargesson, *Birth Defects Res. Part C* **2015**, *105*, 140–156.
[65] X. Yang, Z. Wang, Y. Pei, N. Song, L. Xu, B. Feng, H. Wang, X. Luo, X. Hu, X. Qiu, H. Feng, Y. Yang, Y. Zhou, J. Li, B. Zhou, *Eur. J. Med. Chem.* **2021**, *218*, 113341.
[66] *Instant JChem* was used to predict the physicochemical properties of all the compounds. Instant JChem version 21.2.0, ChemAxon (http://www.chemaxon.com).
[67] O. O. Grygorenko, P. Babenko, D. M. Volochnyuk, O. Raievskyi, I. V. Komarov, *RSC Adv.* **2016**, *6*, 17595–17605.
[68] O. O. Grygorenko, D. Demenko, D. M. Volochnyuk, I. V. Komarov, *New J. Chem.* **2018**, *42*, 8355–8365.
[69] Deposition Number 2235657 (for **8c**) contains the supplementary crystallographic data for this paper. These data are provided free of charge by the joint Cambridge Crystallographic Data Centre and Fachinformationszentrum Karlsruhe Access Structures service.

[70] E. Benjamin, Y. M. Hijji, *J. Chem.* **2017**, *2017*, 6436185.

[71] E. Skolia, C. G. Kokotos, *ACS Org. Inorg. Au* **2022**, DOI 10.1021/acsorginorgau.2c00053.

[72] J. L. He Qiang, *Synthesis* **2021**, *54*, 925–942.

[73] S. Ahuja, S. Jockusch, A. Ugrinov, J. Sivaguru, *Eur. J. Org. Chem.* **2020**, 1478–1481.

[74] N. Kumar, R. R. Reddy, N. Eghbarieha, A. Masarwa, *Chem. Commun.* **2020**, *56*, 13–25.

[75] I. Fleming, *Molecular Orbitals and Organic Chemical Reactions*, Wiley, Chichester, **2010**, 70–72.

[76] J. Hioe, H. Zipse, *Org. Biomol. Chem.* **2010**, *8*, 3609–3617.

[77] W. L. F. Armarego, C. L. L. Chai, *Purification of Laboratory Chemicals*, Elsevier, Oxford **2003**.

[78] Y. Nishihara, Y. Okada, J. Jiao, M. Suetsugu, M.-T. Lan, M. Kinoshita, M. Iwasaki, K. Takagi, *Angew. Chem. Int. Ed.* **2011**, *50*, 8660–8664.

[79] K. Jaiswal, K. Groutchik, D. Bawari, R. Dobrovetsky, *ChemCatChem* **2022**, *14*, e202200004.

[80] H. Kinoshita, H. Takahashi, K. Miura, *Org. Lett.* **2013**, *15*, 2962–2965.

[81] L. Wang, J. M. Lear, S. M. Rafferty, S. C. Fosu, D. A. Nagib, *Science* **2018**, *362*, 225–229.

[82] I. Gazić-Smilović, E. Casas-Arcé, S. J. Roseblade, U. Nettekoven, A. Zanotti-Gerosa, M. Kovačevič, Z. Časar, *Angew. Chem. Int. Ed.* **2012**, *51*, 1014–1018.

[83] C.-I. Lee, J. Zhou, O. V. Ozerov, *J. Am. Chem. Soc.* **2013**, *135*, 3560–3566.

[84] H. E. Ho, N. Asao, Y. Yamamoto, T. Jin, *Org. Lett.* **2014**, *16*, 4670–4673.

[85] F. Possémé, M. Deligny, F. Carreaux, B. Carboni, *J. Org. Chem.* **2007**, *72*, 984–989.

[86] T. León, E. Fernández, *Chem. Commun.* **2016**, *52*, 9363–9366.

[87] A. Robertson, D. Philp, N. Spencer, *Tetrahedron* **1999**, *55*, 11365–11384.

[88] F. Feist, S. L. Walden, J. Alves, S. V. Kunz, A. S. Micallef, A. J. Brock, J. C. McMurtrie, T. Weil, J. P. Blinco, C. Barner-Kowollik, *Angew. Chem. Int. Ed.* **2021**, *60*, 10402–10408.

[89] S. V. Shelar, N. P. Argade, *Org. Biomol. Chem.* **2021**, *19*, 6160–6169.

[90] P. Wessig, D. Freyse, D. Schuster, A. Kelling, *Eur. J. Org. Chem.* **2020**, *2020*, 1732–1744.

[91] G. Deng, Y. Chen, *Macromolecules* **2004**, *37*, 18–26.

[92] I. A. P. Linares, K. T. de Oliveira, J. R. Perussi, *Dyes Pigm.* **2017**, *145*, 518–527.

[93] R. M. de Figueiredo, R. Fröhlich, M. Christmann, P. Oczipka, *Synthesis* **2008**, *2008*, 1316–1318.

[94] R. Shintani, W.-L. Duan, T. Hayashi, *J. Am. Chem. Soc.* **2006**, *128*, 5628–5629.

[95] K. Rix, G. H. Kelsall, K. Hellgardt, K. K. (Mimi) Hii, *ChemSusChem* **2015**, *8*, 665–671.

[96] A. Phillips, C. Nasveschuk, J. Henderson, Y. Liang, C. Chen, M. Duplessis, M. He, K. Lazarski, **2017**, WO/2017/197051.

[97] G. M. Sheldrick, *Acta Crystallogr. Sect. A* **2015**, *71*, 3–8.

[98] O. V. Dolomanov, L. J. Bourhis, R. J. Gildea, J. A. K. Howard, H. Puschmann, *J. Appl. Crystallogr.* **2009**, *42*, 339–341.

[99] CrysAlisPro Software System, Rigaku Oxford Diffraction, 2022. https://www.rigaku.com/products/crystallography/crysalis.

Manuscript received: June 4, 2023
Accepted manuscript online: July 2, 2023
Version of record online: ■■, ■■

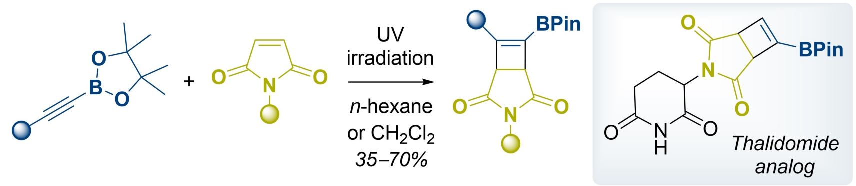

A photochemical [2+2] cycloaddition of alkynyl boronates and maleimides is described as a convenient method for the synthesis of polysubstituted borylated cyclobutenes tolerating a wide range of functional groups. Physicochemical and structural properties of the products obtained provide rationale for their application as phthalimide isosteric replacements, for example, in Thalidomide. Mechanistic studies confirm that the [2+2] cycloaddition proceeds through initial excitation of the maleimide component.

*O. S. Liashuk, Prof. Dr. O. O. Grygorenko, Prof. Dr. Y. M. Volovenko, Prof. Dr. J. Waser**

1 – 9

Photochemical [2+2] Cycloaddition of Alkynyl Boronates

Table of contents

General

The solvents were purified according to the standard procedures.[1] Starting materials were obtained from commercial sources. UV photochemical transformations were performed using commercially available Rayonet® RPR-100 photochemical reactor with installed RPR-3500A lamps. Visible light photochemical transformations were performed using commercially available Kessil® PR160L-440 nm lamps. ^{1}H, ^{11}B, ^{13}C, and ^{19}F NMR spectra were recorded on NMR spectrometers at 600 MHz for protons, 151 MHz for carbon-13 or at 400 MHz for protons, 128 MHz for boron-11, 101 MHz for carbon-13, and 376 MHz for fluorine-19. Chemical shifts are reported in parts per million (ppm) downfield from tetramethylsilane (TMS) as internal standards. Coupling constants (*J*) are given in Hz. Spectra are reported as follows: chemical shift (δ, ppm), multiplicity, integration, and coupling constants (Hz). Preparative flash chromatography was performed using SiliaFlash® Irregular Silica Gel P60, 40–63 µm, 60 Å (R12030B) as the stationary phase. High-performance liquid chromatography (HPLC) purification was performed using XBridge® Prep C18 column (5 µm particle size, 130 Å pore size, 150 × 19 column size (length × inner diameter)). High resolution mass spectroscopy (HRMS) was performed on Waters XEVO G2-S QTOF instrument (electrospray ionization (ESI) or atmospheric pressure chemical ionization (APCI)) and Orbitrap Exploris™ 240 Mass Spectrometer (soft ionization by chemical reaction in transfer (SICRIT)). Infrared spectra (IR) were measured on JASCO (FT/IR-4100) Fourier Transform Infrared Spectrometer. Fluorescence excitation and emission spectra were collected using a Cary Eclipse fluorescence spectrometer (Agilent) with a 150 W xenon lamp as excitation source and a 3-nm bandpass filter for excitation and emission. All fluorescence samples were measured in 4-mm path-length quartz cuvettes (Starna). CCDC contain the supporting crystallographic data for this paper. These data can be obtained free of charge from The Cambridge Crystallographic Data Centre viawww.ccdc.cam.ac.uk/data_request/cif.

*Table S1. Structures of starting materials **4** and **7***

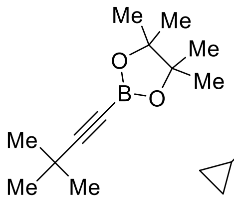

4a

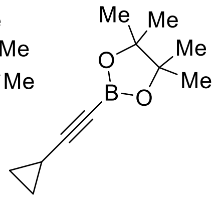

4b

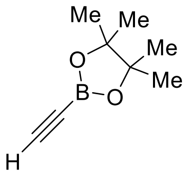

4c

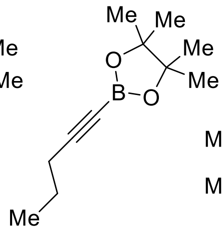

4d

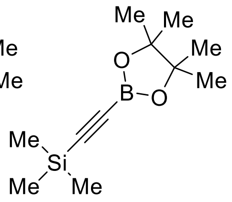

4e

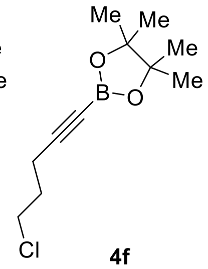

4f

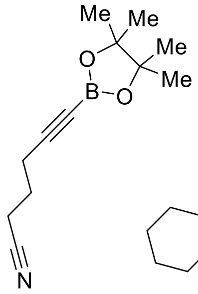

4g

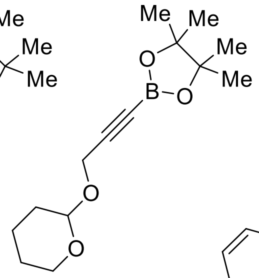

4h

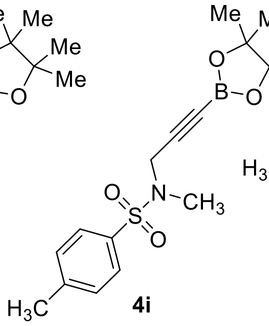

4i

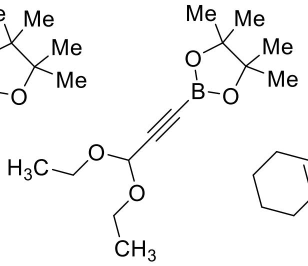

4j

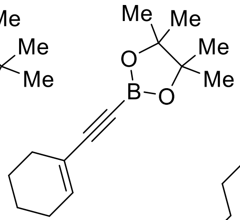

4k

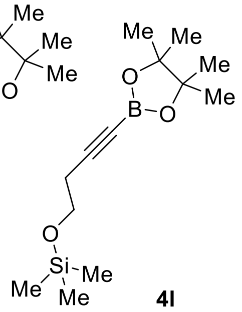

4l

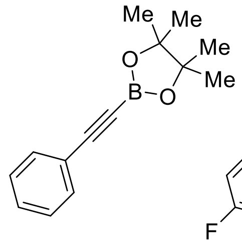

4m

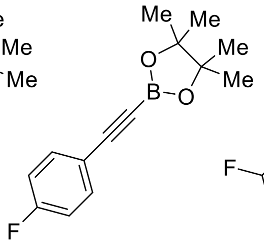

4n

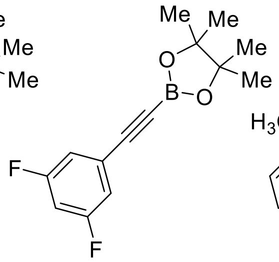

4o

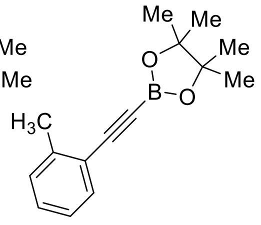

4p

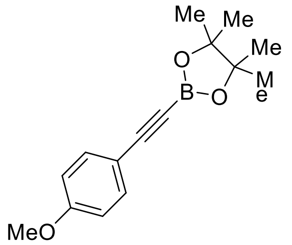

4q

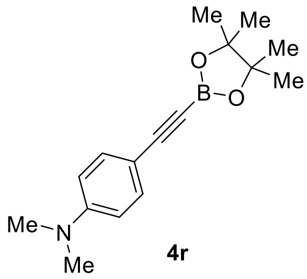

4r

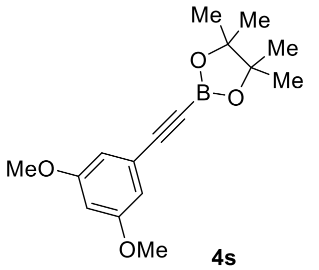

4s

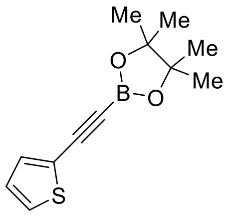

4t

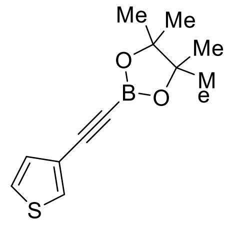

4u

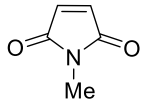

7a

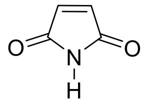

7b

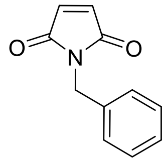

7c

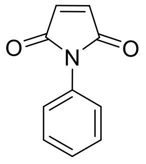

7d

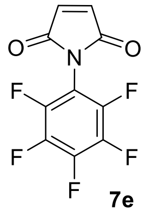

7e

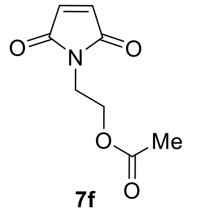

7f

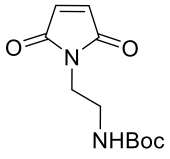

7g

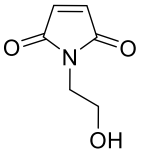

7h

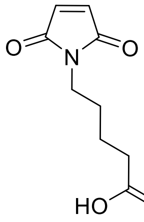

7i

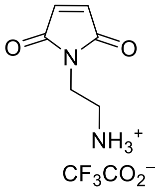

7j

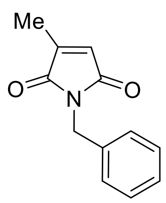

7k

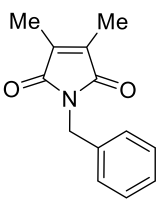

7m

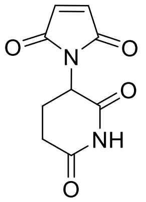

7n

Synthesis of starting materials

Maleimides **7a**,**b**,**d** were obtained from Sigma-Aldrich and used without additional purification. Alkynyl boronates **4a–u** and maleimides **7c,e–l** were prepared according to literature procedures. Yields of the obtained products and corresponding spectra are in full accordance with previously reported data. Previously unknown substrates **4g**, **4i**, **4o** and **4s** were obtained using the following procedure.

Preparation of alkynylboronates **4**

To a solution of the corresponding acetylene derivative (1.2 equiv, 6 mmol) in THF (0.6 M) at –78 °C under an argon atmosphere, *n*-BuLi was added dropwise (1.2 equiv, 1.6 M in hexanes, 6 mmol). The reaction was stirred for 1 h. Then, the resulting mixture was added using a cannula to a solution of 2-isopropoxy-4,4,5,5-tetramethyl-1,3,2-dioxaborolane (1 equiv, 5 mmol) in THF (0.5 M) under an argon atmosphere at –78 °C. After being stirred for 2 h, the reaction mixture was quenched with 2.0 M HCl·Et_2O (3.15 mL, 1.26 equiv, 6.3 mmol), and the mixture was warmed at rt with an additional 1 h of stirring. The solvent was evaporated under vacuum and pentane (10 mL) was added to the residue to remove the lithium salts by simple filtration. The solvent was evaporated again, affording the target product.

General note: It is known that carbons linked to the boron atom are difficult to be observed by ^{13}C NMR due to a broadening of the signal caused by the quadrupole moment of ^{11}B nuclei. Therefore, they are not listed in the characterization data.

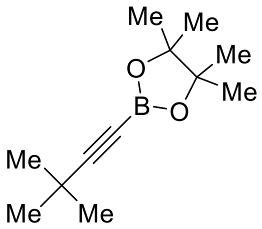

4a. Yellow waxy solid. 0.786 g, 3.78 mmol, 63% yield. ^{1}H NMR (500 MHz, $CDCl_3$) δ = 1.33 (s, 9H, CH_3), 1.01 (s, 12H, CH_3). ^{13}C NMR (125 MHz, $CDCl_3$) δ = 101.9 (br), 84.1, 28.3, 21.9, 19.8. The NMR spectra are consistent with literature data.[2] HRMS (Sicrit plasma/LTQ-Orbitrap) m/z: $[M + H]^+$ Calcd for $C_{12}H_{22}BO_2^+$: 209.1707; Found: 209.1706.

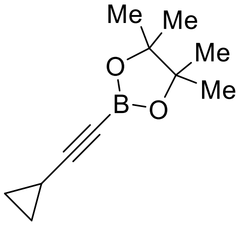

4b. Yellow waxy solid. 0.829 g, 4.32 mmol, 72% yield. ^{1}H NMR (400 MHz, $CDCl_3$) δ = 1.26 (m, 13H, CH_3 and CH), 0.79-0.83 (m, 4H, 2×CH_2). ^{13}C NMR (101 MHz, $CDCl_3$) δ = 107.9 (br), 83.8, 24.5, 8.7. The NMR spectra are consistent with literature data.[3] HRMS (Sicrit plasma/LTQ-Orbitrap) m/z: $[M + H]^+$ Calcd for $C_{11}H_{18}BO_2^+$: 193.1394; Found: 193.1392.

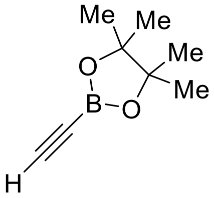

4c. Compound was prepared according to a reported procedure by Miura.[4]

^{1}H NMR (400 MHz, $CDCl_3$) δ = 1.28 (s, 12H, CH_3), 2.48 (s, 1H, CH). ^{13}C NMR (150 MHz, $CDCl_3$): δ = 24.6, 57.2, 84.5, 90.1 (br). The NMR spectra are consistent with literature data.[5] HRMS (Sicrit plasma/LTQ-Orbitrap) m/z: $[M + H]^+$ Calcd for $C_8H_{14}BO_2^+$: 153.1081; Found: 153.1080.

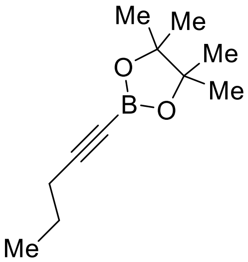

4d. Colorless oil. 0.698 g, 3.60 mmol, 60% yield. ^{1}H NMR (400 MHz, $CDCl_3$) δ = 2.20 (t, J = 7.1 Hz, 2H, CH_2), 1.53 (sept, J = 7.2 Hz, 2H, CH_2), 1.24 (s, 12H, CH_3), 0.95 (t, J = 7.4 Hz, 3H, CH_3). ^{13}C NMR (101 MHz, $CDCl_3$) δ = 104.7 (br), 83.8, 24.5, 21.4, 21.3, 13.3. The NMR spectra are consistent with literature data.[6] HRMS (Sicrit plasma/LTQ-Orbitrap) m/z: $[M + H]^+$ Calcd for $C_{11}H_{20}BO_2^+$: 195.1551; Found: 195.1554.

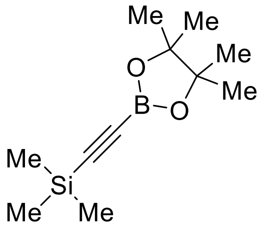

4e. Yellowish oil. 1.06 g, 4.74 mmol, 79% yield. ^{1}H NMR (400 MHz, $CDCl_3$): δ = 1.22 (s, 12H, CH_3), 0.13 (s, 9H, CH_3). ^{13}C NMR (101 MHz, $CDCl_3$): δ = 111.0 (br), 84.2, 24.5, -0.7. The NMR spectra are consistent with literature data.[3] HRMS (Sicrit plasma/LTQ-Orbitrap) m/z: $[M + H]^+$ Calcd for $C_{11}H_{22}BO_2Si^+$: 225.1477; Found: 225.1478.

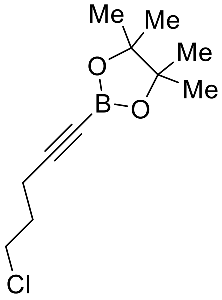

4f. Yellow liquid. 0.807 g, 3.54 mmol, 59% yield. ^{1}H NMR (500 MHz, $CDCl_3$): δ = 3.61 (t, J = 6.5 Hz, 2H, CH_2), 2.43 (t, J = 6.5 Hz, 2H, CH_2), 1.95 (p, J = 6.5 Hz, 2H, CH_2), 1.24 (s, 12H, CH_3). ^{13}C NMR (126 MHz, $CDCl_3$): δ 102.8 (br), 84.3, 43.6, 31.0, 24.8, 17.1. The NMR spectra are consistent with literature data.[7] HRMS (Sicrit plasma/LTQ-Orbitrap) m/z: $[M + H]^+$ Calcd for $C_{11}H_{19}BClO_2^+$: 229.1161; Found: 229.1159.

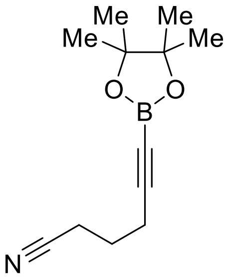

4g. Yellow oil. 2.73 g, 9.35 mmol, 75% purity (25% starting alkyne), 78% yield. Yellow waxy solid. g, mmol, % yield. ^{1}H NMR (400 MHz, $CDCl_3$) δ = 2.50 (t, *J* = 7.2 Hz, 2H, CH_2), 2.44 (t, *J* = 6.7 Hz, 2H, CH_2), 1.88 (quint, *J* = 7.0 Hz, 2H, CH_2), 1.26 (s, 12H Hz, CH_3). ^{13}C NMR (101 MHz, $CDCl_3$) δ 118.9, 101.4, 84.3, 18.6, 16.2 (signals of BPin carbons could not be unambiguously extracted due to overlapping with impurities). IR (v_{max}, cm^{-1}) 3404 (w), 2981 (m), 2942 (w), 2880 (w), 2251 (w), 2212 (w), 1519 (m), 1477 (s), 1456 (s), 1383 (s), 1341 (s), 1274 (w), 1217 (w), 1145 (s), 1051 (w), 983 (m), 853 (m). HRMS (Sicrit plasma/LTQ-Orbitrap) m/z: $[M + H]^+$ Calcd for $C_{12}H_{18}BNNaO_2^+$ 242.1323; Found 242.1324.

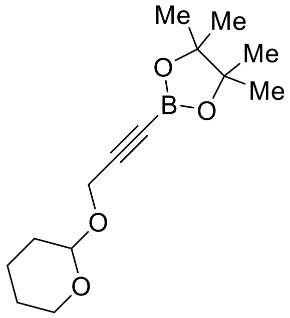

4h. Yellowish viscous oil. 0.845 g, 3.18 mmol, 53% yield. ^{1}H NMR (400 MHz, $CDCl_3$) δ = 4.81 (t, J = 3.2 Hz, 1H, CH), 4.28 (d, J = 3.2 Hz, 2H, CH_2), 3.83-3.77 (m, 1H, CH_2), 3.54-3.48 (m, 1H, CH_2), 1.84-1.70 (m, 2H, CH_2), 1.69-1.48 (m, 2H, CH_2), 1.26 (s, 12H, CH_3); ^{13}C NMR (101 MHz, $CDCl_3$) δ = 98.9, 96.5, 84.3, 61.8, 54.1, 30.1, 25.3, 24.6, 18.9. The NMR spectra are consistent with literature data.[8] HRMS (Sicrit plasma/LTQ-Orbitrap) m/z: $[M + H]^+$ Calcd for $C_{14}H_{24}BO_4^+$: 267.1762; Found: 267.1764.

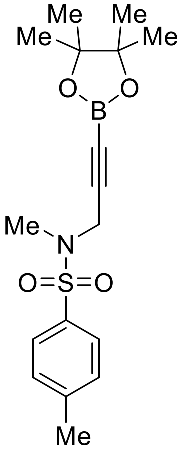

4i. Yellow waxy solid. 1.20 g, 3.44 mmol, 100% purity (recrystallization from heptane, 10 mL), 57% yield. Yellow waxy solid. g, mmol, % yield. ^{1}H NMR (400 MHz, $CDCl_3$) δ = 7.70 (d, *J* = 8.3 Hz, 2H, Ar*H*), 7.30 (d, *J* = 8.0 Hz, 2H, Ar*H*), 4.05 (s, 2H, CH_2), 2.81 (s, 3H, CH_3), 2.42 (s, 3H, CH_3), 1.23 (s, 12H, CH_3). ^{13}C NMR (101 MHz, $CDCl_3$) δ = 143.6, 133.9, 129.6, 128.0, 84.4, 40.5, 34.6, 24.6, 21.6.IR (v_{max}, cm^{-1}) 2981 (w), 2883 (w), 2216 (w), 1698 (m), 1381 (m), 1337 (s), 1164 (s), 1142 (m), 983 (w), 919 (m), 854 (w), 748 (m). HRMS (Sicrit plasma/LTQ-Orbitrap) m/z: $[M + H]^+$ Calcd for $C_{17}H_{24}BNNaO_4S^+$ 372.1411; Found 372.1412.

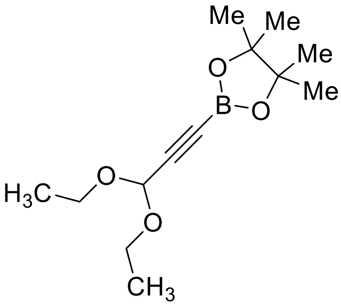

4j. Yellow oil. 0.533 g, 2.10 mmol, 35% yield. ^{1}H NMR (400 MHz, $CDCl_3$) δ = 5.29 (s, 1H, C*H*), 3.73 (dq, J = 7.1, 9.5 Hz, 2H, C*H*$_2$), 3.64 (dq, J = 7.1, 9.5 Hz, 2H, C*H*$_2$), 1.27 (s, 12H, C*H*$_3$), 1.22 (t, J = 7.1 Hz, 6H, C*H*$_3$). ^{13}C NMR (101 MHz, $CDCl_3$) δ = 96.4 (br), 91.1, 84.5, 83.0, 61.1, 24.6, 24.5, 15.0. The NMR spectra are consistent with literature data.[9] HRMS (Sicrit plasma/LTQ-Orbitrap) m/z: [M + H]$^+$ Calcd for $C_{13}H_{24}BO_4^+$: 255.1762; Found: 255.1763.

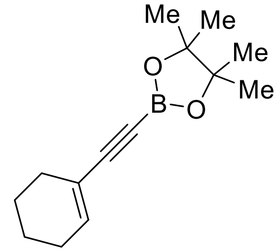

4k. Yellow liquid. 0.932 g, 4.02 mmol, 67% yield. ^{1}H NMR (400 MHz, $CDCl_3$) δ = 6.30 (m, 1H, C*H*), 2.08-2.13 (m, 4H, C*H*$_2$), 1.54-1.62 (m, 4H, C*H*$_2$), 1.27 (s, 12H, C*H*$_3$). ^{13}C NMR (101 MHz, $CDCl_3$) δ = 139.1, 120.3, 104.3 (br), 84.3, 28.8, 26.0, 24.9, 22.3, 21.5. The NMR spectra are consistent with literature data.[3,8] HRMS (Sicrit plasma/LTQ-Orbitrap) m/z: [M + H]$^+$ Calcd for $C_{14}H_{22}BO_2^+$: 233.1707; Found: 233.1707.

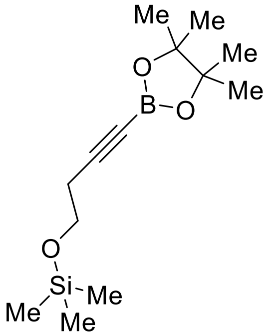

4l. Colorless oil. 0.402 g, 1.50 mmol, 25% yield. ^{1}H NMR (500 MHz, C_6D_6): δ = 3.50 (t, 2H, J = 7.0 Hz, C*H*$_2$), 2.28 (t, 2H, J = 7.0 Hz, C*H*$_2$), 0.98 (s, 12H, C*H*$_3$), 0.01 (s, 9H, C*H*$_3$). ^{13}C NMR (126 MHz, C_6D_6): δ = 101.4 (br), 83.7, 61.1, 24.7, 24.2, -0.4. The NMR spectra are consistent with literature data.[7] HRMS (Sicrit plasma/LTQ-Orbitrap) m/z: [M + H]$^+$ Calcd for $C_{13}H_{26}BO_3Si^+$: 269.1739; Found: 269.1741.

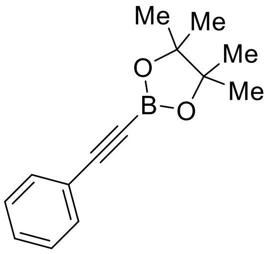

4m. Colorless waxy solid. 0.985 g, 4.32 mmol, 72% yield. ^{1}H NMR (400 MHz, $CDCl_3$) δ = 7.52-7.54 (m, 2H, Ar*H*), 7.29-7.38 (m, 3H, Ar*H*), 1.32 (s, 12H, C*H*$_3$). ^{13}C NMR (101 MHz, $CDCl_3$) δ = 132.6, 129.4, 128.3, 121.9, 101.8 (br), 84.4, 24.7. The NMR spectra are consistent with literature data.[3] HRMS (Sicrit plasma/LTQ-Orbitrap) m/z: [M + H]$^+$ Calcd for $C_{14}H_{18}BO_2^+$: 229.1324; Found: 229.1325.

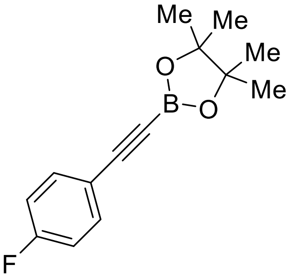

4n. Yellow oil. 1.03 g, 4.20 mmol, 70% yield. ^{1}H NMR (400 MHz, $CDCl_3$) δ = 7.51 (m, 2H, Ar*H*), 7.0 (t, J = 8.7 Hz, 2H, Ar*H*), 1.32 (s, 12H, C*H*$_3$). ^{13}C NMR (101 MHz, $CDCl_3$): δ = 24.7, 84.5, 100.7 (br), 115.7 (d, J = 22.2 Hz), 118.0, 134.6 (d, J = 8.5 Hz), 161.9, 163.2 (d, J = 252.1 Hz). The NMR spectra are consistent with literature data.[3,8] HRMS (Sicrit plasma/LTQ-Orbitrap) m/z: [M + H]$^+$ Calcd for $C_{14}H_{17}BFO_2^+$: 247.1300; Found: 247.1301.

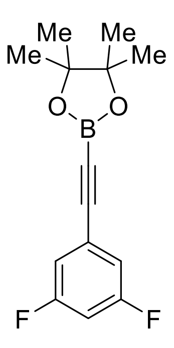

4o. Yellow waxy solid. 1.61 g, 3.03 mmol, 70% purity, 71% yield. g, mmol, % yield. ^{1}H NMR (400 MHz, $CDCl_3$) δ = 7.11 – 6.94 (m, 2H, Ar*H*), 6.87 – 6.75 (m, 1H, Ar*H*), 1.31 (s, 12H, C*H*$_3$). ^{13}C NMR (101 MHz, $CDCl_3$) δ = 162.6 (d, J = 249.5), 161.2 (d, J = 249.1), 124.5 (t, J = 11.6), 115.4 (dd, J = 19.5, 7.3), 105.7 (t, J = 25.3), 98.7, 84.7, 24.7. ^{19}F NMR (376 MHz, $CDCl_3$) δ = -109.1 – -109.2 (m). IR (ν_{max}, cm^{-1}) 2981 (m), 2935 (w), 2207 (m), 1617 (m), 1588 (m), 1476 (m), 1459 (m), 1371 (s), 1325 (s), 1295 (s), 1141 (s), 988 (m), 856 (s). HRMS (Sicrit plasma/LTQ-Orbitrap) m/z: [M + H]$^+$ Calcd for $C_{14}H_{16}BF_2O_2^+$ 265.1206; Found 265.1207.

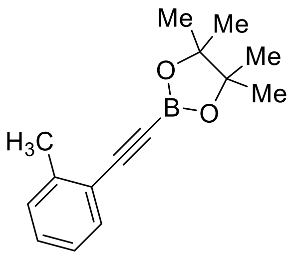

4p. Yellowish waxy solid. 0.958 g, 3.96 mmol, 66% yield. ^{1}H NMR (400 MHz, CDCl$_3$) δ = 7.50 (d, J = 7.6 Hz, 1H, Ar*H*), 7.27-7.23 (m, 1H, Ar*H*), 7.19-7.10 (m, 2H, Ar*H*), 2.48 (s, 3H, C*H*$_3$), 1.33 (s, 12H, C*H*$_3$). ^{13}C NMR (101 MHz, CDCl$_3$) δ = 141.1, 132.9, 129.3, 129.2, 125.3, 121.6, 100.5 (br), 84.2, 24.7, 20.7. The NMR spectra are consistent with literature data.[8] HRMS (Sicrit plasma/LTQ-Orbitrap) m/z: [M + H]$^+$ Calcd for $C_{15}H_{20}BO_2^+$: 243.1551; Found: 243.1550.

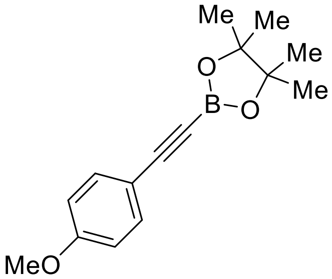

4q. Orange waxy solid. 0.758 g, 2.94 mmol, 49% yield. ^{1}H NMR (400 MHz, CDCl$_3$) δ = 7.47 (d, J = 8.9 Hz, 2H, Ar*H*), 6.82 (d, J = 8.8 Hz, 2H, Ar*H*), 3.80 (s, 3H, C*H*$_3$), 1.31 (s, 12H, C*H*$_3$). ^{13}C NMR (101 MHz, CDCl$_3$) δ = 24.8, 55.4, 84.4, 102.3 (br), 114.1, 133.7, 134.4, 160.6. The NMR spectra are consistent with literature data.[3,8] HRMS (Sicrit plasma/LTQ-Orbitrap) m/z: [M + H]$^+$ Calcd for $C_{15}H_{20}BO_3^+$: 259.1500; Found: 259.1498.

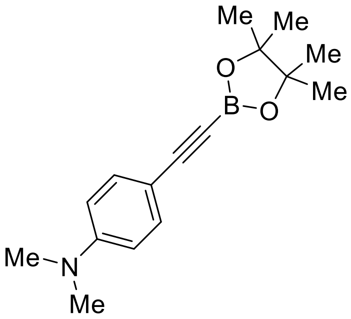

4r. Brownish waxy solid. 0.731 g, 2.70 mmol, 45% yield. ^{1}H NMR (400 MHz, CDCl$_3$) δ = 7.40 (d, J = 9.06 Hz, 2H, Ar*H*), 6.58 (d, J = 9.06 Hz, 2H, Ar*H*), 2.96 (s, 6H, C*H*$_3$), 1.30 (s, 12H, C*H*$_3$). ^{13}C NMR (101 MHz, CDCl$_3$) δ = 150.7, 133.9, 111.3, 108.0, 103.9 (br), 84.0, 39.9, 24.6. The NMR spectra are consistent with literature data.[3] HRMS (Sicrit plasma/LTQ-Orbitrap) m/z: [M + H]$^+$ Calcd for $C_{16}H_{23}BNO_2^+$: 272.1816; Found: 272.1818.

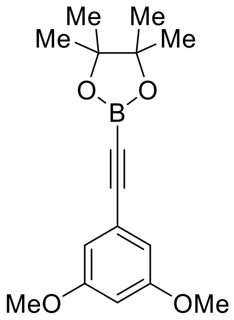

4s. Yellow waxy solid. 1.19 g, 2.88 mmol, 80% purity, 60% yield. g, mmol, % yield. ^{1}H NMR (400 MHz, CDCl$_3$) δ = 6.72 (d, *J* = 2.3, 2H, Ar*H*), 6.50 (t, *J* = 2.3, 1H, Ar*H*), 3.78 (s, 6H, C*H*$_3$), 1.35 (s, 12H, C*H*$_3$). ^{13}C NMR (101 MHz, CDCl$_3$) δ = 160.4, 123.1, 110.2, 103.1, 101.7, 84.5, 55.4, 24.7. IR (v$_{max}$, cm^{-1}) 2979 (m), 2938 (w), 2197 (m), 1591 (s), 1458 (s), 1372 (m), 1323 (s), 1292 (s), 1206 (s), 1141 (s), 1063 (m), 981 (m), 852 (m). HRMS (Sicrit plasma/LTQ-Orbitrap) m/z: [M + H]$^+$ Calcd for $C_{16}H_{22}BO_4^+$ 269.1606; Found 269.1608.

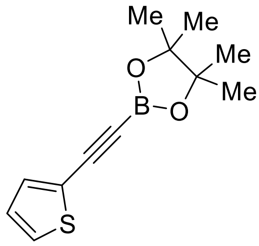

4t. Brown oil. 0.519 g, 2.22 mmol, 37% yield. ^{1}H NMR (400 MHz, CDCl$_3$) δ = 7.34 (d, J = 3.6 Hz, 1H, Ar*H*), 7.30 (d, J = 5.2 Hz, 1H, Ar*H*), 6.97 (dd, J = 5.2, 3.6 Hz, 1H, Ar*H*), 1.32 (s, 12H, C*H*$_3$); ^{13}C NMR (101 MHz, CDCl$_3$) δ = 134.4, 128.8, 126.9, 121.7, 84.5, 24.7. The NMR spectra are consistent with literature data.[8] HRMS (Sicrit plasma/LTQ-Orbitrap) m/z: [M + H]$^+$ Calcd for $C_{12}H_{16}BO_2S^+$: 235.0959; Found: 235.0957.

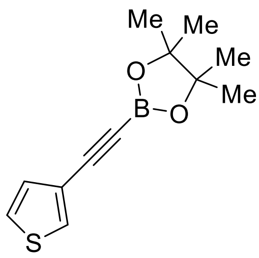

4u. Yellow oil. 0.576 g, 2.46 mmol, 41% yield. ^{1}H NMR (400 MHz, CDCl$_3$) δ = 7.59 (dd, J = 3.2, 1.1 Hz, 1H, Ar*H*), 7.24 (dd, J = 5.0, 3.1 Hz, 1H, Ar*H*), 7.15 (dd, J = 5.1, 1.2 Hz, 1H, Ar*H*), 1.30 (s, 12H, C*H*$_3$). ^{13}C NMR (101 MHz, CDCl$_3$) δ = 131.7, 130.2, 125.4, 121.1, 103.4 (br), 84.4, 83.2, 24.7. The NMR spectra are consistent with literature data.[10] HRMS (Sicrit plasma/LTQ-Orbitrap) m/z: [M + H]$^+$ Calcd for $C_{12}H_{16}BO_2S^+$: 235.0959; Found: 235.0959.

Preparation of maleimides 7

To the solution of maleic anhydride (588 mg, 6.00 mmol) in EtOAc (10 mL) corresponding amine (6.00 mmol) was added in one portion and the reaction mixture was stirred at 80 °C for 6 h. After cooling the reaction mixture to rt the organic solvent was evaporated under reduced pressure to dryness. Obtained waxy residue was dissolved in AcOH (30 mL) and acetice anhydride (3 mL) was added in one portion. The resulting solution was heated to 120 °C and kept at 120 °C for 12 h. After cooling the reaction mixture to rt the reaction mixture was poured on crushed ice/water mixture, and the obtained suspension was filtered. Desired product **7** was obtained after drying of the solid on air overnight without any additional purification.

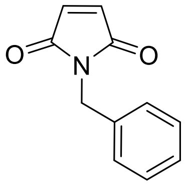

7c. White solid. 0.897 g, 4.80 mmol, 80% yield. ^{1}H NMR (400 MHz, DMSO) δ = 7.41-7.22 (m, 5H, ArH), 7.08 (s, 2H, CH_2), 4.61 (s, 2H, CH_2). ^{13}C NMR (101 MHz, DMSO[D$_6$]) δ = 170.5, 136.2, 134.2, 128.7, 128.4, 127.9, 41.4. The NMR spectra are consistent with literature data.[11] HRMS (ESI/QTOF) m/z: [M + Na]$^+$ Calcd for $C_{11}H_9NO_2Na^+$: 210.0525; Found: 210.0526.

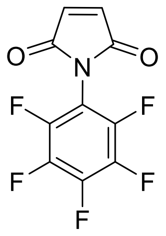

7e. Beige solid. 0.0.817 g, 3.12 mmol, 52% yield. ^{1}H NMR (600 MHz, CDCl$_3$) δ = 6.98 (s, 2H, CH). ^{13}C NMR (151 MHz, CDCl$_3$) δ = 166.9, 146.9 (ddq, J = 165.12 12.4, 4.1 Hz), 142.3 (dtt, J = 258.2, 13.2, 4.5 Hz) , 138.0 (br), 135.5, 106.4 (br). ^{19}F NMR (565 MHz, CDCl$_3$) δ: -142.8 – -143.1 (m), -151.0 (t, J = 21.3 Hz), -160.6 – -161.3 (m). The NMR spectra are consistent with literature data.[12] HRMS (ESI/QTOF) m/z: [M + Na]$^+$ Calcd for $C_{10}H_2F_5NO_2Na^+$: 285.9898; Found: 286.0000.

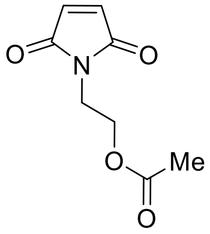

7f. Yellowish solid. 0.768 g, 4.20 mmol, 70% yield. ^{1}H NMR (400 MHz, CDCl$_3$,) δ = 6.71 (s, 2 H, CH), 4.22 (t, J = 5.4 Hz, 2H, CH_2), 3.77 (t, J = 5.4 Hz, 2H, CH_2), 2.01 (s, 3H, CH_3). ^{13}C NMR (CDCl$_3$, 101 MHz) δ = 177.1, 170.9, 60.8, 37.9, 28.1, 20.7. The NMR spectra are consistent with literature data.[13] HRMS (ESI/QTOF) m/z: [M + Na]$^+$ Calcd for $C_8H_9NO_4Na^+$: 206.0424; Found: 206.0423.

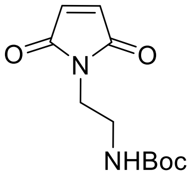

7g. Brownish solid. 0.547 g, 2.28 mmol, 38% yield. ^{1}H NMR (400 MHz, CDCl$_3$) δ = 6.70 (s, 2H, CH), 4.82 (br s, 1H, NH), 3.59–3.70 (m, 2H, CH_2), 2.23–2.37 (m, 2H, CH_2), 1.38 (s, 9H, CH_3), ^{13}C NMR (101 MHz, CDCl$_3$) δ = 170.8, 134.1, 79.4, 39.3, 37.9, 28.2. The NMR spectra are consistent with literature data.[14] HRMS (ESI/QTOF) m/z: [M + Na]$^+$ Calcd for $C_{11}H_{16}N_2O_4Na^+$: 263.1002; Found: 263.1002.

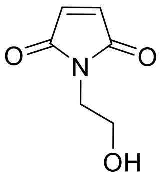

7h. Compound was obtained from 0.200 g of **7f** by the reported procedure.[15] Beige solid. 0.110 g, 0.781 mmol, 71% yield. ^{1}H NMR (400 MHz, DMSO) δ = 7.01(s, 2H, CH), 4.78 (br s, 1H, OH), 3.46 (br s, 4H, CH_2). ^{13}C NMR (101 MHz, DMSO) δ = 171.1, 134.5, 57.9, 39.9. The NMR spectra are consistent with literature data. [15,16] HRMS (ESI/QTOF) m/z: [M + Na]$^+$ Calcd for $C_6H_7NO_3Na^+$: 164.0318; Found: 164.0317.

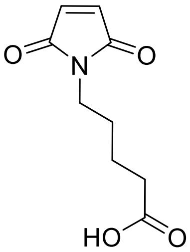

7i. Colorless solid. 1.18 g, 3.72 mmol, 62% yield. ^{1}H NMR (500 MHz, $CDCl_3$) δ = 6.69 (s, 2H, C*H*), 3.53 (t, J = 6.8 Hz, 2H, C*H*$_2$), 2.37 (t, J = 7.1 Hz, 2H, C*H*$_2$), 1.69–1.55 (m, 4H, C*H*$_2$). ^{13}C NMR (125 MHz, $CDCl_3$) δ = 179.1, 170.8, 134.0, 37.3, 33.3, 27.8, 21.7. The NMR spectra are consistent with literature data.[17] HRMS (ESI/QTOF) m/z: $[M + Na]^+$ Calcd for $C_9H_{11}NO_4Na^+$: 220.0580; Found: 220.0579.

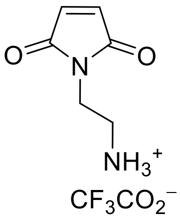

7j. Compound was obtained from 0.200 g of **7g** by the reported procedure. [14] Beige solid. 0.165 g, 0.65 mmol, 78% yield. ^{1}H NMR (400 MHz, DMSO) δ = 8.04 (br s, 3H, C*H*$_3$), 7.05 (s, 2H, C*H*), 3.66 (t, J = 5.9 Hz, 2H, C*H*$_2$), 2.99 (t, J = 5.8 Hz, 2H, C*H*$_2$). ^{13}C NMR (101 MHz, DMSO) δ = 171.0, 134.8, 37.5, 35.0. The NMR spectra are consistent with literature data.[14] HRMS (ESI/QTOF) m/z: $[M]^+$ Calcd for $C_6H_9N_2O_2^+$: 141.0659; Found: 141.0660.

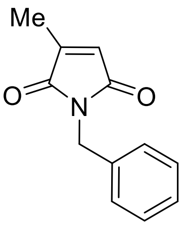

7k. Orange oil. 0.446 g, 2.22 mmol, 37% yield. ^{1}H NMR (400 MHz, $CDCl_3$) δ = 7.35-7.24 (m, 5H, Ar*H*), 6.33 (q, J = 1.8 Hz, 1H, C*H*), 4.65 (s, 2H, C*H*), 2.07 (d, J = 1.8 Hz, 3H, C*H*$_3$). ^{13}C NMR (400 MHz, $CDCl_3$) δ = 171.5, 170.5, 145.7, 136.4, 128.6, 128.4, 127.7, 127.4, 41.5, 11.0. The NMR spectra are consistent with literature data.[18] HRMS (ESI/QTOF) m/z: $[M + Na]^+$ Calcd for $C_{12}H_{11}NO_2Na^+$: 224.0682; Found: 224.0680.

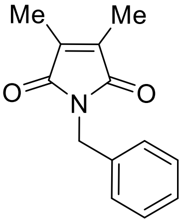

7m. Orange oil. 0.658 g, 3.06 mmol, 51% yield. ^{1}H NMR (400 MHz, $CDCl_3$) δ = 7.25–7.35 (m, 5H, Ar*H*), 4.66 (s, 2H, C*H*$_2$), 1.97 (s, 6H, C*H*$_3$). ^{13}C NMR (101 MHz, $CDCl_3$) δ = 171.8, 137.3, 136.7, 129.3, 128.6, 128.4, 127.7, 41.5, 8.7. The NMR spectra are consistent with literature data.[19] HRMS (ESI/QTOF) m/z: $[M + Na]^+$ Calcd for $C_{13}H_{13}NO_2Na^+$: 238.0838; Found: 238.0839.

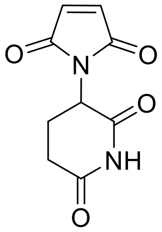

7n. White solid. 0.524 g, 2.52 mmol, 42% yield. ^{1}H NMR (400 MHz, DMSO) δ = 11.07 (s, 1H, N*H*), 7.12 (s, 2H, C*H*), 4.93-4.98 (m, 1H, C*H*), 2.79- 2.88 (m, 1H, C*H*$_2$), 2.53- 2.58 (m, 1H, C*H*$_2$), 2.36- 2.46 (m, 1H, C*H*$_2$), 1.94- 1.99 (m, 1H, C*H*$_2$). The NMR spectra are consistent with literature data.[20] HRMS (ESI/QTOF) m/z: $[M + Na]^+$ Calcd for $C_9H_8N_2O_4Na^+$: 231.0376; Found: 231.0376.

General Procedure for the Preparation of Products **8** and **9**

Method A. Reaction in *n*-hexane.

A suspension of corresponding maleimide (0.100 mmol, 1 equiv.), alkynyl boronate (0.100 mmol, 1 equiv.), and thioxanthone (2.1 mg, 0.010 mmol, 0.1 equiv.) in *n*-hexane (2 mL) was placed into a glass tube, closed with rubber septum and degassed by three vacuum pumping-nitrogen purge cycles. The resulting solution was irradiated in a Rayonet® reactor (λ_{max} = 350 nm) placed at a 3 cm distance from the vessel (see Photos S1 and S2 for the experimental setup) at rt for 12 h. The precipitate (maleimide dimer **10**) was filtered off, and the filtrate was evaporated in vacuo. The crude material was dissolved in minimal amounts of pentane (1–2 mL) and stored in refrigerator for 24 h. The precipitate was decanted, washed with cold pentane (3×1 mL) and dried under air to give product **8**.

Method B.* Reaction in CH_2Cl_2.

A solution of the corresponding maleimide (0.100 mmol, 1 equiv.), alkynyl boronate **1a–o** (0.300 mmol, 3 equiv.), and thioxanthone (2.1 mg, 0.010 mmol, 0.1 equiv.) in CH_2Cl_2 (2 mL) was placed in a glass tube, closed with a rubber septum and degassed by three vacuum pumping-nitrogen purge cycles. The resulting solution was irradiated in a Rayonet® reactor (λ_{max} = 350 nm) placed at a 3 cm distance from the vessel (see Photos S1 and S2 for the experimental setup) at rt for 12 h. After the reaction was complete, the organic solvent was evaporated under reduced pressure to dryness. The obtained semi-solid material was triturated with *n*-hexane (5 mL), the precipitate (maleimide dimer **10**) was filtered off, and the filtrate was evaporated in vacuo. The crude product was dissolved in minimal amounts of pentane (1–2 mL) and stored in refrigerator for 24 hrs. The precipitate was decanted, washed with cold pentane (3×1 mL) and dried under air to give product **8**.

*Method B was used for the substrates, insoluble in *n*-hexane, i.e., maleimides **7d,e,l,j,n** and alkynyl boronate **4i**.

Method C.*

A solution of the corresponding maleimide (0.300 mmol, 3 equiv.), arylalkynyl boronate (0.100 mmol, 1 equiv.), and thioxanthone (2.1 mg, 0.010 mmol, 0.1 equiv.) in CH_2Cl_2 (6 mL) was placed in a glass tube, closed with a rubber septum and degassed by three vacuum pumping-nitrogen purge cycles. The resulting solution was irradiated in a Rayonet® reactor (λ_{max} = 350 nm) placed at a 3 cm distance from the vessel (see Photos S1 and S2 for the experimental setup) at rt for 12 h. After the reaction was complete, the organic solvent was evaporated under reduced pressure to dryness. The obtained crude material was purified by column chromatography using pentane/Et_2O gradient (90/10 – 50/50) following by CH_2Cl_2/acetonitrile gradient (100/0 – 70/30).

*Method C was used for aryl-substituted alkynyl boronates **4m–u**.

Product characterization

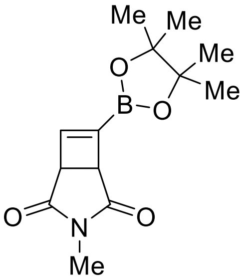

8a. *Method A.* White fluffy solid. 18.4 mg, 0.070 mmol, 70% yield. ^1H NMR (400 MHz, $CDCl_3$) δ 7.07 (d, *J* = 0.8 Hz, 1H, C*H*), 3.86 (d, *J* = 3.1 Hz, 1H, C*H*), 3.84 (dd, *J* = 3.1, 0.8 Hz, 1H, C*H*), 2.96 (s, 3H, CH_3), 1.28 (s, 12H, CH_3). ^{13}C NMR (101 MHz, $CDCl_3$) δ 174.6, 174.3, 152.4, 84.4, 48.5, 47.5, 24.9, 24.8, 24.6. ^{11}B NMR (128 MHz, $CDCl_3$) δ 27.20. IR (ν_{max}, cm^{-1}) 2895 (w), 1768 (w), 1698 (m), 1603 (w), 1429 (w), 1377 (m), 1346 (m), 1278 (w), 1142 (w), 964 (w), 855 (w), 771 (m). HRMS (ESI/QTOF) m/z: [M + Na]$^+$ Calcd for $C_{13}H_{18}BNNaO_4^+$ 286.1221; Found 286.1229.

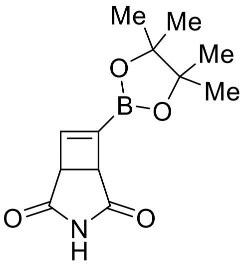

8b. *Method A.* Beige amorphous solid. 10.4 mg, 0.042 mmol, 42% yield. ^1H NMR (400 MHz, $CDCl_3$) δ = 7.55 (s, 1H), 7.07 (s, 1H, C*H*), 3.96 – 3.83 (m, 1H, 2xC*H*), 1.28 (s, 12H, CH_3). ^{13}C NMR (151 MHz, $CDCl_3$) δ = 174.1, 173.7, 152.0, 84.5, 49.9, 48.9, 24.8, 24.6. IR (ν_{max}, cm^{-1}) 2979 (w), 1768 (w), 1715 (m), 1375 (w), 1341 (m), 1142 (w), 964 (w), 852 (w), 767 (w). HRMS (ESI/QTOF) m/z: [M + Na]$^+$ Calcd for $C_{12}H_{16}BNNaO_4^+$ 272.1065; Found 272.1071.

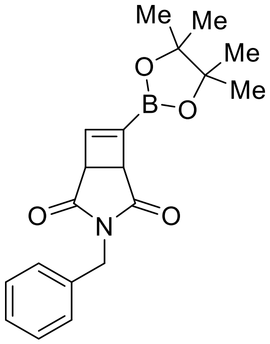

8c. *Method A.* White amorphous solid. 23.6 mg, 0.071 mmol, 71% yield. ^{1}H NMR (400 MHz, $CDCl_3$) δ 7.33 – 7.19 (m, 5H, Ar*H*), 6.99 (d, *J* = 0.8 Hz, 1H. C*H*), 4.54 (s, 2H, C*H*$_2$), 3.88 – 3.57 (m, 2H, 2xC*H*), 1.20 (s, 12H, C*H*$_3$). ^{13}C NMR (101 MHz, $CDCl_3$) δ 174.2, 173.8, 152.4, 135.9, 128.6, 127.8, 84.4, 48.5, 47.6, 42.2, 24.8, 24.6 (carbon signals of phenyl ring are not fully resolved). IR (v_{max}, cm^{-1}) 2979 (w), 2930 (w), 1768 (w), 1704 (s), 1601 (w), 1386 (m), 1340 (s), 1163 (m), 1140 (m), 853 (m). HRMS (ESI/QTOF) m/z: [M + Na]$^+$ Calcd for $C_{19}H_{22}BNNaO_4^+$ 362.1534; Found 362.1541.

*Scale-up for 10 mmol of maleimide **7c**.* Pure product **7c** was obtained by a modified procedure. The suspension obtained after irradiation was filtered, washed with additional amounts of n-hexane (3×15 mL). The obtained solid was washed with Et_2O (4×15 mL). The combined ethereal solutions were evaporated under reduced pressure and dried under air to give pure product (2.24 g, 6.61 mmol, 66% yield). The hexane washings contained still some impure product. After a second recrystallization additional amounts of **8c** (0.25 g, 90% purity) were obtained.

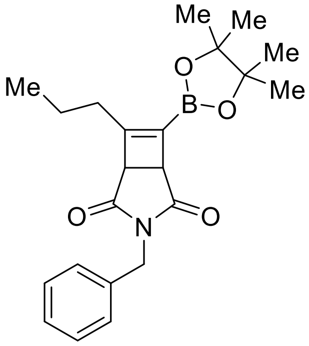

8ca. *Method A.* Beige amorphous solid. 17.1 mg, 0.045 mmol, 45% yield. ^{1}H NMR (400 MHz, $CDCl_3$) δ = 7.34 – 7.27 (m, 5H, Ar*H*), 4.62 (d, *J* = 14.2 Hz, 1H, *H*CH), 4.58 (d, *J* = 14.1 Hz, 1H, HC*H*), 3.73 (d, *J* = 3.1 Hz, 1H, C*H*), 3.68 – 3.63 (m, 1H, C*H*), 2.31 (hept, *J* = 7.3 Hz, 2H, C*H*$_2$), 1.55 – 1.43 (m, 2H, C*H*$_2$), 1.25 (s, 12H, C*H*$_3$), 0.84 (t, *J* = 7.4 Hz, 3H, C*H*$_3$). ^{13}C NMR (101 MHz, $CDCl_3$) δ 175.3, 174.2, 168.6, 136.1, 128.6, 128.5, 127.7, 83.8, 49.4, 43.7, 42.0, 33.2, 24.9, 24.5, 20.0, 13.7. IR (v_{max}, cm^{-1}) 2957 (m), 2922 (m), 2852 (w), 1744 (w), 1462 (w), 1379 (w), 1216 (w), 768 (w). HRMS (ESI/QTOF) m/z: [M + Na]$^+$ Calcd for $C_{22}H_{28}BNNaO_4^+$ 404.2004; Found 404.1999.

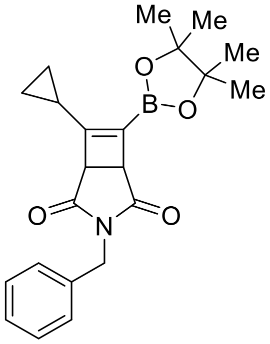

8cb. *Method A.* White amorphous solid. 21.2 mg, 0.056 mmol, 56% yield. ^{1}H NMR (400 MHz, $CDCl_3$) δ = 7.35 – 7.27 (m, 3H, Ar*H*), 7.24 – 7.21 (m, 2H, Ar*H*), 4.61 (d, *J* = 14.2 Hz, 1H, HC*H*), 4.57 (d, *J* = 14.3, 1H, *H*CH), 3.60 (d, *J* = 3.3 Hz, 1H, C*H*), 3.55 (d, *J* = 3.0 Hz, 1H, C*H*), 1.94 – 1.83 (m, 1H), 1.27 (s, 12H), 1.19 – 1.10 (m, 1H), 0.98 – 0.88 (m, 1H), 0.87 – 0.74 (m, 2H). ^{13}C NMR (101 MHz, $CDCl_3$) δ = 175.2, 174.3, 169.5, 136.1, 128.6, 128.5, 127.7, 83.7, 47.4, 42.8, 42.1, 24.9, 24.6, 13.5, 8.0, 7.2. IR (v_{max}, cm^{-1}) 2986 (w), 2959 (w), 1767 (w), 1704 (s), 1636 (w), 1427 (w), 1388 (m), 1335 (m), 1310 (w), 1170 (m), 1142 (m), 968 (w), 854 (w). HRMS (ESI/QTOF) m/z: [M + Na]$^+$ Calcd for $C_{22}H_{26}BNNaO_4^+$ 402.1847; Found 402.1847.

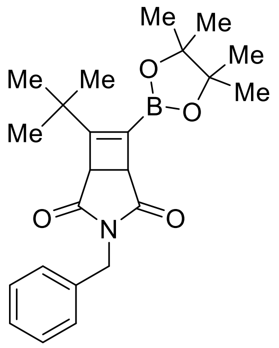

8cc. *Method A.* White amorphous solid.15.8 mg, 0.040 mmol, 40% yield. ^{1}H NMR (400 MHz, $CDCl_3$) δ = 7.41 – 7.10 (m, 5H, Ar*H*), 4.66 (d, *J* = 14.3 Hz, 1H, HC*H*), 4.61 (d, *J* = 14.3 Hz, 1H, *H*CH), 3.78 (d, *J* = 3.2 Hz, 1H, C*H*), 3.58 (d, *J* = 3.2 Hz, 1H, C*H*), 1.29 (s, 12H, CH_3), 1.13 (s, 9H). ^{13}C NMR (101 MHz, $CDCl_3$) δ = 175.4, 174.8, 174.4, 136.2, 128.6, 128.5, 127.7, 84.2, 47.9, 42.8, 42.05, 35.8, 28.5, 25.0, 24.5. ^{11}B NMR (128 MHz, $CDCl_3$) δ = 28.35 – 27.35 (m). IR (v_{max}, cm^{-1}) 3022 (w), 2979 (m), 1767 (w), 1703 (s), 1630 (w), 1386 (m), 1350 (s), 1314 (m), 1216 (m), 1141 (s), 855 (m), 754 (s). HRMS (ESI/QTOF) m/z: [M + Na]$^+$ Calcd for $C_{23}H_{30}BNNaO_4^+$ 418.2160; Found 418.2165.

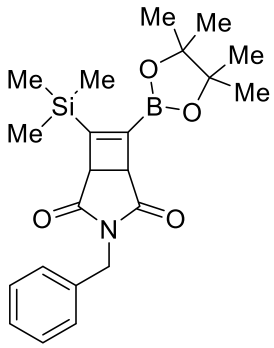

8cd. *Method A.* Yellowish glassy solid. 18.1 mg, 0.044 mmol, 44% yield. ^{1}H NMR (400 MHz, $CDCl_3$) δ = 7.33 – 7.14 (m, 5H, Ar*H*), 4.61 (s, 2H, CH_2), 3.86 (d, *J* = 3.1 Hz, 1H, C*H*), 3.75 (d, *J* = 3.1 Hz, 1H, C*H*), 1.26 (s, 12H, CH_3), 0.14 (s, 9H, CH_3). ^{13}C NMR (101 MHz, $CDCl_3$) δ = 177.4, 176.5 (2xC), 137.9, 130.3, 130.1, 129.4, 85.9, 51.6, 50.2, 43.7, 26.7, 26.3, 0.0. IR (v_{max}, cm^{-1}) 2979 (m), 1766 (w), 1701 (s), 1580 (w), 1385 (m), 1341 (s), 1142 (m), 845 (s), 755 (m). HRMS (ESI/QTOF) m/z: [M + Na]$^+$ Calcd for $C_{22}H_{30}BNNaO_4Si^+$ 434.1929; Found 434.1937.

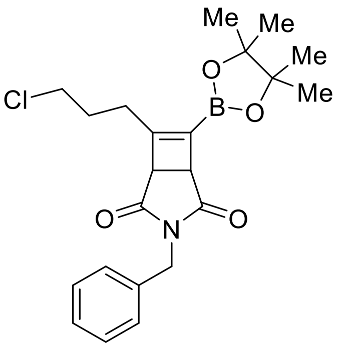

8ce. *Method A.* White amorphous solid. 18.7 mg, 0.045 mmol, 45% yield. ^{1}H NMR (400 MHz, $CDCl_3$) δ = 7.36 – 7.27 (m, 5H, Ar*H*), 4.63 (d, *J* = 14.2 Hz, 1H, HC*H*), 4.57 (d, *J* = 14.2 Hz, 1H, *H*CH), 3.77 – 3.70 (m, 1H), 3.67 (dd, *J* = 3.1, 1.5 Hz, 1H, CH_2), 3.41 (td, *J* = 6.6, 1.7 Hz, 2H, CH_2), 2.50 (t, *J* = 7.4 Hz, 2H, CH_2), 1.97 (p, *J* = 6.9 Hz, 2H, CH_2), 1.26 (s, 12H, CH_3). ^{13}C NMR (101 MHz, $CDCl_3$) δ = 175.0, 174.0, 166.5, 136.0, 128.6, 127.8, 84.0, 49.5, 44.1, 43.9, 42.1, 29.4, 28.7, 24.9, 24.6 (carbon signals of phenyl ring are not fully resolved). IR (v_{max}, cm^{-1}) 2979 (m), 1767 (w), 1701 (s), 1642 (m), 1371 (s), 1338 (m), 1141 (s). HRMS (ESI/QTOF) m/z: [M + Na]$^+$ Calcd for $C_{22}H_{27}BClNNaO_4^+$ 438.1614; Found 438.1621.

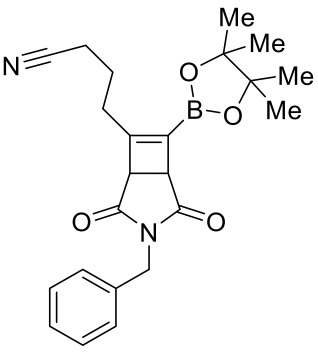

8cf. *Method A.* White amorphous solid. 17.4 mg, 0.043 mmol, 43% yield. ^{1}H NMR (400 MHz, $CDCl_3$) δ = 7.39 – 7.26 (m, 5H, Ar*H*), 4.66 (d, *J* = 14.1 Hz, 1H, HC*H*), 4.55 (d, *J* = 14.1 Hz, 1H, *H*CH), 3.77 – 3.72 (m, 1H, C*H*), 3.69 (dd, *J* = 3.0, 1.5 Hz, 1H, C*H*), 2.47 (h, *J* = 8.2 Hz, 2H, CH_2), 2.11 (t, *J* = 7.2 Hz, 2H, CH_2), 1.95 – 1.73 (m, 2H, CH_2), 1.27 (s, 12H, CH_3). ^{13}C NMR (151 MHz, $CDCl_3$) δ = 174.8, 174.1, 165.5, 136.1, 128.8, 128.8, 128.1, 119.3, 84.3, 49.7, 44.1, 42.2, 30.3, 25.0, 24.7, 22.5, 16.5. IR (v_{max}, cm^{-1}) 2956 (w), 2929 (w), 2870 (w), 2211 (w), 1702 (m), 1456 (w), 1343 (m), 1170 (w), 1145 (w), 853 (w), 769 (w). HRMS (ESI/QTOF) m/z: [M + Na]$^+$ Calcd for $C_{23}H_{27}BN_2NaO_4^+$ 429.1956; Found 429.1963.

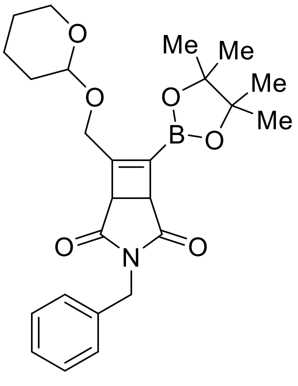

8cg. *Method A.* White amorphous solid. 18.1 mg, 0.040 mmol, 40% yield, mixture of diastereomers. ^{1}H NMR (400 MHz, $CDCl_3$) δ = 7.39 – 7.13 (m, 5H, Ar*H*), 4.71 (t, J = 3.1 Hz, 0.5H, C*H*), 4.65 (t, J = 3.3 Hz, 0.5H, C*H*), 4.60 (s, 2H, benzylic C*H₂*), 4.43 (d, J = 14.3 Hz, 0.5H, HC*H*), 4.35 (d, J = 14.3 Hz, 0.5H, HC*H*), 4.19 (d, J = 14.1 Hz, 0.5H, *H*CH), 4.13 (d, J = 14.4 Hz, 0.5H, *H*CH), 3.92 – 3.78 (m, 2H, CH_2), 3.77 – 3.69 (m, 1H, C*H*), 3.56 – 3.35 (m, 1H, C*H*), 1.96 – 1.76 (m, 1H, aliphatic CH_2), 1.73 – 1.44 (m, 5H, aliphatic CH_2), 1.26 (s, 12H, CH_3). ^{13}C NMR (101 MHz, $CDCl_3$) δ = 174.6, 173.4 and 173.3, 163.1 and 162.8, 136.1, 128.6 and 128.5, 127.7, 98.5 and 97.9, 84.1, 63.3 and 63.0, 61.8 and 61.5, 48.5, 44.6 and 44.5, 42.1, 30.2, 25.4, 24.9, 24.6, 18.9 and 18.7. IR (ν_{max}, cm^{-1}) 2979 (w), 2950 (w), 1768 (w), 1704 (s), 1651 (w), 1364 (m), 1141 (m), 1033 (m), 766 (w). HRMS (ESI/QTOF) m/z: $[M + Na]^+$ Calcd for $C_{25}H_{32}BNNaO_6^+$ 476.2215; Found 476.2227.

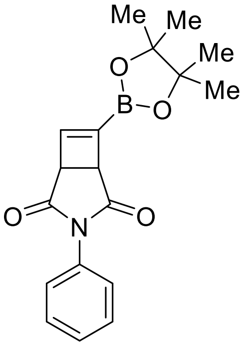

8d. *Method B.* White amorphous solid. 13.0 mg, 0.040 mmol, 40% yield. ^{1}H NMR (400 MHz, $CDCl_3$) δ = 7.58 – 7.28 (m, 5H, Ar*H*), 7.17 (s, 1H, C*H*), 4.14 – 3.82 (m, 2H, 2xC*H*), 1.29 (s, 6H, CH_3), 1.28 (s, 6H, CH_3). ^{13}C NMR (101 MHz, $CDCl_3$) δ = 173.5, 173.3, 152.3, 132.0, 129.1, 128.6, 126.6, 84.5, 48.4, 47.4, 24.9, 24.6. IR (ν_{max}, cm^{-1}) 2958 (w), 2921 (w), 1717 (w), 1599 (w), 1375 (w), 1141 (w), 853 (w), 770 (w). HRMS (ESI/QTOF) m/z: $[M + Na]^+$ Calcd for $C_{18}H_{20}BNNaO_4^+$ 348.1378; Found 348.1366.

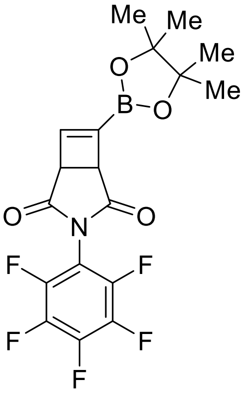

8e. *Method B.* Beige amorphous solid. 14.6 mg, 0.035 mmol, 35% yield. ^{1}H NMR (400 MHz, $CDCl_3$) δ = 7.14 (s, 1H, C*H*), 4.15 – 4.10 (m, 2H, C*H*), 1.29 (s, 6H, CH_3), 1.28 (s, 6H, CH_3) ^{13}C NMR (151 MHz, $CDCl_3$) δ = 171.4, 171.2, 152.1, 145.5 – 144.1 (m), 143.6 – 142.0 (m), 141.3 (t, J = 13.4), 137.9 (dq, J = 256.2, 12.8), 108.11 – 106.75 (m), 84.6, 48.8, 47.9, 24.8, 24.6. ^{19}F NMR (565 MHz, $CDCl_3$) δ = -142.6 (d, J = 22.5), -143.6 (dt, J = 22.3, 5.4), -151.2 (t, J = 21.4), -160.83 (td, J = 22.0, 6.5), -160.94 (td, J = 22.0, 6.5). IR (ν_{max}, cm^{-1}) 2982 (w), 1732 (s), 1522 (s), 1351 (m), 1141 (m), 1062 (w), 990 (m), 766 (m). HRMS (ESI/QTOF) m/z: $[M + H]^+$ Calcd for $C_{18}H_{16}BF_5NO_4^+$ 416.1087; Found 416.1069.

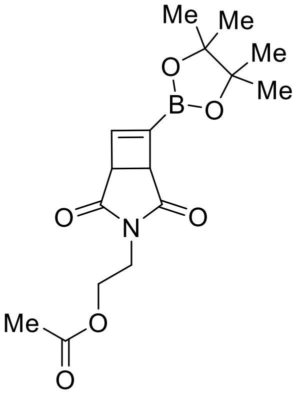

8f. *Method A.* Yellowish amorphous solid. 21.8 mg, 0.065 mmol, 65% yield. ^{1}H NMR (400 MHz, $CDCl_3$) δ = 7.07 (d, J = 0.8 Hz, 1H, Ar*H*), 4.51 – 4.07 (m, 2H, CH_2), 3.92 – 3.82 (m, 2H, 2xC*H*), 3.74 (t, J = 5.3 Hz, 2H, CH_2), 2.00 (s, 3H, CH_3), 1.28 (s, 12H, 4xCH_3). ^{13}C NMR (101 MHz, $CDCl_3$) δ = 174.3, 174.0, 170.8, 152.2, 84.4, 60.7, 48.4, 47.4, 37.7, 24.8, 24.6, 20.8. IR (ν_{max}, cm^{-1}) 2980 (w), 1703 (s), 1387 (m), 1346 (m), 1232 (m), 1141 (m), 767 (w). HRMS (ESI/QTOF) m/z: $[M + Na]^+$ Calcd for $C_{16}H_{22}BNNaO_6^+$ 358.1432; Found 358.1444.

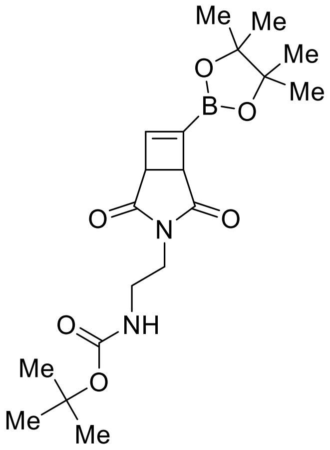

8g. *Method A.* Yellowish amorphous solid. 19.6 mg, 0.050 mmol, 50% yield. ^{1}H NMR (400 MHz, CDCl$_3$) δ = 7.06 (s, 1H, C*H*), 4.79 (s, 1H, N*H*), 3.87 – 3.84 (m, 2H, 2xC*H*), 3.61 (t, *J* = 5.6 Hz, 2H, C*H*$_2$), 3.42 – 3.23 (m, 2H, C*H*$_2$), 1.41 (s, 9H, 3xC*H*$_3$), 1.28 (s, 12H, 4xC*H*$_3$). ^{13}C NMR (151 MHz, CDCl$_3$) δ = 180.8, 174.7, 174.3, 155.9, 152.3, 84.3, 79.3, 48.4, 47.4, 39.1, 38.5, 28.3, 24.8, 24.5. IR (ν_{max}, cm^{-1}) 2979 (w), 2942 (w), 1700 (s), 1393 (m), 1342 (m), 1167 (m), 752 (s). HRMS (ESI/QTOF) m/z: [M + Na]$^+$ Calcd for $C_{19}H_{29}BN_2NaO_6^+$ 415.2011; Found 415.2018.

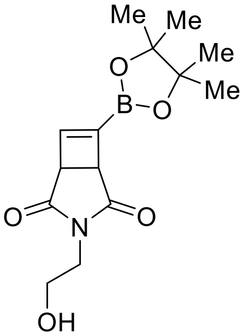

8h. *Method A.* Yellowish glassy solid. 17.6 mg, 0.060 mmol, 60% yield. ^{1}H NMR (400 MHz, CDCl$_3$) δ = 7.07 (s, 1H, C*H*), 3.89 – 3.85 (m, 2H, 2xC*H*), 3.82 – 3.72 (m, 2H, C*H*$_2$), 3.72 – 3.62 (m, 2H, C*H*$_2$), 1.27 (s, 13H, 4xC*H*$_3$ + O*H*). ^{13}C NMR (101 MHz, CDCl$_3$) δ = 175.3, 174.9, 152.4, 84.5, 60.8, 48.4, 47.5, 41.7, 24.8, 24.6. IR (ν_{max}, cm^{-1}) 2986 (w), 1768 (w), 1701 (m), 1602 (w), 1389 (w), 1342 (m), 1166 (w), 1142 (w), 853 (w). HRMS (ESI/QTOF) m/z: [M + Na]$^+$ Calcd for $C_{14}H_{20}BNNaO_5^+$ 316.1327; Found 316.1317

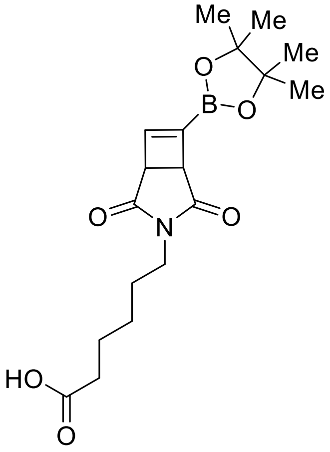

8i. *Method B.* White amorphous solid. 26.1 mg, 0.072 mmol, 72% yield. ^{1}H NMR (400 MHz, CDCl$_3$) δ = 7.07 (d, *J* = 0.9 Hz, 1H, C*H*), 3.98 – 3.75 (m, 2H, 2xC*H*), 3.46 (t, *J* = 7.2 Hz, 2H, C*H*$_2$), 2.32 (t, *J* = 7.4 Hz, 2H, C*H*$_2$), 1.78 – 1.62 (m, 2H, C*H*$_2$), 1.62 – 1.50 (m, 2H, C*H*$_2$), 1.36 – 1.30 (m, 2H, C*H*$_2$), 1.28 (s, 12H, 4xC*H*$_3$). ^{13}C NMR (101 MHz, CDCl$_3$) δ = 177.7, 174.6, 174.3, 152.6, 84.5, 48.4, 47.4, 38.3, 33.5, 27.1, 26.0, 24.9, 24.5, 24.2. IR (ν_{max}, cm^{-1}) 2986 (w), 2944 (w), 1765 (w), 1731 (m), 1701 (s), 1602 (w), 1346 (m), 1216 (w), 1142 (m), 856 (w), 768 (w). HRMS (ESI/QTOF) m/z: [M – CH$_2$COO$^-$]$^+$ Calcd for $C_{18}H_{27}BNO_6^+$ 304.0956; Found 304.0955.

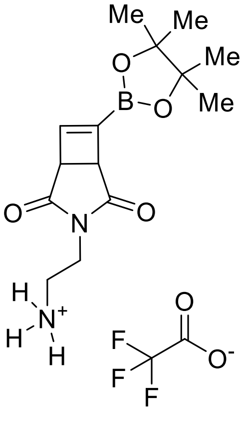

8j. *Method B* (pure product was obtained by trituration with Et$_2$O). Beige amorphous solid. 20.1 mg, 0.051 mmol, 51% yield. ^{1}H NMR (400 MHz, CD$_3$CN) δ = 8.19 – 7.30 (br s, 3H, N*H*$_3$), 6.99 (d, *J* = 1.1 Hz, 1H, C*H*), 3.85 (dd, *J* = 3.1, 1.1 Hz, 1H, C*H*), 3.79 (d, *J* = 3.2 Hz, 1H, C*H*), 3.73 – 3.63 (m, 2H, C*H*$_2$), 3.14 (d, *J* = 5.7 Hz, 2H, C*H*$_2$), 1.24 (s, 12H, 4xC*H*$_3$). ^{13}C NMR (101 MHz, CD$_3$CN) δ = 175.8, 175.3, 152.7, 84.7, 49.3, 48.3, 38.8, 36.7, 24.6, 24.6 (TFA peaks omitted). ^{19}F NMR (376 MHz, CD$_3$CN) δ = -75.84. IR (ν_{max}, cm^{-1}) 2990 (w), 2887 (w), 1699 (s), 1390 (m), 1220 (m). HRMS (ESI/QTOF) m/z: [M]$^+$ Calcd for $C_{14}H_{22}BN_2O_4^+$ 293.1667; Found 293.1671.

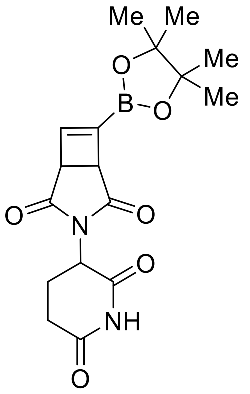

8n. Mixture of isomers. *Method B.* Beige amorphous solid. 24.5 mg, 0.068 mmol, 68% yield. ^{1}H NMR (400 MHz, CDCl$_3$) δ = 8.03 (s, 1H, N*H*), 7.09 (s, 1H, C*H*), 4.90 – 4.71 (m, 1H, C*H*), 4.09 – 3.85 (m, 2H, C*H*$_2$), 3.05 – 2.75 (m, 1H, C*H*), 2.72 – 2.53 (m, 2H, C*H*$_2$), 2.09 – 1.92 (m, 1H, C*H*), 1.28 (s, 12H, 4xC*H*$_3$). ^{13}C NMR (101 MHz, CDCl$_3$) δ = 173.5 and 173.1, 173.3 and 173.2, 170.7, 167.2, 152.2, 84.6 and 84.5, 49.4 and 49.3, 48.4 and 48.2, 47.6 and 47.3, 31.12 and 31.08, 24.8, 24.6, 21.3. IR (ν_{max}, cm^{-1}) 2958 (w), 2925 (w), 2867 (w), 1715 (m), 1460 (w), 1378 (w), 1329 (w), 1267 (w), 1202 (w), 1141 (w), 767 (w). HRMS (ESI/QTOF) m/z: [M + Na]$^+$ Calcd for $C_{17}H_{21}BN_2NaO_6^+$ 383.1385; Found 383.1375.

Double cycloaddition products

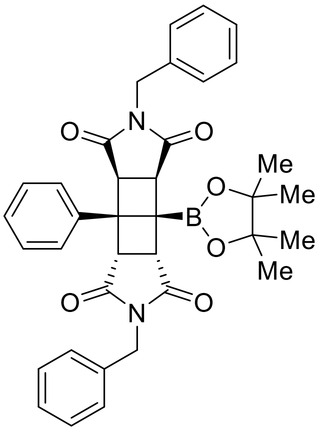

9a. *Method C.* Beige amorphous solid. *R$_f$* = 0.45 (pentane/Et$_2$O). 9.8 mg, 0.016 mmol, 16% yield. ^{1}H NMR (400 MHz, CDCl$_3$) δ = 7.56 – 7.44 (m, 2H, Ar*H*), 7.33 – 7.19 (m, 8H, Ar*H*), 7.19 – 7.10 (m, 3H, Ar*H*), 7.09 – 7.02 (m, 2H, Ar*H*), 4.76 (s, 2H, C*H*$_2$), 4.54 (d, *J* = 13.9 Hz, 1H, HC*H*), 4.40 (d, *J* = 13.9 Hz, 1H, HC*H*), 3.84 (d, *J* = 8.8 Hz, 1H, C*H*), 3.78 (d, *J* = 8.9 Hz, 1H, C*H*), 3.09 (d, *J* = 6.1 Hz, 1H, C*H*), 2.80 (d, *J* = 6.1 Hz, 1H, C*H*), 1.13 (s, 6H, 2xC*H*$_3$), 1.11 (s, 6H, 2xC*H*$_3$). ^{13}C NMR (101 MHz, CDCl$_3$) δ = 176.3, 176.0, 175.2, 174.2, 139.2, 136.0, 135.4, 129.8, 129.4, 128.8, 128.5, 128.3, 128.2, 127.8, 127.6, 126.2, 85.2, 54.1, 48.4, 47.8, 43.0, 42.7, 40.5, 39.7, 24.9, 24.8. IR (ν_{max}, cm^{-1}) 2982 (w), 1772 (w), 1708 (s), 1392 (m), 1342 (m), 1165 (w), 746 (m), 701 (m). HRMS (ESI/QTOF) m/z: [M + Na]$^+$ Calcd for $C_{36}H_{35}BN_2NaO_6^+$ 625.2480; Found 625.2495.

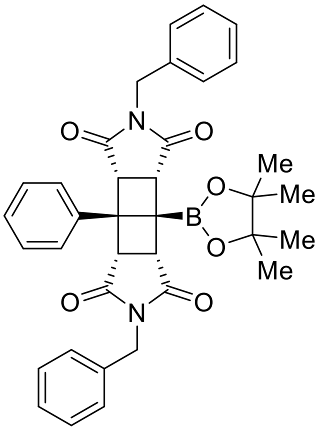

9a'. *Method C.* Beige glassy solid. *R$_f$* = 0.15 (DCM/acetonitrile). 29.4 mg, 0.048 mmol, 48% yield. ^{1}H NMR (400 MHz, CDCl$_3$) δ = 7.24 – 7.10 (m, 11H, Ar*H*), 7.10 – 6.96 (m, 4H, Ar*H*), 4.49 (s, 4H, 2xC*H*$_2$), 3.81 (d, *J* = 6.0 Hz, 2H, C*H*$_2$), 3.45 (d, *J* = 6.0 Hz, 2H, C*H*$_2$), 1.08 (s, 12H, 4xC*H*$_3$). ^{13}C NMR (101 MHz, CDCl$_3$) δ = 175.4, 174.2, 135.5, 134.6, 129.2, 128.5, 127.9, 127.8, 127.6, 127.2, 84.9, 57.1, 51.4, 46.3, 42.6, 25.0. IR (ν_{max}, cm^{-1}) 2958 (w), 2924 (w), 2853 (w), 1769 (w), 1706 (s), 1430 (w), 1394 (m), 1346 (m), 1172 (m). HRMS (ESI/QTOF) m/z: [M + Na]$^+$ Calcd for $C_{36}H_{35}BN_2NaO_6^+$ 625.2480; Found 625.2494.

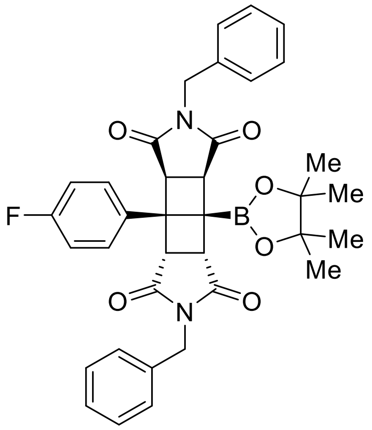

9b. *Method C.* Beige amorphous solid. R_f = 0.41 (pentane/Et_2O). 10.9 mg, 0.017 mmol, 17% yield. ^1H NMR (400 MHz, $CDCl_3$) δ = 7.50 – 7.42 (m, 2H, Ar*H*), 7.34 – 7.19 (m, 8H, Ar*H*), 7.08 – 6.99 (m, 2H, Ar*H*), 6.70 – 6.50 (m, 2H, Ar*H*), 4.72 (s, 2H, C*H*₂), 4.53 (d, *J* = 13.8 Hz, 1H, C*H*), 4.34 (d, *J* = 13.8 Hz, 1H, C*H*), 3.79 (d, *J* = 8.9 Hz, 1H, C*H*), 3.69 (d, *J* = 8.9 Hz, 1H, C*H*), 3.01 (d, *J* = 6.1 Hz, 1H, C*H*), 2.77 (d, *J* = 6.1 Hz, 1H, C*H*), 1.10 (s, 6H, 2xCH_3), 1.09 (s, 6H, 2xCH_3). ^{13}C NMR (101 MHz, $CDCl_3$) δ = 176.2, 175.9, 175.1, 174.1, 161.9 (d, *J* = 247.3 Hz), 136.0, 135.3, 135.0 (d, *J* = 3.1 Hz), 129.9, 129.4, 128.8, 128.5, 128.3, 128.2 (d, *J* = 8.3 Hz), 127.9, 115.1 (d, *J* = 21.5 Hz), 85.3, 53.6, 48.3, 47.8, 43.0, 42.8, 40.5, 39.6, 24.9, 24.8. ^{19}F NMR (376 MHz, $CDCl_3$) δ = -112.9 – -115.6 (m). IR (v_{max}, cm^{-1}) 3029 (w), 2981 (w), 1704 (s), 1388 (m), 1343 (m), 1162 (m), 852 (w), 755 (s). HRMS (ESI/QTOF) m/z: $[M + Na]^+$ Calcd for $C_{36}H_{34}BFN_2NaO_6^+$ 643.2386; Found 643.2395.

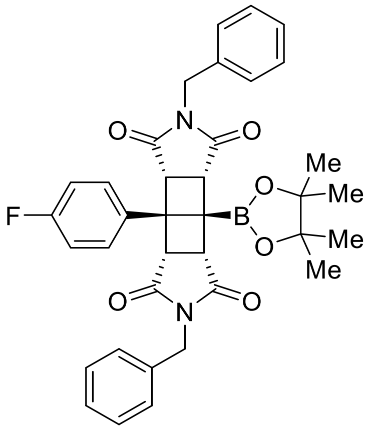

9b'. *Method C.* Yellow glassy solid. R_f = 0.18 (DCM/acetonitrile). 33.8 mg, 0.053 mmol, 53% yield. ^1H NMR (400 MHz, $CDCl_3$) δ = 7.25 – 7.11 (m, 10H, Ar*H*), 7.06 – 6.97 (m, 2H, Ar*H*), 6.67 (t, *J* = 8.7 Hz, 2H, Ar*H*), 4.51 (d, *J* = 14.0 Hz, 2H, C*H*₂), 4.47 (d, *J* = 14.0 Hz, 2H, C*H*₂), 3.78 (d, *J* = 6.0 Hz, 2H, C*H*₂), 3.46 (d, *J* = 6.0 Hz, 2H, C*H*₂), 1.09 (s, 12H, 4xCH_3). ^{13}C NMR (101 MHz, $CDCl_3$) δ = 175.2, 174.0, 161.9 (d, *J* = 247.1 Hz), 135.3, 130.3 (d, *J* = 3.2 Hz), 129.1 (d, *J* = 7.6 Hz), 129.1, 128.4, 127.9, 114.5 (d, *J* = 21.6 Hz), 84.8, 56.5, 51.2, 46.1, 42.5, 24.9. ^{19}F NMR (376 MHz, $CDCl_3$) δ = -113.6 – -115.5 (m). IR (v_{max}, cm^{-1}) 3027 (w), 2986 (w), 2946 (w), 1700 (s), 1391 (s), 1342 (s), 1227 (m), 1166 (m), 748 (s). HRMS (ESI/QTOF) m/z: $[M + Na]^+$ Calcd for $C_{36}H_{34}BFN_2NaO_6^+$ 643.2386; Found 643.2408.

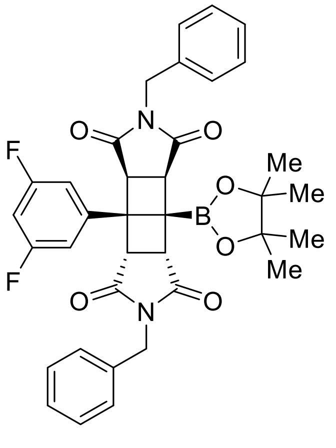

9c. *Method C.* Beige amorphous solid. R_f = 0.44 (pentane/Et_2O). 10.0 mg, 0.016 mmol, 16% yield. ^1H NMR (400 MHz, $CDCl_3$) δ = 7.54 – 7.47 (m, 4H, Ar*H*), 7.33 – 7.27 (m, 3H, Ar*H*), 7.25 – 7.20 (m, 3H, Ar*H*), 6.87 (dd, *J* = 8.2, 2.1 Hz, 2H, Ar*H*), 6.63 (tt, *J* = 8.7, 2.2 Hz, 1H, Ar*H*), 4.77 (s, 2H, C*H*₂), 4.49 (s, 2H, C*H*₂), 3.84 (d, *J* = 8.9 Hz, 1H, C*H*), 3.70 (d, *J* = 8.9 Hz, 1H, C*H*), 3.12 (d, *J* = 6.1 Hz, 1H, C*H*), 2.76 (d, *J* = 6.1 Hz, 1H, C*H*), 1.15 (s, 6H, 2xCH_3), 1.12 (s, 6H, 2xCH_3). ^{13}C NMR (101 MHz, $CDCl_3$) δ = 175.8, 175.4, 174.9, 173.8, 162.9 (dd, *J* = 250.1, 12.7 Hz), 143.3 (t, *J* = 9.0 Hz), 135.9, 135.1, 129.4, 129.2, 128.9, 128.6, 128.5, 127.9, 109.7 (dd, *J* = 18.9, 7.2 Hz), 103.4 (t, *J* = 25.1 Hz), 85.6, 53.3, 48.5, 47.6, 43.1, 42.9, 40.5, 39.5, 24.8, 24.7. ^{19}F NMR (376 MHz, $CDCl_3$) δ = -108.1 – -108.2 (m). IR (v_{max}, cm^{-1}) 2958 (w), 2923 (w), 2853 (w), 1772 (w), 1710 (m), 1624 (w), 1597 (w), 1458 (w), 1435 (w), 1384 (w), 1343 (w), 1166 (w), 1142 (w), 852 (w), 764 (w). HRMS (ESI/QTOF) m/z: $[M + Na]^+$ Calcd for $C_{36}H_{33}BF_2N_2NaO_6^+$ 661.2292; Found 661.2306.

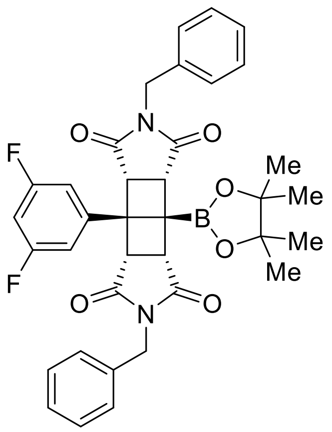

9c'. *Method C.* Yellow glassy solid. R_f = 0.17 (DCM/acetonitrile). 30.1 mg, 0.048 mmol, 48% yield. ^{1}H NMR (400 MHz, CDCl$_3$) δ = 7.24 – 7.16 (m, 6H, Ar*H*), 7.15 – 7.08 (m, 4H, Ar*H*), 6.81 (dd, J = 8.4, 2.2 Hz, 2H, Ar*H*), 6.65 (tt, J = 8.7, 2.2 Hz, 1H, Ar*H*), 4.55 (d, J = 14.1 Hz, 2H, C*H*$_2$), 4.47 (d, J = 14.1 Hz, 2H, C*H*$_2$), 3.79 (d, J = 5.9 Hz, 2H, 2xC*H*), 3.46 (d, J = 5.9 Hz, 2H, 2xC*H*), 1.05 (s, 12H, C*H*$_3$). ^{13}C NMR (151 MHz, CDCl$_3$) δ = 174.8, 173.6, 162.3 (d, J = 249.0 Hz), 162.2 (d, J = 248.6 Hz), 138.3 (t, J = 9.0 Hz), 135.1, 128.7, 128.5, 128.0, 110.8 (dd, J = 26.0, 5.2 Hz), 103.4, 85.1, 56.6, 51.2, 46.1, 42.6, 24.8. ^{19}F NMR (376 MHz, CDCl$_3$) δ = -109.1 (t, J = 8.0 Hz). IR (ν_{max}, cm^{-1}) 2958 (w), 2926 (w), 2870 (w), 1769 (w), 1704 (s), 1514 (w), 1394 (w), 1343 (w), 1249 (w), 1170 (w), 766 (m). HRMS (ESI/QTOF) m/z: [M + Na]+ Calcd for $C_{36}H_{33}BF_2N_2NaO_6^+$ 661.2292; Found 661.2314.

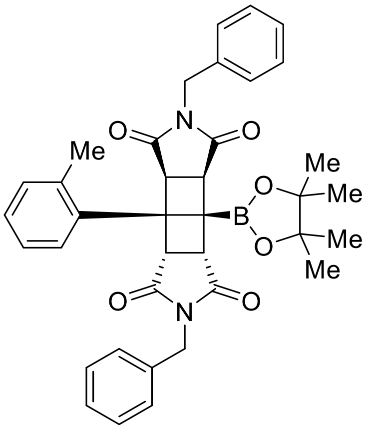

9d. *Method C.* Beige amorphous solid. Reaction was performed on 0.5 mmol scale. R_f = 0.46 (pentane/Et$_2$O). 33.0 mg, 0.054 mmol, 11% yield. ^{1}H NMR (400 MHz, CDCl$_3$) δ = 7.61 – 7.54 (m, 2H, Ar*H*), 7.42 – 7.28 (m, 5H, Ar*H*), 7.23 (dd, J = 8.0, 2.5 Hz, 3H, Ar*H*), 7.20 – 7.12 (m, 3H, Ar*H*), 7.02 – 6.95 (m, 1H, Ar*H*), 4.87 (d, J = 13.6 Hz, 1H, C*H*$_2$), 4.83 (d, J = 13.6 Hz, 1H, C*H*$_2$), 4.50 (s, 2H, C*H*$_2$), 3.98 (d, J = 8.7 Hz, 1H, C*H*), 3.57 (d, J = 8.7 Hz, 1H, C*H*), 3.56 (d, J = 6.0 Hz, 1H, C*H*), 2.81 (d, J = 6.0 Hz, 1H, C*H*), 2.61 (s, 3H, C*H*$_3$), 1.30 (s, 6H, 2x C*H*$_3$), 1.28 (s, 6H, 2xC*H*$_3$). ^{13}C NMR (101 MHz, CDCl$_3$) δ = 176.0, 175.3, 175.3, 174.2, 136.9, 136.9, 136.0, 135.5, 131.6, 129.4, 128.9, 128.8, 128.5, 128.2, 128.2, 127.5, 126.3, 124.6, 85.4, 56.2, 49.0, 45.9, 43.0, 42.6, 40.5, 39.9, 24.9, 24.6, 20.4. IR (ν_{max}, cm^{-1}) 2979 (w), 2885 (w), 1711 (m), 1394 (w), 1343 (w), 1048 (w), 773 (w), 745 (w). HRMS (ESI/QTOF) m/z: [M + Na]$^+$ Calcd for $C_{37}H_{37}BN_2NaO_6^+$ 639.2637; Found 639.2635.

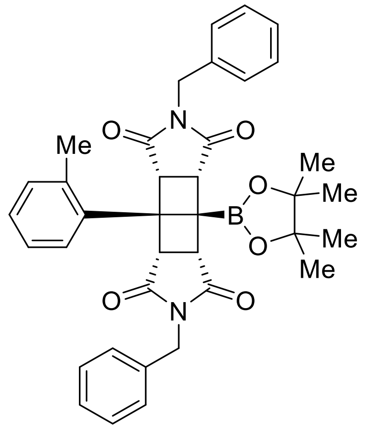

9d'. *Method C.* Yellow glassy solid. Reaction was performed on 0.5 mmol scale. R_f = 0.20 (DCM/acetonitrile). 97.1 mg, 0.157 mmol, 32% yield. ^{1}H NMR (400 MHz, CDCl$_3$) δ = 7.16 – 7.09 (m, 7H, Ar*H*), 7.09 – 6.99 (m, 5H, Ar*H*), 6.81 (d, J = 7.5 Hz, 1H, Ar*H*), 6.70 – 6.49 (m, 1H, Ar*H*), 4.41 (d, J = 14.1 Hz, 2H, C*H*$_2$), 4.33 (d, J = 14.1 Hz, 2H, C*H*$_2$), 3.88 (d, J = 6.0 Hz, 2H, 2xC*H*), 3.36 (d, J = 5.9 Hz, 2H, 2xC*H*), 2.49 (s, 3H, C*H*$_3$), 1.05 (s, 12H, 4xC*H*$_3$). ^{13}C NMR (101 MHz, CDCl$_3$) δ = 175.3, 173.8, 137.4, 135.4, 133.5, 130.6, 128.9, 128.4, 128.1, 127.7, 127.2, 124.5, 84.8, 59.1, 50.2, 46.2, 42.4, 24.9, 21.0. IR (ν_{max}, cm^{-1}) 2958 (w), 1770 (m), 1712 (s), 1393 (m), 1361 (m), 1341 (m), 1173 (m), 854 (m), 741 (m). HRMS (ESI/QTOF) m/z: [M + Na]$^+$ Calcd for $C_{37}H_{37}BN_2NaO_6^+$ 639.2637; Found 639.2637.

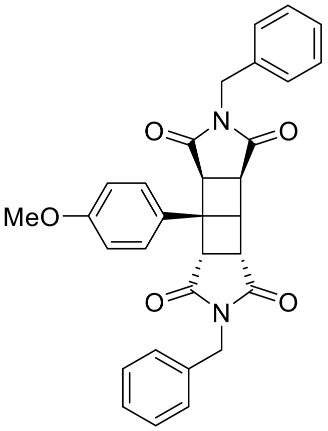

9e. *Method C.* Beige amorphous solid. R_f = 0.40 (pentane/Et_2O). 12.6 mg, 0.015 mmol, 15% yield. ^1H NMR (400 MHz, $CDCl_3$) δ = 7.59 – 7.47 (m, 2H, Ar*H*), 7.35 – 7.27 (m, 4H, Ar*H*), 7.25 – 7.20 (m, 2H, Ar*H*), 7.17 – 7.08 (m, 2H, Ar*H*), 6.77 (d, *J* = 8.7 Hz, 2H, Ar*H*), 6.63 (d, *J* = 8.8 Hz, 2H, Ar*H*), 4.79 (s, 2H, CH_2), 4.42 (s, 2H, CH_2), 3.76 (s, 3H, CH_3), 3.67 (d, *J* = 8.7 Hz, 1H, C*H*), 3.60 (dd, *J* = 8.5, 0.8 Hz, 1H, C*H*), 3.53 (d, *J* = 8.8 Hz, 1H, C*H*), 3.11 (d, *J* = 5.6 Hz, 1H, C*H*), 2.83 (dd, *J* = 5.6, 1.4 Hz, 1H, C*H*). ^{13}C NMR (101 MHz, $CDCl_3$) δ = 176.5, 175.5, 175.4, 173.9, 158.9, 135.9, 135.3, 129.6, 129.4, 129.2, 128.9, 128.6, 128.5, 128.0, 126.8, 114.2, 55.2, 52.6, 48.8, 46.8, 43.0, 42.7, 41.1, 39.0, 37.9. IR ($ν_{max}$, cm^{-1}) 2961 (w), 2925 (w), 2858 (w), 1707 (w), 1512 (w), 1460 (w), 1382 (w), 1253 (w). HRMS (ESI/QTOF) m/z: $[M + Na]^+$ Calcd for $C_{31}H_{26}N_2NaO_5^+$ 529.1734; Found 529.1732.

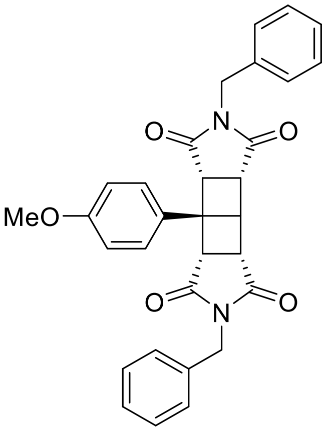

9e'. *Method C.* Yellow glassy solid. R_f = 0.25 (DCM/acetonitrile). 37.8 mg, 0.045 mmol, 45% yield. 1H NMR (400 MHz, CDCl3) δ = 7.31 – 7.21 (m, 2H, Ar*H*), 7.17 – 7.02 (m, 6H, Ar*H*), 6.97 – 6.91 (m, 4H, Ar*H*), 6.60 – 6.36 (m, 2H, Ar*H*), 4.41 (d, J = 14.0 Hz, 2H, CH_2), 4.31 (d, J = 14.0 Hz, 2H, CH_2), 3.70 (s, 3H, CH_3), 3.67 (d, J = 5.5 Hz, 2H, 2xC*H*), 3.38 (dd, J = 5.5, 1.0 Hz, 2H, 2xC*H*), 3.26 (t, J = 1.1 Hz, 1H, C*H*). ^{13}C NMR (101 MHz, $CDCl_3$) δ = 176.3, 174.1, 158.9, 135.2, 128.7, 128.5, 127.8, 125.1, 113.7, 55.6, 55.1, 50.5, 42.9, 42.5 (carbon signals of NBn phenyl ring and aliphatic region are not fully resolved). IR ($ν_{max}$, cm^{-1}) 2972 (w), 2903 (w), 1701 (s), 1516 (w), 1393 (m), 1343 (m), 1251 (w), 1169 (m), 910 (w), 733 (m). HRMS (ESI/QTOF) m/z: $[M + Na]^+$ Calcd for $C_{31}H_{26}N_2NaO_5^+$ 529.1734; Found 529.1737.

Cycloadduct transformations

Suzuki reaction.

Method D. Using pure cyclobutenyl boronate.

Alkenyl boronate **8** (0.147 mmol), het(aryl) halogenide (0.150 mmol), and Na_2CO_3 (31.8 mg, 0.300 mmol) were dissolved in THF/H_2O mixture (9/1 v/v, 3 mL) and the obtained solution was thoroughly degassed by three vacuum pumping-nitrogen purge cycles. $Pd(PPh_3)_4$ (8.5 mg, 0.0073 mmol) was added in one portion and the resulting reaction mixture was heated to 50 °C. After stirring overnight at the same temperature, the organic solvent was evaporated under reduced pressure, and the crude material was partitioned between EtOAc (5 mL) and water (3 mL). The organic layer was washed with brine (3 mL), dried over Na_2SO_4 and evaporated to dryness under reduced pressure. The crude product was purified by column chromatography (*n*-pentane/Et_2O gradient elution, 100/0 – 50/50) to give the desired product.

Method E. One-pot protocol.

A solution of corresponding maleimide **7** (0.150 mmol), alkynyl boronate **4** (0.450 mmol), and thioxanthone (3.1 mg, 0.015 mmol) in appropriate solvent (3 mL) was placed into a glass tube, closed with rubber septum and degassed by three vacuum pumping-nitrogen purge cycles. The resulting solution was irradiated in a Rayonet® reactor (λmax = 350 nm) placed at a 3 cm distance from the vessel (see Figure for the experimental setup) at rt for 12 h. After the reaction was complete, the organic solvent was evaporated under reduced pressure to dryness. The obtained semi-solid material was triturated with n-Hexane/Et_2O (5 mL, 1:1), the precipitate (maleimide dimer **10**) was filtered off, and the filtrate was evaporated in vacuo. The residue was subjected to drying in vacuo (0.1 mmHg) upon heating to 160 °C on a sand bath for 2 h. After cooling to rt, het(aryl) halogenide (0.15 mmol) and Na_2CO_3 (31.8 mg, 0.300 mmol) was added and the mixture was suspended in a THF/H_2O mixture (9/1 v/v, 3 mL). The obtained suspension was thoroughly degassed, $Pd(PPh_3)_4$ (8.5 mg, 0.0073 mmol) was added in one portion and the resulting reaction mixture was heated to 50°C. After stirring overnight at the same temperature, the organic solvent was evaporated under reduced pressure, and the crude material was partitioned between EtOAc (5 mL) and water (3 mL). The organic layer was washed with brine (3 mL), dried over Na_2SO_4 and evaporated to dryness under reduced pressure. The crude product was purified by column chromatography (pentane/Et_2O gradient elution, 100/0 – 50/50) to give the desired product.

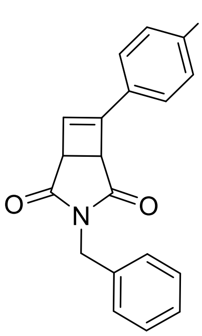

11a. *Method D*. Slightly orange film. R_f = 0.45 (pentane/Et_2O). 26.7 mg, 0.088 mmol, 60% yield. *Method E*: 22.7 mg, 0.075 mmol, 51% yield. ^1H NMR (400 MHz, $CDCl_3$) δ = 7.39 (d, *J* = 8.1 Hz, 2H, Ar*H*), 7.23 (ddd, *J* = 18.1, 7.9, 1.8 Hz, 4H, Ar*H*), 7.19 – 7.14 (m, 1H, Ar*H*), 7.11 (d, *J* = 7.9 Hz, 2H, Ar*H*), 6.41 (d, *J* = 1.1 Hz, 1H, C*H*), 4.57 (d, *J* = 14.3 Hz, 1H, HC*H*), 4.51 (d, *J* = 14.2 Hz, 1H, *H*CH), 4.06 (d, *J* = 3.3 Hz, 1H, C*H*), 3.77 – 3.63 (m, 1H, C*H*), 2.29 (s, 3H, C*H*3). ^{13}C NMR (101 MHz, $CDCl_3$) δ = 175.0, 174.3, 149.1, 139.7, 135.8, 129.4 128.9, 128.6, 128.6, 127.8, 125.5, 125.5, 47.2, 43.7, 42.3, 21.5. IR (ν_{max}, cm^{-1}) 2979 (w), 1703 (m), 1522 (w), 1390 (w), 1343 (w), 1168 (w), 770 (w). HRMS (ESI/QTOF) m/z: $[M + H]^+$ Calcd for $C_{20}H_{18}NO_2^+$ 304.1332; Found 304.1332.

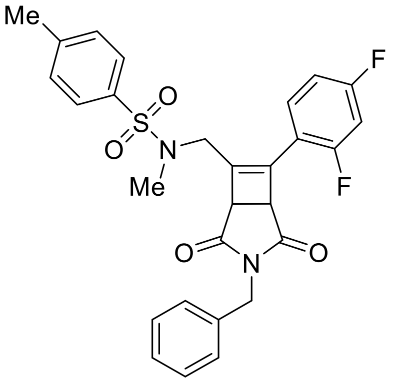

11b. *Method E.* Slightly yellow film. R_f = 0.34 (pentane/Et_2O). 26.7 mg, 0.049 mmol, 34% yield. ^1H NMR (400 MHz, $CDCl_3$) δ = 7.72 – 7.60 (m, 3H, Ar*H*), 7.35 – 7.20 (m, 7H, Ar*H*), 6.95 (tdd, *J* = 8.7, 2.5, 0.7 Hz, 1H, Ar*H*), 6.83 (ddd, *J* = 11.0, 8.7, 2.5 Hz, 1H, Ar*H*), 4.64 (d, *J* = 14.1 Hz, 1H, HC*H*), 4.57 (d, *J* = 14.1 Hz, 1H, *H*CH), 4.11 (d, *J* = 16.2 Hz, 1H, C*H*), 4.02 – 3.93 (m, 1H, C*H*), 3.78 (d, *J* = 16.2 Hz, 1H, C*H*), 3.73 (d, *J* = 3.3 Hz, 1H, C*H*), 2.71 (s, 3H, C*H*3), 2.44 (s, 3H, C*H*3). ^{13}C NMR (151 MHz, $CDCl_3$) δ = 174.0, 173.4, 143.7, 139.3, 137.2, 135.7, 134.1, 130.9 (d, *J* = 4.3 Hz), 129.8, 128.8, 128.7, 128.0, 127.6, 112.2 (dd, *J* = 21.4, 3.3 Hz), 104.5, 48.2, 48.1, 45.2, 45.1, 42.3, 36.3, 29.7, 21.6. ^{19}F NMR (376 MHz, $CDCl_3$) δ = -105.8 (q, *J* = 9.4), -106.5 (p, *J* = 8.6). IR (ν_{max}, cm^{-1}) 2977 (w), 2896 (w), 1703 (m), 1505 (w), 1392 (w), 1343 (w), 1165 (w), 914 (w), 772 (w), 736 (w). HRMS (ESI/QTOF) m/z: $[M + Na]^+$ Calcd for $C_{28}H_{24}F_2N_2NaO_4S^+$ 545.1317; Found 545.1313.

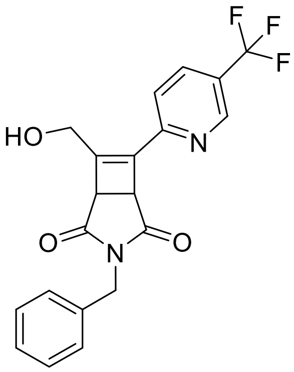

11c. *Method E.* Colorless film (purple after standing overnight). 17.5 mg, 0.045 mmol, 30% yield. The crude material was purified using HPLC (gradient 5 – 95% CH_3CN/H_2O/0.1% TFA, R_t = 15.5 min). During purification, complete removal of the THP protecting group occured. The compound was found to be unstable at rt after 8 h. ^1H NMR (400 MHz, $CDCl_3$) δ = 8.88 – 8.68 (m, 1H, Ar*H*), 8.06 (dd, *J* = 8.2, 1.7 Hz, 1H, Ar*H*), 7.83 (d, *J* = 8.2 Hz, 1H, Ar*H*), 7.42 – 7.27 (m, 5H, Ar*H*), 4.64 (d, *J* = 14.2 Hz, 1H, HC*H*), 4.60 (d, *J* = 14.2 Hz, 1H, *H*CH), 4.58 (s, 2H, C*H*$_2$), 4.10 (q, *J* = 2.7 Hz, 1H, C*H*), 3.89 – 3.85 (m, 1H, C*H*). ^{13}C NMR (101 MHz, $CDCl_3$) δ = 173.8, 172.6, 153.2, 152.4, 145.9 (q, *J* = 3.8 Hz), 138.5, 135.6 (q, *J* = 3.5 Hz), 135.4, 128.8, 128.7, 128.1, 125.7 (q, *J* = 33.3 Hz), 123.0 (q, *J* = 273.2 Hz), 121.7, 60.7, 45.4, 44.2, 42.6. ^{19}F NMR (376 MHz, $CDCl_3$) δ = -62.5, -75.9. HRMS (ESI/QTOF) m/z: $[M + H]^+$ Calcd for $C_{20}H_{16}F_3N_2O_3^+$ 389.1108; Found 389.1101

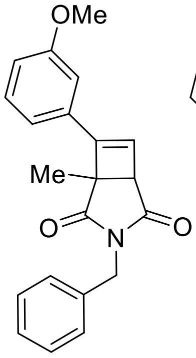

11d

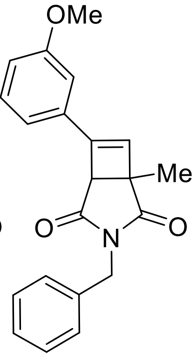

11d'

11d and **11d'.** *Method E.* Slightly yellow film. R_f = 0.29 (pentane/Et_2O). 19.9 mg, 0.060 mmol, 40% yield, **11d** : **11d'** = 2.15 : 1. Signals of individual isomers were assigned by HNMR, HSQC and HMBC spectra. 1 isomer **11d**: ^1H NMR (400 MHz, $CDCl_3$) δ = 7.36 – 7.20 (m, 6H, Ar*H*), 7.18 – 7.13 (m, 1H, Ar*H*), 7.08 (s, 1H, Ar*H*), 6.89 (dd, *J* = 8.2, 2.3 Hz, 1H, Ar*H*), 6.51 (d, *J* = 1.2 Hz, 1H, C*H*), 4.62 (s, 2H, C*H*$_2$), 3.84 (s, 3H, C*H*$_3$), 3.43 (d, *J* = 1.1 Hz, 1H, C*H*), 1.69 (s, 3H, C*H*$_3$). ^{13}C NMR (101 MHz, $CDCl_3$) δ = 177.4, 174.8, 160.0, 153.0, 136.0, 132.5, 130.0, 128.8, 128.5, 127.9, 125.7, 118.6, 115.5, 111.1, 55.4, 53.8, 50.6, 42.4, 15.8. 2 isomer **11d'**. ^1H NMR (400 MHz, $CDCl_3$) δ = 7.36 – 7.20 (m, 6H, Ar*H*), 7.18 – 7.13 (m, 1H, Ar*H*), 7.08 (s, 1H, Ar*H*), 6.89 (dd, *J* = 8.2, 2.3 Hz, 1H, C*H*), 6.57 (s, 1H, C*H*), 4.66 (d, *J* = 14.1 Hz, 1H, HC*H*), 4.57 (d, *J* = 14.2 Hz, 1H, *H*CH), 3.84 (s, 3H, C*H*$_3$), 3.76 (s, 1H. C*H*), 1.59 (s, 3H, C*H*$_3$). ^{13}C NMR (101 MHz, $CDCl_3$) δ = 177.9, 174.1, 147.2, 136.0, 133.0, 132.5, 132.1, 129.9, 128.8, 128.5, 127.9, 118.2, 115.7, 110.6, 55.4, 52.8, 49.7, 42.4, 16.2 (carbon signals of NBn phenyl ring are not fully resolved). IR (v_{max}, cm^{-1}) 2977 (w), 2903 (w), 1703 (m), 1393 (w), 1343 (w), 1224 (w), 772 (m). HRMS (ESI/QTOF) m/z: $[M + H]^+$ Calcd for $C_{21}H_{20}NO_3^+$ 334.1438; Found 334.1438.

Pd/C – catalyzed reduction

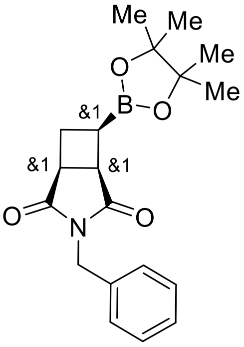

Alkenyl boronate **8c** (50.0 mg, 0.147 mmol) was dissolved in MeOH and 10% Pd/C (5 mg, 10% weight) was added under N_2 atmosphere. The obtained suspension was stirred overnight under H_2 atmosphere, then filtered through a pad of celite, and the solvent was evaporated under reduced pressure. Drying of the product under high vacuum (0.01 mmHg) resulted in solid product **12** (46.2 mg, 0.135 mmol, 92% yield) with minor impurities.

^1H NMR (400 MHz, $CDCl_3$) δ = 7.46 – 7.27 (m, 5H, Ar*H*), 4.72 (d, *J* = 14.2 Hz, 1H, HC*H*), 4.65 (d, *J* = 14.3 Hz, 1H, *H*CH), 3.42 – 3.26 (m, 2H, 2xC*H*), 2.76 – 2.61 (m, 1H, C*H*), 2.54 (ddt, *J* = 14.7, 10.3, 5.9 Hz, 1H, C*H*), 2.25 – 2.12 (m, 1H, C*H*), 1.20 (s, 6H, 2xC*H*$_3$), 1.17 (s, 6H, 2xC*H*$_3$). ^{13}C NMR (101 MHz, $CDCl_3$) δ = 179.7, 178.8, 136.1, 128.6, 128.5, 127.7, 84.0, 42.4, 39.7, 38.2, 25.0, 24.7, 24.3. IR (v_{max}, cm^{-1}) 2981 (w), 2946 (w), 2875 (w), 1769 (w), 1704 (s), 1381 (m), 1341 (m), 1221 (w), 1170 (w), 1145 (w), 852 (w). HRMS (ESI/QTOF) m/z: [M + Na]$^+$ Calcd for $C_{19}H_{24}BNNaO_4^+$ 364.1691; Found 364.1677

Reduction of the carbonyl groups

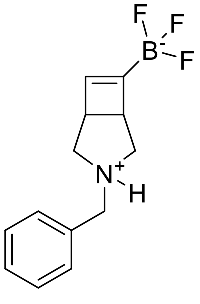

To the pre-cooled to 0 °C stock solution of $LiAlH_4$ (1 M in THF, 1.2 mL) under N_2 atmosphere, a solution of alkenyl boronate **8c** (100 mg, 0.294 mmol) in THF (5 mL) was added in a dropwise manner. After complete addition of the reagent, the reaction mixture was slowly heated to gentle reflux and stirred at the same temperature overnight. The obtained thick suspension was cooled to 0 °C with an ice-water bath and the excess of the reagent was quenched with 5% aq NaOH (2 mL). The obtained precipitate was filtered, washed with THF (2×5 mL) and suspended in a MeOH/H_2O mixture (10 mL, 7:3), followed by the addition of solid KHF_2 (188 mg, 2.40 mmol) in one portion. After additional stirring for 4 h, the solvents were evaporated to dryness in vacuo and the obtained solid material was suspended in refluxing acetone (10 mL). The suspension was filtered, the precipitate was washed with additional amounts of hot acetone (3×5 mL) and the combined organic solutions were evaporated in vacuo to approximately 1 mL volume. The obtained cloudy solution was triturated with Et_2O (5 mL) and chilled in the fridge for 2 hrs. The obtained suspension was filtered, washed with additional amounts of Et_2O (2×5 mL) and dried subsequently under air (2 hrs) and high vacuum (0.01 mmHg, 2 hrs) to give the desired product **13** (51.1 mg, 0.173 mmol, 59% yield) as a white solid.

^{1}H NMR (400 MHz, acetone-*d*$_6$) δ = 7.59 – 7.46 (m, 2H, Ar*H*), 7.44 – 7.33 (m, 3H, Ar*H*), 5.80 (s, 1H, C*H*), 4.26 (d, *J* = 13.3 Hz, 1H, HC*H*), 4.22 (d, *J* = 13.4 Hz, 1H, *H*CH), 3.35 (d, *J* = 10.3 Hz, 1H, *H*CH), 3.33 – 3.29 (m, 1H, C*H*), 3.29 – 3.25 (m, 1H, C*H*), 3.22 (d, *J* = 10.6 Hz, 1H, HC*H*), 2.57 (dd, *J* = 10.2, 6.6 Hz, 2H, *H*CH). ^{13}C NMR (101 MHz, acetone-*d*$_6$) δ = 134.0, 133.8 (q, *J* = 4.5 Hz), 58.0, 54.2, 54.1, 45.9, 44.5 (carbon signals of phenyl ring are not fully resolved). ^{19}F NMR (376 MHz, acetone-*d*$_6$) δ = -142.5. ^{11}B NMR (128 MHz, acetone-*d*$_6$) δ = 2.61 – -2.15 (m). IR (ν_{max}, cm^{-1}) 2958 (w), 1207 (w), 1062 (w), 1000 (w), 770 (w). HRMS (ESI/QTOF) m/z: [M + Na]$^+$ Calcd for $C_{13}H_{15}BF_3NNa^+$ 276.1142; Found 276.1138.

Oxidation at the C–B bond

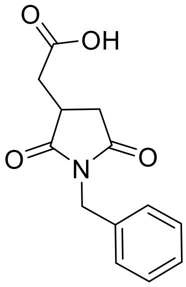

Alkenyl boronate **8c** (50.0 mg, 0.147 mmol) was dissolved in THF (2 mL), followed by the subsequent addition of H_2O (1 mL), NaH_2PO_4 (52.9 mg, 0.441 mmol), and $NaBO_3{\cdot}4H_2O$ (67.8 mg, 0.441 mmol). After the reaction was complete, the solvents were evaporated to dryness and re-evaporated with distilled water (3 mL) 2 times. The crude material was triturated with water, obtained precipitate was filtered, washed with additional amounts of water (2×2mL) and dried on air to give pure **14** (34.1 mg, 0.138 mmol, 94% yield) as a white amorphous solid.

^{1}H NMR (400 MHz, DMSO) δ = 12.52 (s, 1H, O*H*), 7.65 – 6.94 (m, 5H, Ar*H*), 4.59 (d, *J* = 15.2 Hz, 1H, HC*H*), 4.52 (d, *J* = 15.2 Hz, 1H, *H*CH), 3.15 (dq, *J* = 10.1, 5.4 Hz, 1H, C*H*), 2.87 (dd, *J* = 17.9, 9.3 Hz, 1H, HC*H*), 2.80 – 2.62 (m, 2H, 2x*H*CH), 2.57 – 2.50 (m, 1H, *H*CH). ^{1}H NMR (400 MHz, $CDCl_3$) δ = 7.46 – 7.29 (m, 5H, Ar*H*), 4.73 (d, *J* = 14.1 Hz, 1H, HC*H*), 4.68 (d, *J* = 14.2 Hz, 1H, *H*CH), 3.13 (dddd, *J* = 9.6, 7.2, 4.1, 2.7 Hz, 1H, C*H*), 3.03 – 2.81 (m, 3H, 3x*H*CH), 2.55 (dd, *J* = 18.1, 5.5 Hz, 1H, HC*H*). ^{13}C NMR (101 MHz, DMSO) δ = 179.8, 177.1, 173.1, 136.7, 128.8, 127.7, 127.7, 41.9, 36.3, 34.5, 34.0. IR (ν_{max}, cm^{-1}) 2986 (w), 2889 (w), 1739 (m), 1523 (m), 1351 (w), 1144 (w), 993 (w), 770 (m). HRMS (ESI/QTOF) m/z: [M – H$^+$]$^-$ Calcd for $C_{13}H_{14}NO_4^-$ 246.0772; Found 246.0771.

Protodeborylation

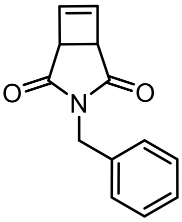

Alkenyl boronate **8c** (20.0 mg, 0.0600 mmol) was suspended in 37% aq HCl and stirred at gentle reflux overnight. Evaporation of the solvent and purification of the crude material with HPLC (gradient 5 – 95% CAN/H_2O/0.1% TFA, R_t = 12.3 min).results in product **15** (6.4 mg, 0.030 mmol, 50% yield) as a thin colorless film.

^1H NMR (400 MHz, $CDCl_3$) δ = 7.29 – 7.20 (m, 5H, Ar*H*), 6.37 (d, *J* = 0.5 Hz, 2H, 2xC*H*), 4.55 (s, 2H), 3.74 (d, *J* = 0.5 Hz, 2H, 2xC*H*). ^{13}C NMR (201 MHz, $CDCl_3$) δ = 174.3, 139.4, 135.7, 128.6, 128.5, 127.9, 47.7, 42.2. IR (ν_{max}, cm^{-1}) 2982 (w), 2892 (w), 1702 (m), 1388 (w), 1343 (w), 1145 (w), 1062 (w), 777 (w). HRMS (APCI/QTOF) m/z: $[M + H]^+$ Calcd for $C_{13}H_{12}NO_2^+$ 214.0863; Found 214.0861.

[3+2] cycloaddition

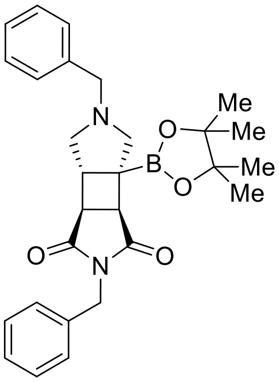

Method F. Alkenyl boronate **8c** (50.0 mg, 0.147 mmol), *N*-benzyl-1-methoxy-*N*-((trimethylsilyl)methyl)methanamine **16** (42 mg, 0.17 mmol), and LiF (11.4 mg, 0.438 mmol) were mixed in DMSO (1 mL), and the reaction mixture was placed into pre-heated to 110 °C oil bath. The reaction progress was monitored by ^1H NMR. Upon the completion of the reaction, the precipitate was filtered off through a paper filter, and the DMSO filtrate was extracted with hexanes (2×5 mL). The combined extracts were washed with H2O (2×5 mL), brine (2×5 mL), dried over Na_2SO_4, filtered, and evaporated in vacuo. The residue was subjected to drying in vacuo (0.1 mmHg) upon heating to 160 °C on a sand bath for 2 h. Purification with column chromatography (pentane/Et_2O 100/0 – 50/50) results in **17** (38.9 mg, 0.081 mmol, 55% yield) as a slightly orange oil.

Method G. Alkenyl boronate **8c** (50.0 mg, 0.147 mmol) and *N*-benzyl-1-methoxy-*N*-((trimethylsilyl)methyl)methanamine **16** (42 mg, 0.17 mmol) were mixed in CH_2Cl_2 (1 mL) and cooled with ice/water bath. Trifluoroacetic acid (1.1 μL, 0.015 mmol) was added in one portion and the reaction was stirred for 2 h. After the reaction was complete, the organic solvents were evaporated in vacuo. The residue was subjected to drying in vacuo (0.1 mmHg) upon heating to 160 °C on a sand bath for 2 h.

Purification with column chromatography (pentane/Et_2O 100/0 – 50/50) results in **17** (43.2 mg, 0.089 mmol, 61% yield) as a slightly orange oil.
^1H NMR (400 MHz, $CDCl_3$) δ = 7.44 – 7.27 (m, 9H, Ar*H*), 7.25 – 7.21 (m, 1H, Ar*H*), 4.69 (d, *J* = 14.2 Hz, 1H, HC*H*), 4.63 (d, *J* = 14.2 Hz, 1H, *H*CH), 3.75 (d, *J* = 13.2 Hz, 1H, HC*H*), 3.64 (d, *J* = 13.1 Hz, 1H, *H*CH), 3.09 (d, *J* = 10.3 Hz, 1H, HC*H*), 3.05 (d, *J* = 9.8 Hz, 1H, *H*CH), 3.02 – 2.96 (m, 2H, 2xC*H*), 2.84 (dd, *J* = 5.3, 1.9 Hz, 1H, C*H*), 2.19 (d, *J* = 10.3 Hz, 1H, *H*CH), 2.17 (dd, *J* = 9.4, 5.9 Hz, 1H, *H*CH), 1.17 (s, 6H, 2xCH_3), 1.15 (s, 6H, 2xCH_3). ^{13}C NMR (101 MHz, $CDCl_3$) δ = 179.5, 178.9, 139.3, 136.1, 128.7, 128.5, 128.4, 128.3, 127.7, 127.0, 84.0, 61.3, 59.5, 58.9, 45.1, 43.1, 43.0, 42.5, 24.9, 24.7. IR (ν_{max}, cm^{-1}) 2957 (w), 2923 (w), 2791 (w), 1699 (w), 1394 (w), 1338 (w), 1215 (w), 1145 (w), 762 (w). HRMS (ESI/QTOF) m/z: $[M + H]^+$ Calcd for $C_{28}H_{34}BN_2O_4^+$ 473.2606; Found 473.2608.

Preparation of potassium trifluoroborate **8cl**

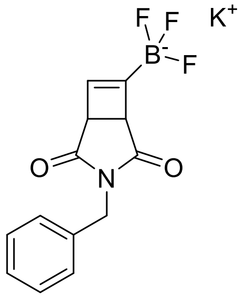

Method H. Alkenyl boronate **8c** (100.0 mg, 0.294 mmol) was dissolved in MeOH (10 mL) and an aqueous solution of KHF_2 (94 mg, 1.2 mmol, 5 mL H_2O) was added in one portion. After additional stirring for 4 h, the solvents were evaporated to dryness in vacuo and the obtained solid material was suspended in refluxing acetone (10 mL). The suspension was filtered, the precipitate was washed with additional amounts of hot acetone (3×5 mL) and the combined organic solutions were evaporated in vacuo to approximately 1 mL volume. The obtained cloudy solution was triturated with Et_2O (5 mL) and chilled in the fridge for 2 h. The obtained suspension was filtered, washed with additional amounts of Et_2O (2×5 mL) and dried subsequently under air (2 h) and high vacuum (0.01 mmHg, 2 h) to give the desired product **8cl** (81.6 mg, 0.256 mmol, 87% yield) as a white solid.

Method I. One pot. The crude reaction mixture from Method **A** (0.294 mmol of maleimide) after UV irradiation was filtered and the precipitate was suspended in MeOH/H_2O (15 mL, 2:1) mixture. The suspension was filtered, and solid KHF_2 (94 mg, 1.2 mmol) was added to the filtrate in one portion. After analogous work up the desired product **8cl** (66.6 mg, 0.208 mmol, 71% yield) was obtained as a beige solid.

^{1}H NMR (400 MHz, DMSO) δ = 7.45 – 7.13 (m, 5H, Ar*H*), 6.10 (s, 1H, C*H*), 4.51 (d, *J* = 15.1 Hz, 1H, HC*H*), 4.44 (d, *J* = 15.1 Hz, 1H, *H*CH), 3.60 (s, 1H, C*H*), 3.51 (d, *J* = 2.7 Hz, 1H, C*H*). ^{1}H NMR (400 MHz, CD_3CN) δ = 7.41 – 7.02 (m, 5H, Ar*H*), 6.15 (s, 1H, C*H*), 4.52 (d, *J* = 15.0 Hz, 1H, HC*H*), 4.44 (d, *J* = 15.0 Hz, 1H, *H*CH), 3.67 – 3.44 (m, 2H, 2xC*H*). ^{13}C NMR (101 MHz, CD_3CN) δ = 177.8, 177.2, 137.5, 135.8 (q, *J* = 4.6 Hz), 129.0, 128.0, 127.9, 48.5, 47.0, 41.6. ^{19}F NMR (376 MHz, DMSO) δ = -138.4 – -142.8 (m). IR (ν_{max}, cm^{-1}) 2361 (w), 2337 (w), 1762 (w), 1696 (s), 1602 (w), 1498 (w), 1429 (w), 1396 (m), 1355 (m), 1255 (w), 1189 (m), 972 (m). HRMS (ESI/QTOF) m/z: $[M]^-$ Calcd for $C_{13}H_{10}BF_3NO_2^-$ 280.0762; Found 280.0769.

Reaction with Langlois reagent

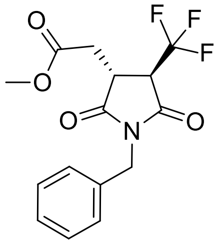

In air, potassium organotrifluoroborate (100 mg, 0.313 mmol), $NaSO_2CF_3$ (146 mg, 0.939 mmol), and CuCl (31 mg, 0.313 mmol) were weighed in a 2–5 mL MW vial equipped with a stirrring bar. MeOH (1 mL), CH_2Cl_2 (1 mL), and distilled H_2O (0.8 mL) were subsequently added, and the tube was sealed with a tap open to air by a needle. This solution was cooled to 0 °C, and TBHP (0.22 mL, 70% in H_2O, 1.6 mmol) was slowly added. The reaction was allowed to warm to rt and stirred at rt for 12 h. The reaction mixture was diluted with Et_2O (10 mL), and this solution was washed subsequently with saturated $NaHCO_3$ (aq) (5 mL) and 5% $Na_2S_2O_3$ (aq) (5 mL). The organic layer was dried ($MgSO_4$), filtered, evaporated under reduced and purified by flash column chromatography (pentane/Et_2O 100/0 – 50/50) to afford pure product **18** (21.6 mg, 0.063 mmol, 20% yield) as s colorless thin film.

^{1}H NMR (400 MHz, $CDCl_3$) δ = 7.49 – 7.28 (m, 5H, Ar*H*), 4.72 (d, *J* = 14.3 Hz, 1H, HC*H*), 4.69 (d, *J* = 14.1 Hz, 1H, *H*CH), 4.03 (qd, *J* = 9.2, 3.1 Hz, 1H, C*H*), 3.53 (s, 3H, C*H*$_3$), 3.27 (ddd, *J* = 9.4, 6.7, 3.1 Hz, 1H, C*H*), 2.97 – 2.72 (m, 2H, C*H*$_2$). ^{13}C NMR (151 MHz, $CDCl_3$) δ = 176.1, 174.9, 173.5, 135.4, 128.9, 128.7, 128.1, 125.9, 53.1, 48.5, 42.9, 37.4, 31.4. ^{19}F NMR (376 MHz, $CDCl_3$) δ = -65.51 (d, *J* = 9.2). IR (ν_{max}, cm^{-1}) 2957 (w), 2925 (w), 2856 (w), 1746 (w), 1702 (w), 1458 (w), 1220 (w), 772 (w). HRMS (ESI/QTOF) m/z: $[M + Na]^+$ Calcd for $C_{17}H_{16}F_3NNaO_4^+$ 352.0767; Found 352.0775.

Epoxidation

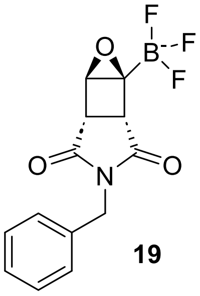
19

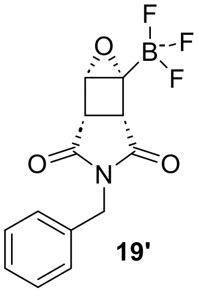
19'

To the pre-cooled to 0 °C solution of potassium cyclobutenyl trifluoroborate **8c** (100 mg, 0.313 mmol) in acetone (10 mL), a freshly prepared solution of DMDO (8.5 mL, ca. 0.5 mmol)[2] was added in a dropwise manner. The obtained solution was left overnight in an open flask and with intensive stirring. Trituration of the colorless solution with Et_2O (10 mL) with subsequent filtration and drying of the precipitate on air results in mixture of compounds **19** and **19'** (100.7 mg, 0.301 mmol, 96% yield, ca. 1:3) as a white solid.

trans-Isomer **19**: ^{1}H NMR (400 MHz, DMSO) δ = 7.46 – 7.00 (m, 5H, Ar*H*), 4.51 (s, 2H, CH_2), 3.83 (d, *J* = 1.4 Hz, 1H, C*H*), 3.29 (dd, *J* = 7.3, 1.5 Hz, 1H, C*H*), 2.99 (d, *J* = 7.3 Hz, 1H, C*H*).

cis-Isomer **19'**: ^{1}H NMR (400 MHz, DMSO) δ = 7.54 – 7.00 (m, 5H, Ar*H*), 4.63 (d, *J* = 15.1 Hz, 1H, HC*H*), 4.45 (d, *J* = 15.1 Hz, 1H, *H*CH), 3.67 (d, *J* = 2.8 Hz, 1H, C*H*), 3.16 (d, *J* = 3.4 Hz, 1H, C*H*), 2.82 (t, *J* = 3.1 Hz, 1H, C*H*).

Isomers mixture (signals not resolved). ^{13}C NMR (101 MHz, DMSO) δ = 175.5, 174.7, 136.9 and 136.7, 128.8, 127.7, 127.6, 127.5 and 127.5, 55.6 and 53.0, 51.0, 50.3, 42.1 and 41.7. ^{19}F NMR (376 MHz, DMSO) δ = -142.4 – -142.9 (m), -143.5 – -144.1 (m). ^{11}B NMR (128 MHz, DMSO) δ = 2.2 – -1.1 (m). IR (ν_{max}, cm^{-1}) 2974 (w), 2881 (w), 1696 (s), 1398 (m), 1352 (m), 1164 (m), 1020 (m), 1001 (m), 772 (w). HRMS (ESI/QTOF) m/z: $[M]^-$ Calcd for $C_{13}H_{10}BF_3NO_3^-$ 296.0711; Found 296.0716.

Reaction condition optimization studies

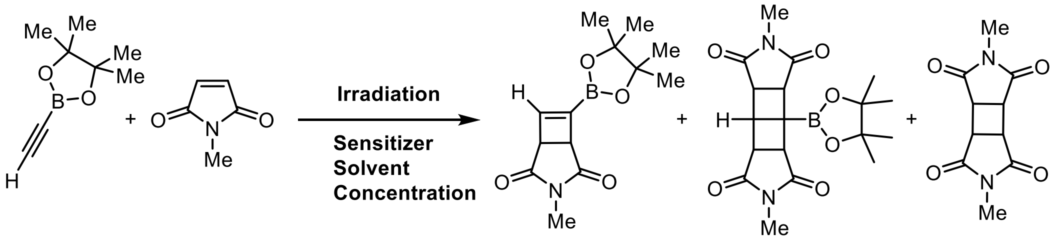

4c **7a** **8a** **9a** **10c**

0.05 mmol

Scheme S1. The reaction studied

General Procedure for the Optimization studies

A solution of the corresponding maleimide (0.050 mmol, 1 equiv.), alkynyl boronate (0.050 mmol, 1 equiv.), and photosensitizer (0.010 mmol, 0.1 equiv.) in investigated solvent (2 mL) was placed in a glass tube, closed with a rubber septum and degassed by three vacuum pumping-nitrogen purge cycles. The resulting mixture was irradiated in a Rayonet® reactor (λ_{max} = 350 nm) or with a Kessil lamp (440 or 467 nm) placed at a 3 cm distance from the vessel (see Photos S1 and S2 for the experimental setup) at rt for 12 h. After the reaction was complete, the organic solvent was evaporated under reduced pressure to dryness and the crude mixture was analysed by qNMR using 1,3,5-trimethoxybenzene as internal standard.

Table S2. Influence of irradiation wavelength

Entry	λ, nm	solvent	C, M	Additive (%)	8a, %[a]	9a, %	10c, %	Conversion of 4c, %
1	350	CH_3CN	0.05	BP (10%)[b]	24	16	13	53
2	350	CH_3CN	0.05	TX (10%)[b]	28	15	16	54[c]
3	No light source	CH_3CN	0.05	(–) [b]	0	0	0	0
4	350	CH_3CN	0.05	(–)	27	19	15	57[d]
5	440	CH_3CN	0.05	(–)	0	0	0	0
6	467	CH_3CN	0.05	(–)	0	0	0	0

[a] Here and below: ^{1}H NMR yield is given; standard – 1,3,5-trimethoxybenzene
[b] Here and below: BP – benzophenone, TX – thioxanthone, (–) – no sensitizer
[c] 8 h; [d] 48 h

Table S3. Influence of sensitizer amount

Entry	λ, nm	solvent	*c*, M	Additive (%)	8a, %	9a, %	10c, %	Conversion of 4c, %
1	350	CH_3CN	0.05	TX (5%)	22	19	16	57
2	350	CH_3CN	0.05	TX (10%)	24	16	13	53
3	350	CH_3CN	0.05	TX (25%)	22	17	15	53
4	350	CH_3CN	0.05	TX (50%)	24	16	14	53
5	350	CH_3CN	0.05	TX (100%)	24	14	15	52

Table S4. Concentration effect

Entry	λ, nm	solvent	C, M	Additive (%)	8a, %	9a, %	10c, %	Conversion of 4c, %
1	350	CH_3CN	0.01	TX (10%)	39	27	22	83
2	350	CH_3CN	0.05	TX (10%)	24	16	13	53
3	350	CH_3CN	0.5	TX (10%)	30	40	30	100
4	350	CH_3CN	1	TX (10%)	11	0	11	100

Table S5. Solvent effect

Entry	λ, nm	solvent	*c*, M	Additive (%)	8a, %	9a, %	Conversion of 4c, %
1	350	CH_3CN	0.05	TX (10%)	13	10	54
2[a]	350	CH_3CN	0.05	TX (10%)	42	6	51
3	350	Acetone	0.05	TX (10%)	30	27	78
4	350	MeOH	0.05	TX (10%)	decomposition		
5	350	DMSO	0.05	TX (10%)	decomposition		
6	350	DCM	0.05	TX (10%)	51	31	100
7[a]	350	DCM	0.05	TX (10%)	78	6	100
8	350	EtOAc	0.05	TX (10%)	21	34	100
9	350	Toluene	0.05	TX (10%)	100[b]	0	100[2]
10	350	*n*-Hexane	0.05	TX (10%)	85	<1	100

[a] *3 eq. of alkynyl boronate*; [b] *Complex mixture was formed probably due to reaction of intermediates with the solvent.*

Influence of the boronate protection group on the reaction outcome

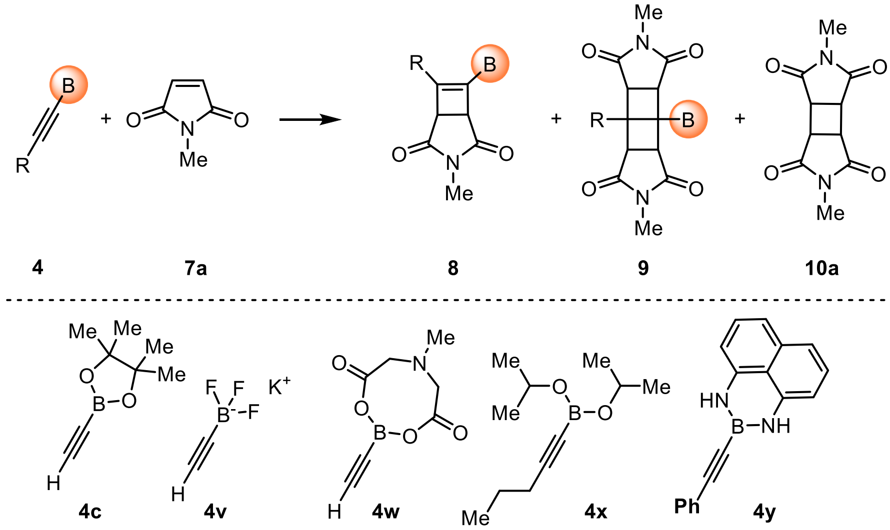

Table S6. *The reaction studied and alkynyl boronate substrates*

Table S7. Studies on the boron protection group-dependent reactivity

Entry	**Alkynyl boronate**	**λ, nm**	**solvent**	***c*, M**	**Additive (%)**	**8, %**	**9, %**	**10a, %**	**Conversion of 4, %**
1	**4c**	350	CH_3CN	0.05	TX (10%)	24	16	13	53
2	**4v**	350	Acetone	0.05	TX (10%)	29	20	7	56
3	**4w**	350	CH_3CN	0.05	TX (10%)	20	22	22	50
4	**4x**	350	CH_3CN	0.05	TX (10%)	decomposition			100
5	**4y**	350	CH_3CN	0.05	TX (10%)	0	0	100	0

Initially, alkynyl trifluoroborates has been considered as more attractive substrates for [2+2] cycloaddition studies due to relatively higher synthetic accessibility, improved the C–B bond stability, and more robust purification procedures. Test experiment utilizing simplest potassium ethynyl trifluoroborate **4v** and *N*-methylmaleimide **7a** (See Table S6, Entry 2) strengthened our confidence – target cyclobutene **8ab** almost completely precipitated from the reaction mixture in 60% yield and excellent 97% purity. More complex substrates show almost the same reactivity, comparable or even superior to corresponding alkynyl boropinacolates (See the Main Text). However, all attempts to separate the desired cyclobutenyl trifluoroborates from their mixture with double addition products or remaining starting alkynyl trifluoroborates were unsuccessful, so we had turned our attention back to the reactivity of alkynyl boropinacolates.

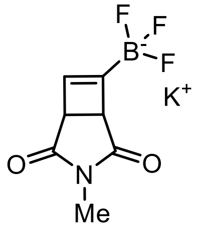

0.5 mmol scale
65% by NMR
(19%)
Isolated yield 60%

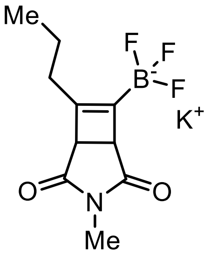

67% by NMR
(33%)

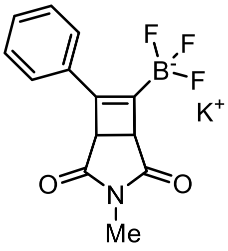

16% by NMR
(42%)

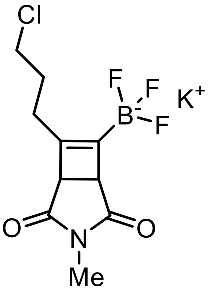

67% by NMR
(33%)

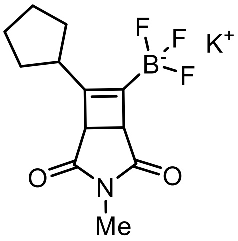

75% by NMR
(15%)

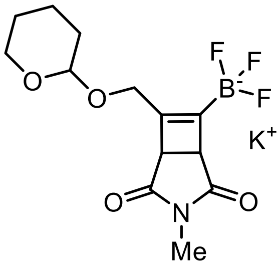

67% by NMR
(31%)

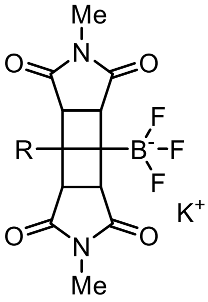

NMR yields of
double addition
products
are given in parentheses

*Table S8. Examples of the products obtained by the direct photochemical reaction of corresponding alkynyltrifluoroborates and N-methylmaleimide **7a***

*Characterization of potassium trifluoro(3-methyl-2,4-dioxo-3-azabicyclo[3.2.0]hept-6-en-6-yl)borate, **8ab***

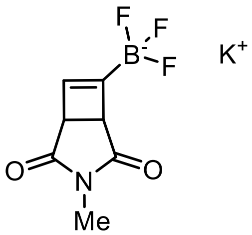

A solution of *N*-methyl maleimide **7a** (11.1 mg, 0.100 mmol, 1 equiv.), potassium ethynyl trifluoroborate (13.2 mg, 0.100 mmol, 1 equiv.), and thioxanthone (2.1 mg, 0.01 mmol) in acetone (2 mL) was placed in a glass tube, closed with rubber septum and degassed by three vacuum pumping-nitrogen purge cycles. Resulting solution was irradiated in Rayonet® reactor (λ_{max} = 350 nm) placed at a 3 cm distance from the vessel (see Photo S1 and Photo S2 for the experimental setup) at rt for 12 h. The precipitate was filtered, washed with Et_2O (3×1 mL) and dried on air to give product **8ab** as a white fluffy solid (14.7 mg, 0.060 mmol, 60% yield). ^{1}H NMR (400 MHz, DMSO) δ = 6.12 – 6.04 (m, 1H, C*H*), 3.57 – 3.52 (m, 1H, C*H*), 3.44 (d, *J* = 2.6 Hz, 1H, C*H*), 2.75 (s, 3H, C*H*$_3$). ^{13}C NMR (101 MHz, DMSO) δ = 177.1, 176.2, 135.1, 48.0, 46.4, 24.5. ^{19}F NMR (376 MHz, DMSO) δ = -138.2 – -141.8 (br). HRMS (ESI/QTOF) m/z: [M]$^-$ Calcd for $C_7H_6BF_3NO_2^-$ 204.0449; Found 204.0443.

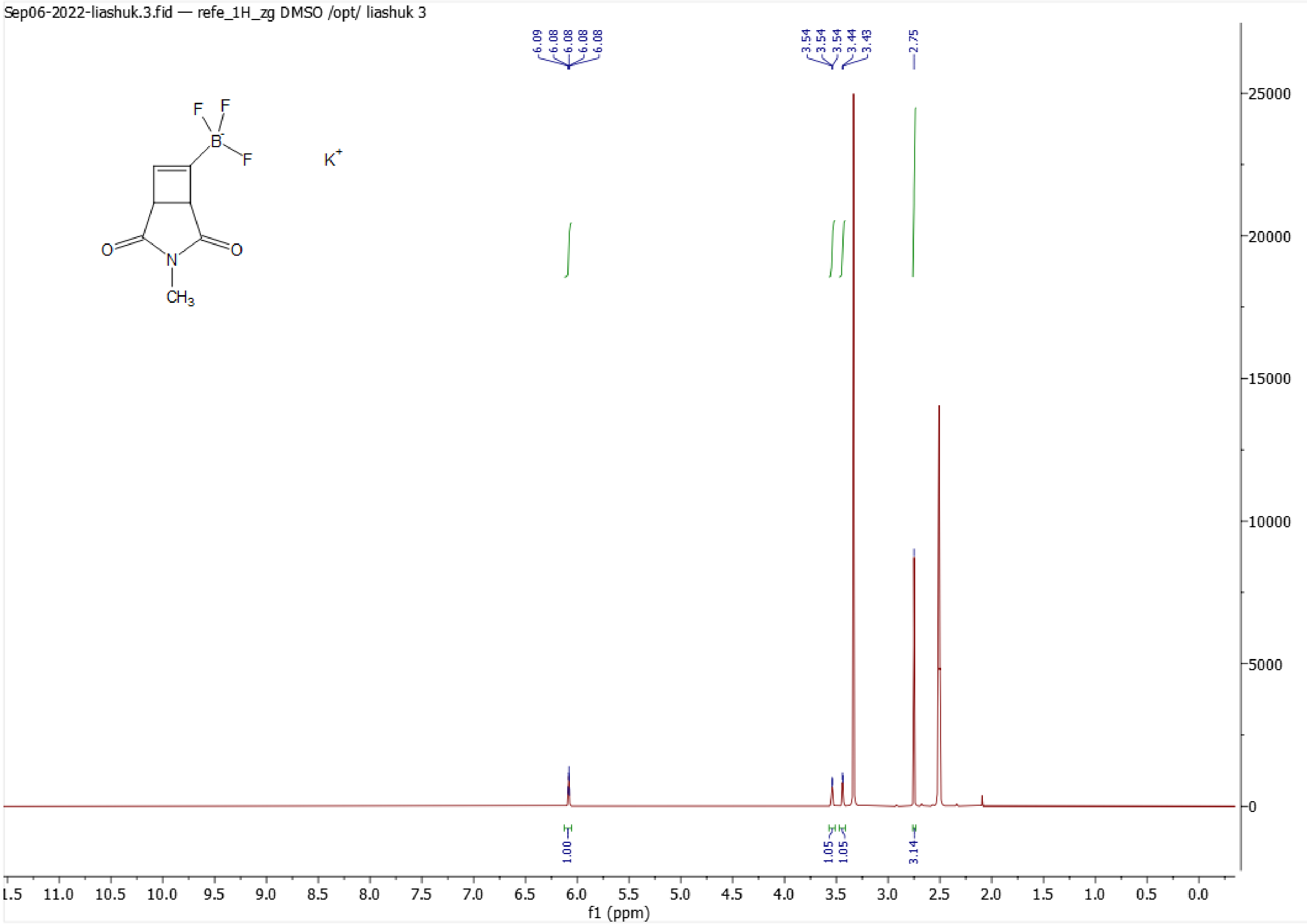

Spectrum 1. Potassium trifluoro(3-methyl-2,4-dioxo-3-azabicyclo[3.2.0]hept-6-en-6-yl)borate ***8ab****, ^{1}H NMR (400 MHz, DMSO-d_6)*

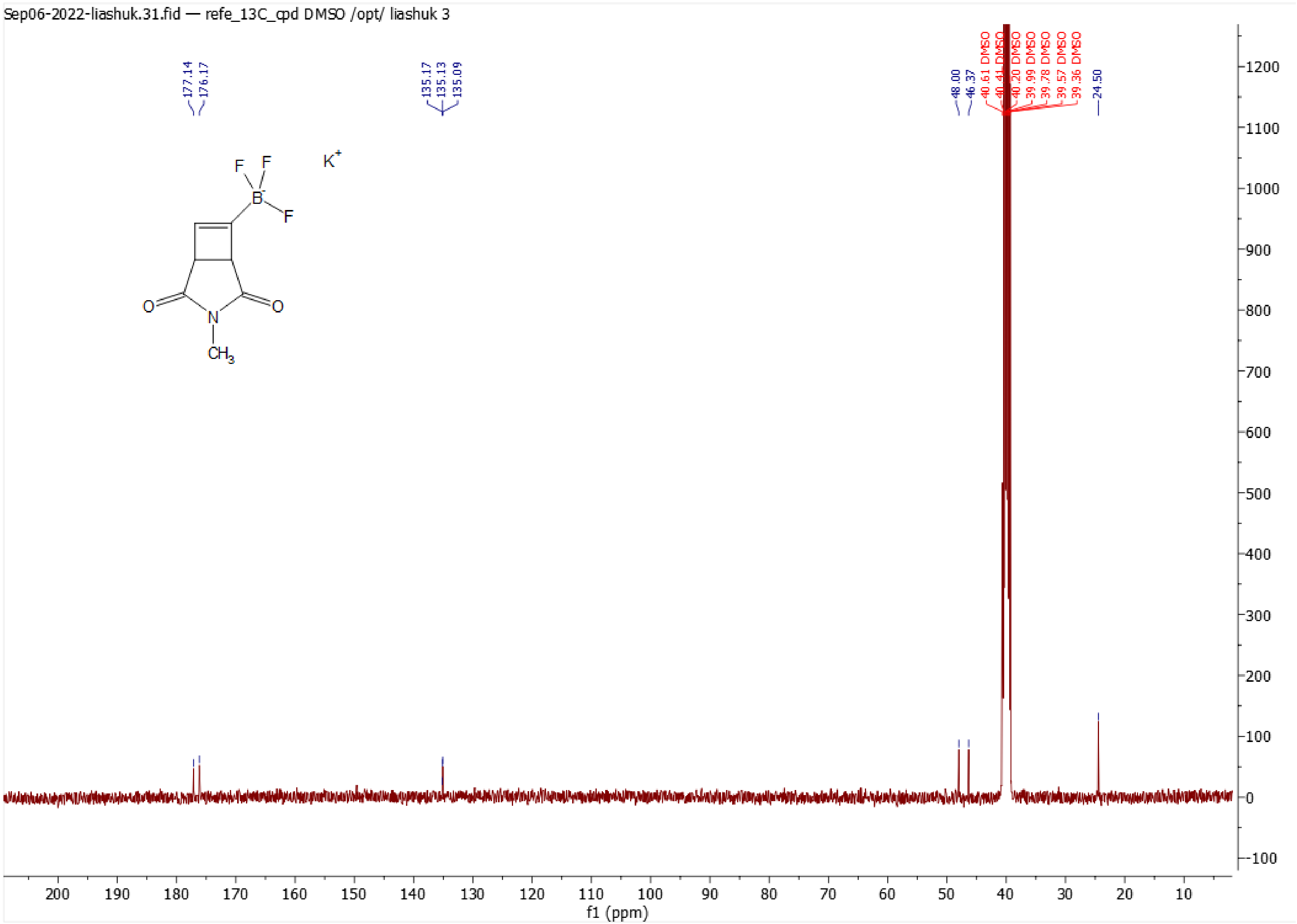

Spectrum 2. Potassium trifluoro(3-methyl-2,4-dioxo-3-azabicyclo[3.2.0]hept-6-en-6-yl)borate ***8ab****,* *^{13}C NMR (101 MHz, DMSO-d_6)*

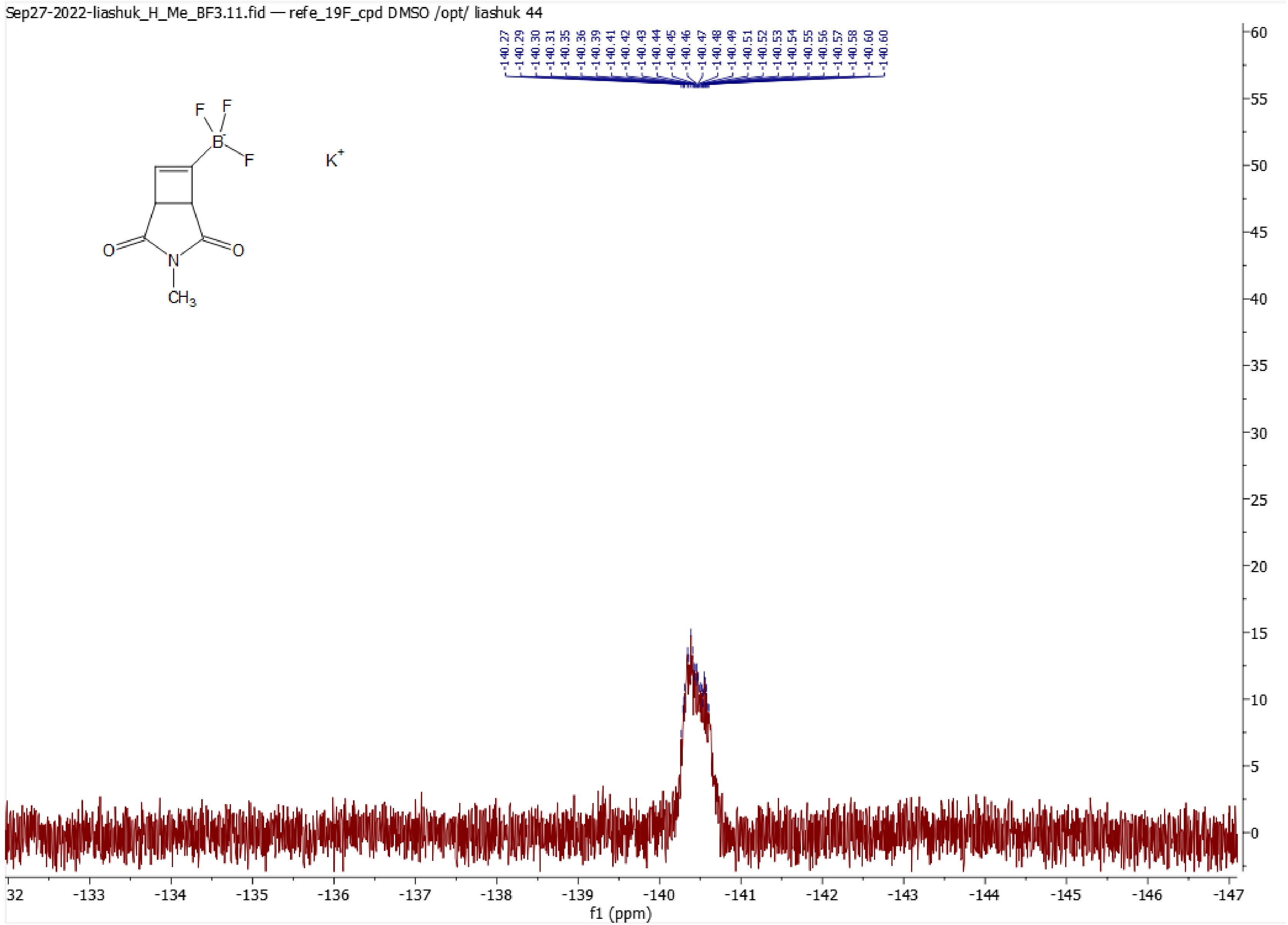

Spectrum 3. Potassium trifluoro(3-methyl-2,4-dioxo-3-azabicyclo[3.2.0]hept-6-en-6-yl)borate ***8ab****,* *^{19}F NMR (376 MHz, DMSO-d_6)*

Reaction limitations

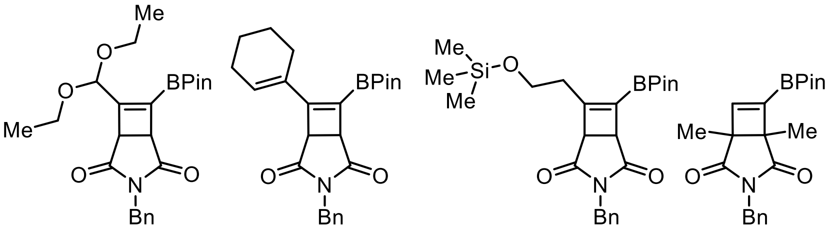

8ci, 25% (NMR)
unstable

8cj, 0%

8ck, 0%

8m, 0%

Table S9. Unsuccesfull experiments

Non-maleimide scope of the reaction

With optimized conditions in hand, the applicability of the developed protocol was tested on a range of electron-deficient and electron-donor alkenes (Table S9). Unfortunately, no desired product was formed in any case.

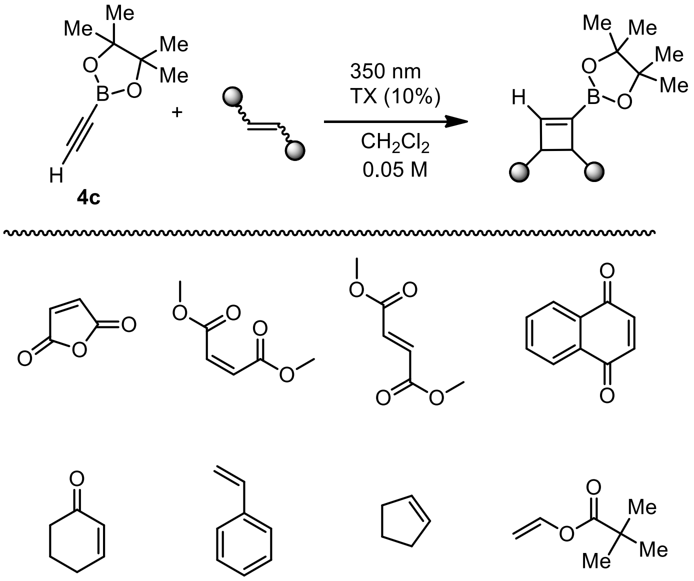

*Table S10. Substrates, that do not undergo the photochemical [2+2] cycloaddition with alkynyl boronate **4c** under the developed conditions*

Studies on the [2+2] cycloaddition of aryl flanked ethynyl boronates

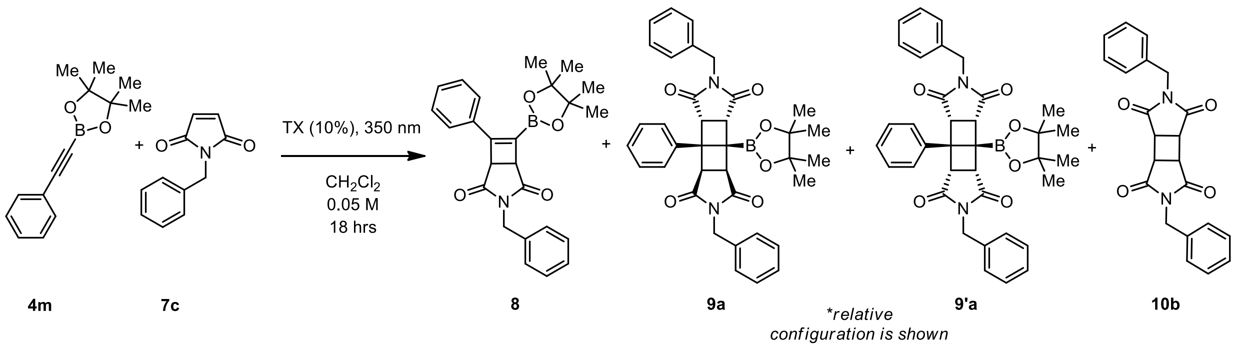

Scheme 2. The reaction studied

Table S11. Optimization studies for the reaction of aryl substituted ethynylboronate ***4m*** *and N-benzylmaleimide* ***7c***

Entry	7c, equiv.	λ, nm	solvent	*c*, M	Additive (%)	8, %	9a/9'a, %	10b, %	Conversion of 4m, %
1	1	350	CH_3CN	0.05	TX (10%)	<1	35	19	50
2	1	350	CH_2Cl_2	0.05	TX (10%)	<1	40	13	56
3	1[1]	350	CH_2Cl_2	0.05	TX (10%)	<1	38	25	80
3	1	350	*n*-hexane	0.05	TX (10%)	0	0	20	15
4	0.3	350	CH_2Cl_2	0.05	TX (10%)	<1	10	8	25
5	3	350	CH_2Cl_2	0.05	TX (10%)	<5	65	95	100
6	1	350	CH_2Cl_2	0.05	-	0	0	7	20
7	1	350	CH_2Cl_2	0.01	TX (10%)	<1	43	7	60

0.3 mmol reaction setup visualization

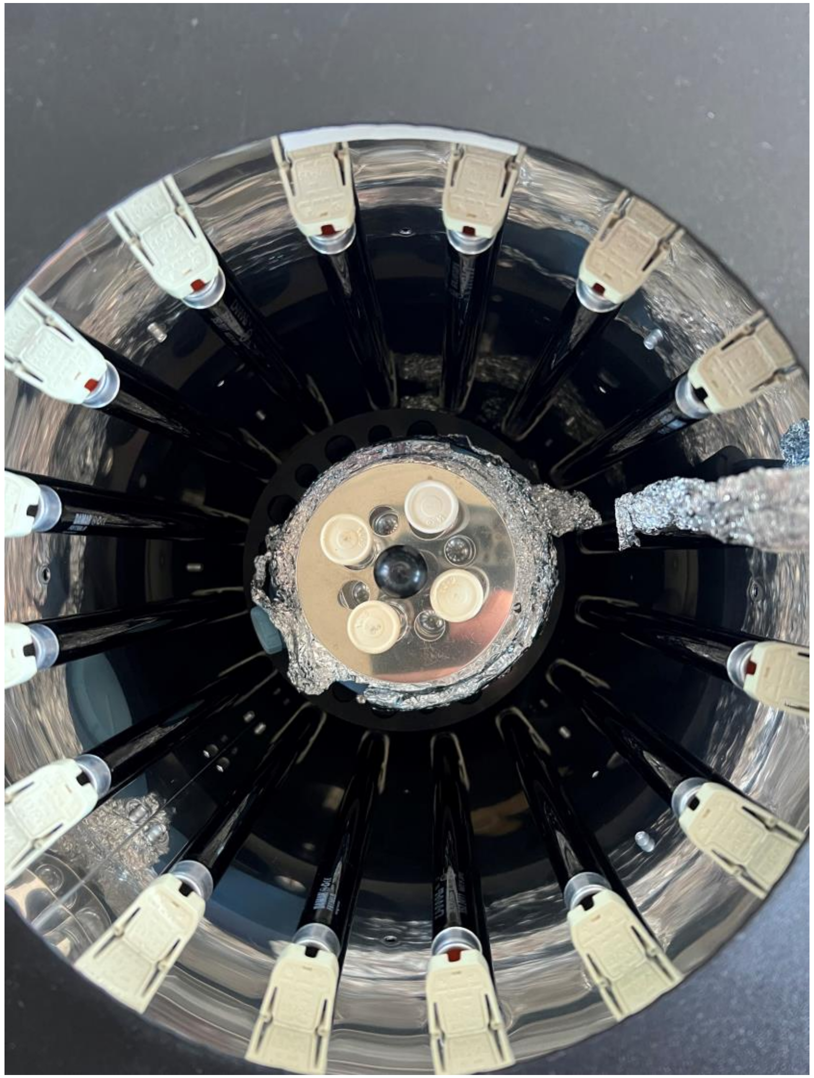

Photo S1. Top view

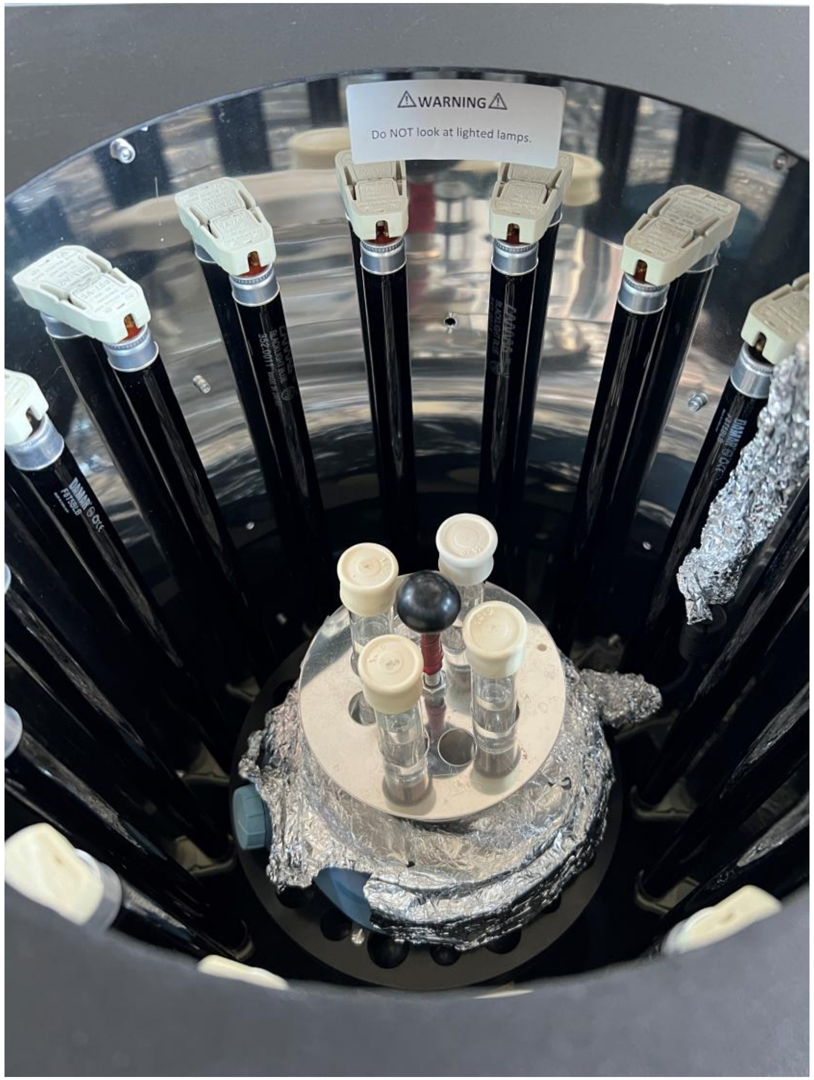

Photo S2. Side view

10 mmol scale-up reaction setup visualization

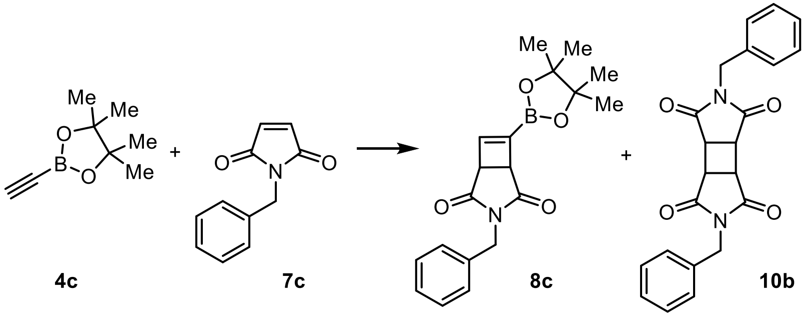

Scheme S3. The reaction studied

Photo S3. Reaction mixture before irradiation; partly insoluble N-benzylmaleimide could be observed on the bottom of the bulb

Photo S4. Irradiation process

Photo S5. Reaction mixture after 24 hrs of irradiation

Mechanistic investigations

Triplet quenching

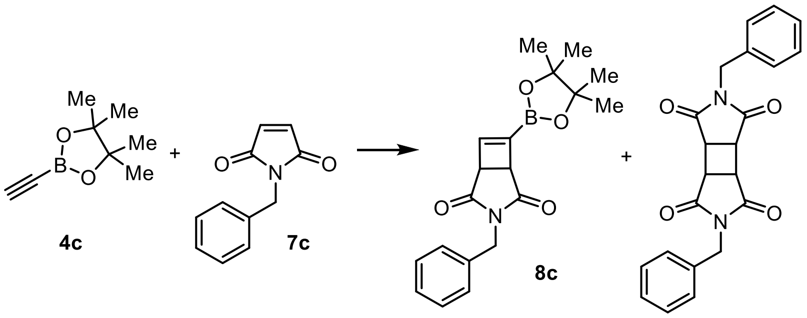

Scheme S4. The reaction studied

Table S12. Triplet and radical quenching for the reaction of alkynyl boronate **4c** and N-benzyl maleimide **7c**

Entry	Conditions	Alkyne conversion, %	Maleimide conversion, %	Product 8c yield, %
1	Typical	100.0	100.0	76.3
2	Air [a]	44.3	100.0	45.3
3	O_2 [a]	40.2	100.0	38.1
4	TEMPO [b]	100.0	100.0	41.2
5	Ni(acac)$_2$	100.0	7.0	0

[a] *instead of N_2 atmosphere in classic conditions* [b] *1 eq TEMPO was used, other conditions remain unchanged*

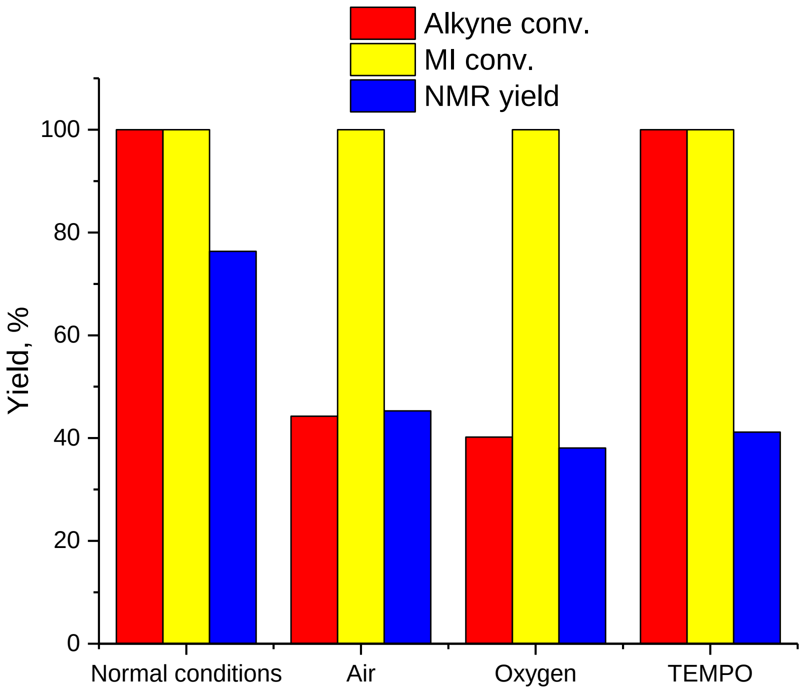

Figure S1. Dependence of the yield and SM conversions from the presence of quenchers for alkynyl boronate **4c**

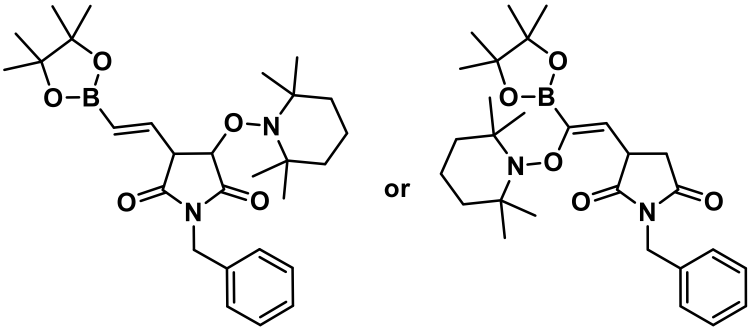

Chemical Formula: $C_{28}H_{41}BN_2O_5$
Exact Mass: 496.3109

Figure S2 . Possible TEMPO adduct of the 1,4-biradical intermediate

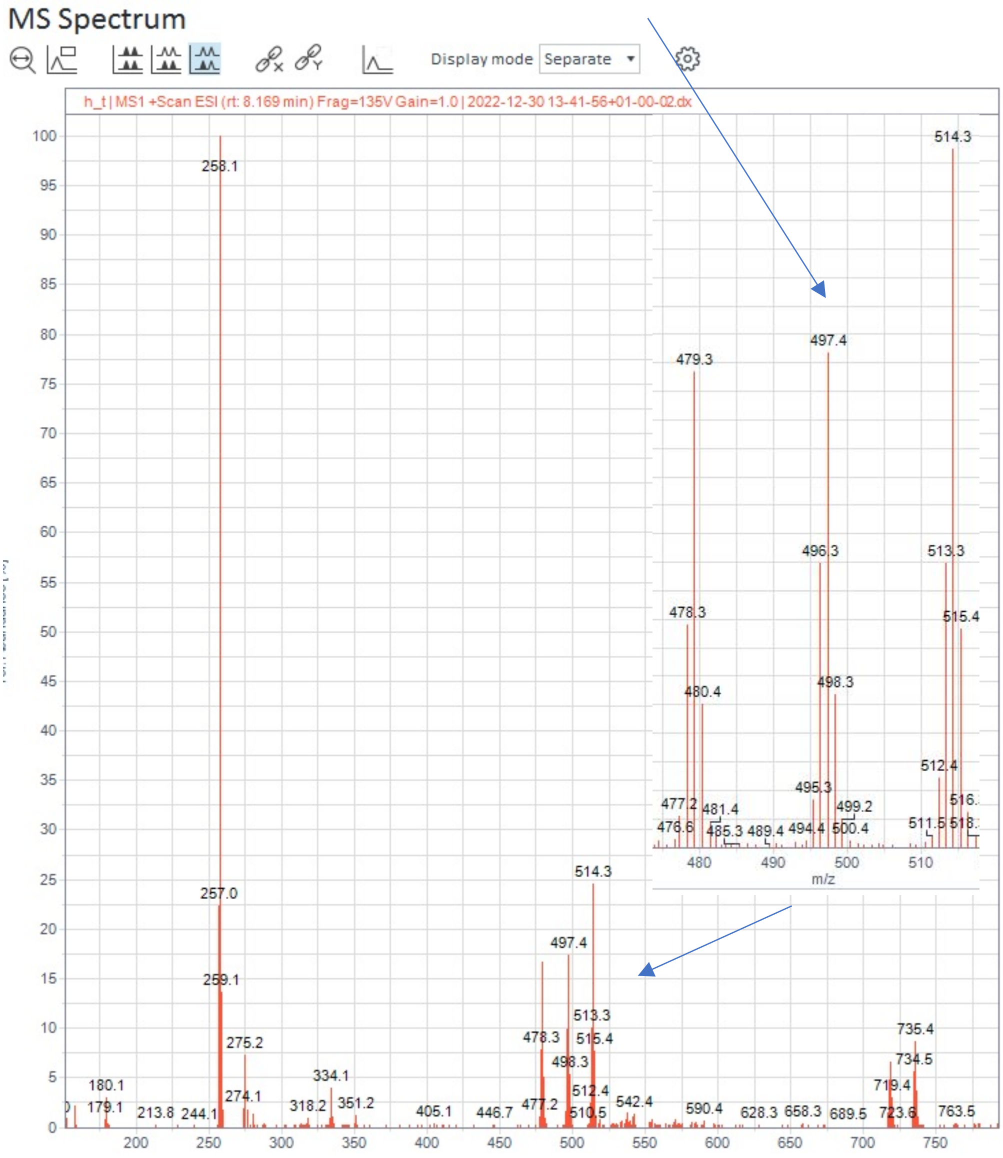

MS Spectrum

Display mode Separate

h_t | MS1 +Scan ESI (rt: 8.169 min) Frag=135V Gain=1.0 | 2022-12-30 13-41-56+01-00-02.dx

Spectrum 4 Mass-spectrum of the selected LCMS peak

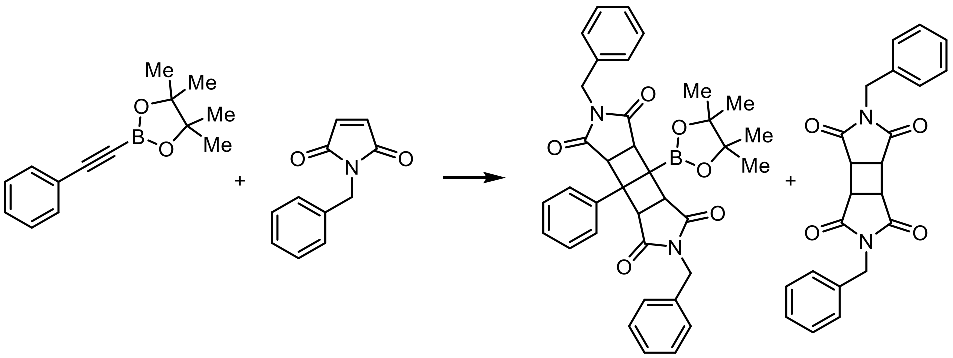

Scheme S5. The reaction studied

*Table S13. Triplet and radical quenching for the reaction of alkynyl boronate **4m** and N-benzyl maleimide **7c***

Entry	Conditions	Alkyne conversion, %	Maleimide conversion, %	Product 9a/9'a yield, %
1	typical cond	34.3	100.0	57.2
2	Air [a]	58.8	100.0	18.9
3	O_2 [a]	100.0	100.0	17.9
4	TEMPO [b]	49.6	49.7	10.2
5	Ni(acac)$_2$	100.0	5.0	0

[a] *instead of N_2 atmosphere in classic conditions* [b] *1 eq TEMPO was used, other conditions remain unchanged*

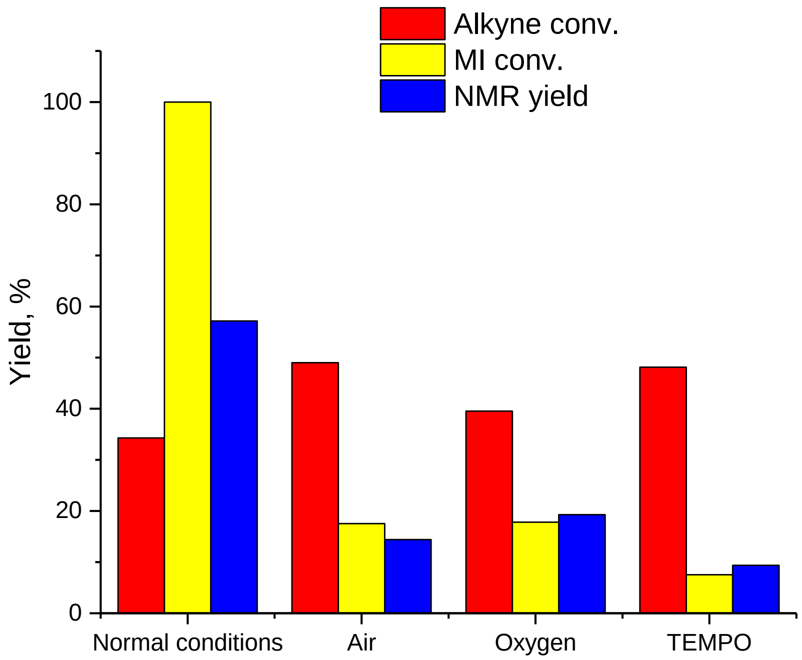

*Figure S3. Dependence of the yield and SM conversions from the presence of quenchers for alkynyl boronate **4m***

Visible light experimentation

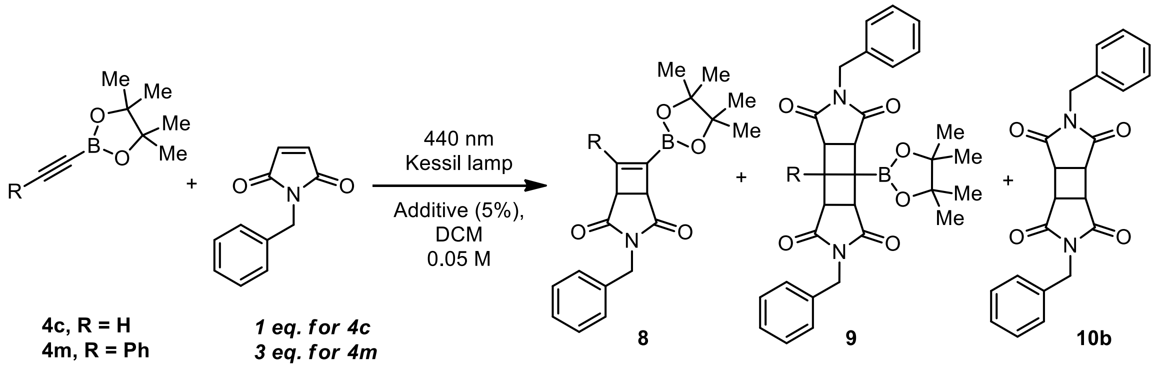

Scheme 6. The reaction studied

*Table S14. Visible-light promoted examples of [2+2] cycloaddition of alkynylboronates 4c and 4m with N-benzylmaleimide **7c***

Entry	**SM**	**Additive**	**E_t, kcal/mol**	**$E_{1/2}$ (M^+/M^*), V**	**$E_{1/2}$ (M^*/M^-), V**	**8, %**	**9, %**	**Conversion of alkyne 4, %**
1	**4c**	-	-	-	-	0	0	0
2[a]	**4c**	-	-	-	-	46	0	90
3	**4c**	TX	65.5	-1.61	1.77	63	<5	80
4	**4c**	Ir(dFppy)$_3$	63.5	-1.46	0.75	90	0	100
5	**4c**	3CzClIPn	60.1	1.49	-1.24	5	0	80
6	**4c**	fac-Ir(ppy)$_3$	58.1	-1.73	0.31	15	0	80
7	**4c**	Ru(bpy)$_3$	49	-0.81	0.77	0	0	100
8	**4m**	Ir(dFppy)$_3$	63.5	-1.46	0.75	0	20	55
9[b]	**4c**	Ir(dFppy)$_3$	63.5	-1.46	0.75	30	2	40

Reaction conditions: 0.1 mmol of alkyne, CH_2Cl_2, 0.05 M, 44 W Kessil lamp, 2 cm from the reaction vessel, 12 hrs.

[a] 360 nm instead of 440 nm irradiation wavelength
[b] 2 mmol of **4c** was used

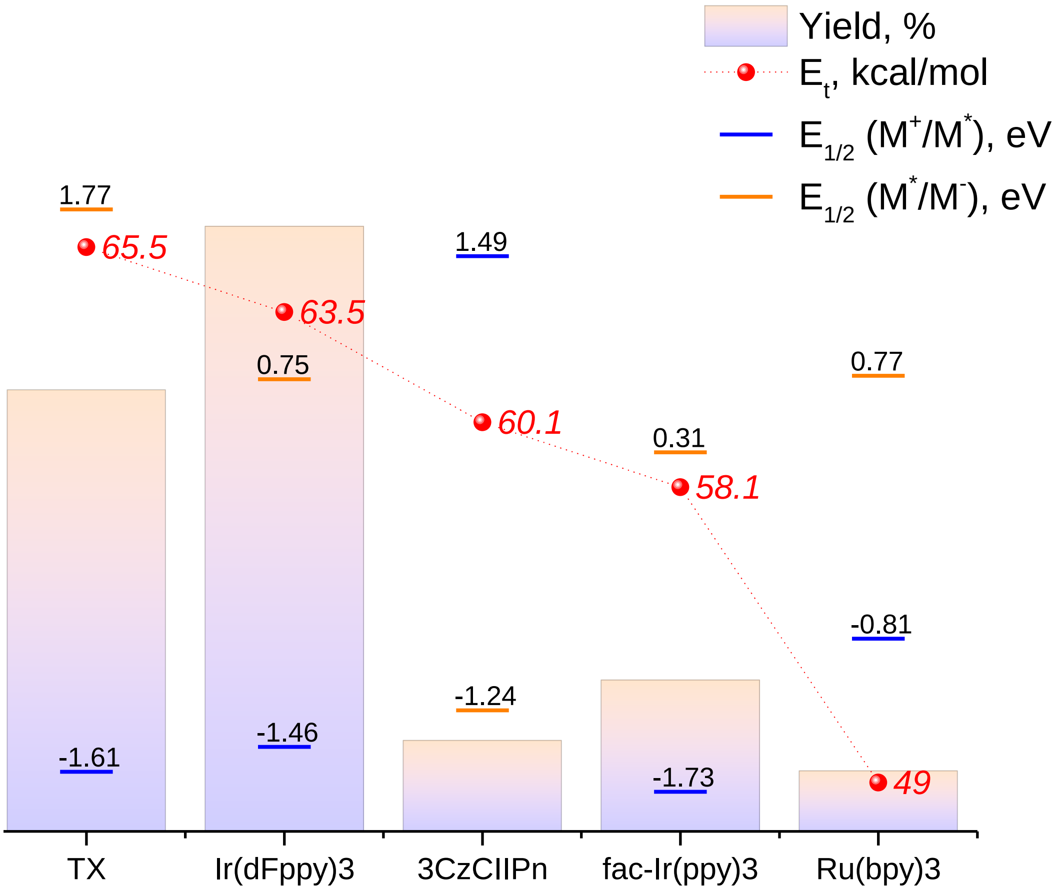

Figure S4 . Graphical representation of the observed correlation between reaction yield, triplet energy and redox potentials of the used photocatalysts

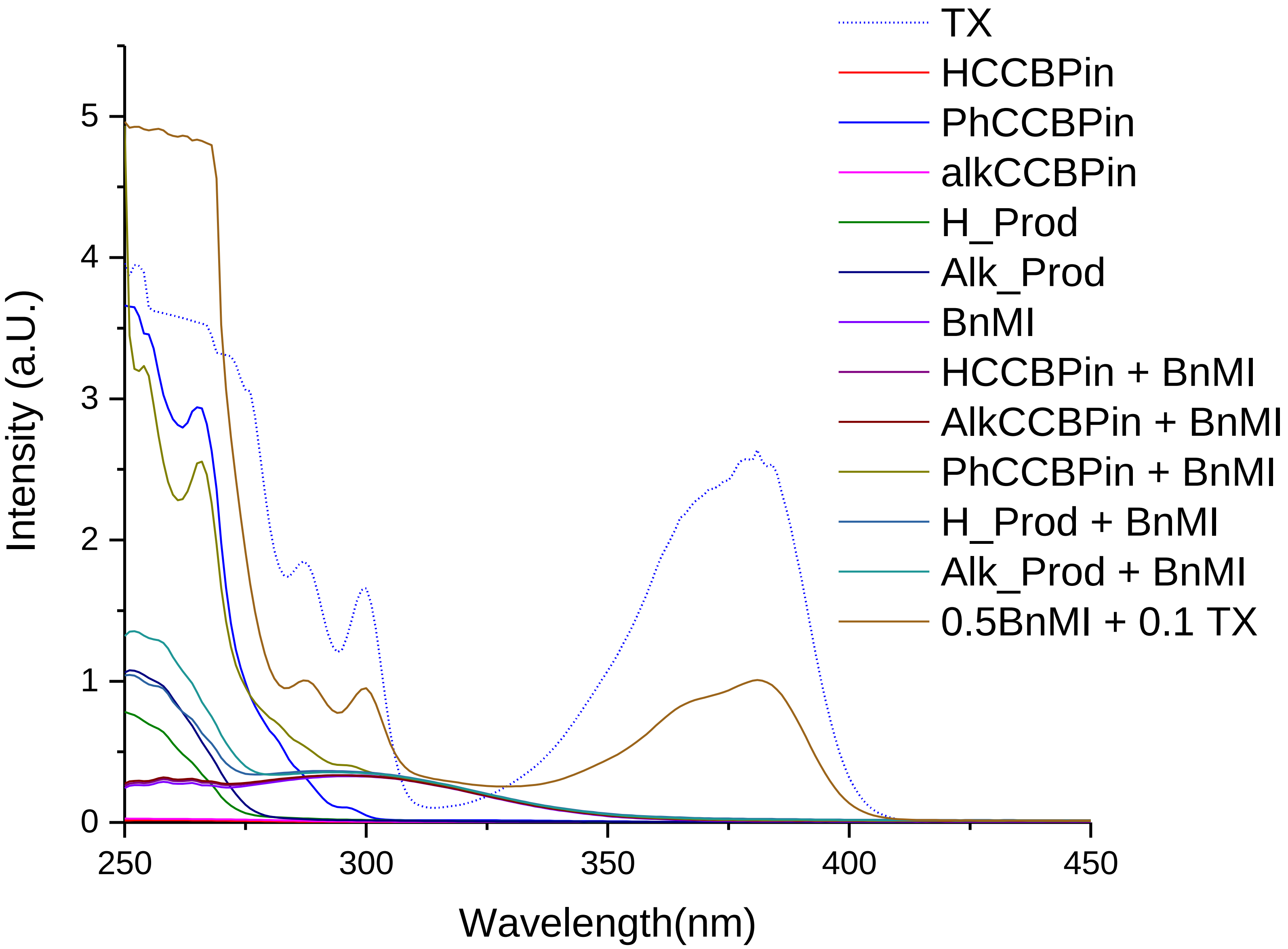

Figure S5. Absorption spectra of the investigated compounds and their mixtures

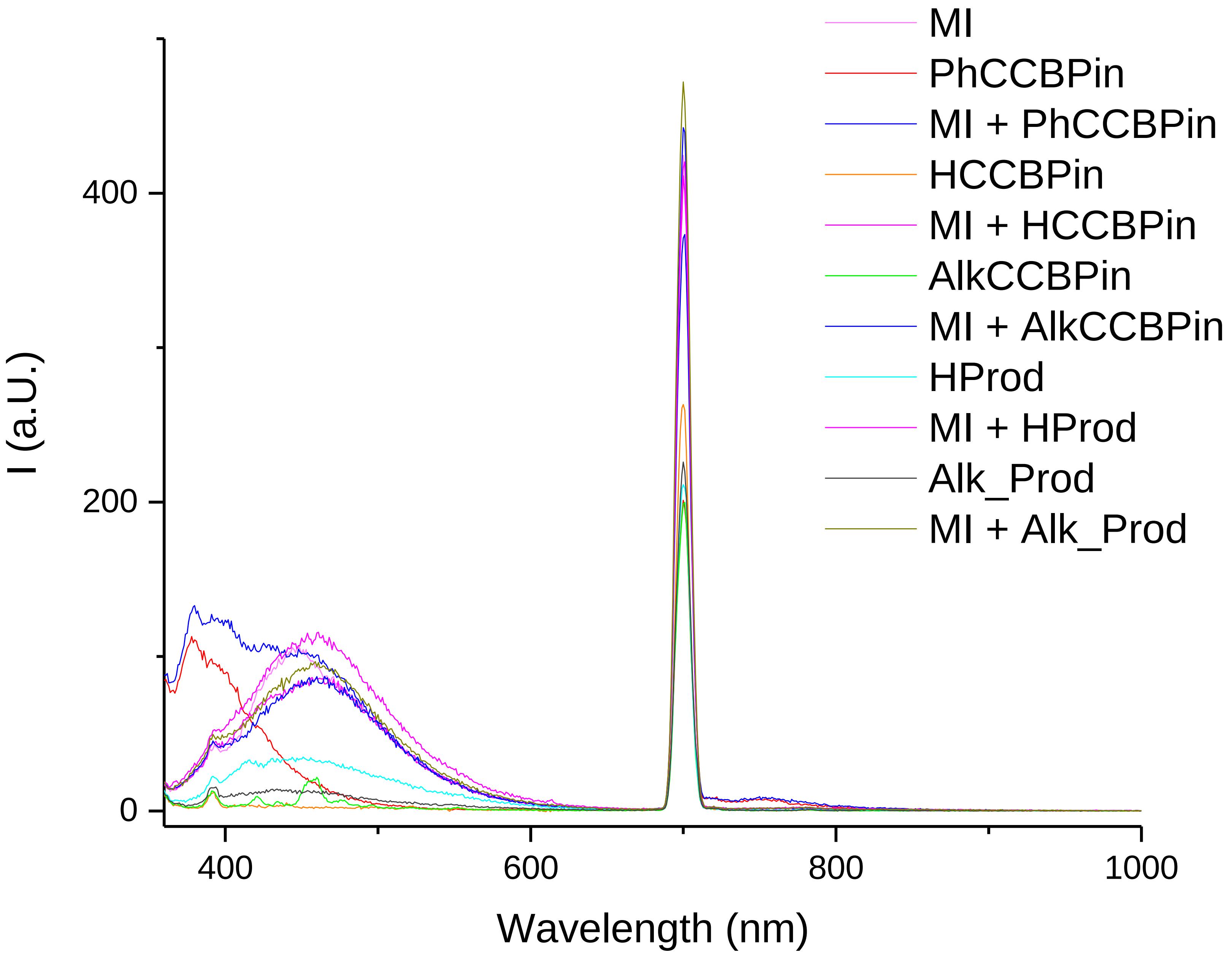

Figure S6. Emission spectra of the investigated compounds and their mixtures

Regioselectivity studies

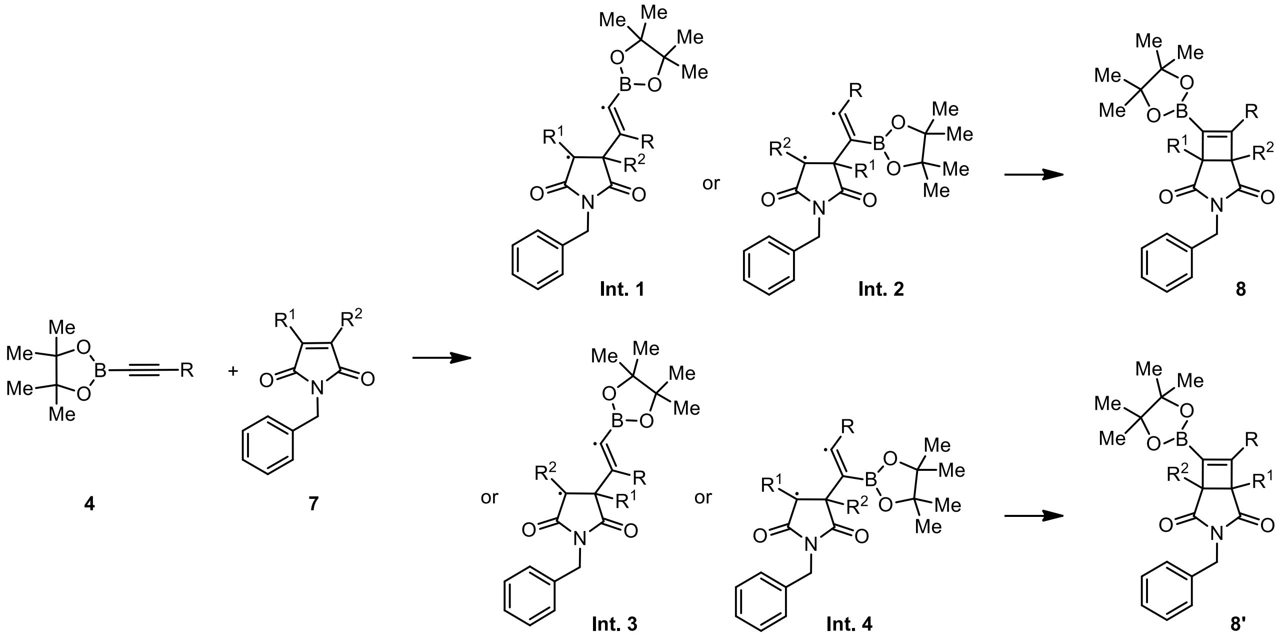

Scheme S7. The reaction studied

Table S15. Regioselectivity studies

#	Alkyne, R	Maleimide			Product 8 (9)	Product 8′
		#	R^1	R^2	NMR yield, %	NMR yield, %
1	**4c**, H	**7c**	H	H	80	–
2		**7k**	H	Me	18	42
3		**7m**	Me	Me	0	–
4	**4b**, *c*-C_3H_5	**7c**	H	H	80	
5		**7k**	H	Me	12	33
6		**7m**	Me	Me	0	
7	**4m**, Ph	**7c**	H	H	65[a]	–
8		**7k**	H	Me	0	0
9		**7m**	Me	Me	0	–

[a] Compounds **9a** and **9′a** were obtained

Cross-cycloaddition experiment

To check the possibility of photoexcitation of arylcyclobutenyl boronate double bond, a cross-cycloaddition experiment was performed. Based on previous results, *N*-phenyl maleimide has low reactivity towards the triple bond as compared to the double bond of unsaturated boronates and reacts significantly slower in comparison with N-benzyl substituted maleimide. In that case, a reaction of alkynyl boronate **4m** with the mixture of *N*-benzyl and *N*-phenyl maleimide will unambiguously starts from the formation of *N*-benzyl maleimide-derived cyclobutenyl boronate. If the cyclobutene double bond was excitated upon irradiation, the second addition would occur in a non-selective manner with *N*-phenyl or *N*-benzyl maleimide.

The obtained results disprove the proposed hypothesis and revealed unusual selectivity of aryl- and alkyl-substituted maleimides towards double and triple bonds (See Scheme S10 and Table S16).

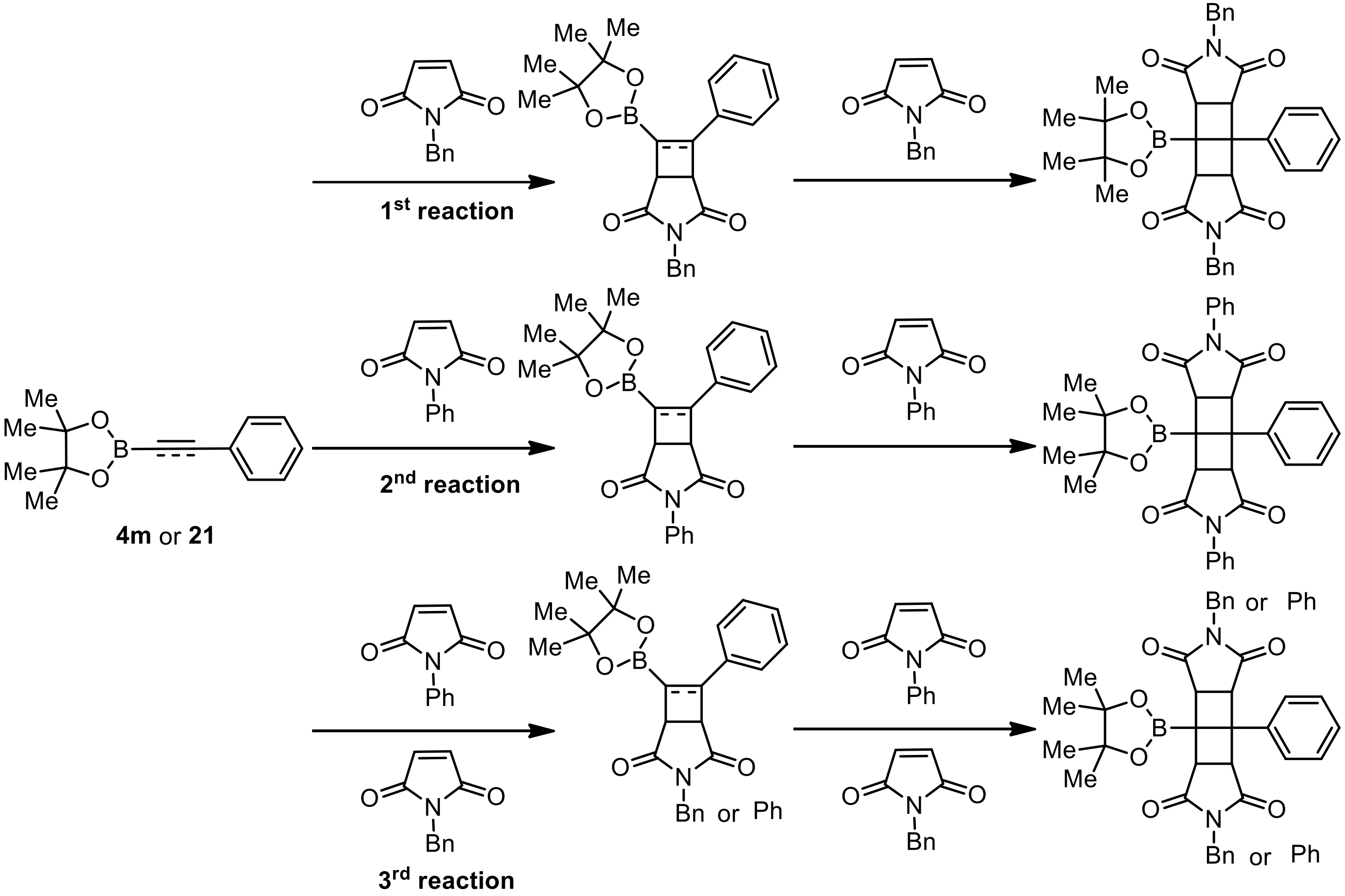

Scheme S8. Hypothetical products in cross-cycloaddition experiments

Table S16. Results of cross-cycloaddition experiments

Entry	**Maleimide**	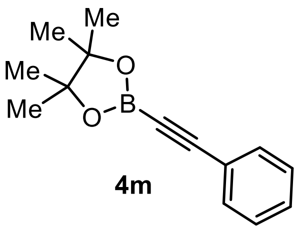 **4m**	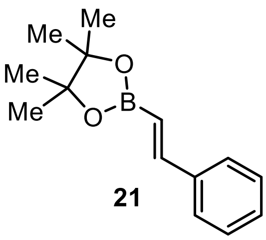 **21**	**Alkyne 4m + alkene 21 mixture**
1	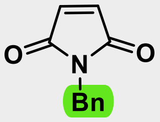 3 eq.	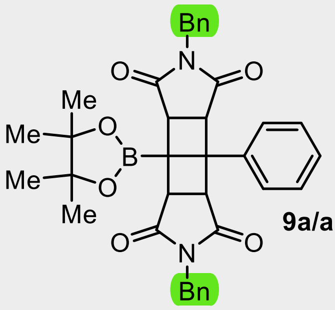 **9a/a'** NMR yield 54% Decomposed 30% SM 15%	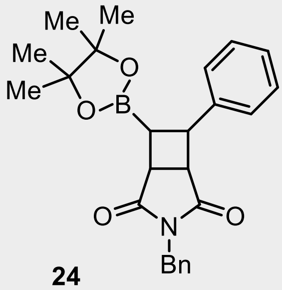 **24** NMR yield 80% Decomposed 0% SM 18%	Conversion 80% alkene **9a/9'a**: alkane **24** = 1 : 1
2	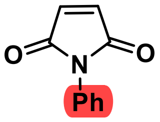 3 eq.	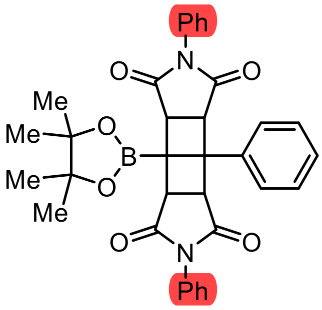 NMR yield <5% Decomposed 37% SM 55%	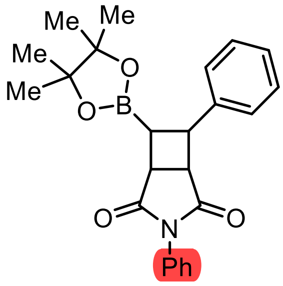 NMR yield 84% Decomposed 0% SM 0%	Alkyne **4m** conversion 0% Alkene **21** conversion 100% Yield 79%
3	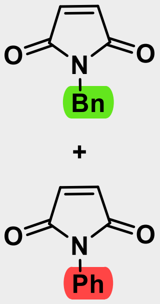 3 eq. and 3 eq.	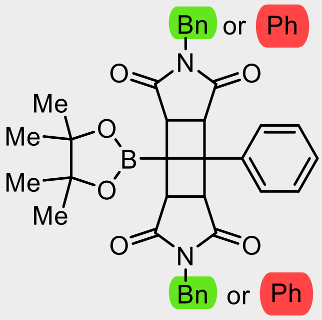 Conversion 100% **(N-Ph)$_2$: (N-Bn)(N-Ph) : (N-Bn)$_2$ = 0: 6 : 1** (by LCMS)	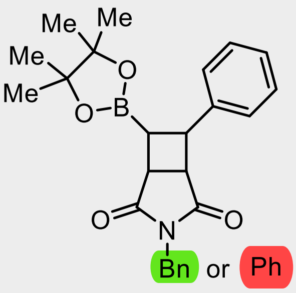 Conversion 100% **N-Ph : N-Bn = 10 : 1** (by ^{1}H NMR)	(–)

Plausible mechanism

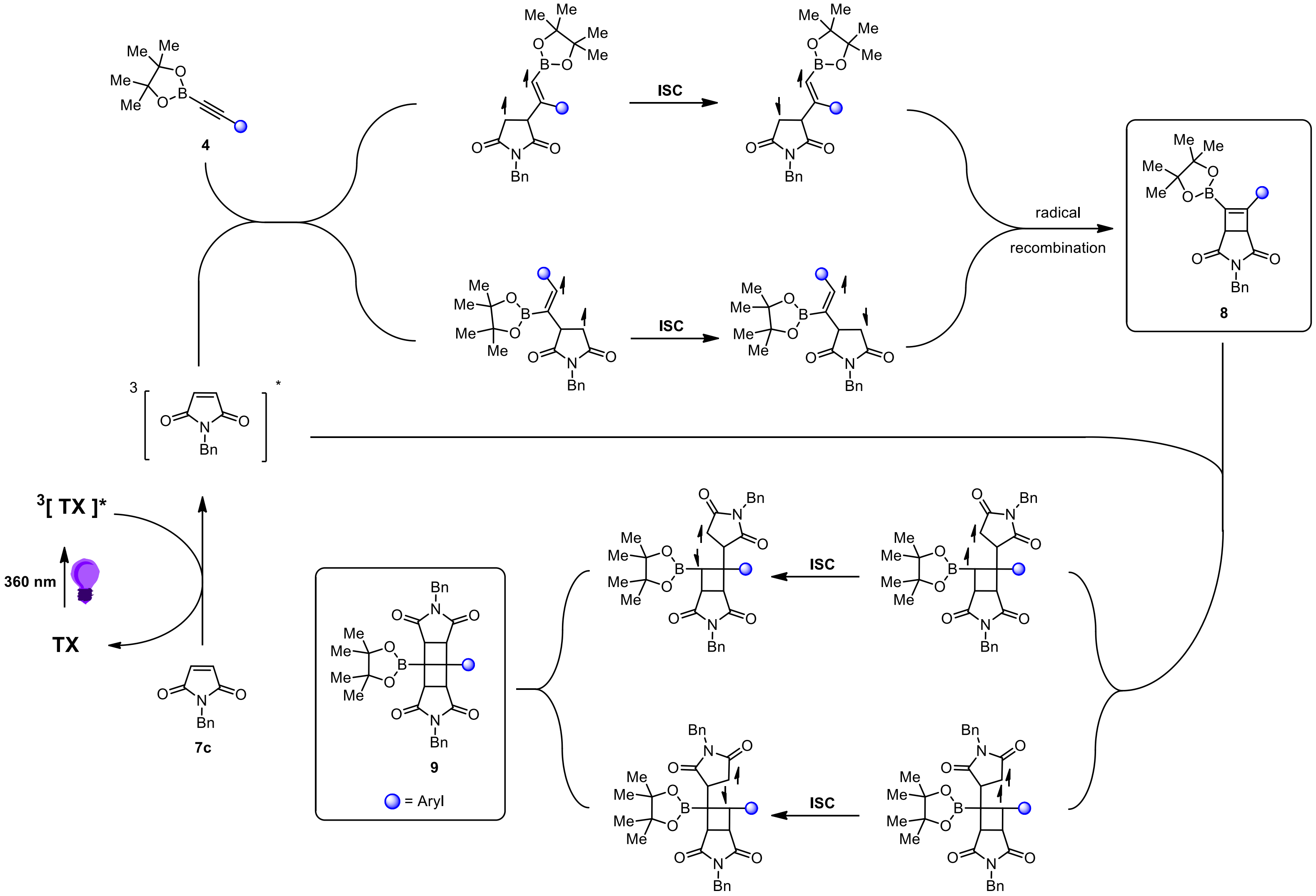

Scheme S9. Proposed general mechanism.

Spectra table

Copies of NMR spectra

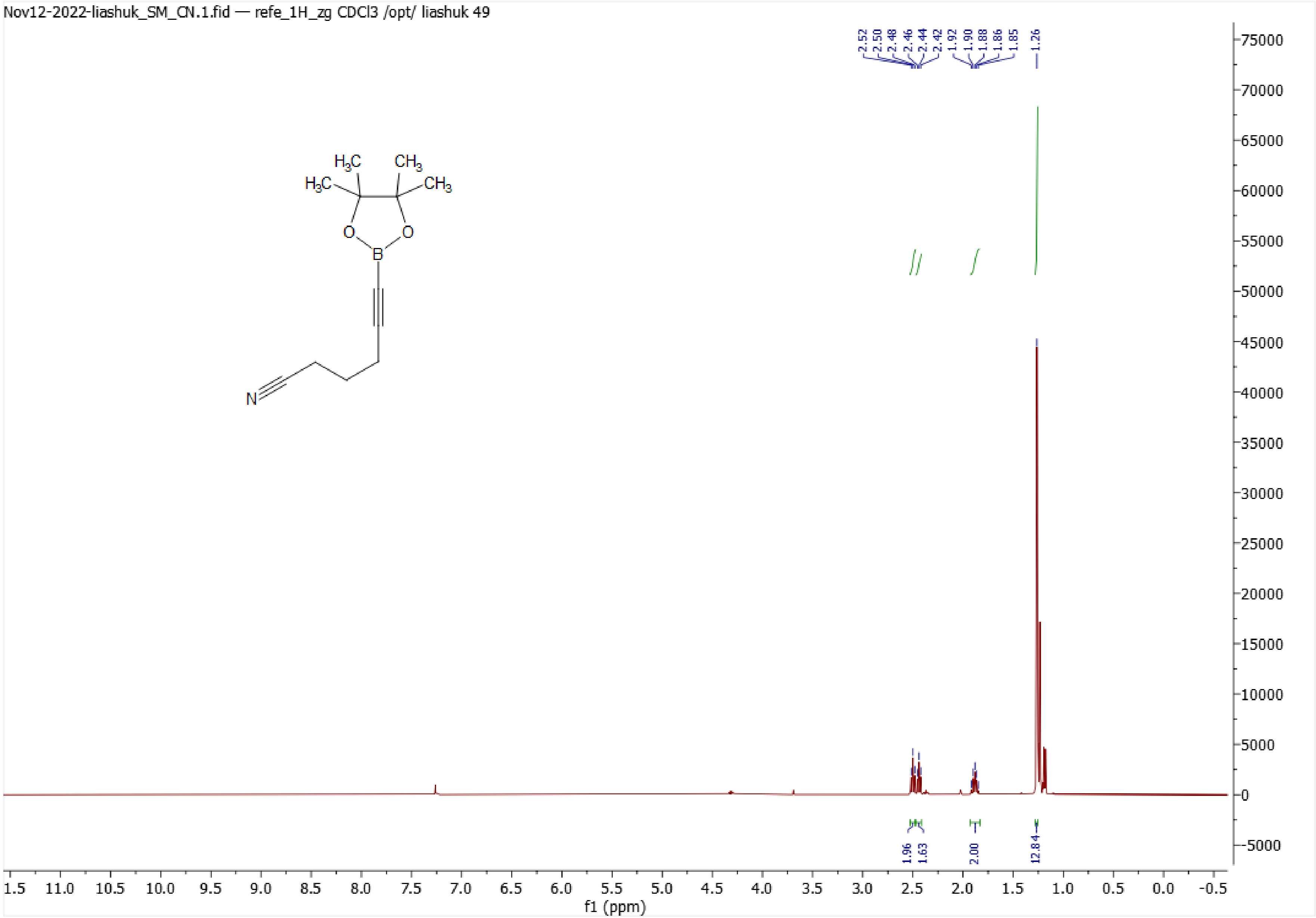

Spectrum 5. 6-(4,4,5,5-tetramethyl-1,3,2-dioxaborolan-2-yl)hex-5-ynenitrile ***4g****, ^{1}H NMR (400 MHz, $CDCl_3$)*

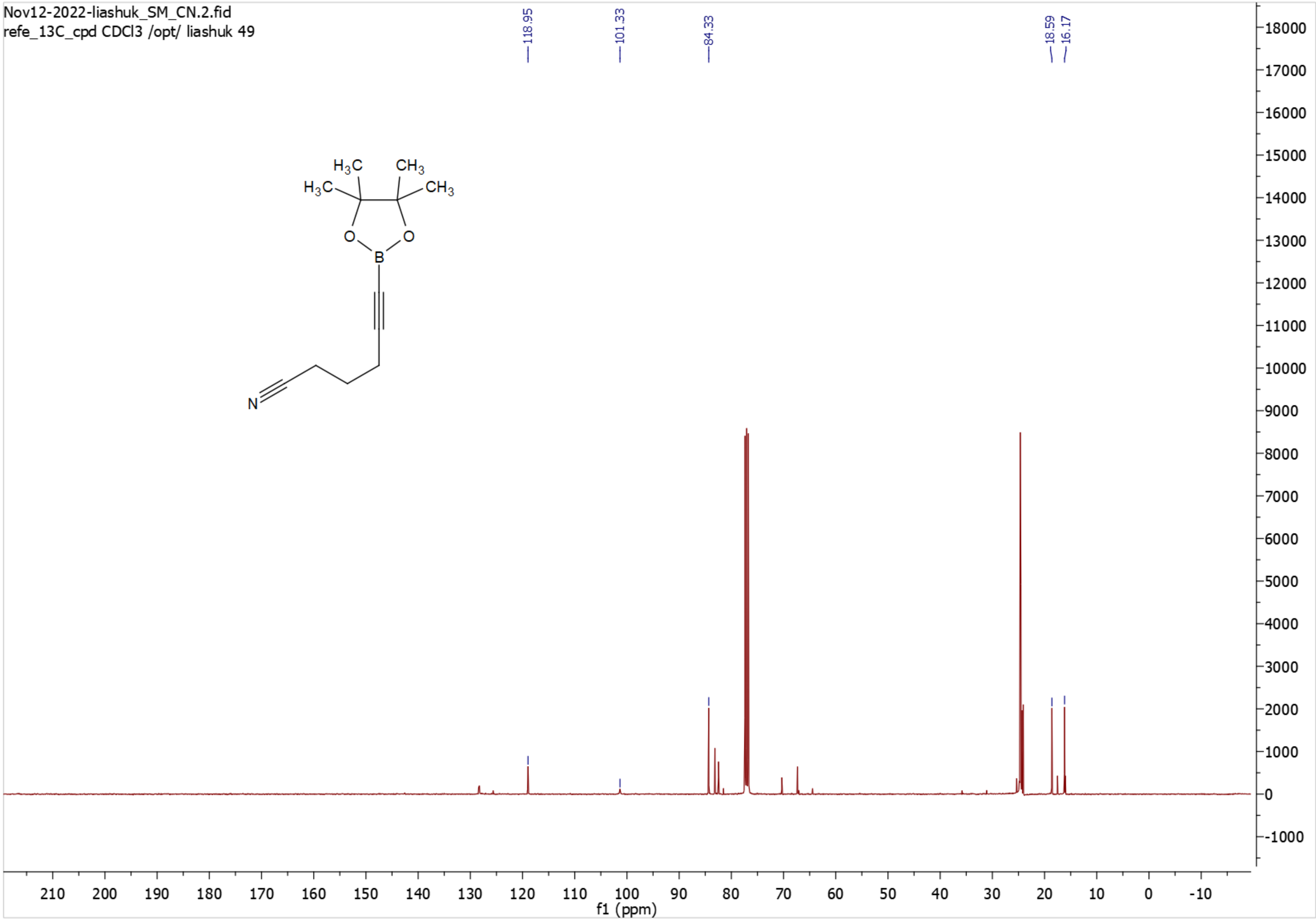

*Spectrum 6, 6-(4,4,5,5-tetramethyl-1,3,2-dioxaborolan-2-yl)hex-5-ynenitrile **4g**, ^{13}C NMR (101 MHz, CDCl$_3$)*

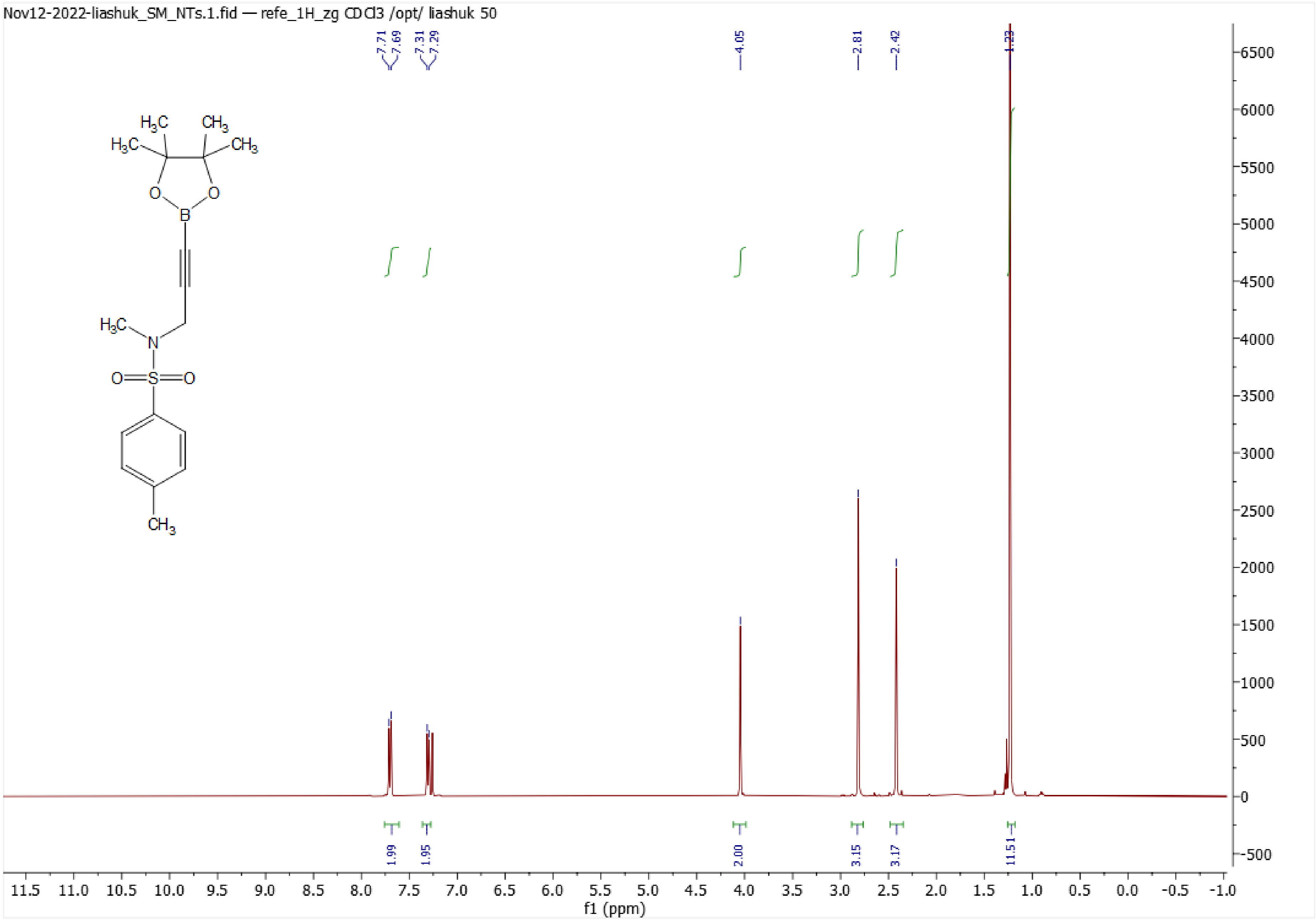

*Spectrum 7. N,4-dimethyl-N-(3-(4,4,5,5-tetramethyl-1,3,2-dioxaborolan-2-yl)prop-2-yn-1-yl)benzenesulfonamide **4i**, ^{1}H NMR (400 MHz, $CDCl_3$)*

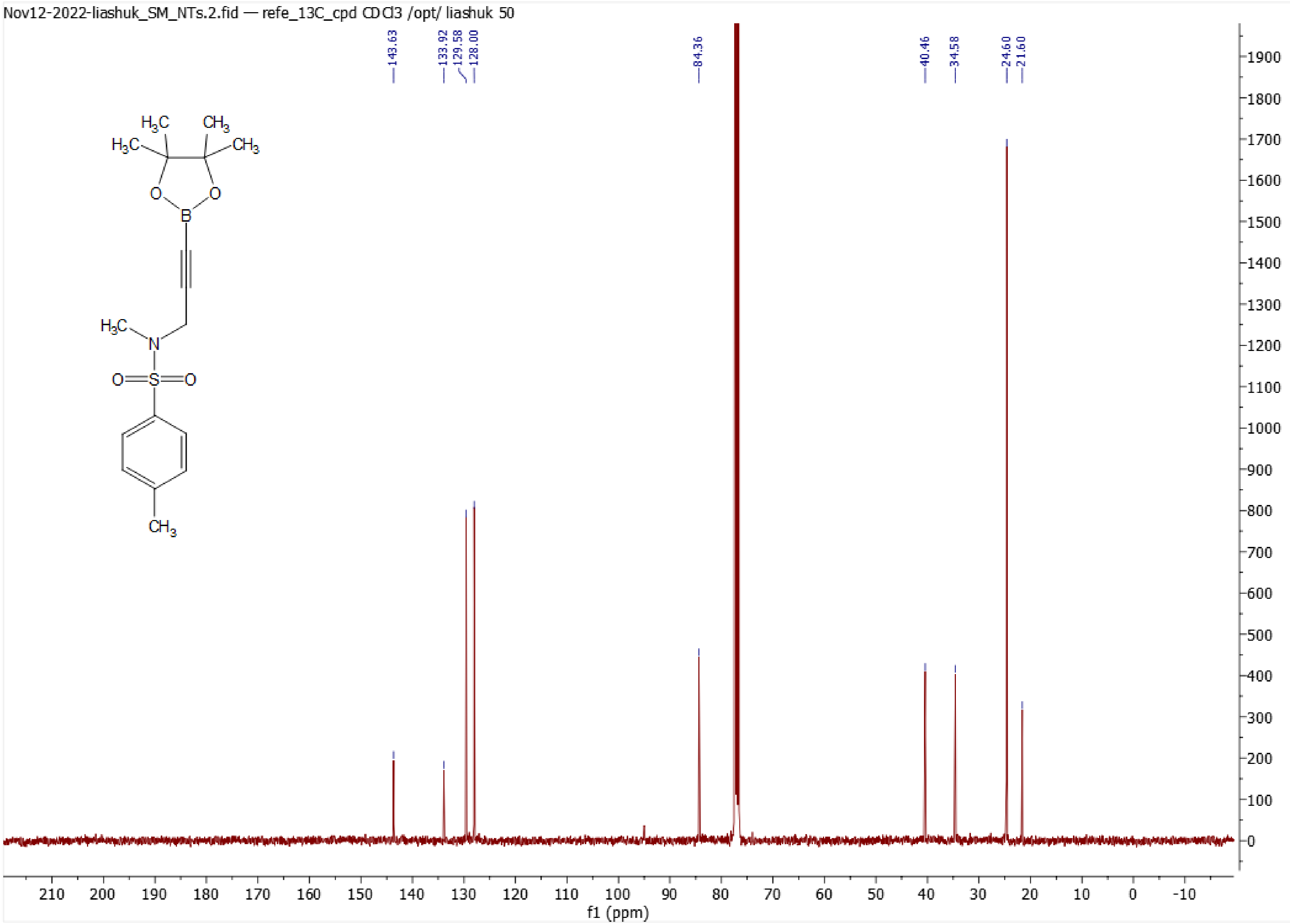

*Spectrum 8. N,4-dimethyl-N-(3-(4,4,5,5-tetramethyl-1,3,2-dioxaborolan-2-yl)prop-2-yn-1-yl)benzenesulfonamide **4i**, ^{13}C NMR (101 MHz, $CDCl_3$)*

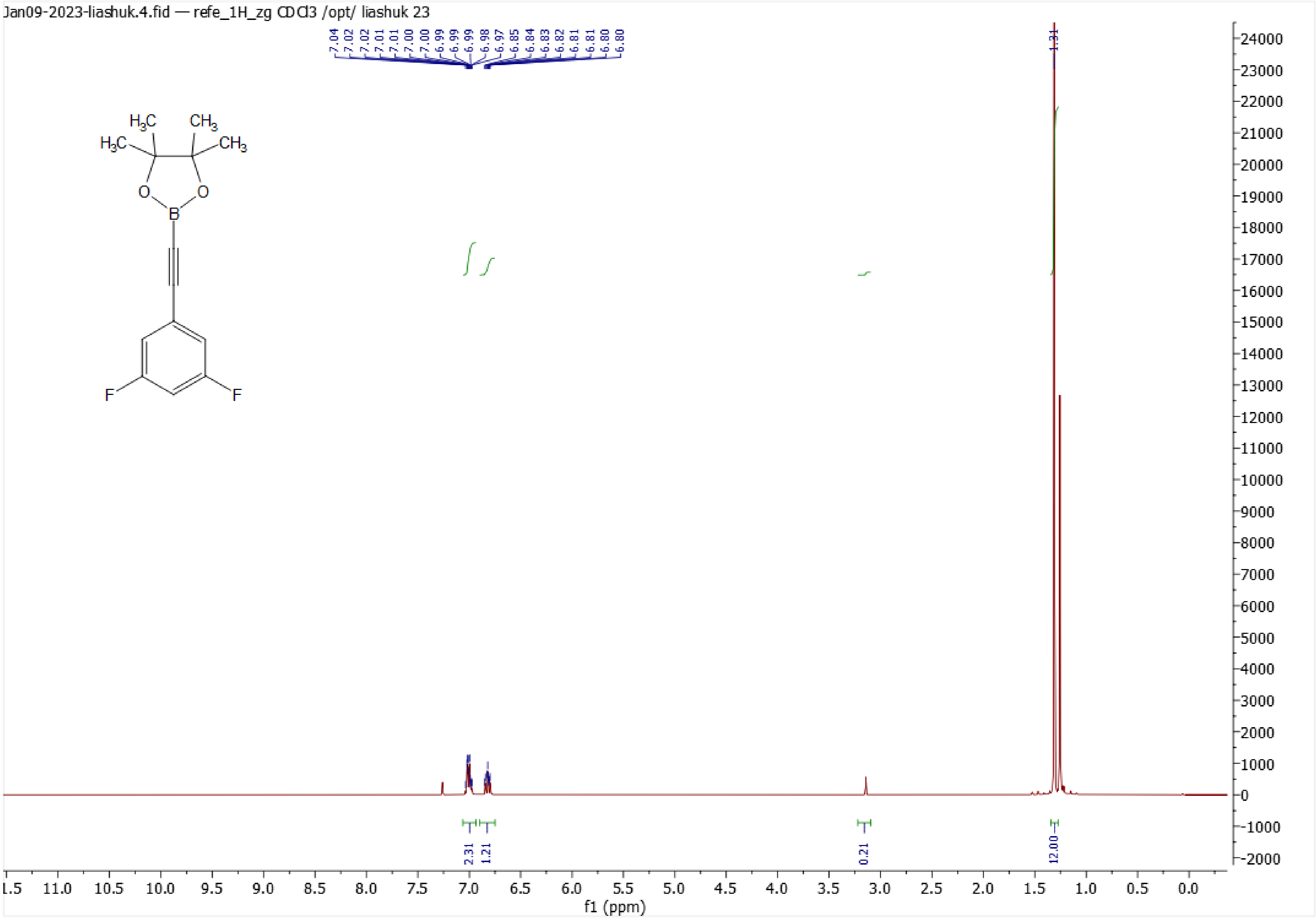

Spectrum 9. 2-((3,5-difluorophenyl)ethynyl)-4,4,5,5-tetramethyl-1,3,2-dioxaborolane ***4o****, ^{1}H NMR (400 MHz, CDCl$_3$)*

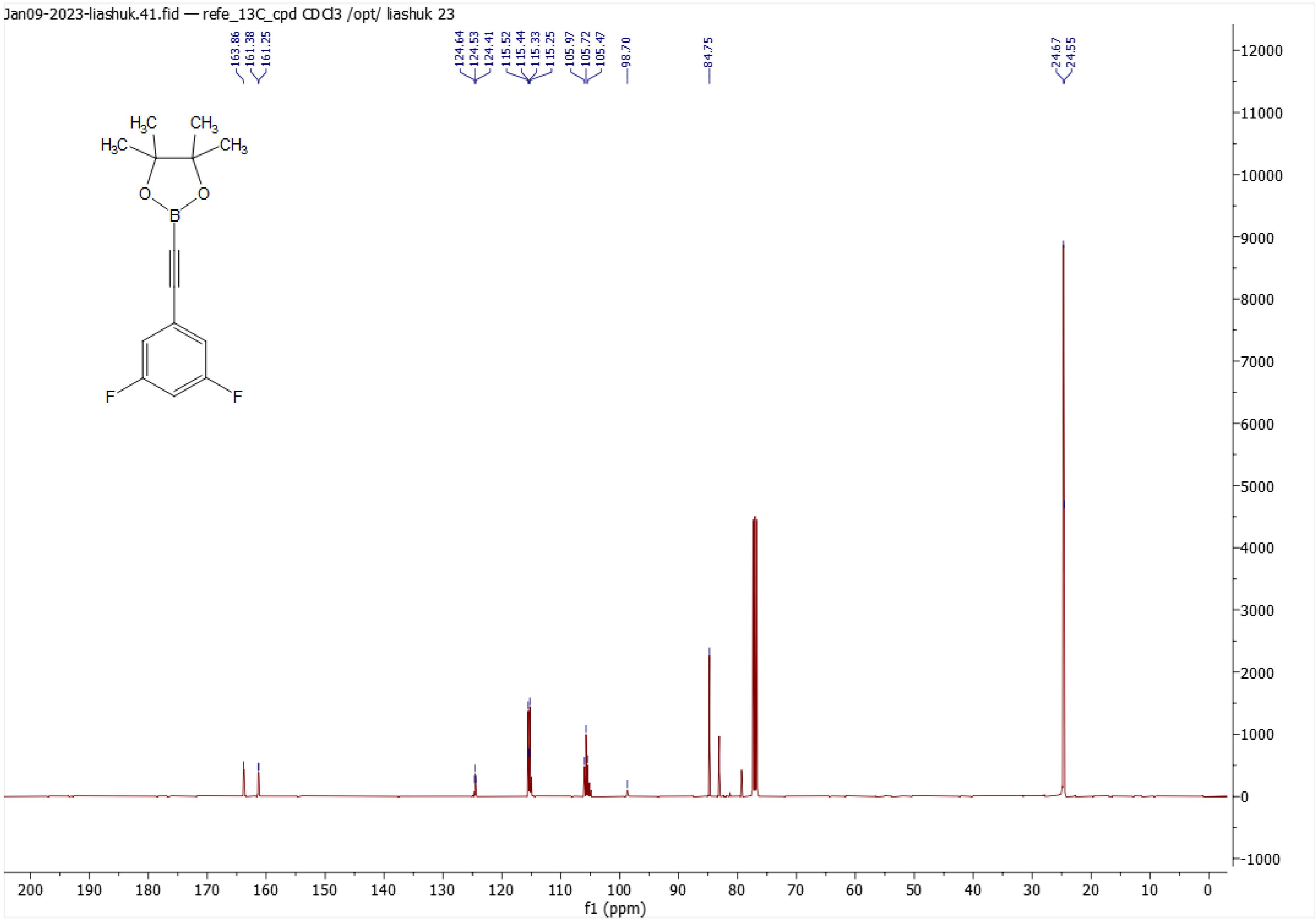

*Spectrum 10. 2-((3,5-difluorophenyl)ethynyl)-4,4,5,5-tetramethyl-1,3,2-dioxaborolane **4o**, ^{13}C NMR (101 MHz, CDCl$_3$)*

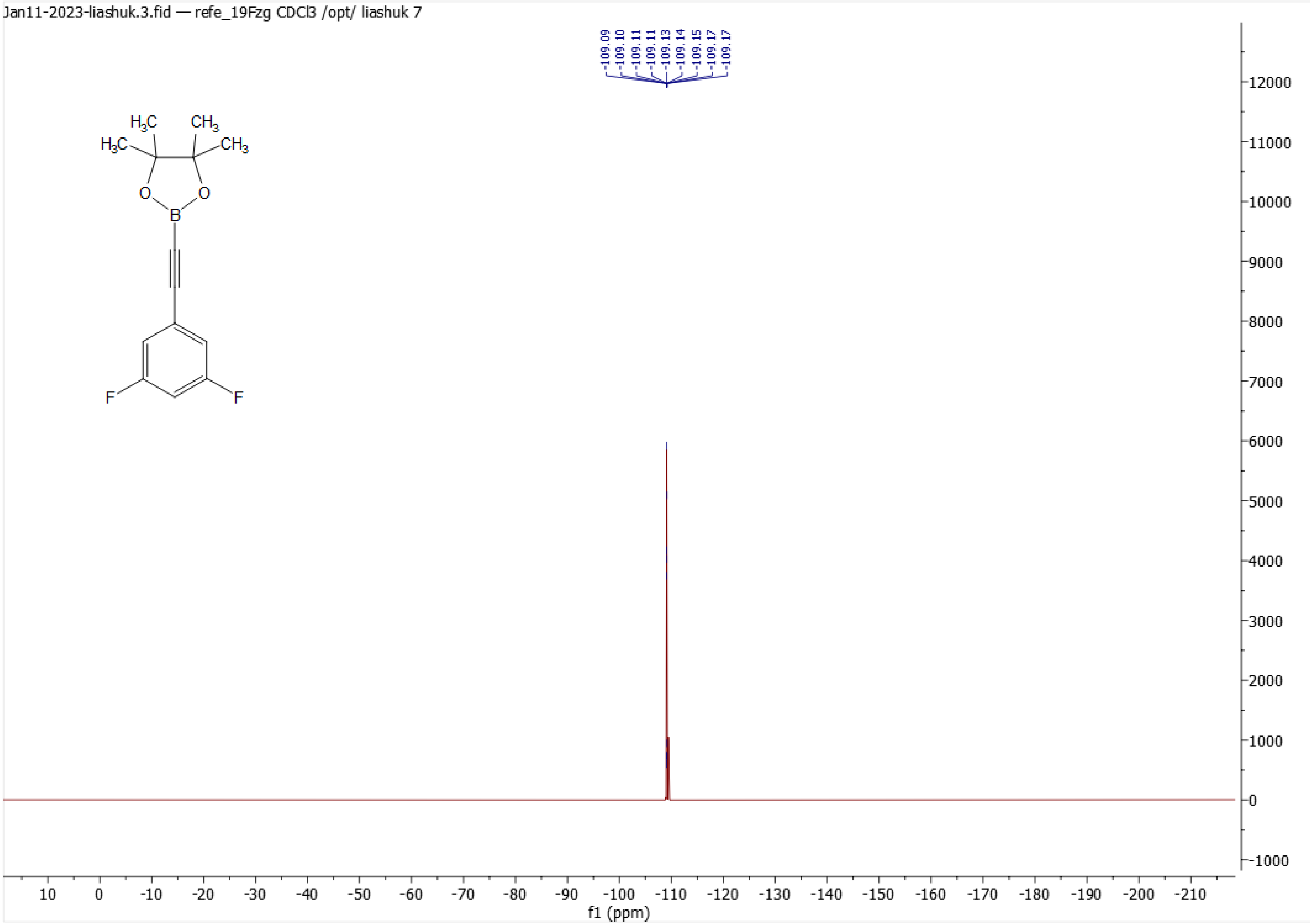

Spectrum 11. 2-((3,5-difluorophenyl)ethynyl)-4,4,5,5-tetramethyl-1,3,2-dioxaborolane ***4o****, ^{19}F NMR (376 MHz, CDCl$_3$)*

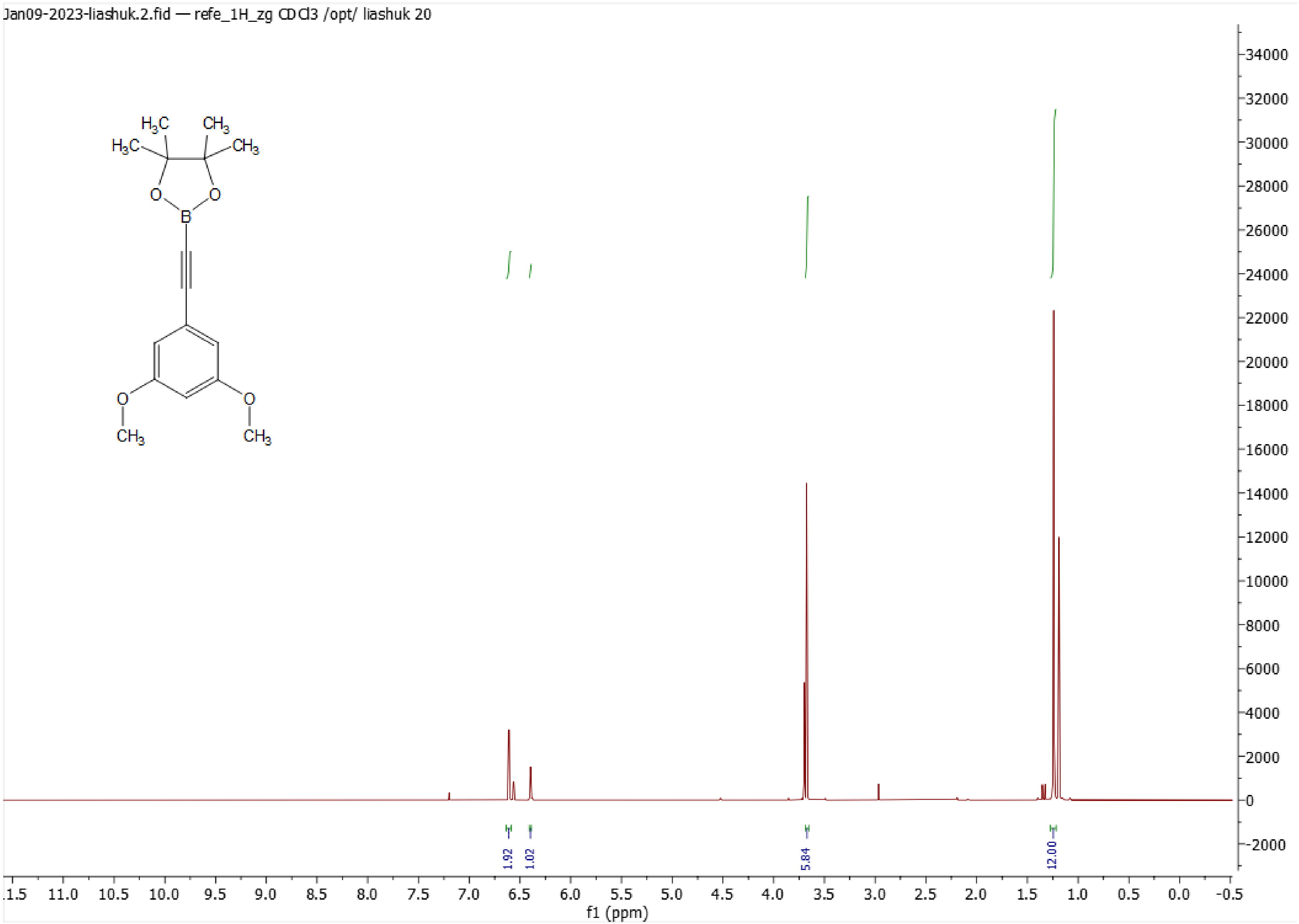

Spectrum 12. 2-((3,5-dimethoxyphenyl)ethynyl)-4,4,5,5-tetramethyl-1,3,2-dioxaborolane ***4q****, ^{1}H NMR (400 MHz, $CDCl_3$)*

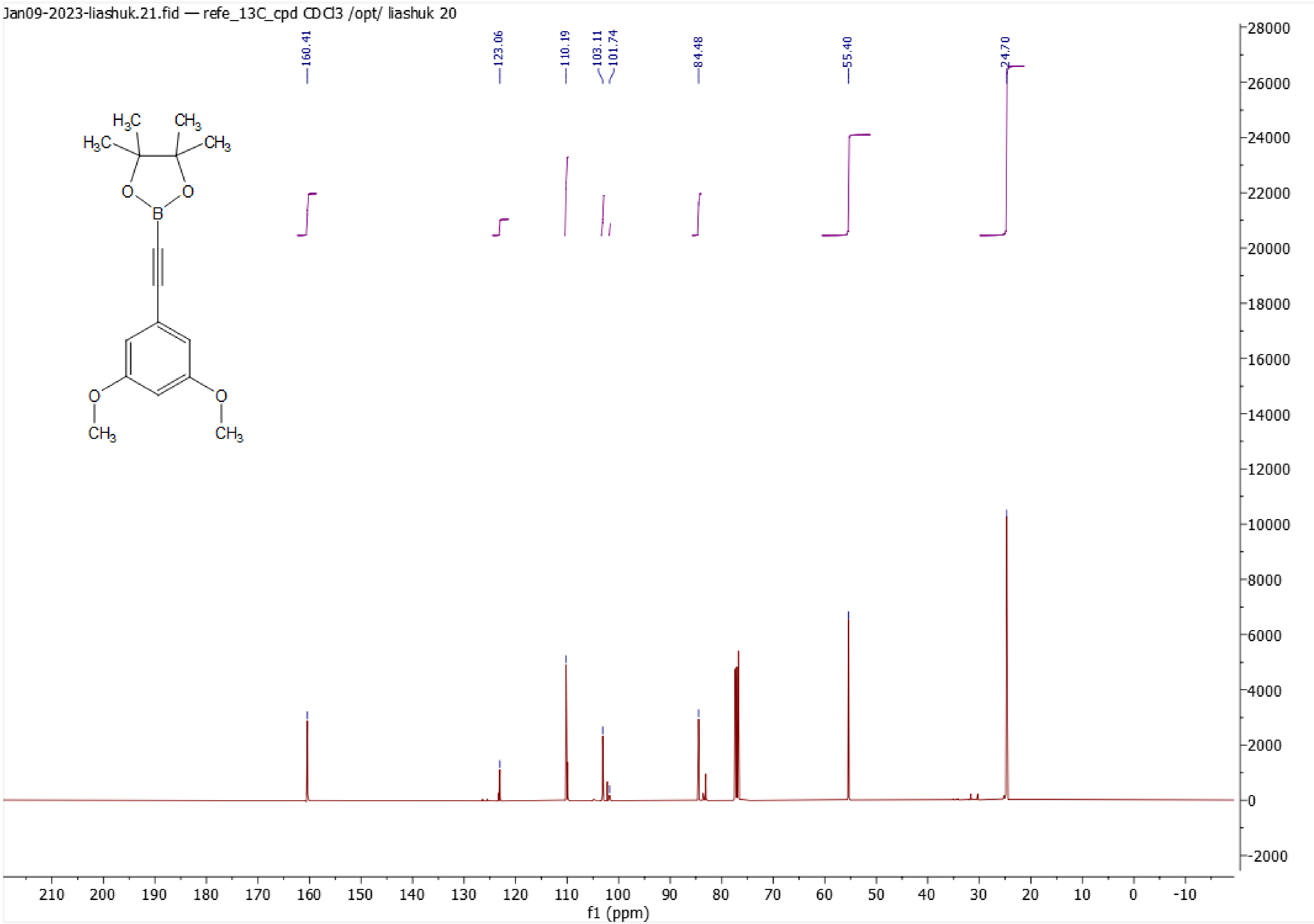

Spectrum 13. 2-((3,5-dimethoxyphenyl)ethynyl)-4,4,5,5-tetramethyl-1,3,2-dioxaborolane ***4q****, ^{13}C NMR (101 MHz, $CDCl_3$)*

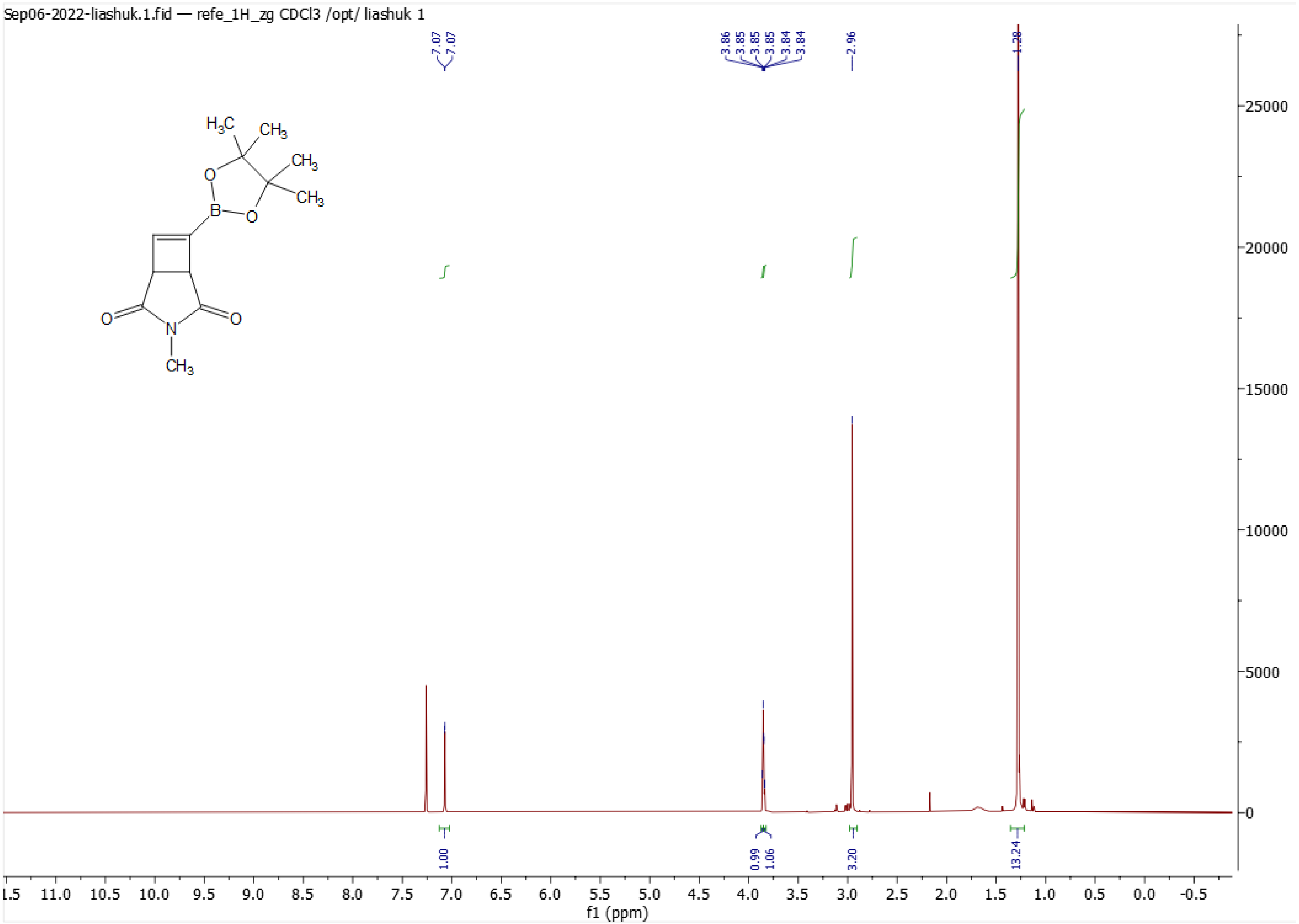

*Spectrum 14. 3-methyl-6-(4,4,5,5-tetramethyl-1,3,2-dioxaborolan-2-yl)-3-azabicyclo[3.2.0]hept-6-ene-2,4-dione **8a**, ^{1}H NMR (400 MHz, $CDCl_3$)*

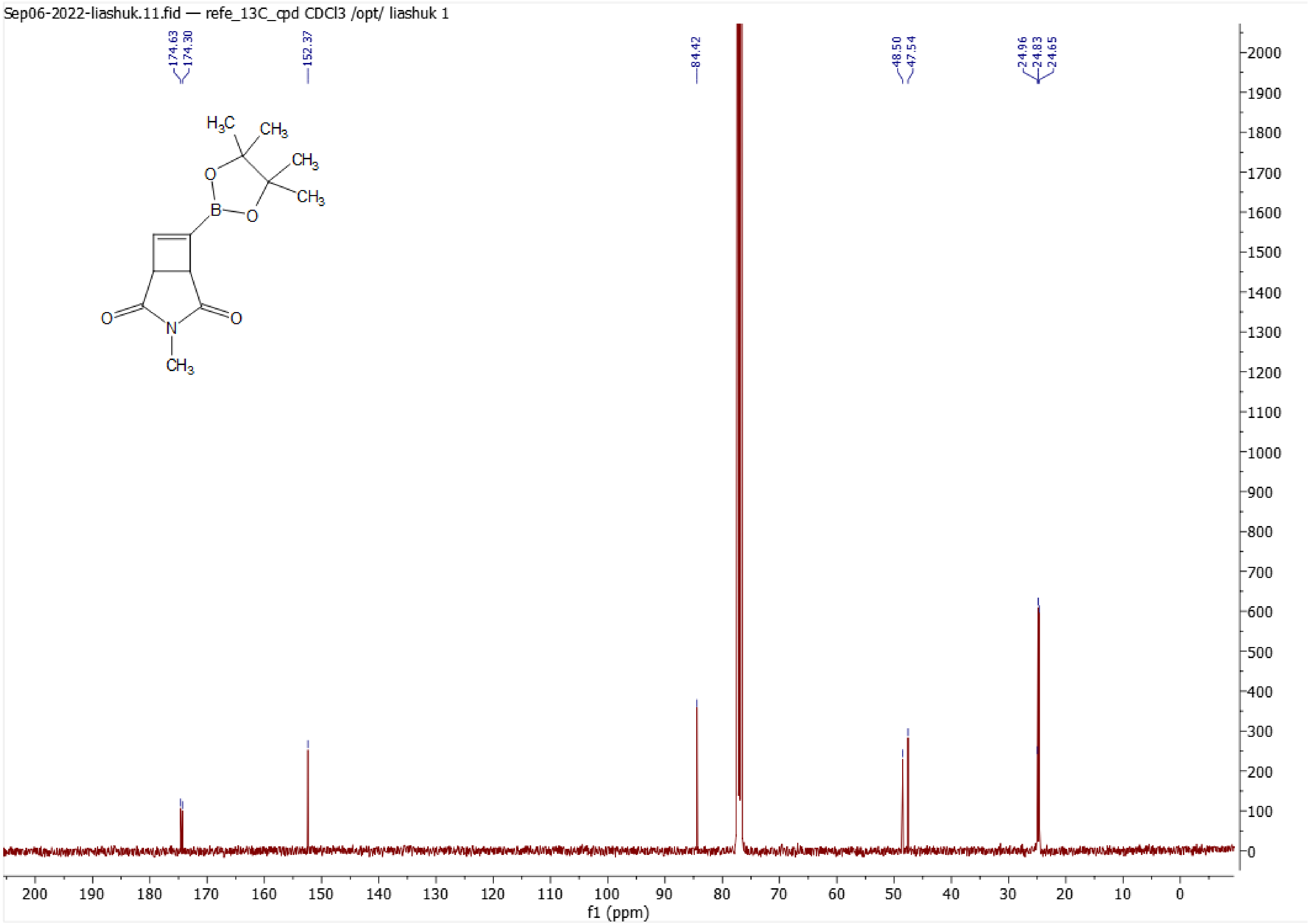

Spectrum 15. 3-methyl-6-(4,4,5,5-tetramethyl-1,3,2-dioxaborolan-2-yl)-3-azabicyclo[3.2.0]hept-6-ene-2,4-dione ***8a****, ^{13}C NMR (101 MHz, CDCl$_3$)*

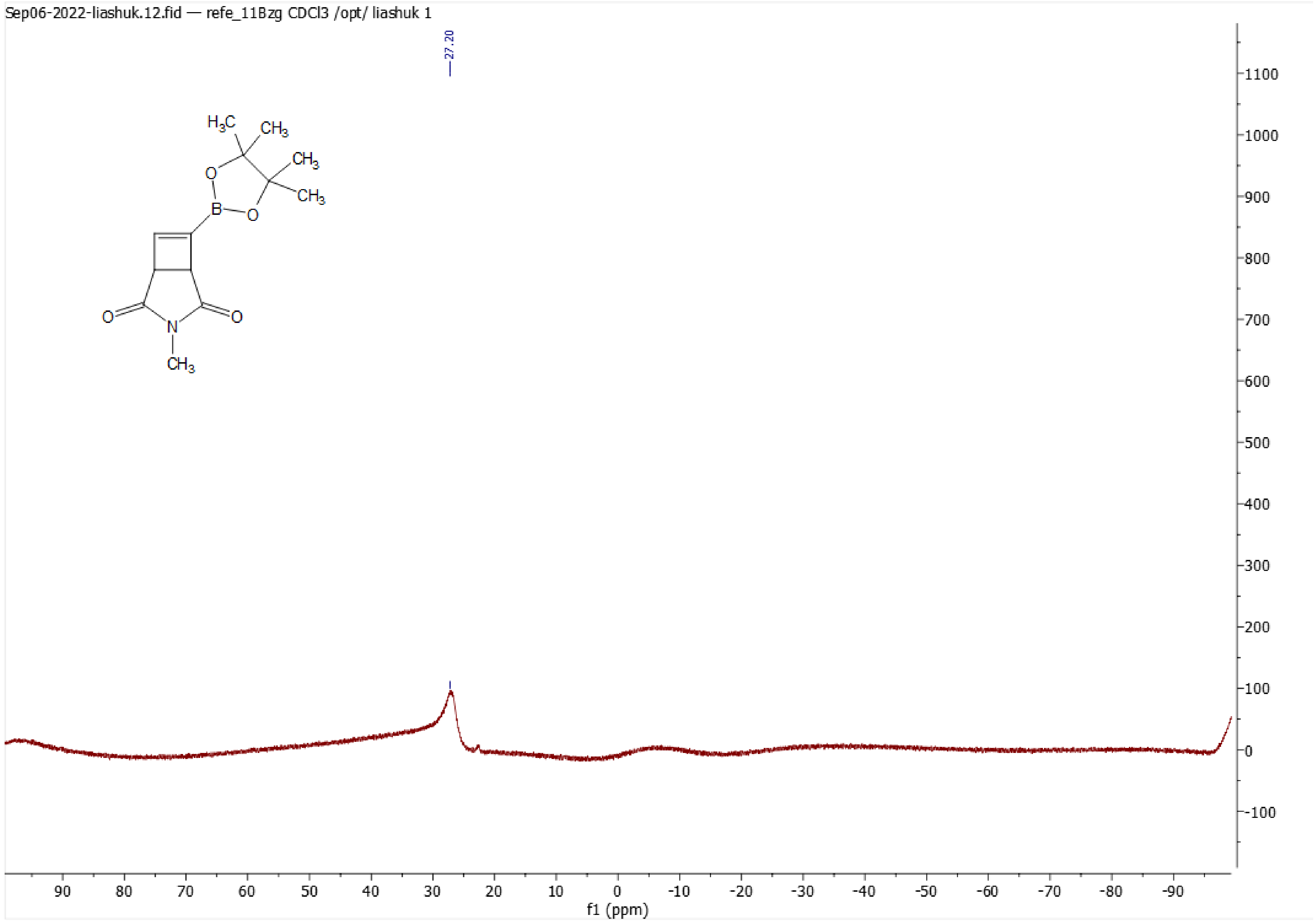

Spectrum 16. 3-methyl-6-(4,4,5,5-tetramethyl-1,3,2-dioxaborolan-2-yl)-3-azabicyclo[3.2.0]hept-6-ene-2,4-dione ***8a****, ^{11}B NMR (128 MHz, CDCl$_3$)*

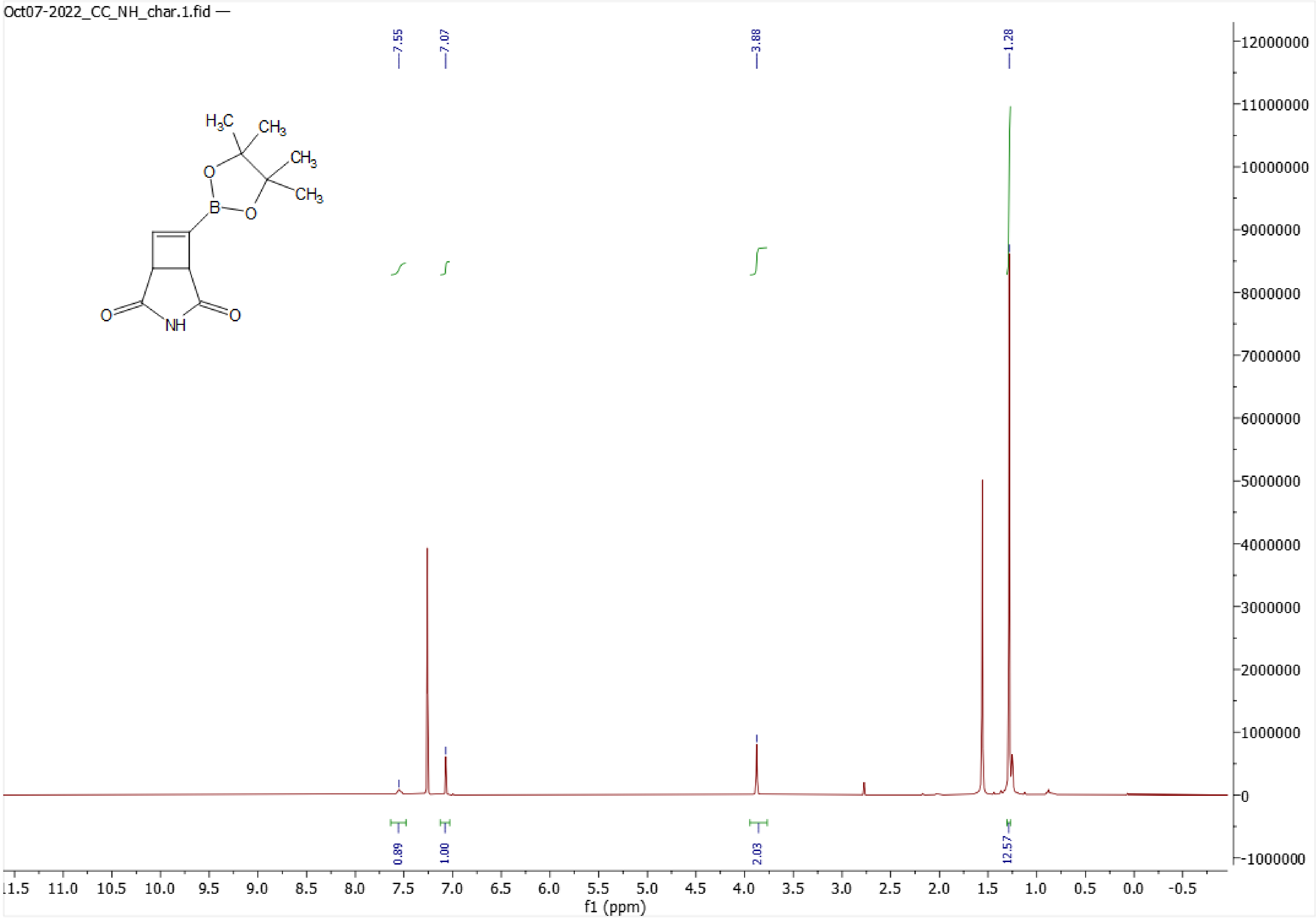

Spectrum 17. 6-(4,4,5,5-tetramethyl-1,3,2-dioxaborolan-2-yl)-3-azabicyclo[3.2.0]hept-6-ene-2,4-dione ***8b****,* ^{1}*H NMR (400 MHz,* $CDCl_3$*)*

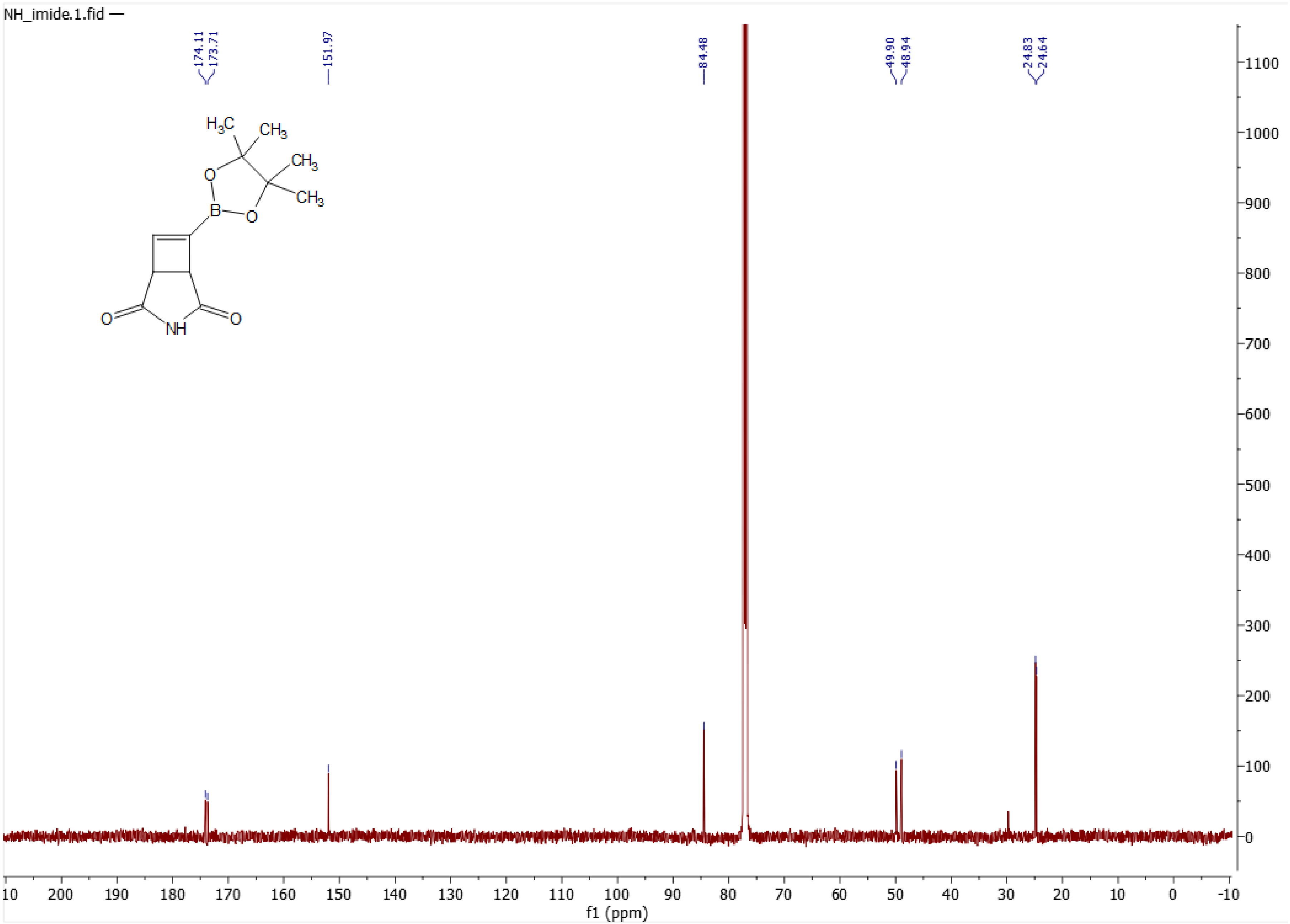

Spectrum 18. 6-(4,4,5,5-tetramethyl-1,3,2-dioxaborolan-2-yl)-3-azabicyclo[3.2.0]hept-6-ene-2,4-dione ***8b****,* ^{13}*C NMR (151 MHz, CDCl*$_3$*)*

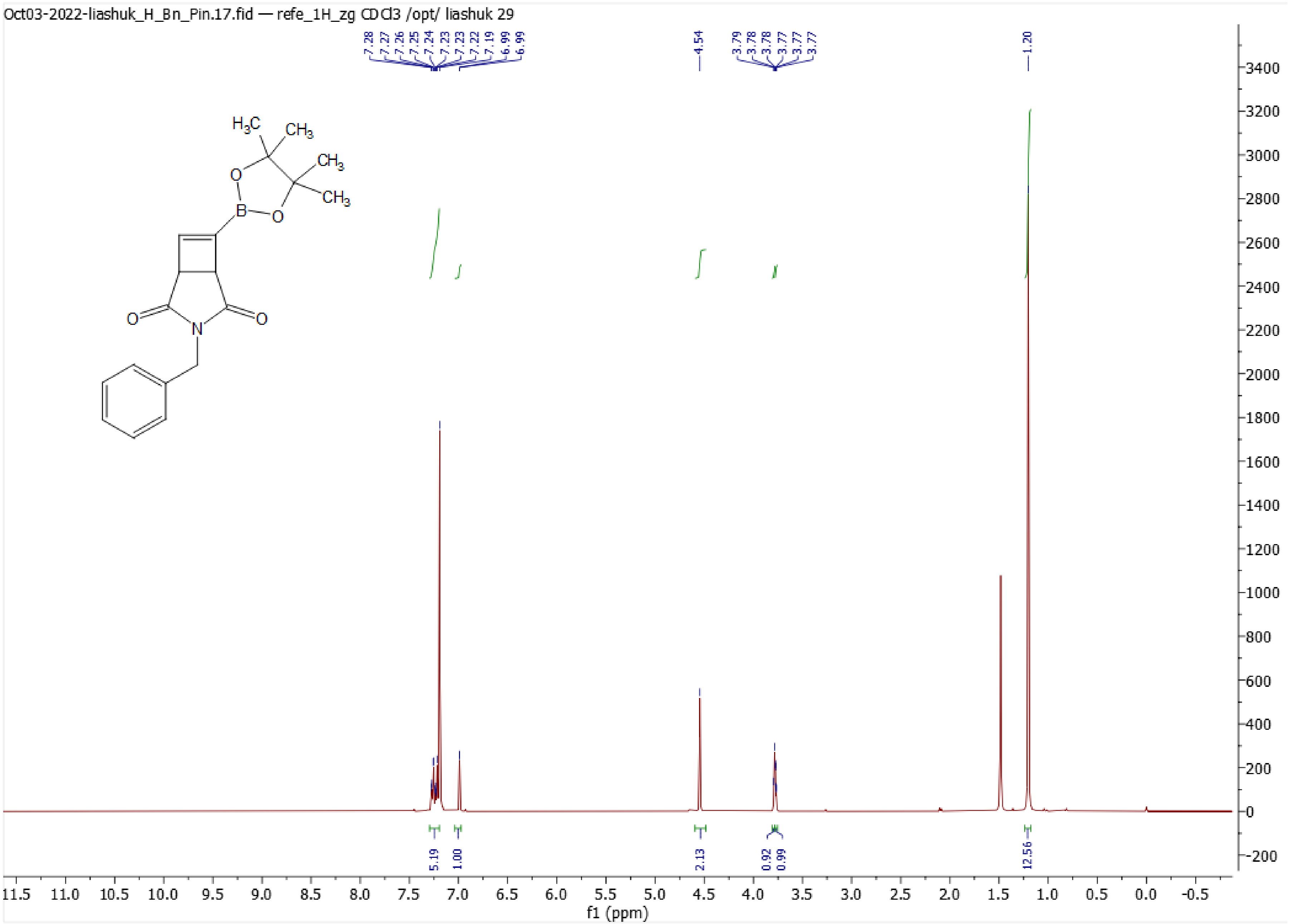

Spectrum 19. 3-benzyl-6-(4,4,5,5-tetramethyl-1,3,2-dioxaborolan-2-yl)-3-azabicyclo[3.2.0]hept-6-ene-2,4-dione ***8c****, ^{1}H NMR (400 MHz, CDCl$_3$)*

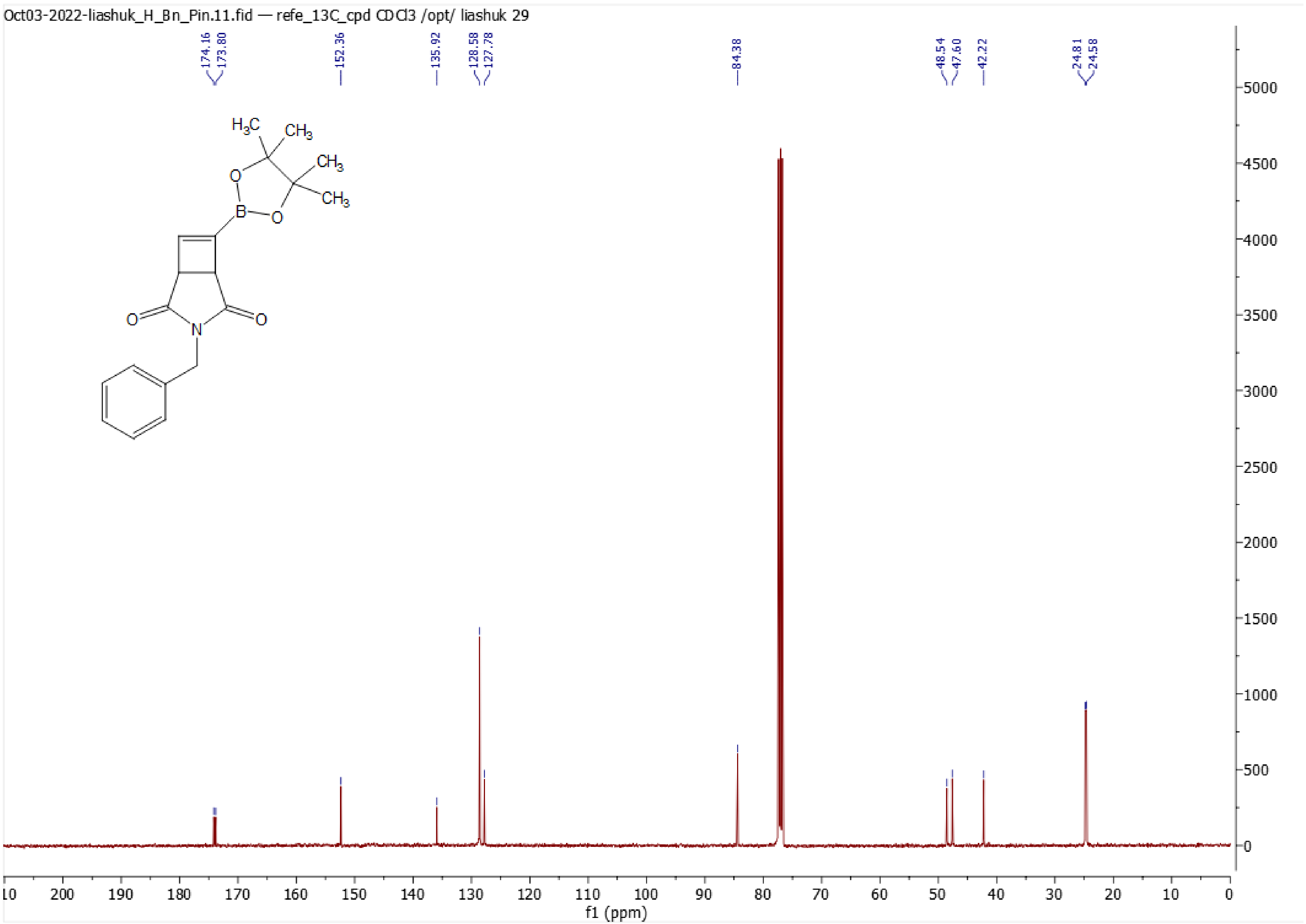

Spectrum 20. 3-benzyl-6-(4,4,5,5-tetramethyl-1,3,2-dioxaborolan-2-yl)-3-azabicyclo[3.2.0]hept-6-ene-2,4-dione ***8c****, ^{13}C NMR (101 MHz, CDCl$_3$)*

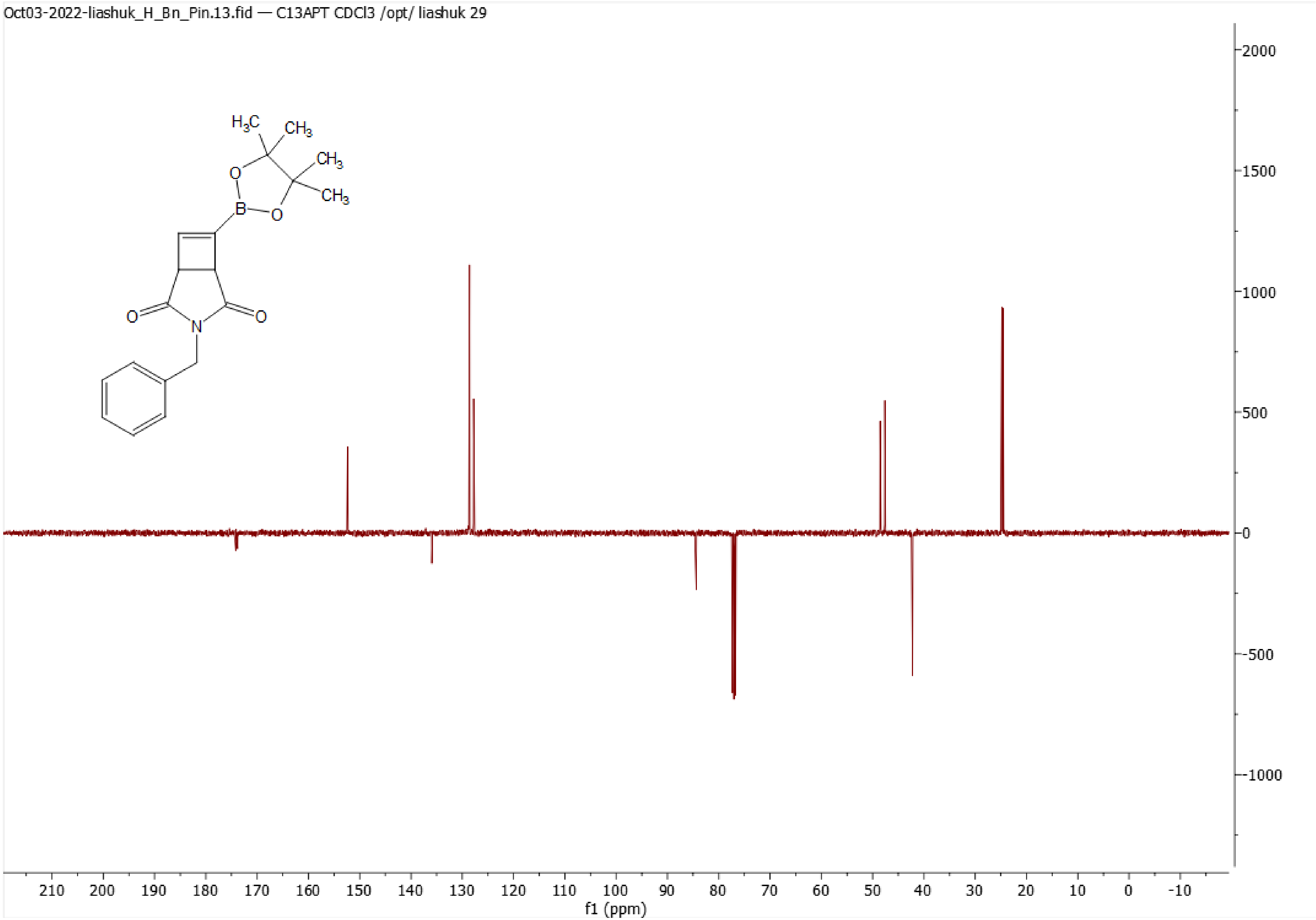

*Spectrum 21. 3-benzyl-6-(4,4,5,5-tetramethyl-1,3,2-dioxaborolan-2-yl)-3-azabicyclo[3.2.0]hept-6-ene-2,4-dione **8c**, ^{13}C APT (101 MHz, $CDCl_3$)*

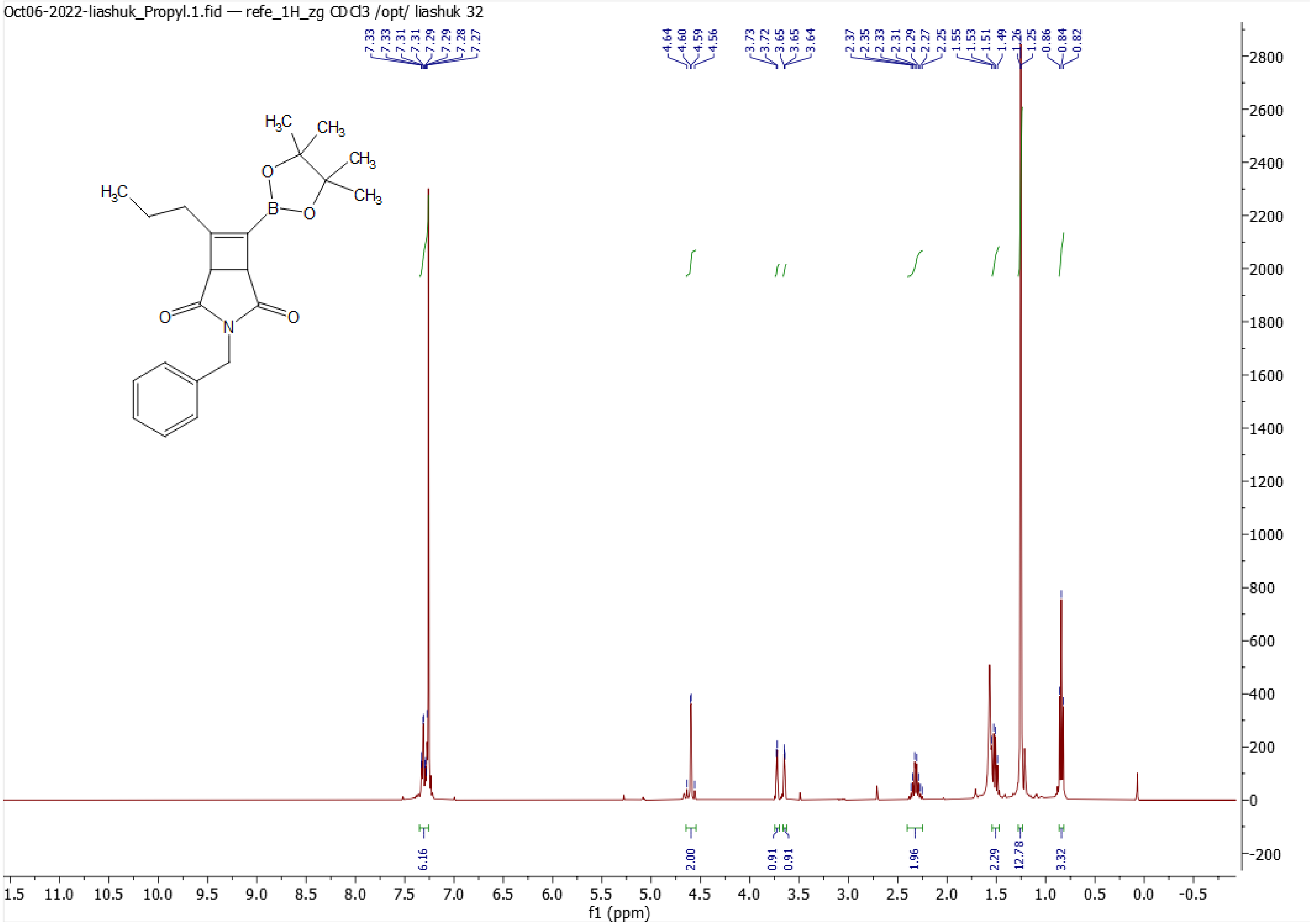

*Spectrum 22. 3-benzyl-6-propyl-7-(4,4,5,5-tetramethyl-1,3,2-dioxaborolan-2-yl)-3-azabicyclo[3.2.0]hept-6-ene-2,4-dione **8ca**, ^{1}H NMR (400 MHz, $CDCl_3$)*

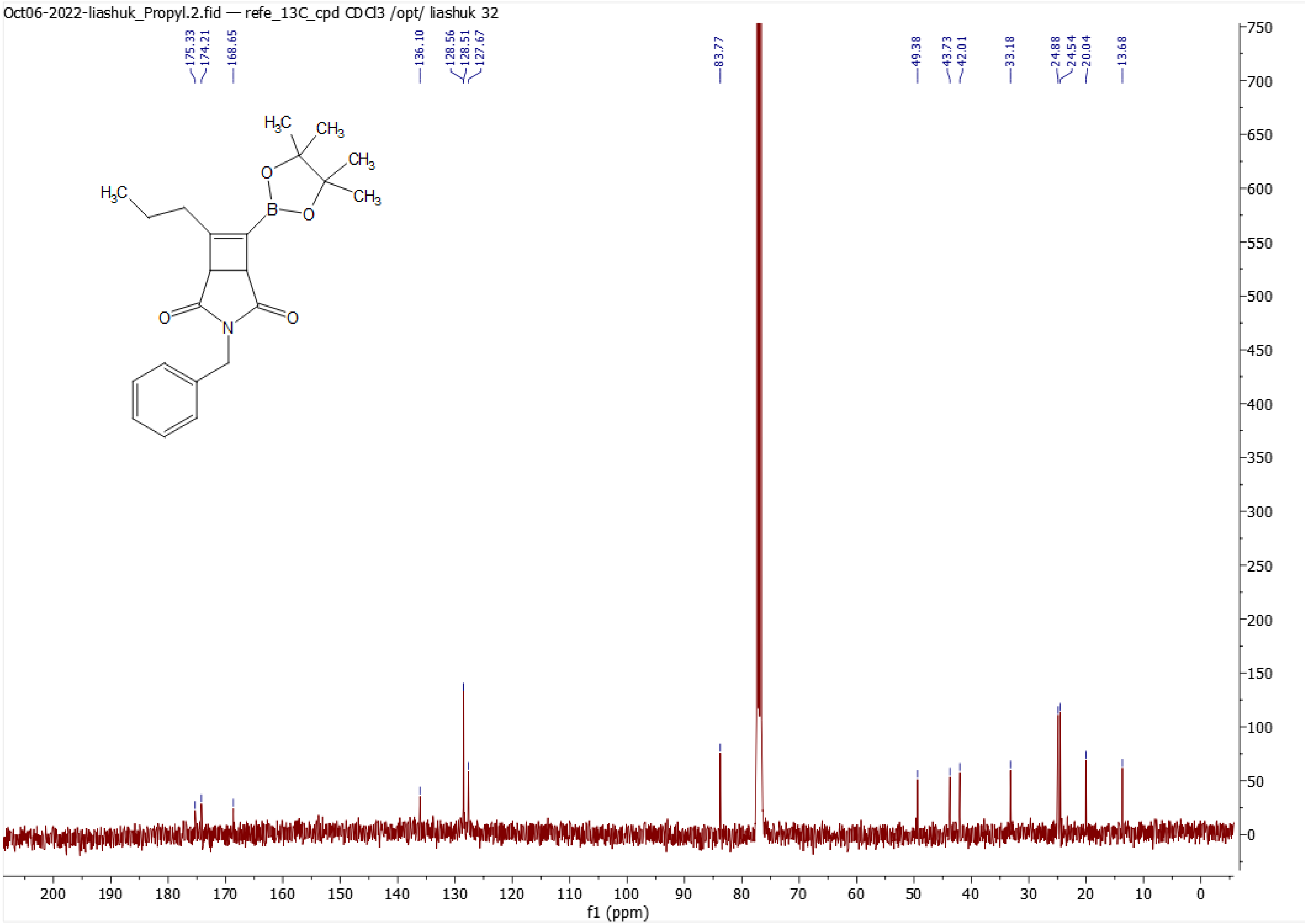

Spectrum 23. 3-benzyl-6-propyl-7-(4,4,5,5-tetramethyl-1,3,2-dioxaborolan-2-yl)-3-azabicyclo[3.2.0]hept-6-ene-2,4-dione ***8ca****, ^{13}C NMR (101 MHz, CDCl$_3$)*

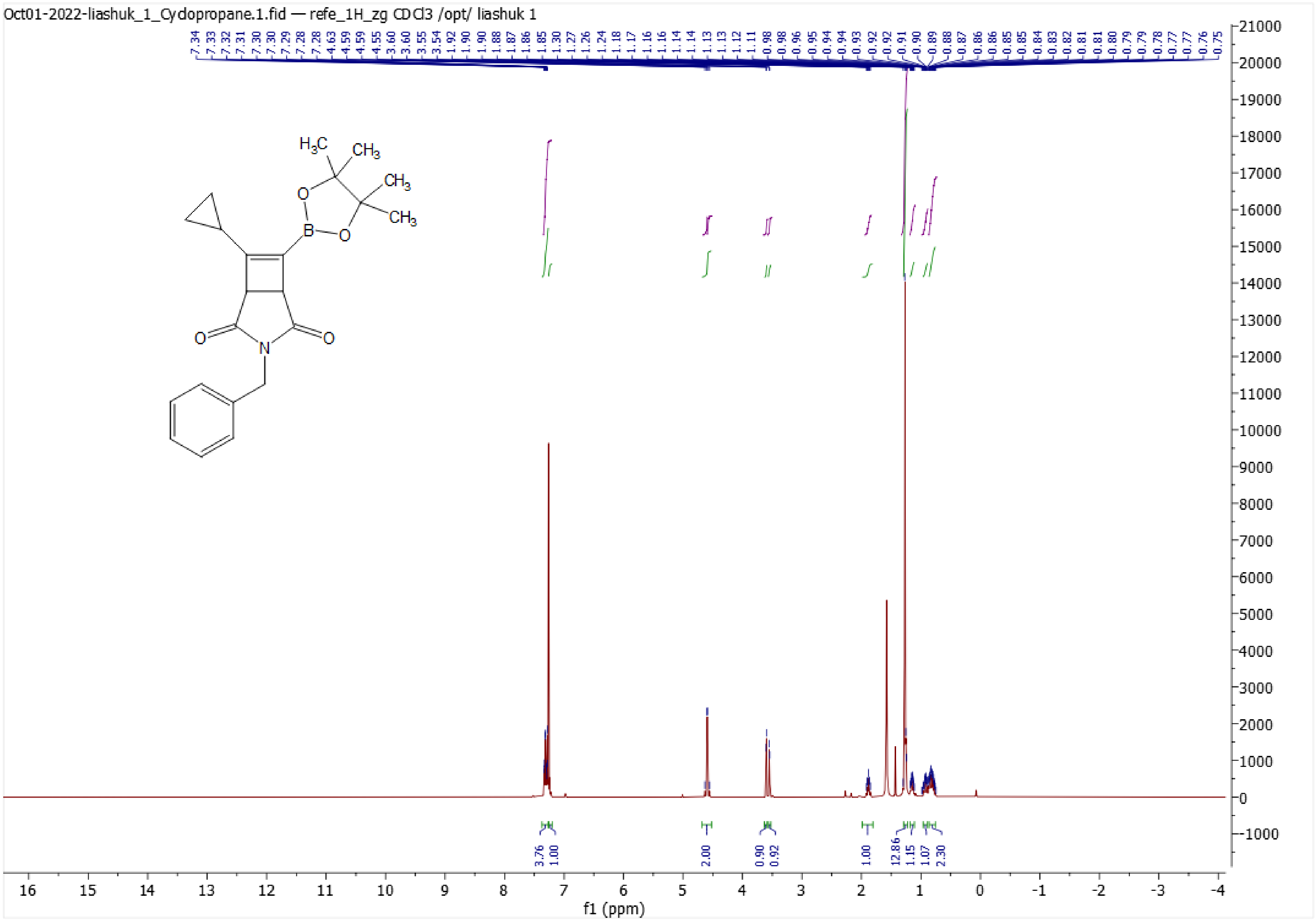

Spectrum 24. 3-benzyl-6-cyclopropyl-7-(4,4,5,5-tetramethyl-1,3,2-dioxaborolan-2-yl)-3-azabicyclo[3.2.0]hept-6-ene-2,4-dione ***8cb***, *^{1}H NMR (400 MHz, $CDCl_3$)*

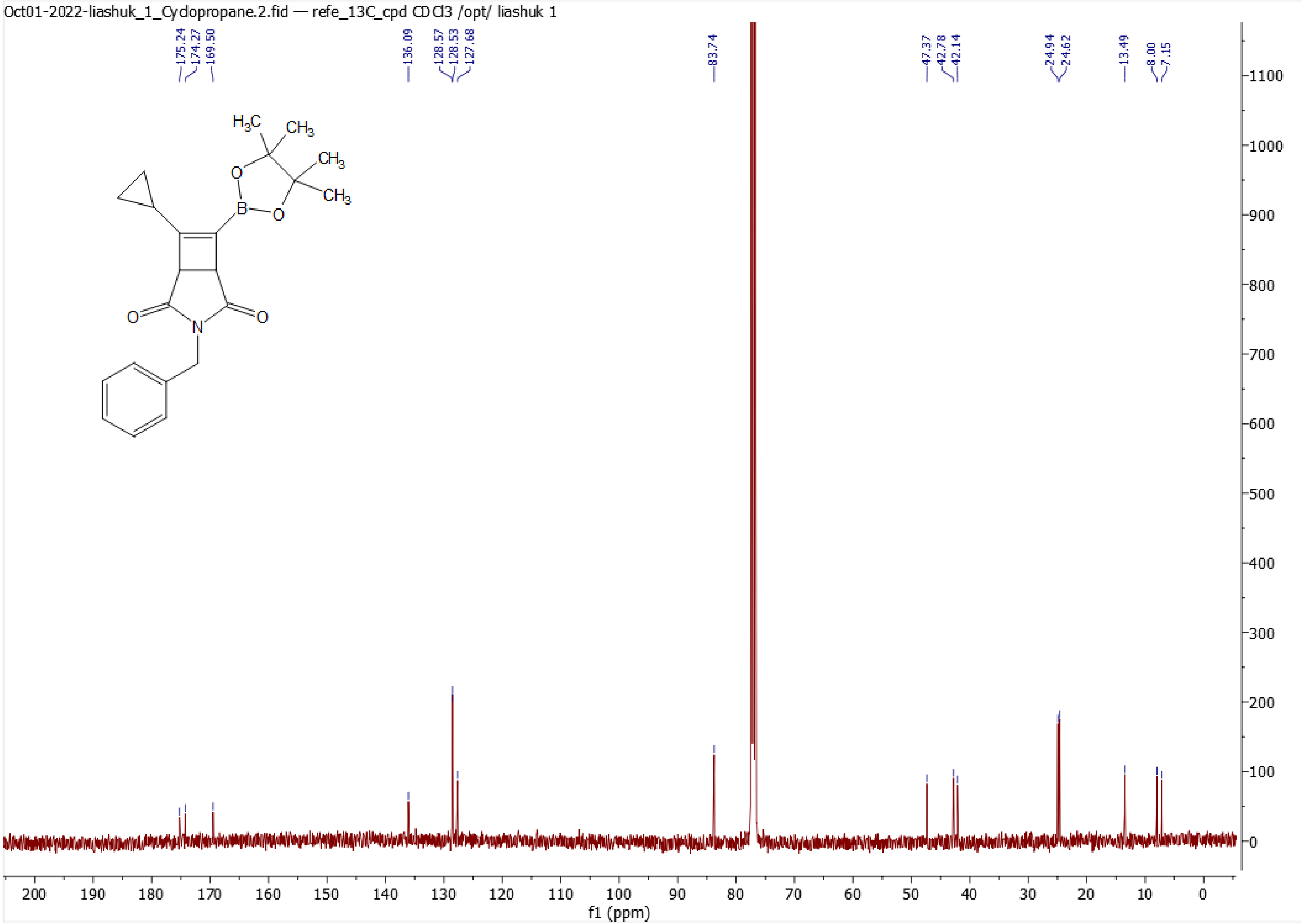

*Spectrum 25. 3-benzyl-6-cyclopropyl-7-(4,4,5,5-tetramethyl-1,3,2-dioxaborolan-2-yl)-3-azabicyclo[3.2.0]hept-6-ene-2,4-dione **8cb**, ^{13}C NMR (101 MHz, $CDCl_3$)*

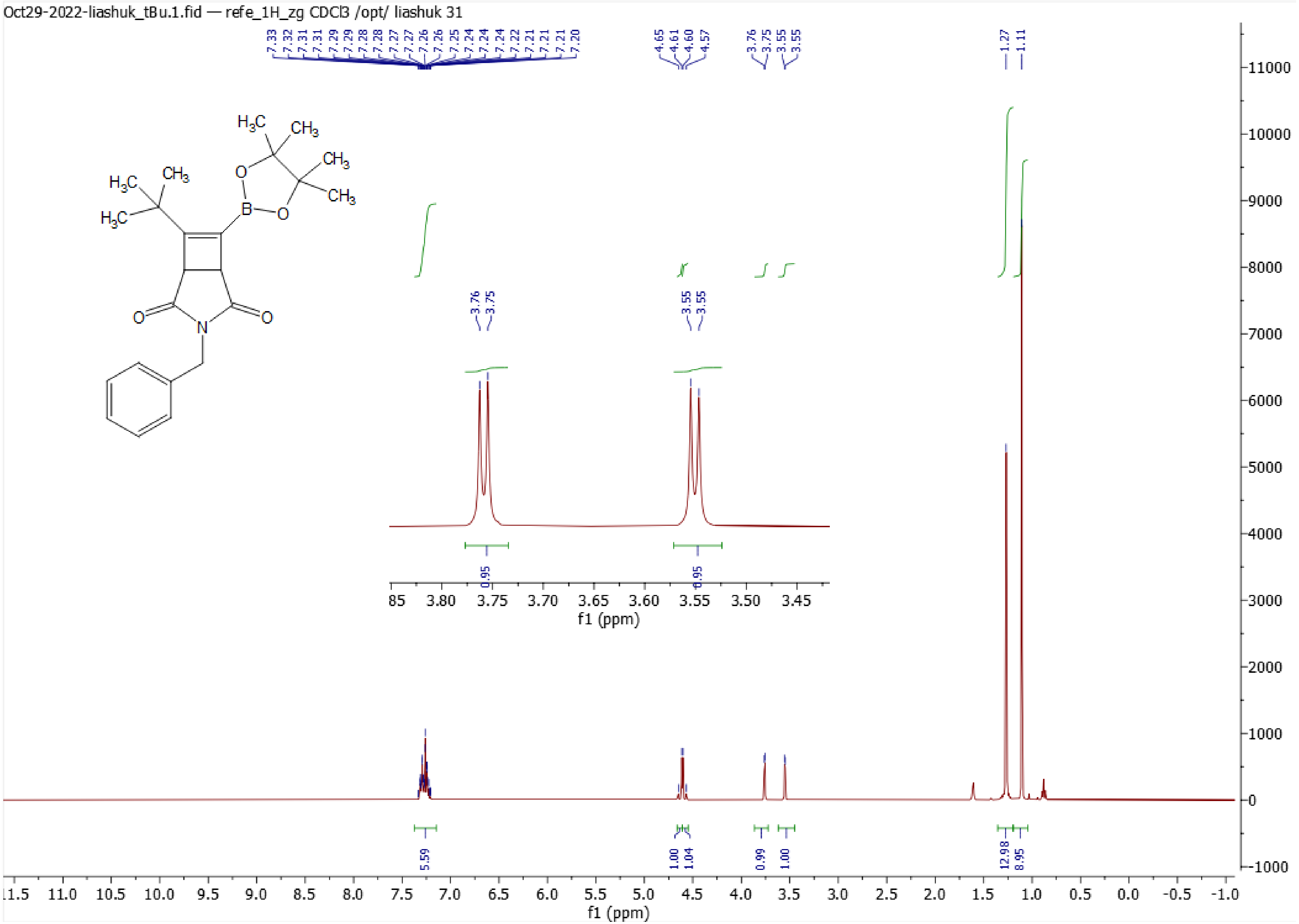

Spectrum 26. 3-benzyl-6-(tert-butyl)-7-(4,4,5,5-tetramethyl-1,3,2-dioxaborolan-2-yl)-3-azabicyclo[3.2.0]hept-6-ene-2,4-dione ***8cc****, ^{1}H NMR (400 MHz, $CDCl_3$)*

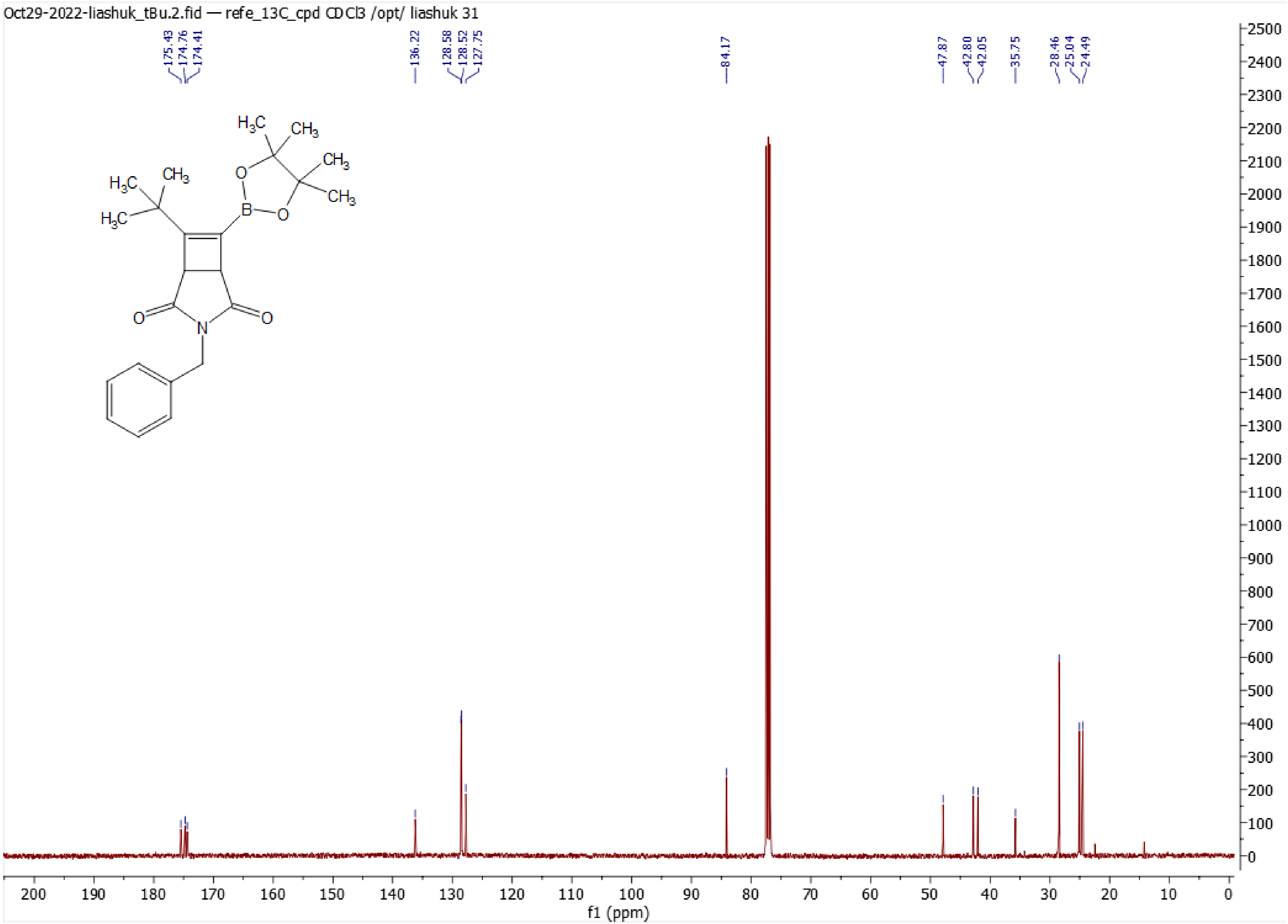

Spectrum 27. 3-benzyl-6-(tert-butyl)-7-(4,4,5,5-tetramethyl-1,3,2-dioxaborolan-2-yl)-3-azabicyclo[3.2.0]hept-6-ene-2,4-dione ***8cc***, *^{13}C NMR (101 MHz, CDCl$_3$)*

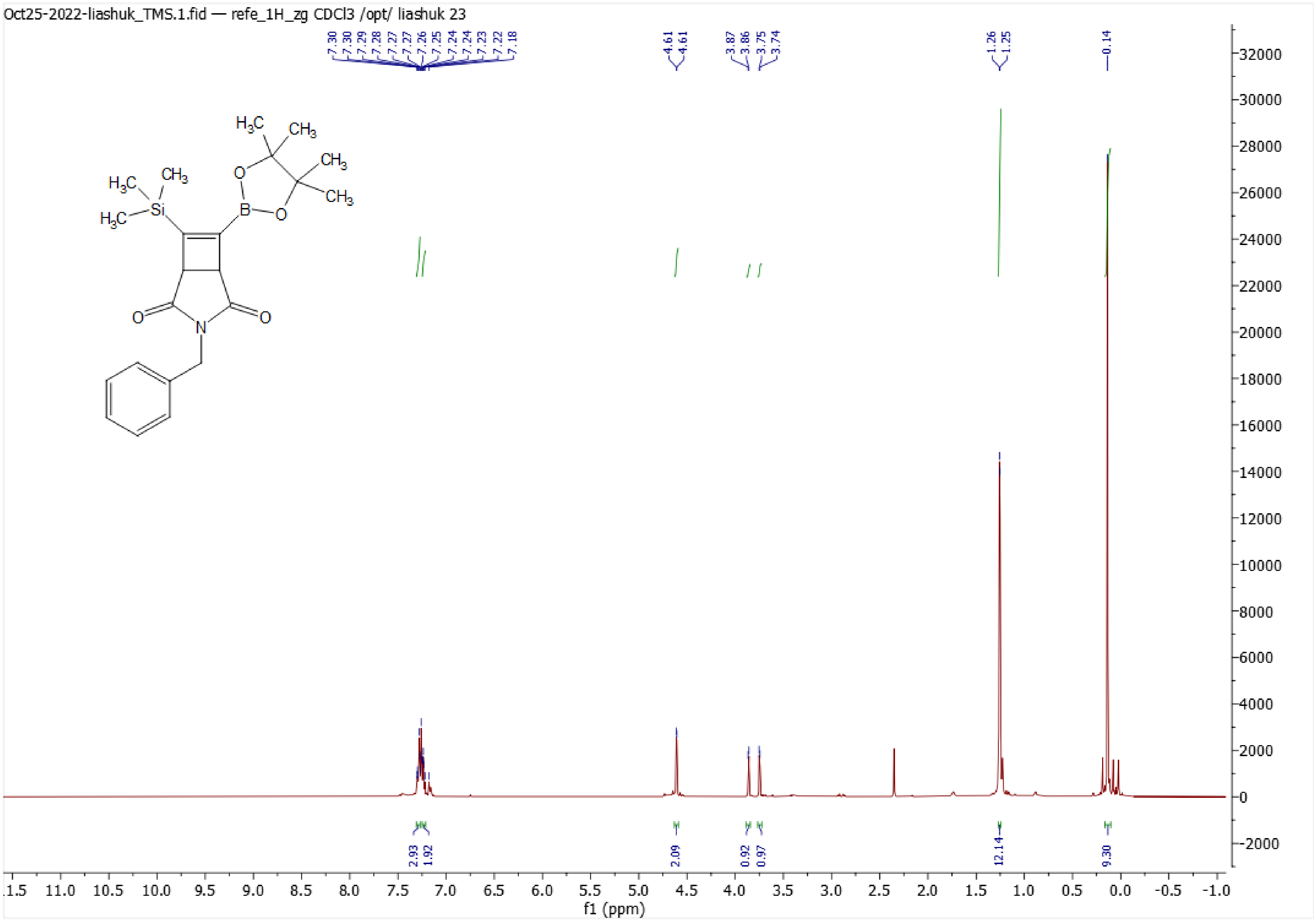

Spectrum 28. 3-benzyl-6-(4,4,5,5-tetramethyl-1,3,2-dioxaborolan-2-yl)-7-(trimethylsilyl)-3-azabicyclo[3.2.0]hept-6-ene-2,4-dione ***8cd****, ^{1}H NMR (400 MHz, CDCl$_3$)*

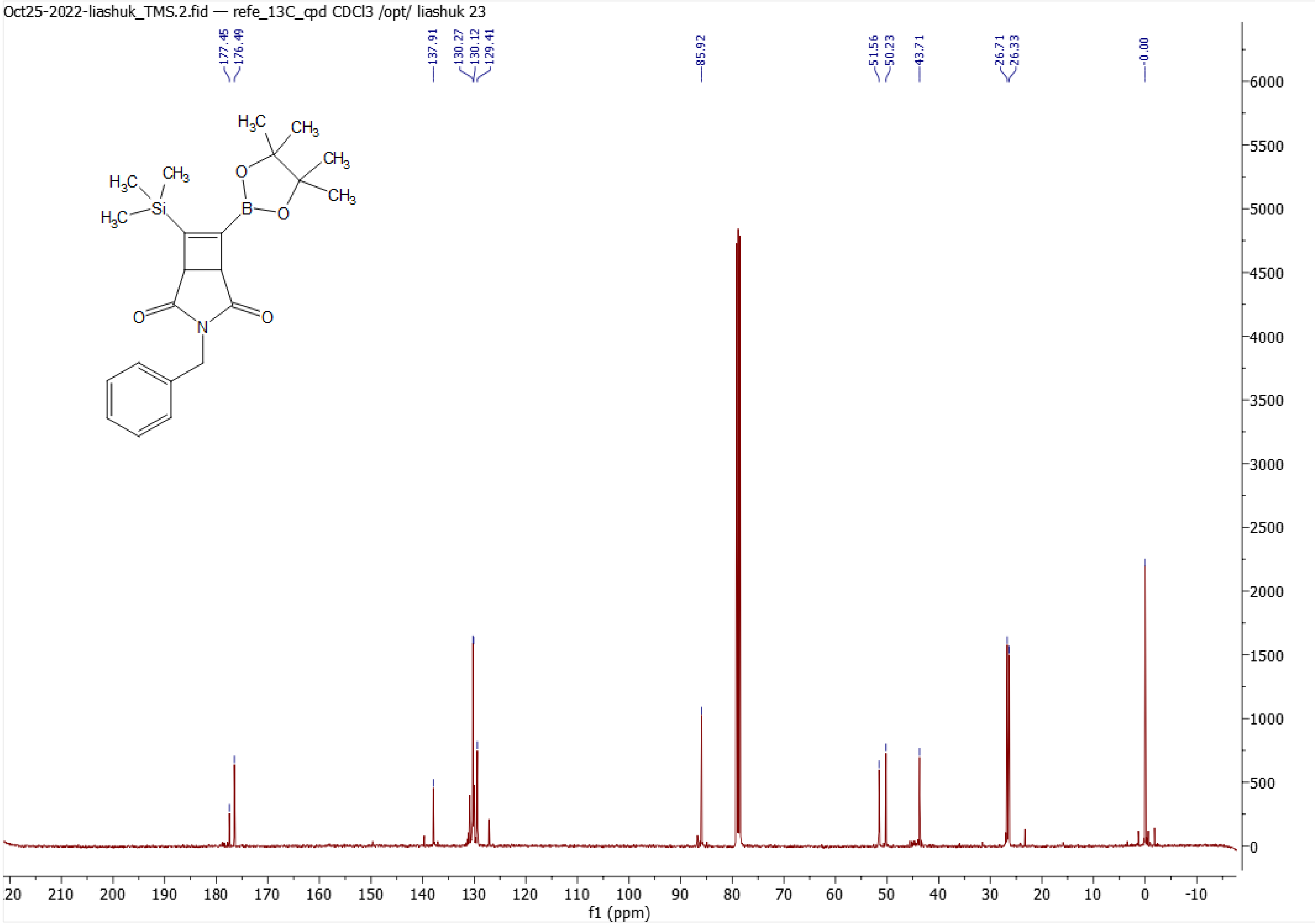

*Spectrum 29. 3-benzyl-6-(4,4,5,5-tetramethyl-1,3,2-dioxaborolan-2-yl)-7-(trimethylsilyl)-3-azabicyclo[3.2.0]hept-6-ene-2,4-dione **8cd**, ^{13}C NMR (101 MHz, CDCl$_3$)*

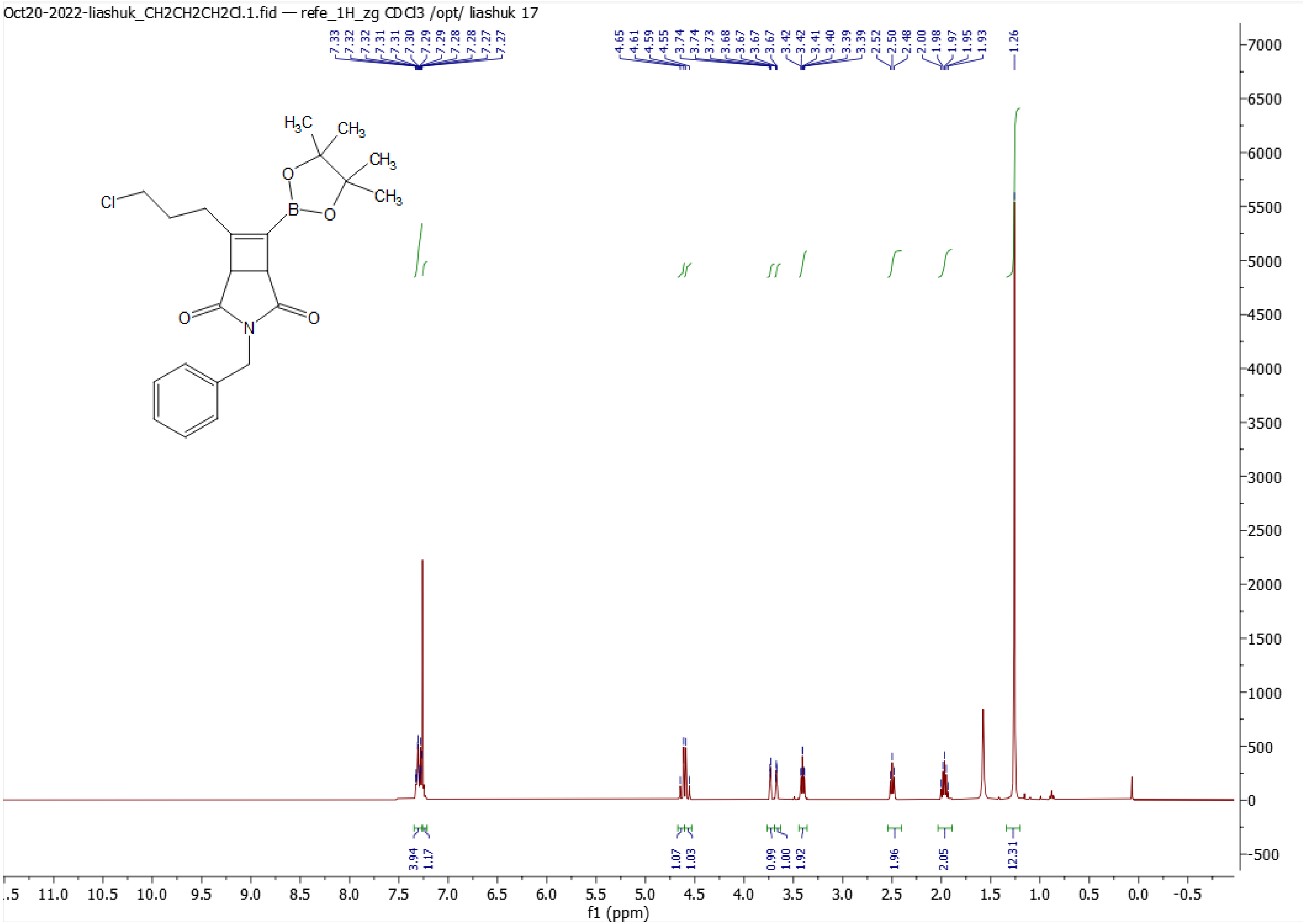

Spectrum 30. 3-benzyl-6-(3-chloropropyl)-7-(4,4,5,5-tetramethyl-1,3,2-dioxaborolan-2-yl)-3-azabicyclo[3.2.0]hept-6-ene-2,4-dione ***8ce****, ^{1}H NMR (400 MHz, $CDCl_3$)*

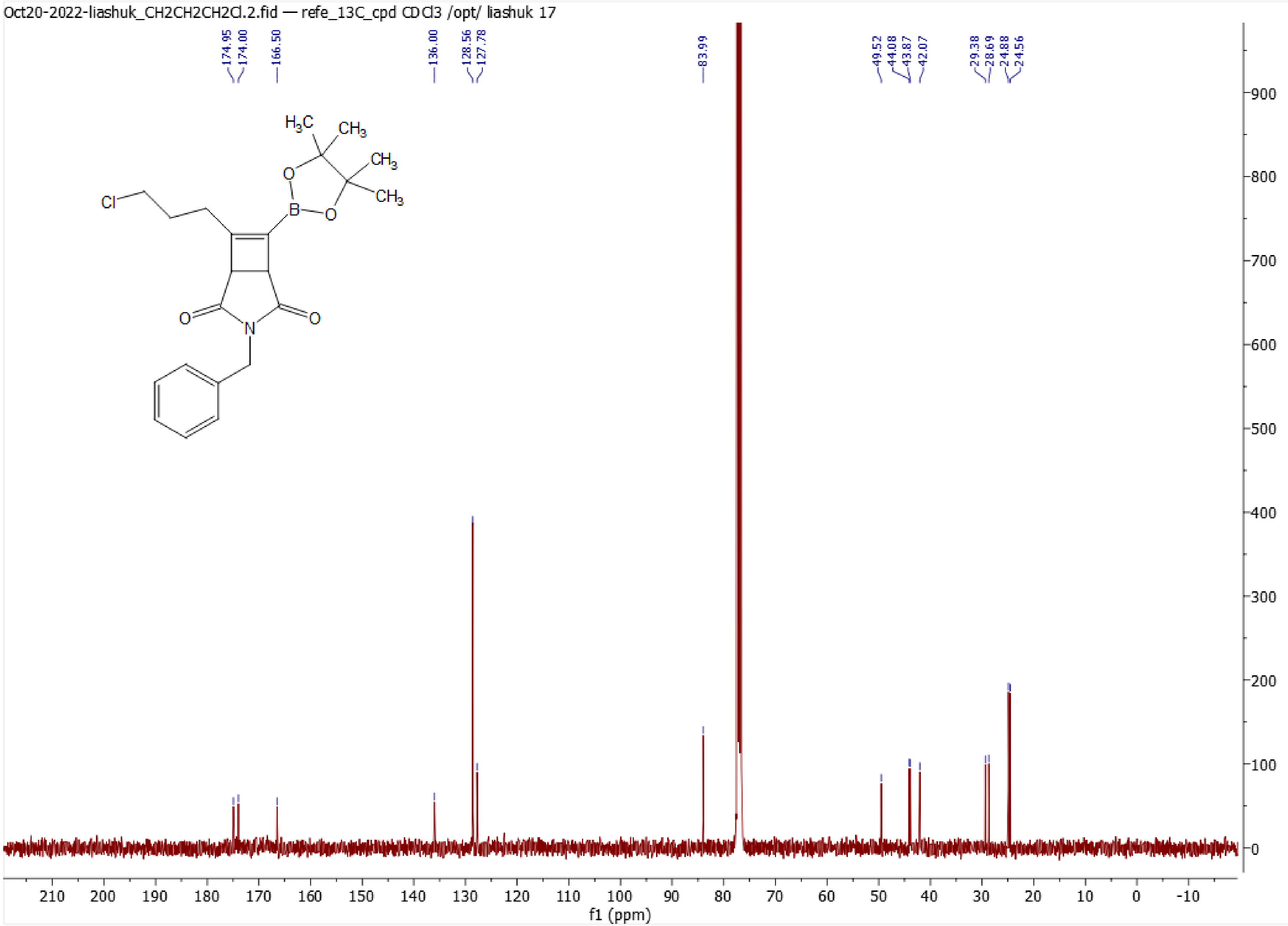

*Spectrum 31. 3-benzyl-6-(3-chloropropyl)-7-(4,4,5,5-tetramethyl-1,3,2-dioxaborolan-2-yl)-3-azabicyclo[3.2.0]hept-6-ene-2,4-dione **8ce**, ^{13}C NMR (101 MHz, CDCl$_3$)*

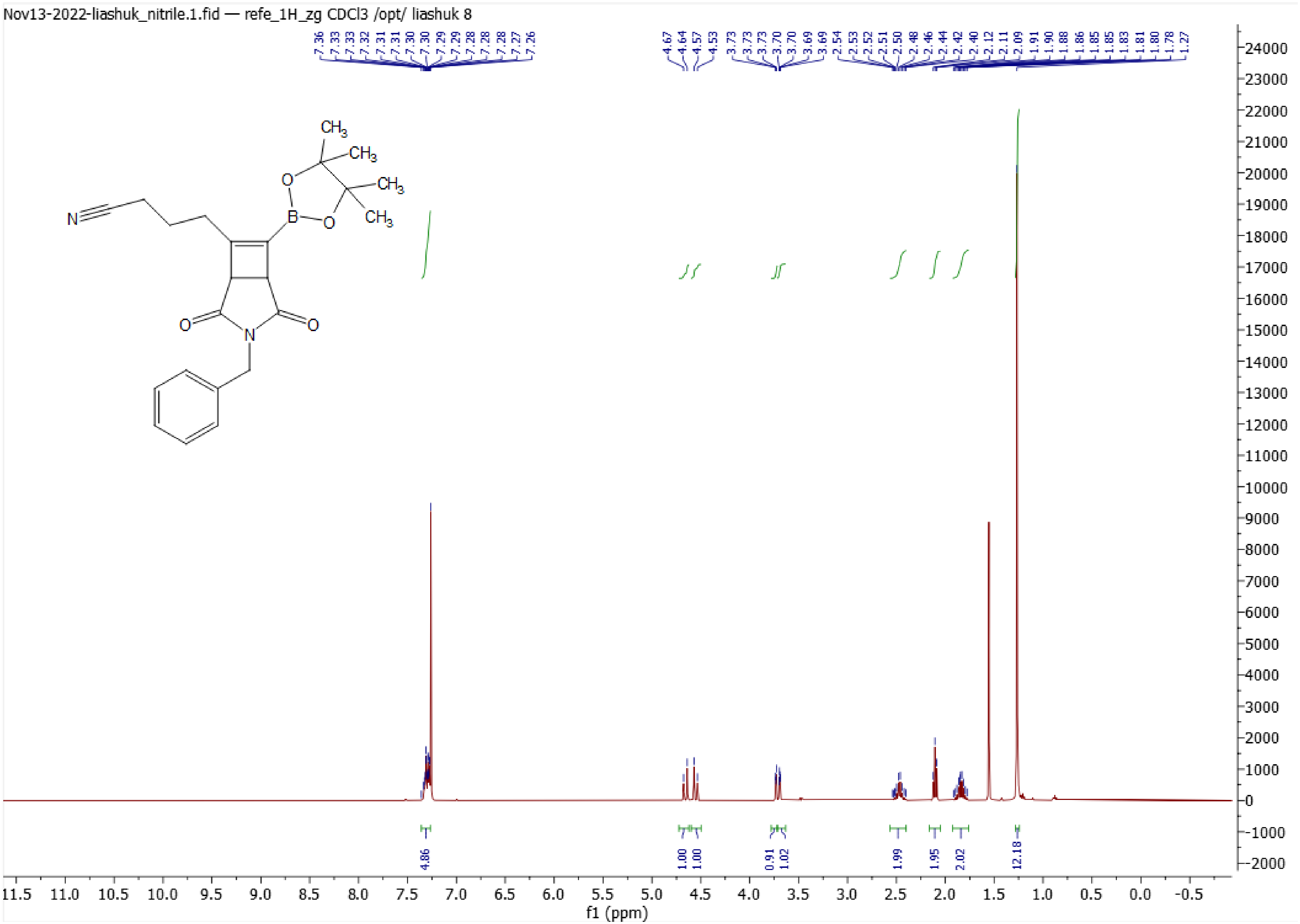

Spectrum 32. 4-(3-benzyl-2,4-dioxo-7-(4,4,5,5-tetramethyl-1,3,2-dioxaborolan-2-yl)-3-azabicyclo[3.2.0]hept-6-en-6-yl)butanenitrile ***8cf****, ^{1}H NMR (400 MHz, CDCl$_3$)*

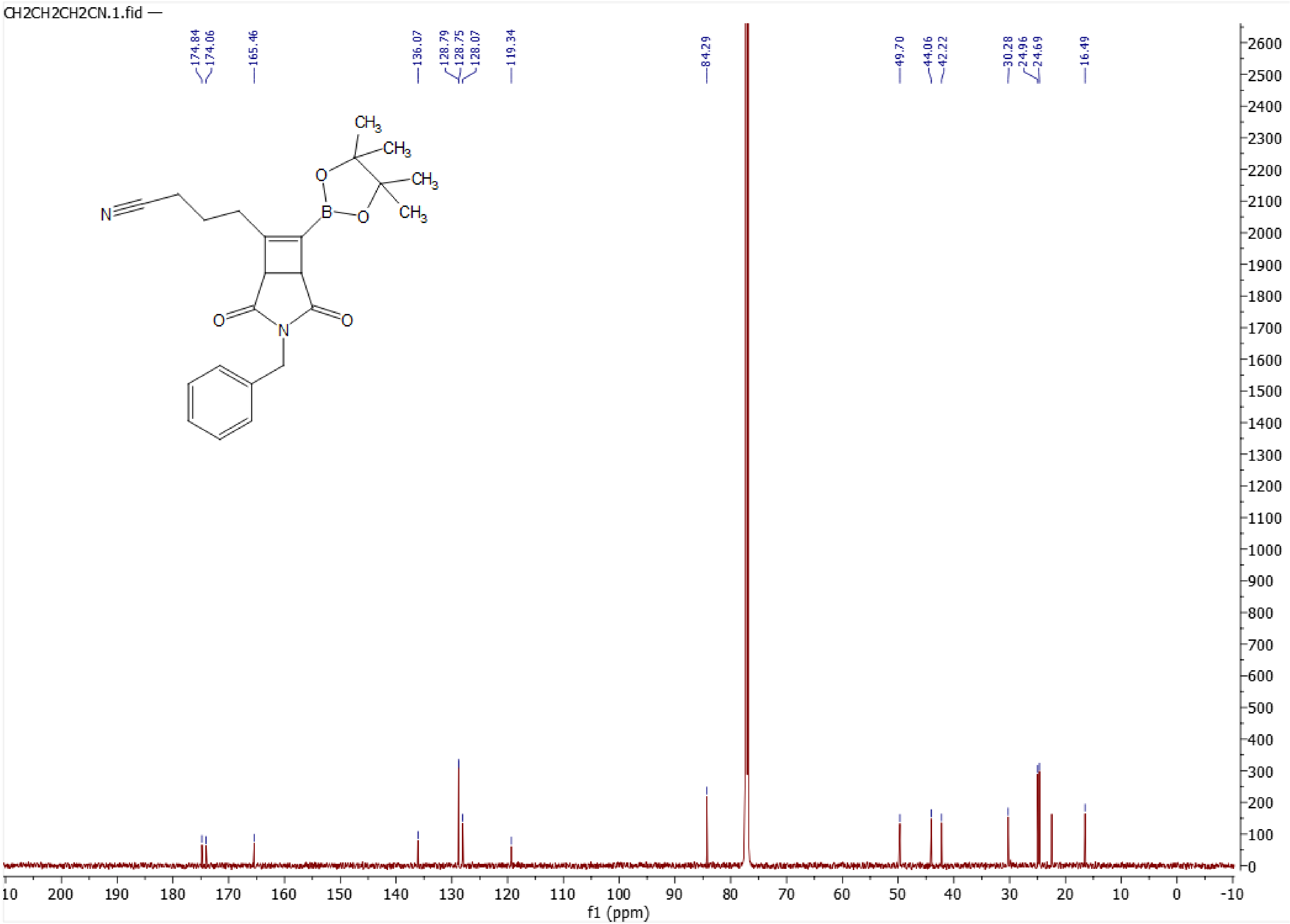

Spectrum 33. 4-(3-benzyl-2,4-dioxo-7-(4,4,5,5-tetramethyl-1,3,2-dioxaborolan-2-yl)-3-azabicyclo[3.2.0]hept-6-en-6-yl)butanenitrile ***8cf***, *^{13}C NMR (151 MHz, $CDCl_3$)*

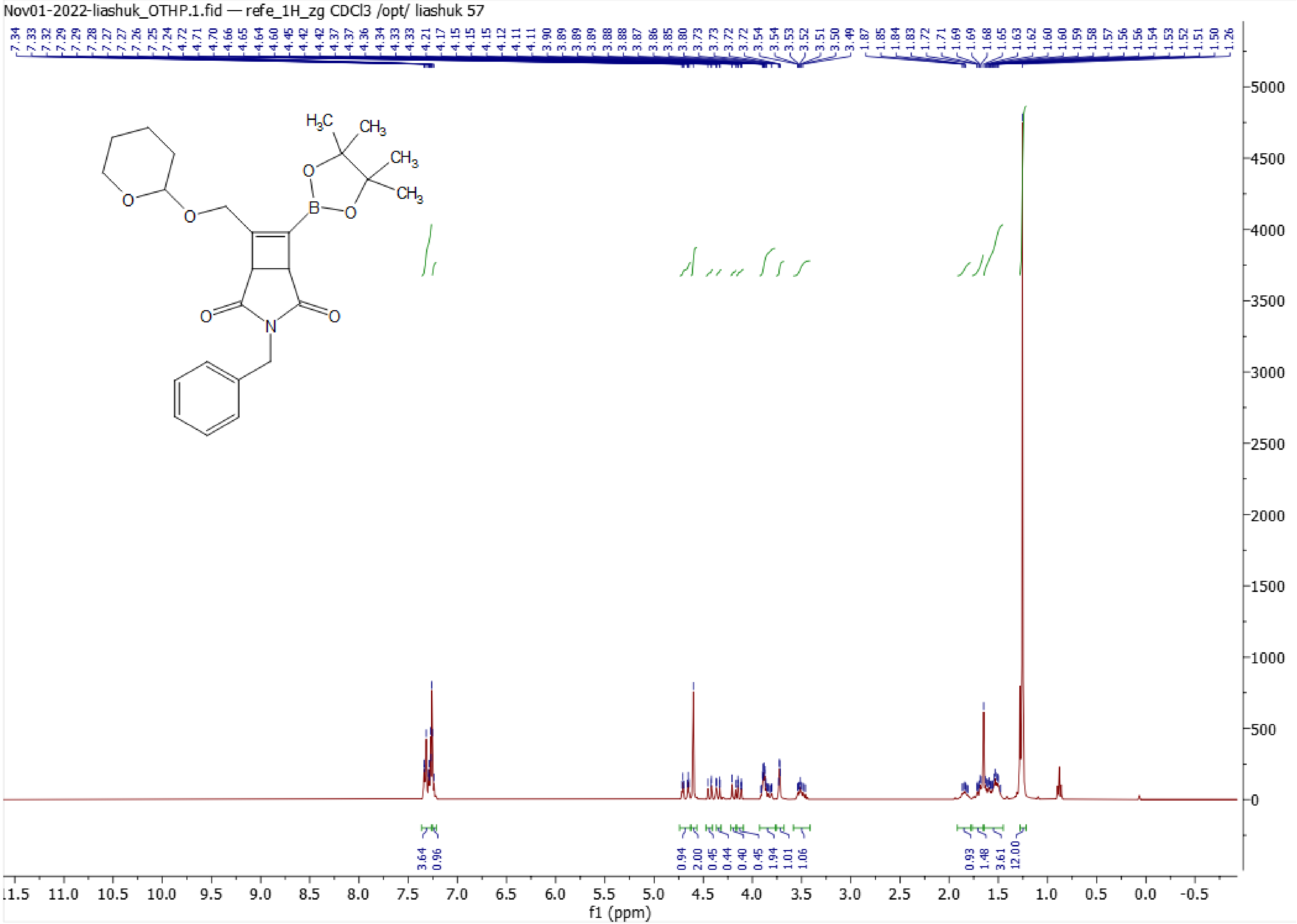

*Spectrum 34. 3-benzyl-6-(((tetrahydro-2H-pyran-2-yl)oxy)methyl)-7-(4,4,5,5-tetramethyl-1,3,2-dioxaborolan-2-yl)-3-azabicyclo[3.2.0]hept-6-ene-2,4-dione **8cg**, ^{1}H NMR (400 MHz, $CDCl_3$)*

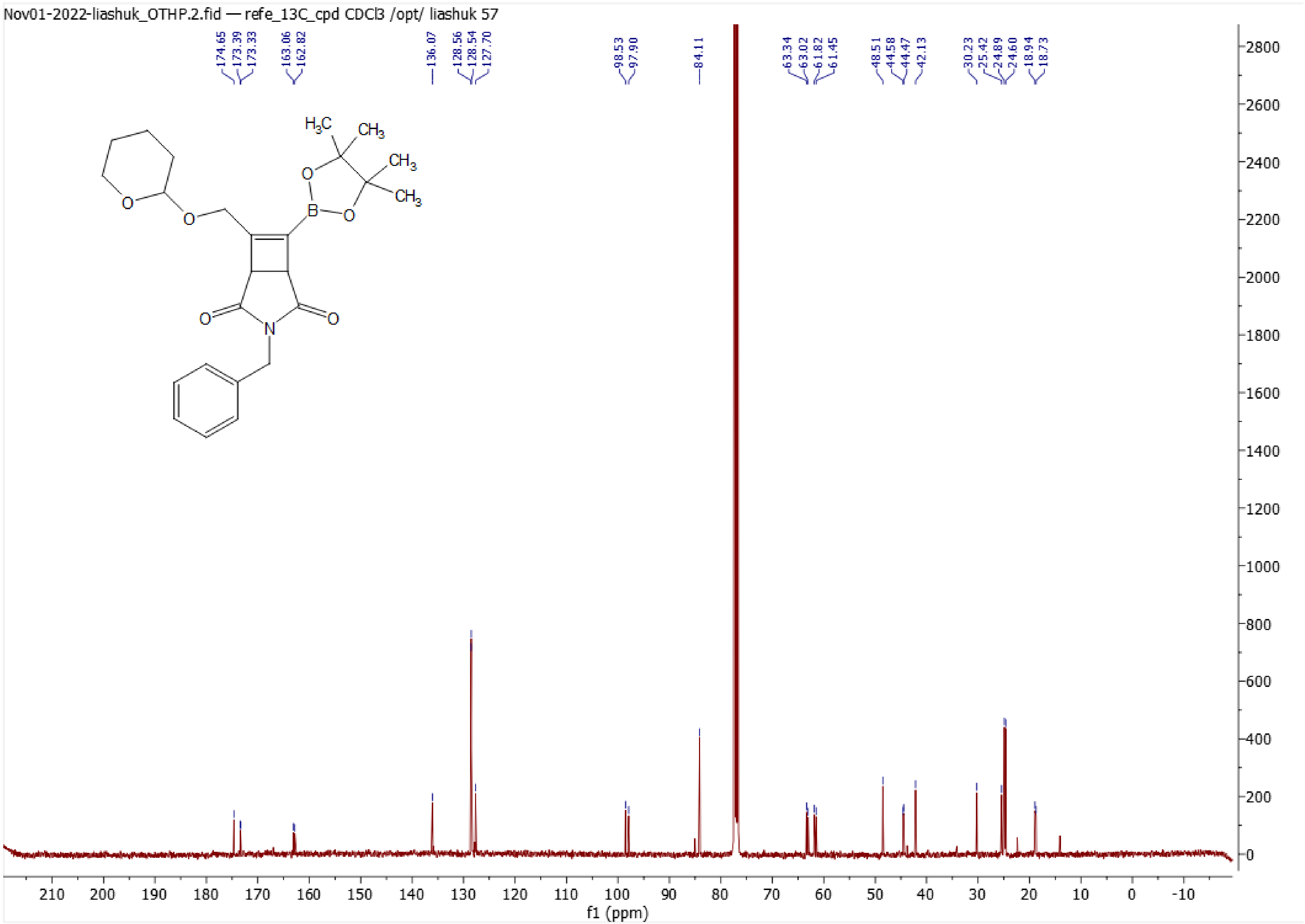

Spectrum 35. 3-benzyl-6-(((tetrahydro-2H-pyran-2-yl)oxy)methyl)-7-(4,4,5,5-tetramethyl-1,3,2-dioxaborolan-2-yl)-3-azabicyclo[3.2.0]hept-6-ene-2,4-dione ***8cg****,* *^{13}C NMR (101 MHz, $CDCl_3$)*

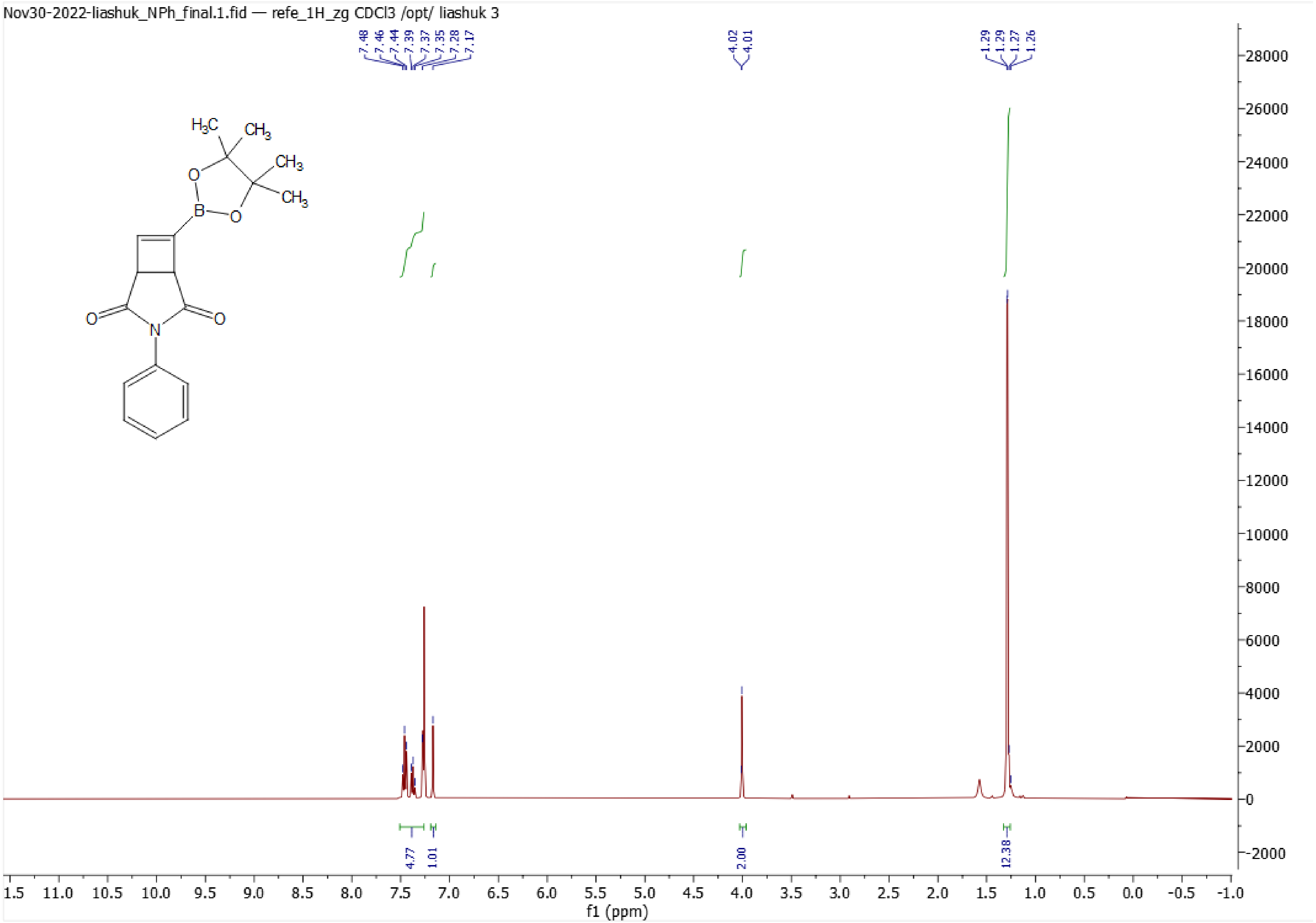

Spectrum 36. 3-phenyl-6-(4,4,5,5-tetramethyl-1,3,2-dioxaborolan-2-yl)-3-azabicyclo[3.2.0]hept-6-ene-2,4-dione ***8d****,* ^{1}*H NMR (400 MHz,* $CDCl_3$*)*

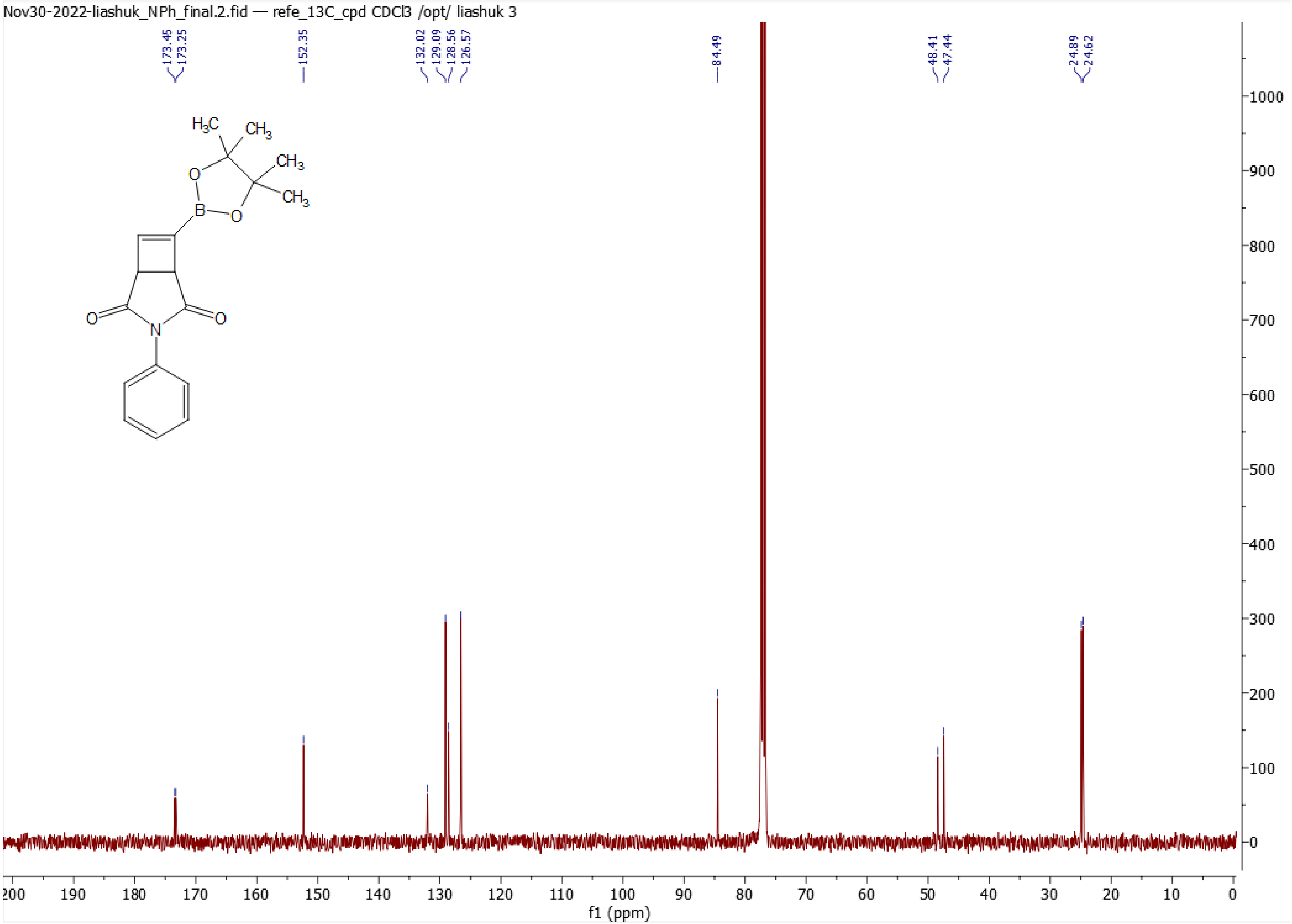

Spectrum 37. 3-phenyl-6-(4,4,5,5-tetramethyl-1,3,2-dioxaborolan-2-yl)-3-azabicyclo[3.2.0]hept-6-ene-2,4-dione ***8d****, ^{13}C NMR (101 MHz, $CDCl_3$)*

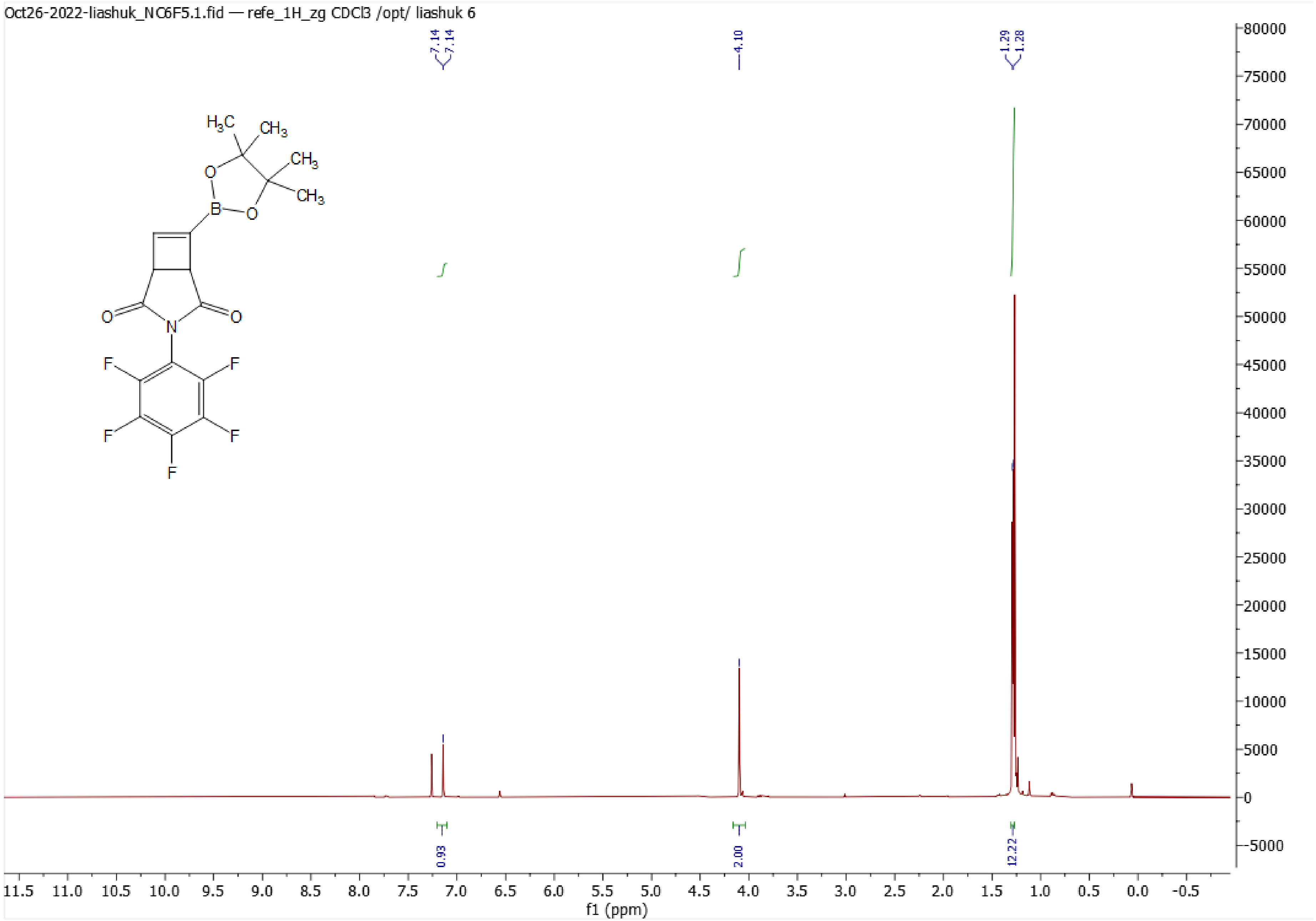

Spectrum 38. 3-(perfluorophenyl)-6-(4,4,5,5-tetramethyl-1,3,2-dioxaborolan-2-yl)-3-azabicyclo[3.2.0]hept-6-ene-2,4-dione ***8e****,* ^{1}*H NMR (400 MHz,* $CDCl_3$*)*

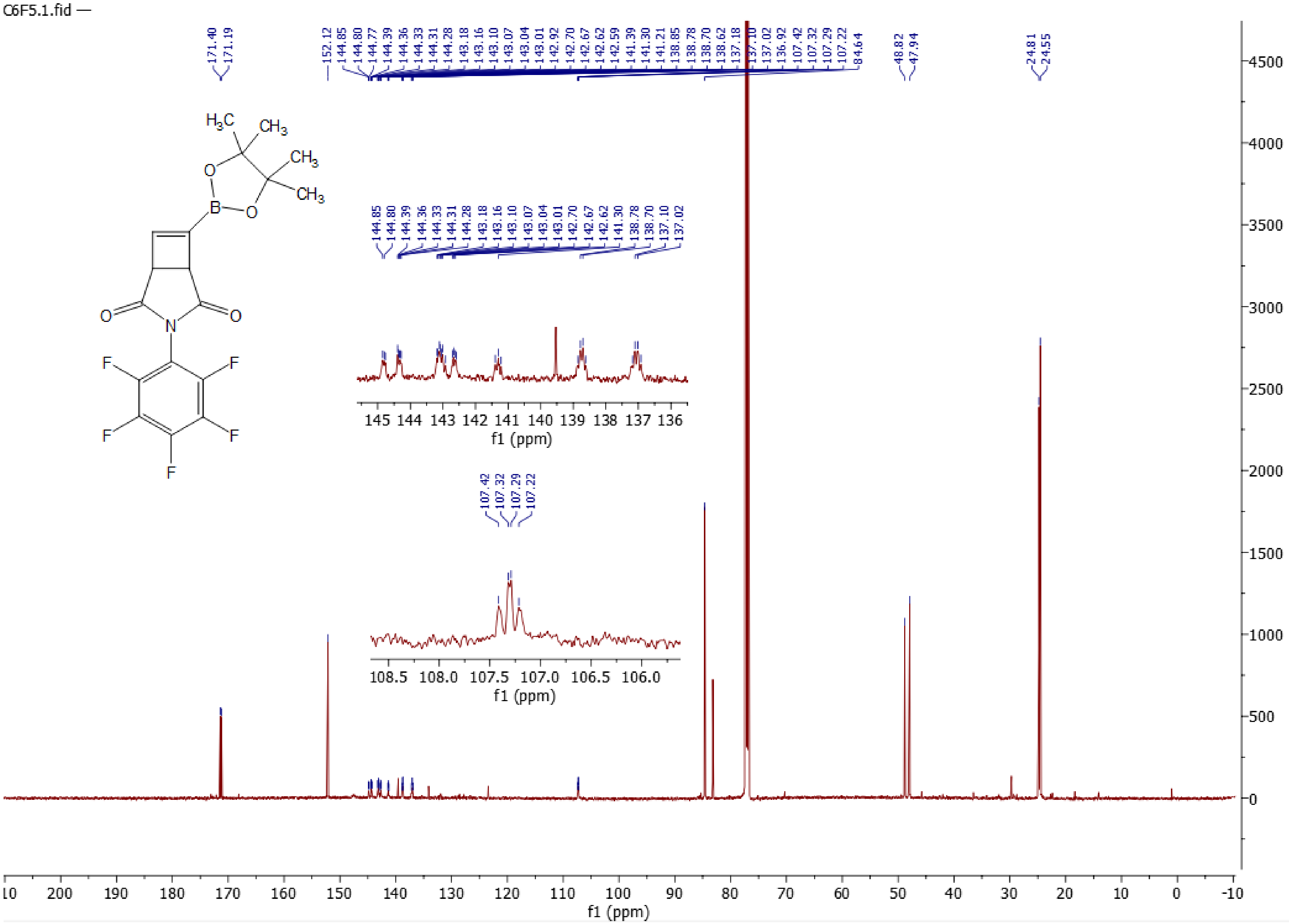

*Spectrum 39. 3-(perfluorophenyl)-6-(4,4,5,5-tetramethyl-1,3,2-dioxaborolan-2-yl)-3-azabicyclo[3.2.0]hept-6-ene-2,4-dione **8e**, ^{13}C NMR (151 MHz, $CDCl_3$)*

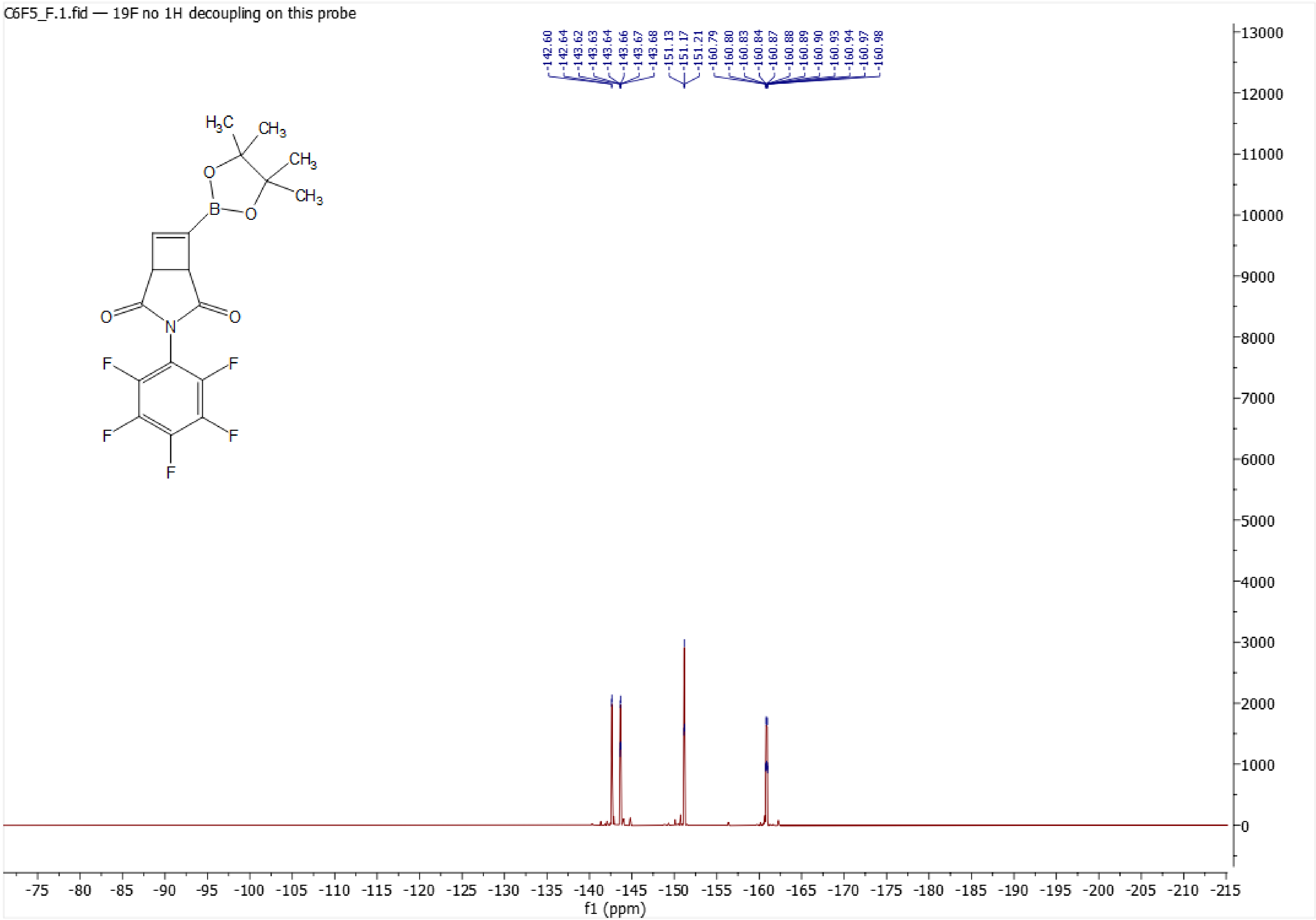

Spectrum 40. 3-(perfluorophenyl)-6-(4,4,5,5-tetramethyl-1,3,2-dioxaborolan-2-yl)-3-azabicyclo[3.2.0]hept-6-ene-2,4-dione ***8e***, *^{19}F NMR (565 MHz, $CDCl_3$)*

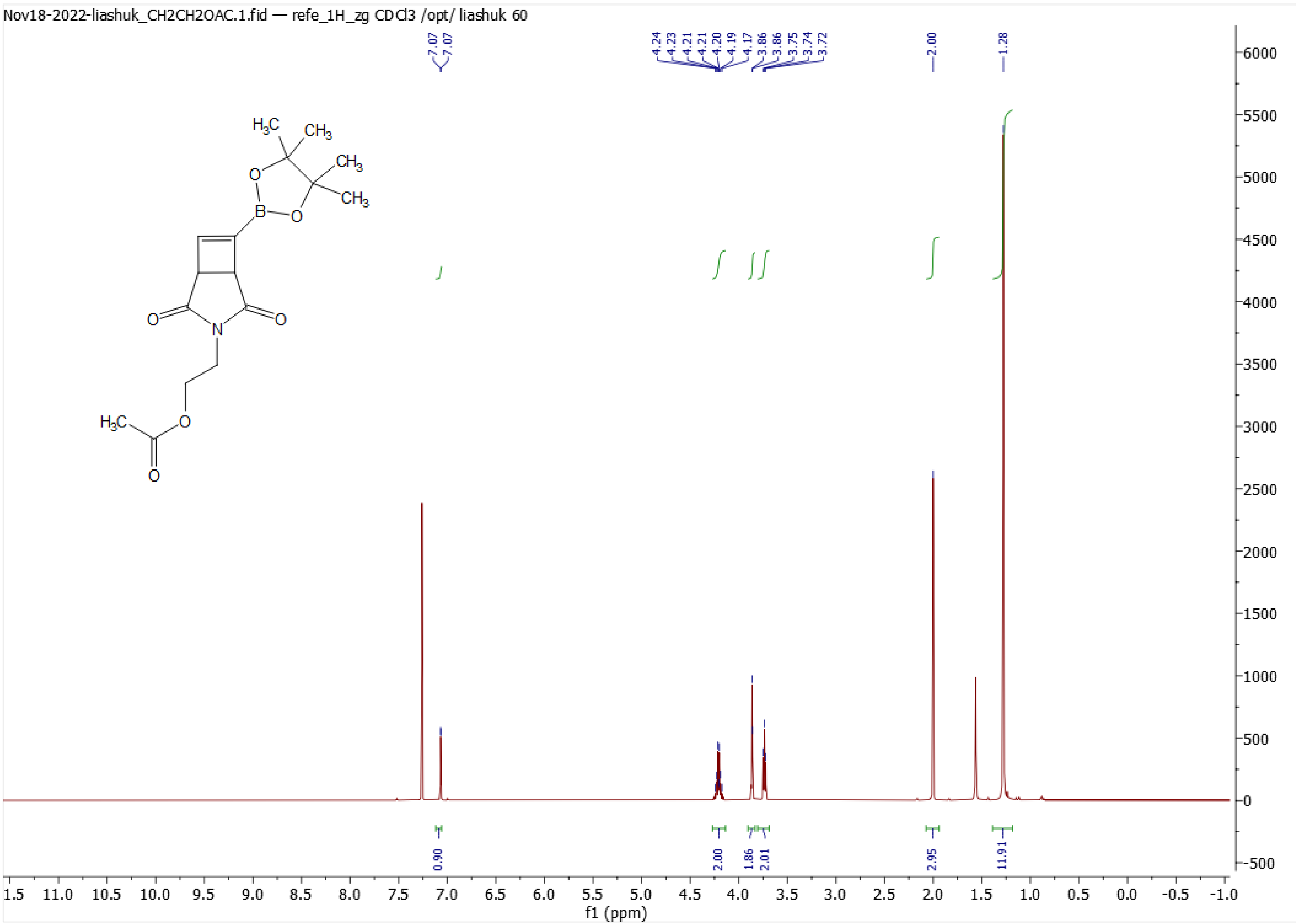

*Spectrum 41. 2-(2,4-dioxo-6-(4,4,5,5-tetramethyl-1,3,2-dioxaborolan-2-yl)-3-azabicyclo[3.2.0]hept-6-en-3-yl)ethyl acetate **8f**, ^{1}H NMR (400 MHz, CDCl$_3$)*

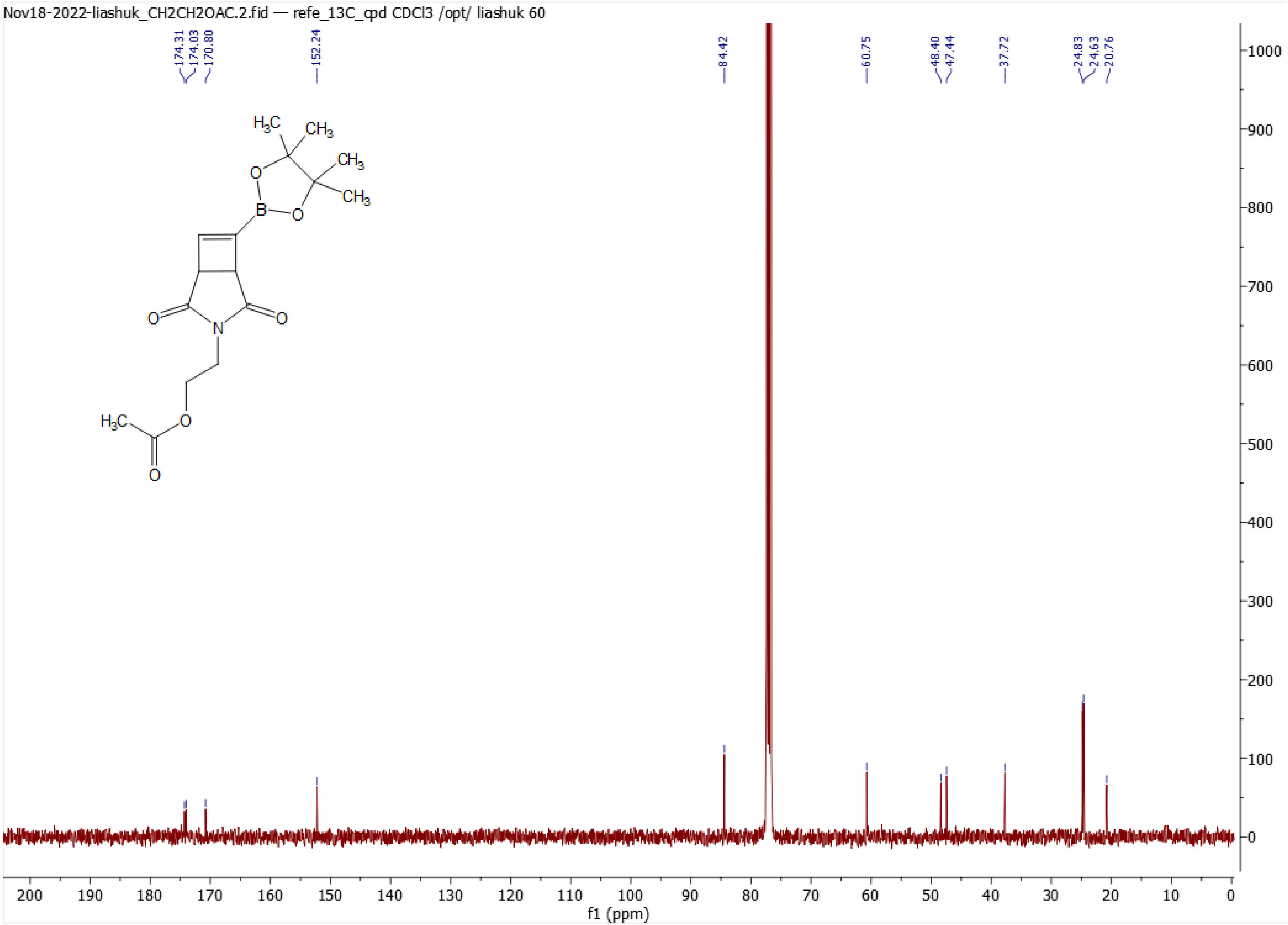

Spectrum 42. 2-(2,4-dioxo-6-(4,4,5,5-tetramethyl-1,3,2-dioxaborolan-2-yl)-3-azabicyclo[3.2.0]hept-6-en-3-yl)ethyl acetate ***8f***, *^{13}C NMR (101 MHz, CDCl$_3$)*

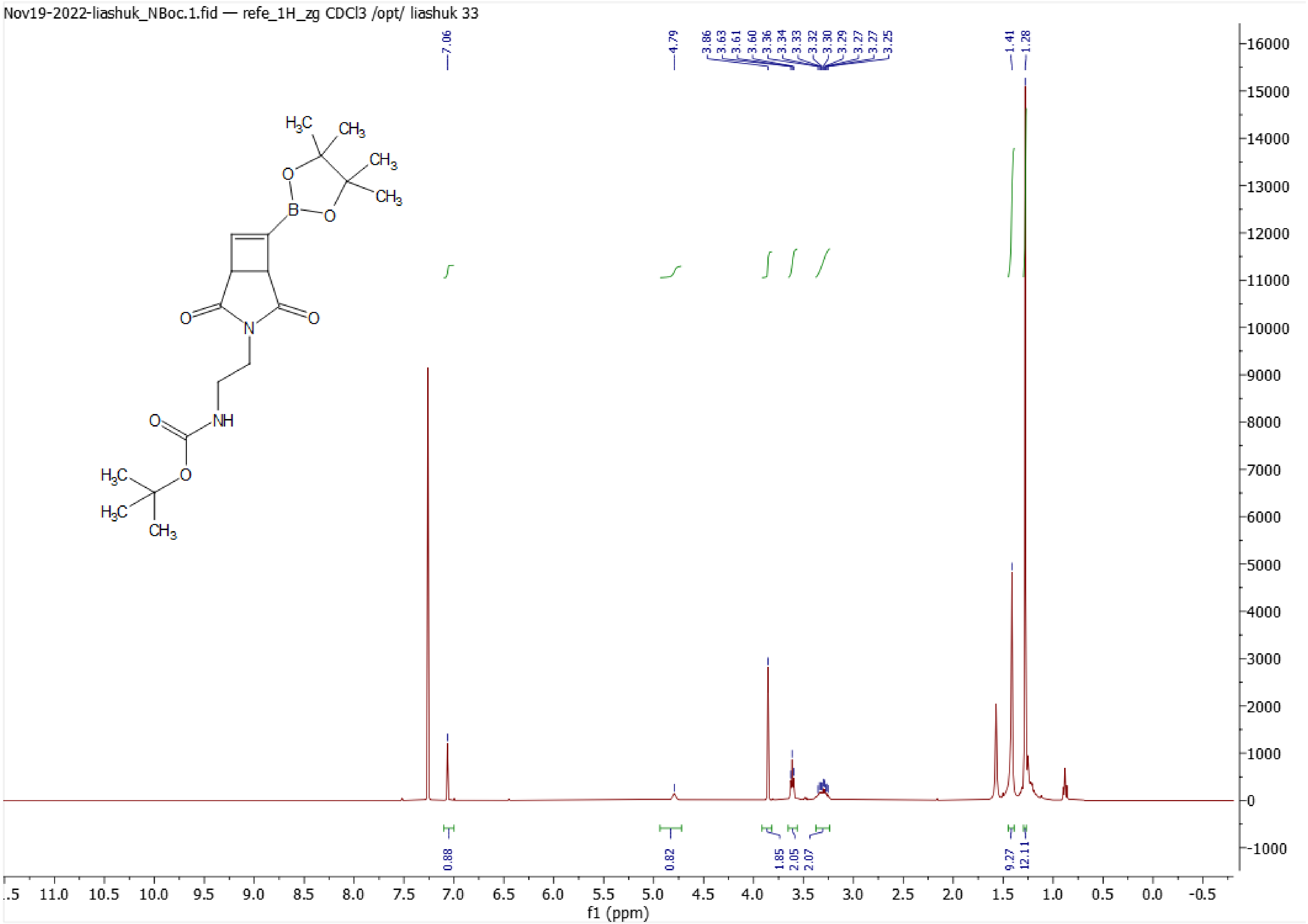

Spectrum 43. tert-butyl (2-(2,4-dioxo-6-(4,4,5,5-tetramethyl-1,3,2-dioxaborolan-2-yl)-3-azabicyclo[3.2.0]hept-6-en-3-yl)ethyl)carbamate ***8g****, ^{1}H NMR (400 MHz, CDCl$_3$)*

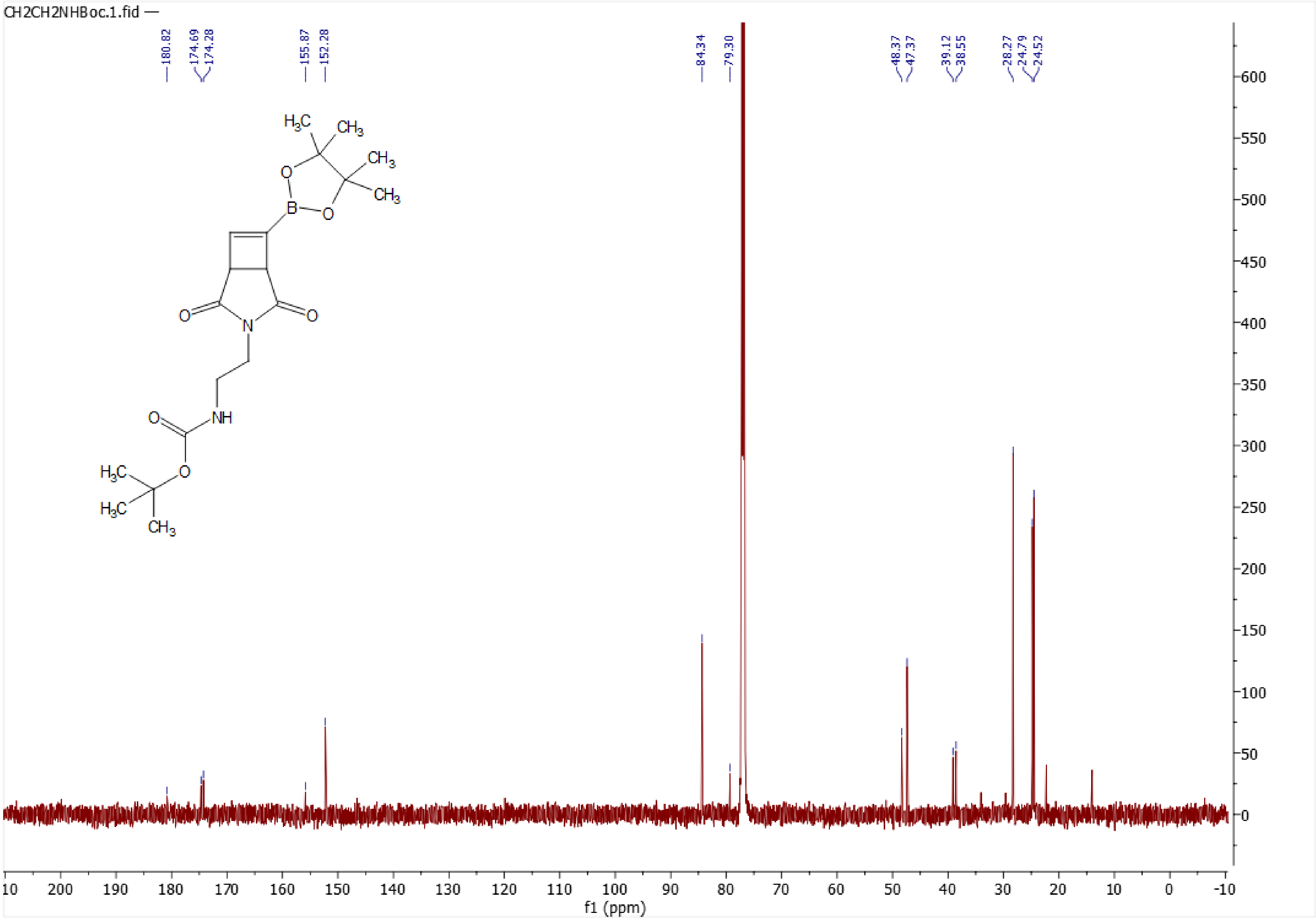

Spectrum 44. tert-butyl (2-(2,4-dioxo-6-(4,4,5,5-tetramethyl-1,3,2-dioxaborolan-2-yl)-3-azabicyclo[3.2.0]hept-6-en-3-yl)ethyl)carbamate ***8g****, ^{13}C NMR (151 MHz, CDCl$_3$)*

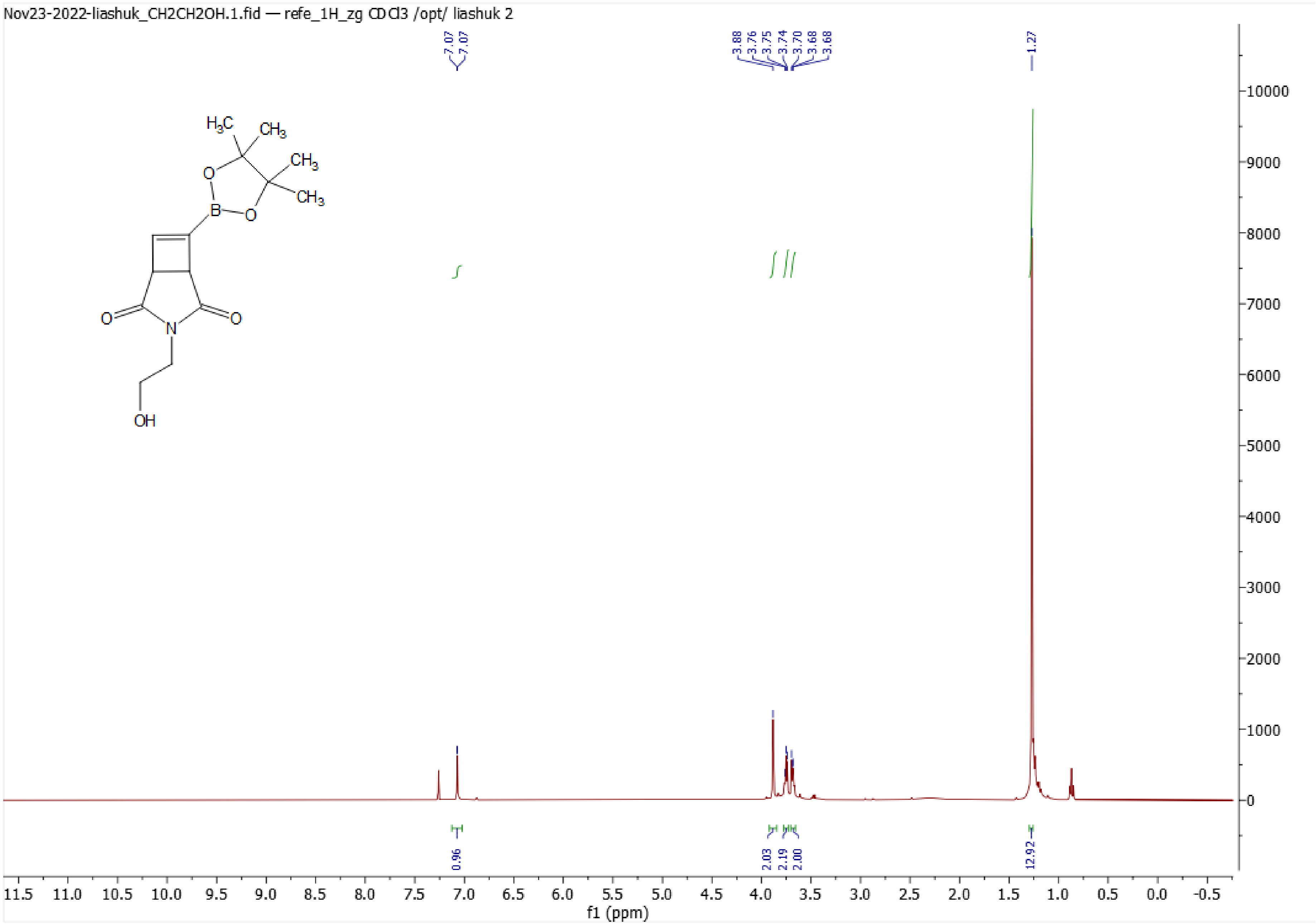

Spectrum 45. 3-(2-hydroxyethyl)-6-(4,4,5,5-tetramethyl-1,3,2-dioxaborolan-2-yl)-3-azabicyclo[3.2.0]hept-6-ene-2,4-dione ***8h***, *^{1}H NMR (400 MHz, $CDCl_3$)*

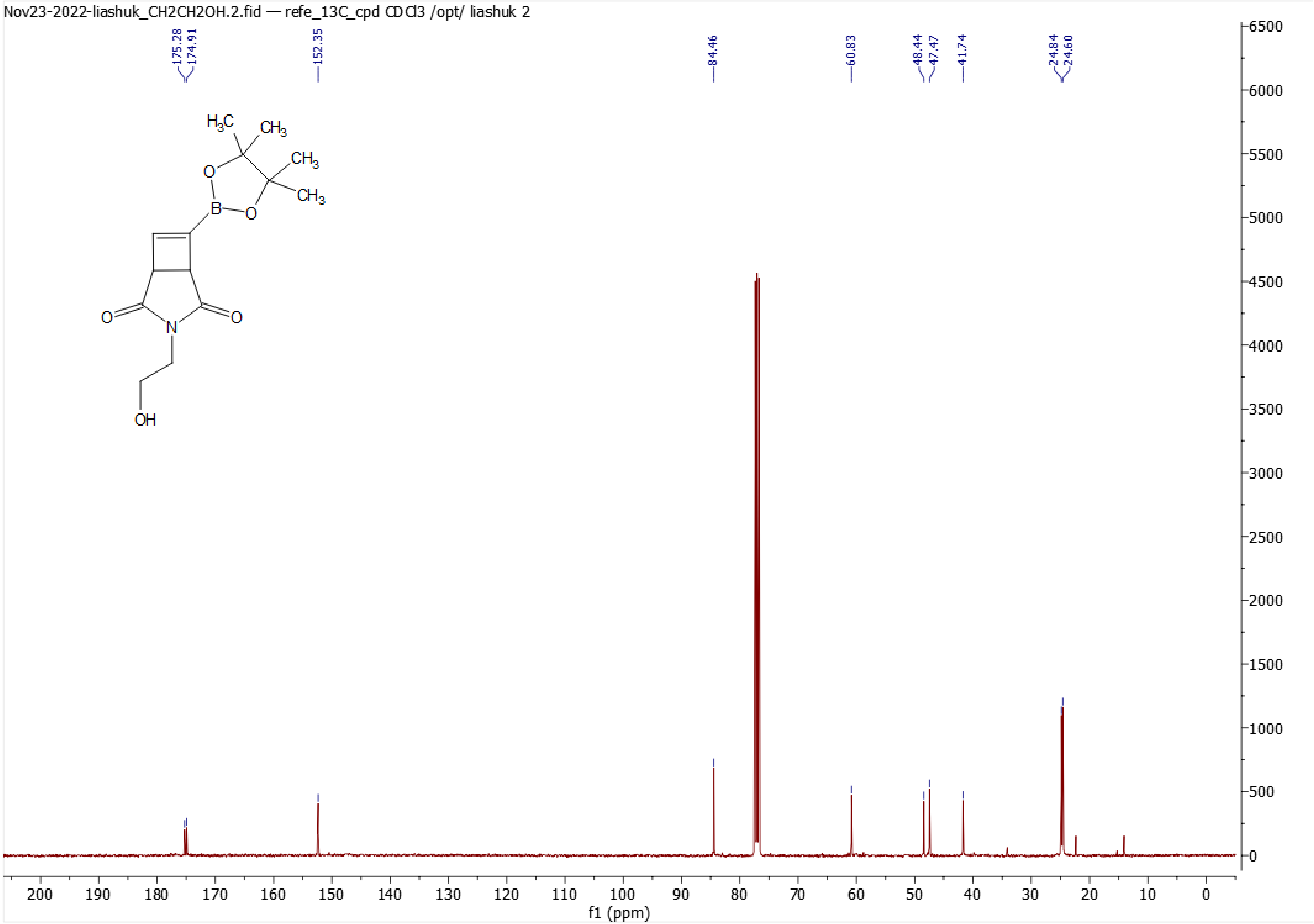

*Spectrum 46. 3-(2-hydroxyethyl)-6-(4,4,5,5-tetramethyl-1,3,2-dioxaborolan-2-yl)-3-azabicyclo[3.2.0]hept-6-ene-2,4-dione **8h**, ^{13}C NMR (101 MHz, CDCl$_3$)*

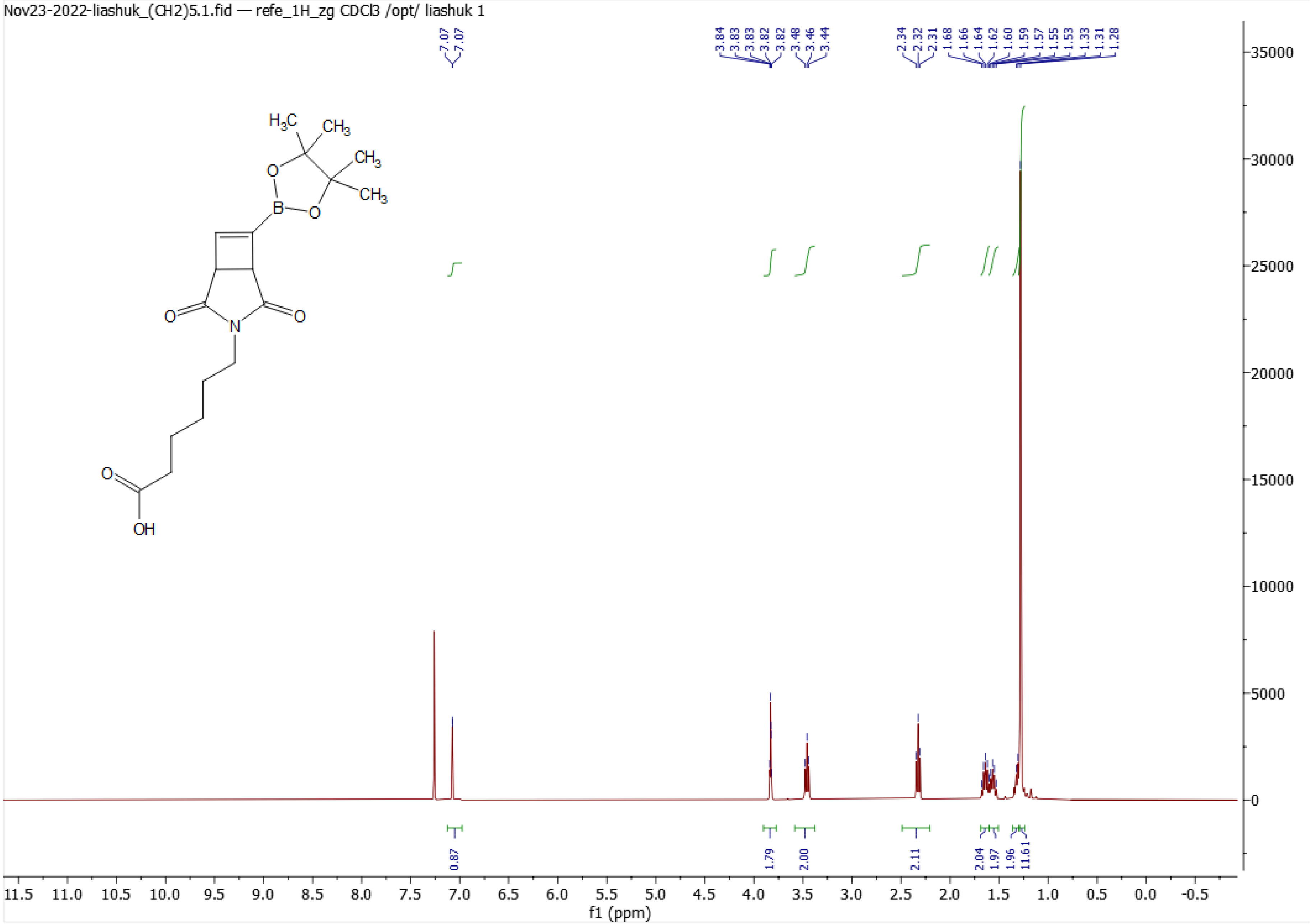

Spectrum 47. 6-(2,4-dioxo-6-(4,4,5,5-tetramethyl-1,3,2-dioxaborolan-2-yl)-3-azabicyclo[3.2.0]hept-6-en-3-yl)hexanoic acid **8i**, ^{1}H NMR (400 MHz, $CDCl_3$)

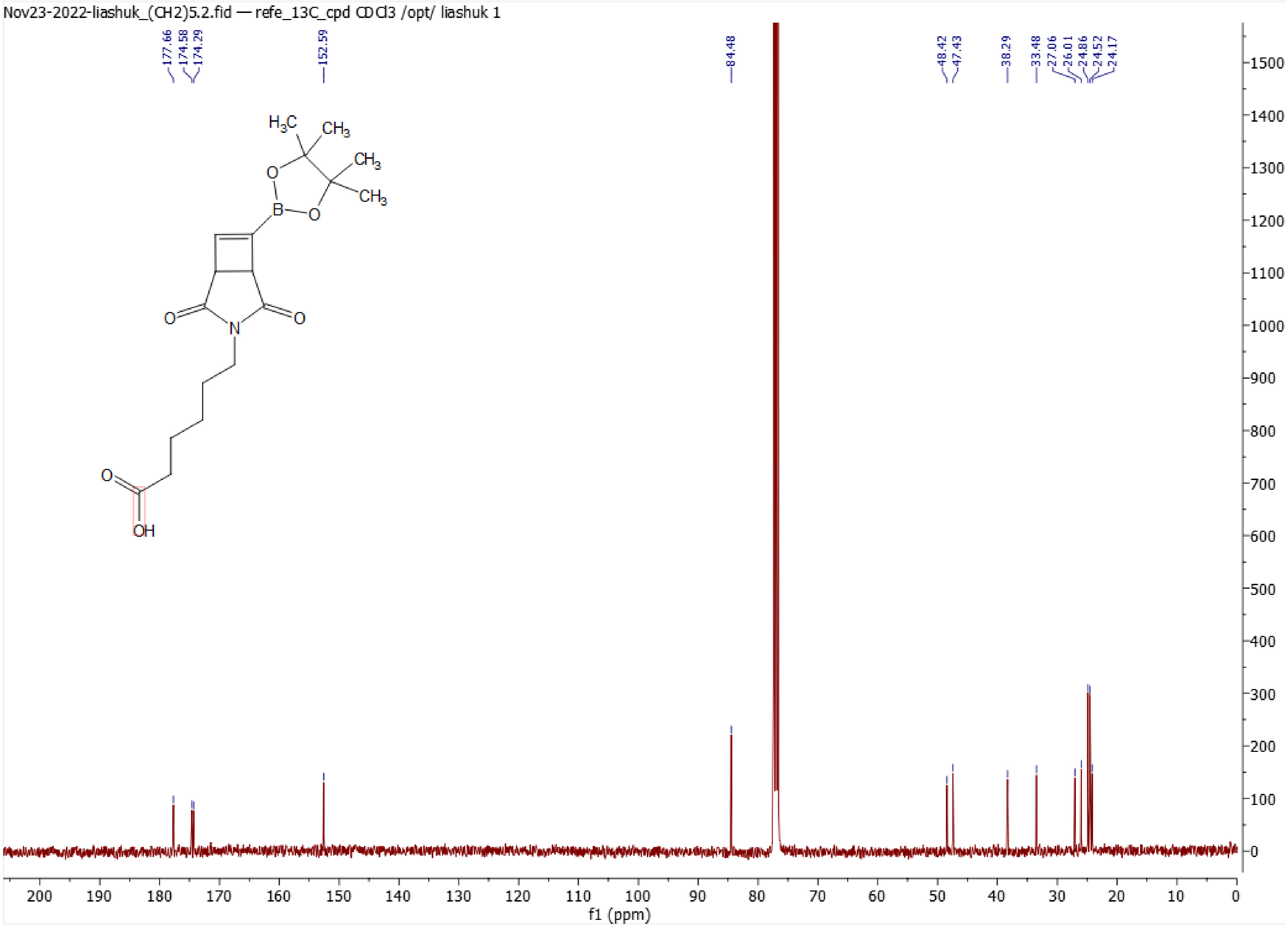

Spectrum 48. 6-(2,4-dioxo-6-(4,4,5,5-tetramethyl-1,3,2-dioxaborolan-2-yl)-3-azabicyclo[3.2.0]hept-6-en-3-yl)hexanoic acid **8i**, ^{13}C NMR (101 MHz, CDCl$_3$)

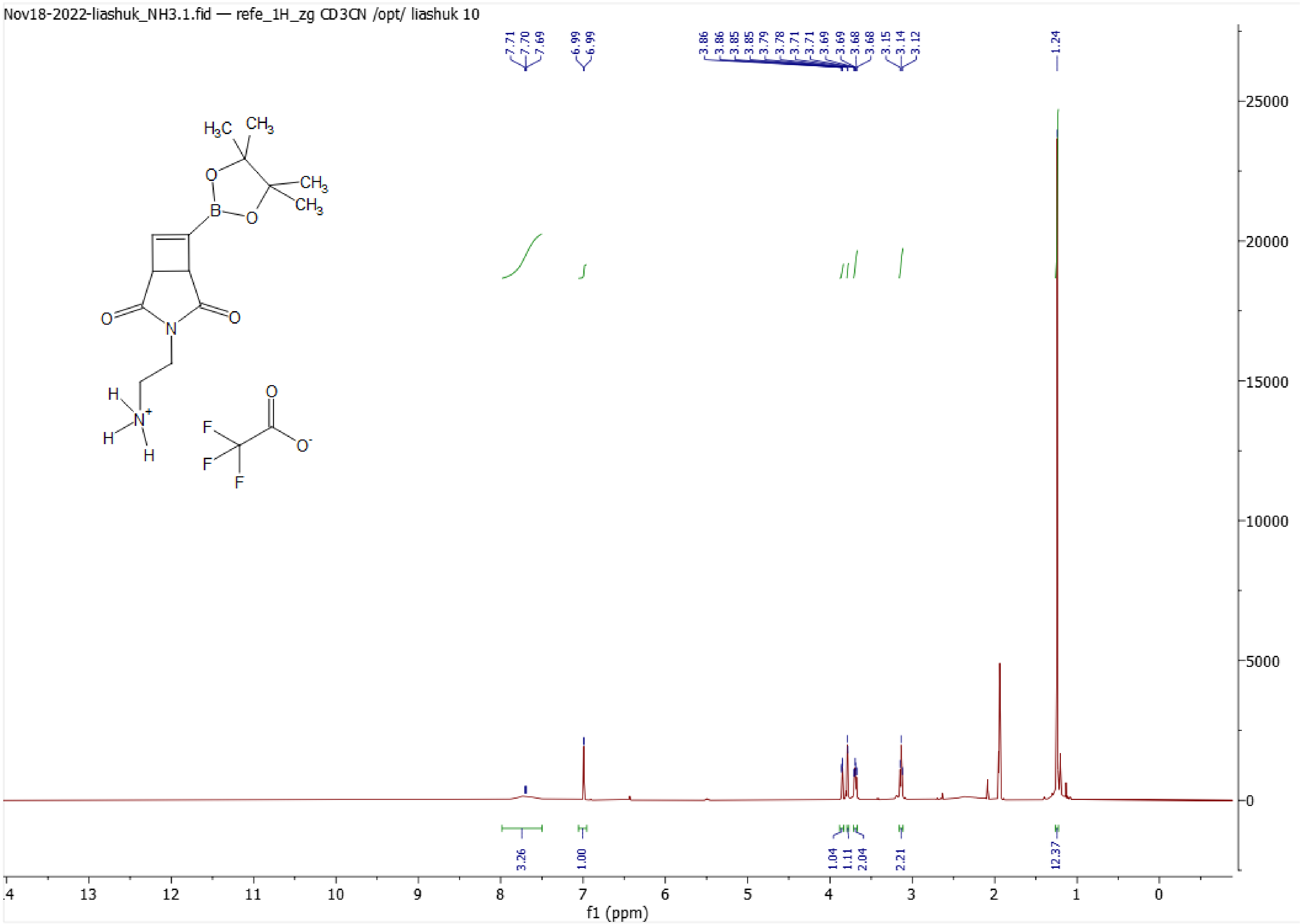

Spectrum 49. 2-(2,4-dioxo-6-(4,4,5,5-tetramethyl-1,3,2-dioxaborolan-2-yl)-3-azabicyclo[3.2.0]hept-6-en-3-yl)ethan-1-aminium trifluoroacetate ***8j****, ^{1}H NMR (400 MHz, CD_3CN)*

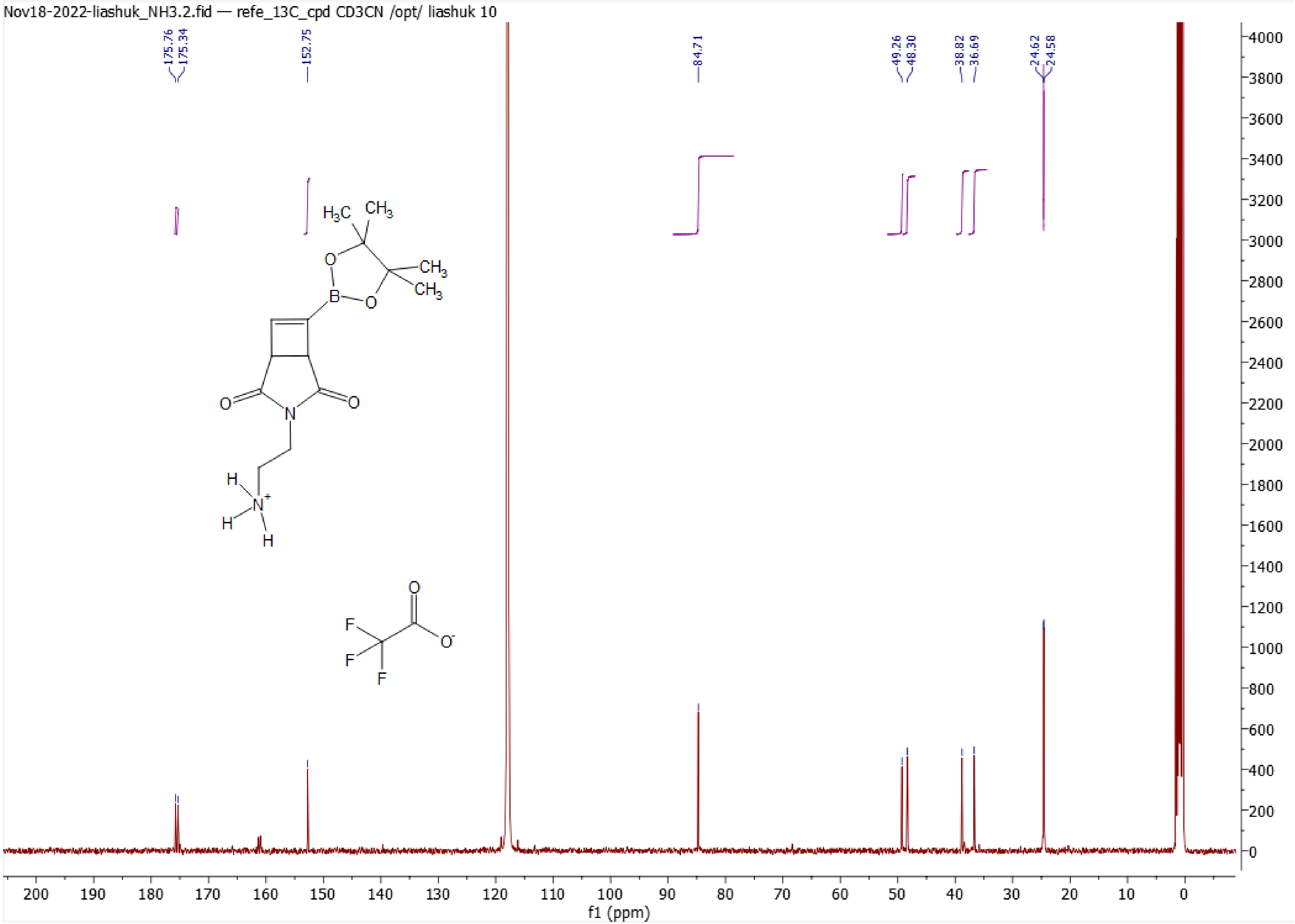

Spectrum 50. 2-(2,4-dioxo-6-(4,4,5,5-tetramethyl-1,3,2-dioxaborolan-2-yl)-3-azabicyclo[3.2.0]hept-6-en-3-yl)ethan-1-aminium trifluoroacetate ***8j****, ^{13}C NMR (101 MHz, CD$_3$CN)*

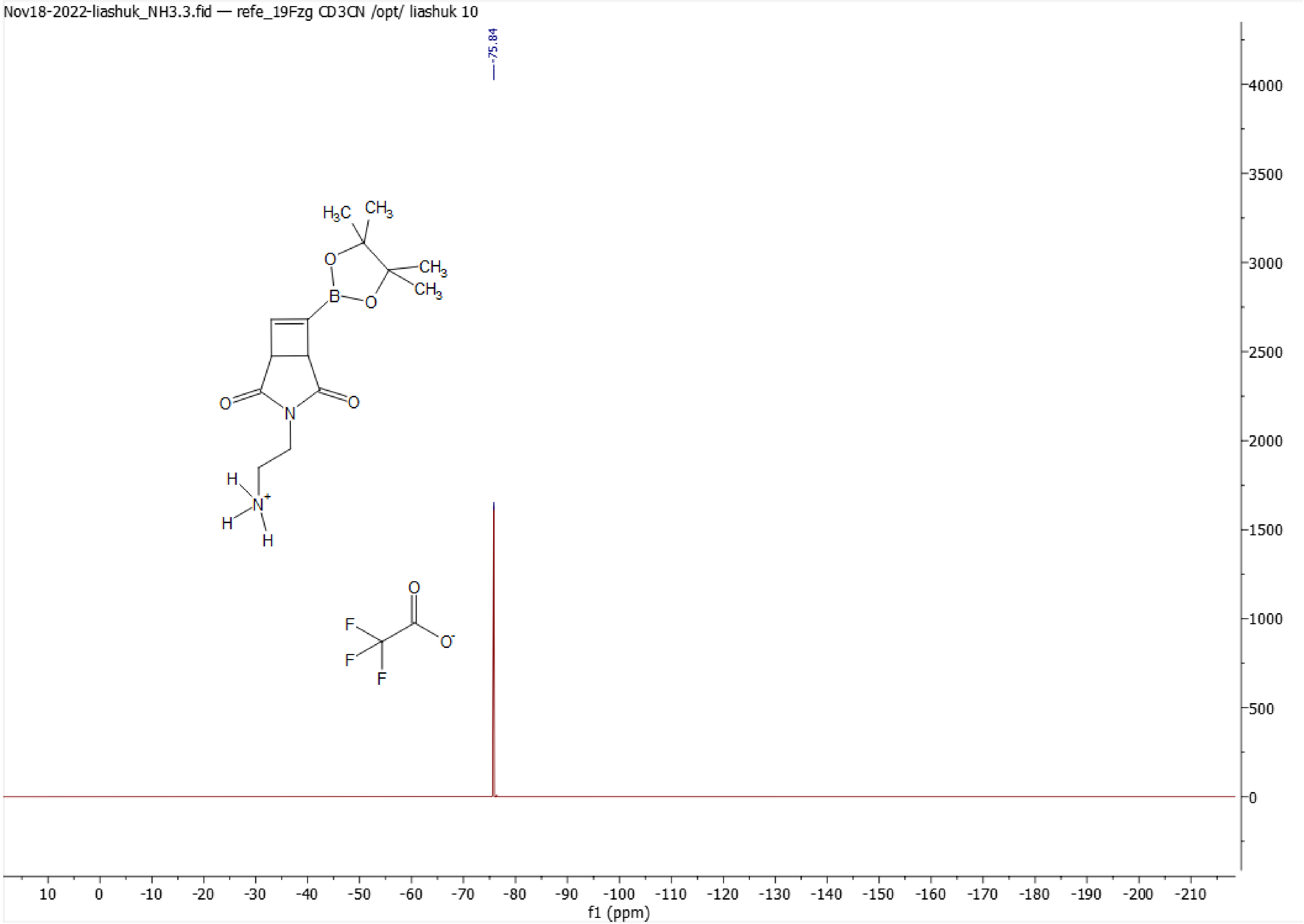

*Spectrum 51. 2-(2,4-dioxo-6-(4,4,5,5-tetramethyl-1,3,2-dioxaborolan-2-yl)-3-azabicyclo[3.2.0]hept-6-en-3-yl)ethan-1-aminium trifluoroacetate **8j**, ^{19}F NMR (376 MHz, CD_3CN)*

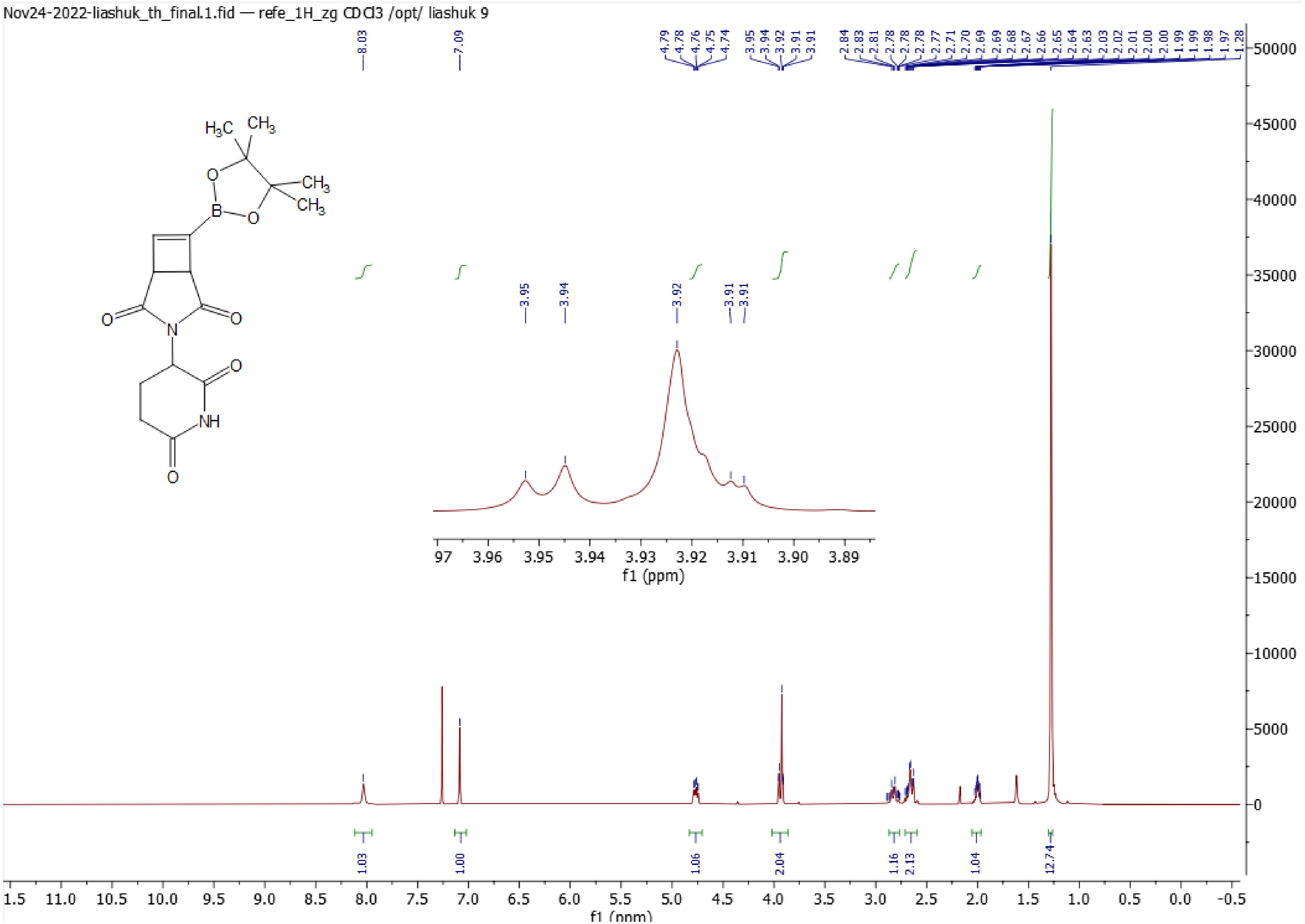

Spectrum 52. 3-(2,6-dioxopiperidin-3-yl)-6-(4,4,5,5-tetramethyl-1,3,2-dioxaborolan-2-yl)-3-azabicyclo[3.2.0]hept-6-ene-2,4-dione **8n**, ^1H NMR (400 MHz, $CDCl_3$)

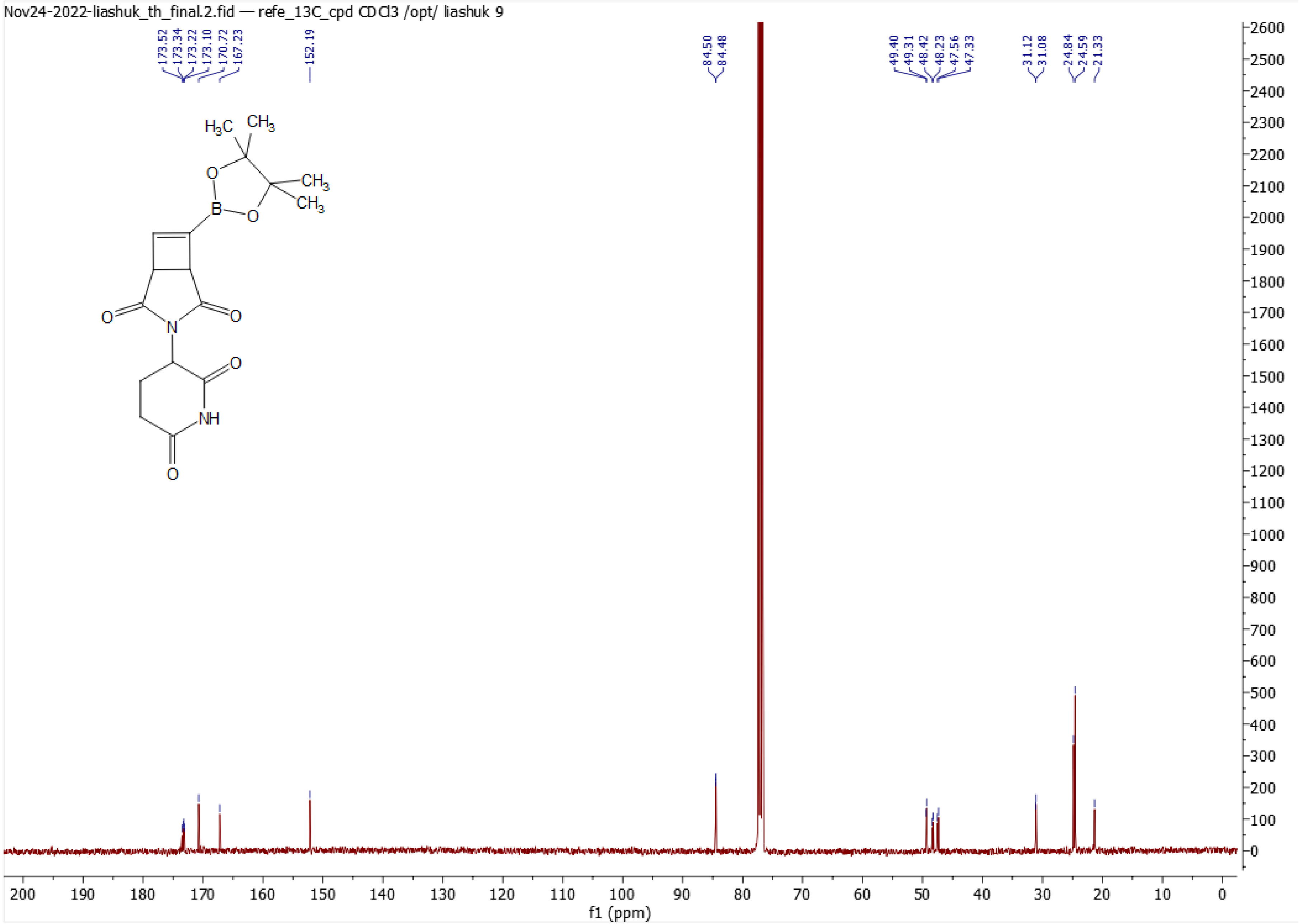

Spectrum 53. 3-(2,6-dioxopiperidin-3-yl)-6-(4,4,5,5-tetramethyl-1,3,2-dioxaborolan-2-yl)-3-azabicyclo[3.2.0]hept-6-ene-2,4-dione ***8n****, ^{13}C NMR (101 MHz, CDCl$_3$)*

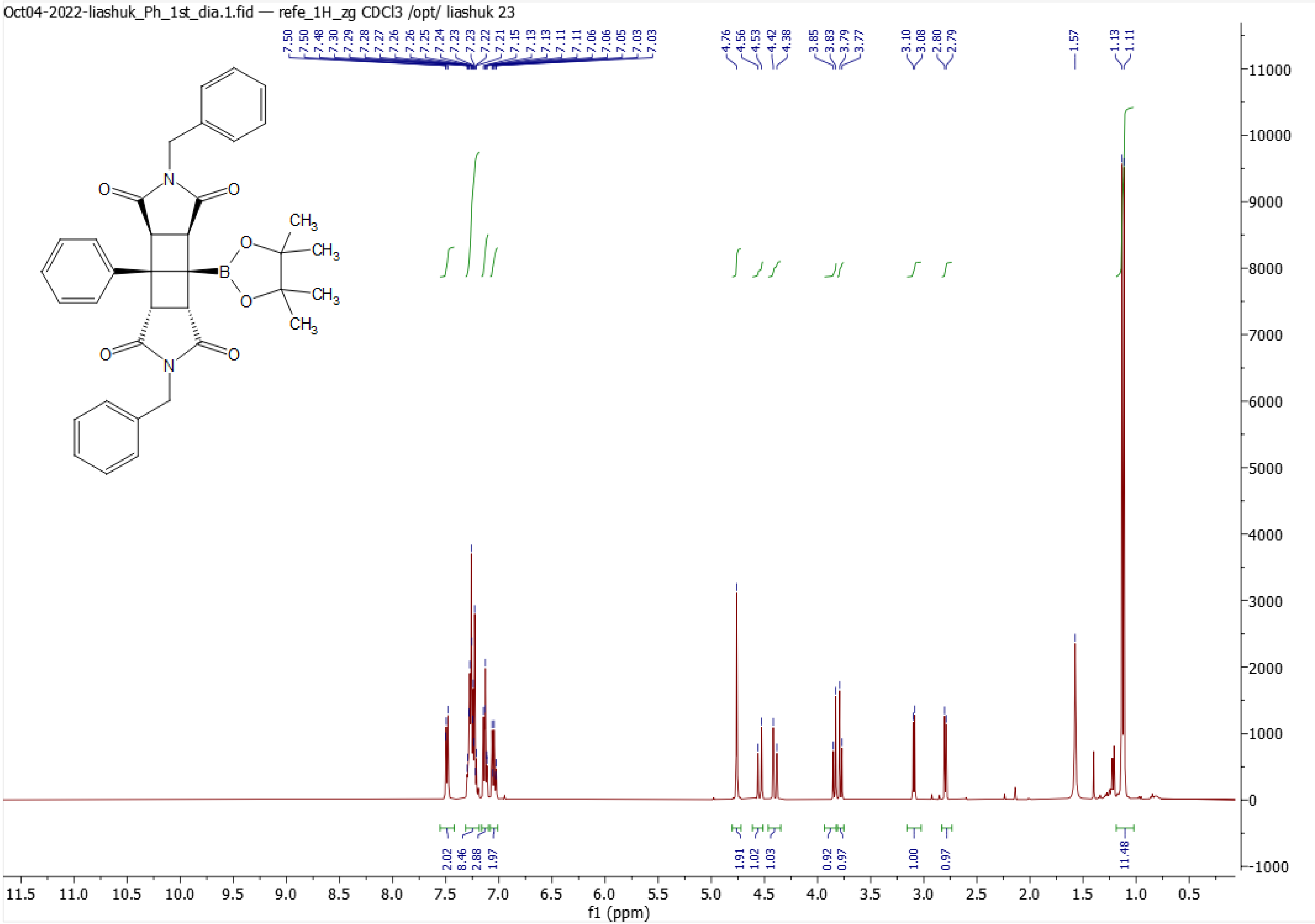

Spectrum 54. (2S,6R,8R,12S)-4,10-dibenzyl-1-phenyl-7-(4,4,5,5-tetramethyl-1,3,2-dioxaborolan-2-yl)-4,10-diazatetracyclo[5.5.0.02,6.08,12]dodecane-3,5,9,11-tetrone ***9a****, ^{1}H NMR (400 MHz, CDCl$_3$)*

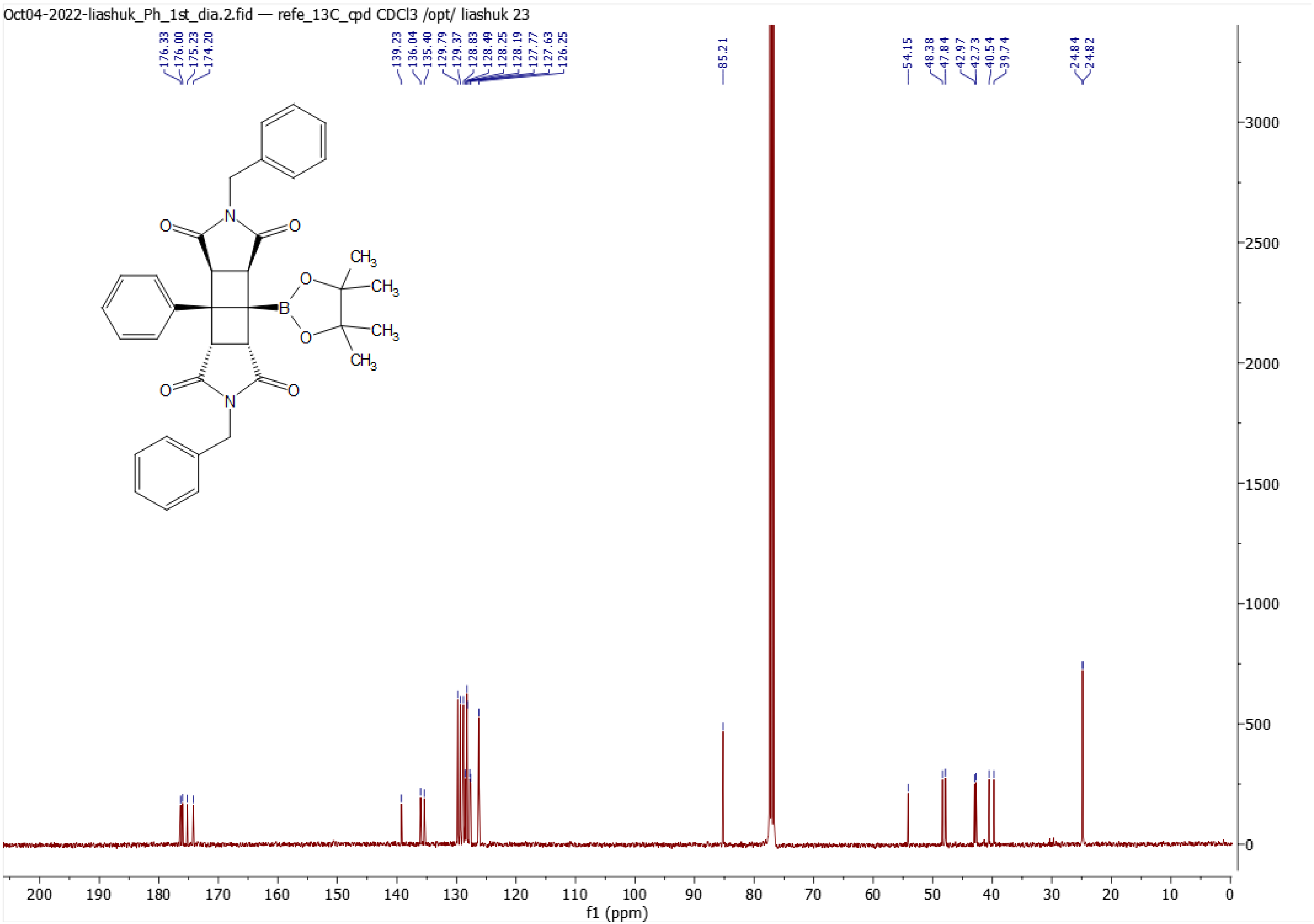

Spectrum 55. (2S,6R,8R,12S)-4,10-dibenzyl-1-phenyl-7-(4,4,5,5-tetramethyl-1,3,2-dioxaborolan-2-yl)-4,10-diazatetracyclo[5.5.0.02,6.08,12]dodecane-3,5,9,11-tetrone ***9a****, ^{13}C NMR (101 MHz, CDCl$_3$)*

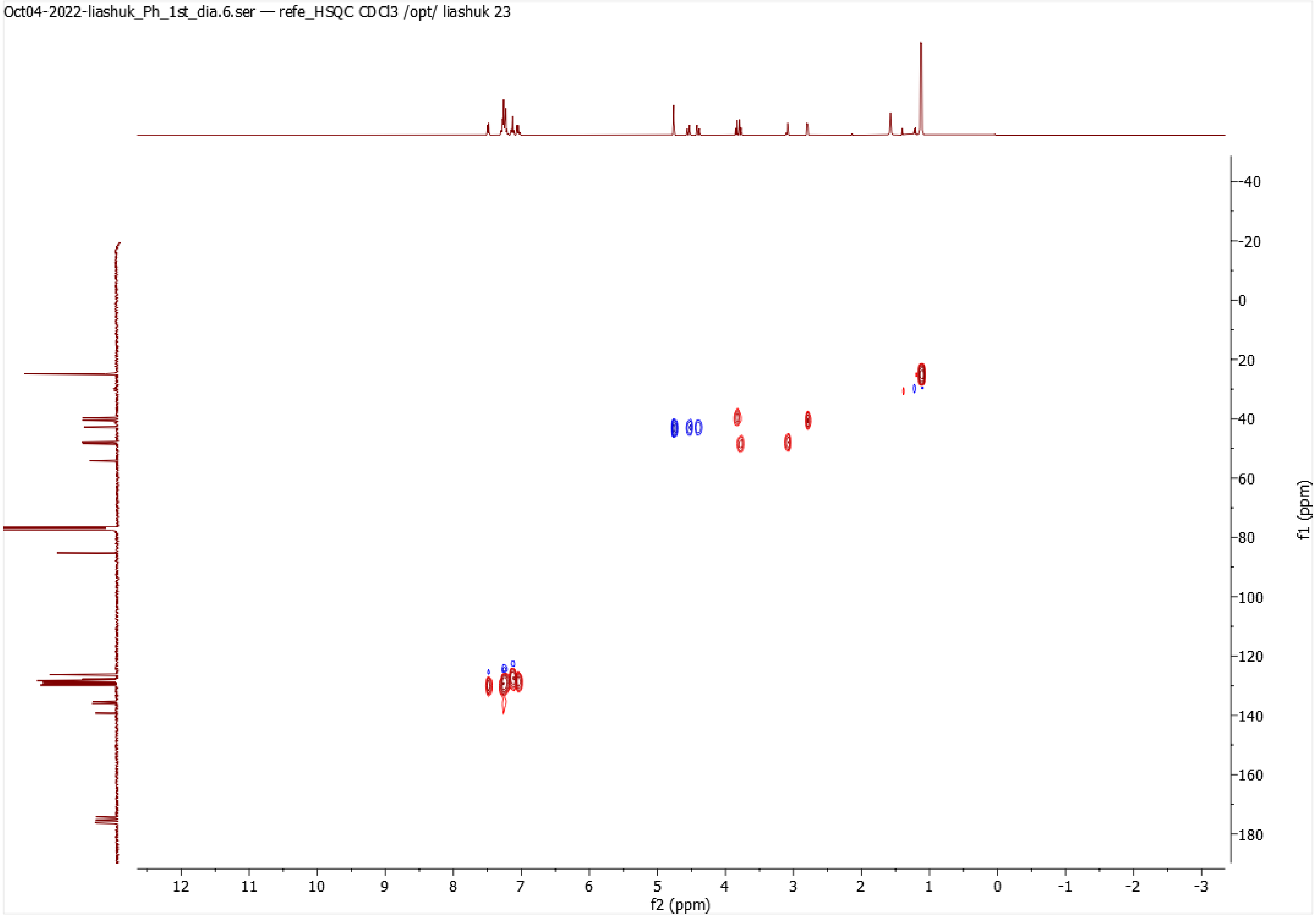

Spectrum 56. (2S,6R,8R,12S)-4,10-dibenzyl-1-phenyl-7-(4,4,5,5-tetramethyl-1,3,2-dioxaborolan-2-yl)-4,10-diazatetracyclo[5.5.0.02,6.08,12]dodecane-3,5,9,11-tetrone ***9a****, HSQC (400/101 MHz, $CDCl_3$), full spectrum*

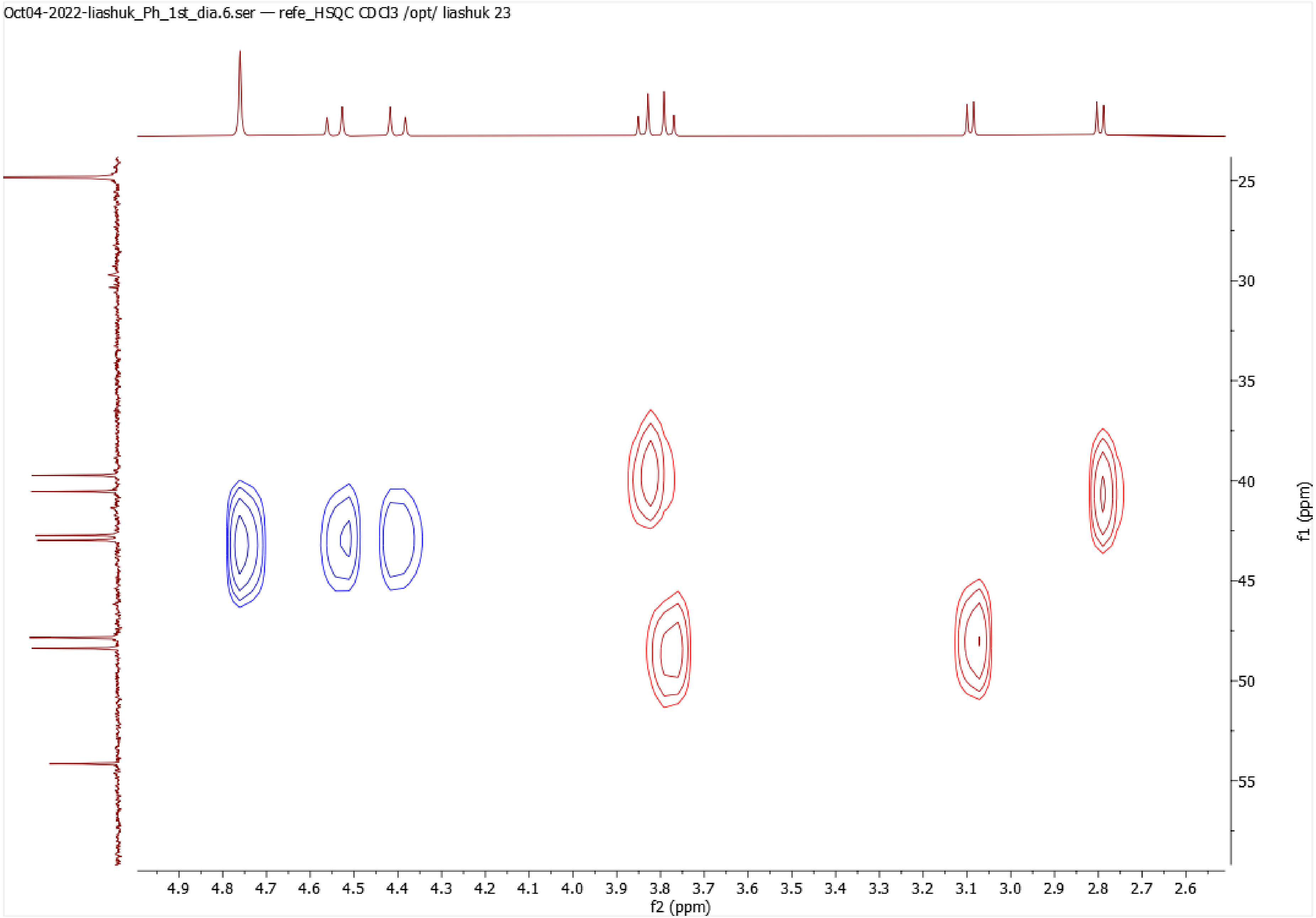

*Spectrum 57. (2S,6R,8R,12S)-4,10-dibenzyl-1-phenyl-7-(4,4,5,5-tetramethyl-1,3,2-dioxaborolan-2-yl)-4,10-diazatetracyclo[5.5.0.02,6.08,12]dodecane-3,5,9,11-tetrone **9a**, HSQC (400/101 MHz, $CDCl_3$), aliphatic region*

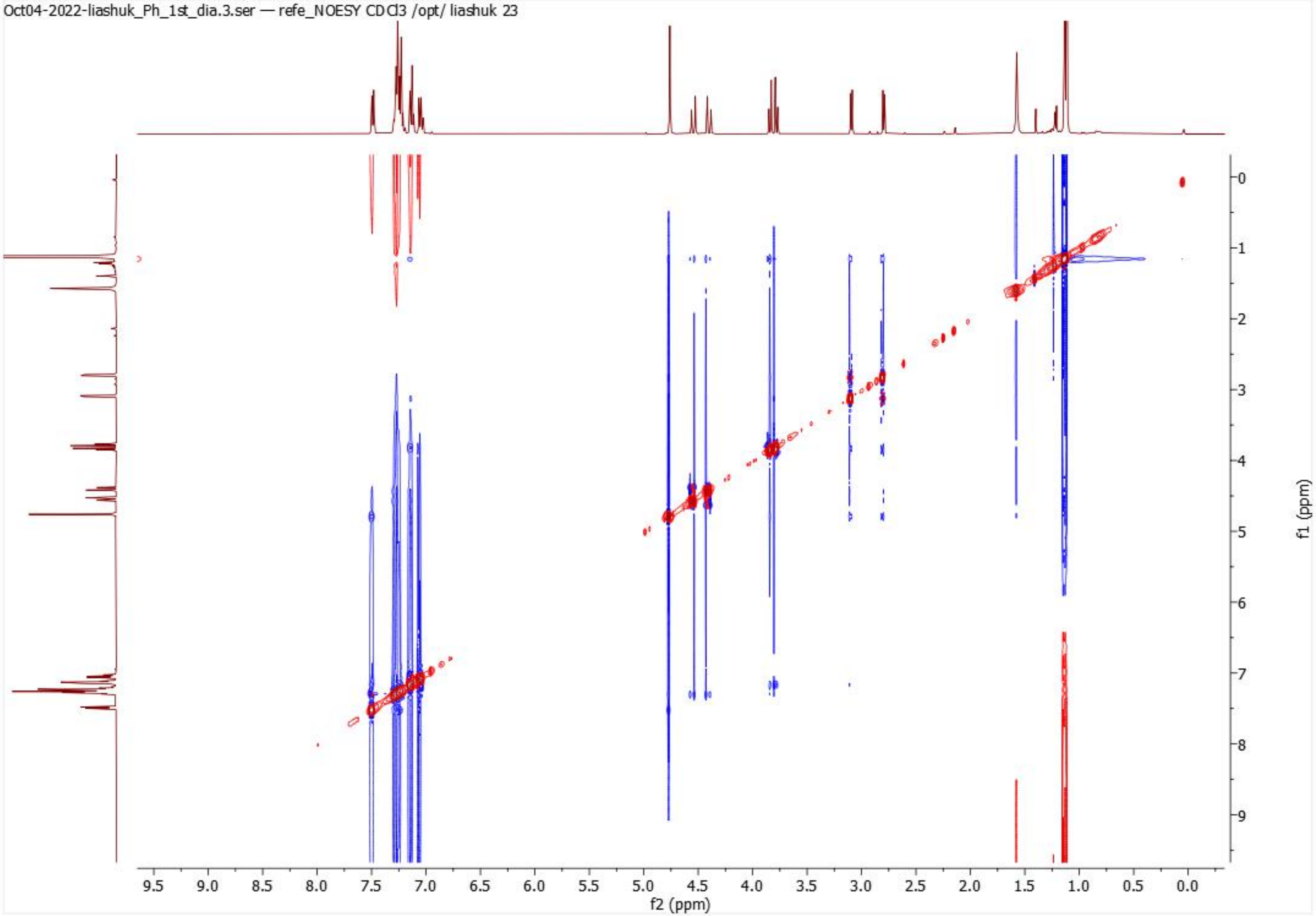

Spectrum 58. (2S,6R,8R,12S)-4,10-dibenzyl-1-phenyl-7-(4,4,5,5-tetramethyl-1,3,2-dioxaborolan-2-yl)-4,10-diazatetracyclo[5.5.0.02,6.08,12]dodecane-3,5,9,11-tetrone ***9a****, NOESY (400 MHz, $CDCl_3$)*

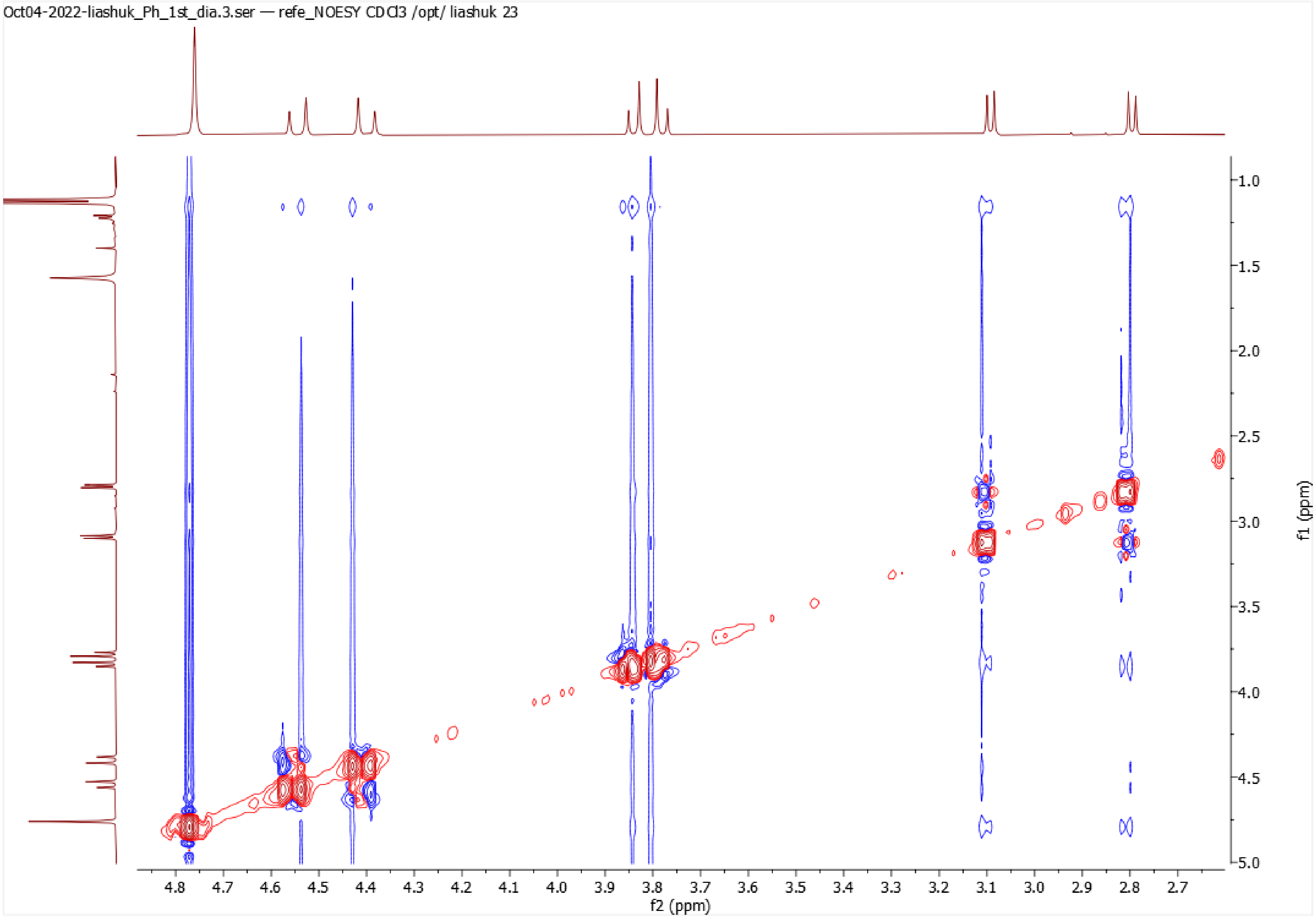

*Spectrum 59. (2S,6R,8R,12S)-4,10-dibenzyl-1-phenyl-7-(4,4,5,5-tetramethyl-1,3,2-dioxaborolan-2-yl)-4,10-diazatetracyclo[5.5.0.02,6.08,12]dodecane-3,5,9,11-tetrone **9a**, NOESY (400 MHz, $CDCl_3$), aliphatic region*

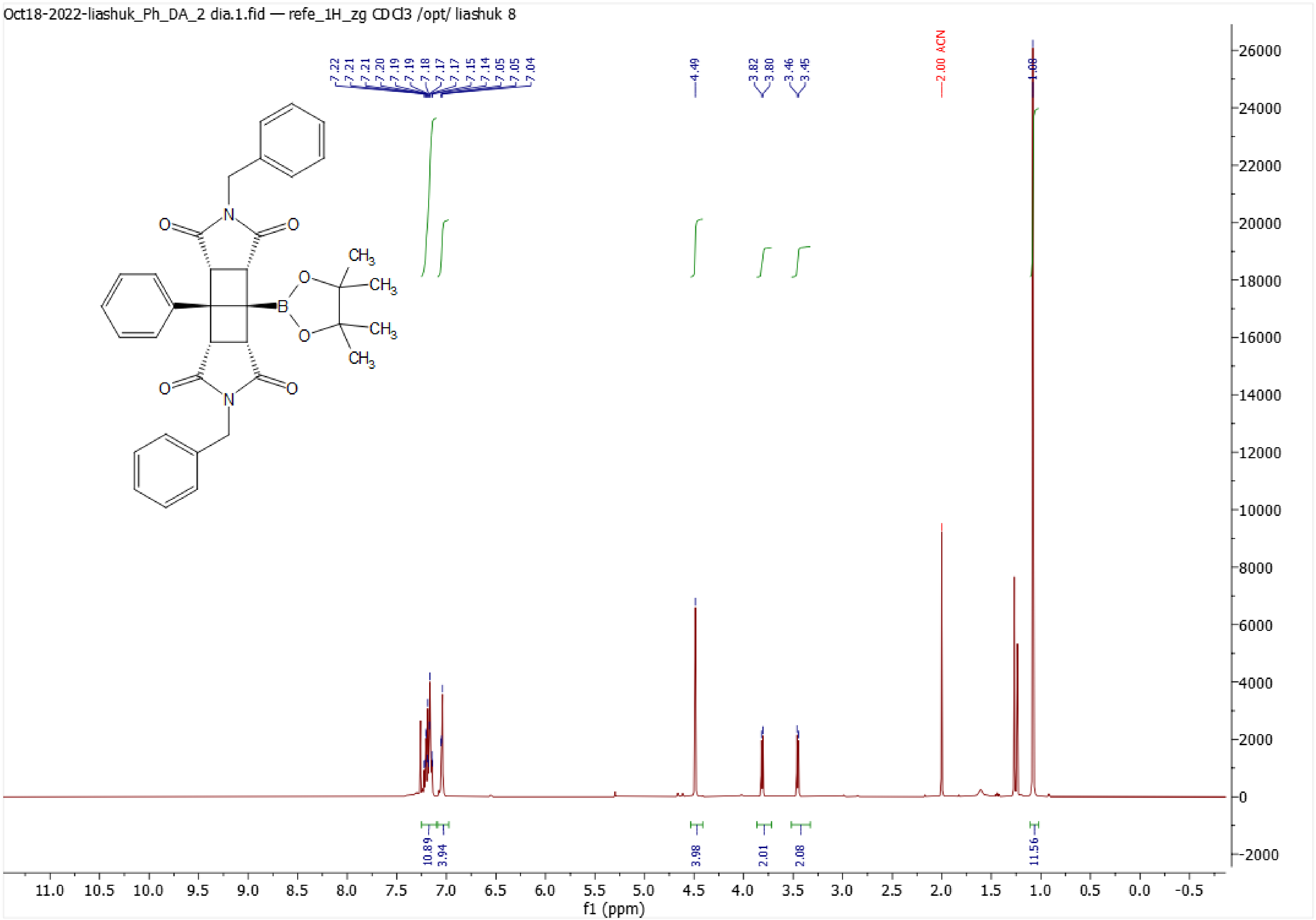

*Spectrum 60. (1R,2R,6S,7R,8R,12S)-4,10-dibenzyl-1-phenyl-7-(4,4,5,5-tetramethyl-1,3,2-dioxaborolan-2-yl)-4,10-diazatetracyclo[5.5.0.02,6.08,12]dodecane-3,5,9,11-tetrone **9'a**, ^{1}H NMR (400 MHz, CDCl$_3$)*

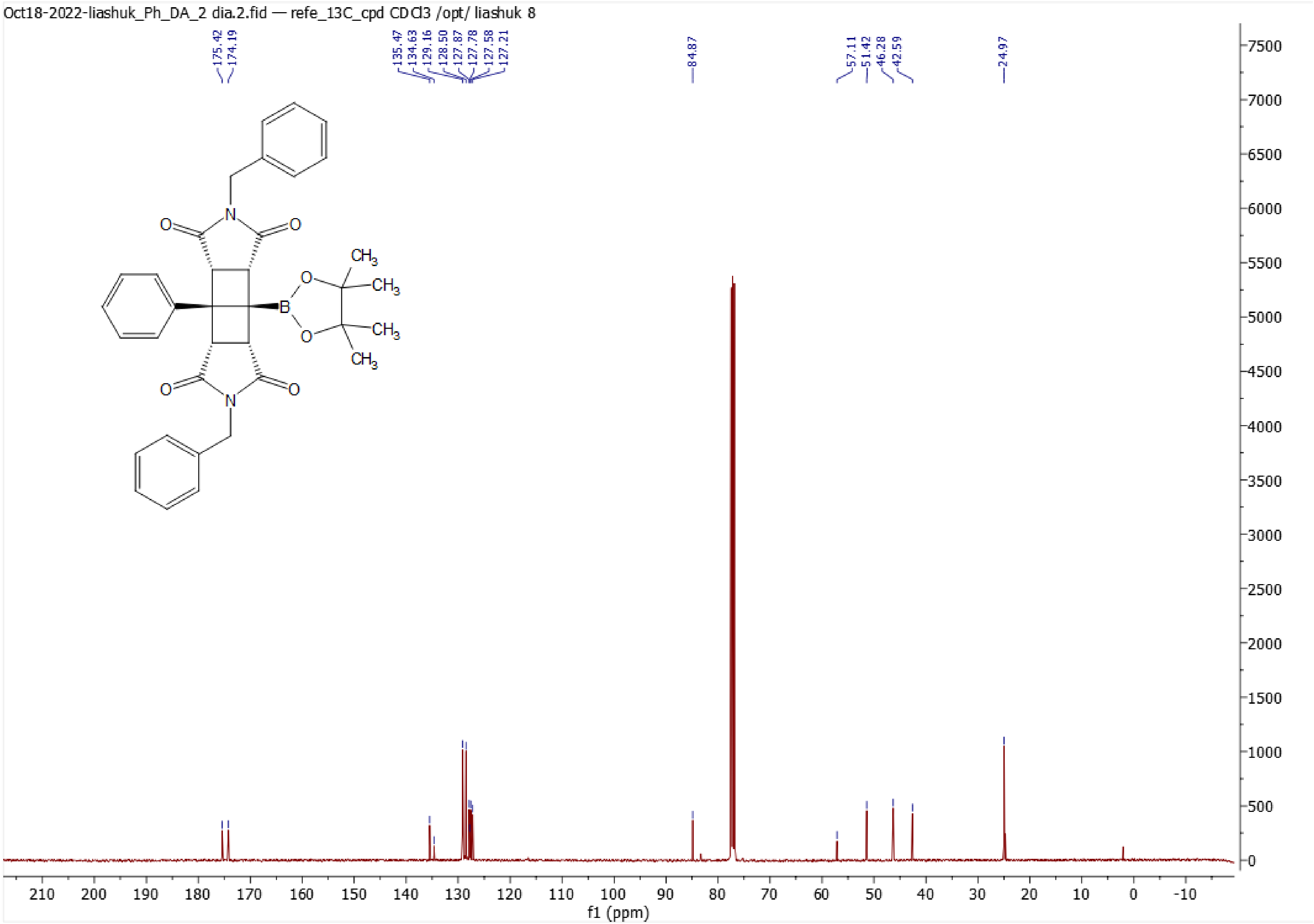

*Spectrum 61. (1r,2R,6S,7r,8R,12S)-4,10-dibenzyl-1-phenyl-7-(4,4,5,5-tetramethyl-1,3,2-dioxaborolan-2-yl)-4,10-diazatetracyclo[5.5.0.02,6.08,12]dodecane-3,5,9,11-tetrone **9a'**, ^{13}C NMR (101 MHz, CDCl$_3$)*

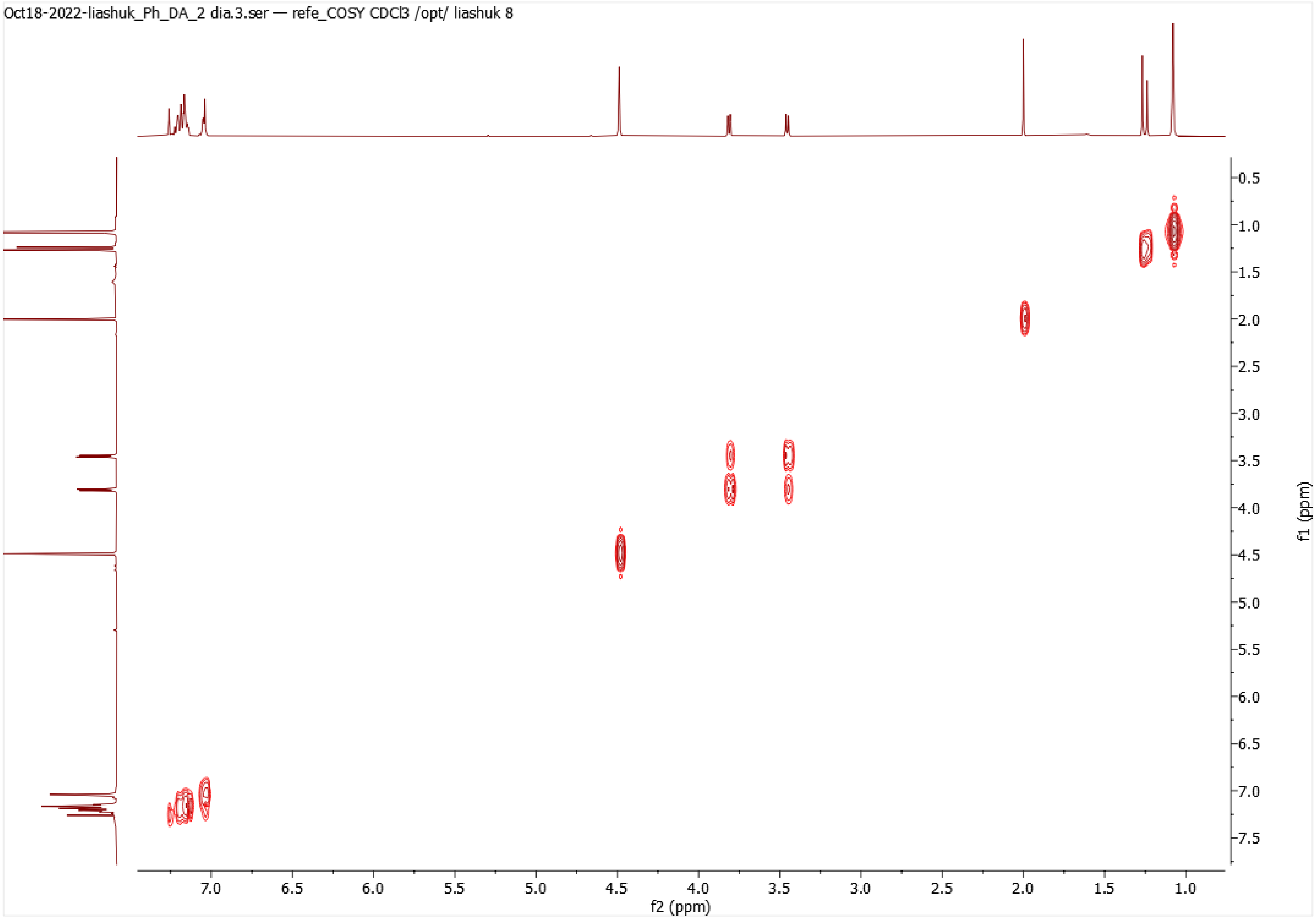

*Spectrum 62. (1r,2R,6S,7r,8R,12S)-4,10-dibenzyl-1-phenyl-7-(4,4,5,5-tetramethyl-1,3,2-dioxaborolan-2-yl)-4,10-diazatetracyclo[5.5.0.02,6.08,12]dodecane-3,5,9,11-tetrone **9a'**, COSY (400 MHz, CDCl3)*

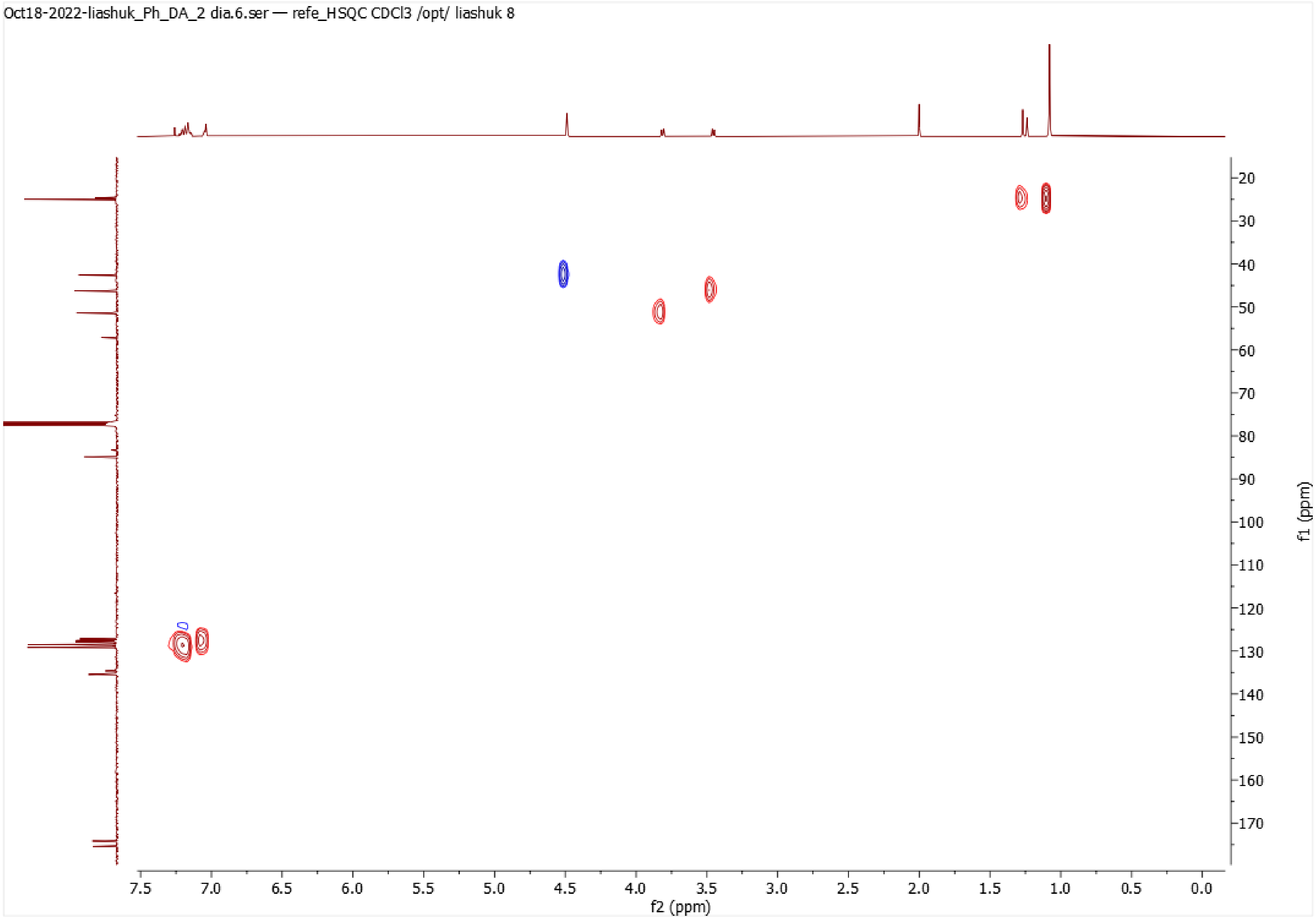

*Spectrum 63. (1r,2R,6S,7r,8R,12S)-4,10-dibenzyl-1-phenyl-7-(4,4,5,5-tetramethyl-1,3,2-dioxaborolan-2-yl)-4,10-diazatetracyclo[5.5.0.02,6.08,12]dodecane-3,5,9,11-tetrone **9a'**, HSQC (400/101 MHz, CDCl3)*

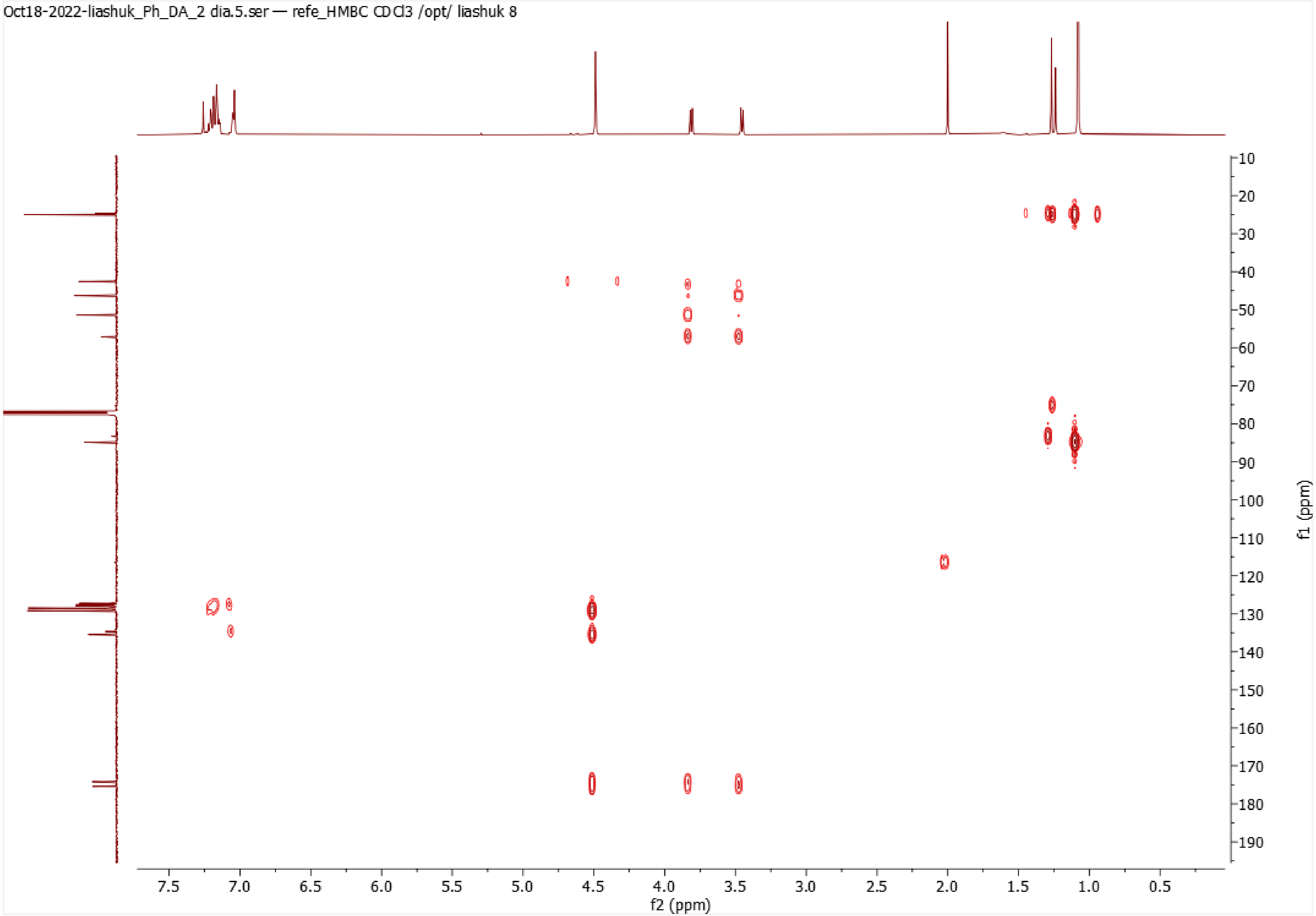

*Spectrum 64. (1r,2R,6S,7r,8R,12S)-4,10-dibenzyl-1-phenyl-7-(4,4,5,5-tetramethyl-1,3,2-dioxaborolan-2-yl)-4,10-diazatetracyclo[5.5.0.02,6.08,12]dodecane-3,5,9,11-tetrone **9a'**, HMBC (400/101 MHz, CDCl3)*

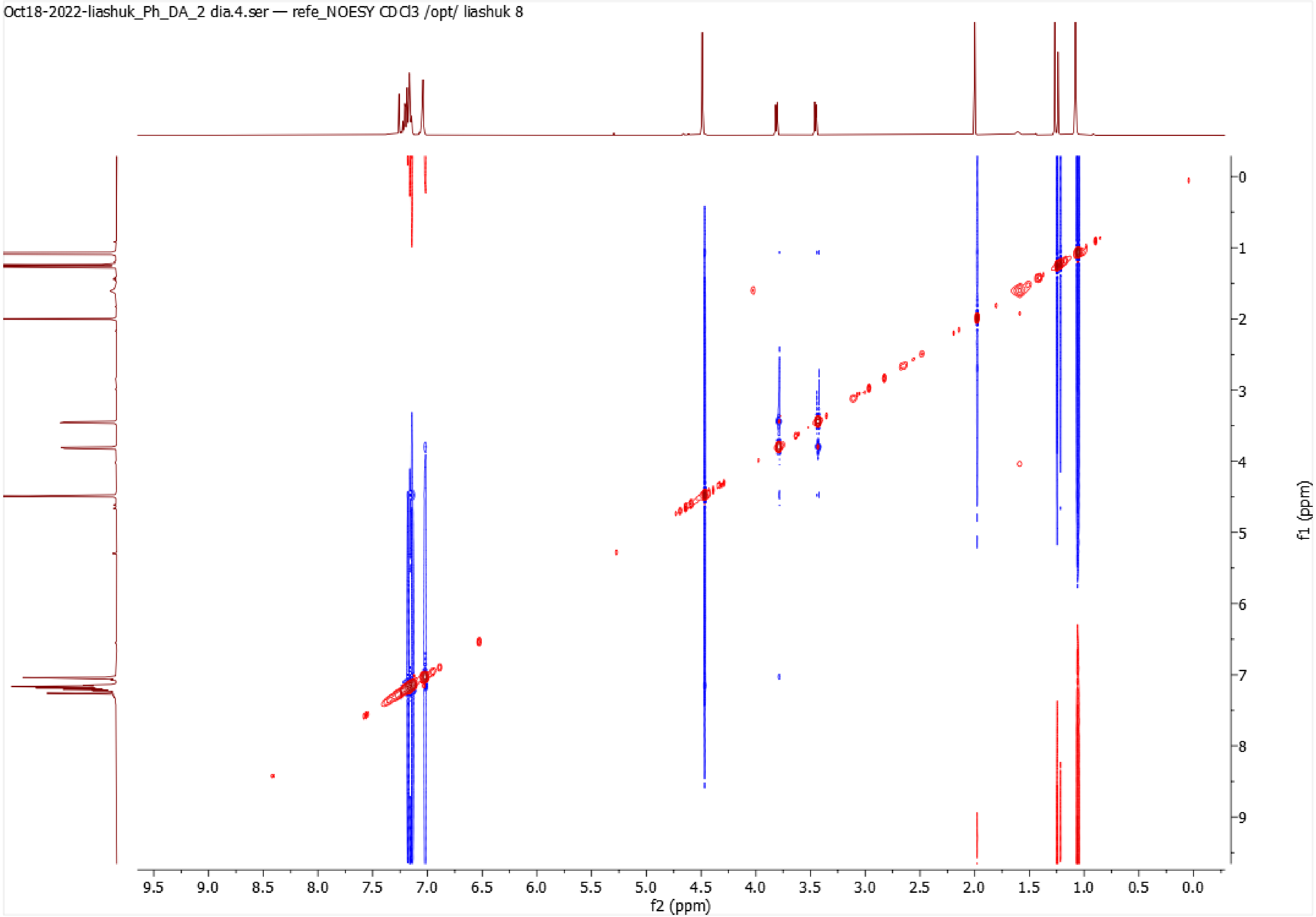

Spectrum 65. (1R,2R,6S,7R,8R,12S)-4,10-dibenzyl-1-phenyl-7-(4,4,5,5-tetramethyl-1,3,2-dioxaborolan-2-yl)-4,10-diazatetracyclo[5.5.0.02,6.08,12]dodecane-3,5,9,11-tetrone **9a'**, NOESY (400 MHz, CDCl3)

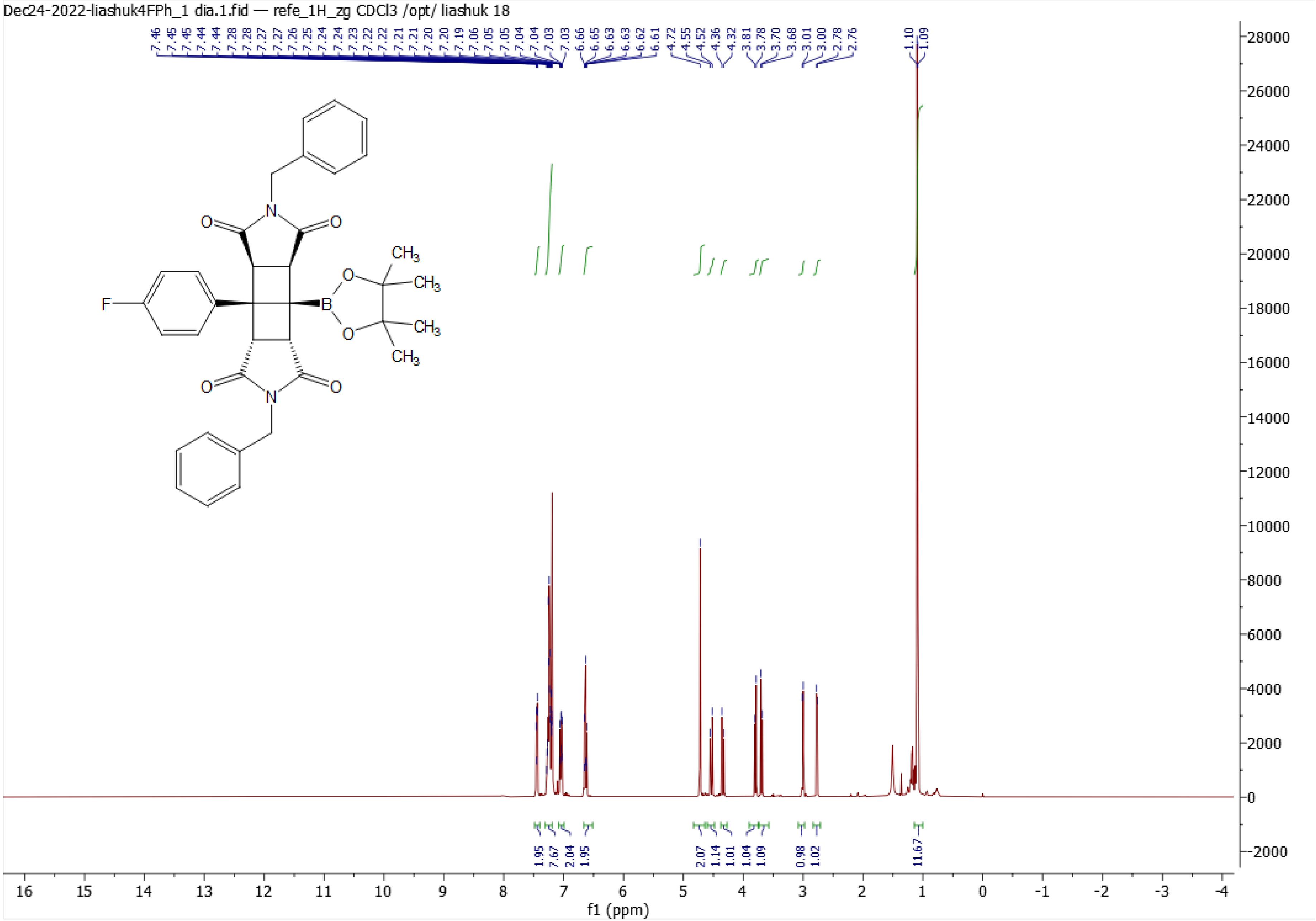

*Spectrum 66. (2S,6R,8R,12S)-4,10-dibenzyl-1-(4-fluorophenyl)-7-(4,4,5,5-tetramethyl-1,3,2-dioxaborolan-2-yl)-4,10-diazatetracyclo[5.5.0.02,6.08,12]dodecane-3,5,9,11-tetrone **9b**, ^{1}H NMR (400 MHz, $CDCl_3$)*

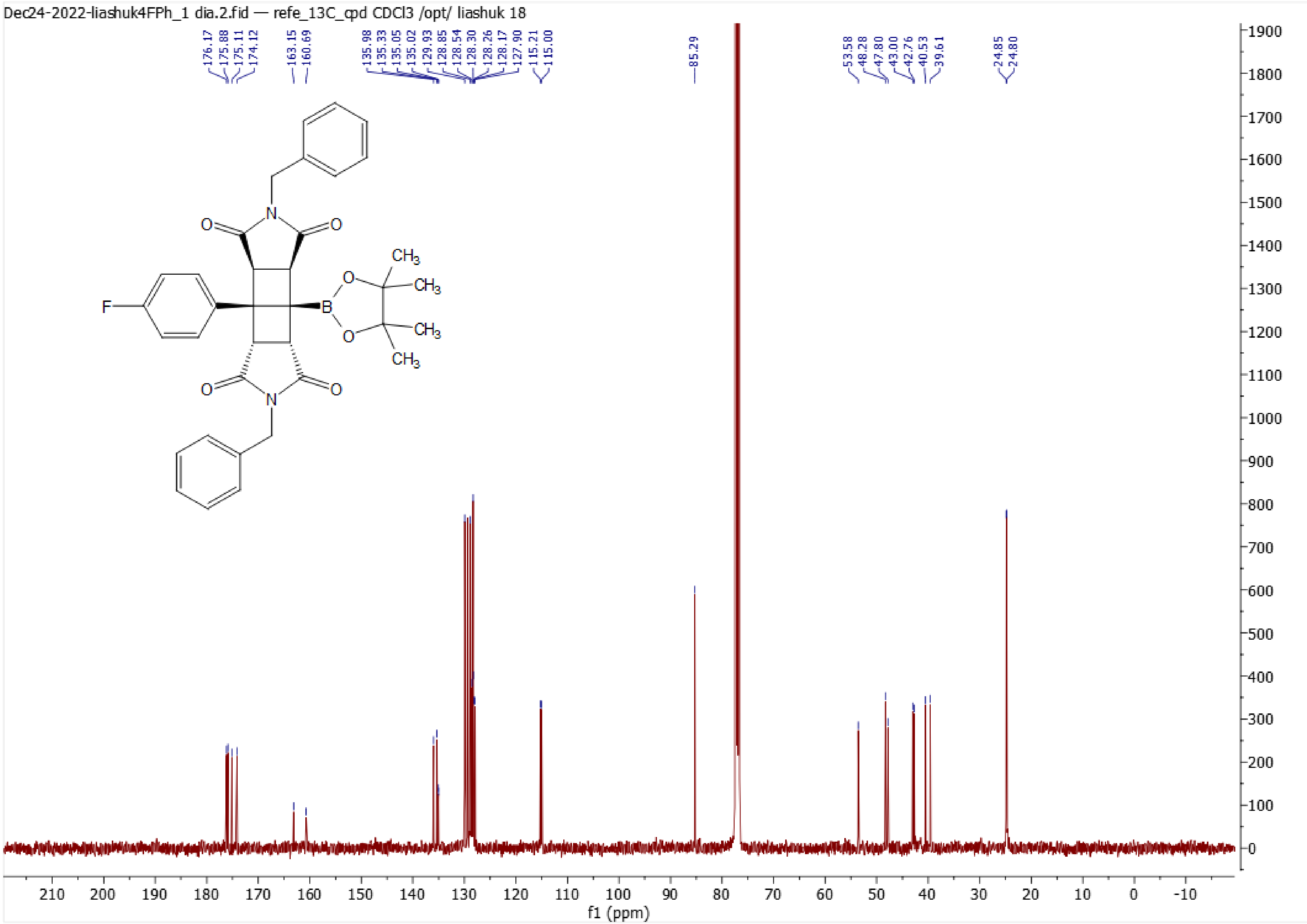

*Spectrum 67. (2S,6R,8R,12S)-4,10-dibenzyl-1-(4-fluorophenyl)-7-(4,4,5,5-tetramethyl-1,3,2-dioxaborolan-2-yl)-4,10-diazatetracyclo[5.5.0.02,6.08,12]dodecane-3,5,9,11-tetrone **9b**, ^{13}C NMR (101 MHz, CDCl$_3$)*

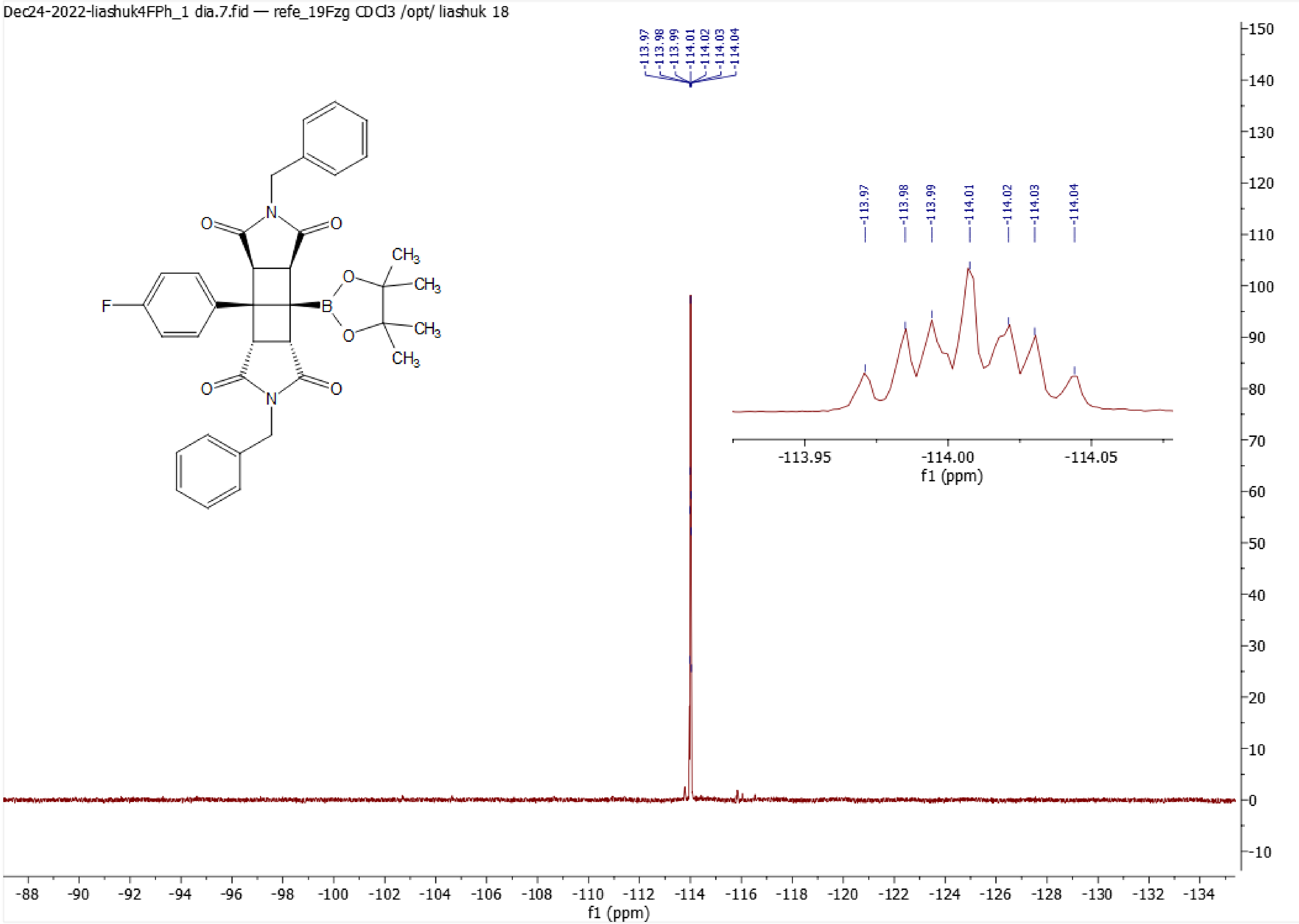

Spectrum 68. (2S,6R,8R,12S)-4,10-dibenzyl-1-(4-fluorophenyl)-7-(4,4,5,5-tetramethyl-1,3,2-dioxaborolan-2-yl)-4,10-diazatetracyclo[5.5.0.02,6.08,12]dodecane-3,5,9,11-tetrone ***9b**, ^{19}F NMR (376 MHz, CDCl$_3$)*

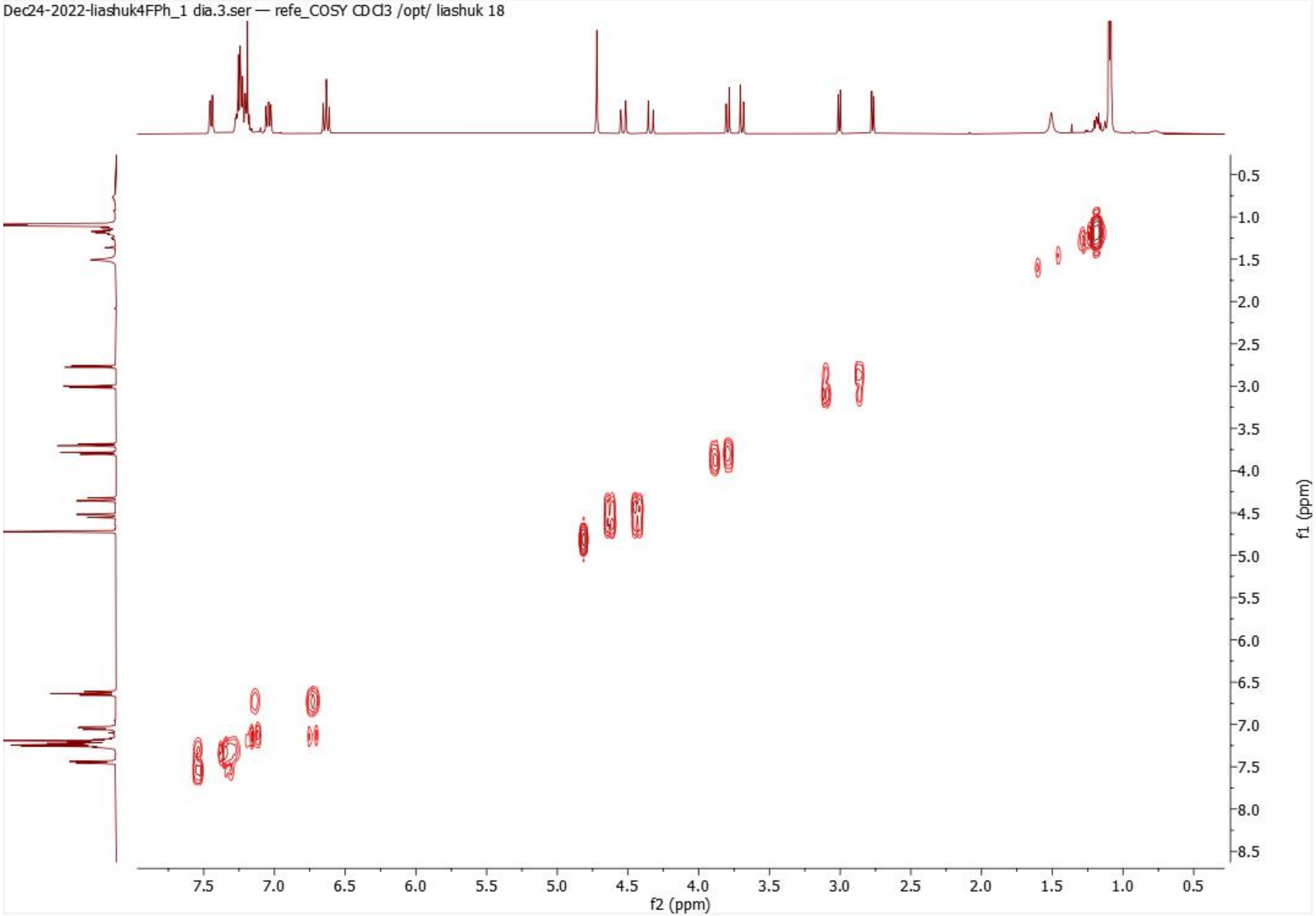

Spectrum 69. (2S,6R,8R,12S)-4,10-dibenzyl-1-(4-fluorophenyl)-7-(4,4,5,5-tetramethyl-1,3,2-dioxaborolan-2-yl)-4,10-diazatetracyclo[5.5.0.02,6.08,12]dodecane-3,5,9,11-tetrone ***9b****, COSY (400 MHz, CDCl3)*

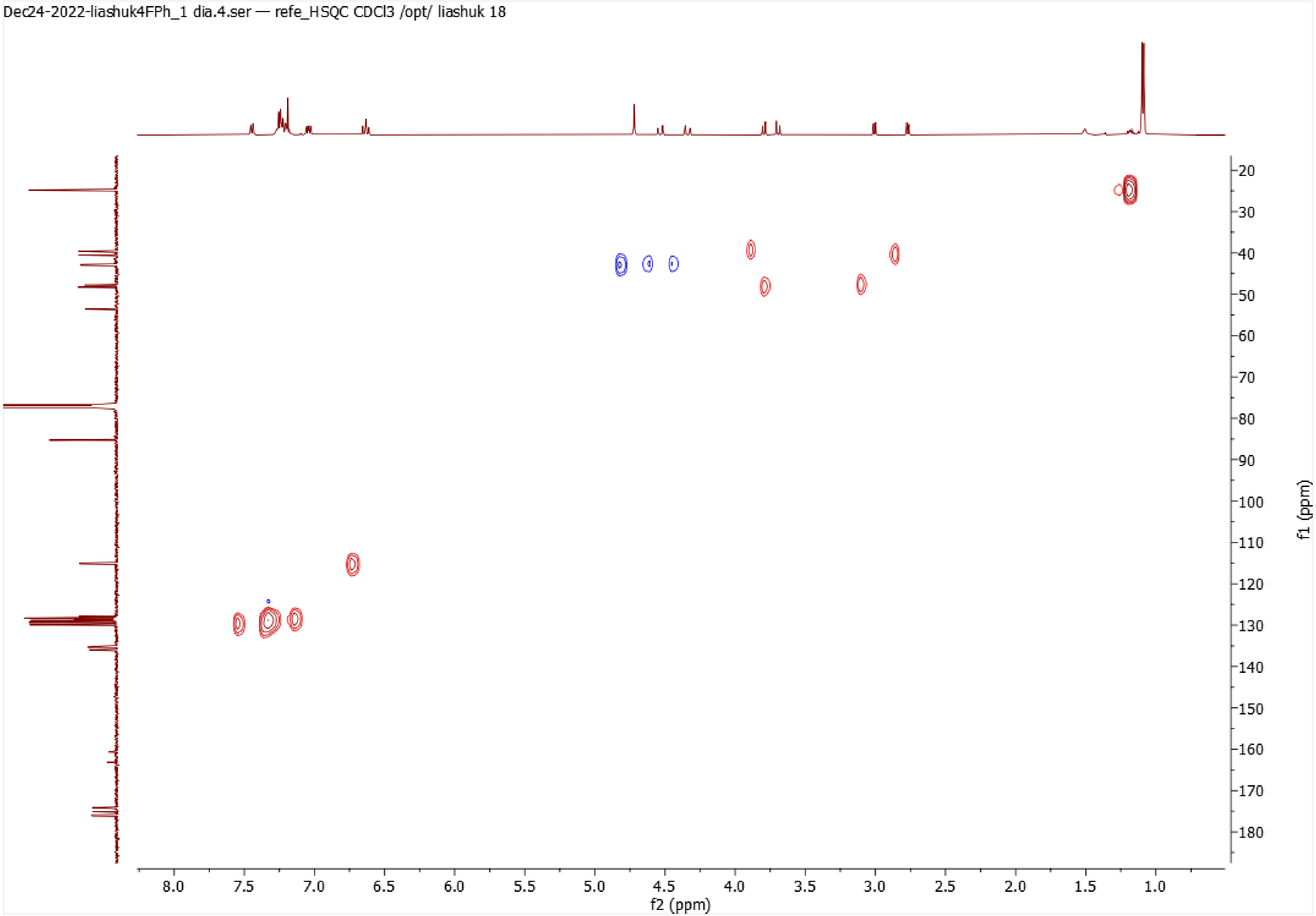

*Spectrum 70. (2S,6R,8R,12S)-4,10-dibenzyl-1-(4-fluorophenyl)-7-(4,4,5,5-tetramethyl-1,3,2-dioxaborolan-2-yl)-4,10-diazatetracyclo[5.5.0.02,6.08,12]dodecane-3,5,9,11-tetrone **9b**, HSQC (400/101 MHz, CDCl3)*

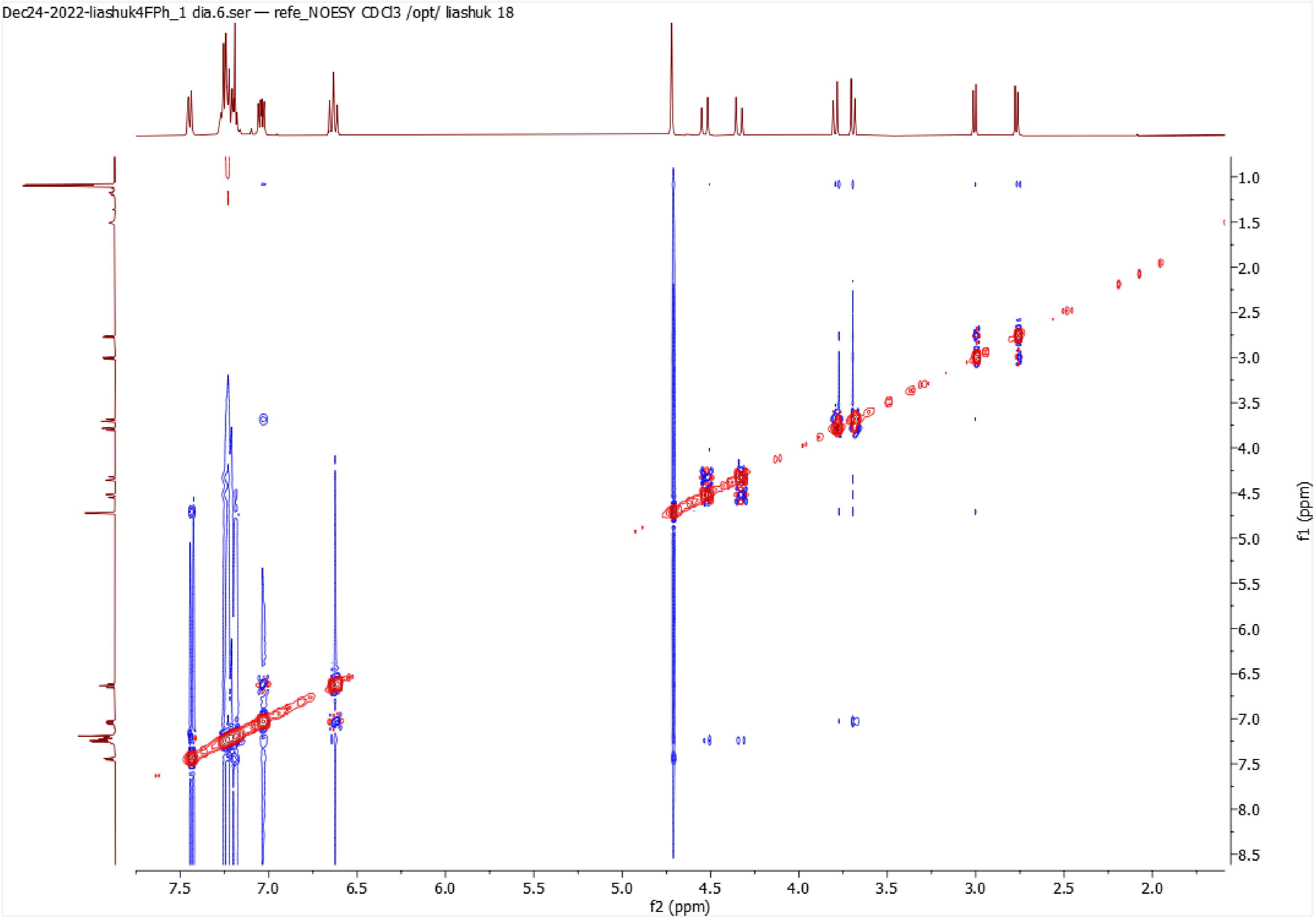

Spectrum 71. (2S,6R,8R,12S)-4,10-dibenzyl-1-(4-fluorophenyl)-7-(4,4,5,5-tetramethyl-1,3,2-dioxaborolan-2-yl)-4,10-diazatetracyclo[5.5.0.02,6.08,12]dodecane-3,5,9,11-tetrone ***9b****, NOESY (400 MHz, CDCl3)*

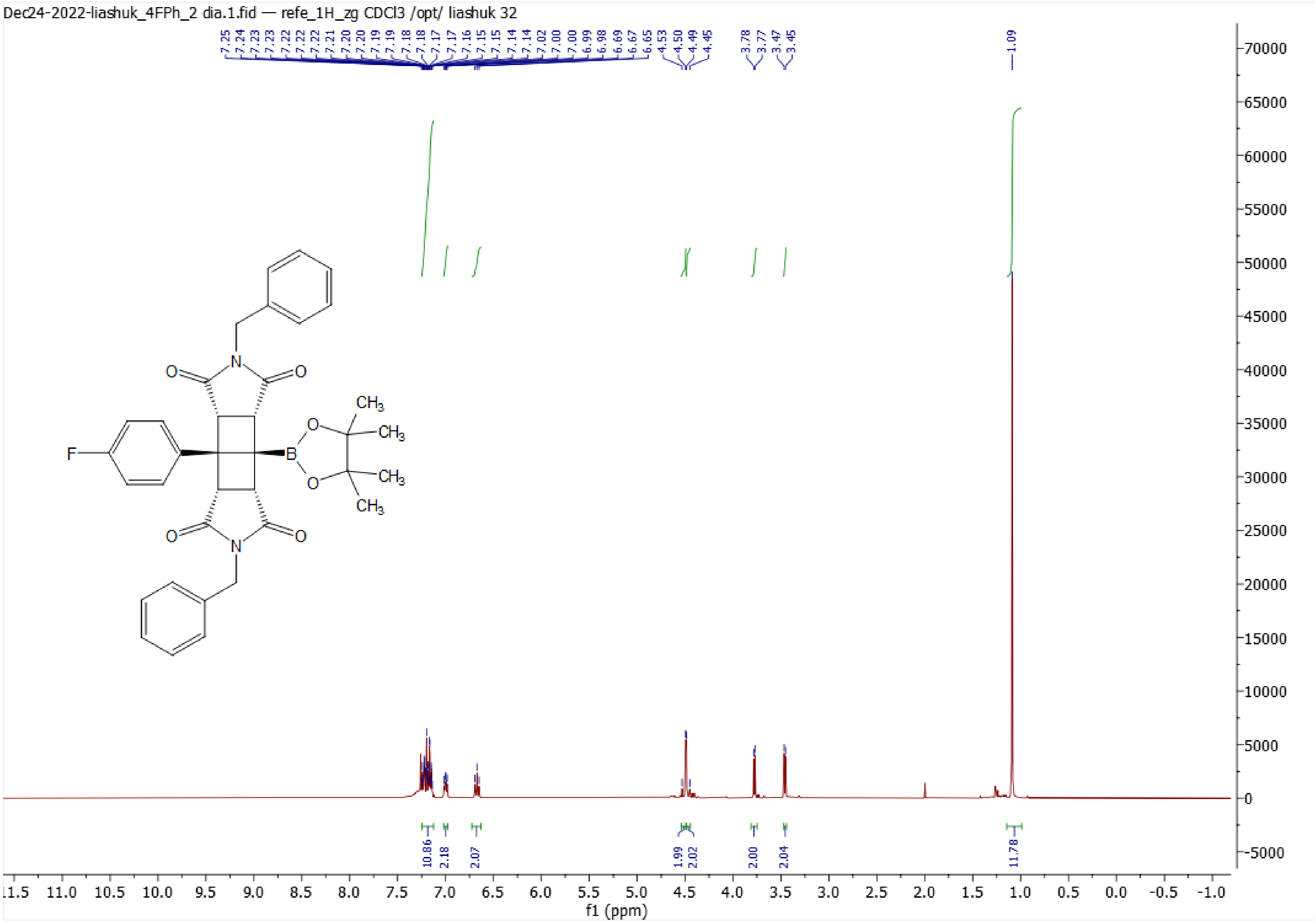

Spectrum 72. (1r,2R,6S,7r,8R,12S)-4,10-dibenzyl-1-(4-fluorophenyl)-7-(4,4,5,5-tetramethyl-1,3,2-dioxaborolan-2-yl)-4,10-diazatetracyclo[5.5.0.02,6.08,12]dodecane-3,5,9,11-tetrone ***9b'****, ^{1}H NMR (400 MHz, CDCl$_3$)*

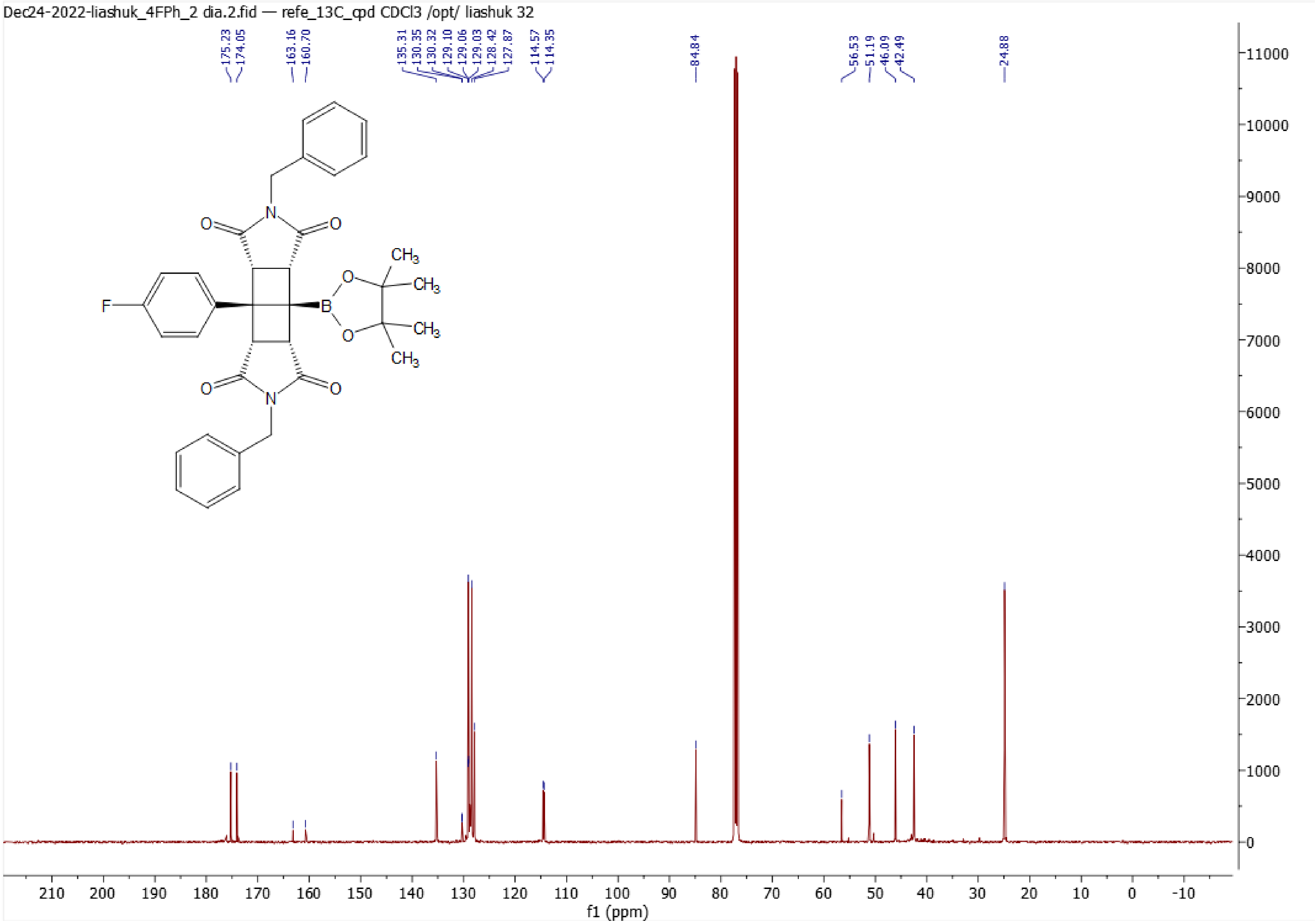

Spectrum 73. (1r,2R,6S,7r,8R,12S)-4,10-dibenzyl-1-(4-fluorophenyl)-7-(4,4,5,5-tetramethyl-1,3,2-dioxaborolan-2-yl)-4,10-diazatetracyclo[5.5.0.02,6.08,12]dodecane-3,5,9,11-tetrone ***9b'***, *^{13}C NMR (101 MHz, CDCl$_3$)*

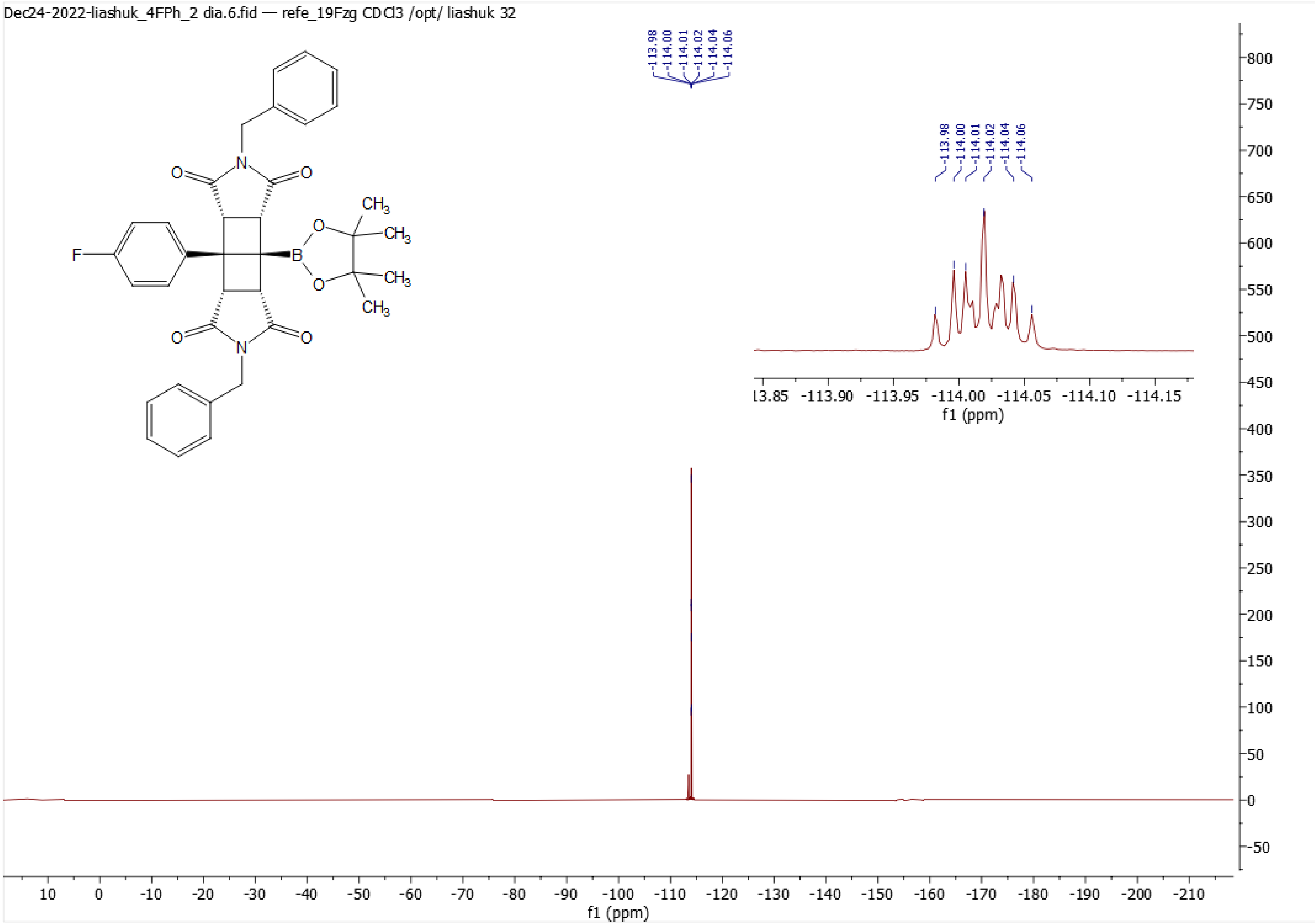

*Spectrum 74. (1r,2R,6S,7r,8R,12S)-4,10-dibenzyl-1-(4-fluorophenyl)-7-(4,4,5,5-tetramethyl-1,3,2-dioxaborolan-2-yl)-4,10-diazatetracyclo[5.5.0.02,6.08,12]dodecane-3,5,9,11-tetrone **9b'**, ^{19}F NMR (376 MHz, CDCl$_3$)*

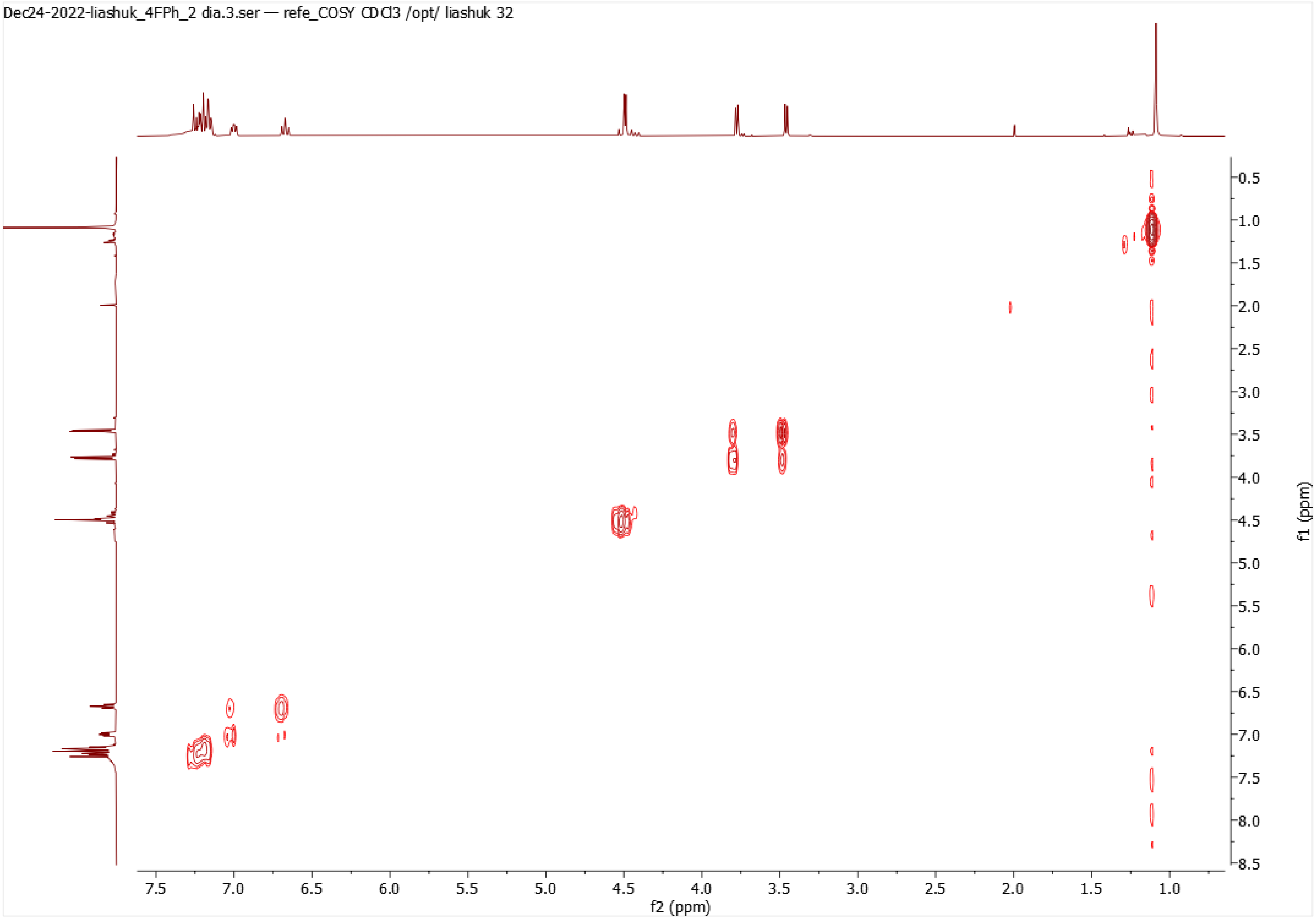

Spectrum 75. (1r,2R,6S,7r,8R,12S)-4,10-dibenzyl-1-(4-fluorophenyl)-7-(4,4,5,5-tetramethyl-1,3,2-dioxaborolan-2-yl)-4,10-diazatetracyclo[5.5.0.02,6.08,12]dodecane-3,5,9,11-tetrone ***9b'****, COSY (400 MHz, CDCl3)*

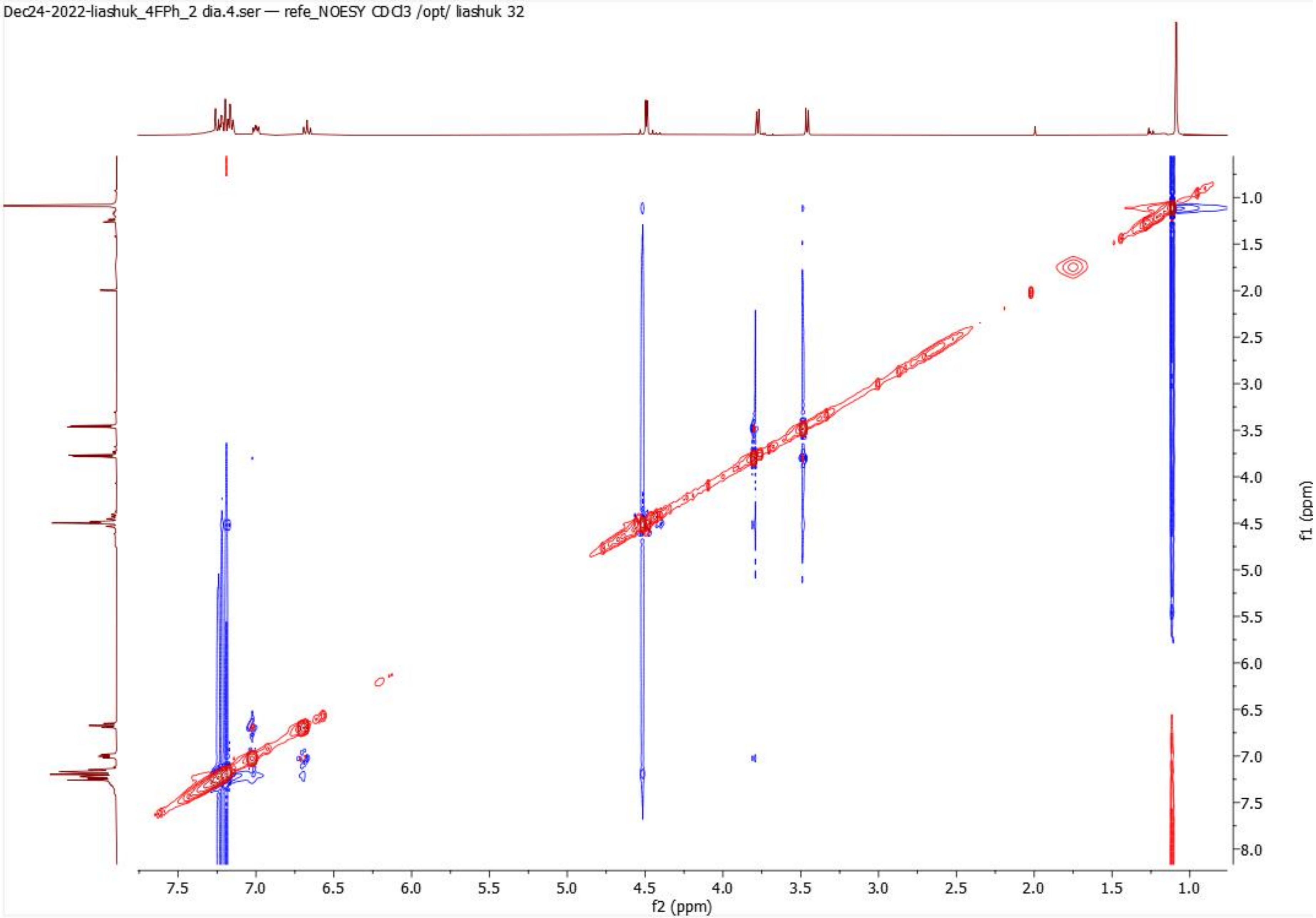

*Spectrum 76. (1r,2R,6S,7r,8R,12S)-4,10-dibenzyl-1-(4-fluorophenyl)-7-(4,4,5,5-tetramethyl-1,3,2-dioxaborolan-2-yl)-4,10-diazatetracyclo[5.5.0.02,6.08,12]dodecane-3,5,9,11-tetrone **9b'**, NOESY (400 MHz, CDCl3)*

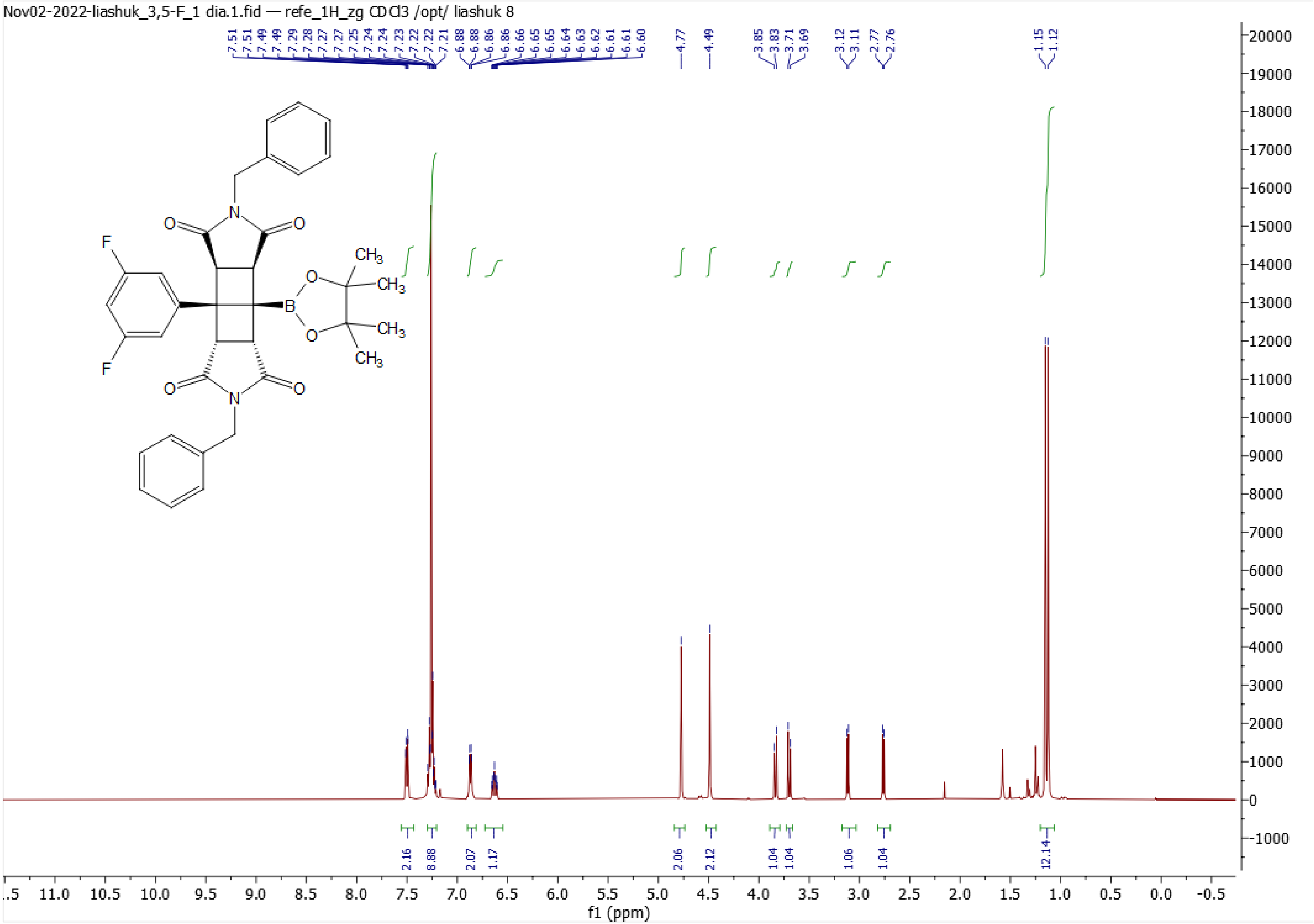

Spectrum 77. (2S,6R,8R,12S)-4,10-dibenzyl-1-(3,5-difluorophenyl)-7-(4,4,5,5-tetramethyl-1,3,2-dioxaborolan-2-yl)-4,10-diazatetracyclo[5.5.0.02,6.08,12]dodecane-3,5,9,11-tetrone ***9c***, *^{1}H NMR (400 MHz, CDCl$_3$)*

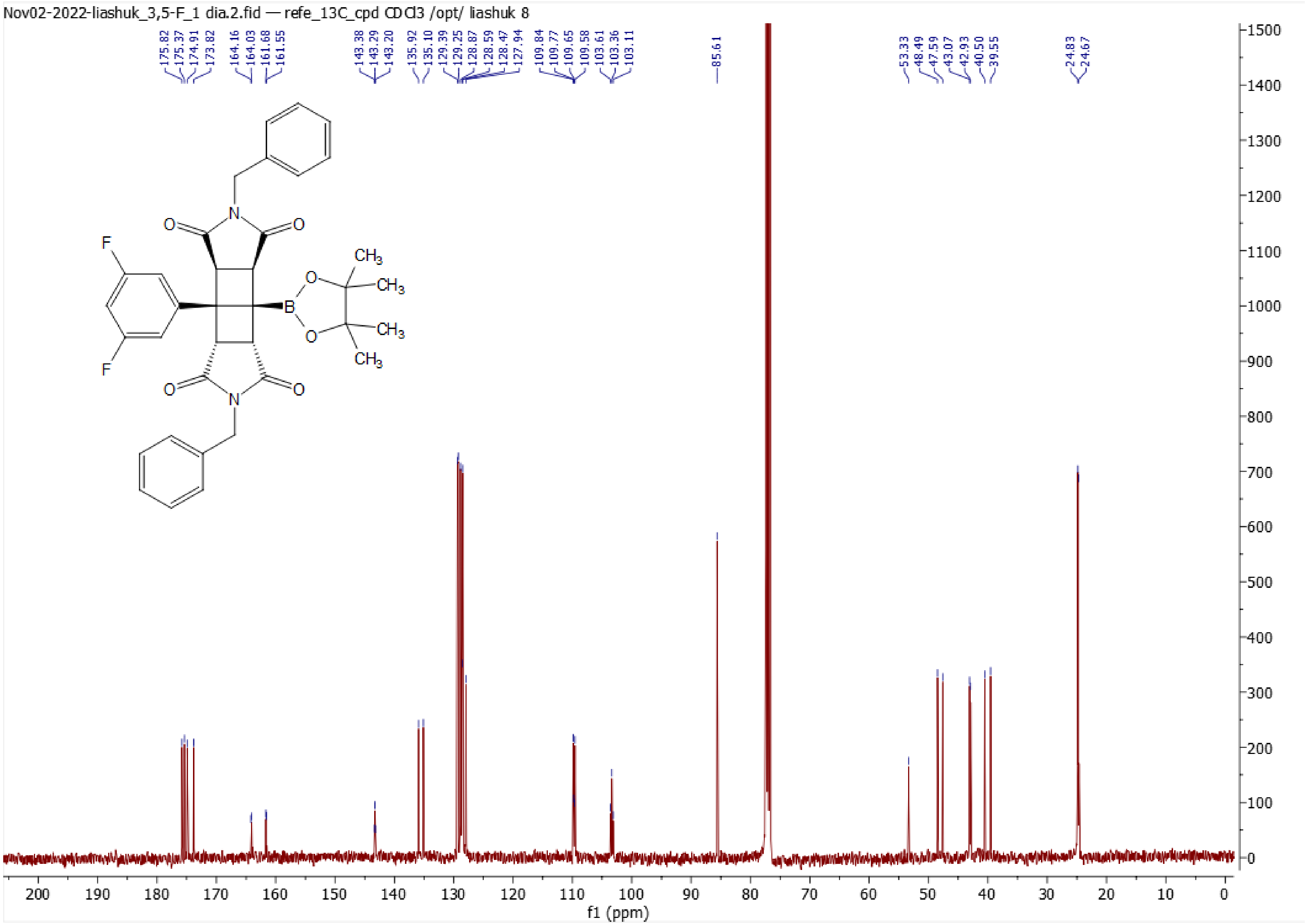

*Spectrum 78. (2S,6R,8R,12S)-4,10-dibenzyl-1-(3,5-difluorophenyl)-7-(4,4,5,5-tetramethyl-1,3,2-dioxaborolan-2-yl)-4,10-diazatetracyclo[5.5.0.02,6.08,12]dodecane-3,5,9,11-tetrone **9c**, ^{13}C NMR (101 MHz, CDCl$_3$)*

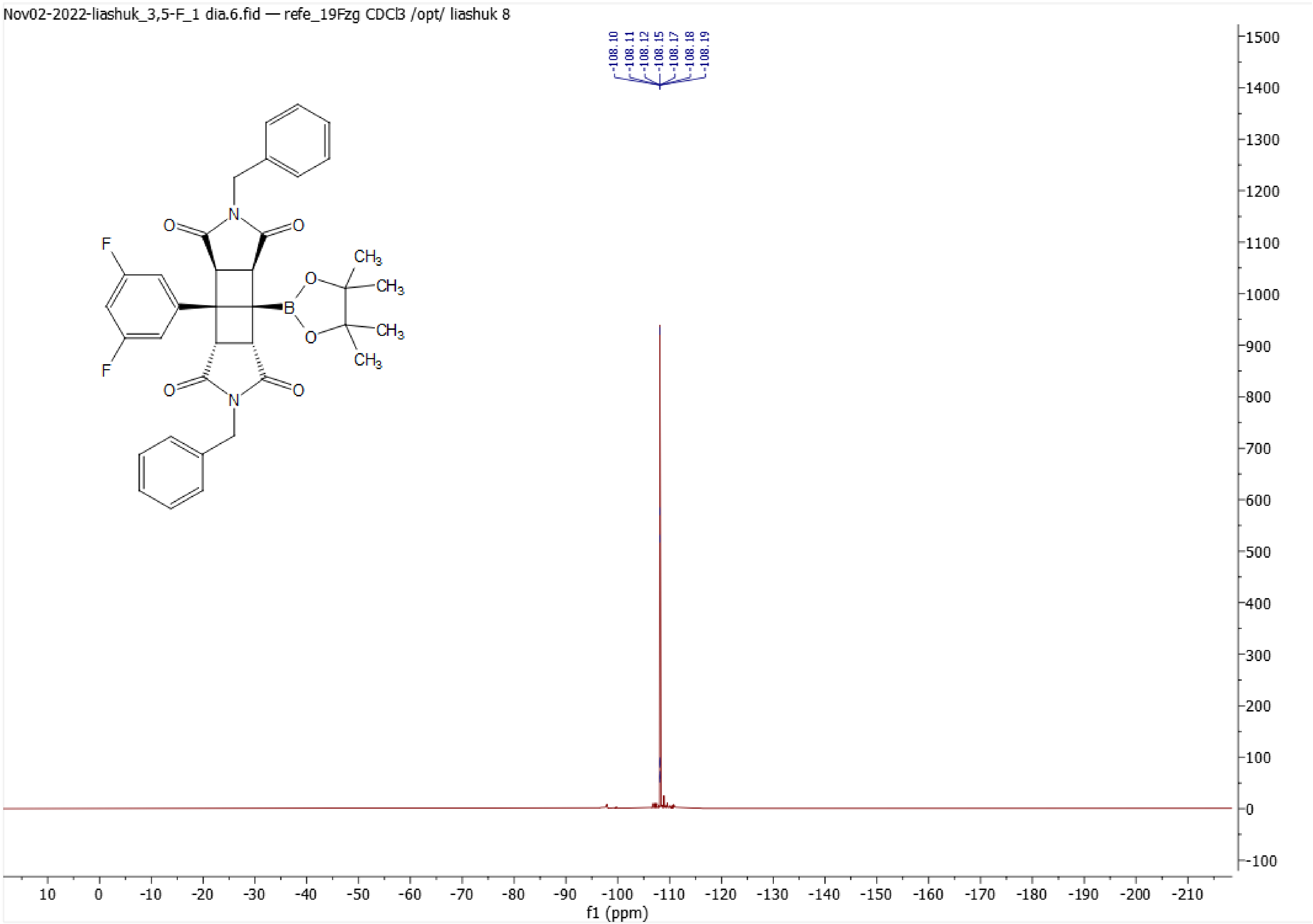

Spectrum 79. (2S,6R,8R,12S)-4,10-dibenzyl-1-(3,5-difluorophenyl)-7-(4,4,5,5-tetramethyl-1,3,2-dioxaborolan-2-yl)-4,10-diazatetracyclo[5.5.0.02,6.08,12]dodecane-3,5,9,11-tetrone ***9c****, ^{19}F NMR (376 MHz, $CDCl_3$)*

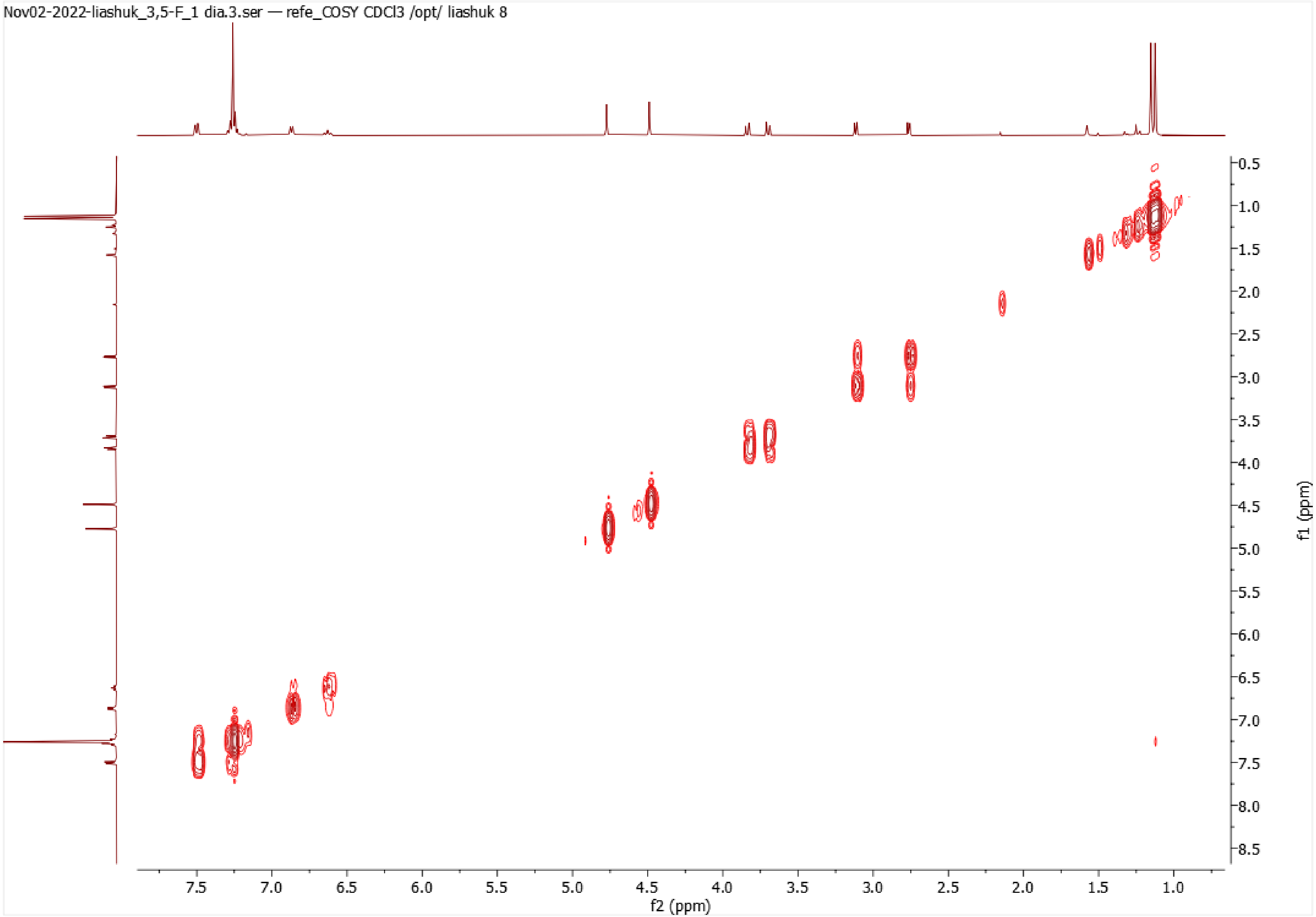

Spectrum 80. (2S,6R,8R,12S)-4,10-dibenzyl-1-(3,5-difluorophenyl)-7-(4,4,5,5-tetramethyl-1,3,2-dioxaborolan-2-yl)-4,10-diazatetracyclo[5.5.0.02,6.08,12]dodecane-3,5,9,11-tetrone ***9c****, COSY (400 MHz, CDCl3)*

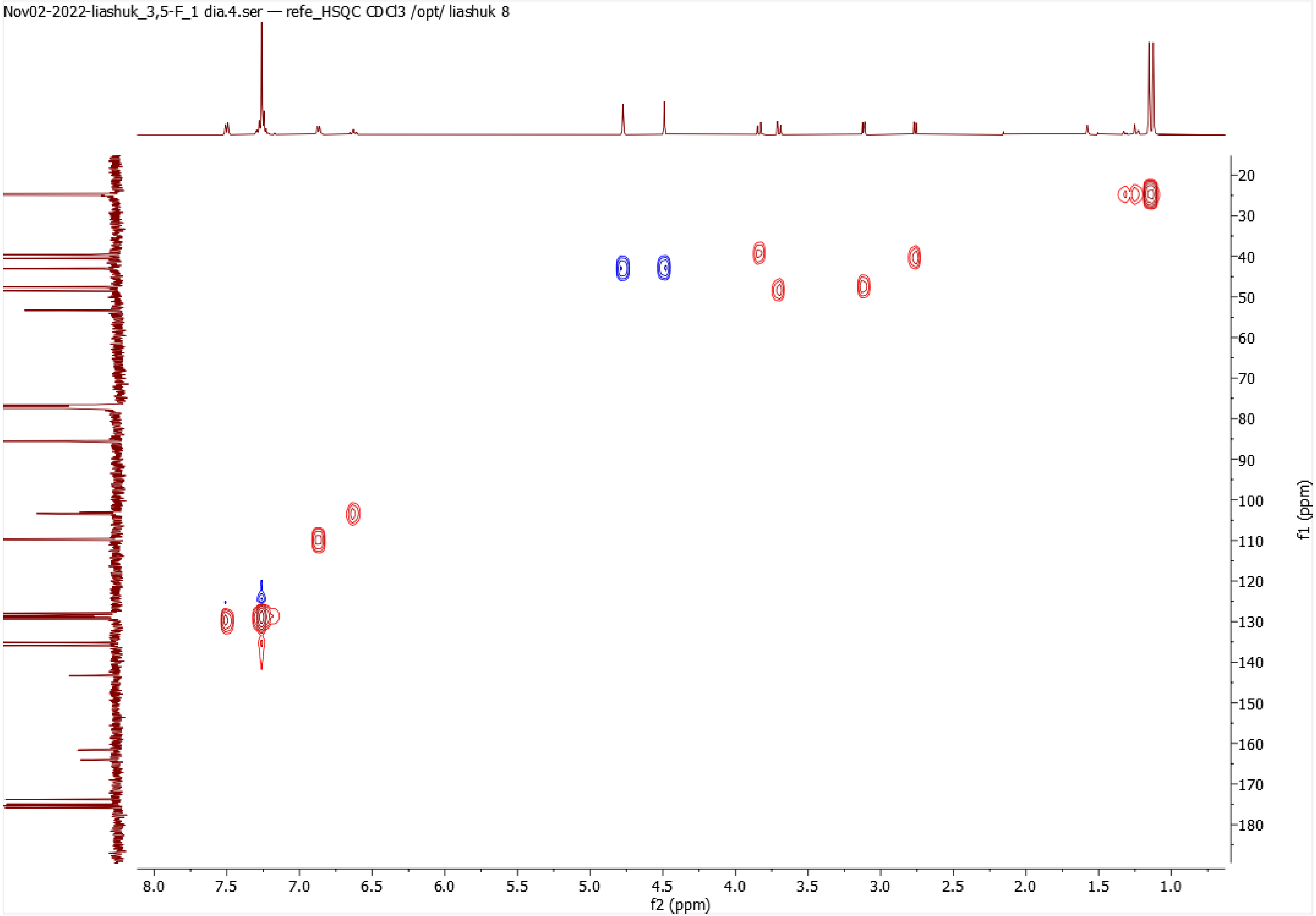

*Spectrum 81. (2S,6R,8R,12S)-4,10-dibenzyl-1-(3,5-difluorophenyl)-7-(4,4,5,5-tetramethyl-1,3,2-dioxaborolan-2-yl)-4,10-diazatetracyclo[5.5.0.02,6.08,12]dodecane-3,5,9,11-tetrone **9c**, HSQC (400/101 MHz, CDCl3)*

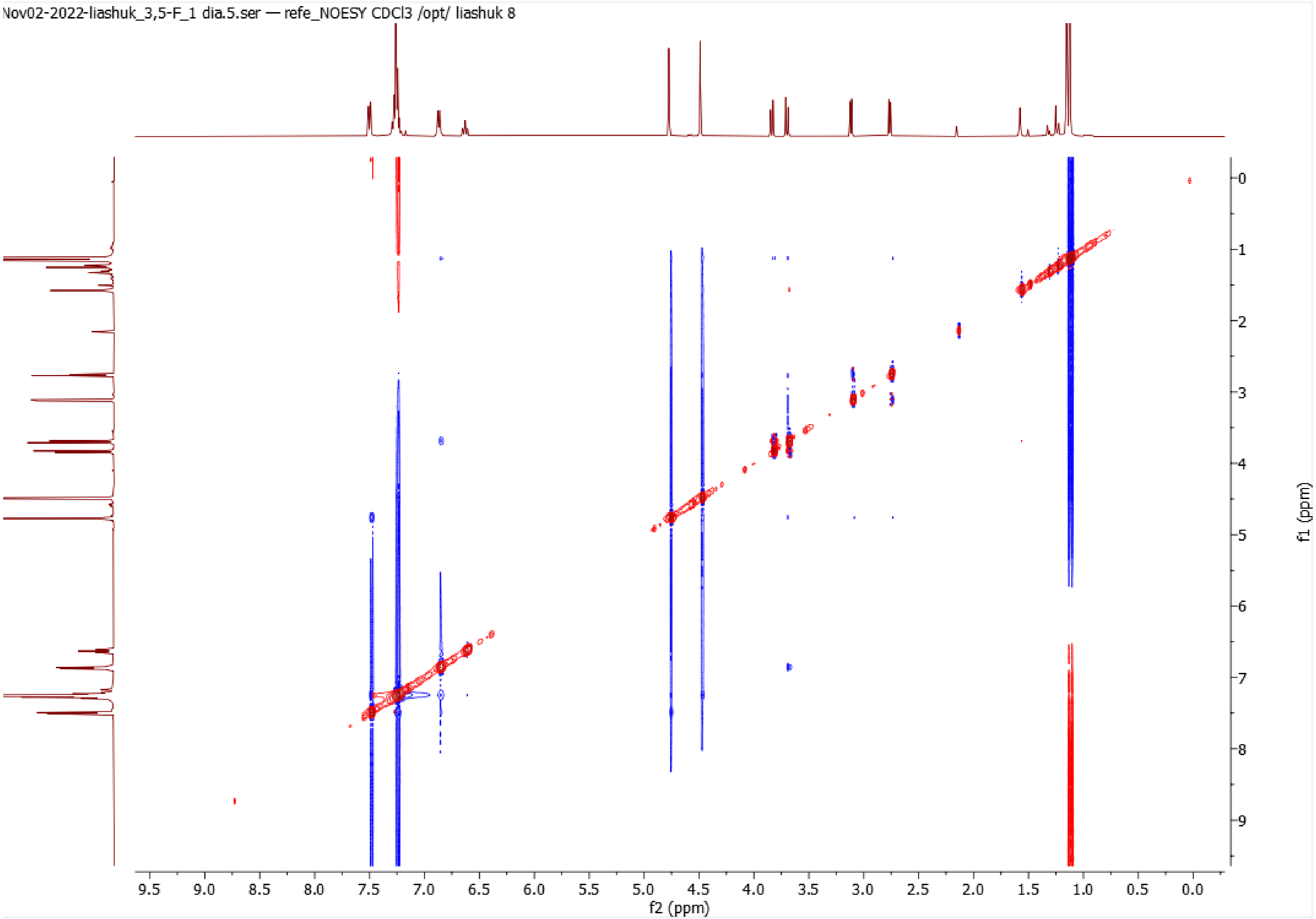

*Spectrum 82. (2S,6R,8R,12S)-4,10-dibenzyl-1-(3,5-difluorophenyl)-7-(4,4,5,5-tetramethyl-1,3,2-dioxaborolan-2-yl)-4,10-diazatetracyclo[5.5.0.02,6.08,12]dodecane-3,5,9,11-tetrone **9c**, NOESY (400 MHz, CDCl3)*

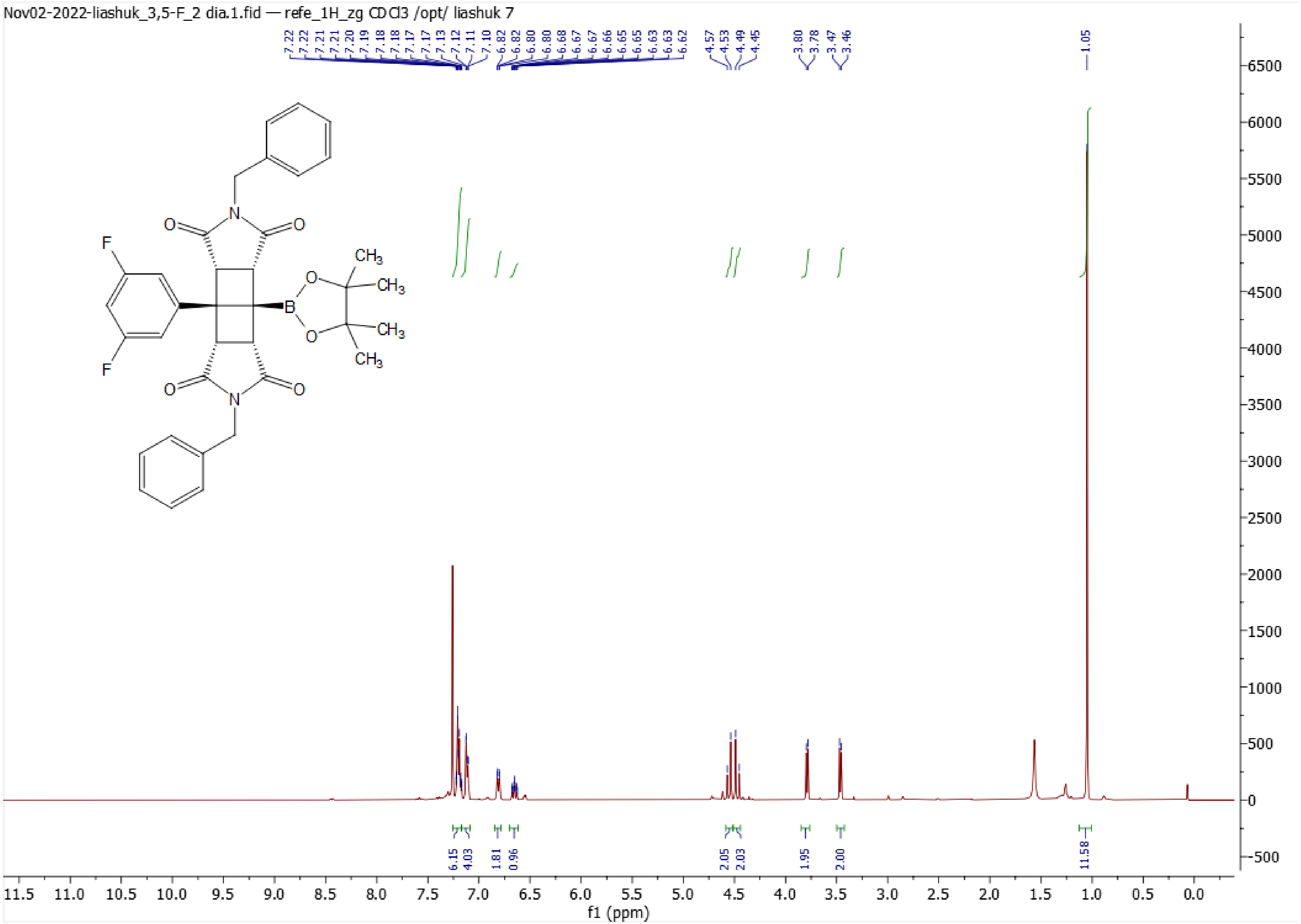

Spectrum 83. (1r,2R,6S,7r,8R,12S)-4,10-dibenzyl-1-(3,5-difluorophenyl)-7-(4,4,5,5-tetramethyl-1,3,2-dioxaborolan-2-yl)-4,10-diazatetracyclo[5.5.0.02,6.08,12]dodecane-3,5,9,11-tetrone ***9c'****,* ^{1}*H NMR (400 MHz, CDCl*$_{3}$*)*

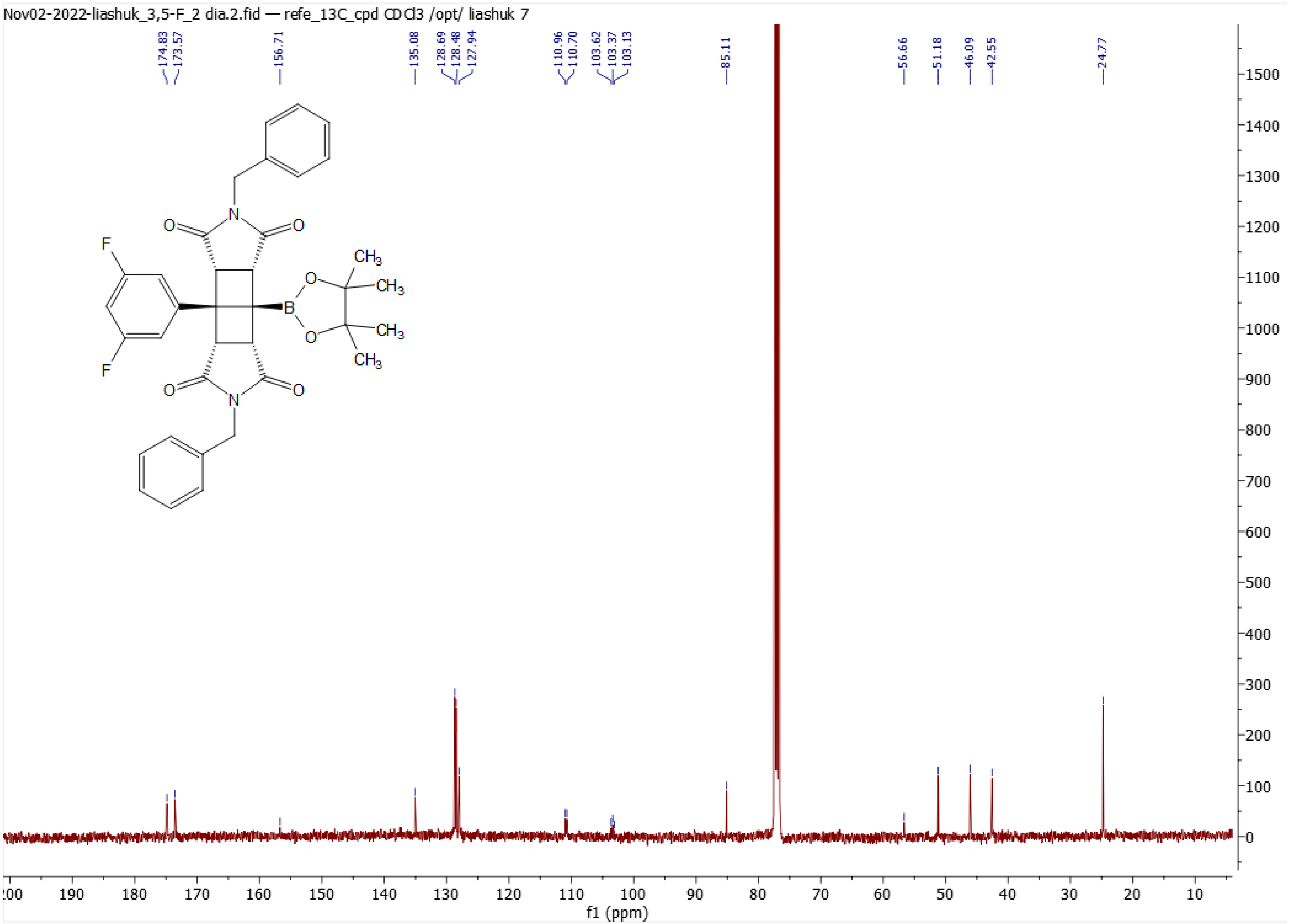

Spectrum 84. (1r,2R,6S,7r,8R,12S)-4,10-dibenzyl-1-(3,5-difluorophenyl)-7-(4,4,5,5-tetramethyl-1,3,2-dioxaborolan-2-yl)-4,10-diazatetracyclo[5.5.0.02,6.08,12]dodecane-3,5,9,11-tetrone ***9c'***, *^{13}C NMR (101 MHz, $CDCl_3$)*

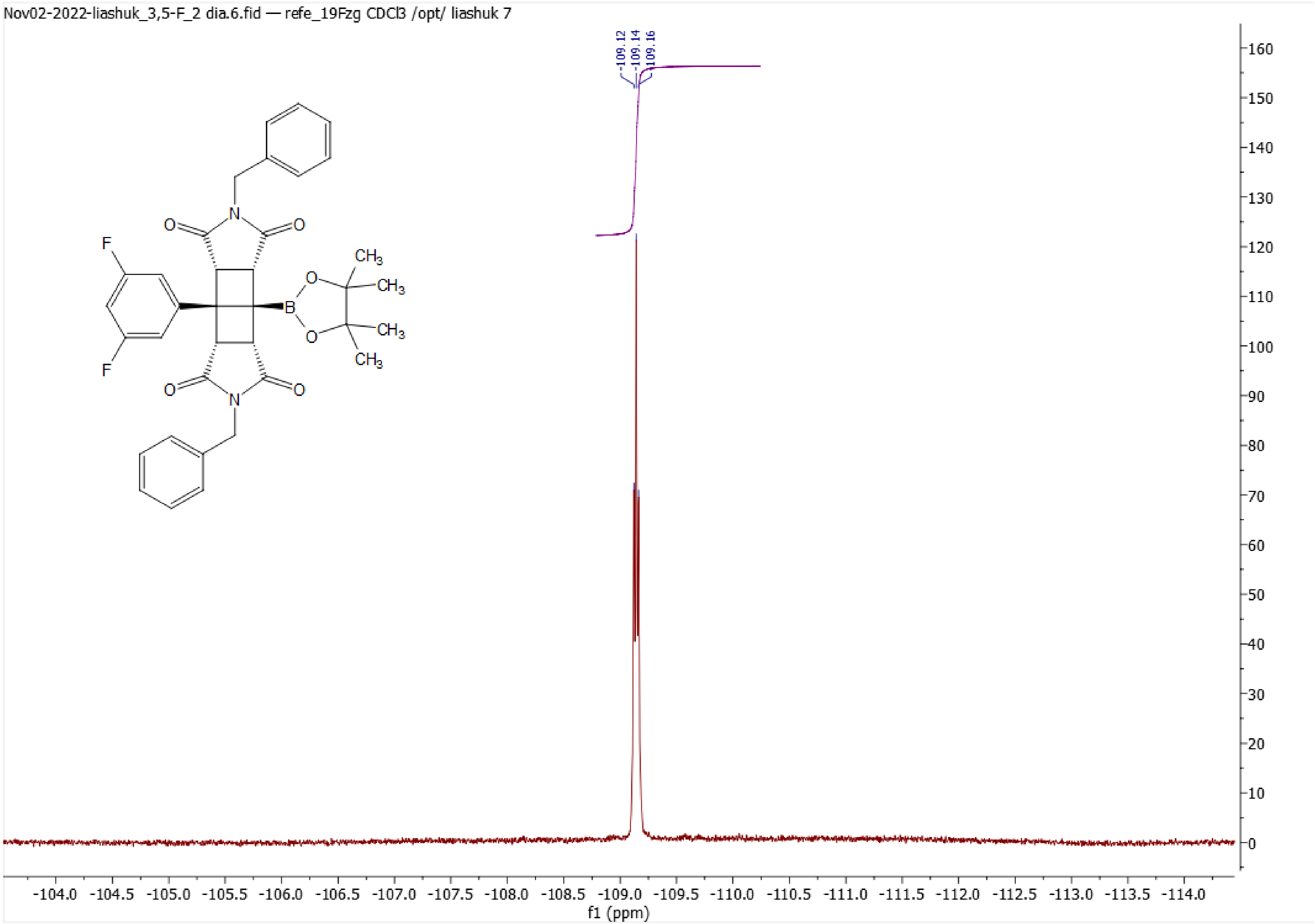

Spectrum 85. (1r,2R,6S,7r,8R,12S)-4,10-dibenzyl-1-(3,5-difluorophenyl)-7-(4,4,5,5-tetramethyl-1,3,2-dioxaborolan-2-yl)-4,10-diazatetracyclo[5.5.0.02,6.08,12]dodecane-3,5,9,11-tetrone ***9c'****,* ^{19}*F NMR (376 MHz,* $CDCl_3$*)*

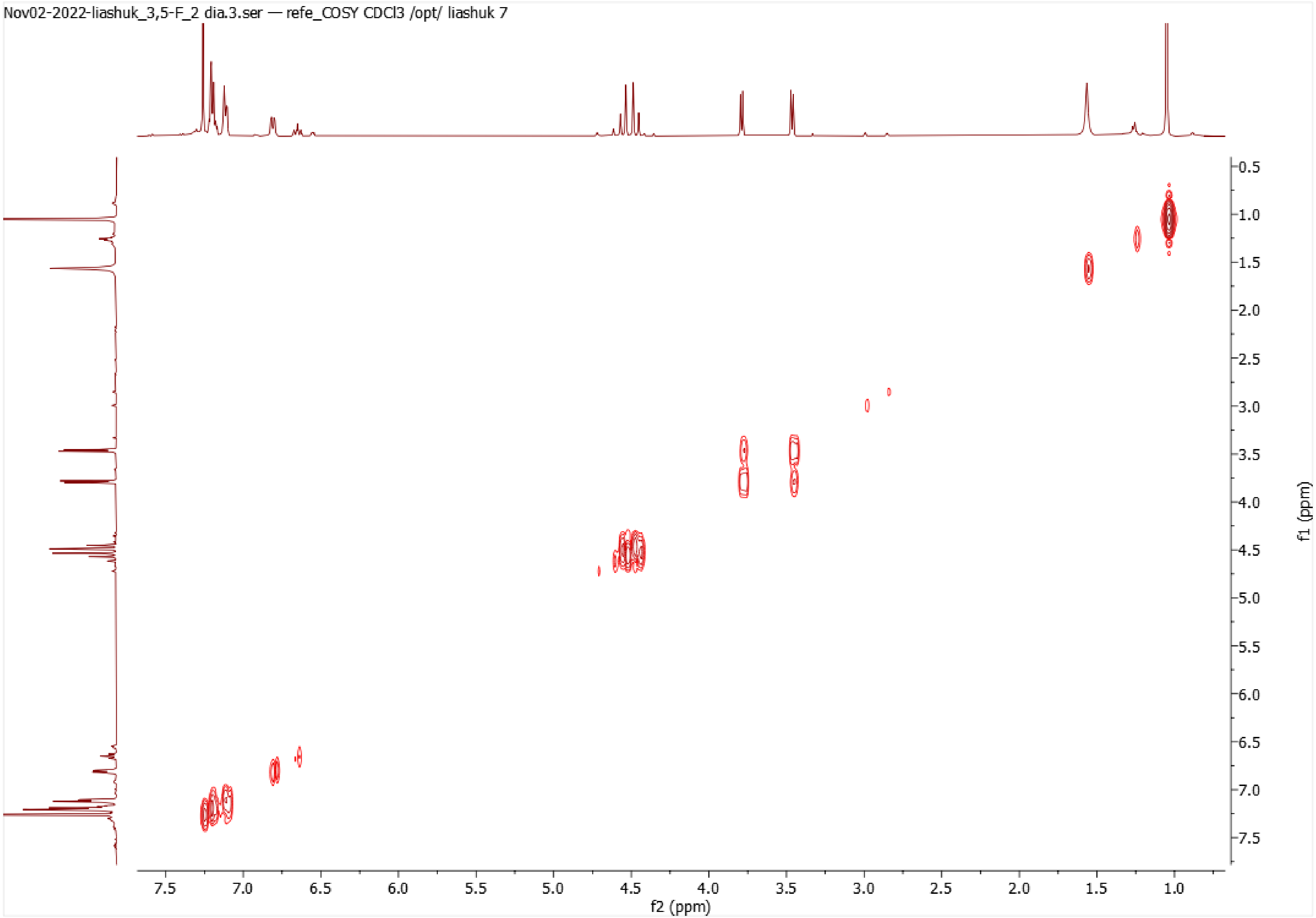

*Spectrum 86. . (1r,2R,6S,7r,8R,12S)-4,10-dibenzyl-1-(3,5-difluorophenyl)-7-(4,4,5,5-tetramethyl-1,3,2-dioxaborolan-2-yl)-4,10-diazatetracyclo[5.5.0.02,6.08,12]dodecane-3,5,9,11-tetrone **9c'**, COSY (400 MHz, CDCl3)*

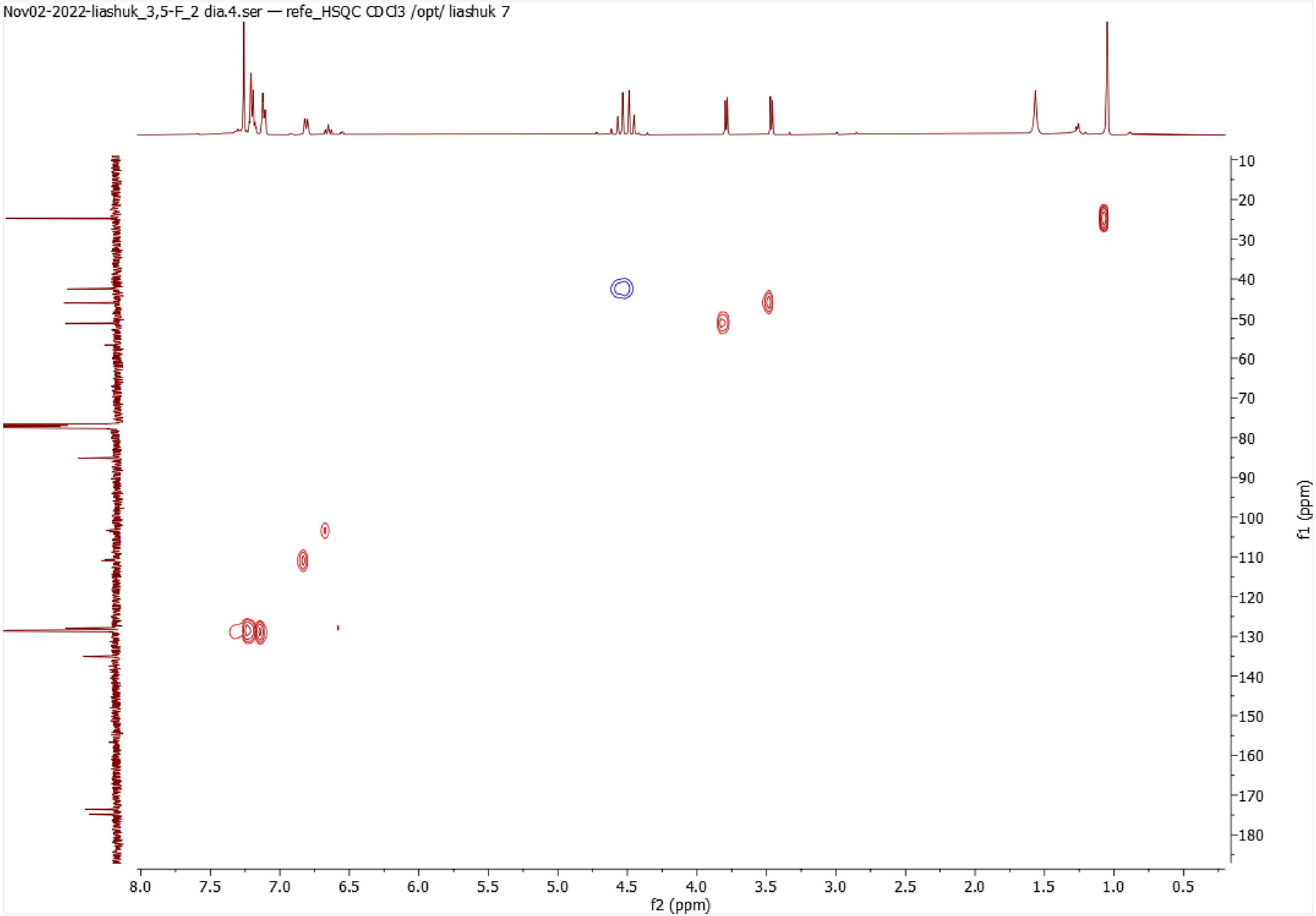

Spectrum 87. (1r,2R,6S,7r,8R,12S)-4,10-dibenzyl-1-(3,5-difluorophenyl)-7-(4,4,5,5-tetramethyl-1,3,2-dioxaborolan-2-yl)-4,10-diazatetracyclo[5.5.0.02,6.08,12]dodecane-3,5,9,11-tetrone ***9c'****, HSQC (400/101 MHz, CDCl3)*

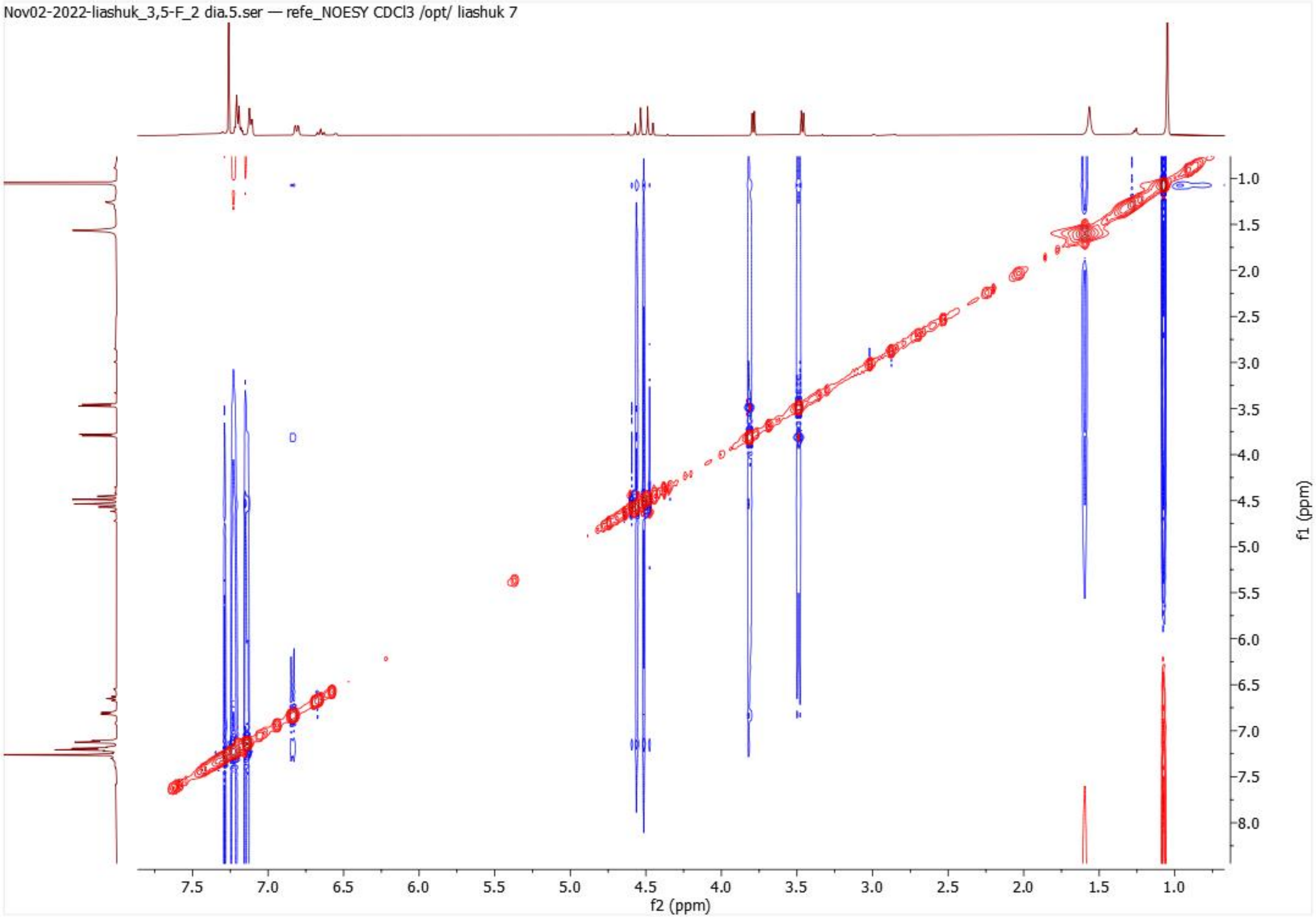

Spectrum 88. (1r,2R,6S,7r,8R,12S)-4,10-dibenzyl-1-(3,5-difluorophenyl)-7-(4,4,5,5-tetramethyl-1,3,2-dioxaborolan-2-yl)-4,10-diazatetracyclo[5.5.0.02,6.08,12]dodecane-3,5,9,11-tetrone ***9c'****, NOESY (400 MHz, CDCl3)*

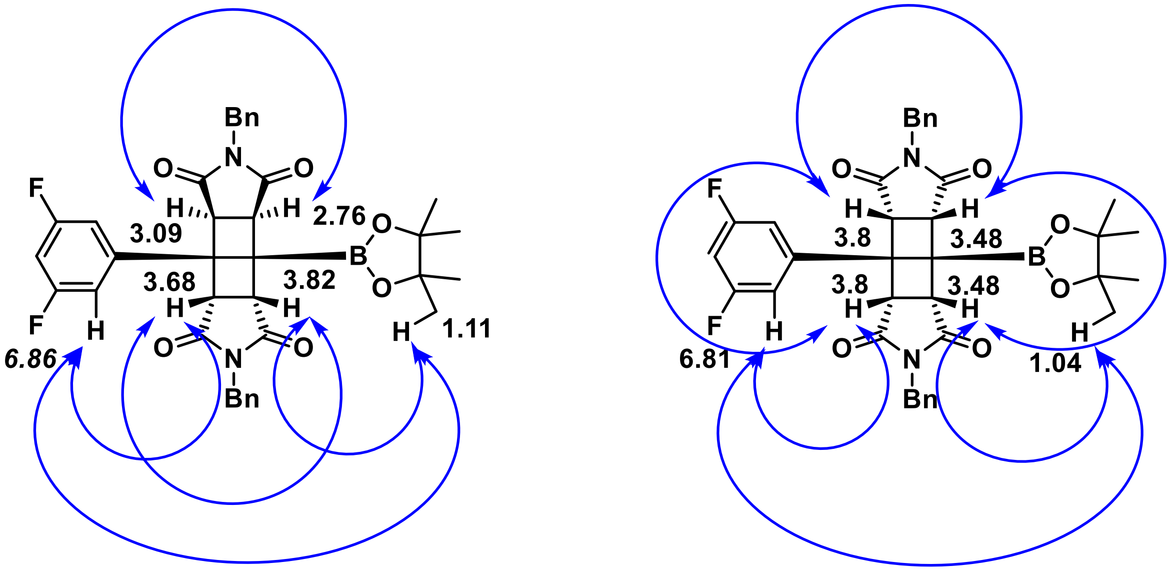

***exo*-*endo*-9c**   ***exo*-*exo*-9c'**

Scheme S10. Representative illustration of nOe correlations for exo-endo and endo-endo isomers (on example of ***9c*** *and* ***9c'****)*

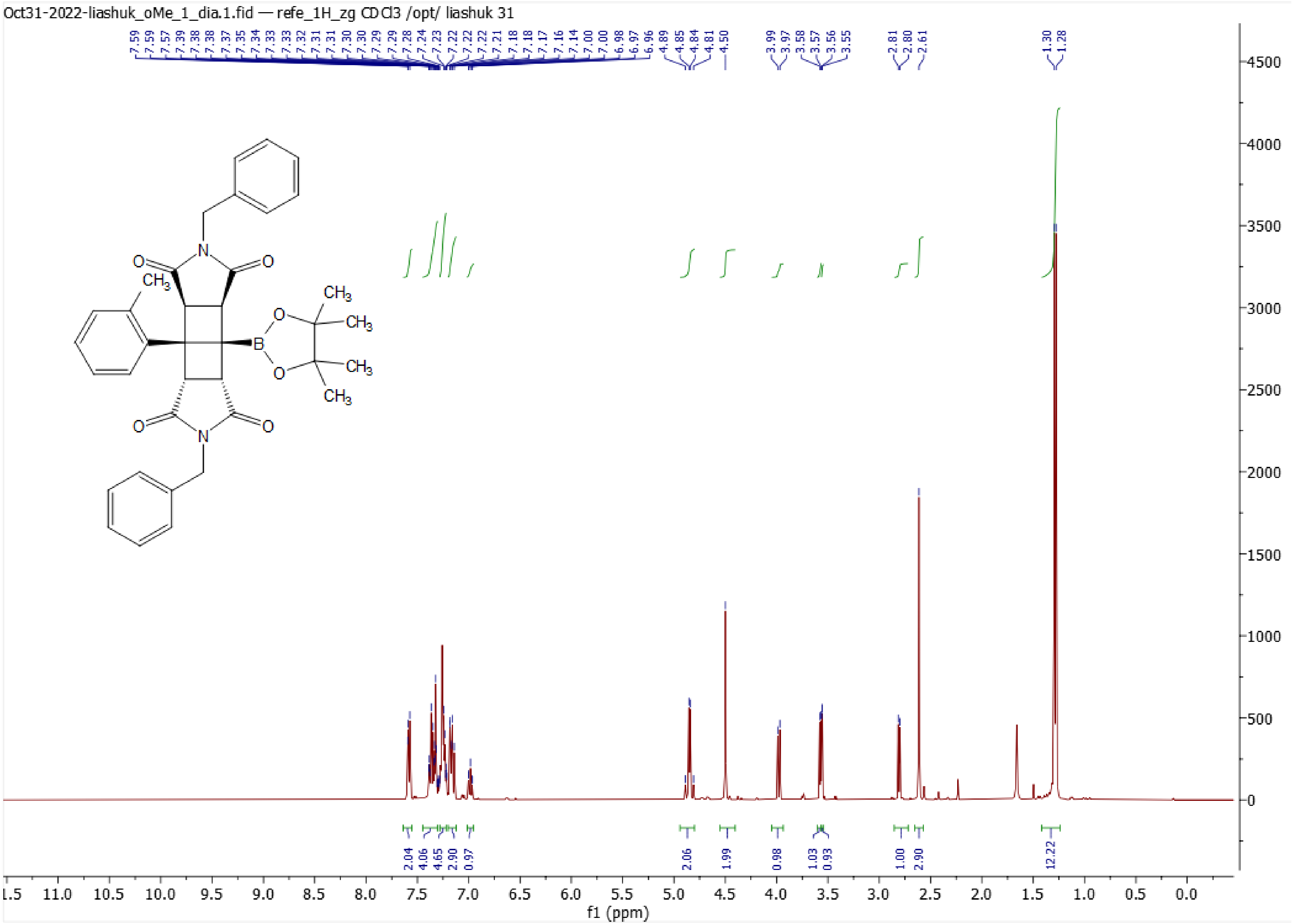

Spectrum 89. (2S,6R,8R,12S)-4,10-dibenzyl-1-(2-methylphenyl)-7-(4,4,5,5-tetramethyl-1,3,2-dioxaborolan-2-yl)-4,10-diazatetracyclo[5.5.0.02,6.08,12]dodecane-3,5,9,11-tetrone **9d**, ^{1}H NMR (400 MHz, $CDCl_3$)

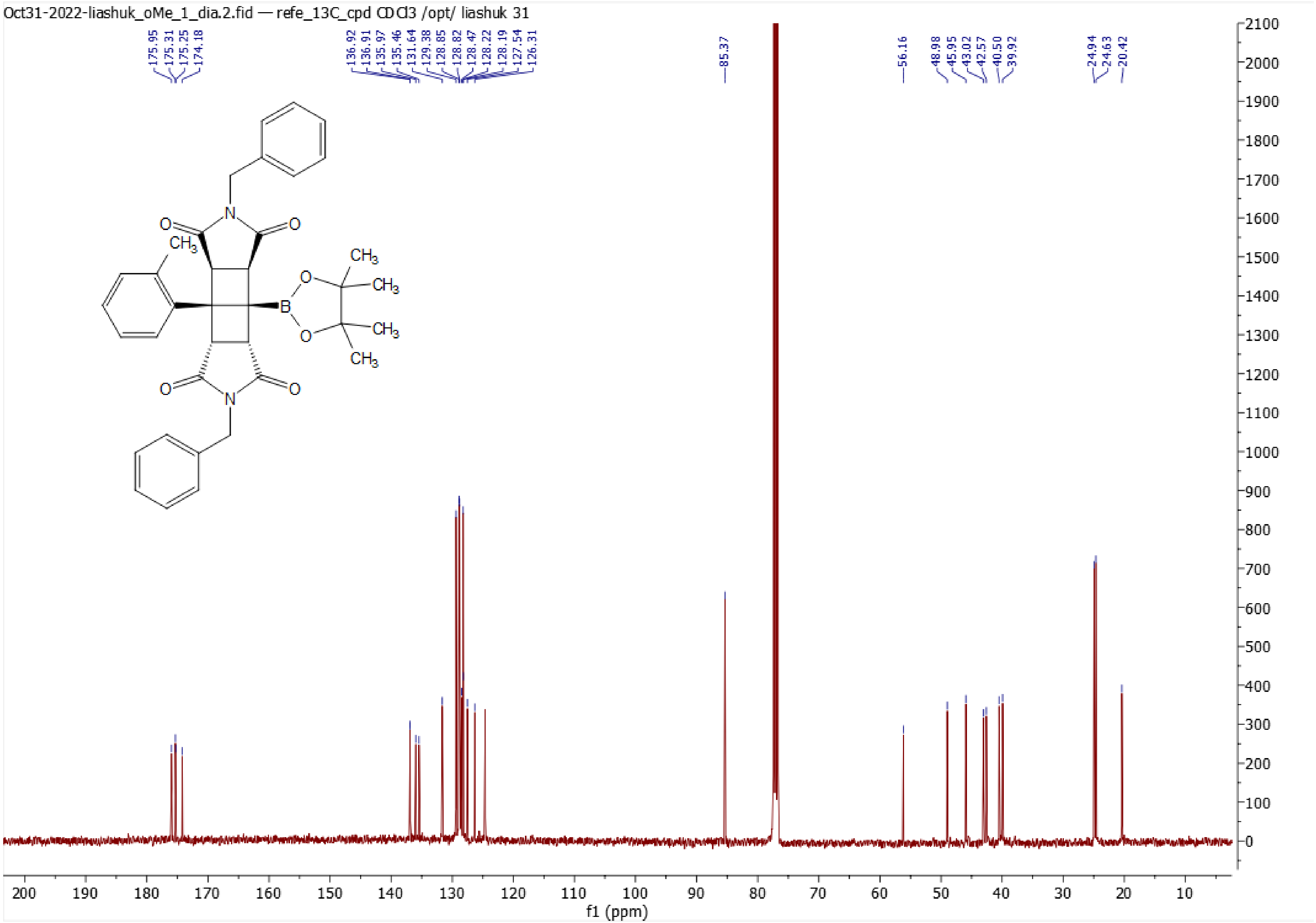

Spectrum 90. (2S,6R,8R,12S)-4,10-dibenzyl-1-(2-methylphenyl)-7-(4,4,5,5-tetramethyl-1,3,2-dioxaborolan-2-yl)-4,10-diazatetracyclo[5.5.0.02,6.08,12]dodecane-3,5,9,11-tetrone ***9d****, ^{13}C NMR (101 MHz, CDCl$_3$)*

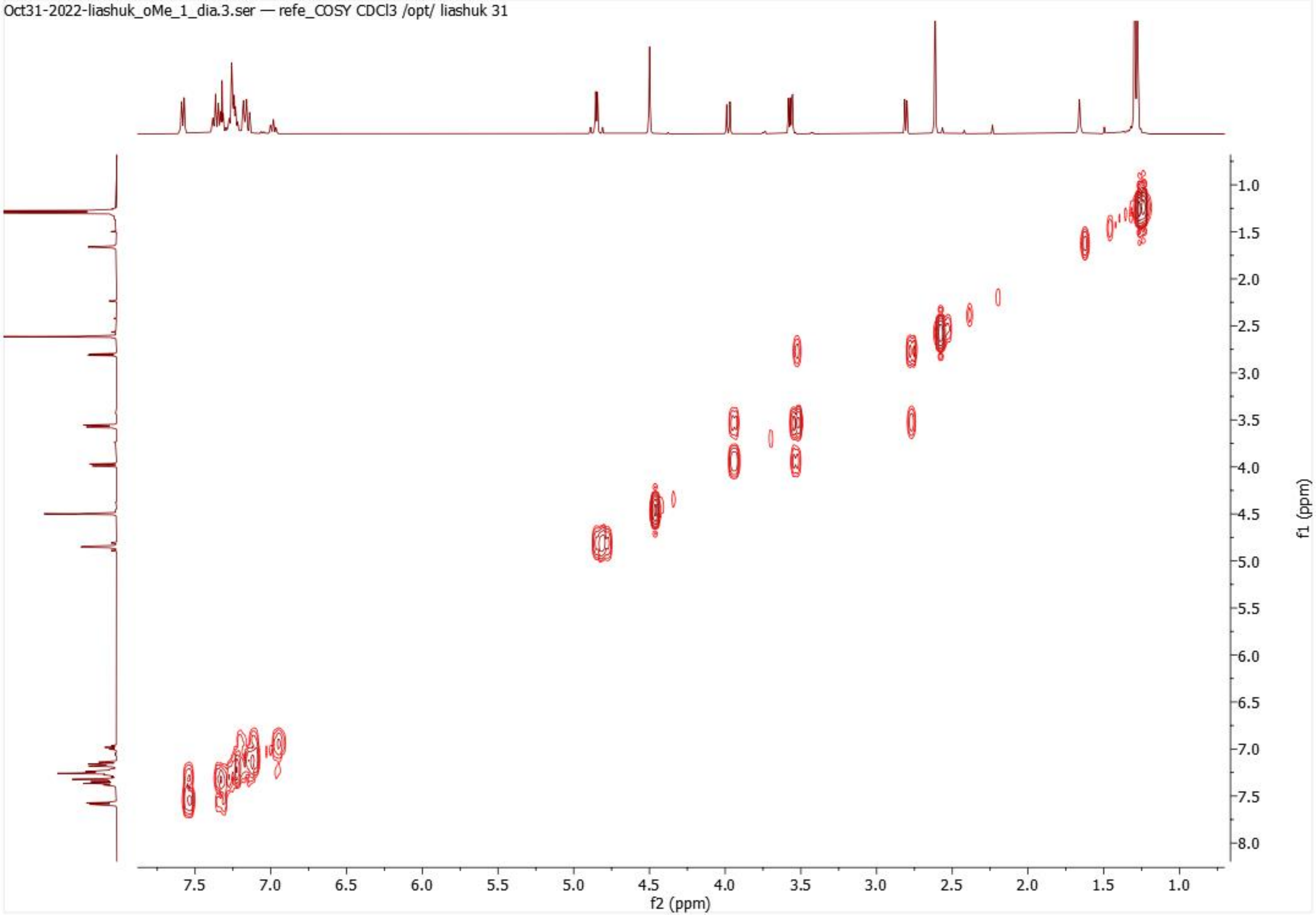

Spectrum 91. (2S,6R,8R,12S)-4,10-dibenzyl-1-(2-methylphenyl)-7-(4,4,5,5-tetramethyl-1,3,2-dioxaborolan-2-yl)-4,10-diazatetracyclo[5.5.0.02,6.08,12]dodecane-3,5,9,11-tetrone ***9d****, COSY (400 MHz, CDCl3)*

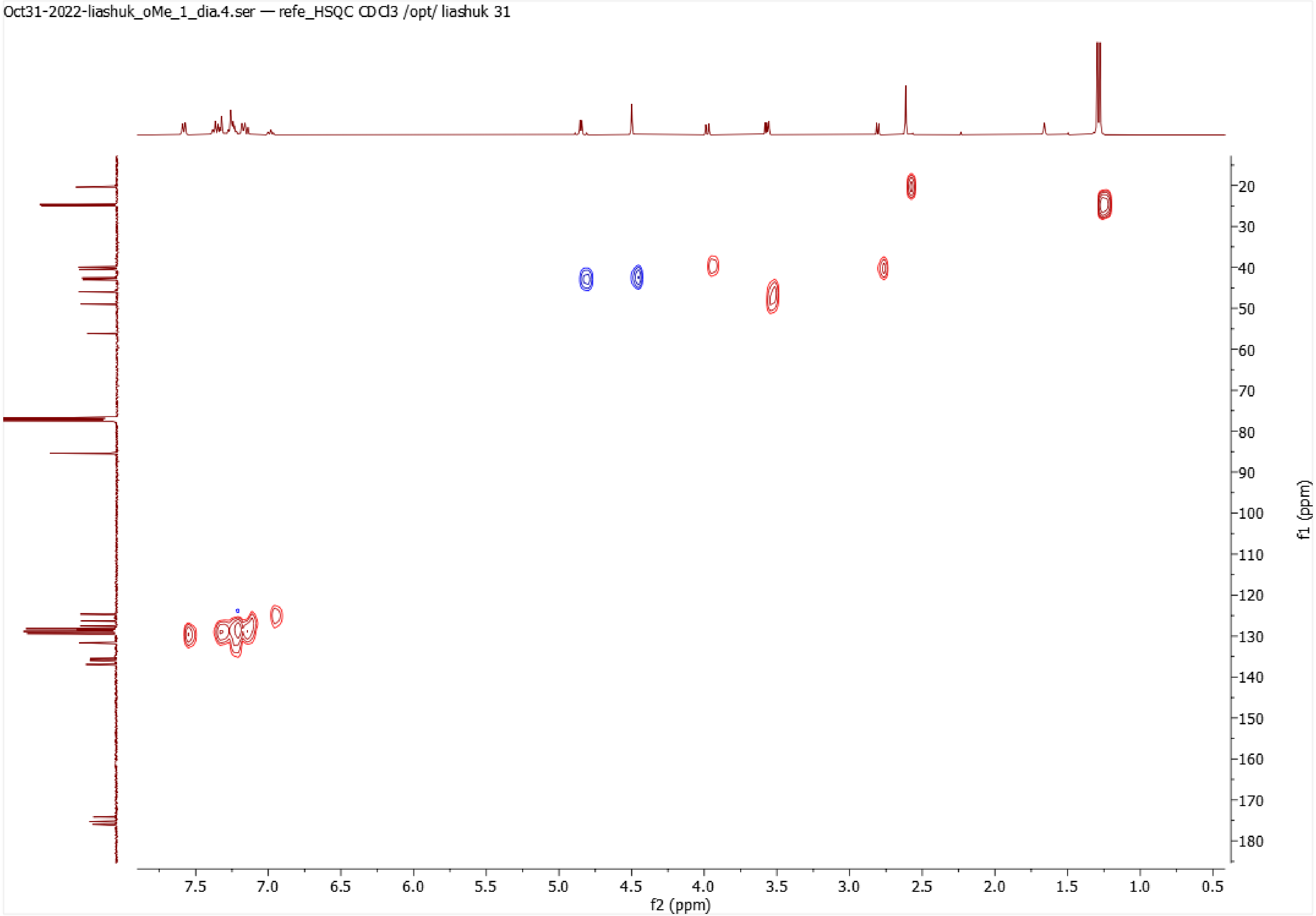

Spectrum 92. (2S,6R,8R,12S)-4,10-dibenzyl-1-(2-methylphenyl)-7-(4,4,5,5-tetramethyl-1,3,2-dioxaborolan-2-yl)-4,10-diazatetracyclo[5.5.0.02,6.08,12]dodecane-3,5,9,11-tetrone ***9d****, HSQC (400/101 MHz, CDCl3)*

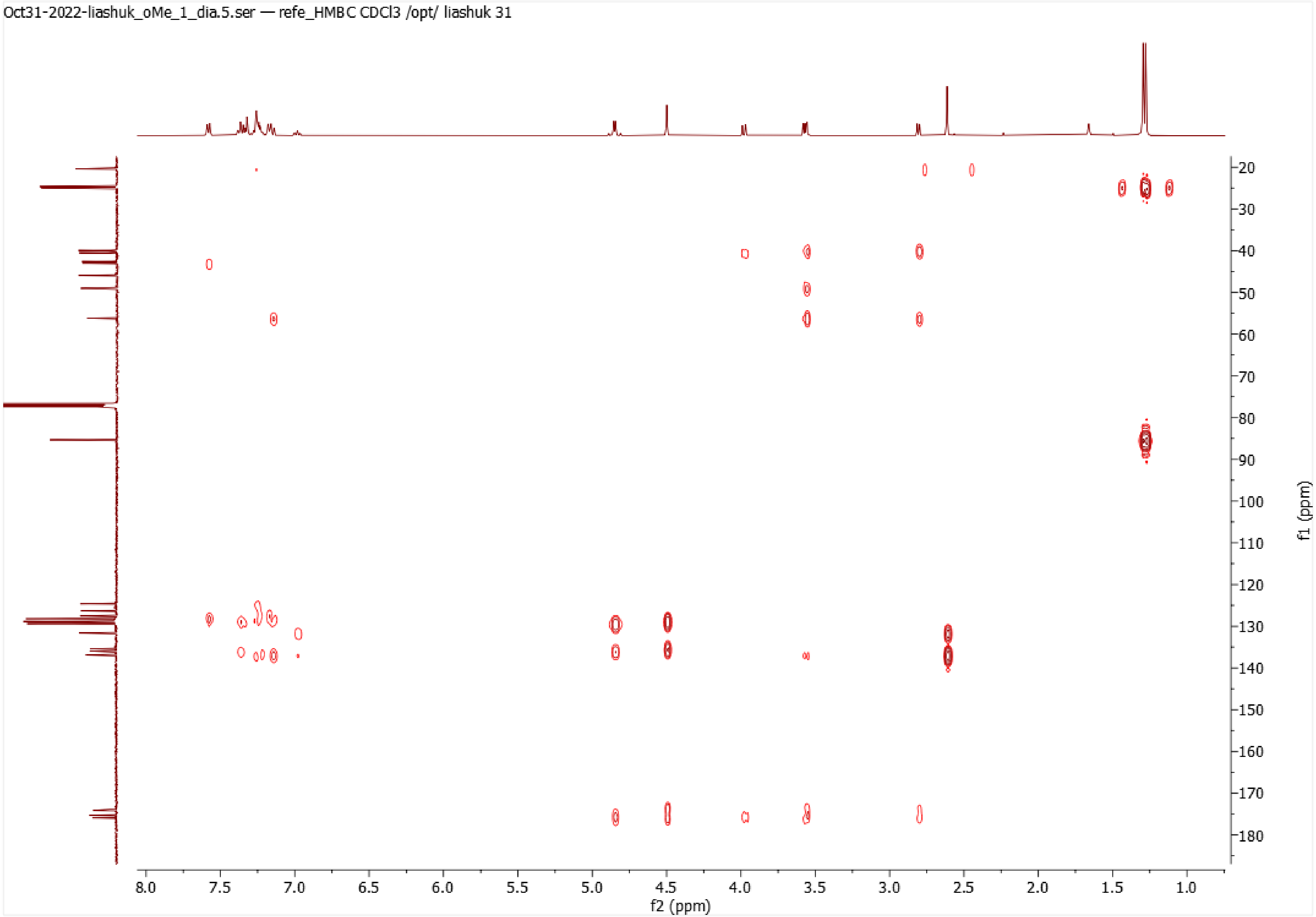

*Spectrum 93. (2S,6R,8R,12S)-4,10-dibenzyl-1-(2-methylphenyl)-7-(4,4,5,5-tetramethyl-1,3,2-dioxaborolan-2-yl)-4,10-diazatetracyclo[5.5.0.02,6.08,12]dodecane-3,5,9,11-tetrone **9d**, HMBC (400/101 MHz, CDCl3)*

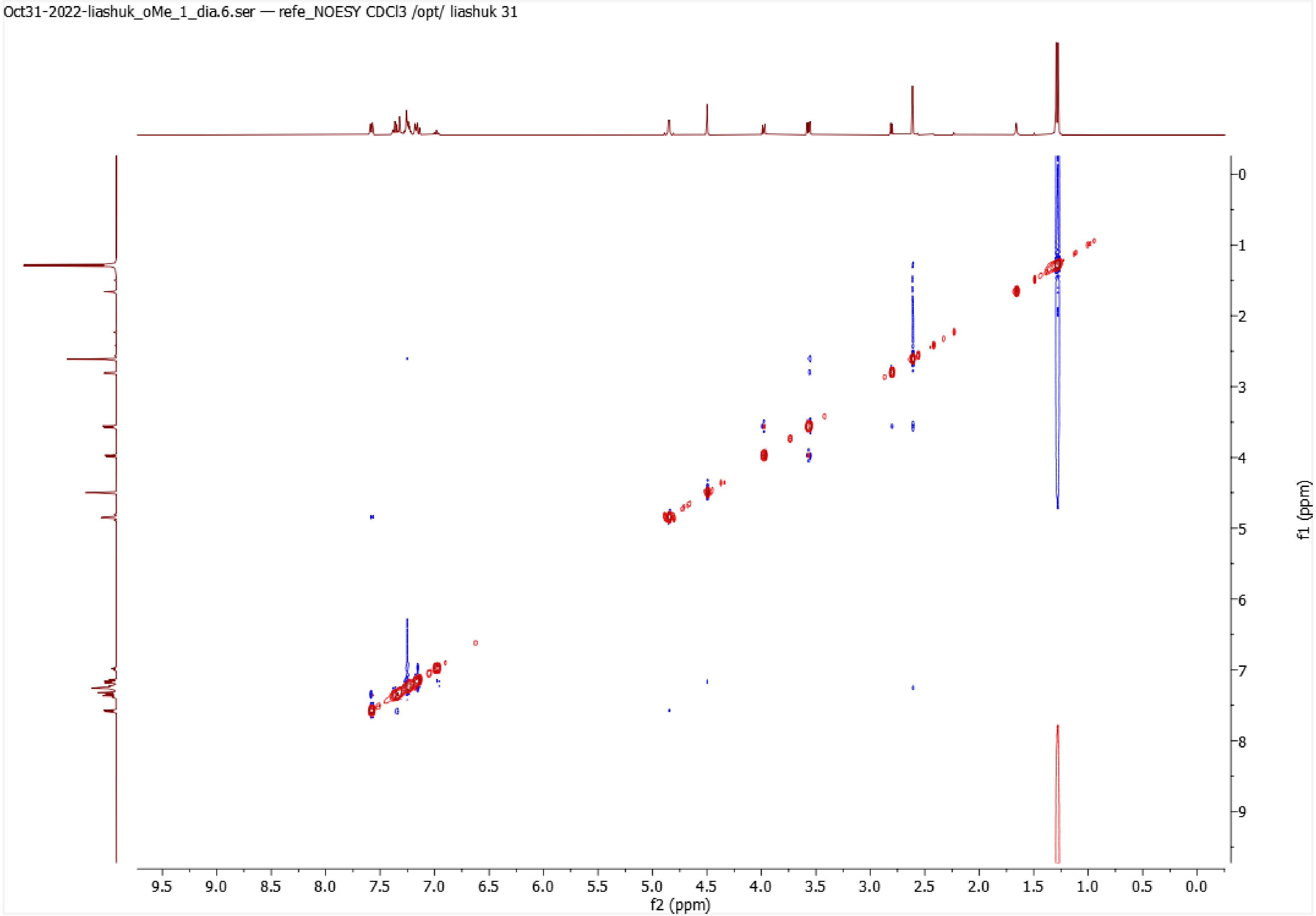

Spectrum 94. (2S,6R,8R,12S)-4,10-dibenzyl-1-(2-methylphenyl)-7-(4,4,5,5-tetramethyl-1,3,2-dioxaborolan-2-yl)-4,10-diazatetracyclo[5.5.0.02,6.08,12]dodecane-3,5,9,11-tetrone ***9d****, NOESY (400 MHz, CDCl3)*

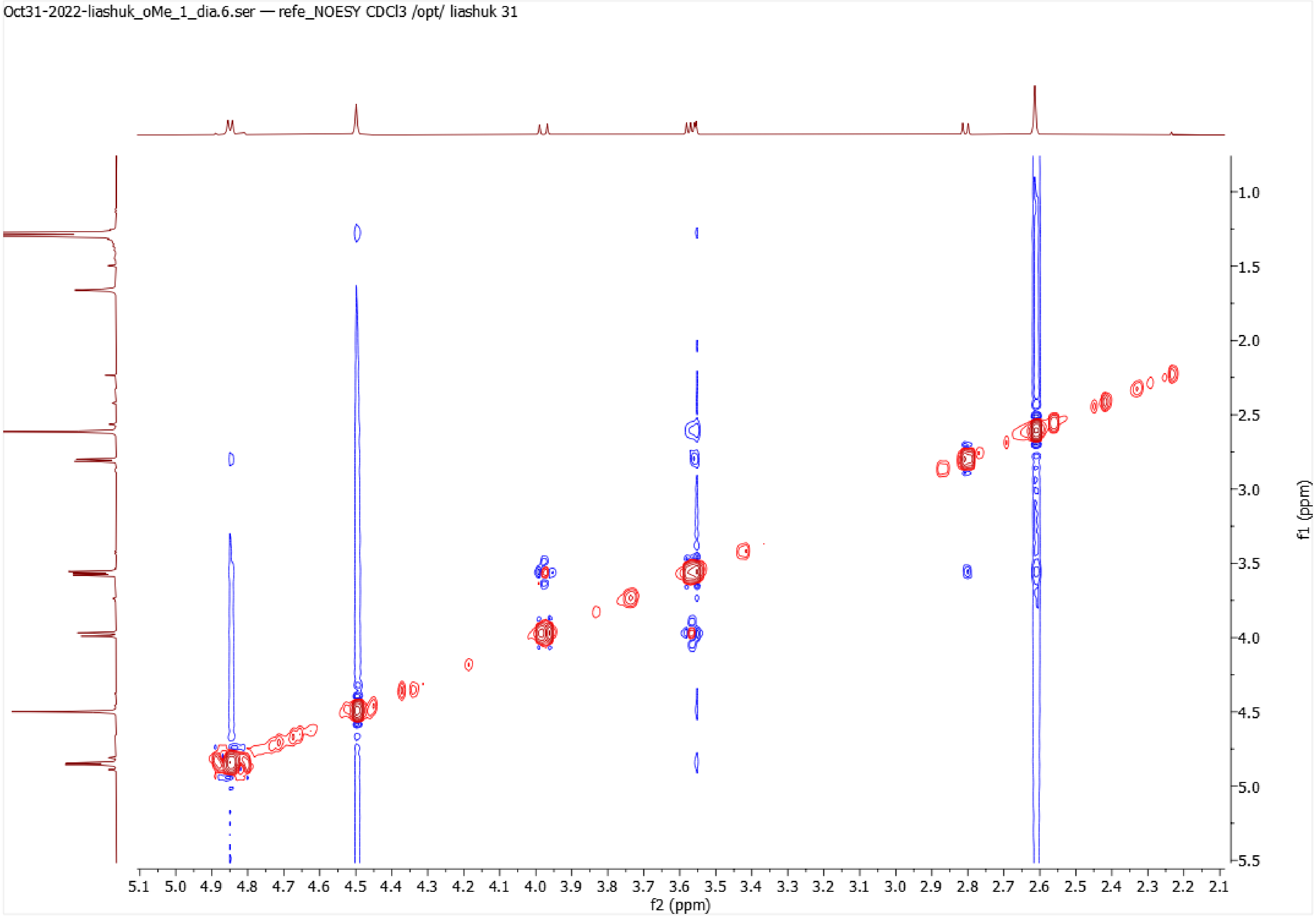

Spectrum 95. (2S,6R,8R,12S)-4,10-dibenzyl-1-(2-methylphenyl)-7-(4,4,5,5-tetramethyl-1,3,2-dioxaborolan-2-yl)-4,10-diazatetracyclo[5.5.0.02,6.08,12]dodecane-3,5,9,11-tetrone ***9d****, NOESY (400 MHz, CDCl3), aliphatic region*

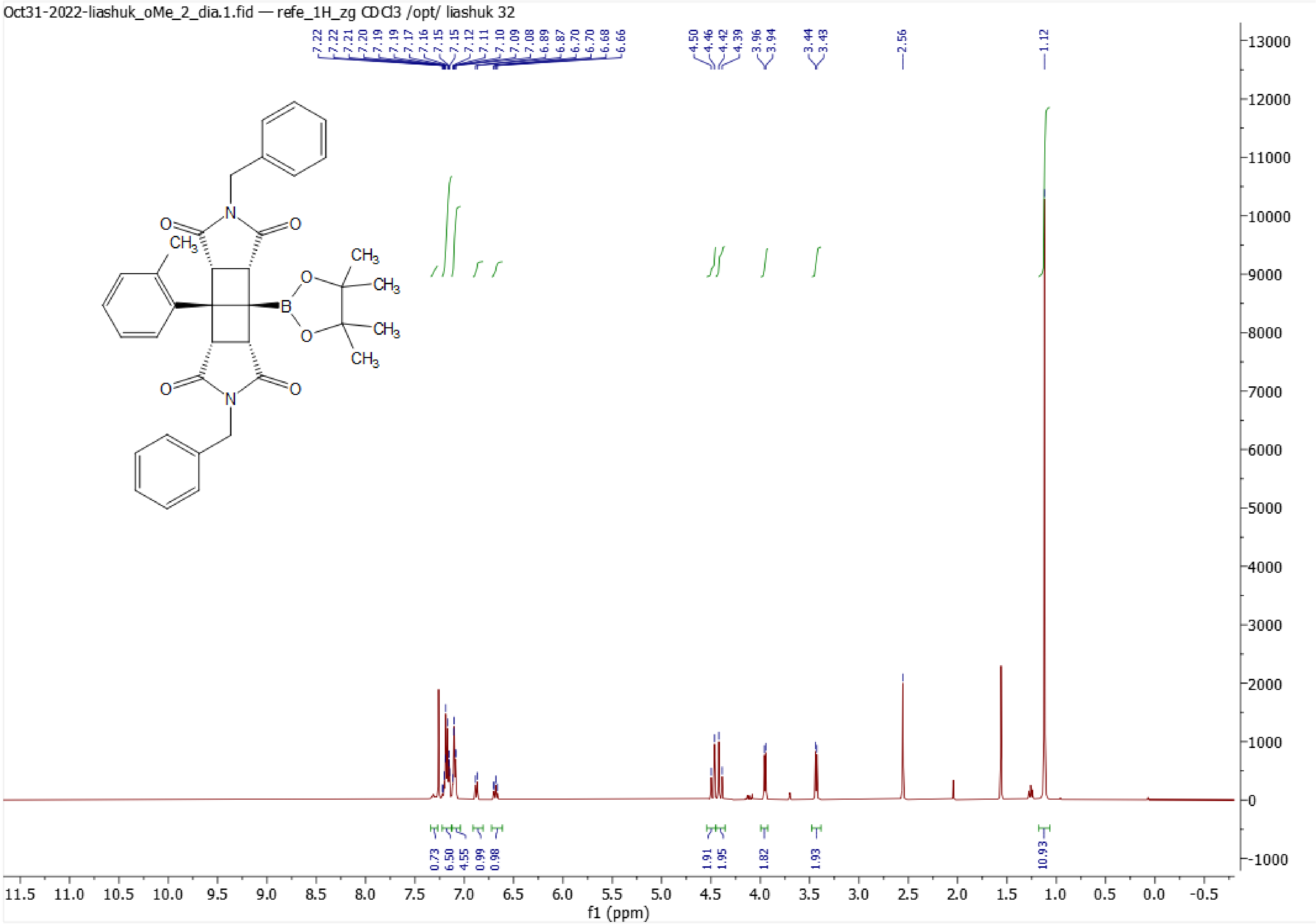

*Spectrum 96. (1r,2R,6S,7r,8R,12S)-4,10-dibenzyl-1-(2-methylphenyl)-7-(4,4,5,5-tetramethyl-1,3,2-dioxaborolan-2-yl)-4,10-diazatetracyclo[5.5.0.02,6.08,12]dodecane-3,5,9,11-tetrone **9d'**, ^{1}H NMR (400 MHz, CDCl$_3$)*

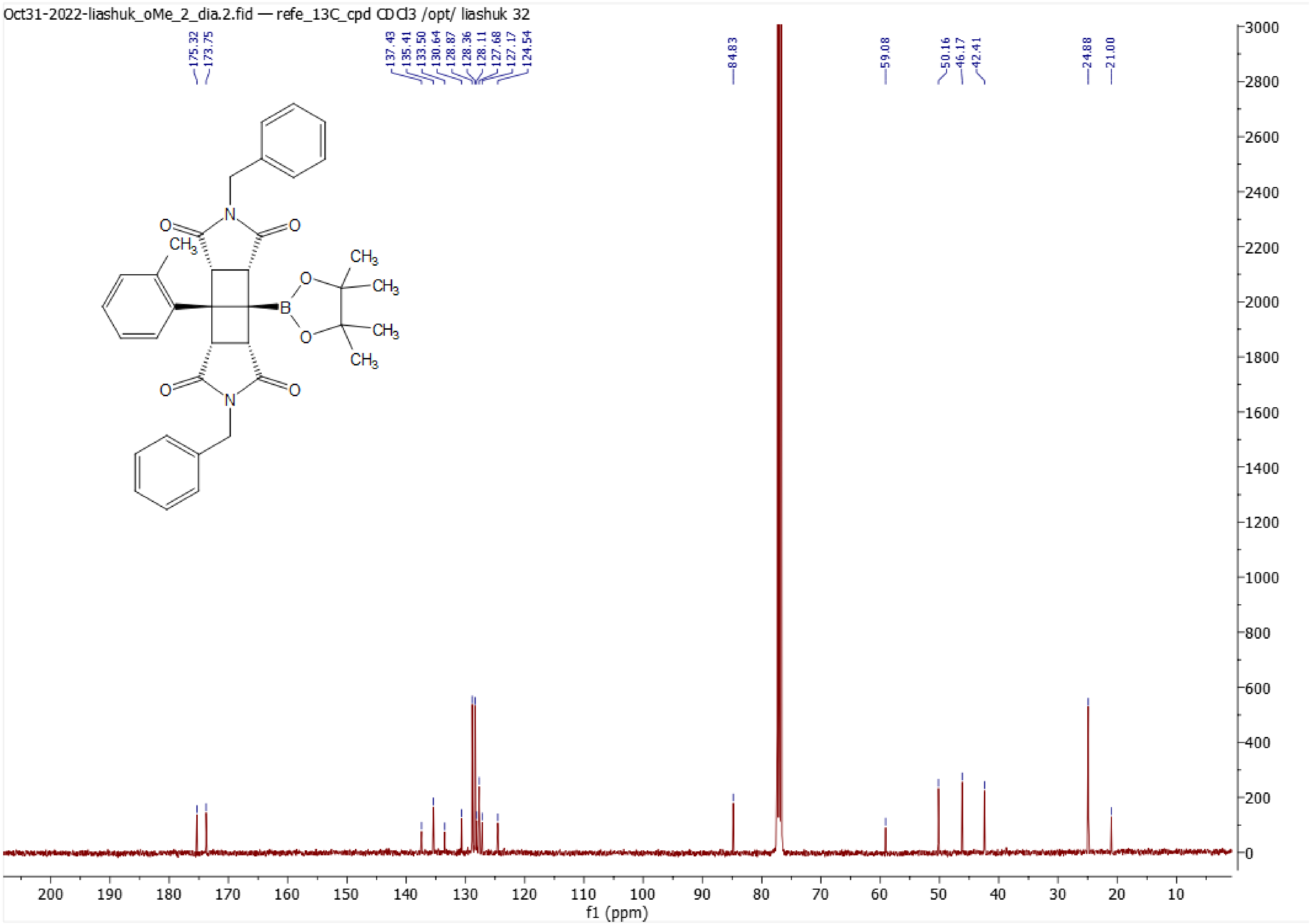

Spectrum 97. (1r,2R,6S,7r,8R,12S)-4,10-dibenzyl-1-(2-methylphenyl)-7-(4,4,5,5-tetramethyl-1,3,2-dioxaborolan-2-yl)-4,10-diazatetracyclo[5.5.0.02,6.08,12]dodecane-3,5,9,11-tetrone ***9d'****. ^{13}C NMR (101 MHz, CDCl$_3$)*

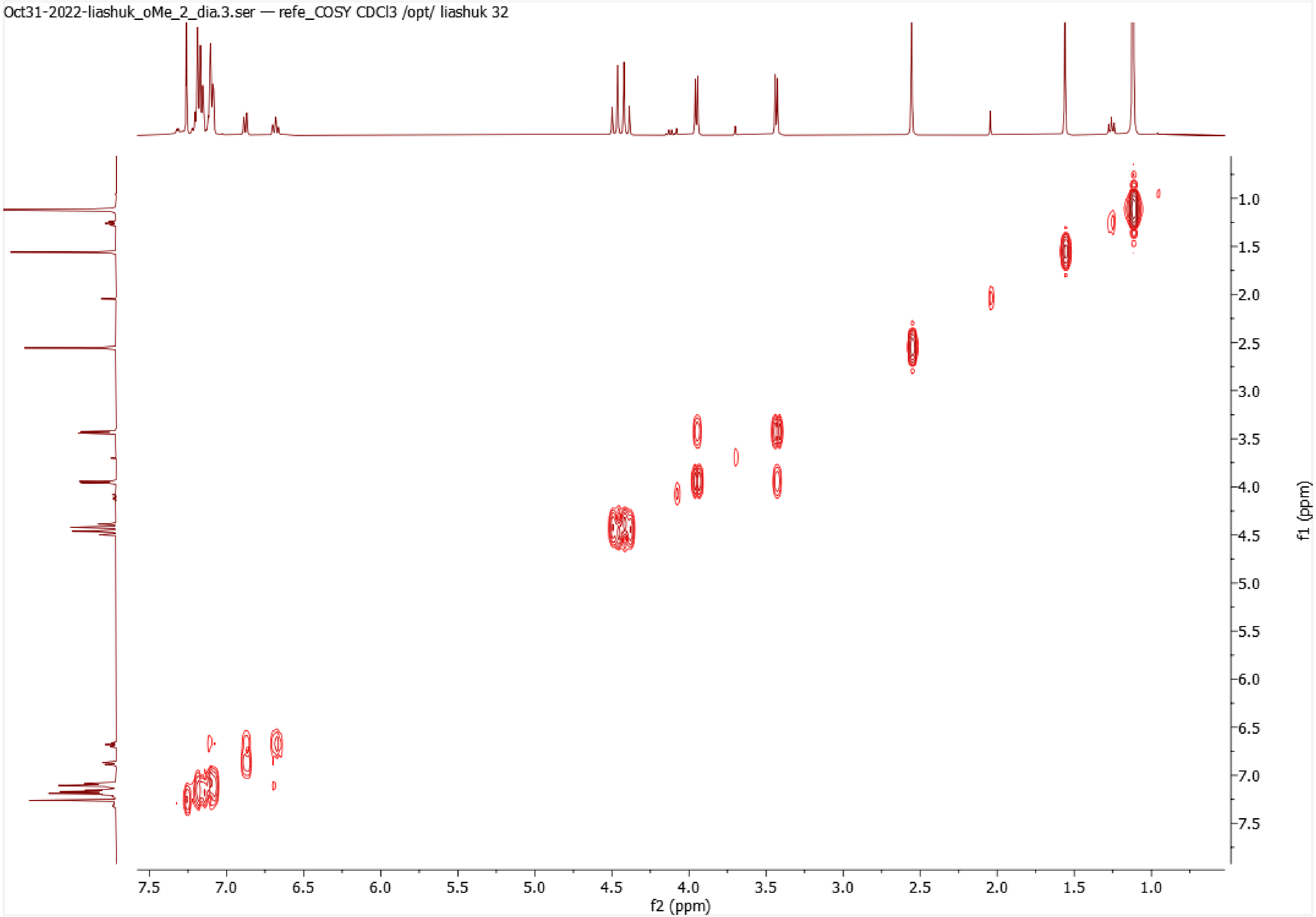

Spectrum 98. (1r,2R,6S,7r,8R,12S)-4,10-dibenzyl-1-(2-methylphenyl)-7-(4,4,5,5-tetramethyl-1,3,2-dioxaborolan-2-yl)-4,10-diazatetracyclo[5.5.0.02,6.08,12]dodecane-3,5,9,11-tetrone ***9d'****, COSY (400 MHz, CDCl3)*

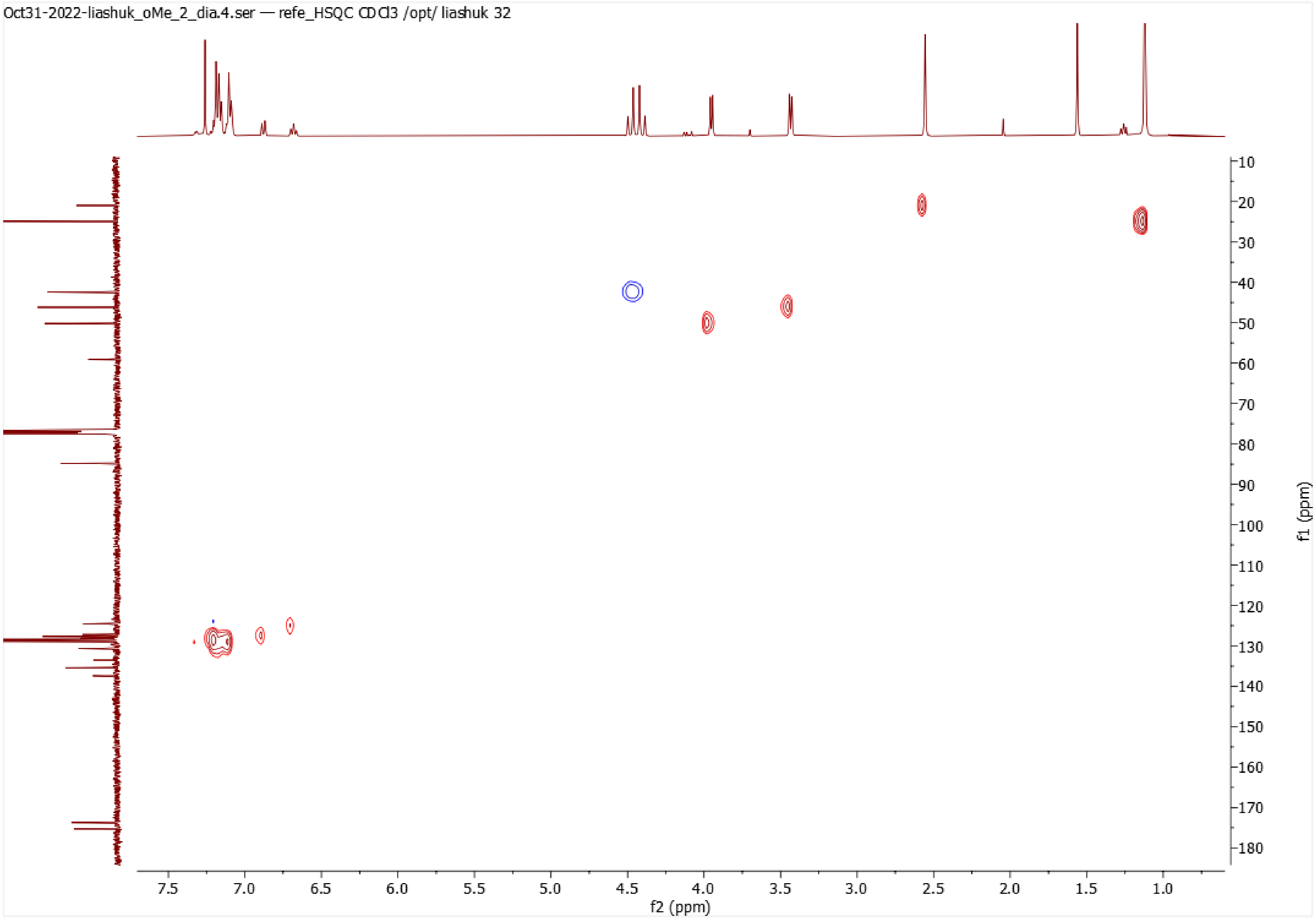

Spectrum 99. (1r,2R,6S,7r,8R,12S)-4,10-dibenzyl-1-(2-methylphenyl)-7-(4,4,5,5-tetramethyl-1,3,2-dioxaborolan-2-yl)-4,10-diazatetracyclo[5.5.0.02,6.08,12]dodecane-3,5,9,11-tetrone ***9d'****, HSQC (400/101 MHz, CDCl3)*

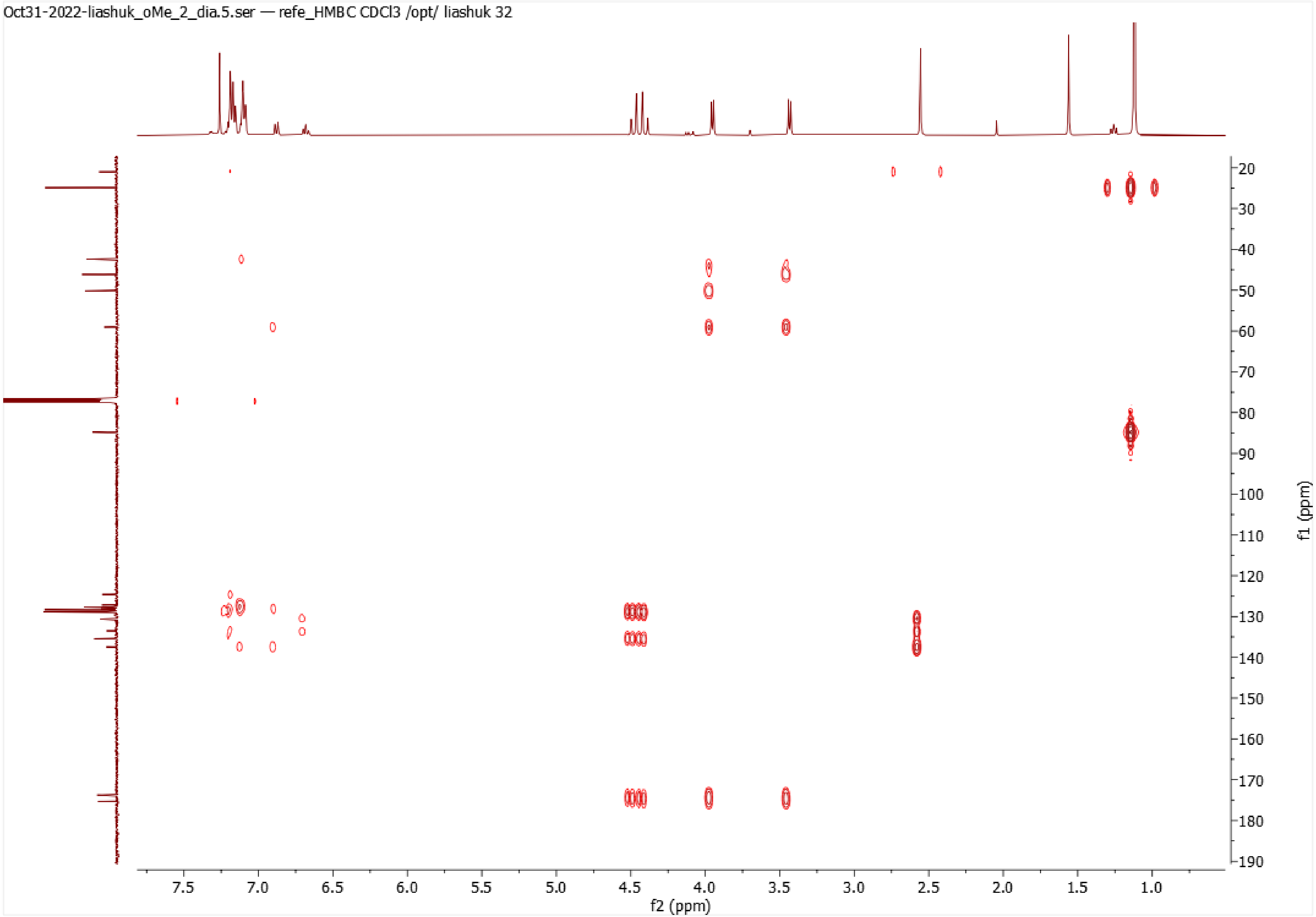

*Spectrum 100. (1r,2R,6S,7r,8R,12S)-4,10-dibenzyl-1-(2-methylphenyl)-7-(4,4,5,5-tetramethyl-1,3,2-dioxaborolan-2-yl)-4,10-diazatetracyclo[5.5.0.02,6.08,12]dodecane-3,5,9,11-tetrone **9d'**, HMBC (400/101 MHz, CDCl3)*

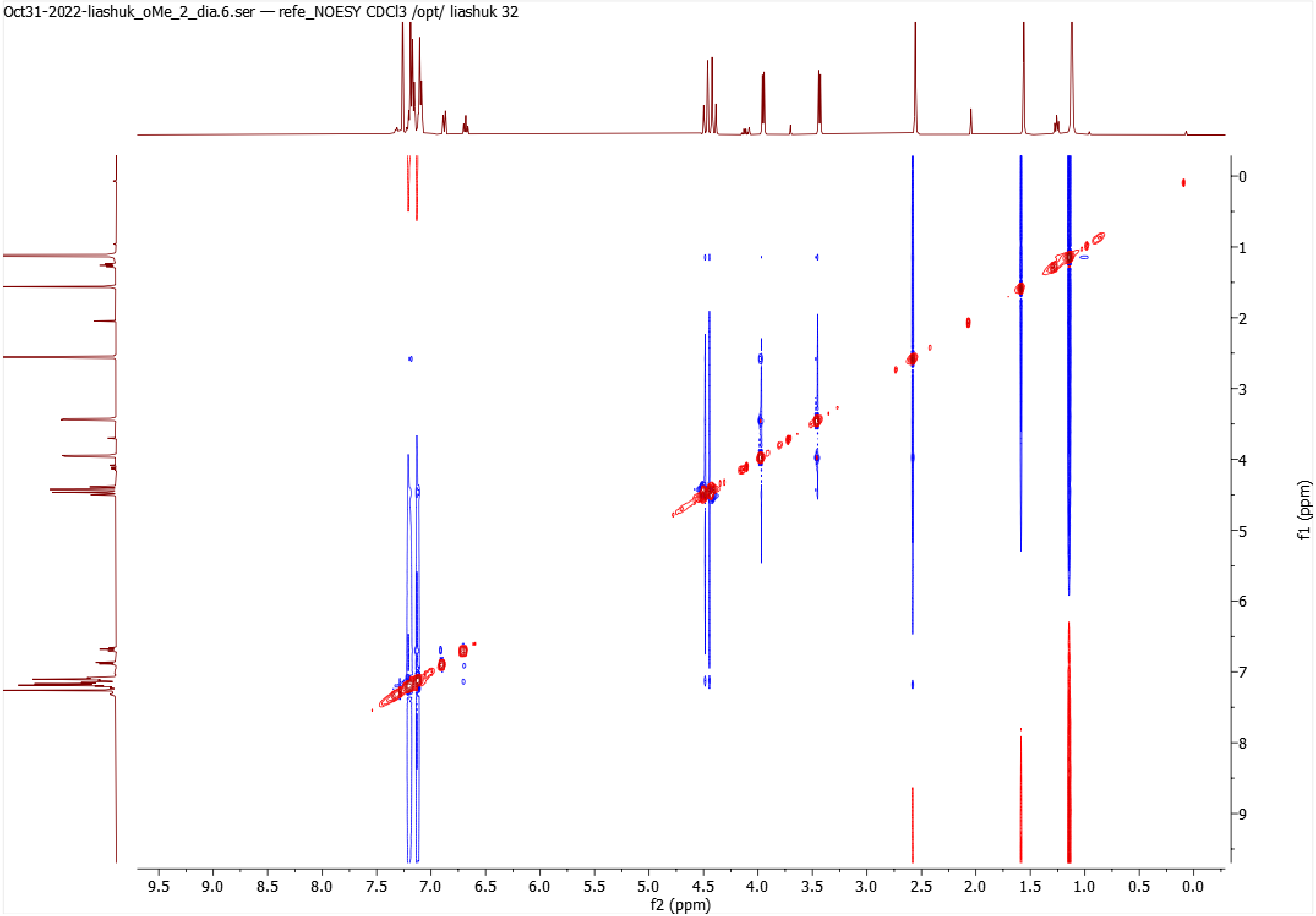

*Spectrum 101. (1r,2R,6S,7r,8R,12S)-4,10-dibenzyl-1-(2-methylphenyl)-7-(4,4,5,5-tetramethyl-1,3,2-dioxaborolan-2-yl)-4,10-diazatetracyclo[5.5.0.02,6.08,12]dodecane-3,5,9,11-tetrone **9d'**, NOESY (400 MHz, CDCl3)*

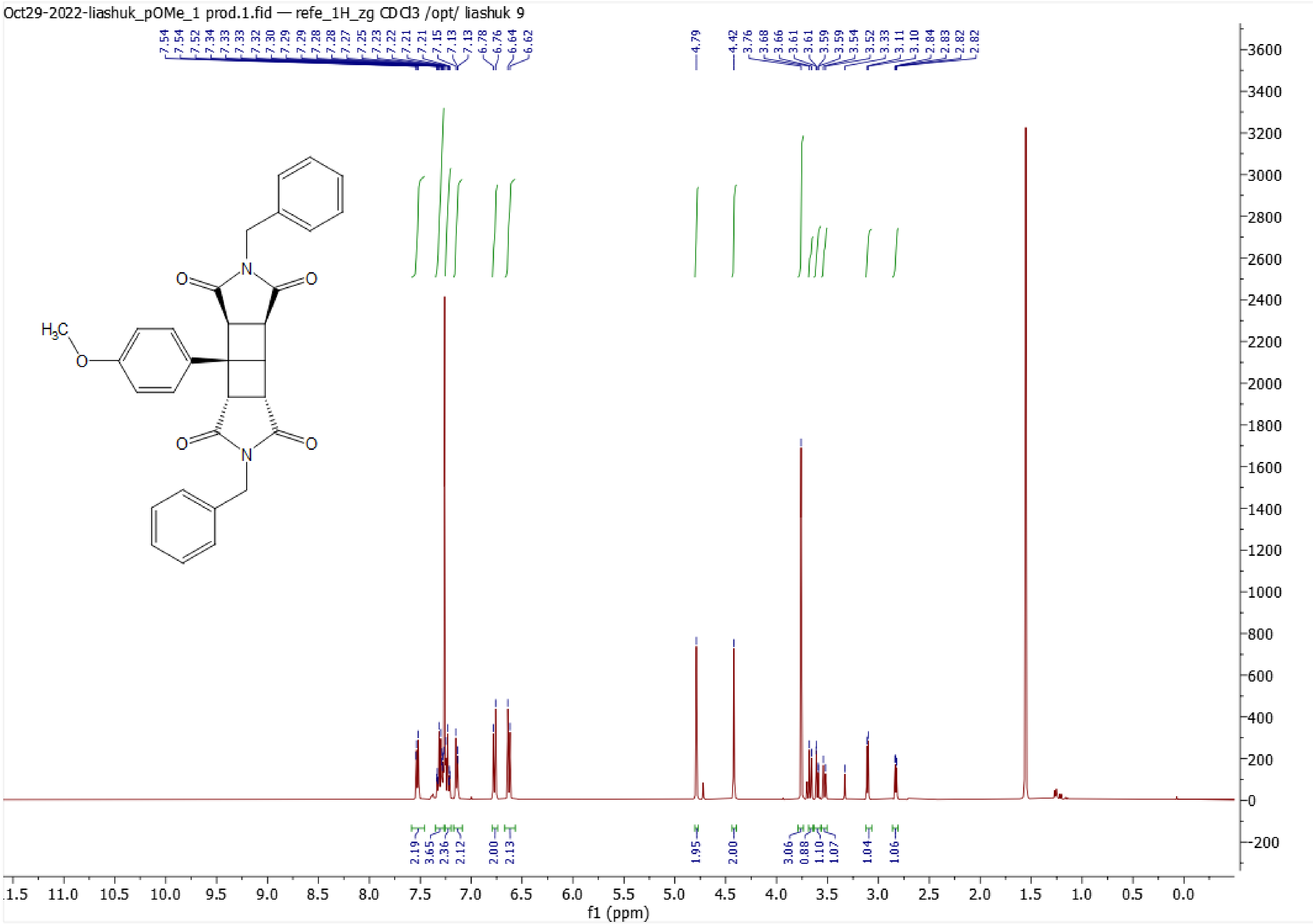

Spectrum 102.(2S,6S,8S,12S)-4,10-dibenzyl-1-(4-methoxyphenyl)-4,10-diazatetracyclo[5.5.0.02,6.08,12]dodecane-3,5,9,11-tetrone ***9e****,* ^{1}*H NMR (400 MHz, CDCl*$_3$*)*

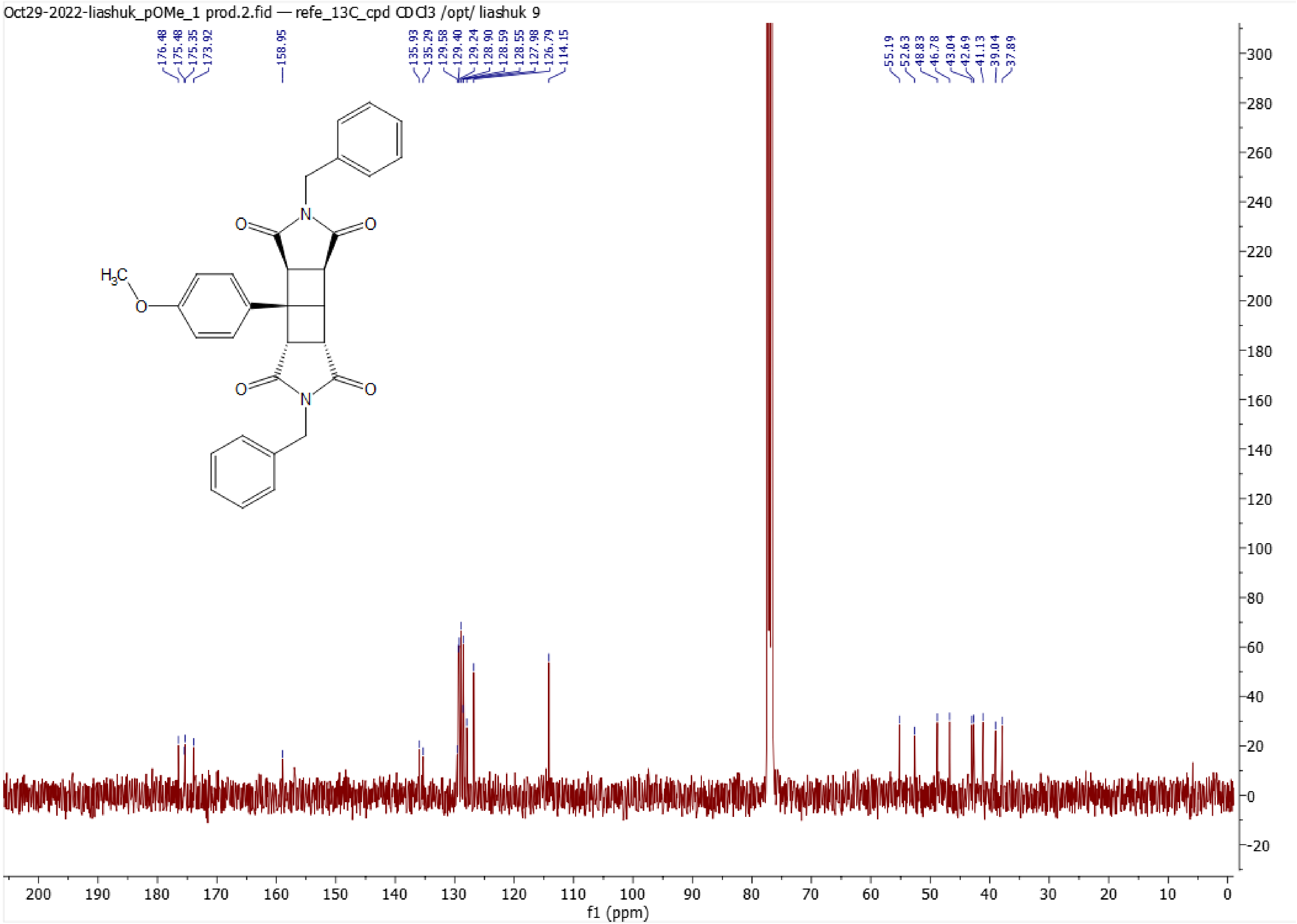

Spectrum 103. (2S,6S,8S,12S)-4,10-dibenzyl-1-(4-methoxyphenyl)-4,10-diazatetracyclo[5.5.0.02,6.08,12]dodecane-3,5,9,11-tetrone ***9e****, ^{13}C NMR (101 MHz, CDCl$_3$)*

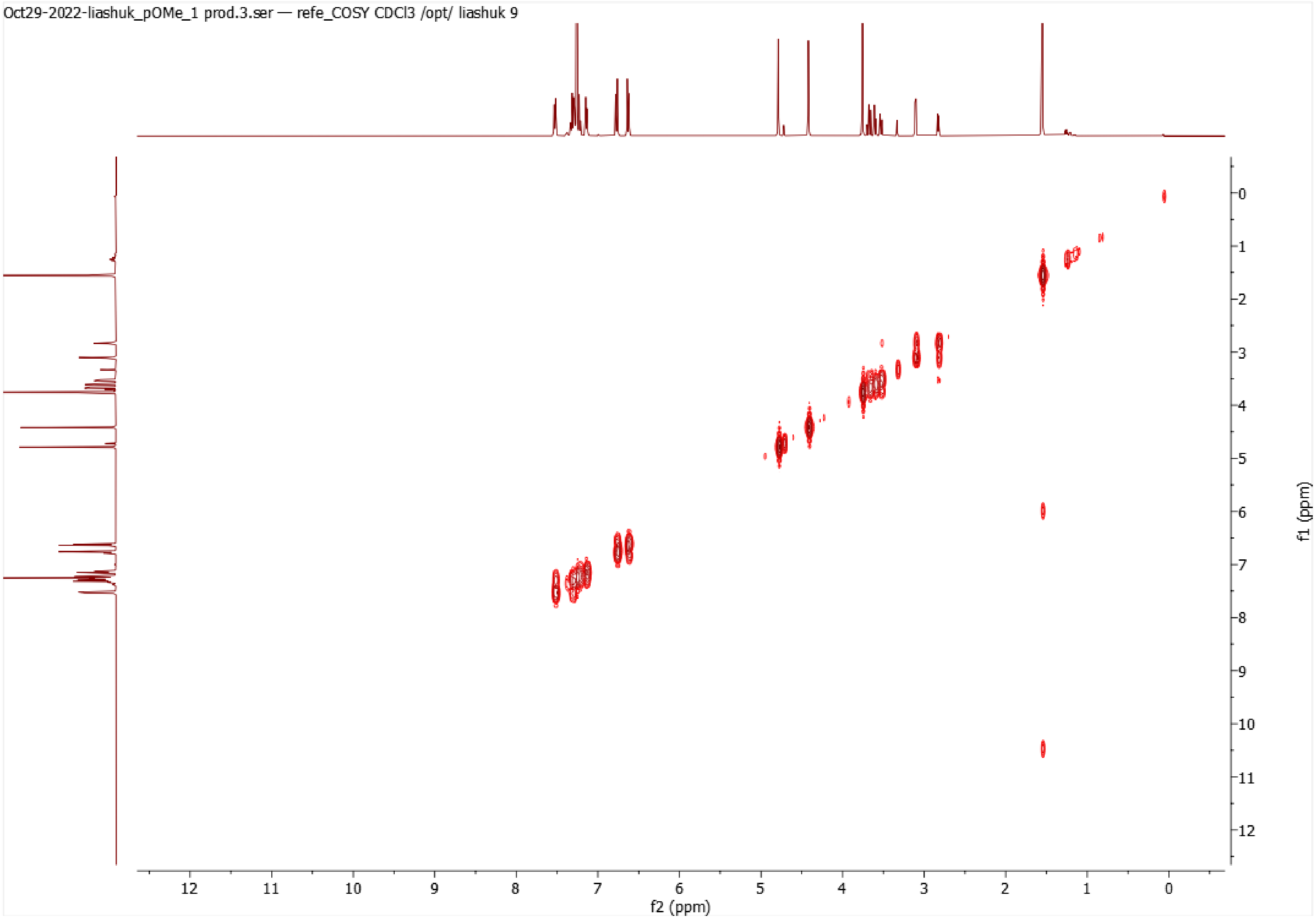

Spectrum 104. (2S,6S,8S,12S)-4,10-dibenzyl-1-(4-methoxyphenyl)-4,10-diazatetracyclo[5.5.0.02,6.08,12]dodecane-3,5,9,11-tetrone ***9e****, COSY (400 MHz, CDCl3)*

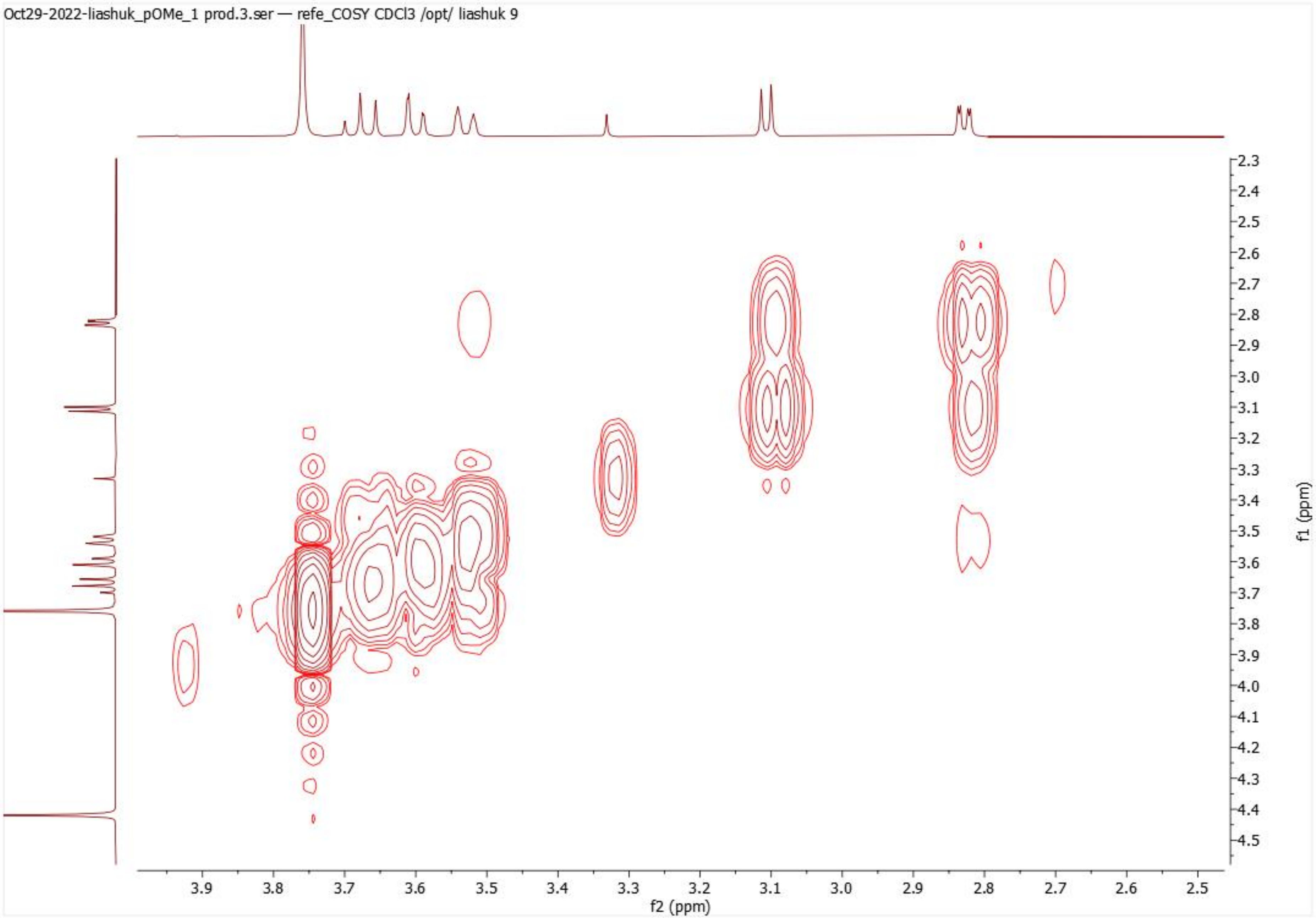

Spectrum 105. (2S,6S,8S,12S)-4,10-dibenzyl-1-(4-methoxyphenyl)-4,10-diazatetracyclo[5.5.0.02,6.08,12]dodecane-3,5,9,11-tetrone ***9e****, COSY (400 MHz, CDCl3), aliphatic region*

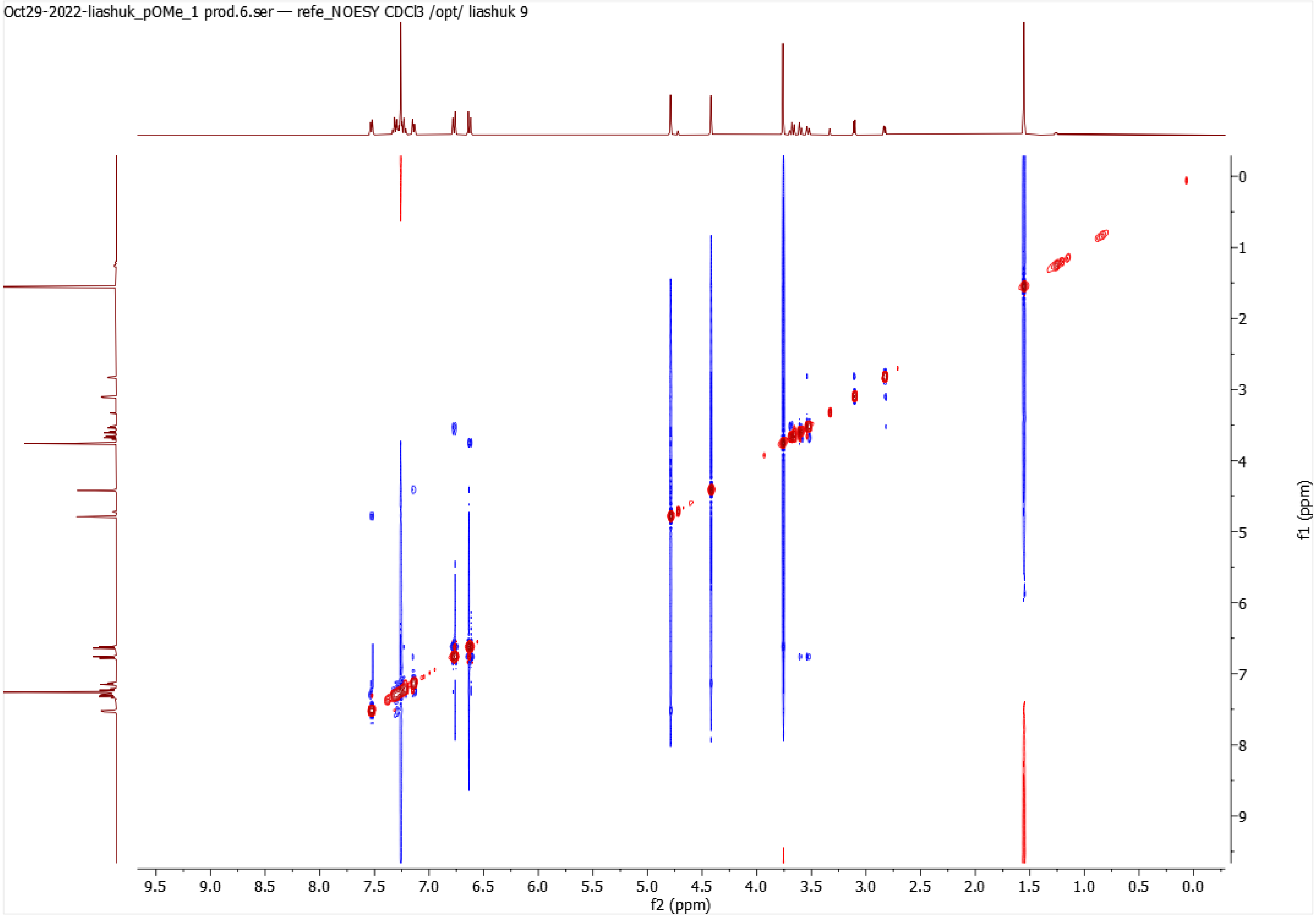

Spectrum 106. (2S,6S,8S,12S)-4,10-dibenzyl-1-(4-methoxyphenyl)-4,10-diazatetracyclo[5.5.0.02,6.08,12]dodecane-3,5,9,11-tetrone ***9e****, NOESY (400 MHz, CDCl3)*

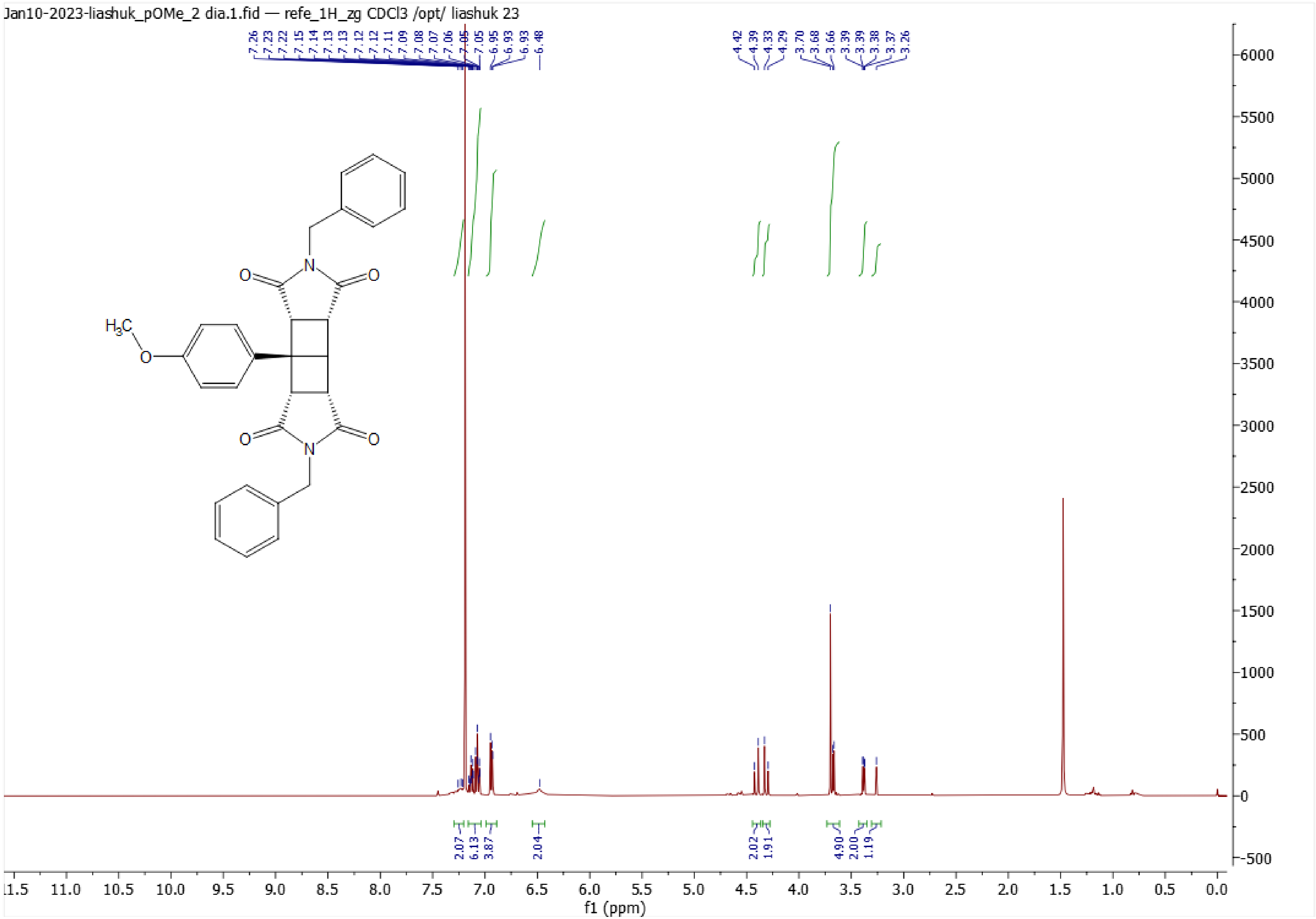

Spectrum 107. (1r,2R,6R,8S,12S)-4,10-dibenzyl-1-(4-methoxyphenyl)-4,10-diazatetracyclo[5.5.0.02,6.08,12]dodecane-3,5,9,11-tetrone ***9e'****, ^{1}H NMR (400 MHz, CDCl$_3$)*

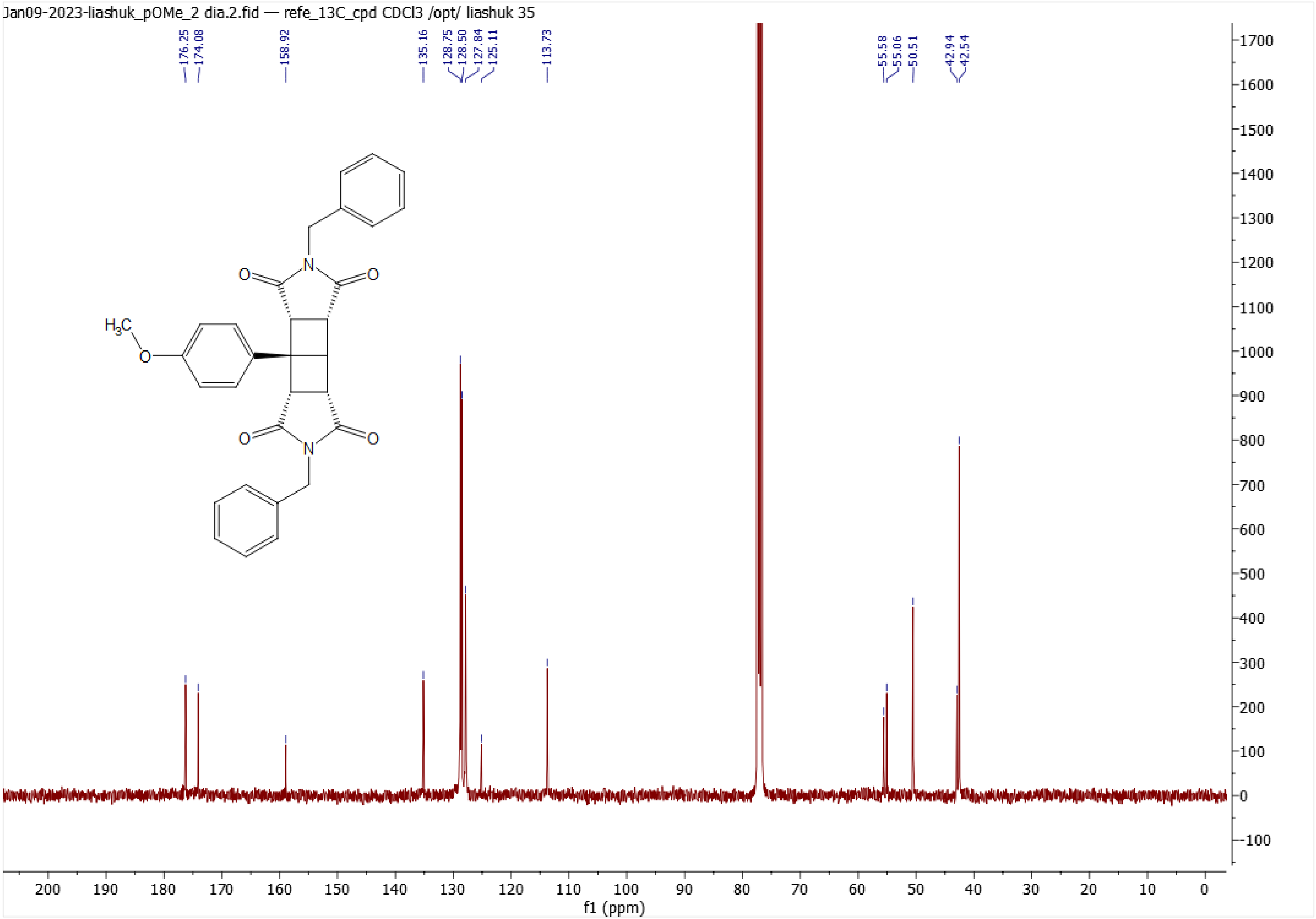

Spectrum 108. (1R,2R,6R,8S,12S)-4,10-dibenzyl-1-(4-methoxyphenyl)-4,10-diazatetracyclo[5.5.0.02,6.08,12]dodecane-3,5,9,11-tetrone ***9e'****, ^{13}C NMR (101 MHz, $CDCl_3$)*

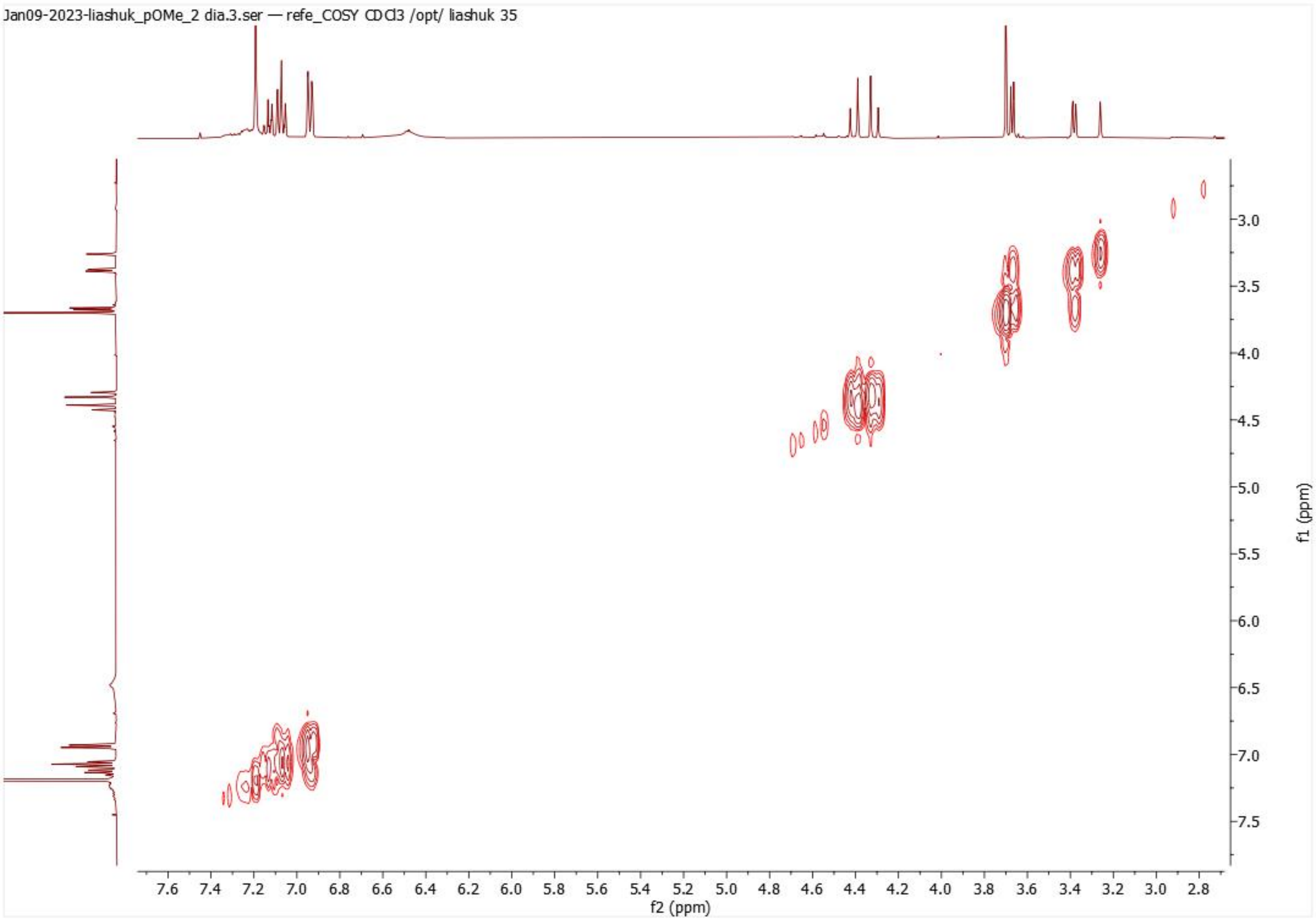

*Spectrum 109. (1r,2R,6R,8S,12S)-4,10-dibenzyl-1-(4-methoxyphenyl)-4,10-diazatetracyclo[5.5.0.02,6.08,12]dodecane-3,5,9,11-tetrone **9e'**, COSY (400 MHz, CDCl3)*

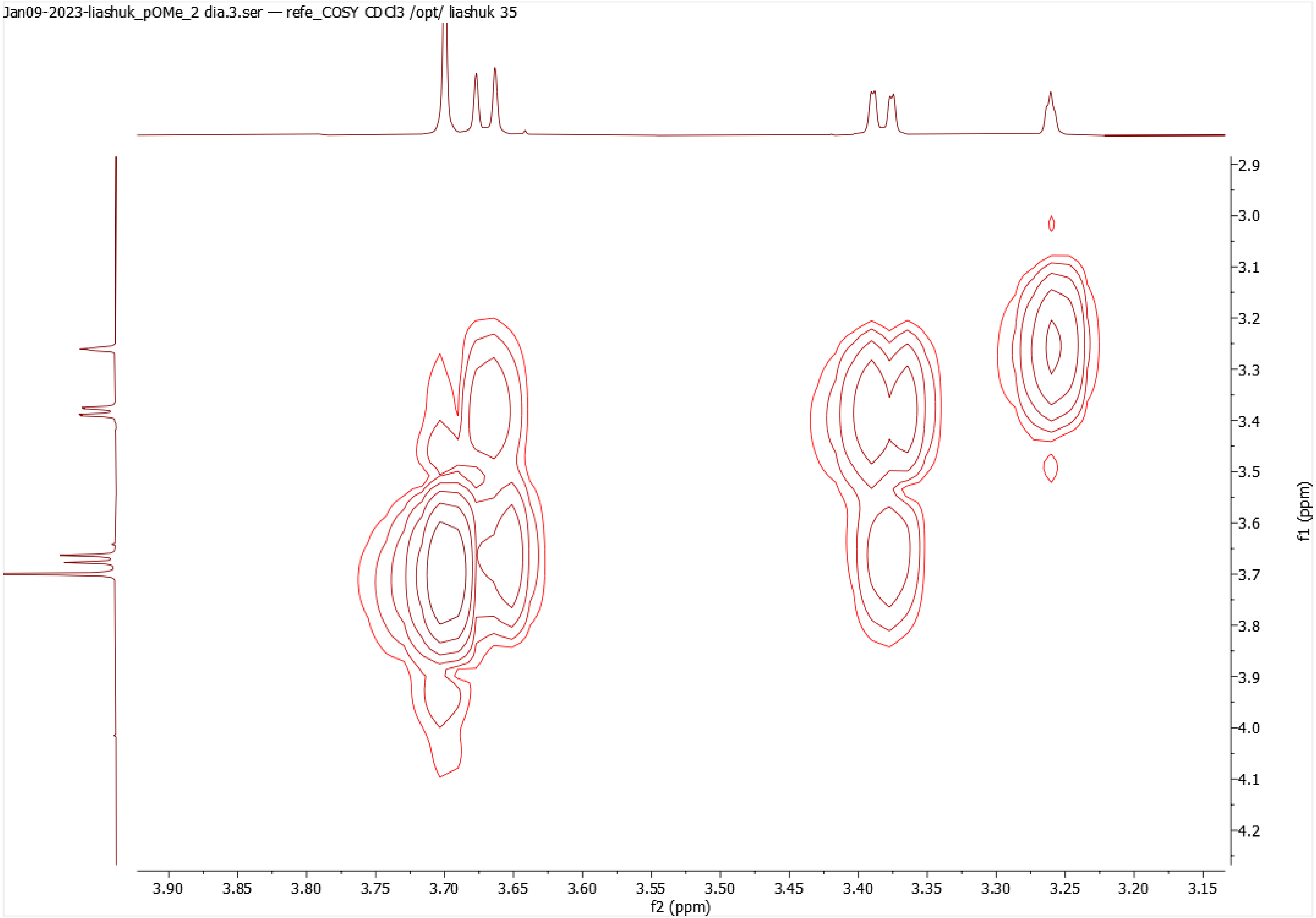

*Spectrum 110. (1r,2R,6R,8S,12S)-4,10-dibenzyl-1-(4-methoxyphenyl)-4,10-diazatetracyclo[5.5.0.02,6.08,12]dodecane-3,5,9,11-tetrone **9e'**, aliphatic region COSY (400 MHz, CDCl3)*

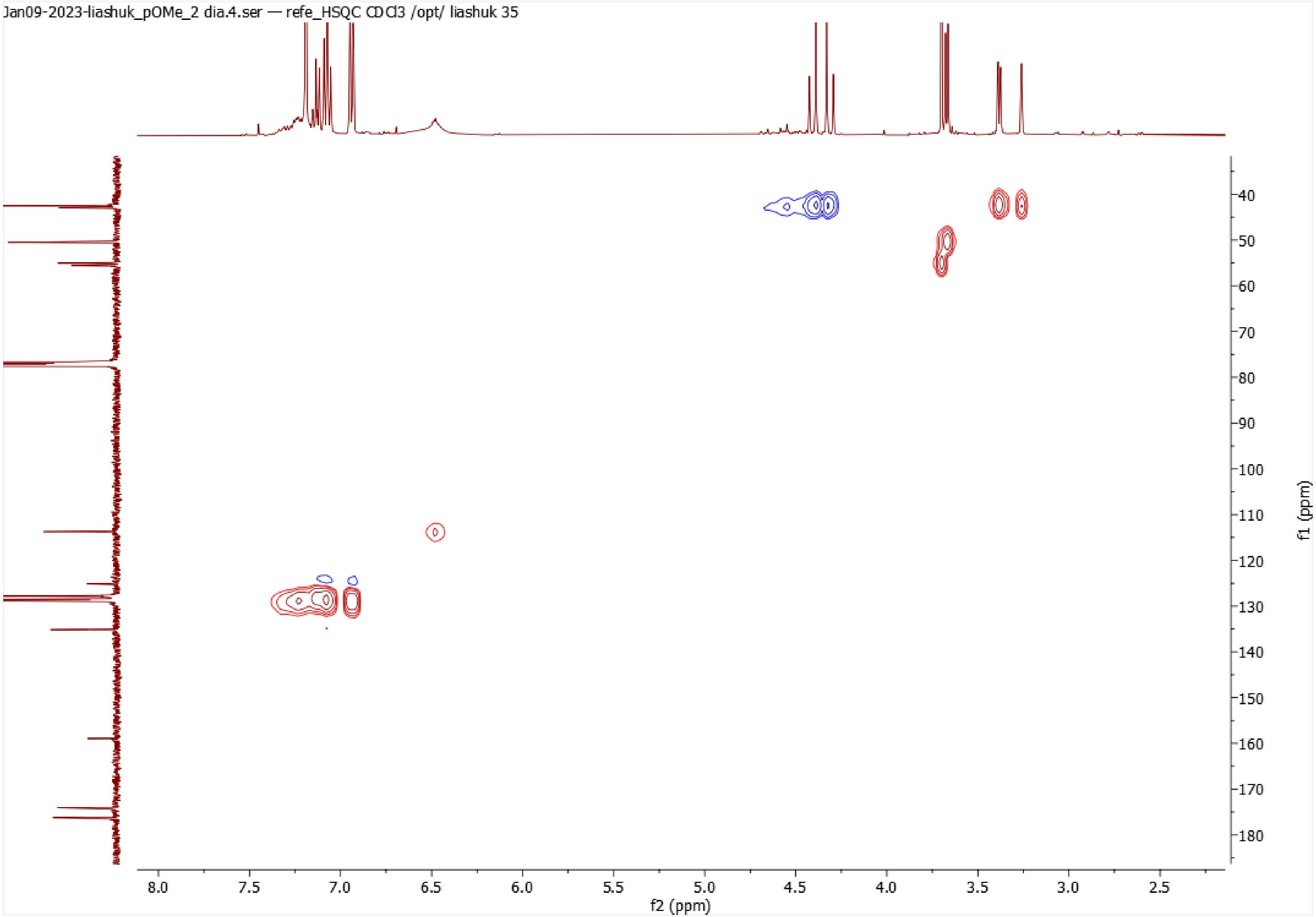

*Spectrum 111. (1r,2R,6R,8S,12S)-4,10-dibenzyl-1-(4-methoxyphenyl)-4,10-diazatetracyclo[5.5.0.02,6.08,12]dodecane-3,5,9,11-tetrone **9e'**, HSQC (400/101 MHz, CDCl3)*

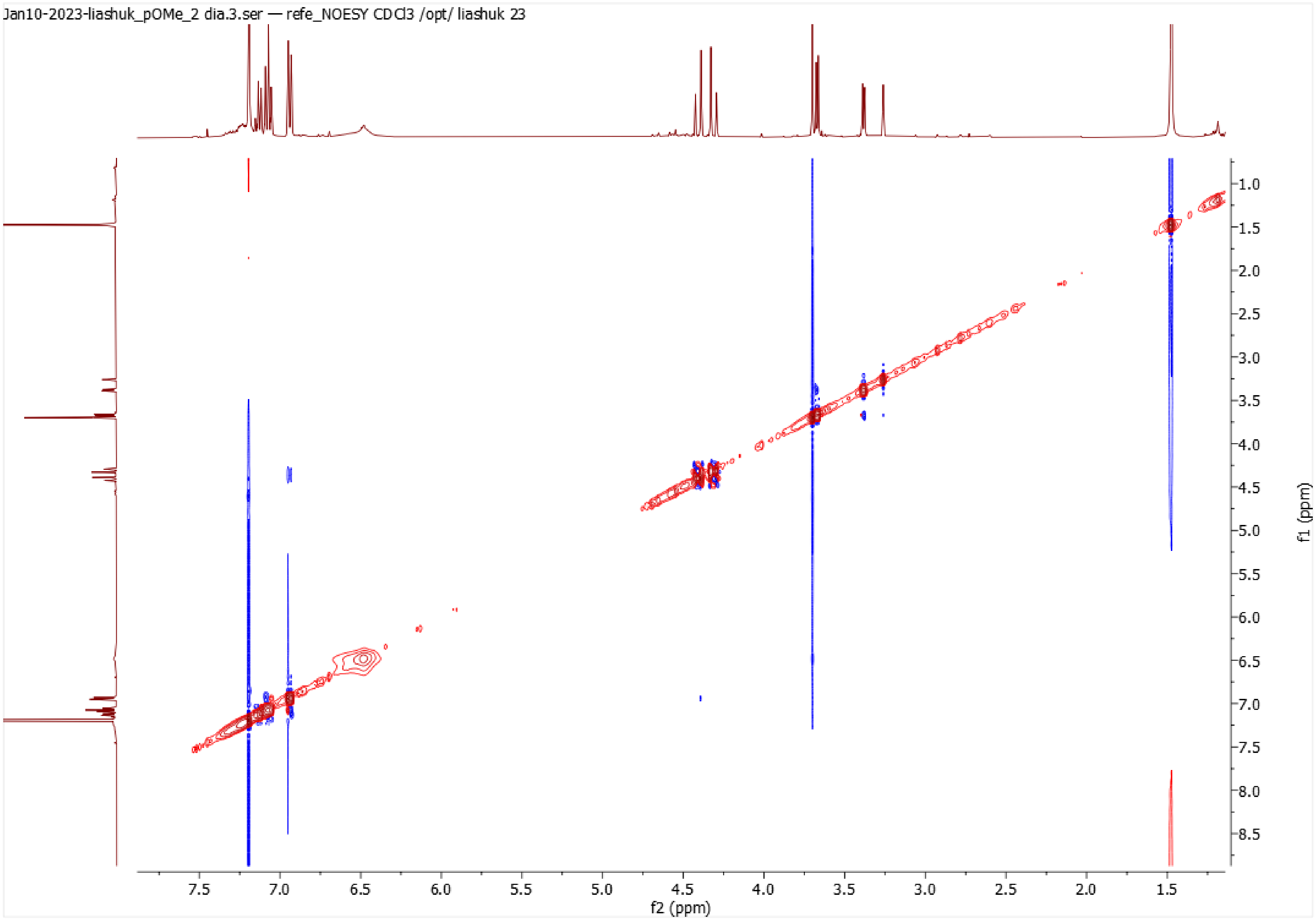

*Spectrum 112. (1r,2R,6R,8S,12S)-4,10-dibenzyl-1-(4-methoxyphenyl)-4,10-diazatetracyclo[5.5.0.02,6.08,12]dodecane-3,5,9,11-tetrone **9e'**, NOESY (400 MHz, CDCl3)*

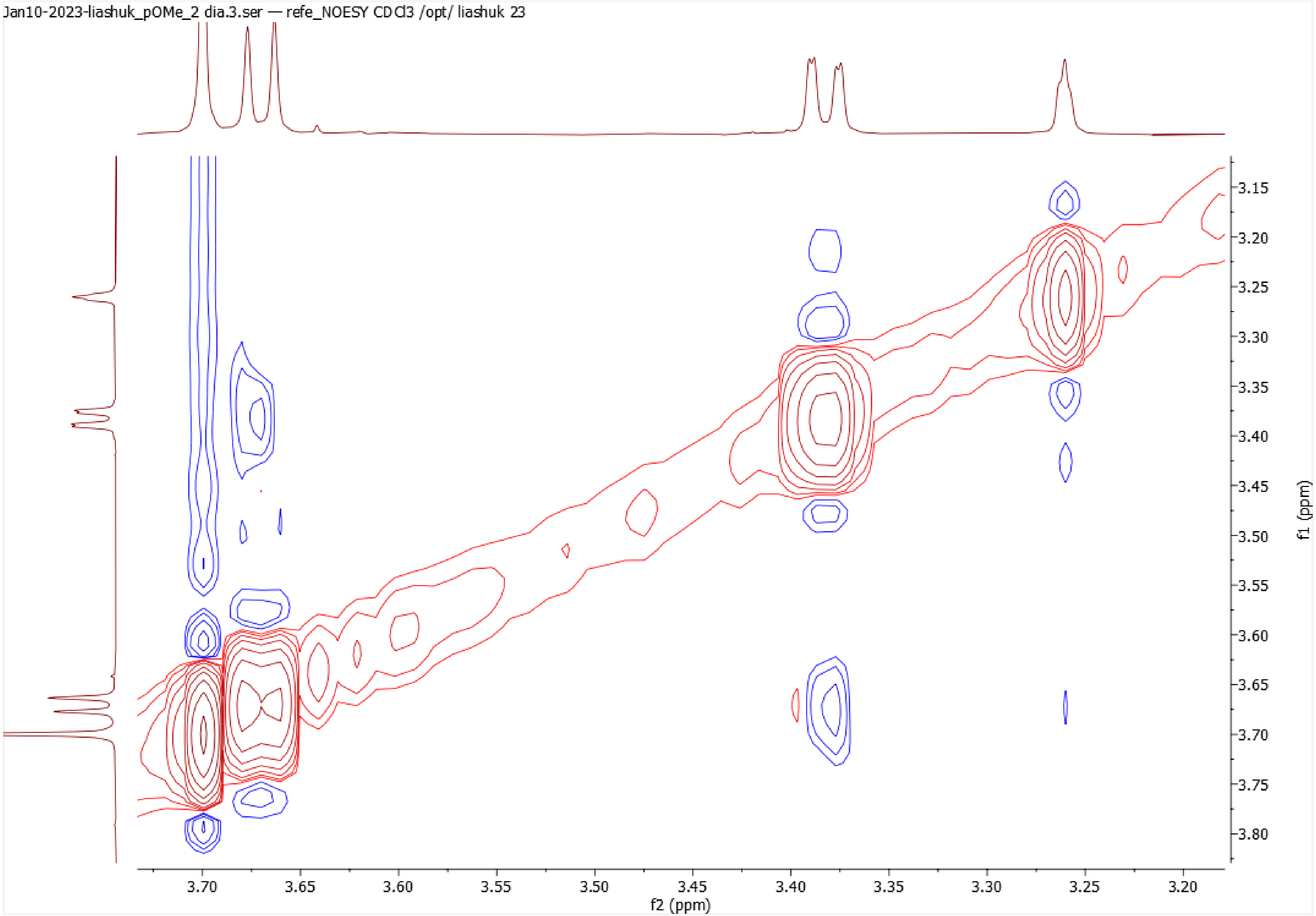

Spectrum 113. (1r,2R,6R,8S,12S)-4,10-dibenzyl-1-(4-methoxyphenyl)-4,10-diazatetracyclo[5.5.0.02,6.08,12]dodecane-3,5,9,11-tetrone ***9e'****, NOESY (400 MHz, CDCl3), aliphatic region*

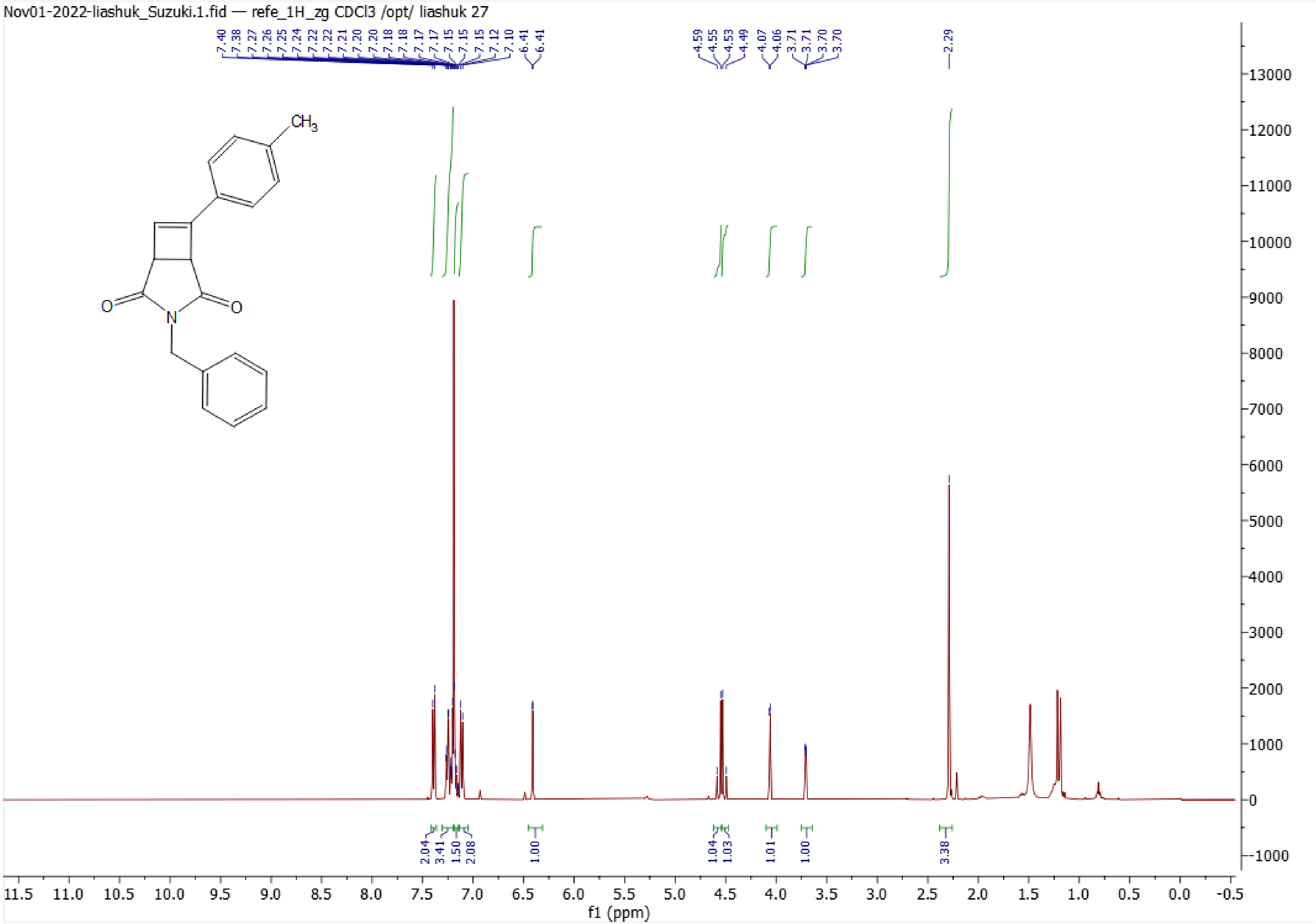

*Spectrum 114. 3-benzyl-6-(p-tolyl)-3-azabicyclo[3.2.0]hept-6-ene-2,4-dione **11a**, ^{1}H NMR (400 MHz, CDCl$_3$)*

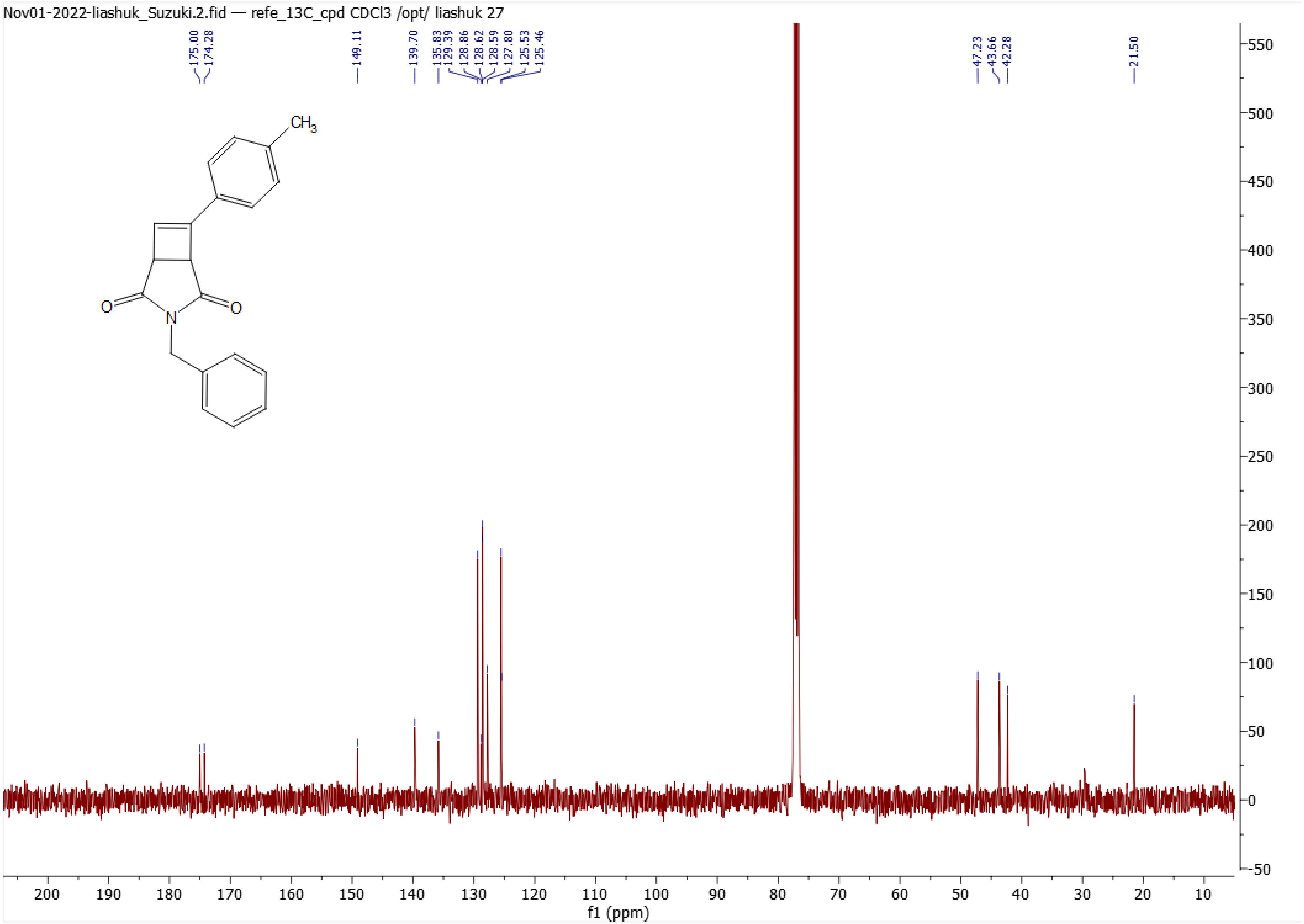

*Spectrum 115. 3-benzyl-6-(p-tolyl)-3-azabicyclo[3.2.0]hept-6-ene-2,4-dione **11a**, ^{13}C NMR (101 MHz, $CDCl_3$)*

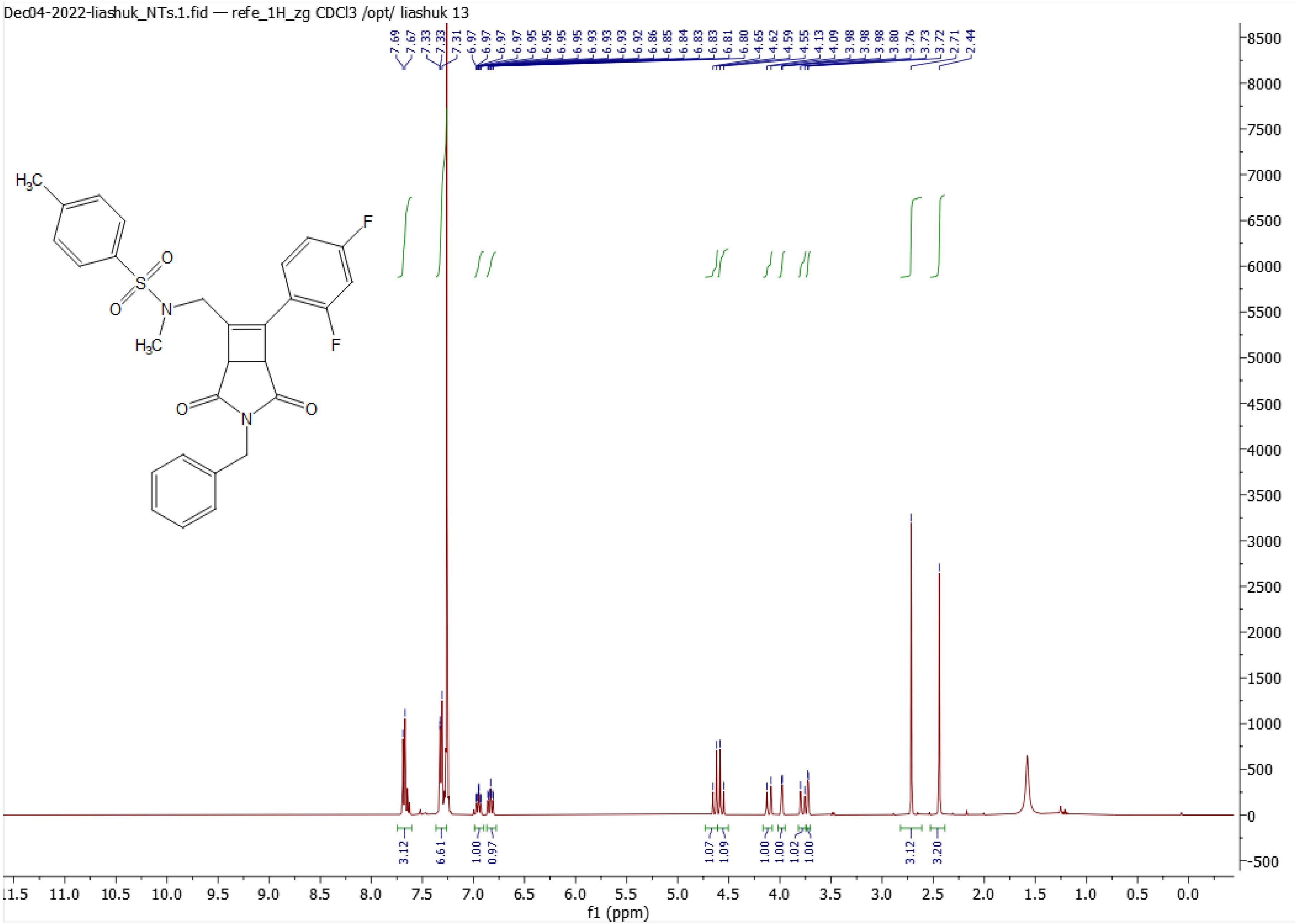

Spectrum 116. N-((3-benzyl-7-(2,4-difluorophenyl)-2,4-dioxo-3-azabicyclo[3.2.0]hept-6-en-6-yl)methyl)-N,4-dimethylbenzenesulfonamide ***11b***, *^{1}H NMR (400 MHz, CDCl$_3$)*

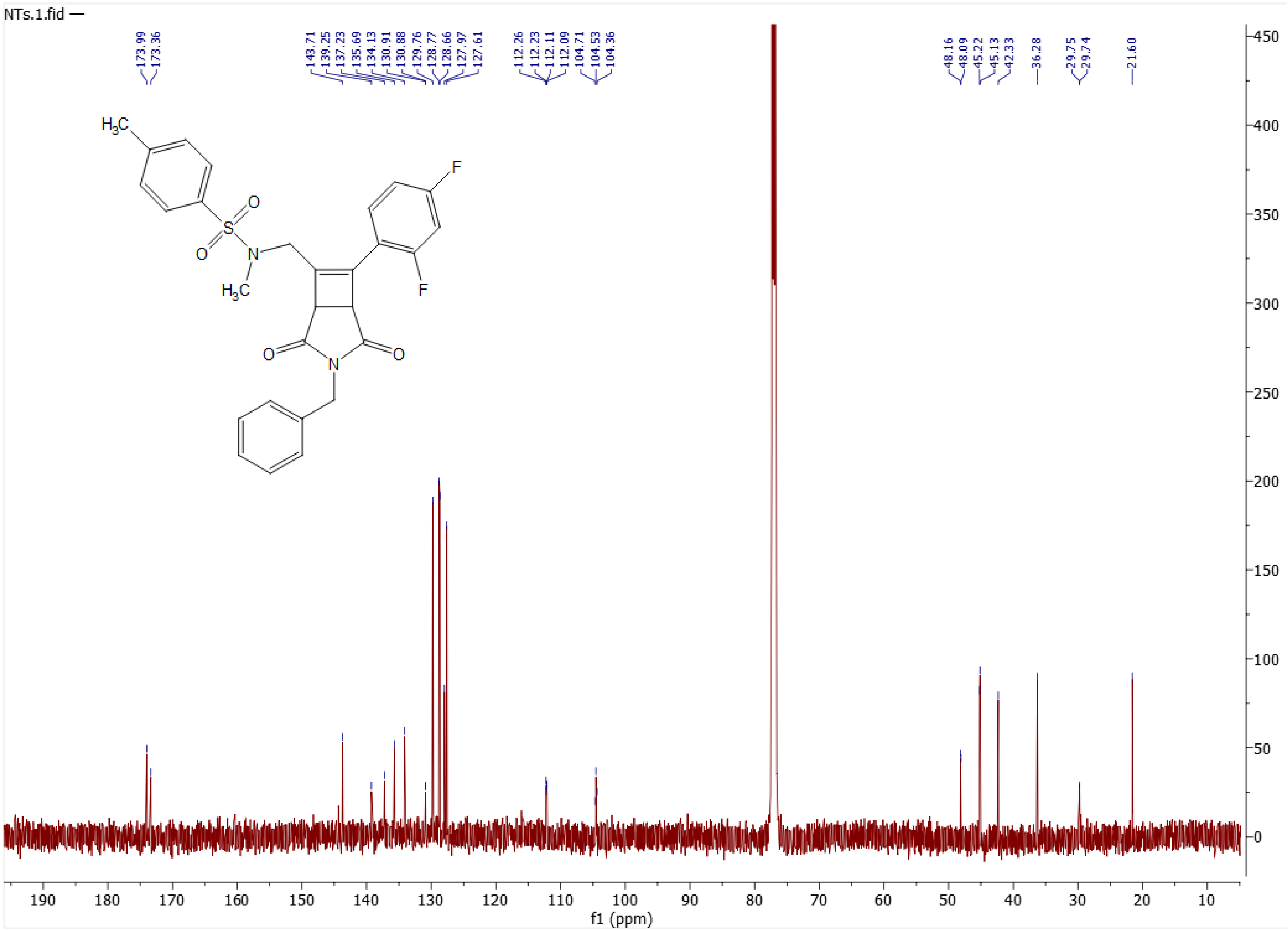

Spectrum 117. N-((3-benzyl-7-(2,4-difluorophenyl)-2,4-dioxo-3-azabicyclo[3.2.0]hept-6-en-6-yl)methyl)-N,4-dimethylbenzenesulfonamide ***11b****, ^{13}C NMR (151 MHz, CDCl$_3$)*

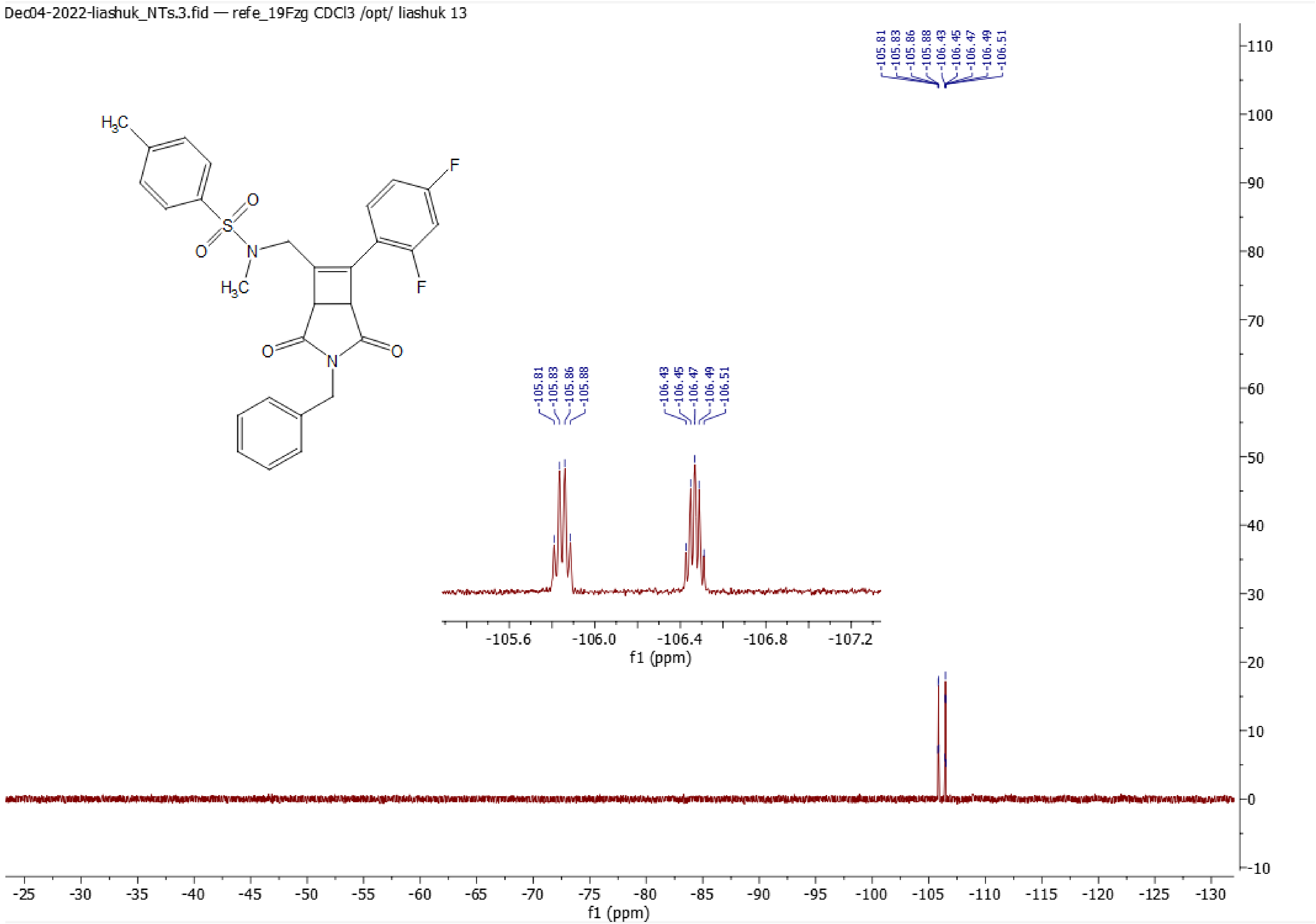

Spectrum 118. N-((3-benzyl-7-(2,4-difluorophenyl)-2,4-dioxo-3-azabicyclo[3.2.0]hept-6-en-6-yl)methyl)-N,4-dimethylbenzenesulfonamide ***11b****,* *^{19}F NMR (376 MHz, CDCl$_3$)*

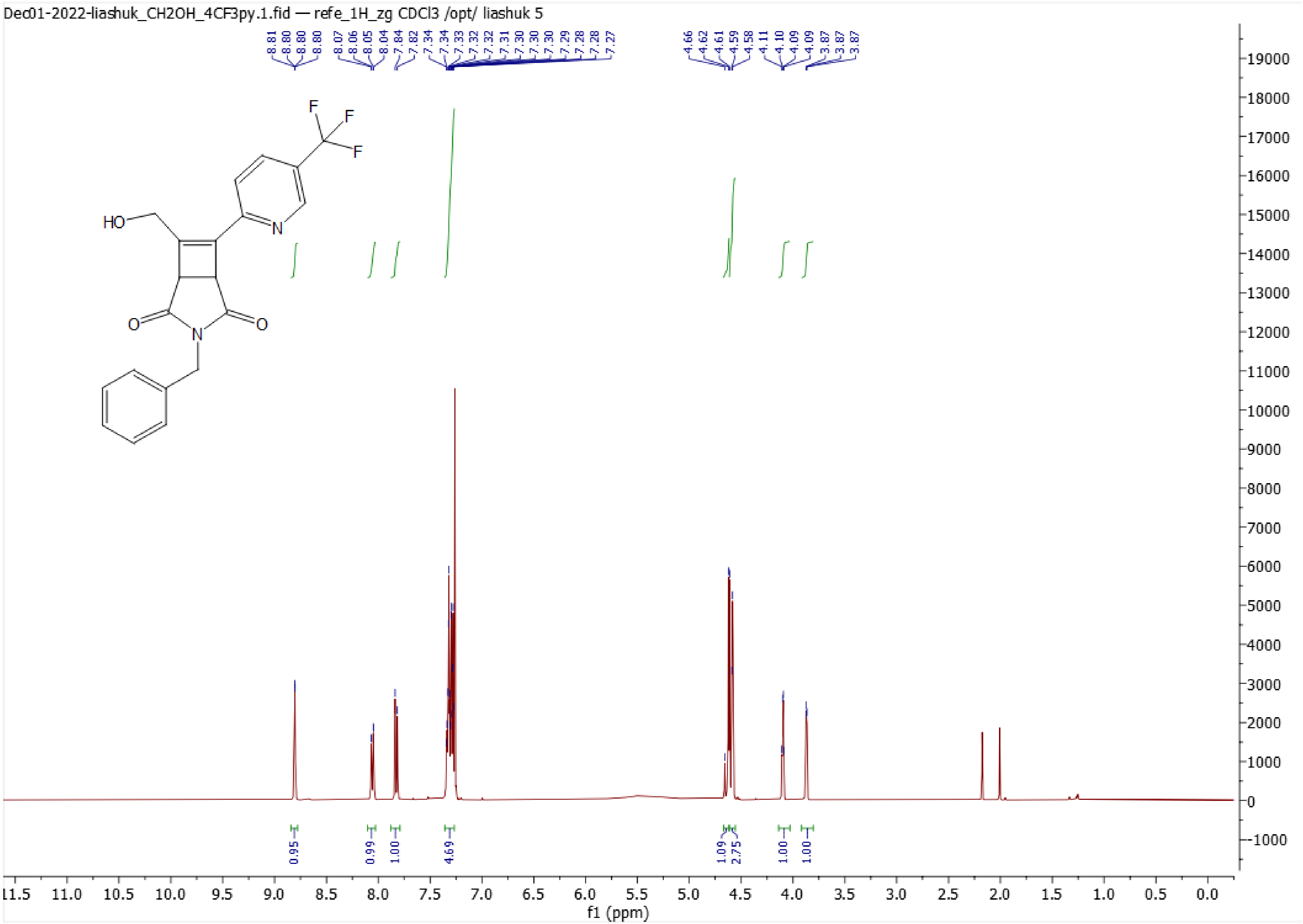

*Spectrum 119. 3-benzyl-6-(hydroxymethyl)-7-(5-(trifluoromethyl)pyridin-2-yl)-3-azabicyclo[3.2.0]hept-6-ene-2,4-dione **11c**, ^{1}H NMR (400 MHz, CDCl$_3$)*

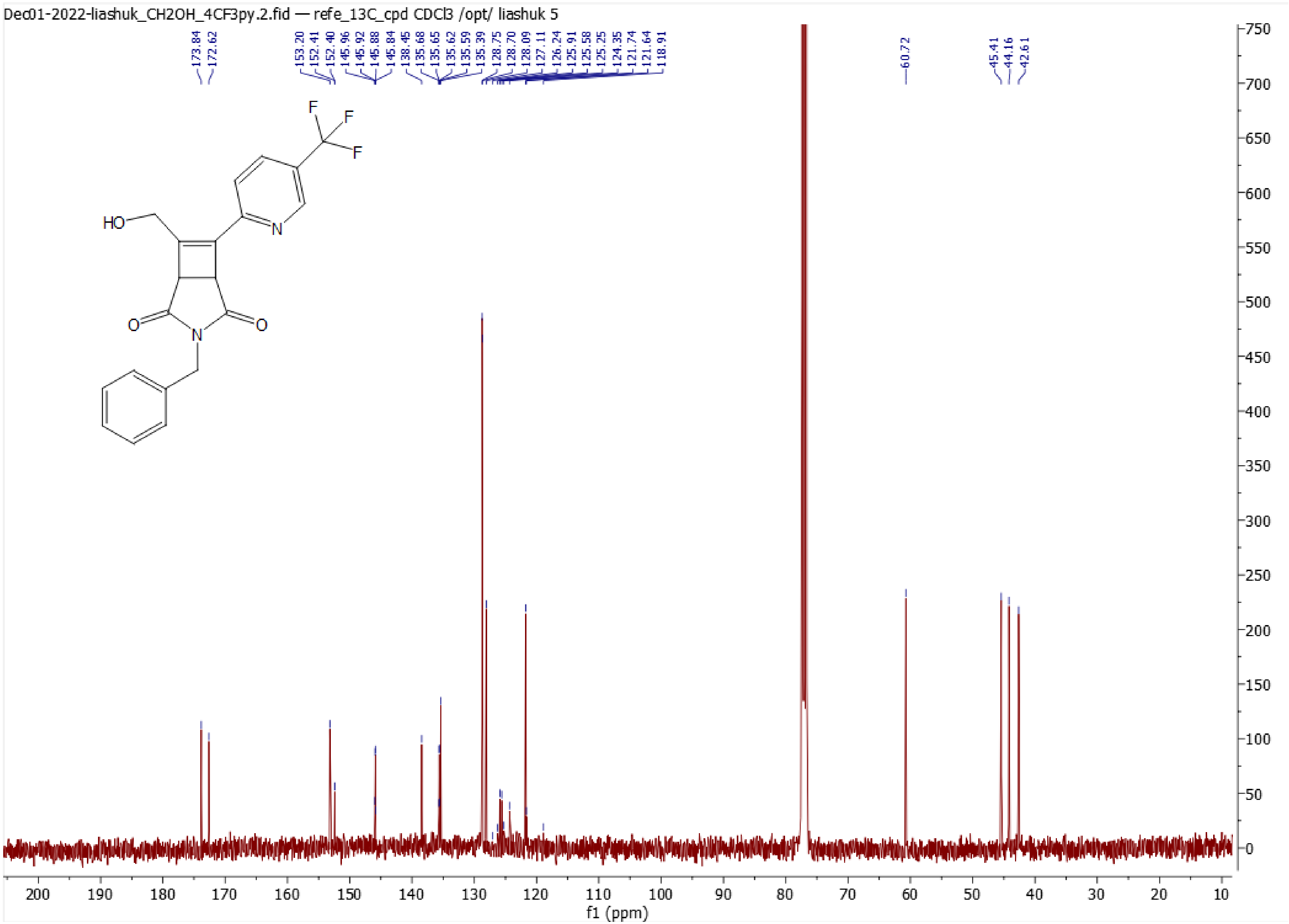

*Spectrum 120. 3-benzyl-6-(hydroxymethyl)-7-(5-(trifluoromethyl)pyridin-2-yl)-3-azabicyclo[3.2.0]hept-6-ene-2,4-dione **11c**, ^{13}C NMR (101 MHz, CDCl$_3$)*

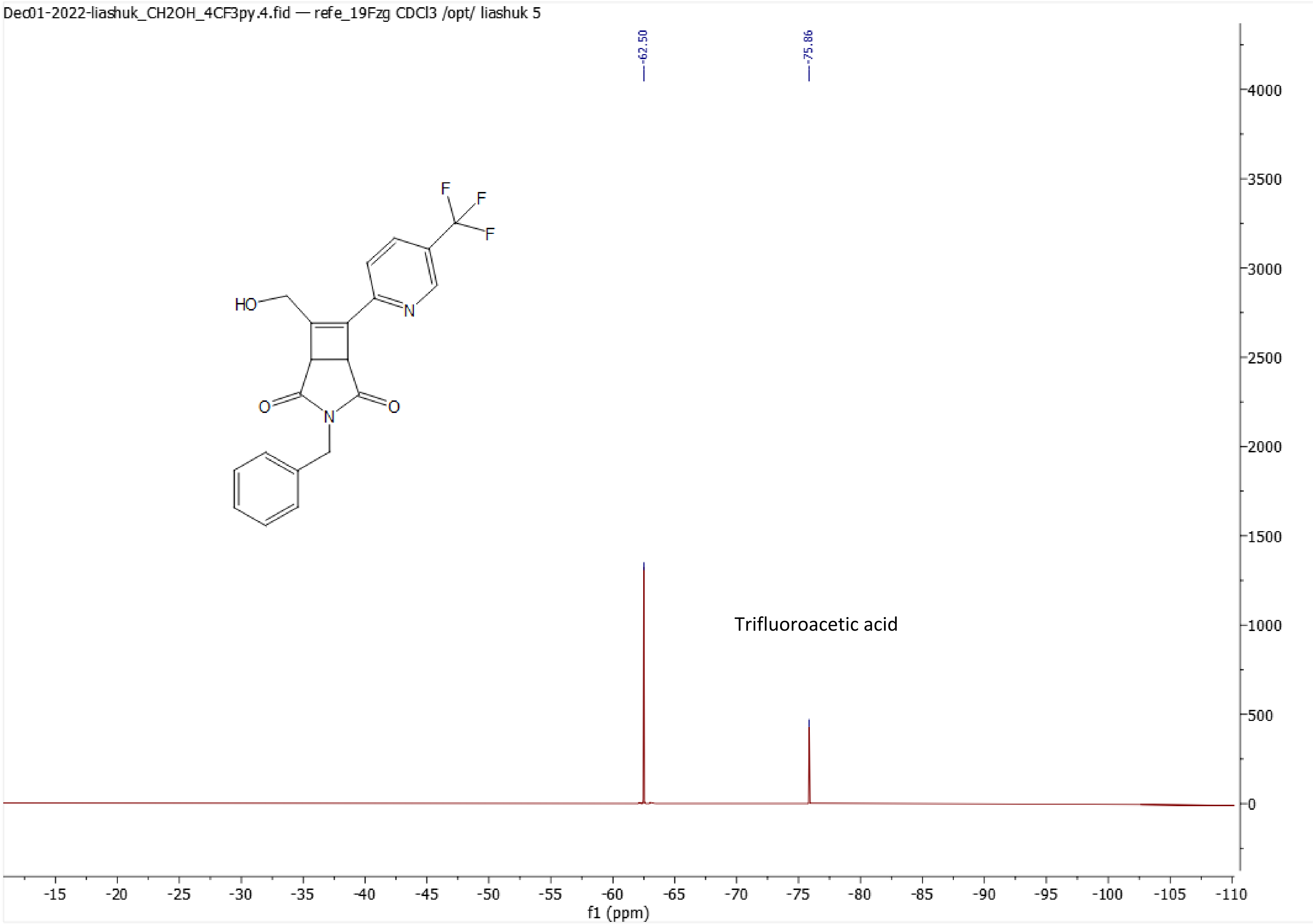

*Spectrum 121. 3-benzyl-6-(hydroxymethyl)-7-(5-(trifluoromethyl)pyridin-2-yl)-3-azabicyclo[3.2.0]hept-6-ene-2,4-dione **11c**, ^{19}F NMR (376 MHz, CDCl$_3$), full spectrum*

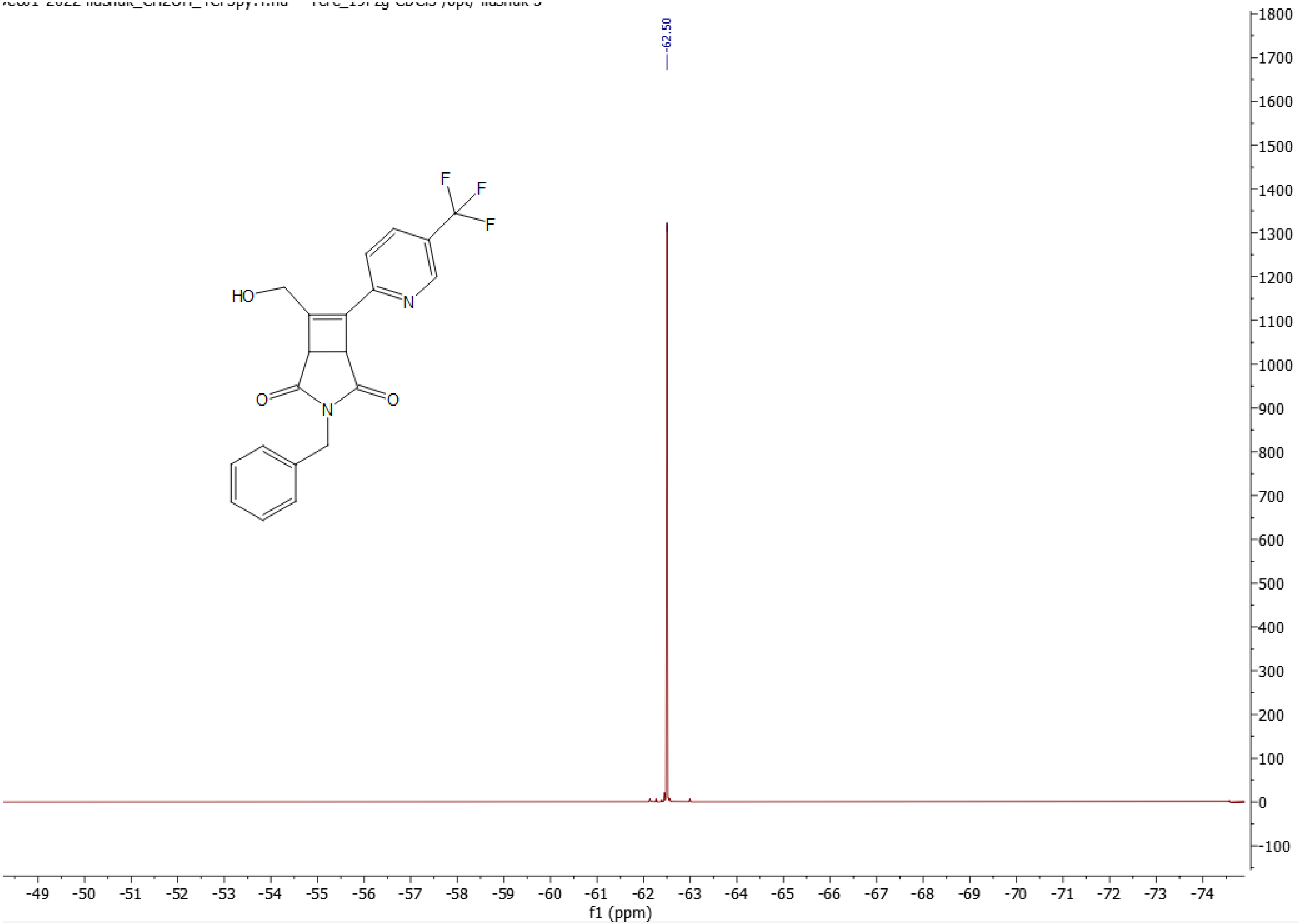

Spectrum 122. 3-benzyl-6-(hydroxymethyl)-7-(5-(trifluoromethyl)pyridin-2-yl)-3-azabicyclo[3.2.0]hept-6-ene-2,4-dione ***11c****, ^{19}F NMR (376 MHz, CDCl$_3$),*

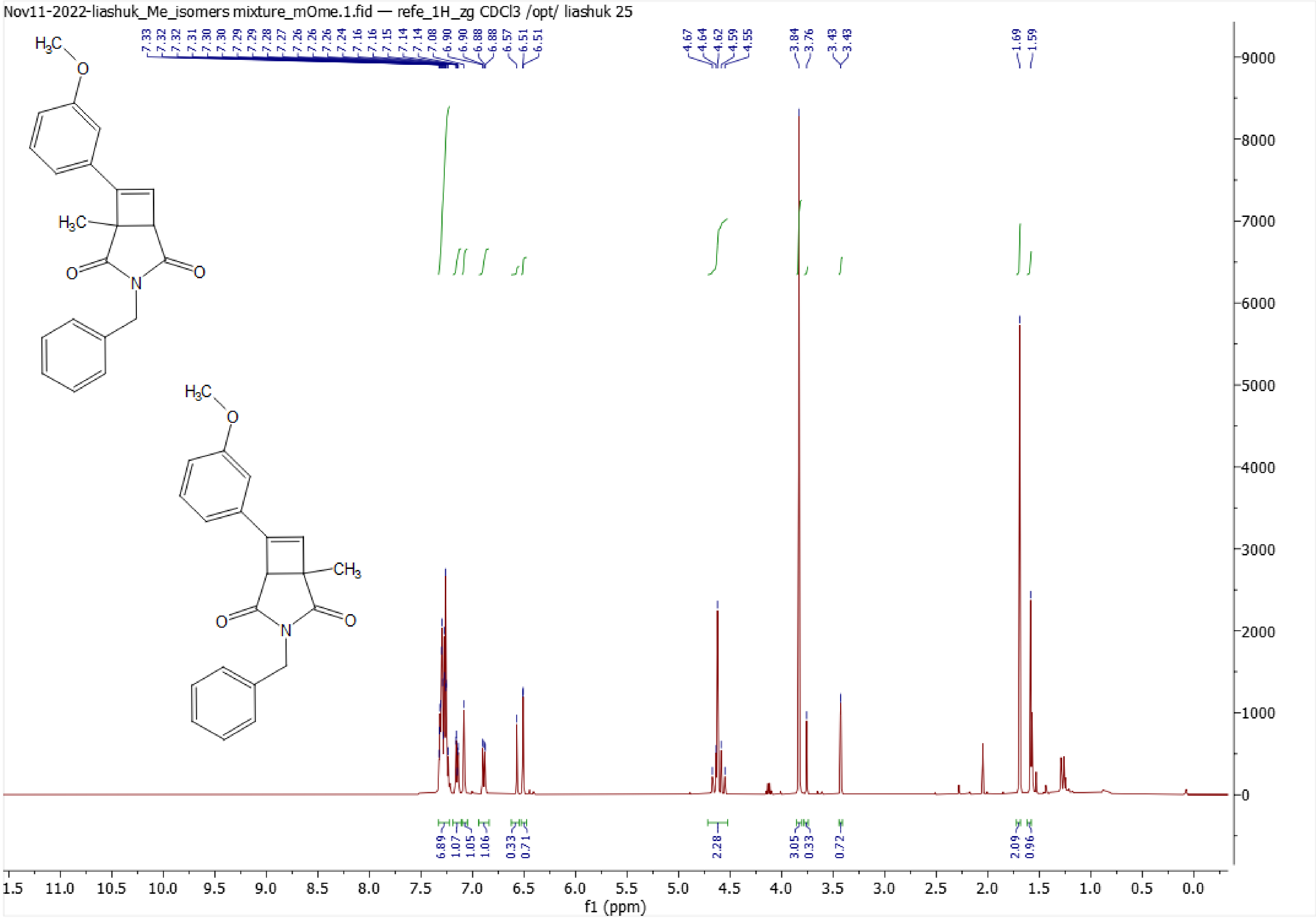

Spectrum 123. 3-benzyl-7-(3-methoxyphenyl)-1-methyl-3-azabicyclo[3.2.0]hept-6-ene-2,4-dione and 3-benzyl-6-(3-methoxyphenyl)-1-methyl-3-azabicyclo[3.2.0]hept-6-ene-2,4-dione **11d** and **11d'**, ^{1}H NMR (400 MHz, CDCl$_3$)

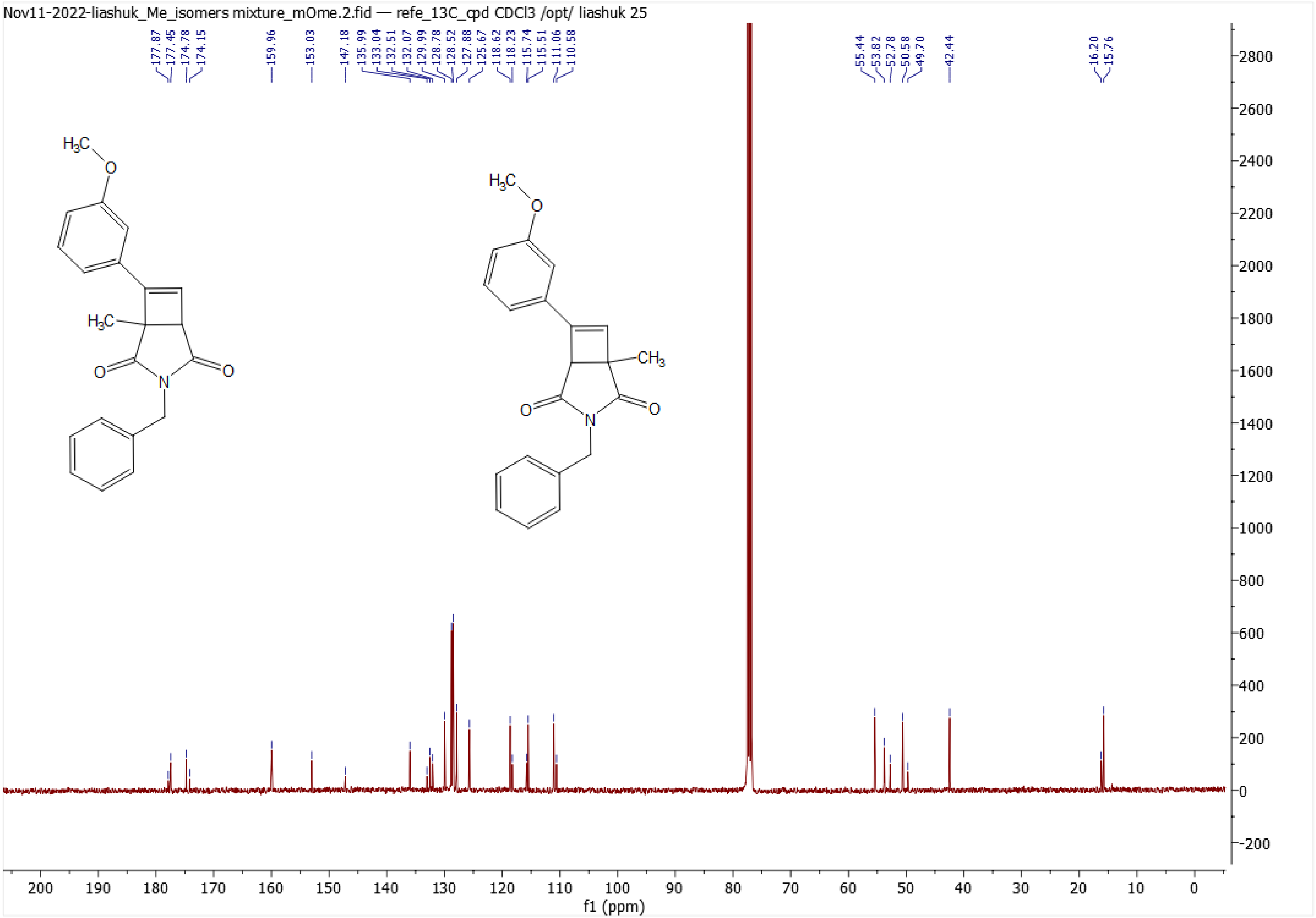

Spectrum 124. 3-benzyl-7-(3-methoxyphenyl)-1-methyl-3-azabicyclo[3.2.0]hept-6-ene-2,4-dione and 3-benzyl-6-(3-methoxyphenyl)-1-methyl-3-azabicyclo[3.2.0]hept-6-ene-2,4-dione ***11d*** *and* ***11d'****, ^{13}C NMR (101 MHz, CDCl$_3$)*

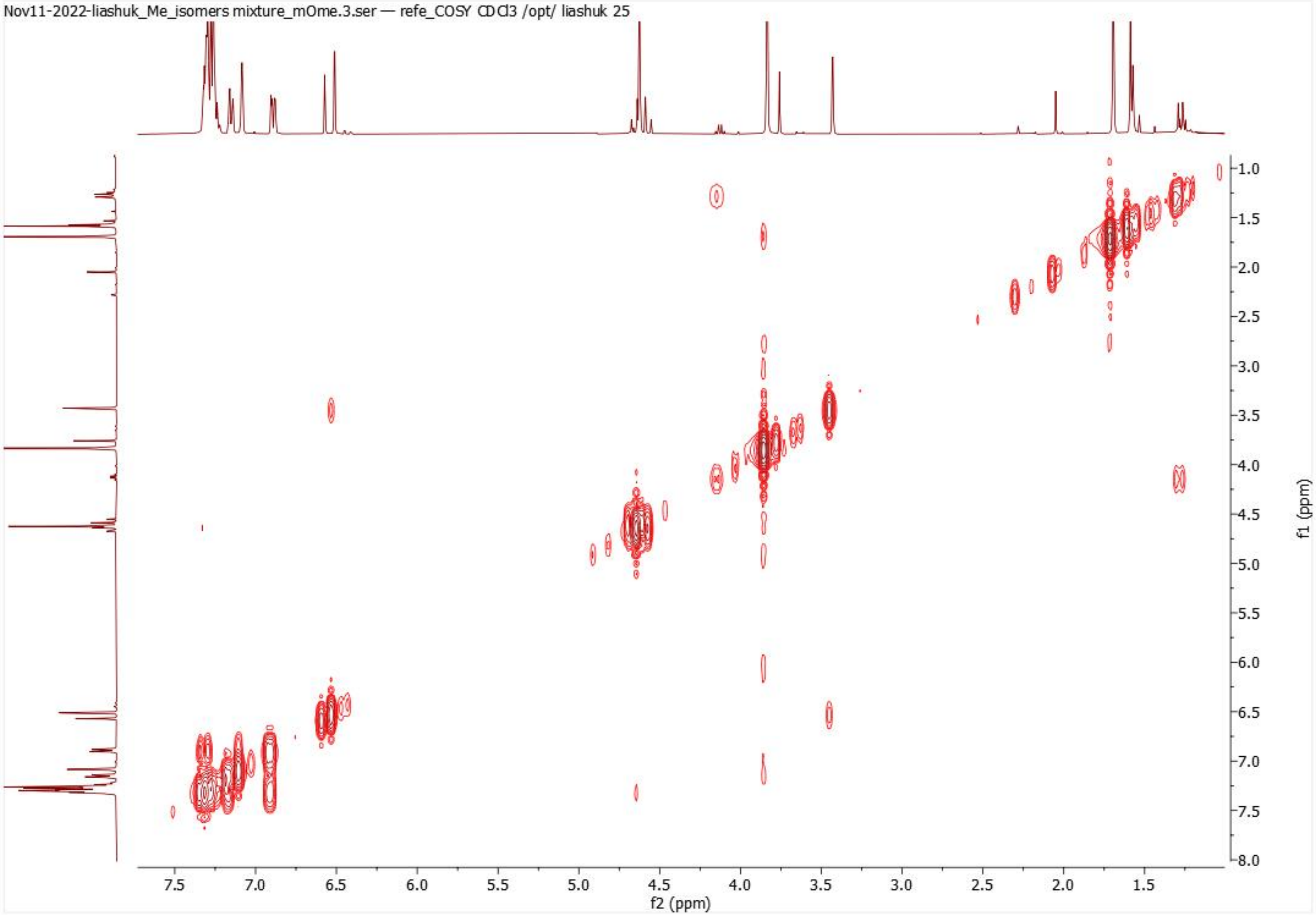

*Spectrum 125. 3-benzyl-7-(3-methoxyphenyl)-1-methyl-3-azabicyclo[3.2.0]hept-6-ene-2,4-dione and 3-benzyl-6-(3-methoxyphenyl)-1-methyl-3-azabicyclo[3.2.0]hept-6-ene-2,4-dione **11d** and **11d'**, COSY (400 MHz, CDCl3)*

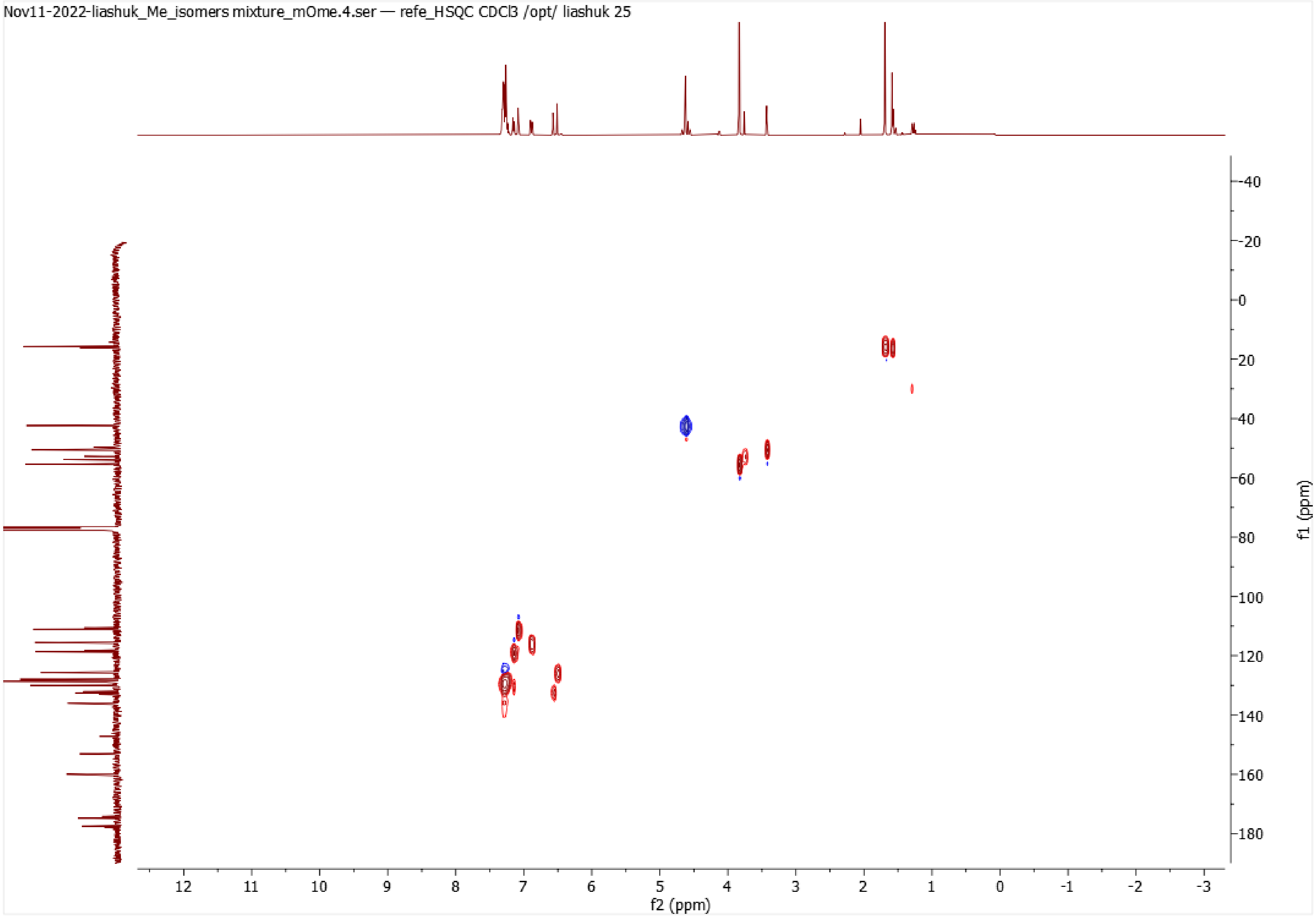

Spectrum 126. 3-benzyl-7-(3-methoxyphenyl)-1-methyl-3-azabicyclo[3.2.0]hept-6-ene-2,4-dione and 3-benzyl-6-(3-methoxyphenyl)-1-methyl-3-azabicyclo[3.2.0]hept-6-ene-2,4-dione ***11d*** *and* ***11d'****, HSQC (400/101 MHz, CDCl3)*

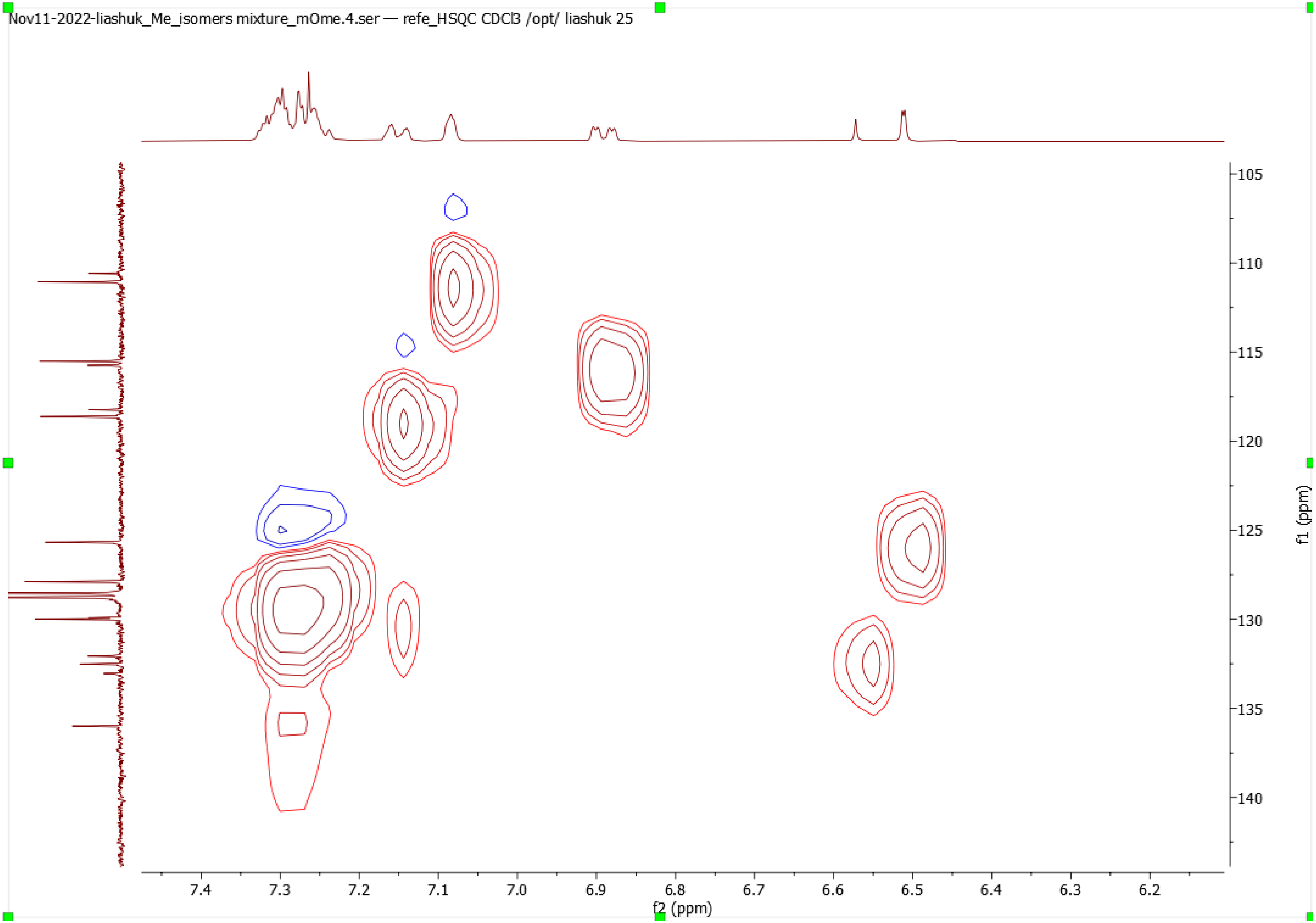

Spectrum 127. 3-benzyl-7-(3-methoxyphenyl)-1-methyl-3-azabicyclo[3.2.0]hept-6-ene-2,4-dione and 3-benzyl-6-(3-methoxyphenyl)-1-methyl-3-azabicyclo[3.2.0]hept-6-ene-2,4-dione **11d** and **11d'**, HSQC (400/101 MHz, CDCl3), aromatic region

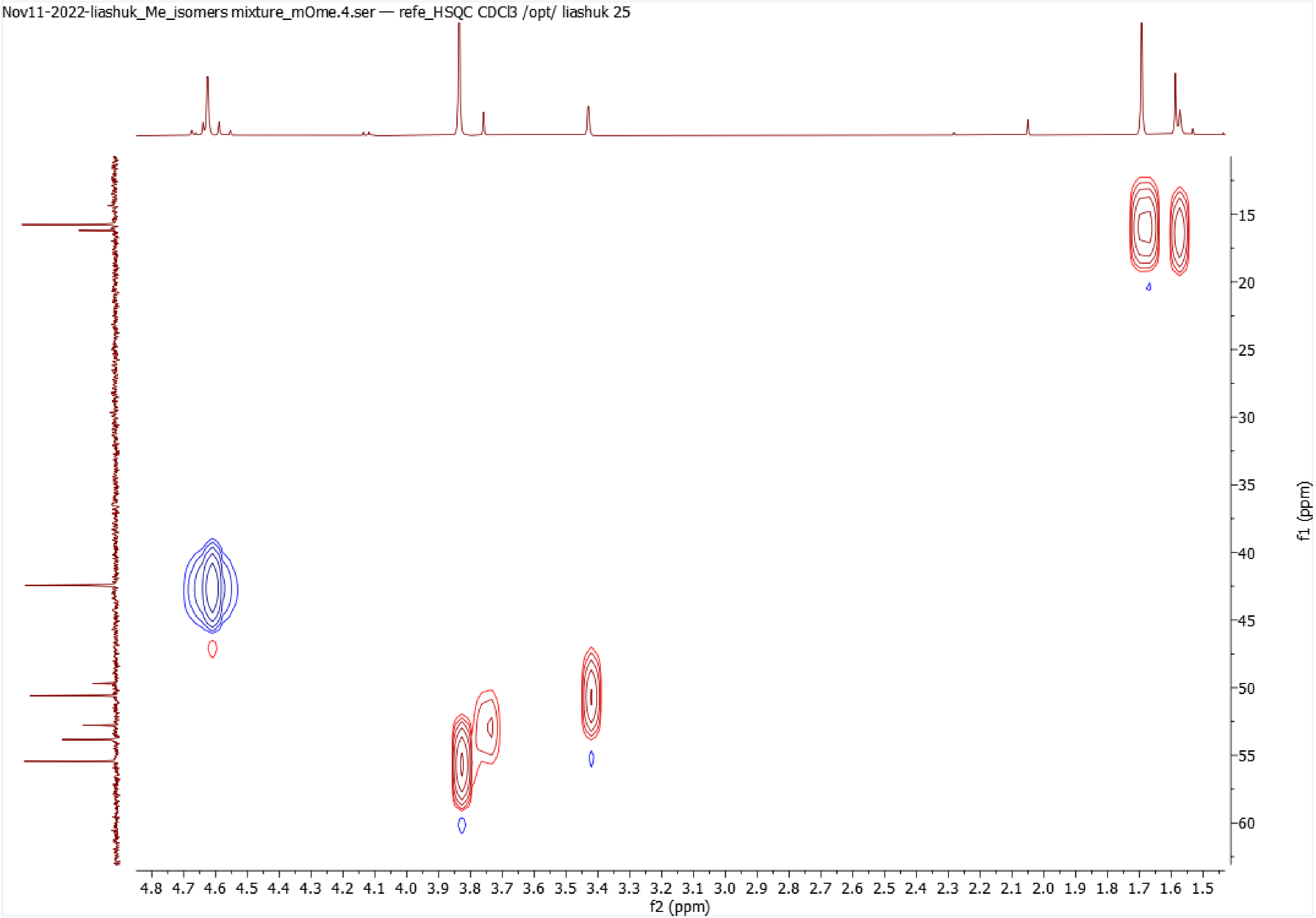

Spectrum 128. 3-benzyl-7-(3-methoxyphenyl)-1-methyl-3-azabicyclo[3.2.0]hept-6-ene-2,4-dione and 3-benzyl-6-(3-methoxyphenyl)-1-methyl-3-azabicyclo[3.2.0]hept-6-ene-2,4-dione ***11d*** *and* ***11d'****, HSQC (400/101 MHz, CDCl3), aliphatic region*

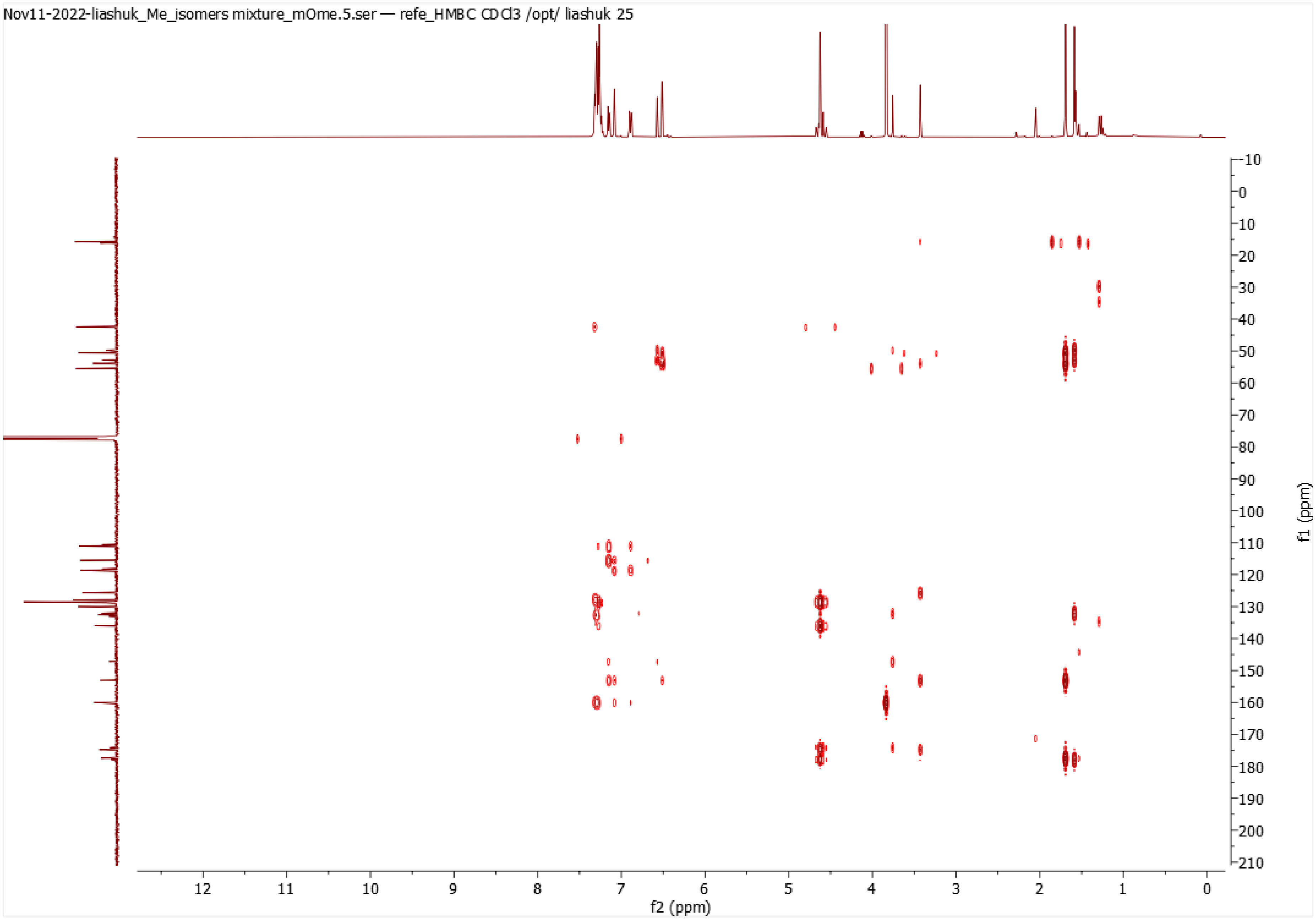

Spectrum 129. 3-benzyl-7-(3-methoxyphenyl)-1-methyl-3-azabicyclo[3.2.0]hept-6-ene-2,4-dione and 3-benzyl-6-(3-methoxyphenyl)-1-methyl-3-azabicyclo[3.2.0]hept-6-ene-2,4-dione ***11d*** *and* ***11d'****, HMBC (400/101 MHz, CDCl3)*

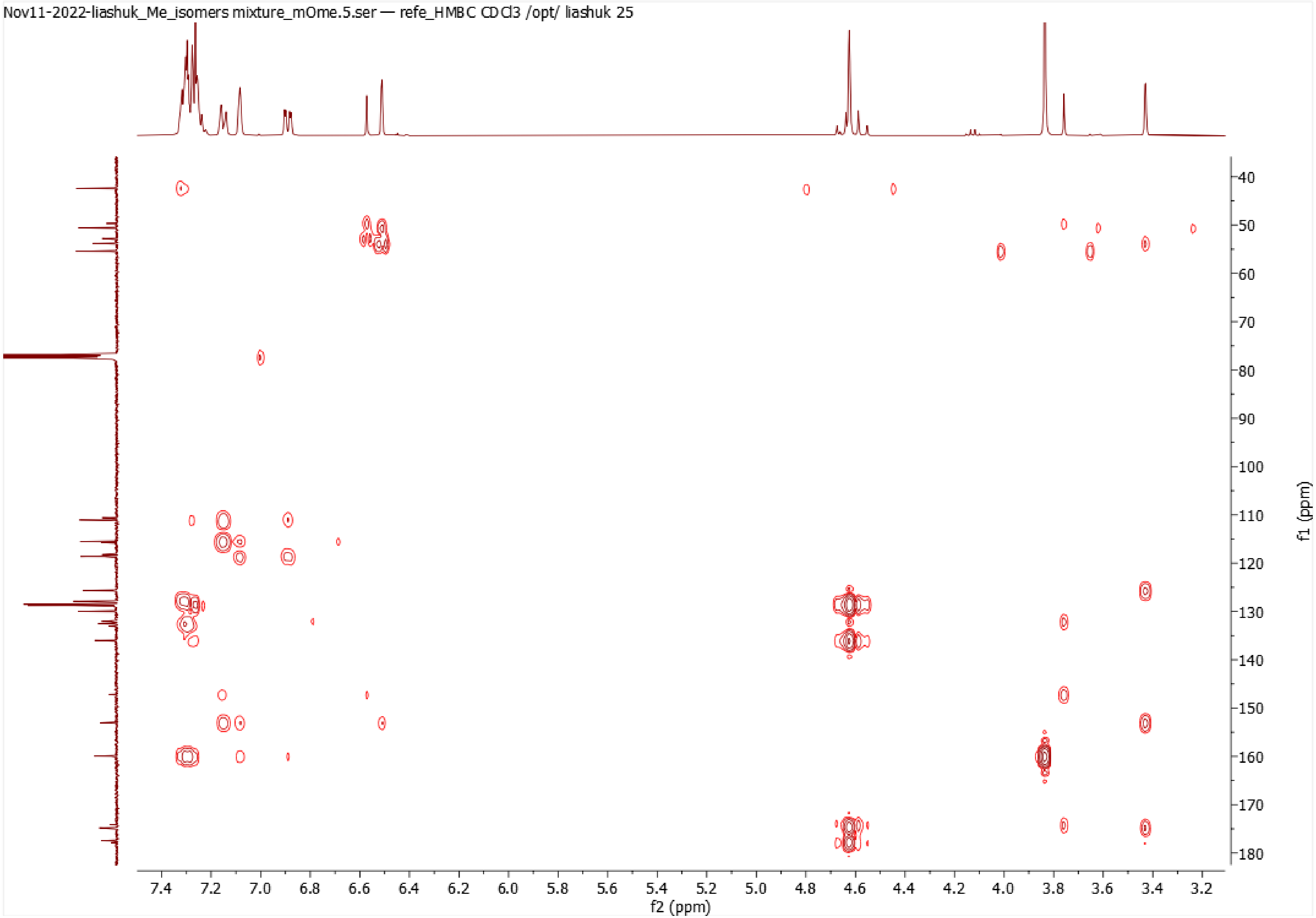

Spectrum 130. 3-benzyl-7-(3-methoxyphenyl)-1-methyl-3-azabicyclo[3.2.0]hept-6-ene-2,4-dione and 3-benzyl-6-(3-methoxyphenyl)-1-methyl-3-azabicyclo[3.2.0]hept-6-ene-2,4-dione ***11d*** *and* ***11d'****, HMBC (400/101 MHz, CDCl3), central region*

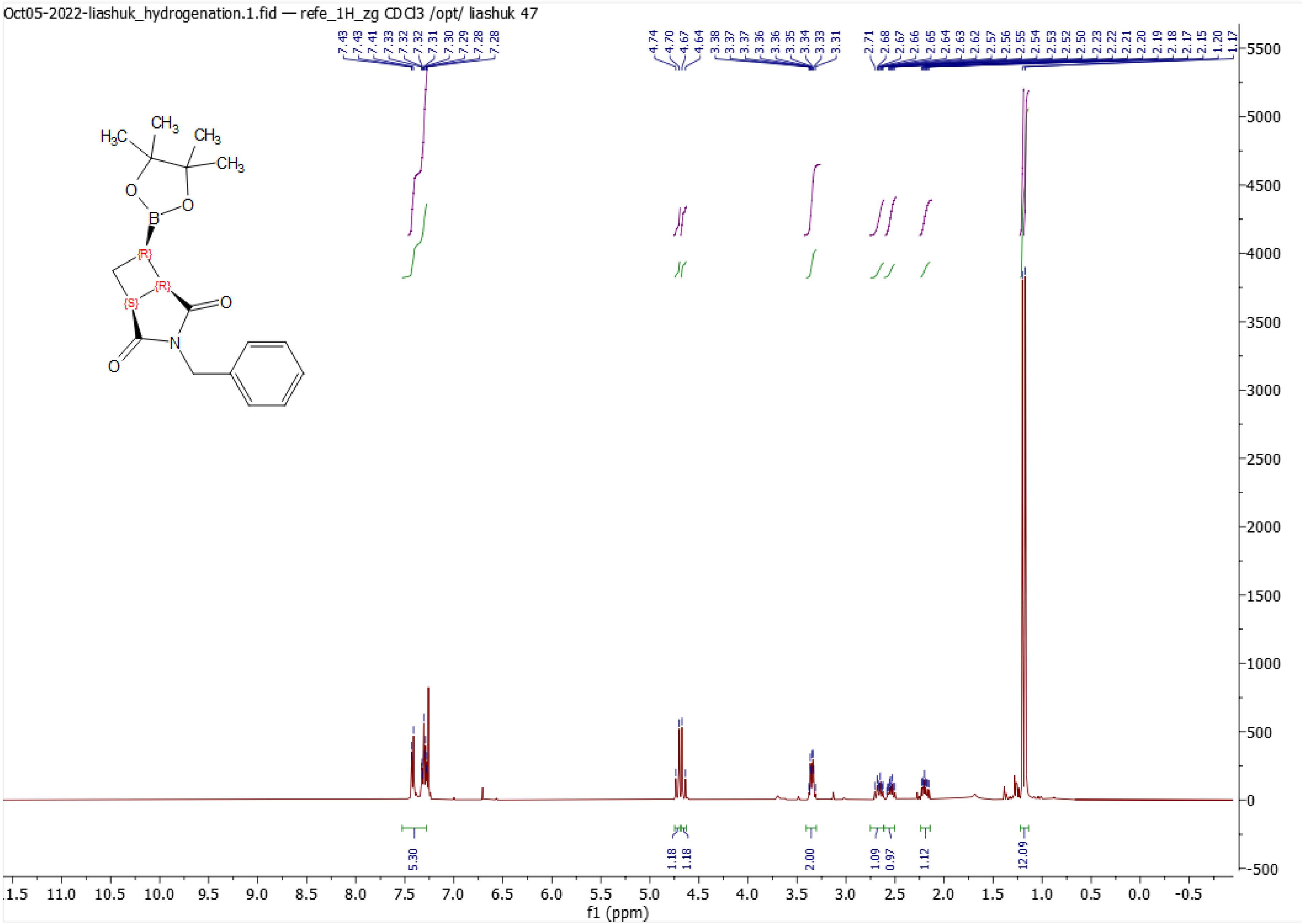

*Spectrum 131. rac-(1R,5S,6S)-3-benzyl-6-(4,4,5,5-tetramethyl-1,3,2-dioxaborolan-2-yl)-3-azabicyclo[3.2.0]heptane-2,4-dione **12**, ^{1}H NMR (400 MHz, $CDCl_3$)*

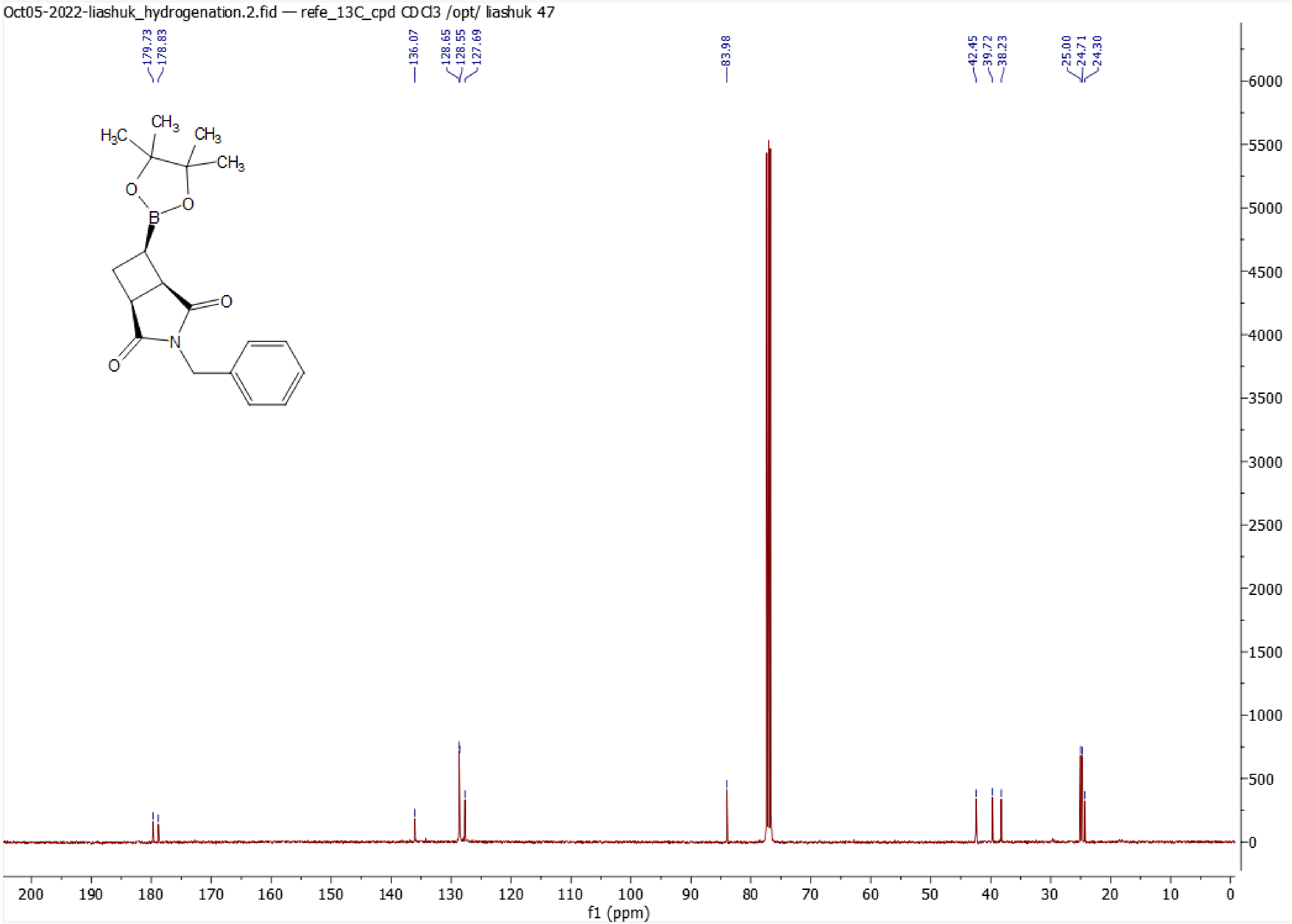

Spectrum 132. rac-(1R,5S,6S)-3-benzyl-6-(4,4,5,5-tetramethyl-1,3,2-dioxaborolan-2-yl)-3-azabicyclo[3.2.0]heptane-2,4-dione ***12***, *^{13}C NMR (101 MHz, CDCl$_3$)*

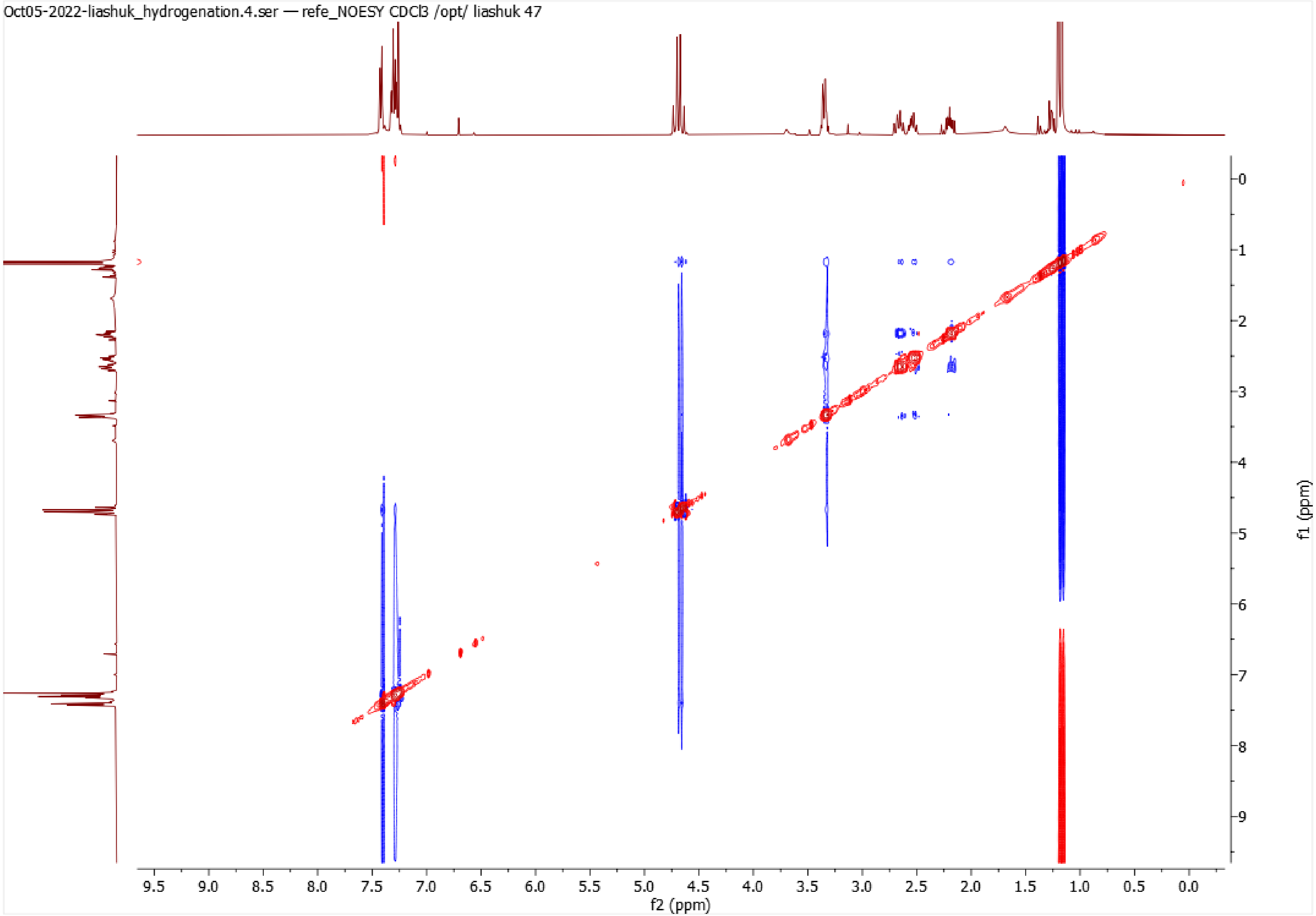

Spectrum 133. rac-(1R,5S,6S)-3-benzyl-6-(4,4,5,5-tetramethyl-1,3,2-dioxaborolan-2-yl)-3-azabicyclo[3.2.0]heptane-2,4-dione ***12****, NOESY (400 MHz, CDCl3)*

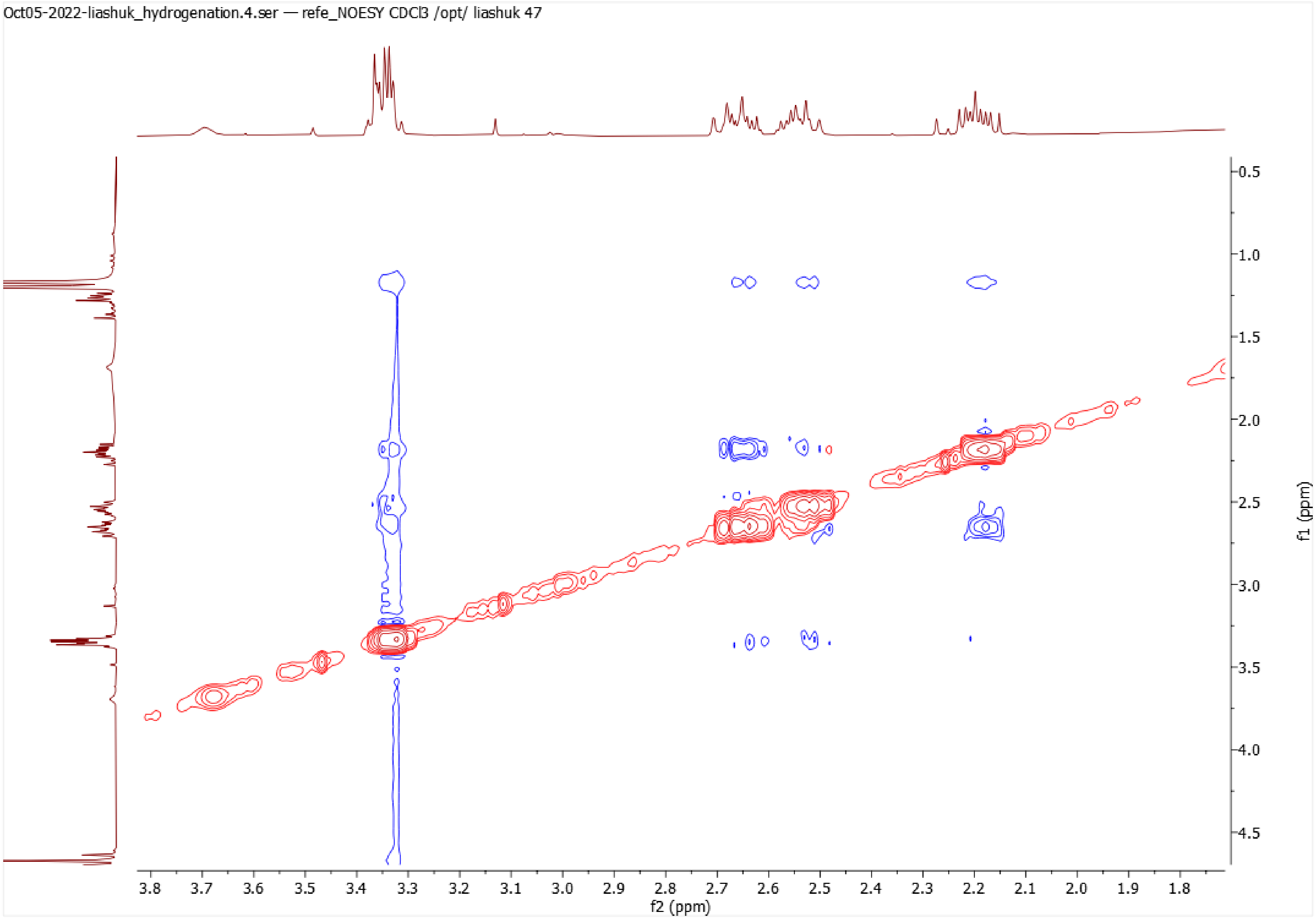

Spectrum 134. rac-(1R,5S,6S)-3-benzyl-6-(4,4,5,5-tetramethyl-1,3,2-dioxaborolan-2-yl)-3-azabicyclo[3.2.0]heptane-2,4-dione ***12****, NOESY (400 MHz, CDCl3), aliphatic region*

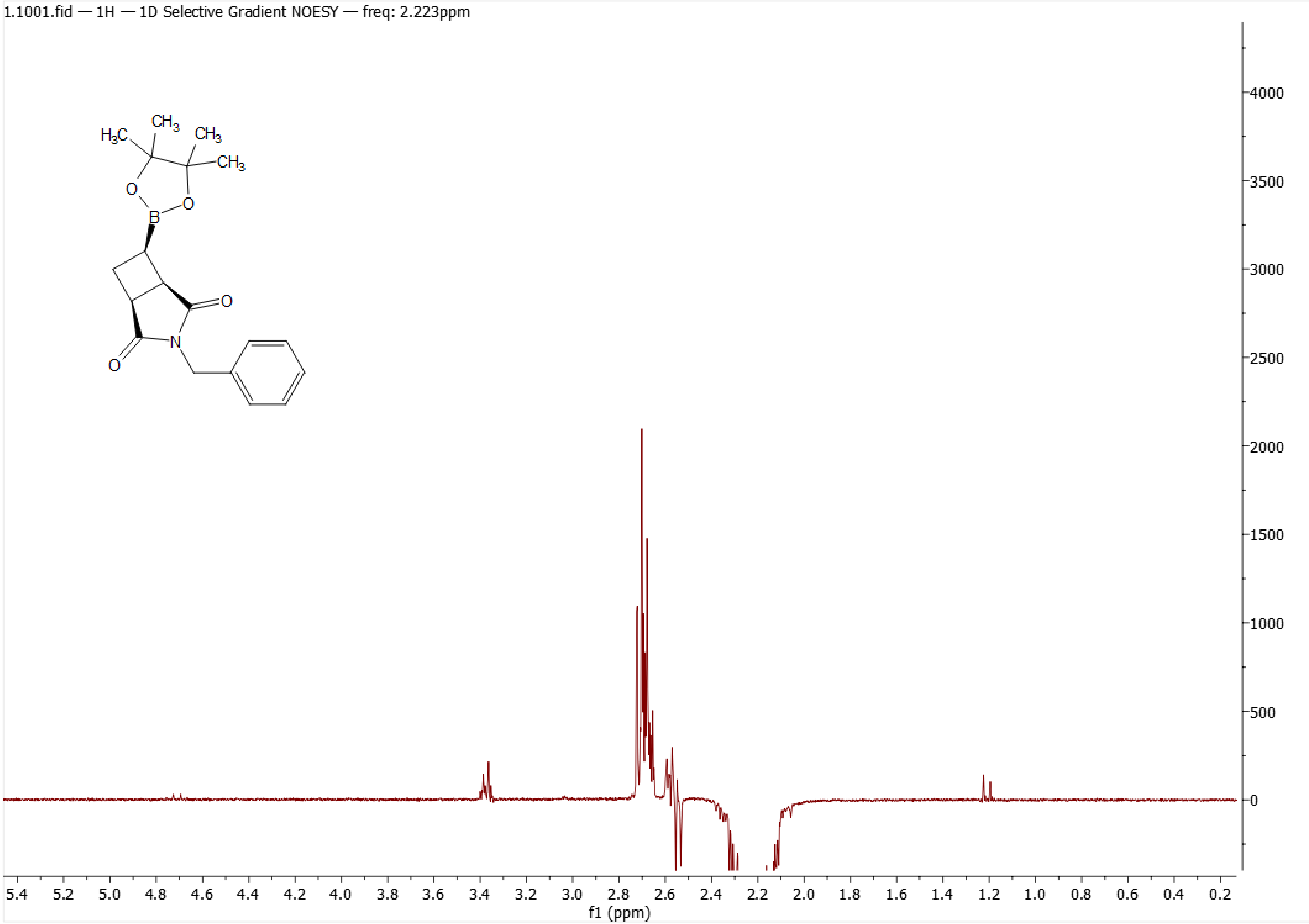

Spectrum 135. rac-(1R,5S,6S)-3-benzyl-6-(4,4,5,5-tetramethyl-1,3,2-dioxaborolan-2-yl)-3-azabicyclo[3.2.0]heptane-2,4-dione ***12****, SelNOE (400 MHz, CDCl3), aliphatic region*

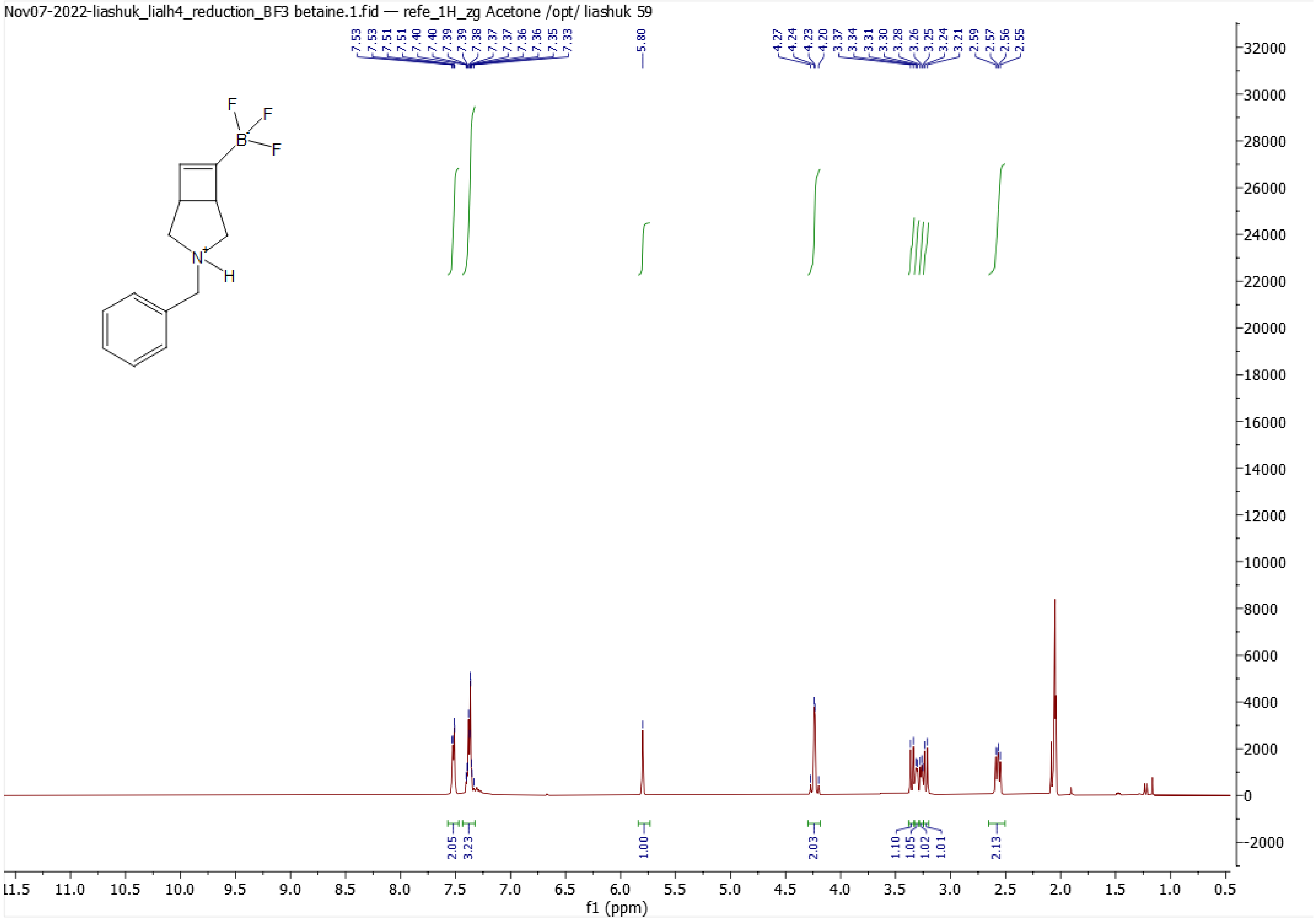

*Spectrum 136. (3-benzyl-3-azabicyclo[3.2.0]hept-6-en-3-ium-6-yl)trifluoroborate **13**, ^{1}H NMR (400 MHz, Acetone-d_6)*

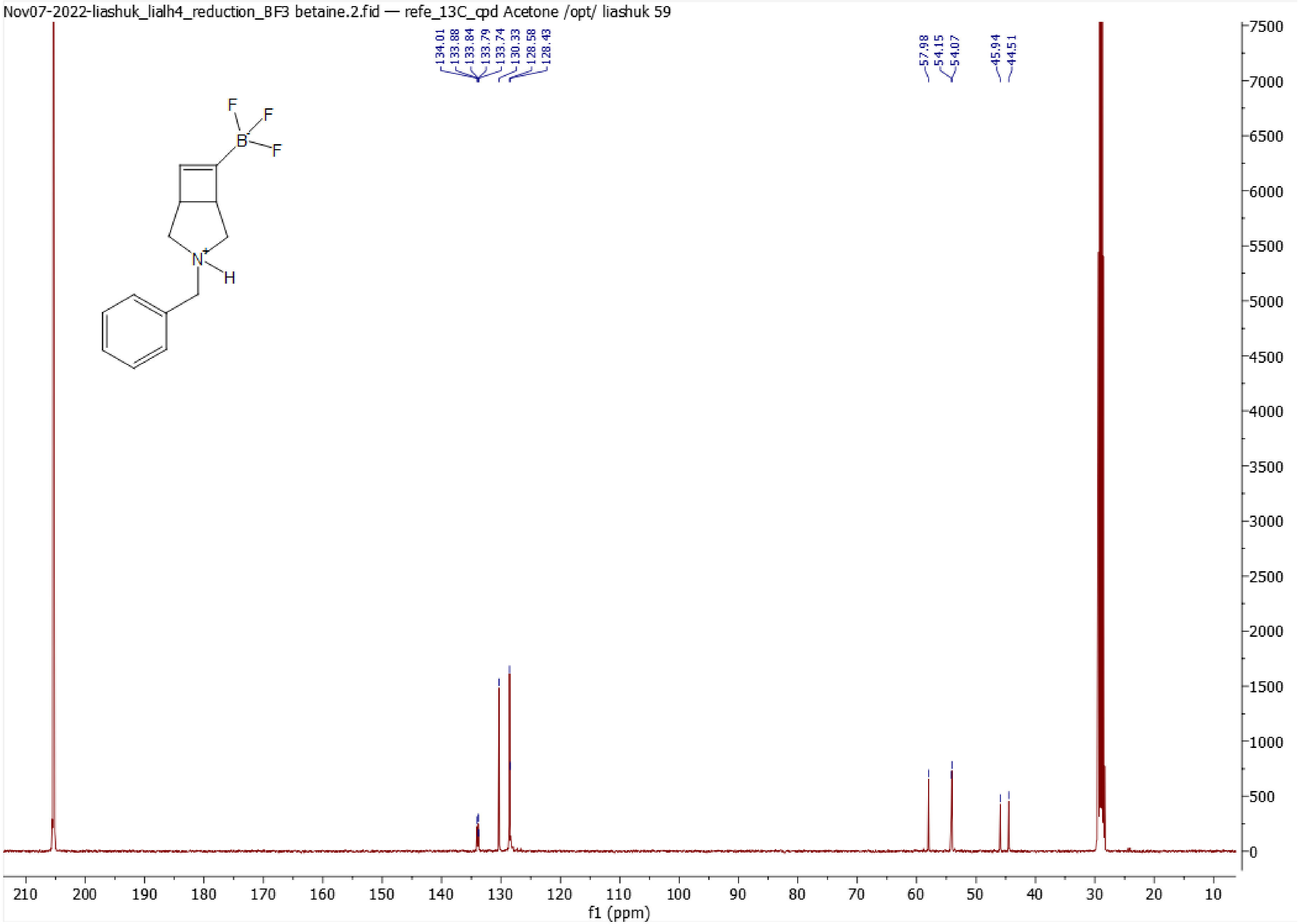

Spectrum 137.(3-benzyl-3-azabicyclo[3.2.0]hept-6-en-3-ium-6-yl)trifluoroborate ***13***, *^{13}C NMR (101 MHz, Acetone-d_6)*

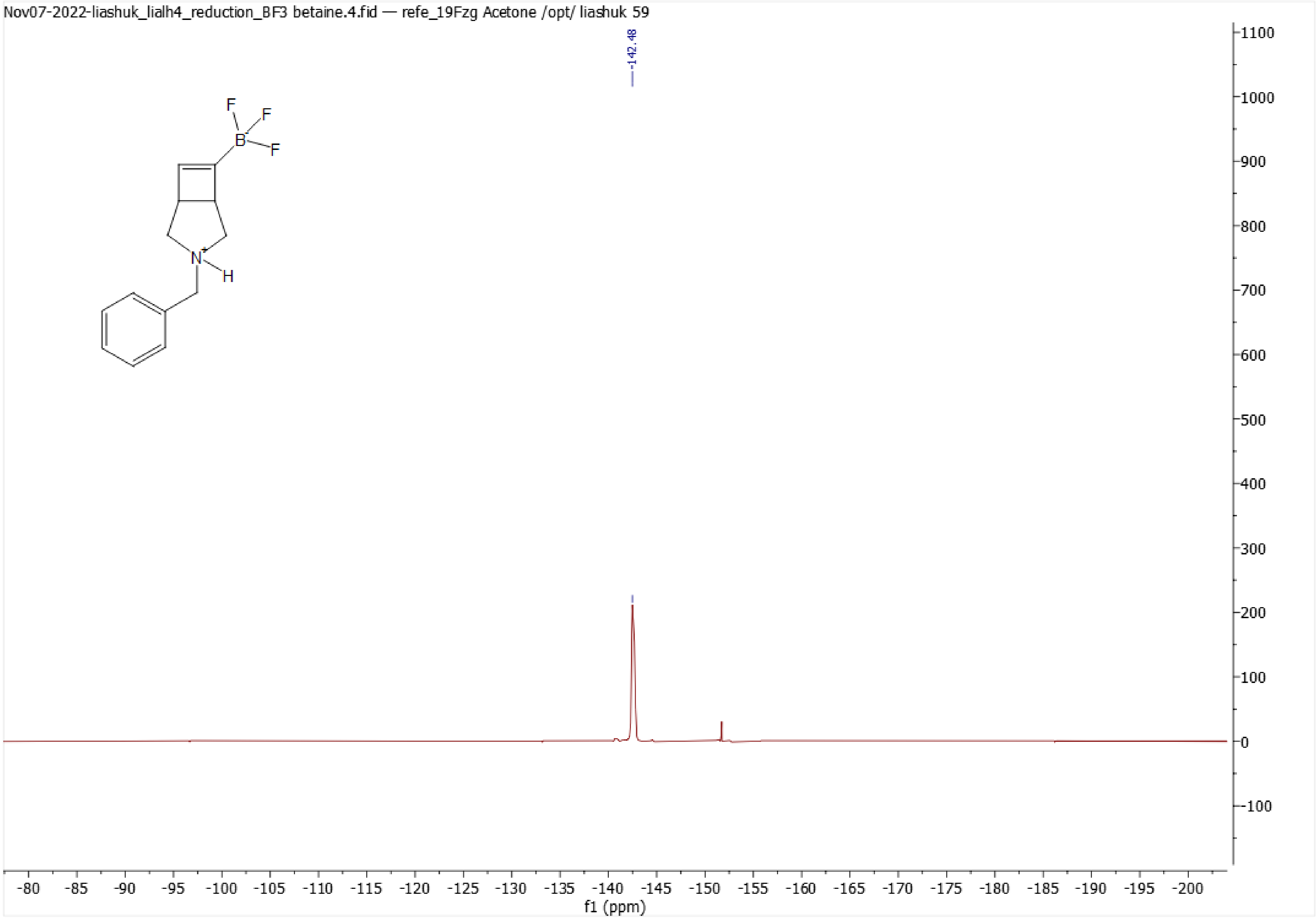

*Spectrum 138. (3-benzyl-3-azabicyclo[3.2.0]hept-6-en-3-ium-6-yl)trifluoroborate **13**, ^{19}F NMR (376 MHz, Acetone-d$_6$)*

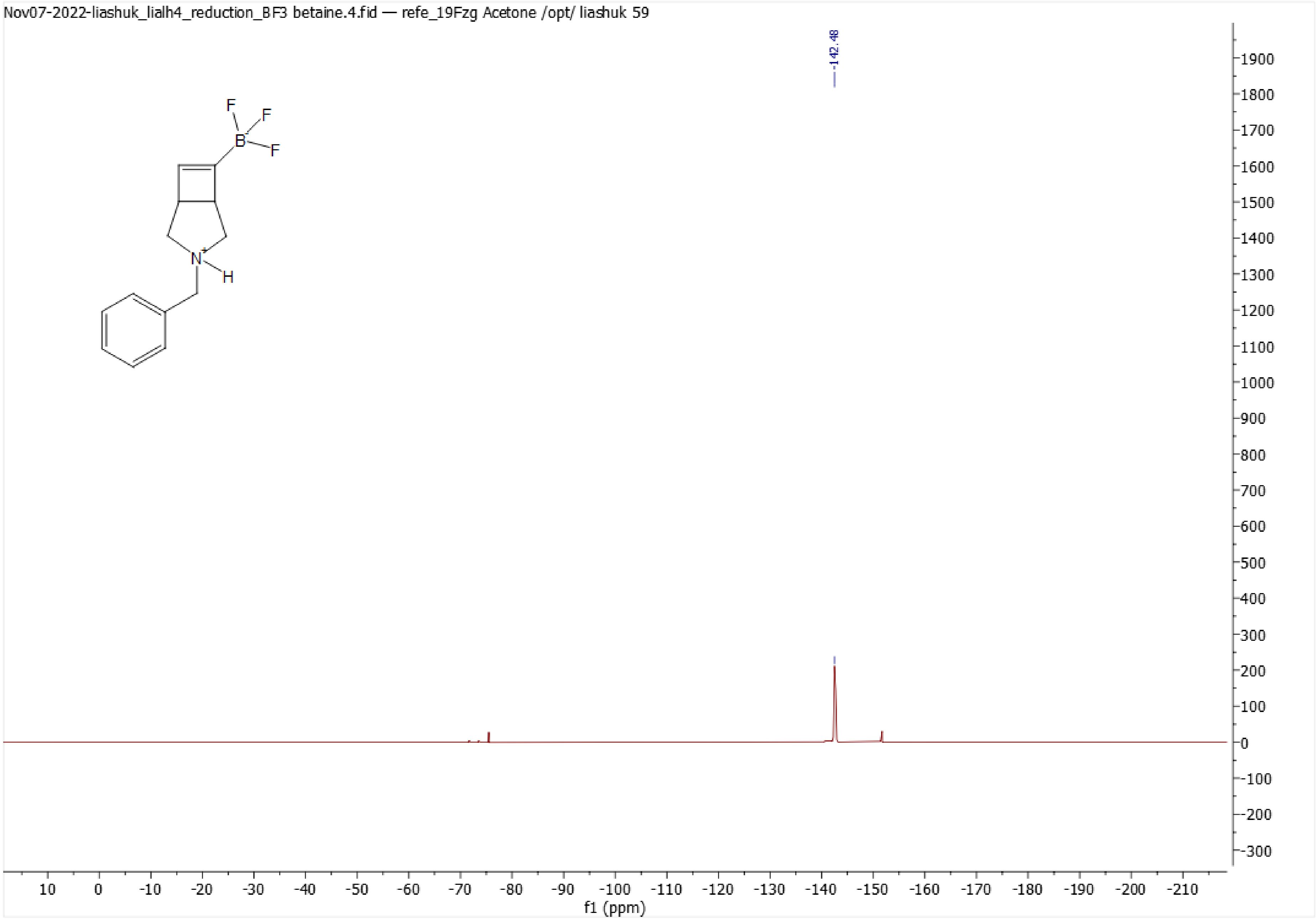

Spectrum 139. (3-benzyl-3-azabicyclo[3.2.0]hept-6-en-3-ium-6-yl)trifluoroborate ***13****, ^{19}F NMR (376 MHz, Acetone-d$_6$), full spectrum*

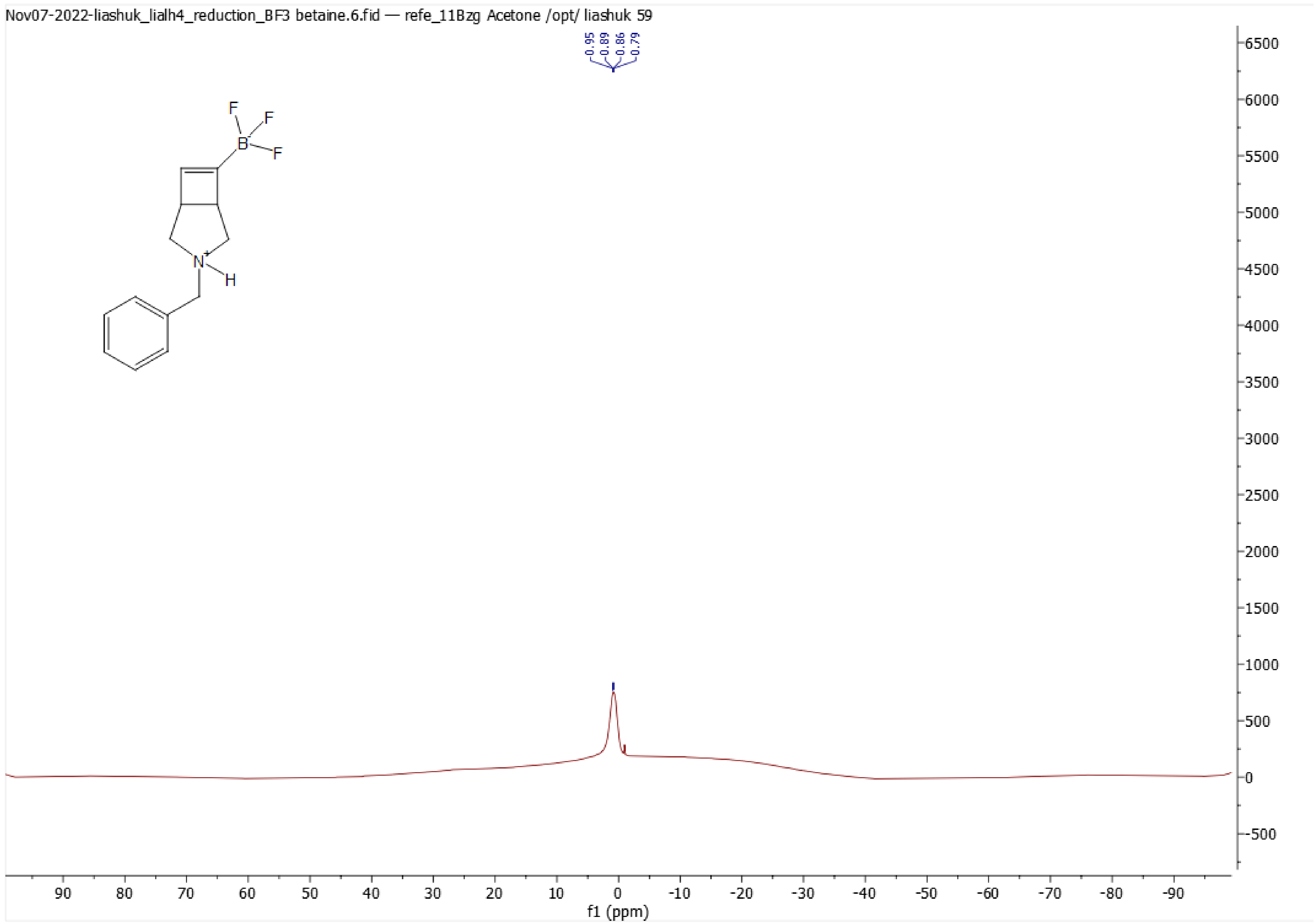

*Spectrum 140. (3-benzyl-3-azabicyclo[3.2.0]hept-6-en-3-ium-6-yl)trifluoroborate **13**, ^{11}B NMR (128 MHz, Acetone-d_6)*

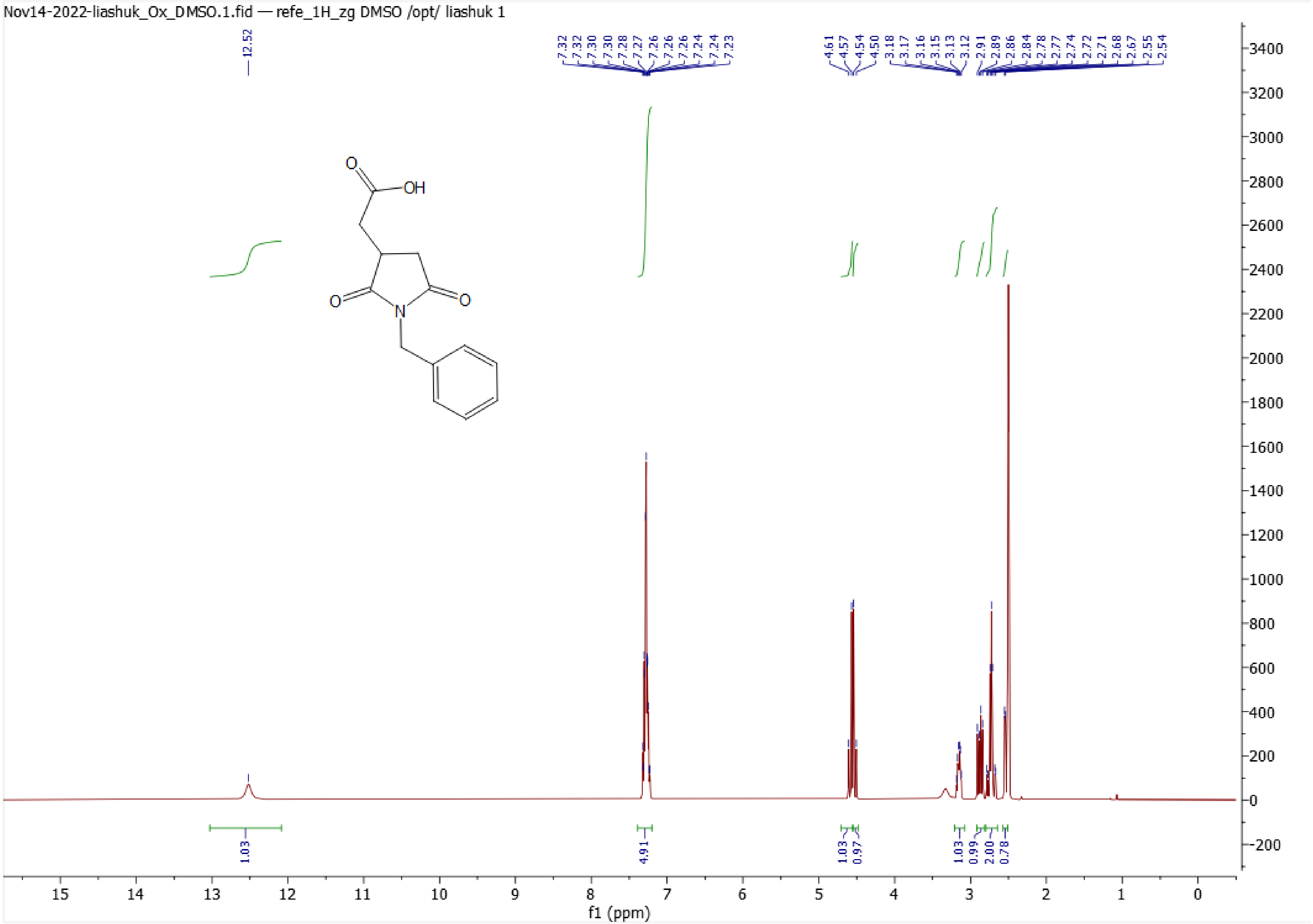

Spectrum 141. 2-(1-benzyl-2,5-dioxopyrrolidin-3-yl)acetic acid ***14****, ^{1}H NMR (400 MHz, DMSO-d_6)*

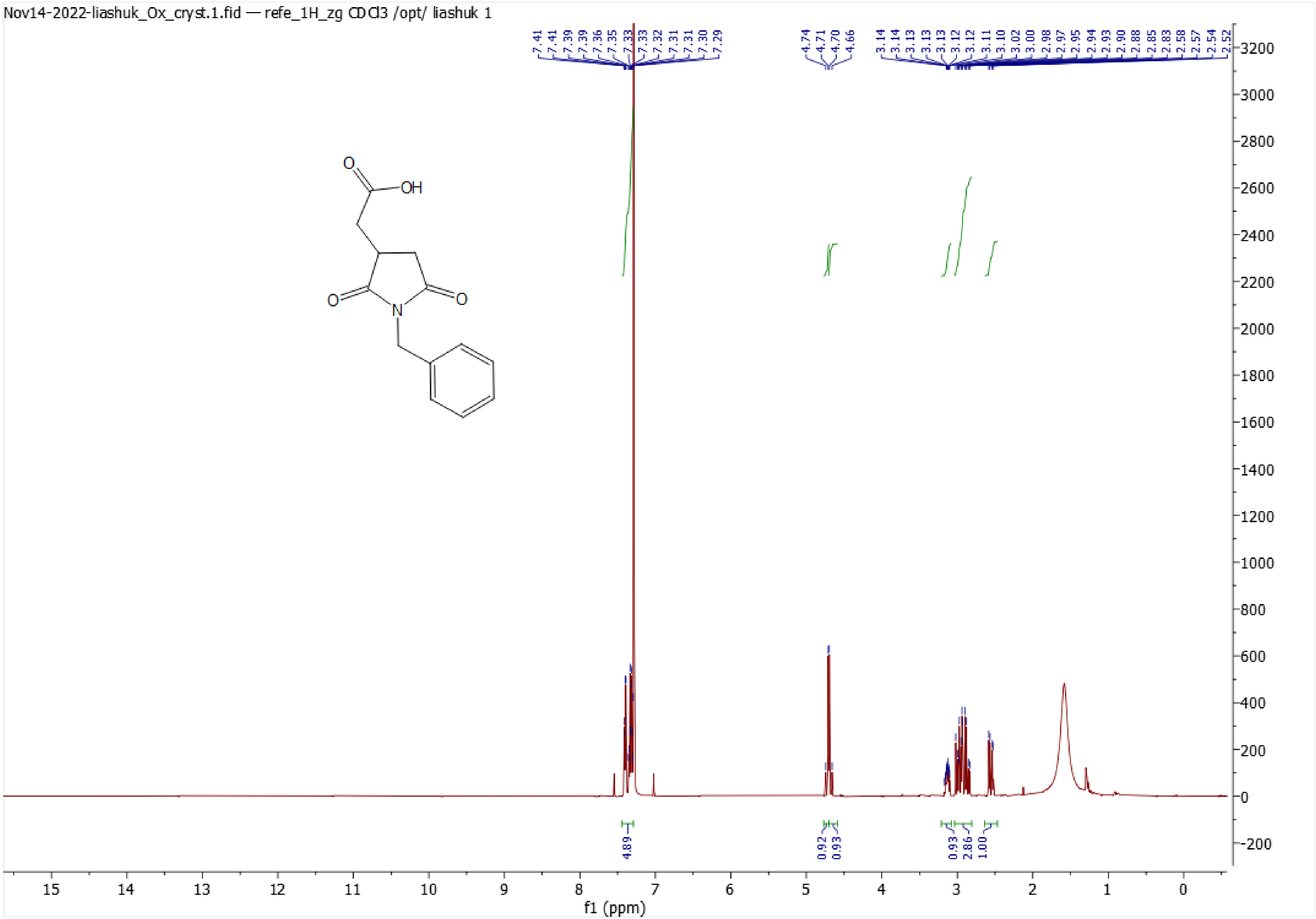

Spectrum 142. 2-(1-benzyl-2,5-dioxopyrrolidin-3-yl)acetic acid ***14****, ^{1}H NMR (400 MHz, $CDCl_3$)*

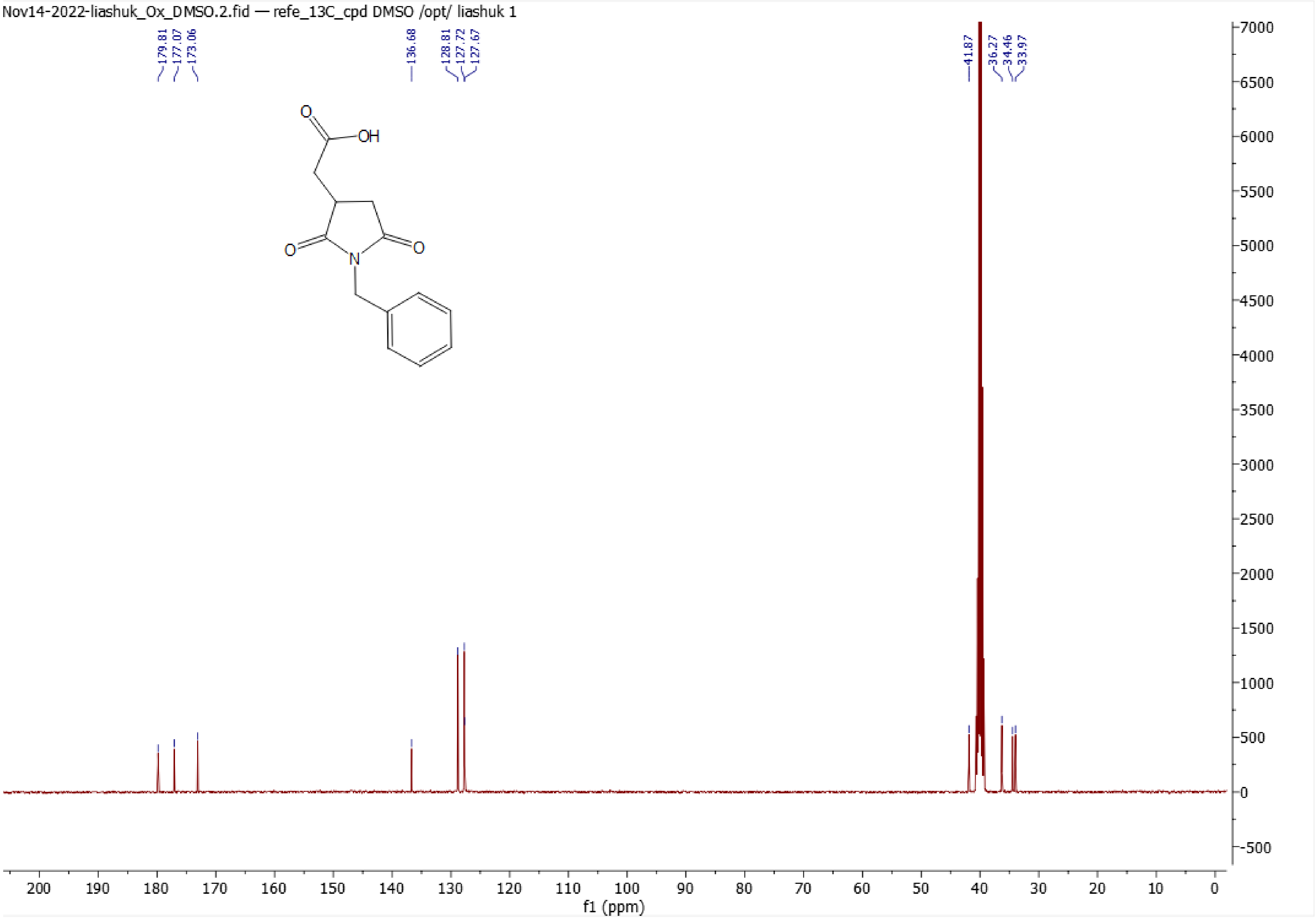

Spectrum 143. 2-(1-benzyl-2,5-dioxopyrrolidin-3-yl)acetic acid ***14****, ^{13}C NMR (101 MHz, DMSO-d$_6$)*

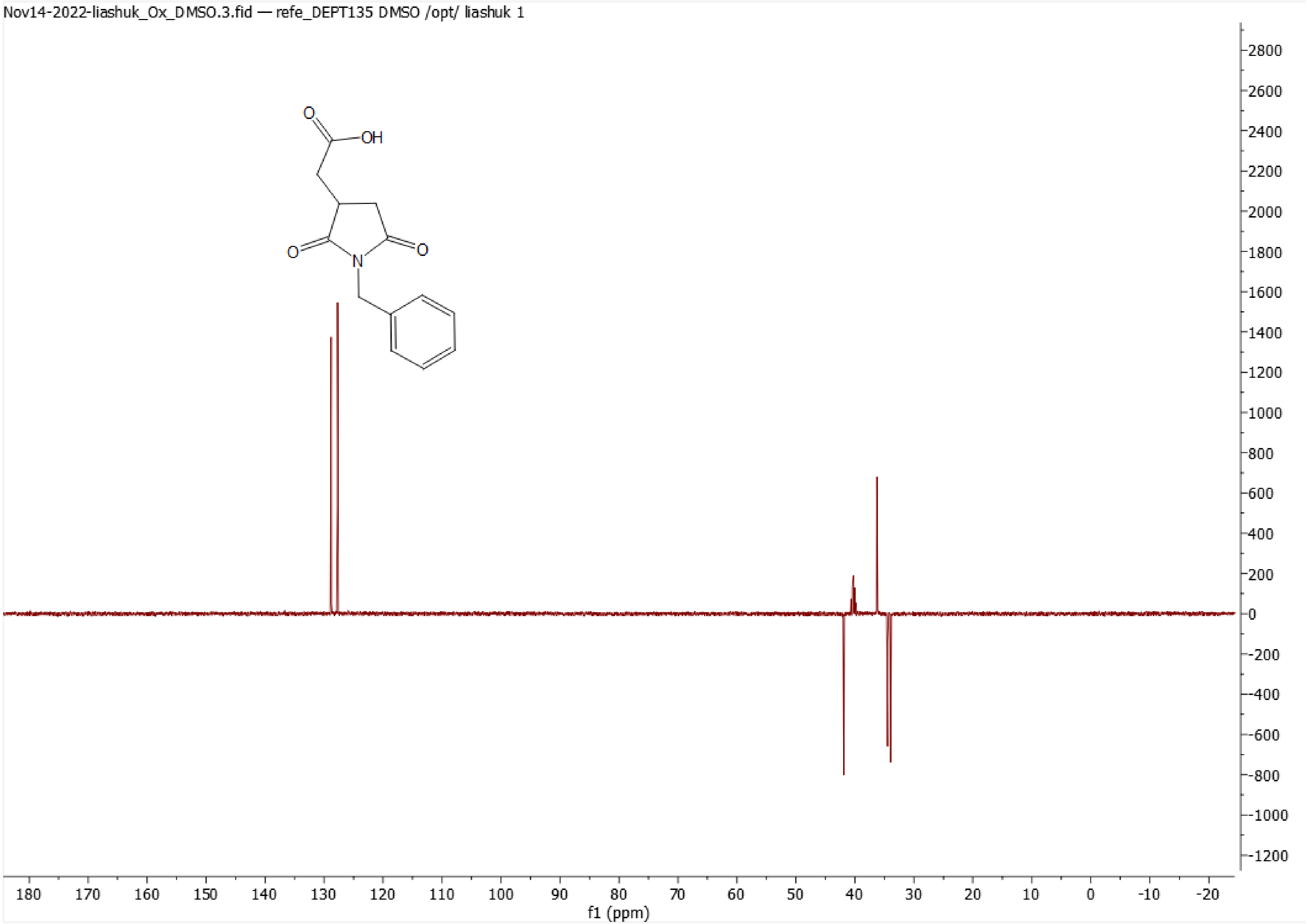

*Spectrum 144. 2-(1-benzyl-2,5-dioxopyrrolidin-3-yl)acetic acid **14**, DEPT135 (101 MHz, DMSO-d_6)*

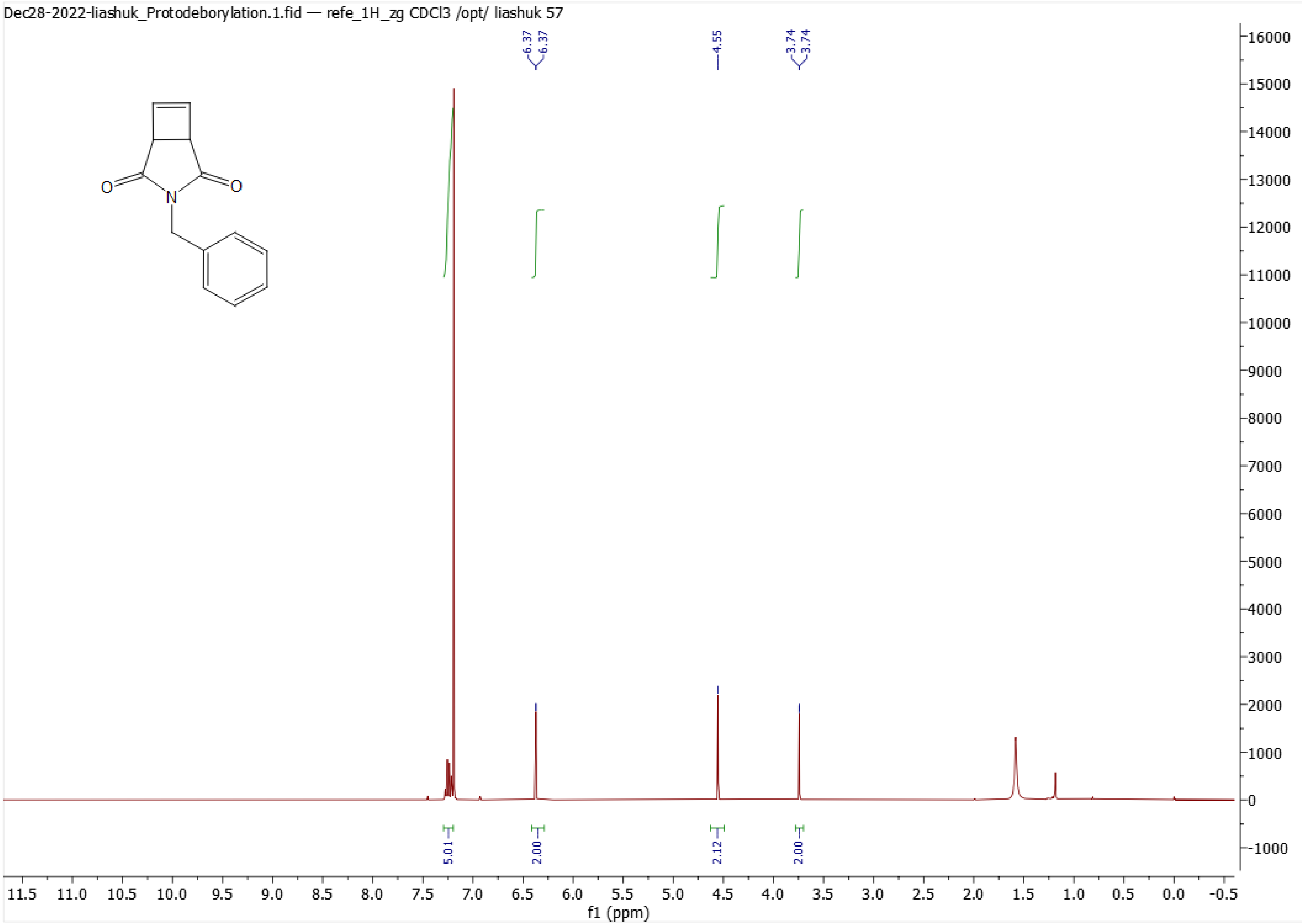

*Spectrum 145. 3-benzyl-3-azabicyclo[3.2.0]hept-6-ene-2,4-dione **15**, ^{1}H NMR (400 MHz, $CDCl_3$)*

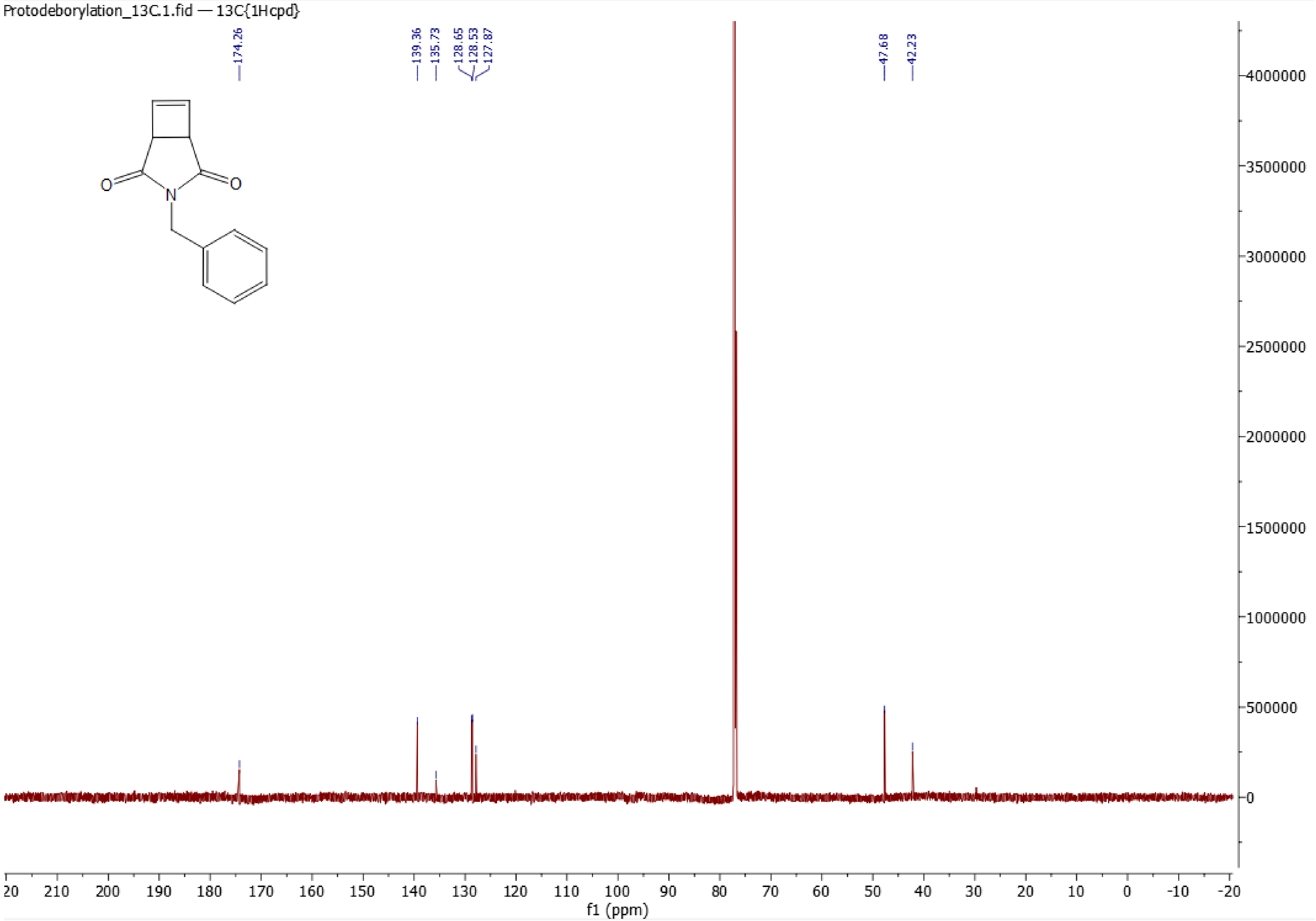

*Spectrum 146. 3-benzyl-3-azabicyclo[3.2.0]hept-6-ene-2,4-dione **15**, ^{13}C NMR (151 MHz, CDCl$_3$)*

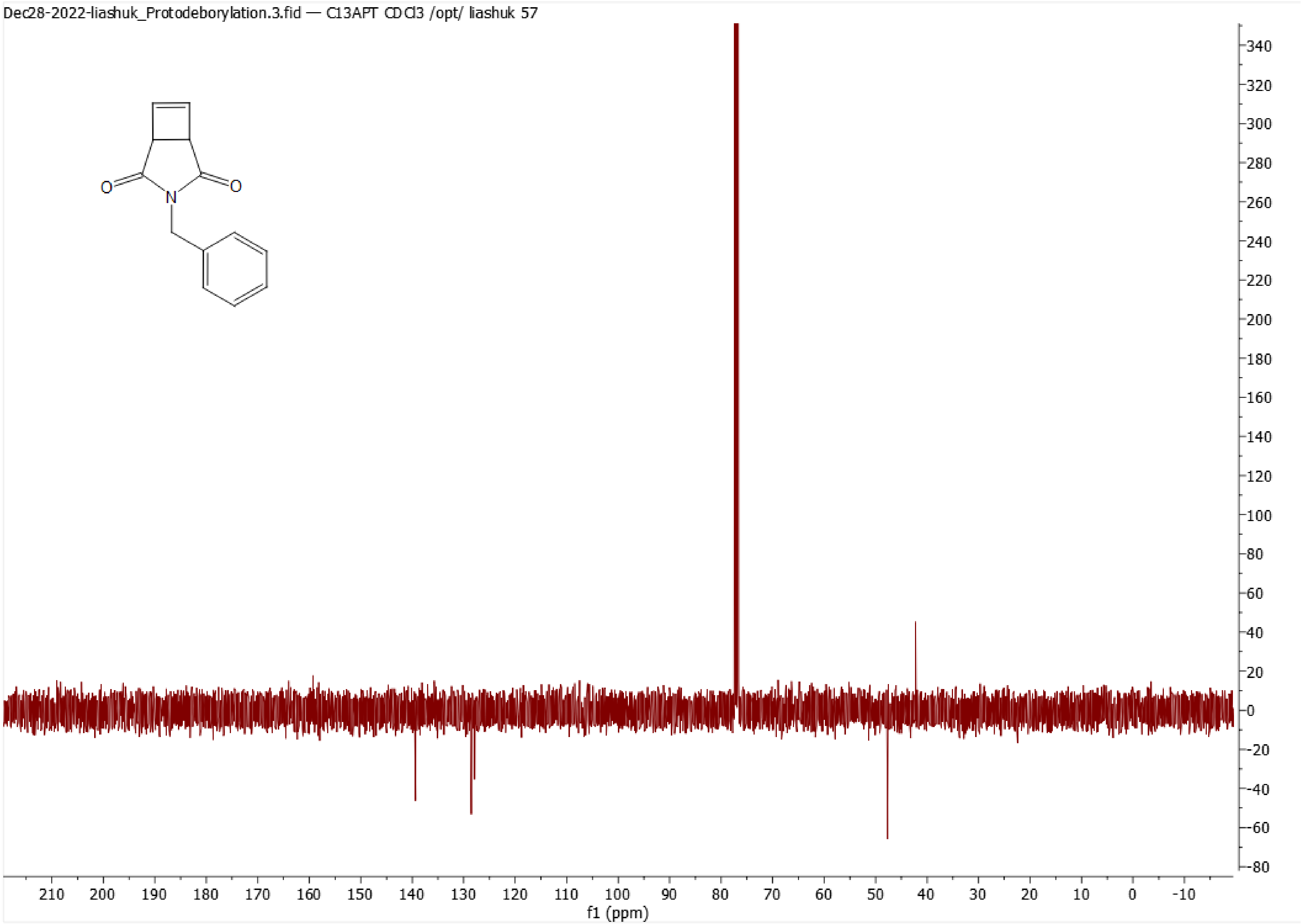

Spectrum 147. 3-benzyl-3-azabicyclo[3.2.0]hept-6-ene-2,4-dione ***15***, *^{13}C APT NMR (151 MHz, CDCl$_3$)*

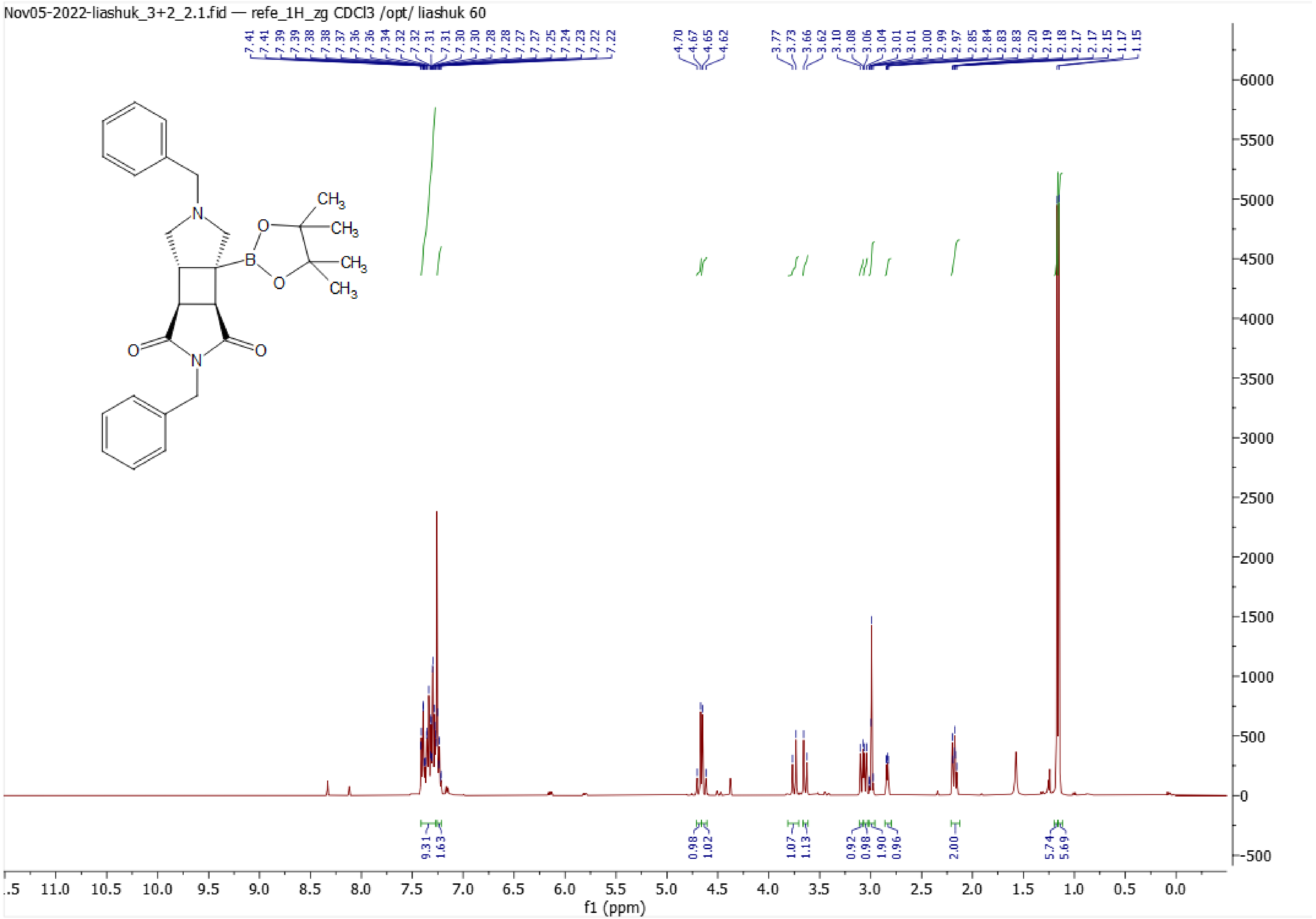

Spectrum 148. rac-(3aR,3bR,6aR,6bR)-2,5-dibenzyl-3b-(4,4,5,5-tetramethyl-1,3,2-dioxaborolan-2-yl)hexahydrocyclobuta[1,2-c:3,4-c']dipyrrole-1,3(2H,3aH)-dione ***17***, *^{1}H NMR (400 MHz, $CDCl_3$)*

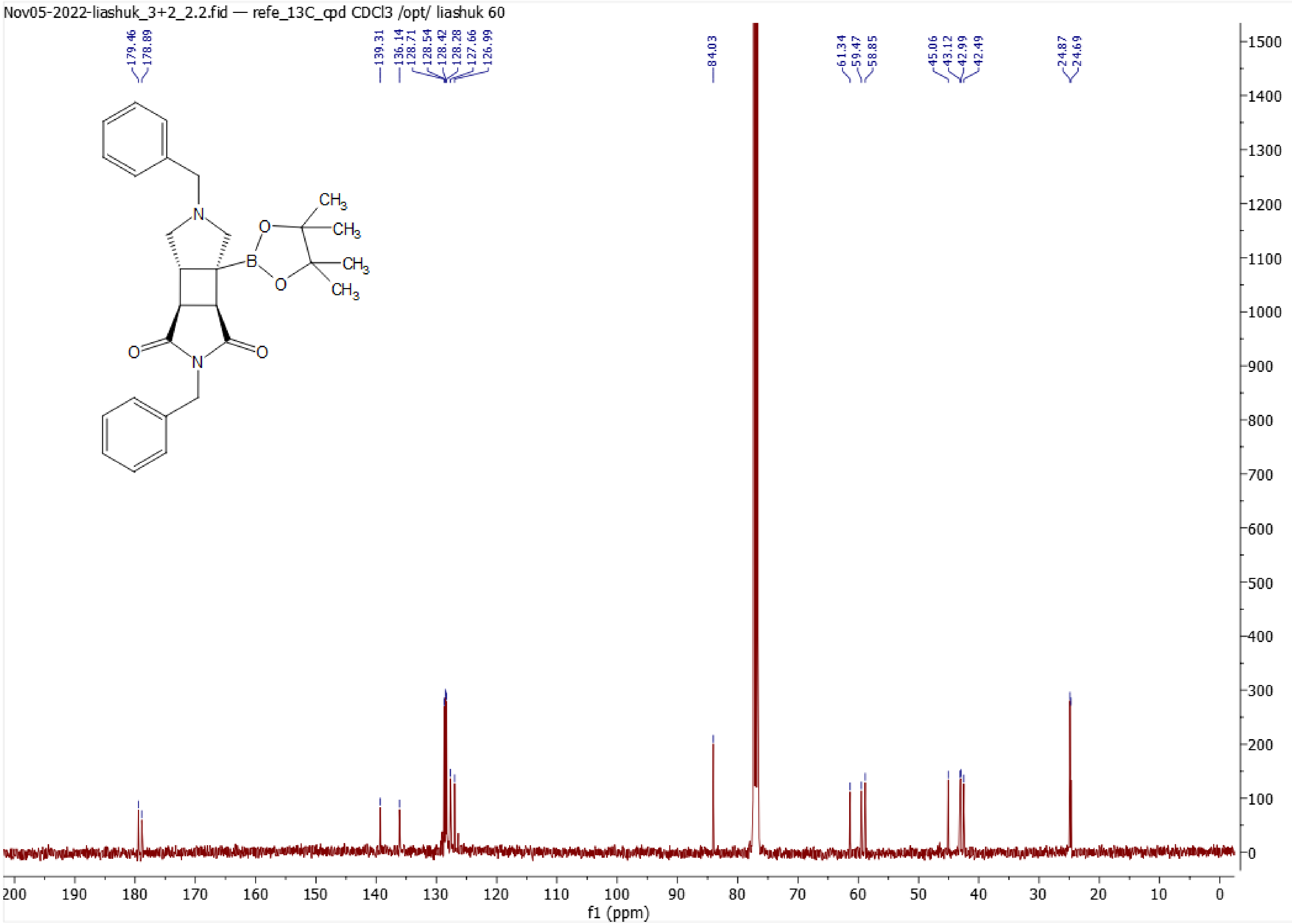

Spectrum 149. rac-(3aR,3bR,6aR,6bR)-2,5-dibenzyl-3b-(4,4,5,5-tetramethyl-1,3,2-dioxaborolan-2-yl)hexahydrocyclobuta[1,2-c:3,4-c']dipyrrole-1,3(2H,3aH)-dione ***17****,* *^{13}C NMR (101 MHz, CDCl$_3$)*

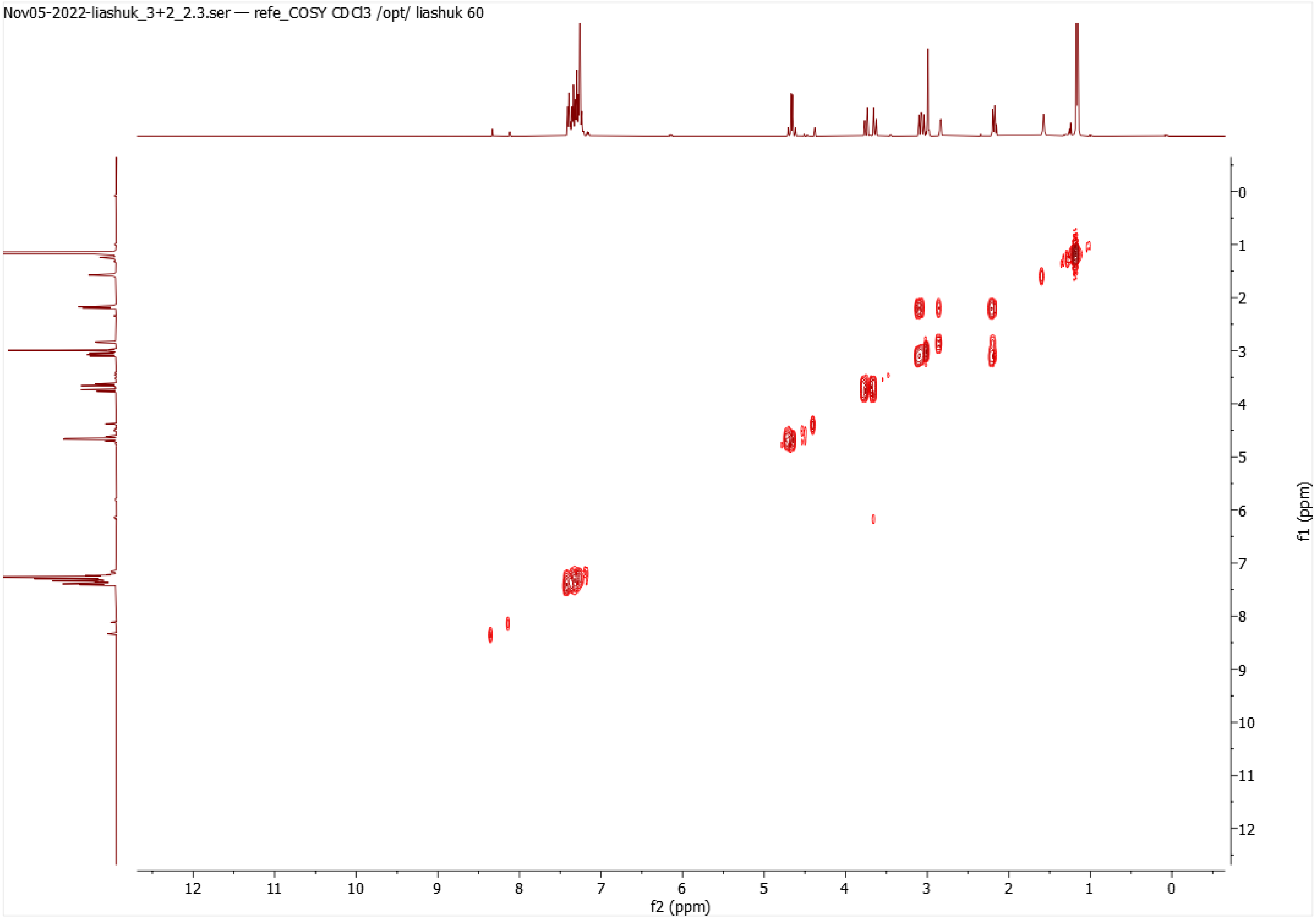

*Spectrum 150. rac-(3aR,3bR,6aR,6bR)-2,5-dibenzyl-3b-(4,4,5,5-tetramethyl-1,3,2-dioxaborolan-2-yl)hexahydrocyclobuta[1,2-c:3,4-c']dipyrrole-1,3(2H,3aH)-dione **17**, COSY (400 MHz, CDCl3)*

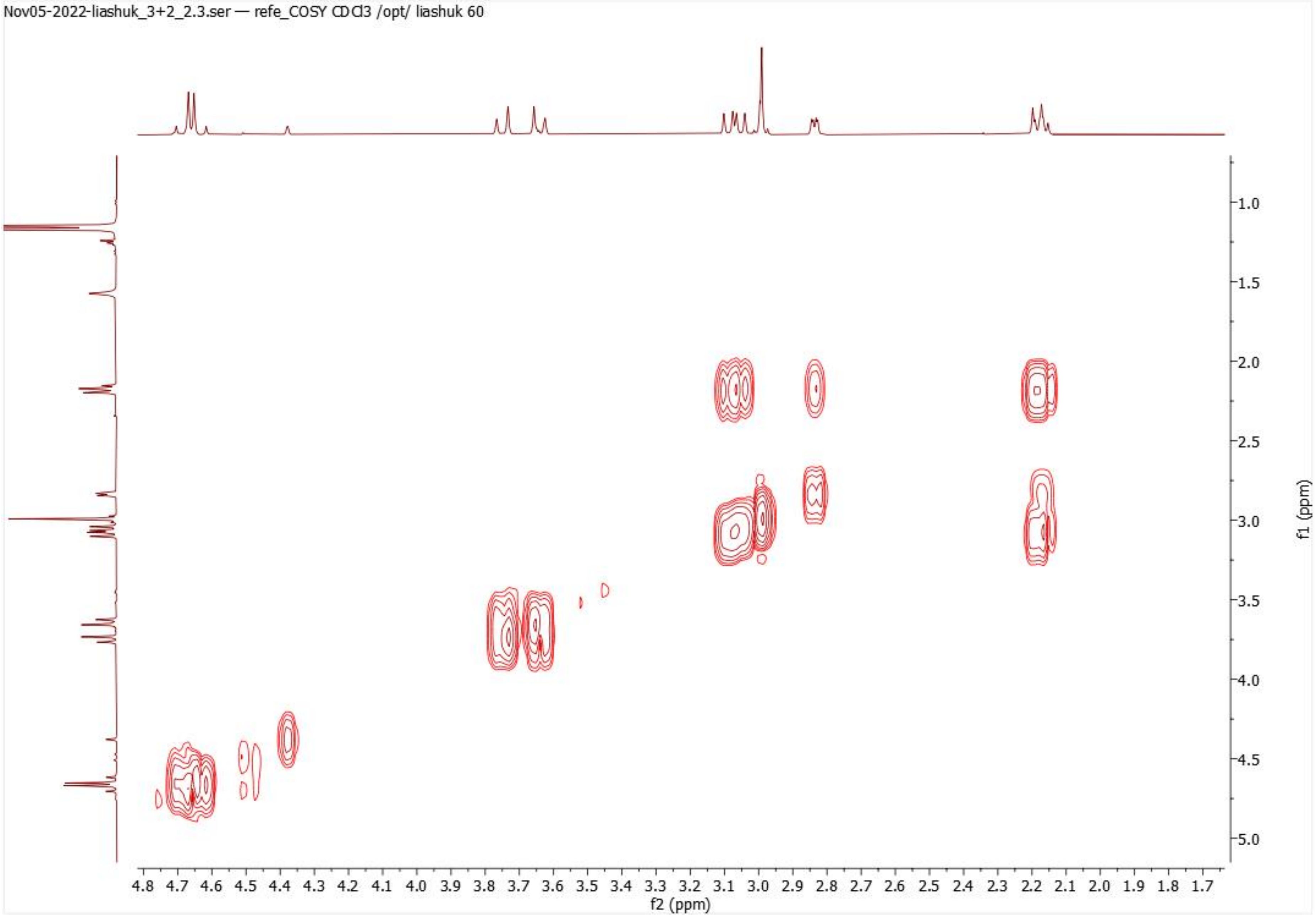

Spectrum 151. rac-(3aR,3bR,6aR,6bR)-2,5-dibenzyl-3b-(4,4,5,5-tetramethyl-1,3,2-dioxaborolan-2-yl)hexahydrocyclobuta[1,2-c:3,4-c']dipyrrole-1,3(2H,3aH)-dione **17**, COSY (400 MHz, CDCl3), aliphatic region

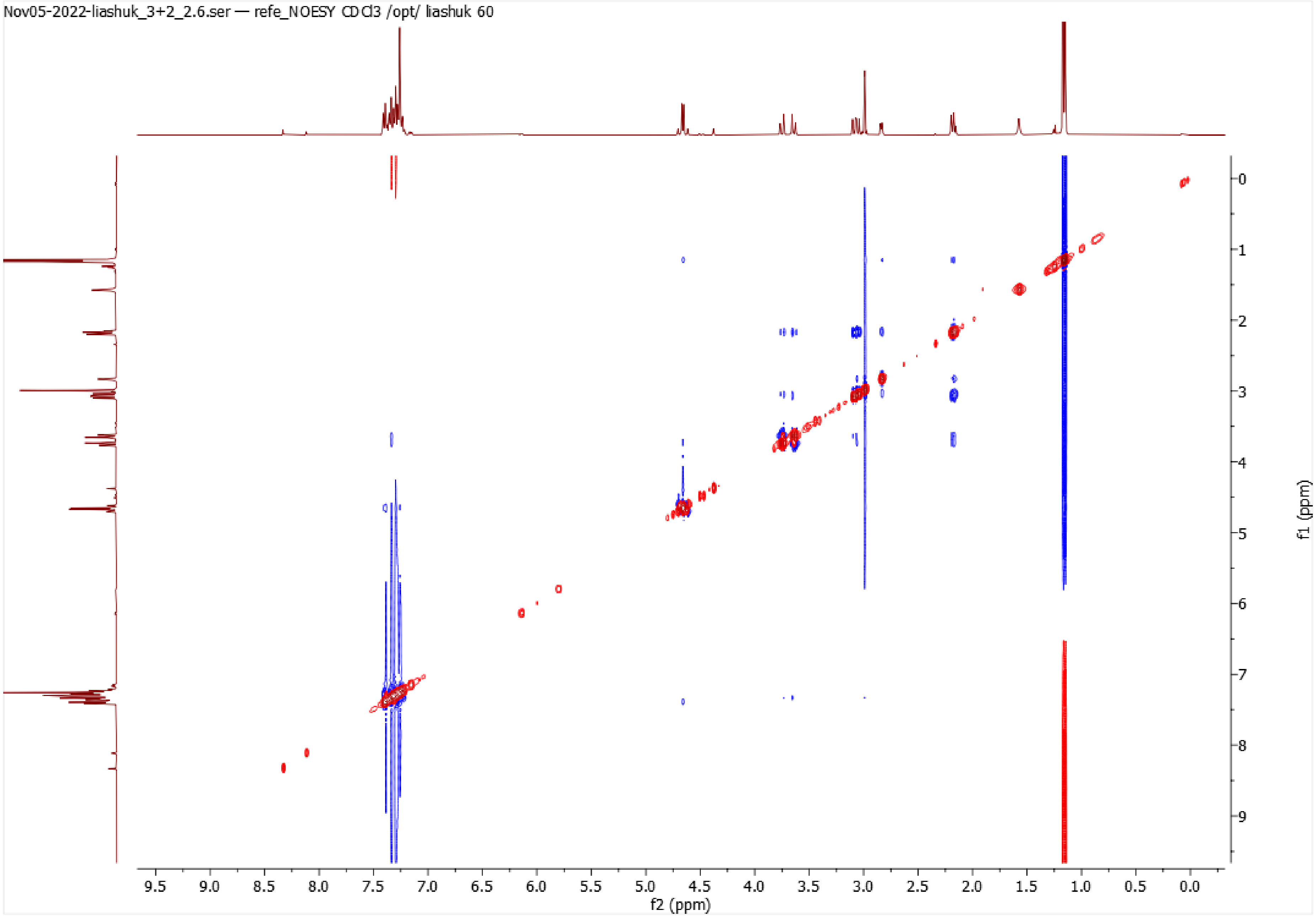

Spectrum 152. rac-(3aR,3bR,6aR,6bR)-2,5-dibenzyl-3b-(4,4,5,5-tetramethyl-1,3,2-dioxaborolan-2-yl)hexahydrocyclobuta[1,2-c:3,4-c']dipyrrole-1,3(2H,3aH)-dione **17**, NOESY (400 MHz, CDCl3)

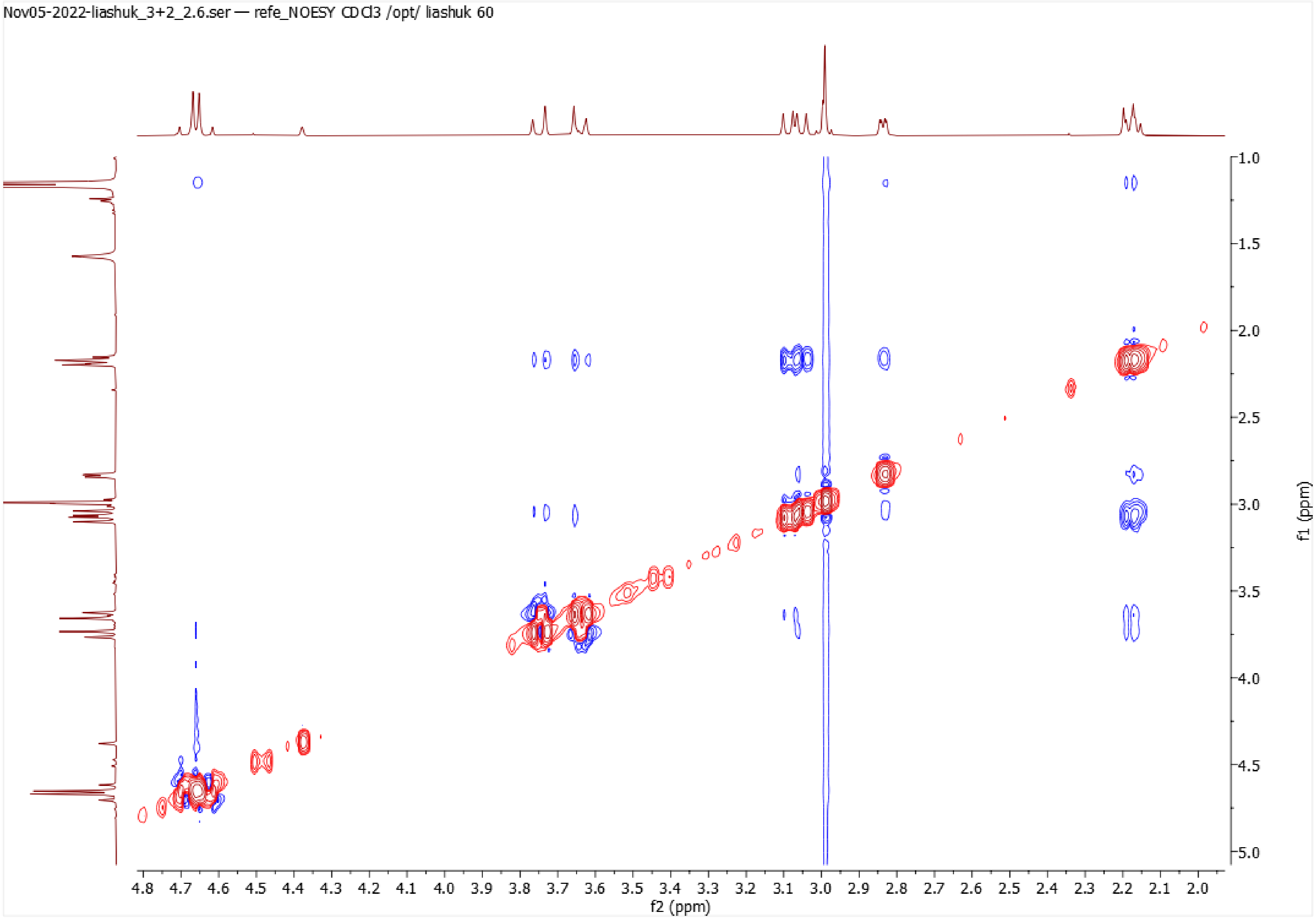

Spectrum 153. rac-(3aR,3bR,6aR,6bR)-2,5-dibenzyl-3b-(4,4,5,5-tetramethyl-1,3,2-dioxaborolan-2-yl)hexahydrocyclobuta[1,2-c:3,4-c']dipyrrole-1,3(2H,3aH)-dione **17**, NOESY (400 MHz, CDCl3), aliphatic region

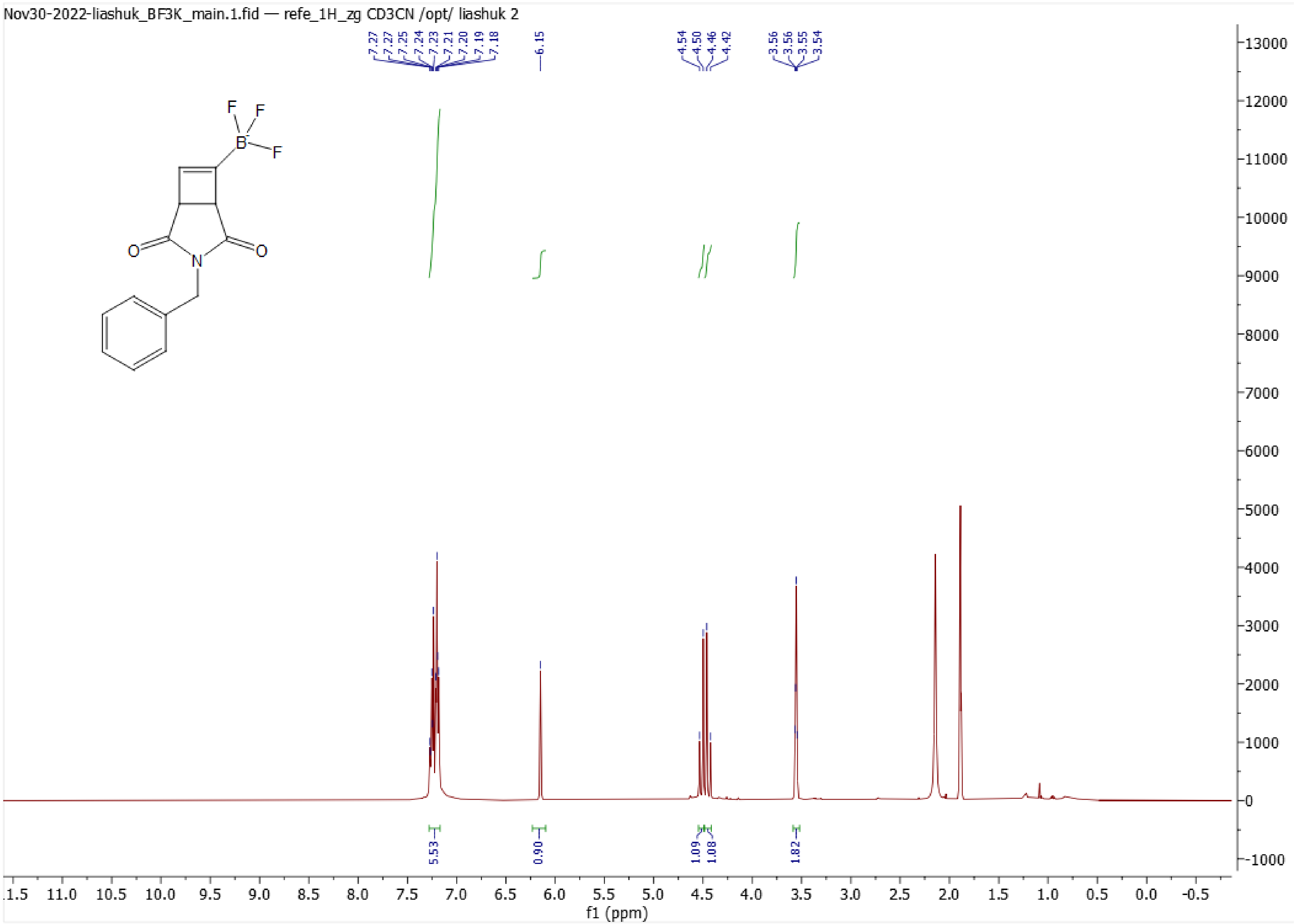

Spectrum 154. Potassium (3-benzyl-2,4-dioxo-3-azabicyclo[3.2.0]hept-6-en-6-yl)trifluoroborate ***8cl****, ^{1}H NMR (400 MHz, CD$_3$CN)*

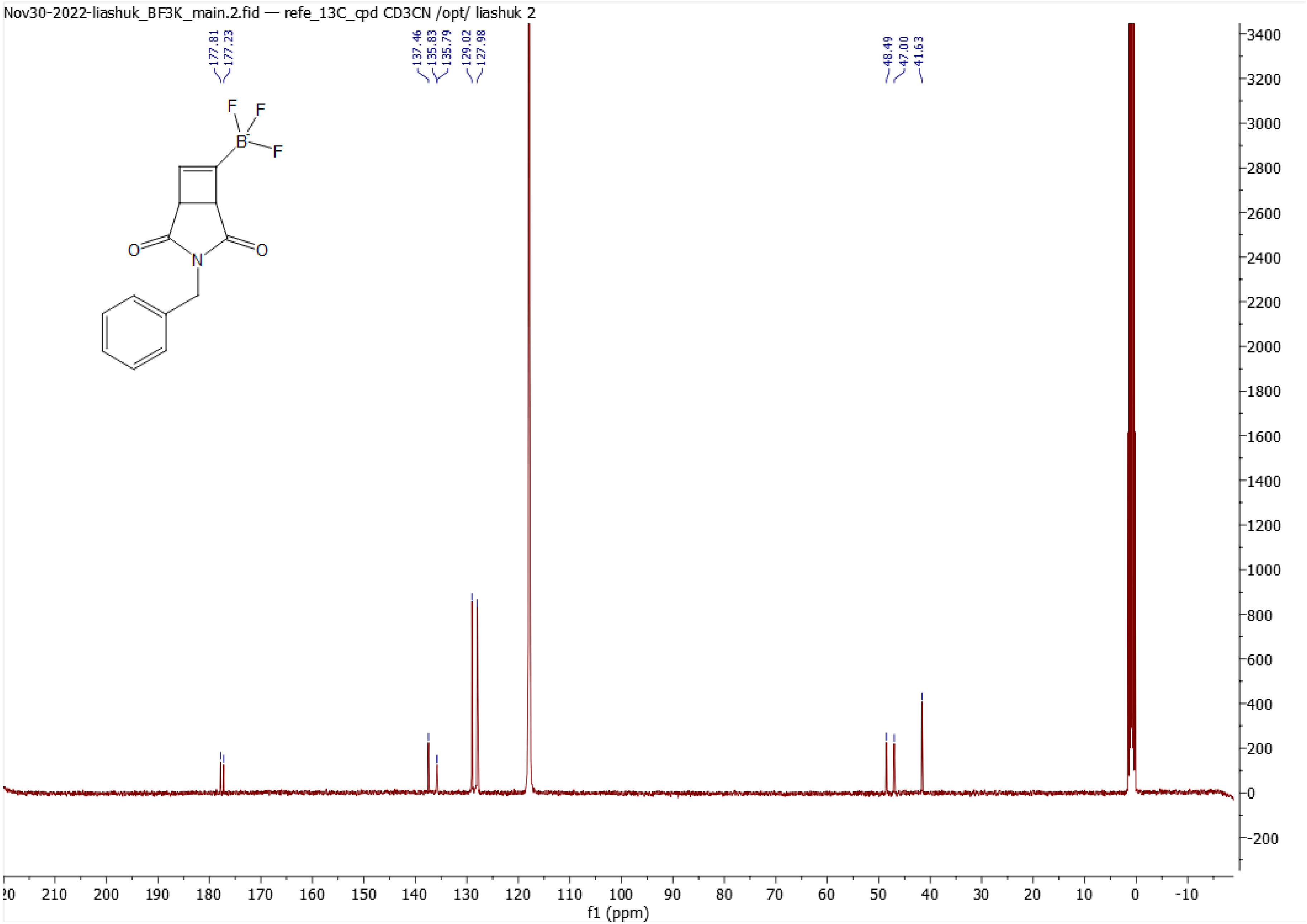

*Spectrum 155. Potassium (3-benzyl-2,4-dioxo-3-azabicyclo[3.2.0]hept-6-en-6-yl)trifluoroborate **8cl**, ^{13}C NMR (101 MHz, CD$_3$CN)*

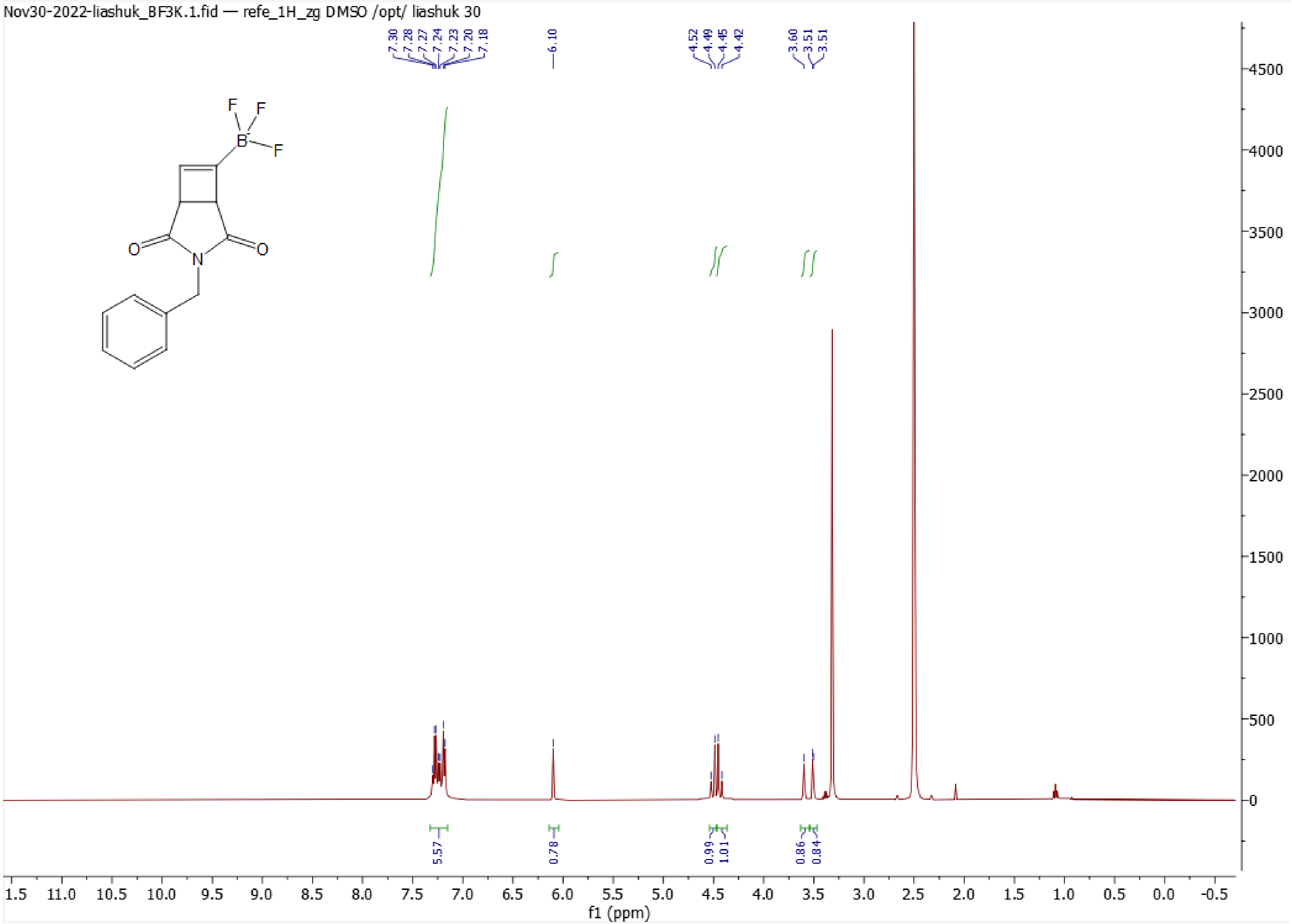

*Spectrum 156.Potassium (3-benzyl-2,4-dioxo-3-azabicyclo[3.2.0]hept-6-en-6-yl)trifluoroborate **8cl**, ^{1}H NMR (400 MHz, DMSO-d_6)*

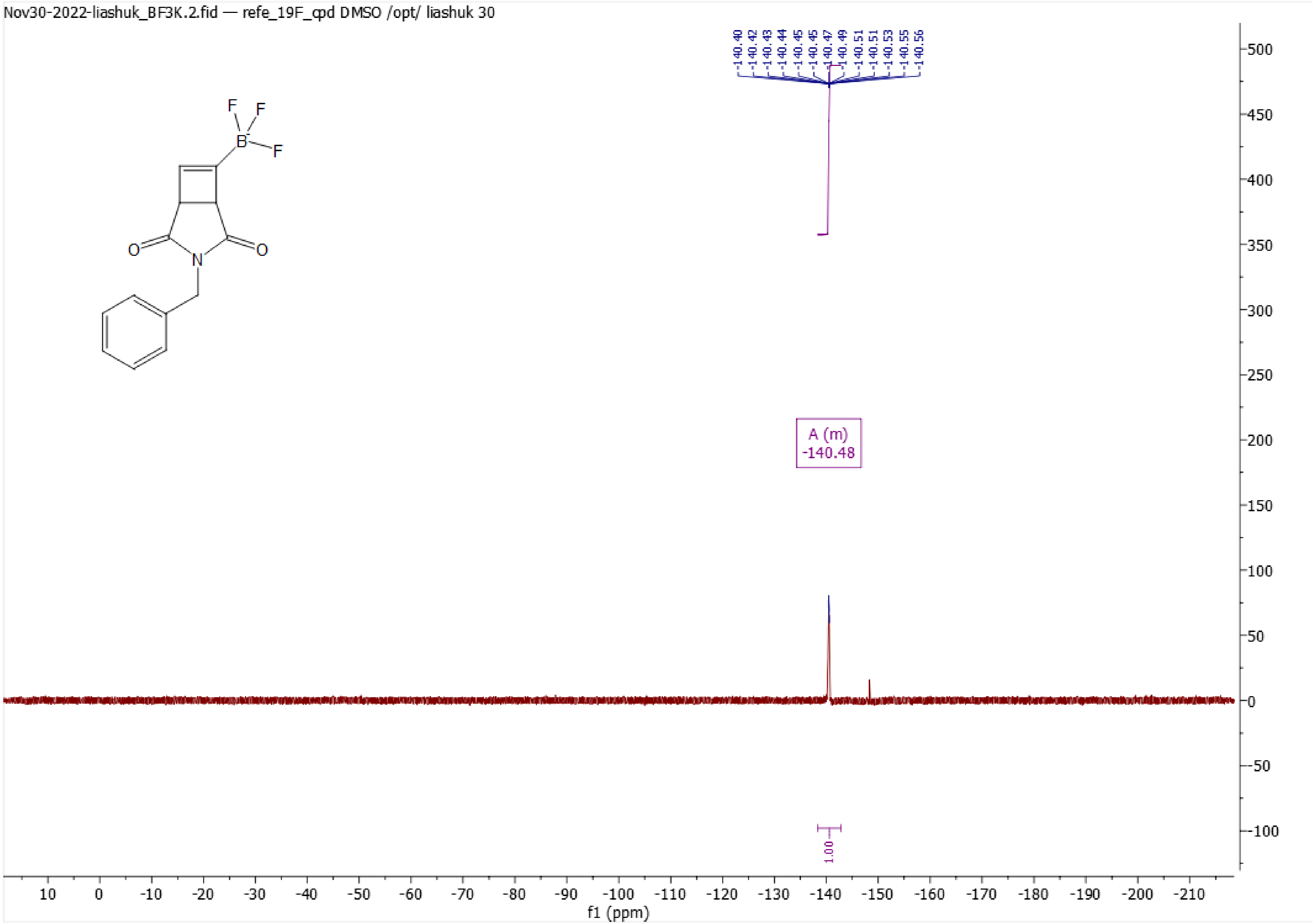

*Spectrum 157. Potassium (3-benzyl-2,4-dioxo-3-azabicyclo[3.2.0]hept-6-en-6-yl)trifluoroborate **8cl**, ^{19}F NMR (376 MHz, DMSO-d_6)*

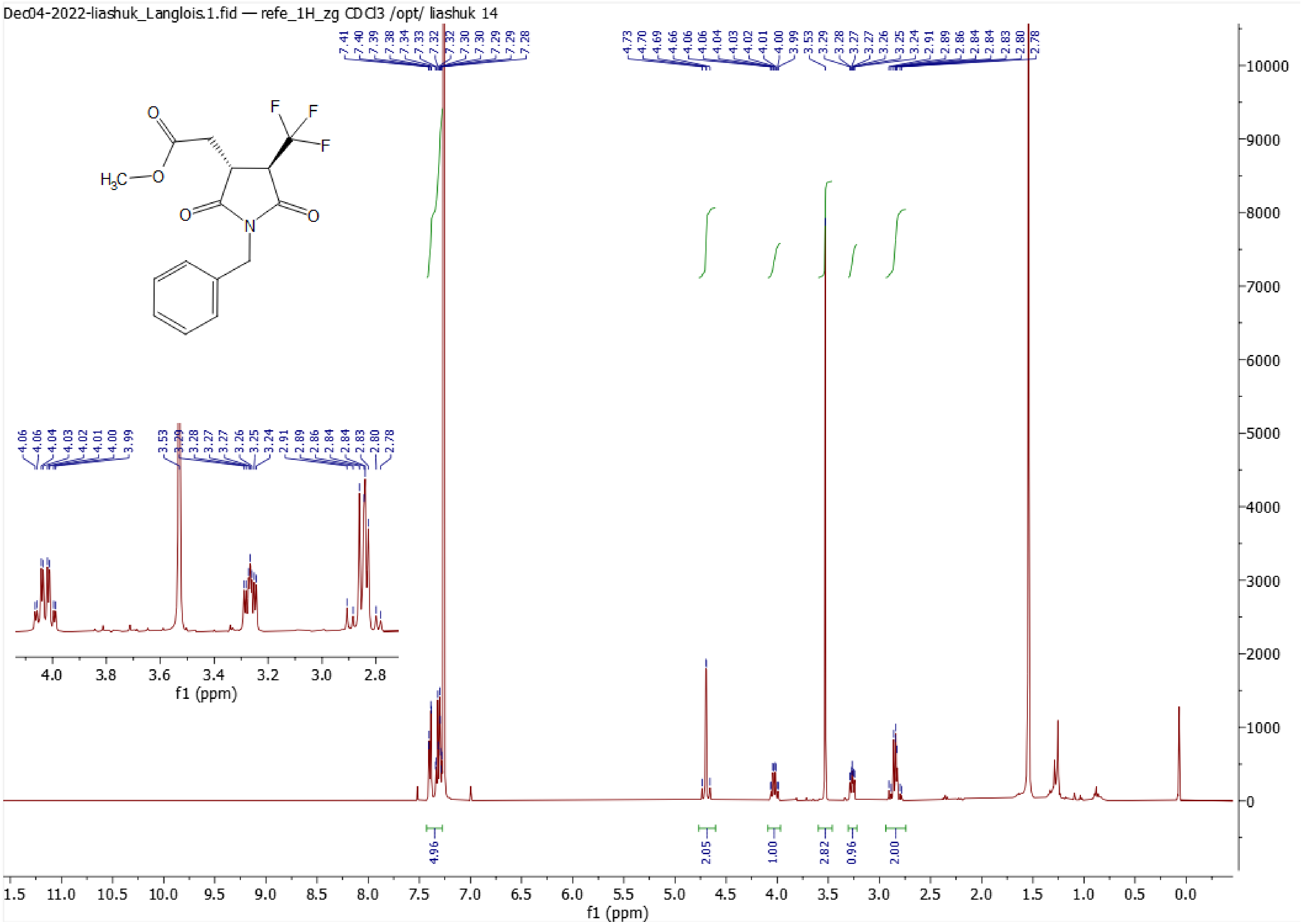

Spectrum 158. rac-methyl 2-((3R,4R)-1-benzyl-2,5-dioxo-4-(trifluoromethyl)pyrrolidin-3-yl)acetate ***18***, *^{1}H NMR (400 MHz, CDCl$_3$)*

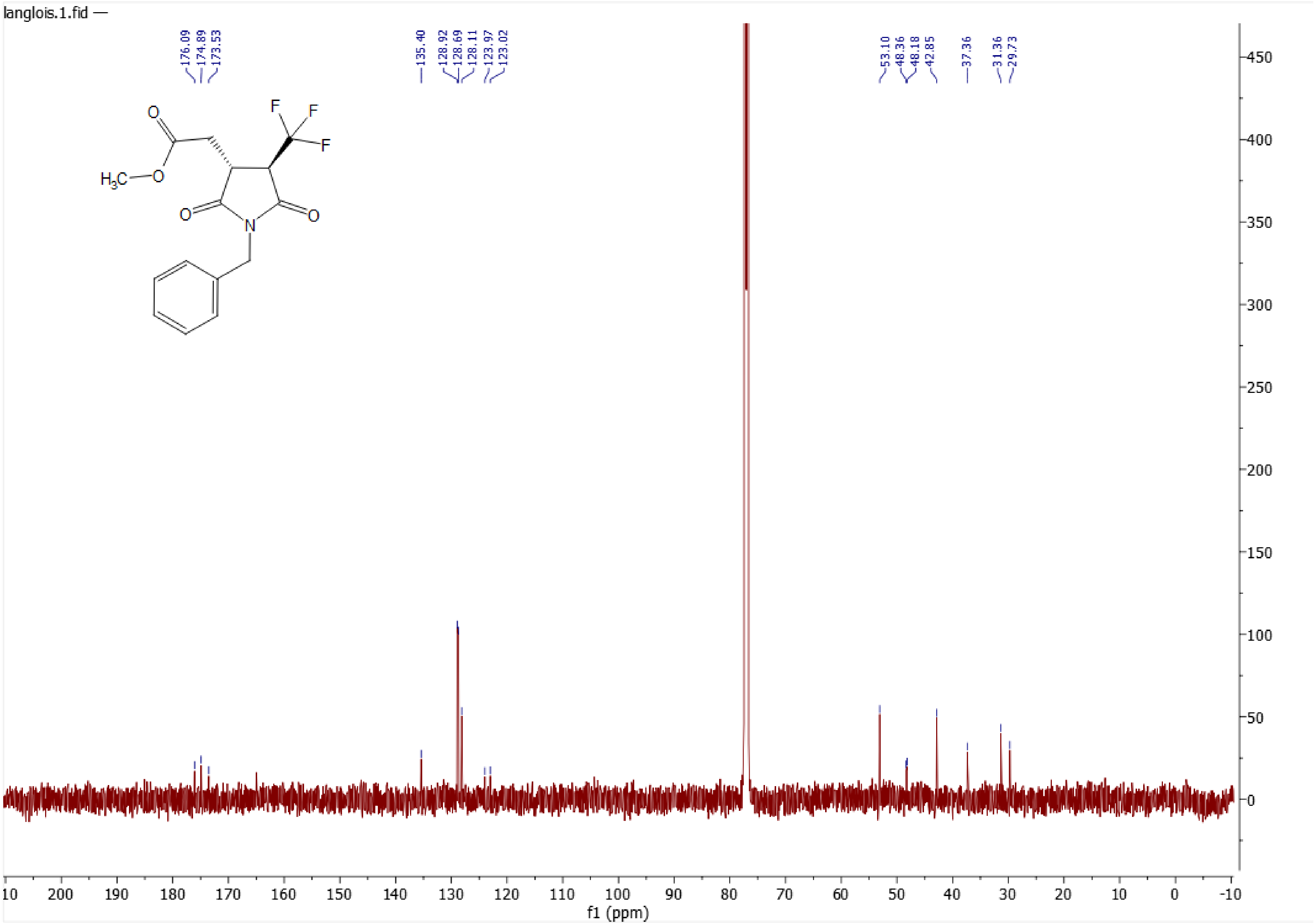

Spectrum 159. rac-methyl 2-((3R,4R)-1-benzyl-2,5-dioxo-4-(trifluoromethyl)pyrrolidin-3-yl)acetate ***18****,* ^{13}*C NMR (151 MHz, CDCl*$_3$*)*

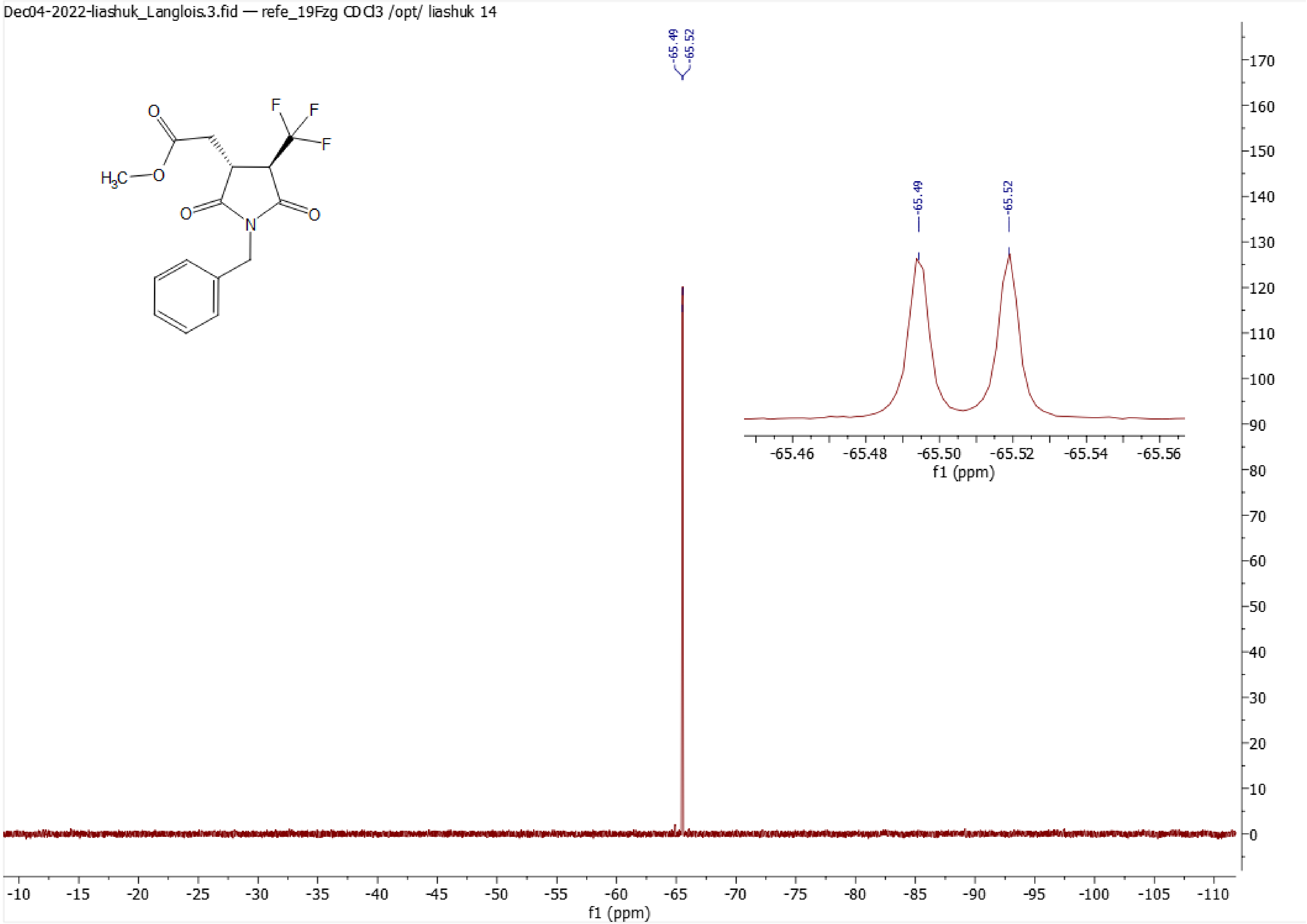

*Spectrum 160. rac-methyl 2-((3R,4R)-1-benzyl-2,5-dioxo-4-(trifluoromethyl)pyrrolidin-3-yl)acetate **18**, ^{19}F NMR (376 MHz, CDCl$_3$)*

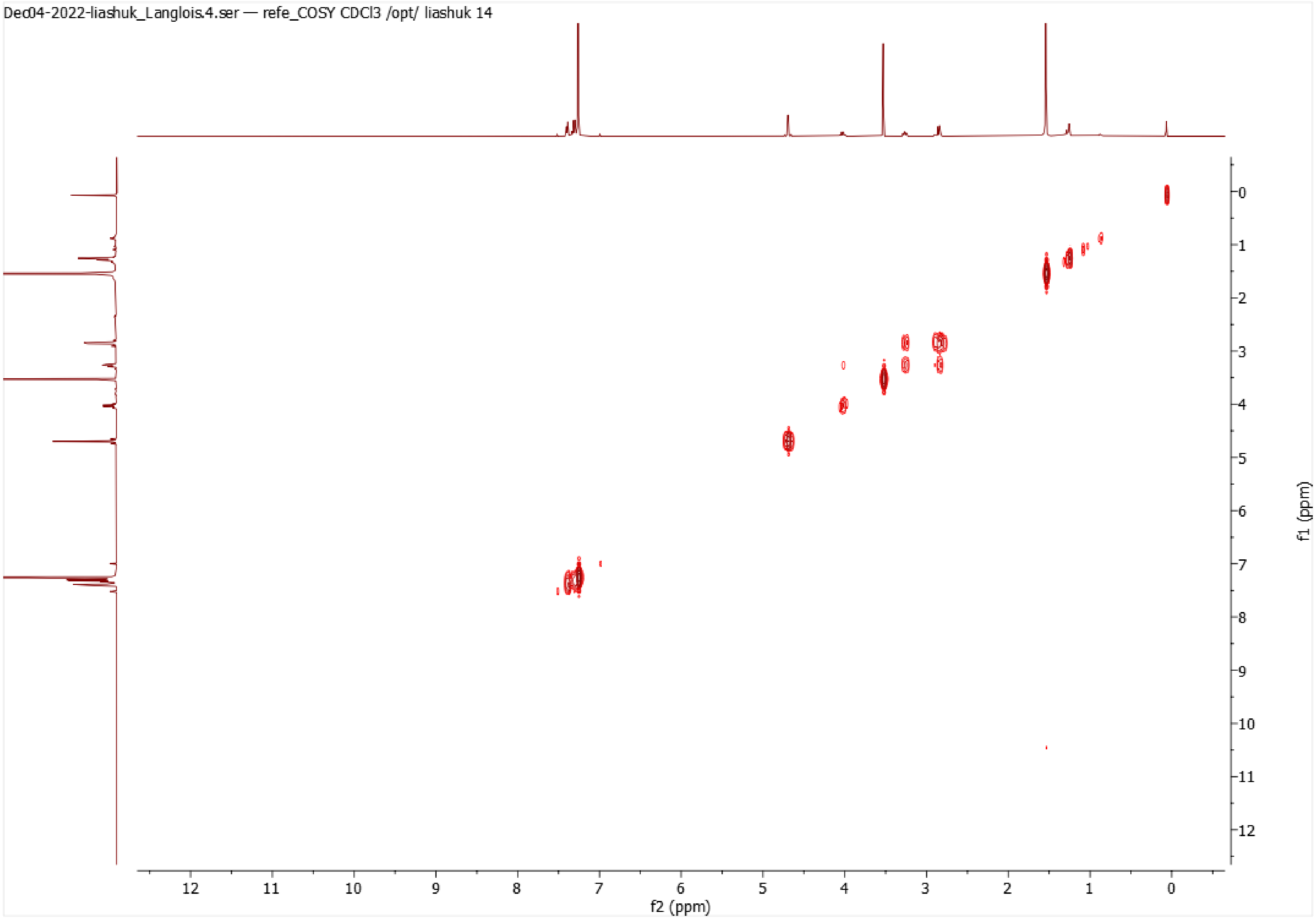

Spectrum 161. rac-methyl 2-((3R,4R)-1-benzyl-2,5-dioxo-4-(trifluoromethyl)pyrrolidin-3-yl)acetate ***18****, COSY (400 MHz, CDCl3)*

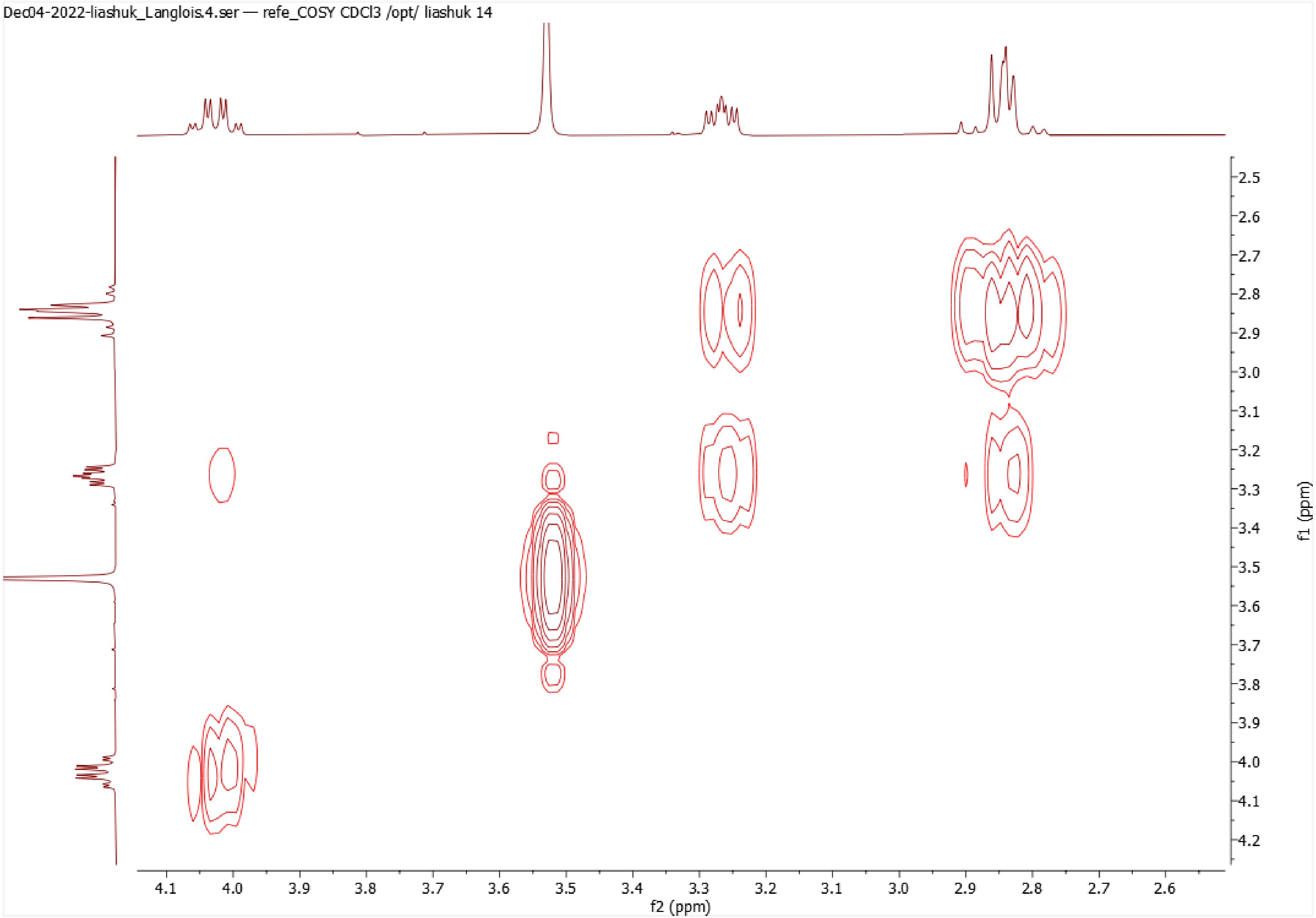

*Spectrum 162. rac-methyl 2-((3R,4R)-1-benzyl-2,5-dioxo-4-(trifluoromethyl)pyrrolidin-3-yl)acetate **18**, COSY (400 MHz, CDCl3), aliphatic region*

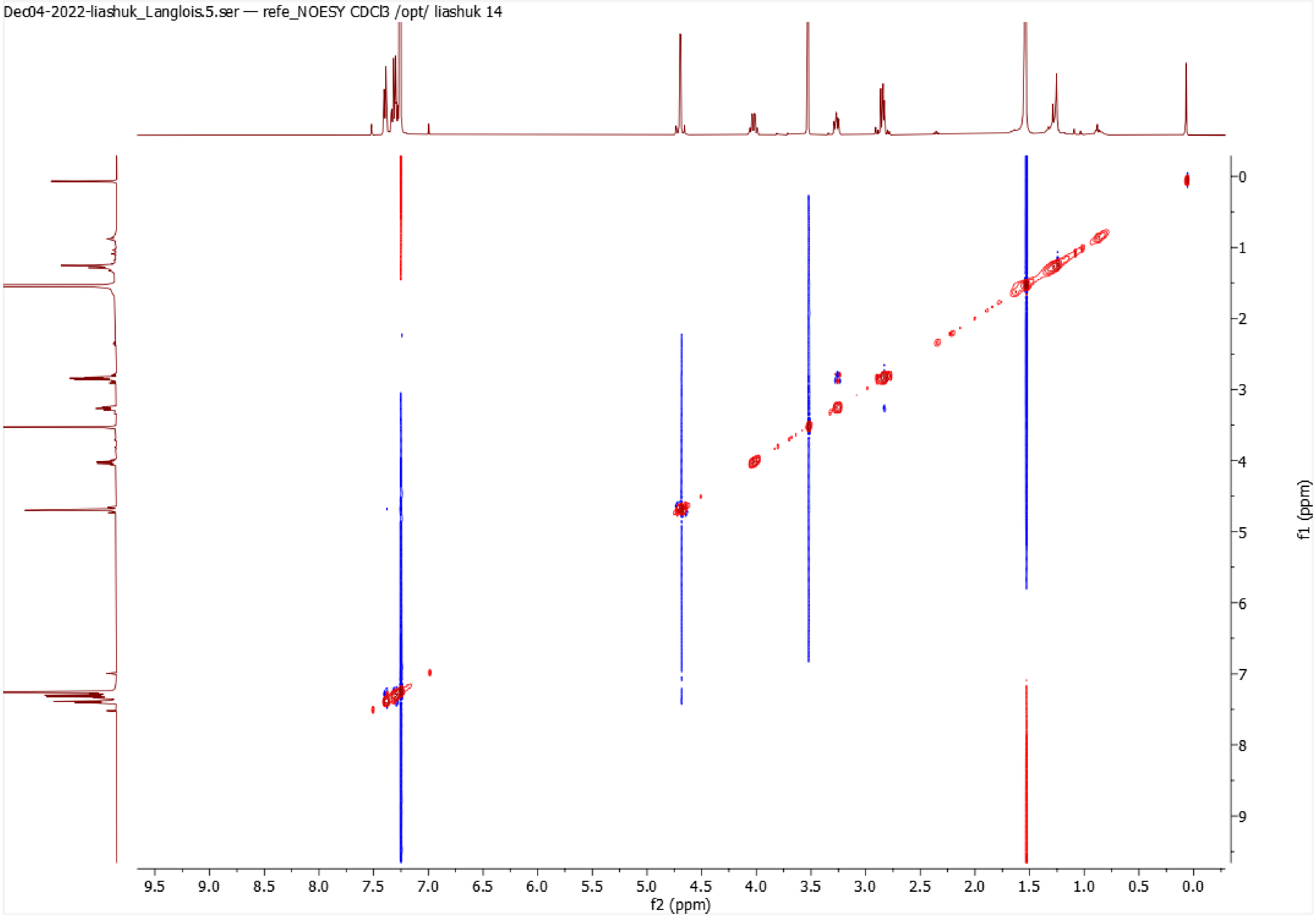

Spectrum 163. rac-methyl 2-((3R,4R)-1-benzyl-2,5-dioxo-4-(trifluoromethyl)pyrrolidin-3-yl)acetate ***18****, NOESY (400 MHz, CDCl3)*

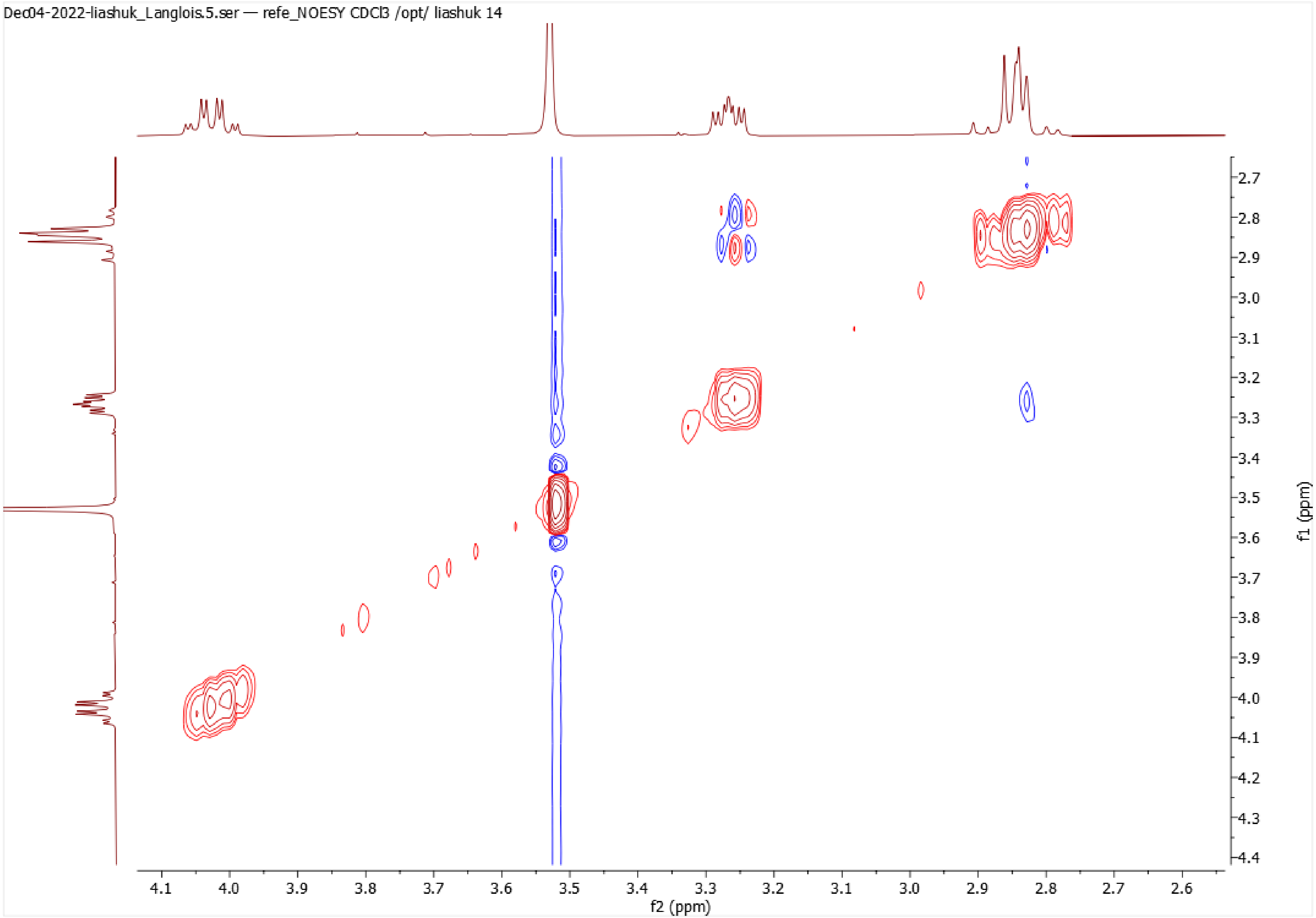

*Spectrum 164. rac-methyl 2-((3R,4R)-1-benzyl-2,5-dioxo-4-(trifluoromethyl)pyrrolidin-3-yl)acetate **18**, NOESY (400 MHz, CDCl3), aliphatic region*

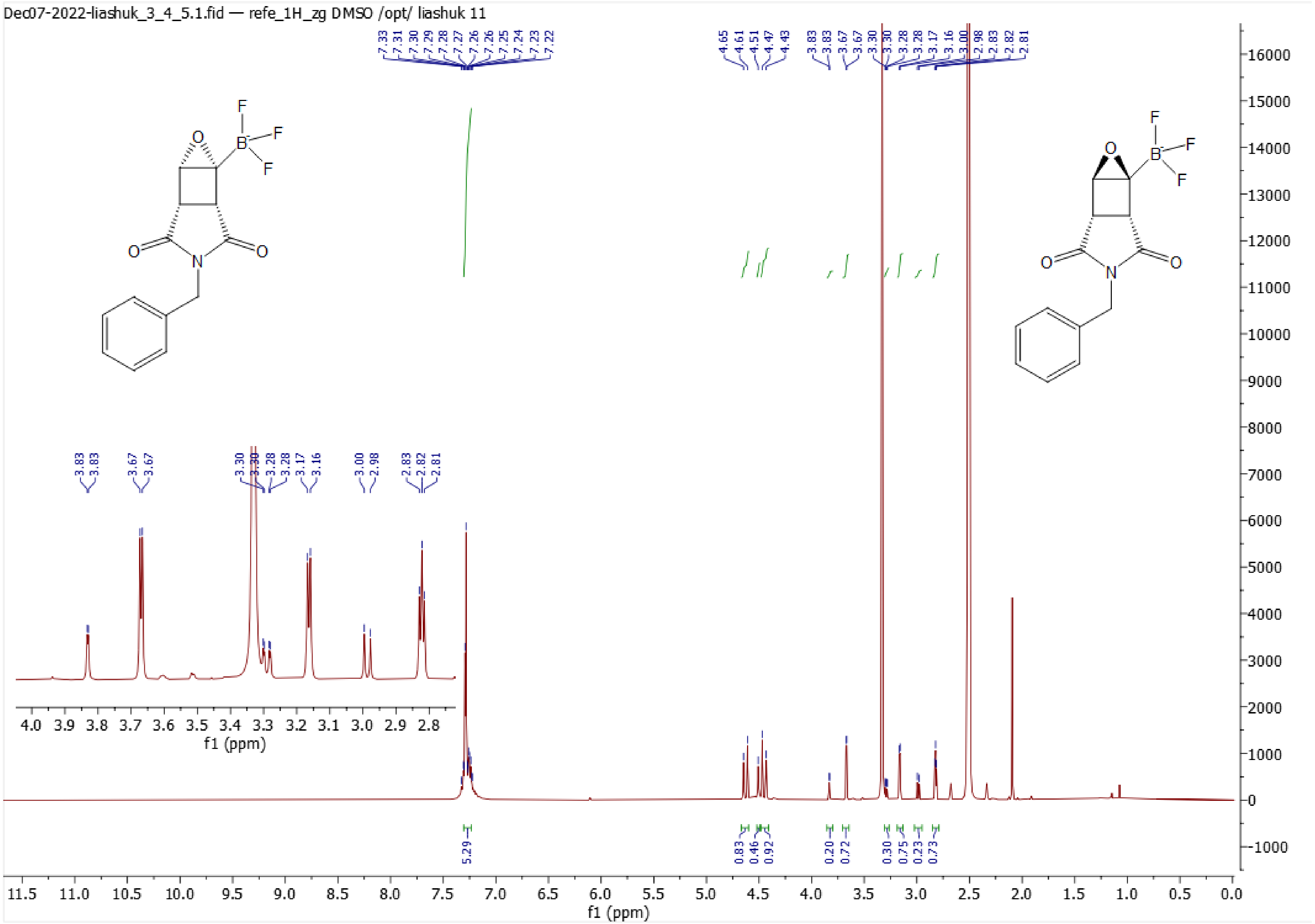

*Spectrum 165. Potassium rac-((1R,2S,4R,5S)-7-benzyl-6,8-dioxo-3-oxa-7-azatricyclo[3.3.0.02,4]octan-2-yl)trifluoroborate and potassium rac-((1R,2R,4S,5S)-7-benzyl-6,8-dioxo-3-oxa-7-azatricyclo[3.3.0.02,4]octan-2-yl)trifluoroborate **19** and **19'**, ^{1}H NMR (400 MHz, DMSO-d_6)*

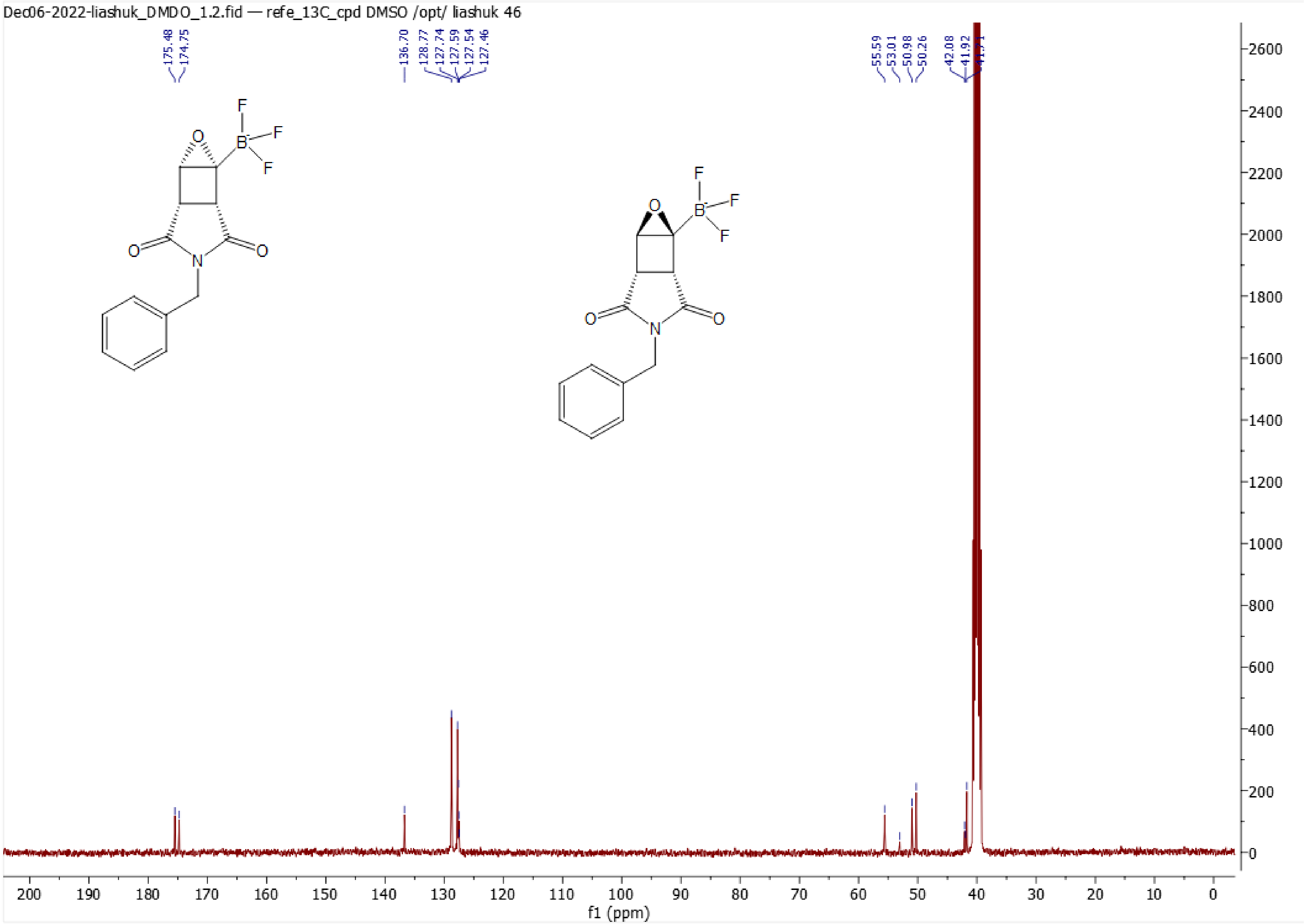

Spectrum 166. Potassium rac-((1R,2S,4R,5S)-7-benzyl-6,8-dioxo-3-oxa-7-azatricyclo[3.3.0.02,4]octan-2-yl)trifluoroborate and potassium rac-((1R,2R,4S,5S)-7-benzyl-6,8-dioxo-3-oxa-7-azatricyclo[3.3.0.02,4]octan-2-yl)trifluoroborate ***19*** *and* ***19'****, ^{13}C NMR (101 MHz, DMSO-d$_6$)*

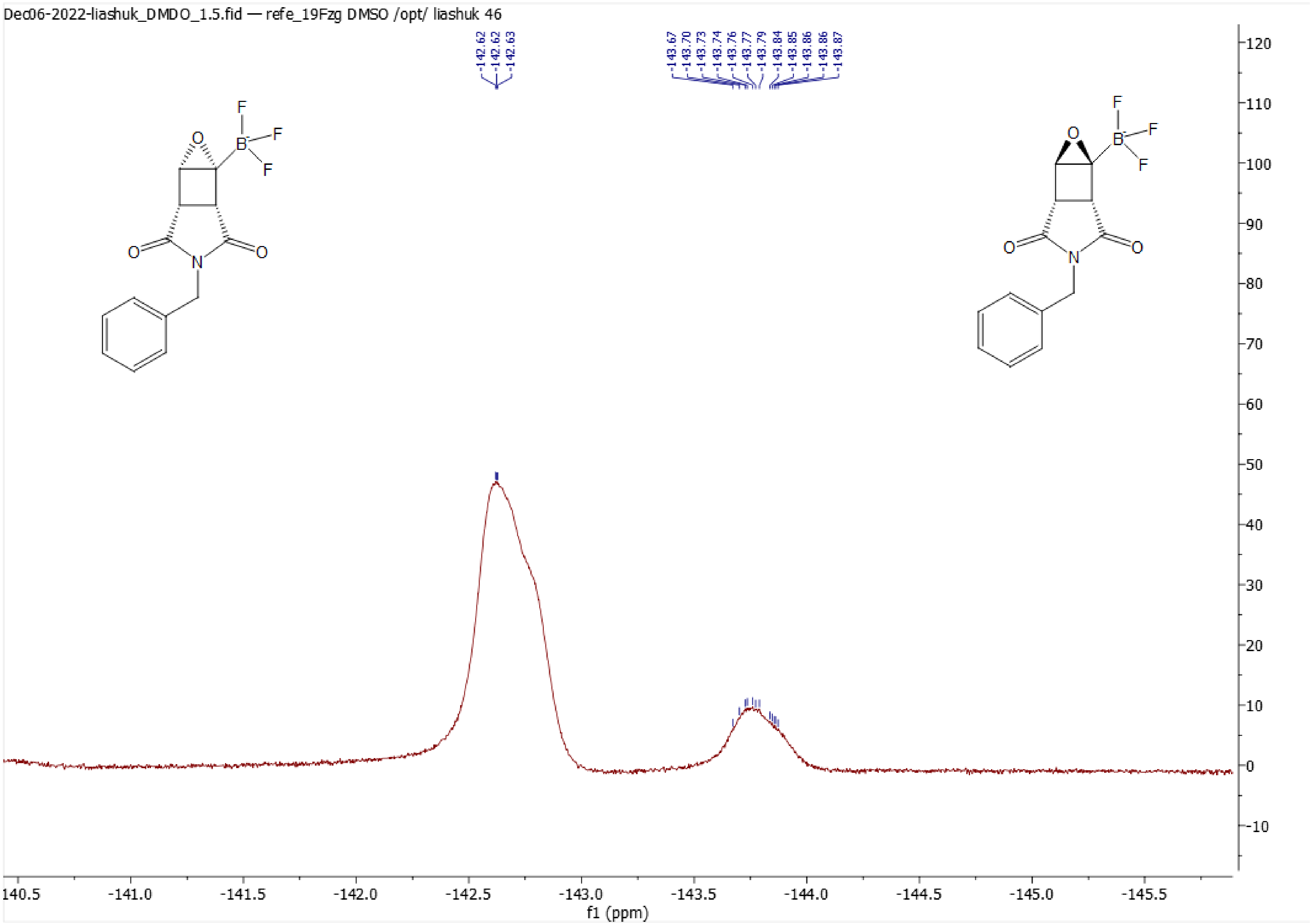

Spectrum 167. Potassium rac-((1R,2S,4R,5S)-7-benzyl-6,8-dioxo-3-oxa-7-azatricyclo[3.3.0.02,4]octan-2-yl)trifluoroborate and potassium rac-((1R,2R,4S,5S)-7-benzyl-6,8-dioxo-3-oxa-7-azatricyclo[3.3.0.02,4]octan-2-yl)trifluoroborate ***19*** *and* ***19'****,* ^{19}*F NMR (376 MHz, DMSO-d*$_6$*)*

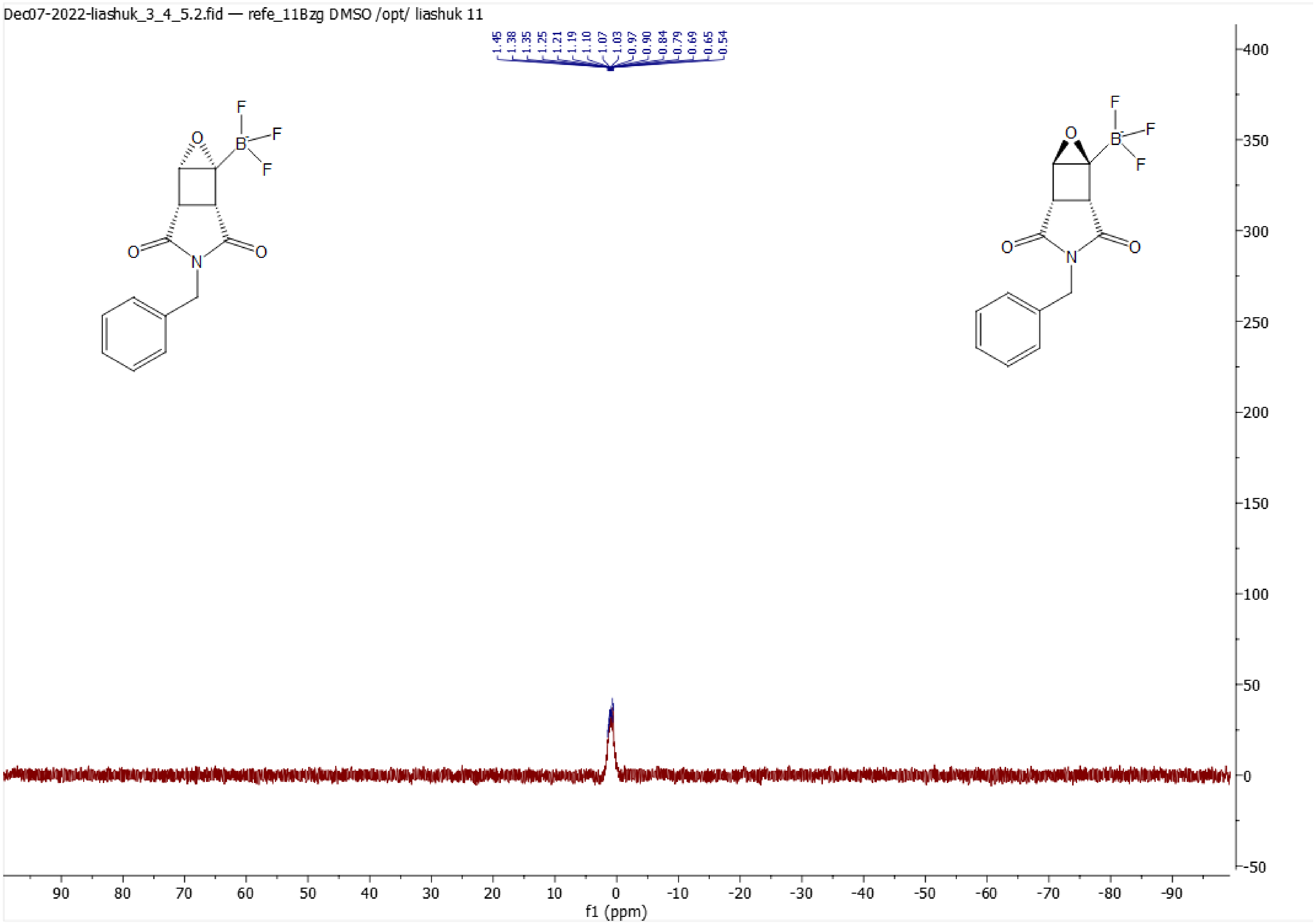

Spectrum 168. Potassium rac-((1R,2S,4R,5S)-7-benzyl-6,8-dioxo-3-oxa-7-azatricyclo[3.3.0.02,4]octan-2-yl)trifluoroborate and potassium rac-((1R,2R,4S,5S)-7-benzyl-6,8-dioxo-3-oxa-7-azatricyclo[3.3.0.02,4]octan-2-yl)trifluoroborate ***19*** *and* ***19'****, ^{11}B NMR (128 MHz, DMSO-d$_6$)*

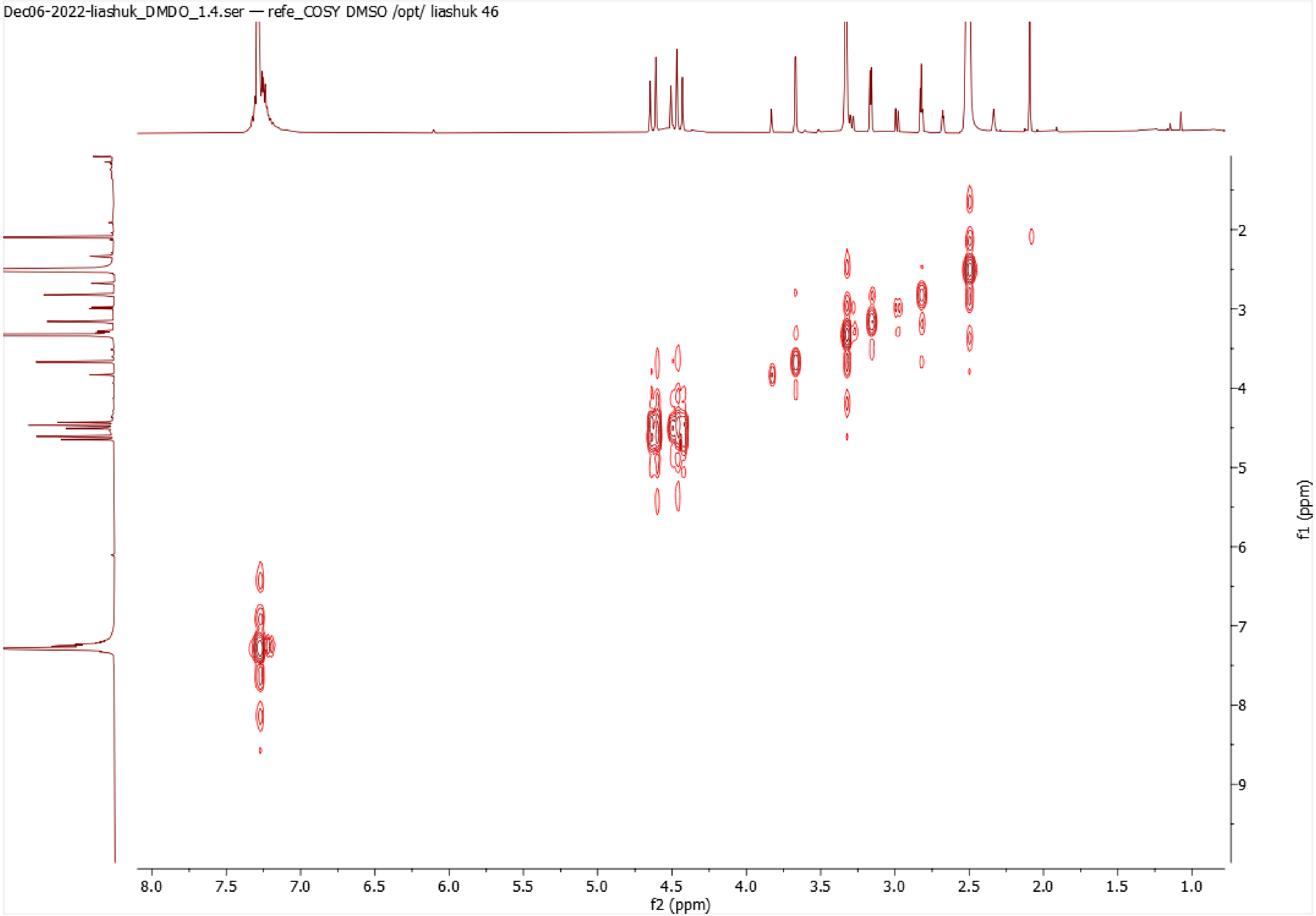

Spectrum 169. Potassium rac-((1R,2S,4R,5S)-7-benzyl-6,8-dioxo-3-oxa-7-azatricyclo[3.3.0.02,4]octan-2-yl)trifluoroborate and potassium rac-((1R,2R,4S,5S)-7-benzyl-6,8-dioxo-3-oxa-7-azatricyclo[3.3.0.02,4]octan-2-yl)trifluoroborate ***19*** *and* ***19'****, COSY (400 MHz, DMSO-d_6)*

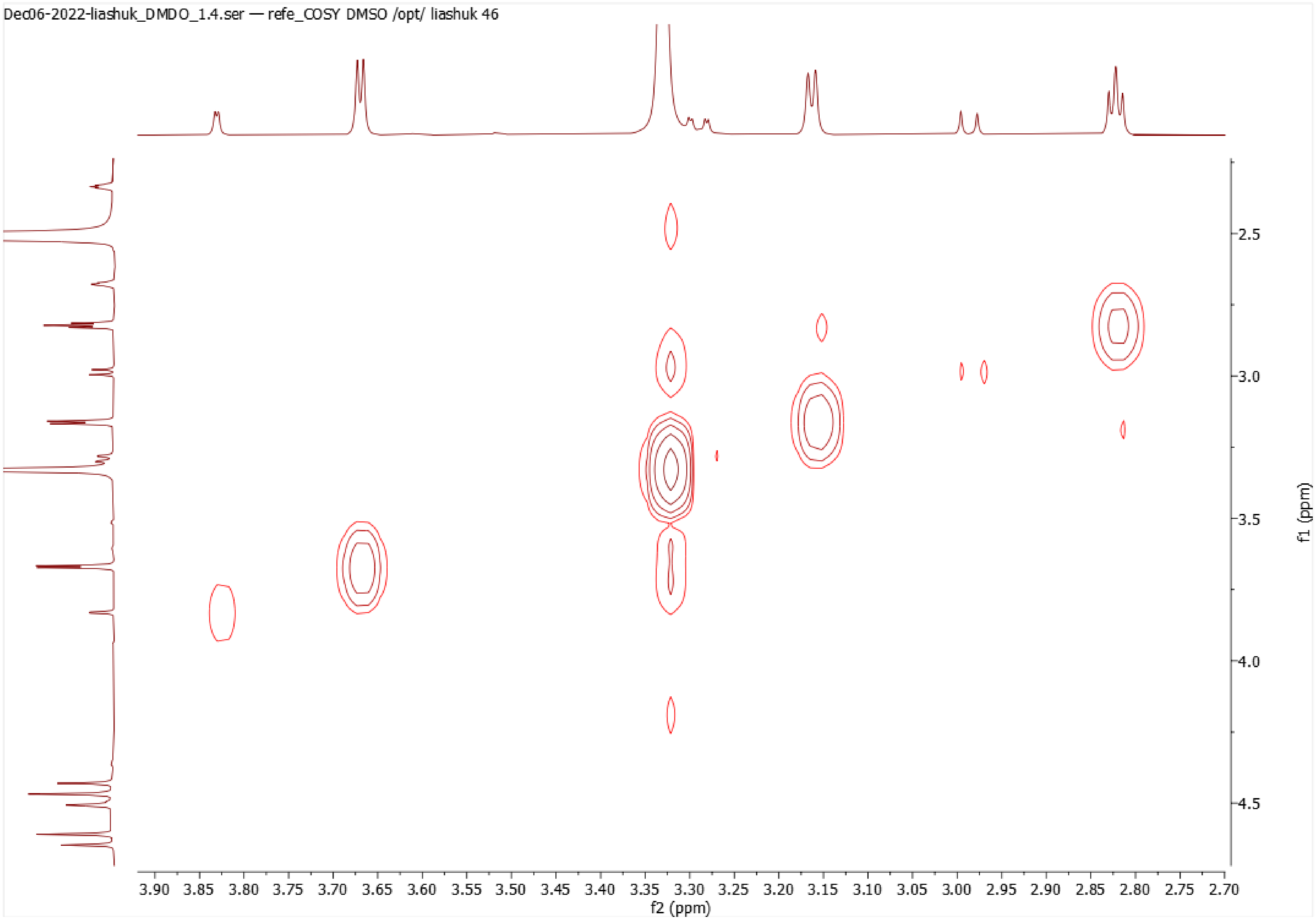

Spectrum 170. Potassium rac-((1R,2S,4R,5S)-7-benzyl-6,8-dioxo-3-oxa-7-azatricyclo[3.3.0.02,4]octan-2-yl)trifluoroborate and potassium rac-((1R,2R,4S,5S)-7-benzyl-6,8-dioxo-3-oxa-7-azatricyclo[3.3.0.02,4]octan-2-yl)trifluoroborate **19** and **19′**, COSY (400 MHz, DMSO-d_6), aliphatic region

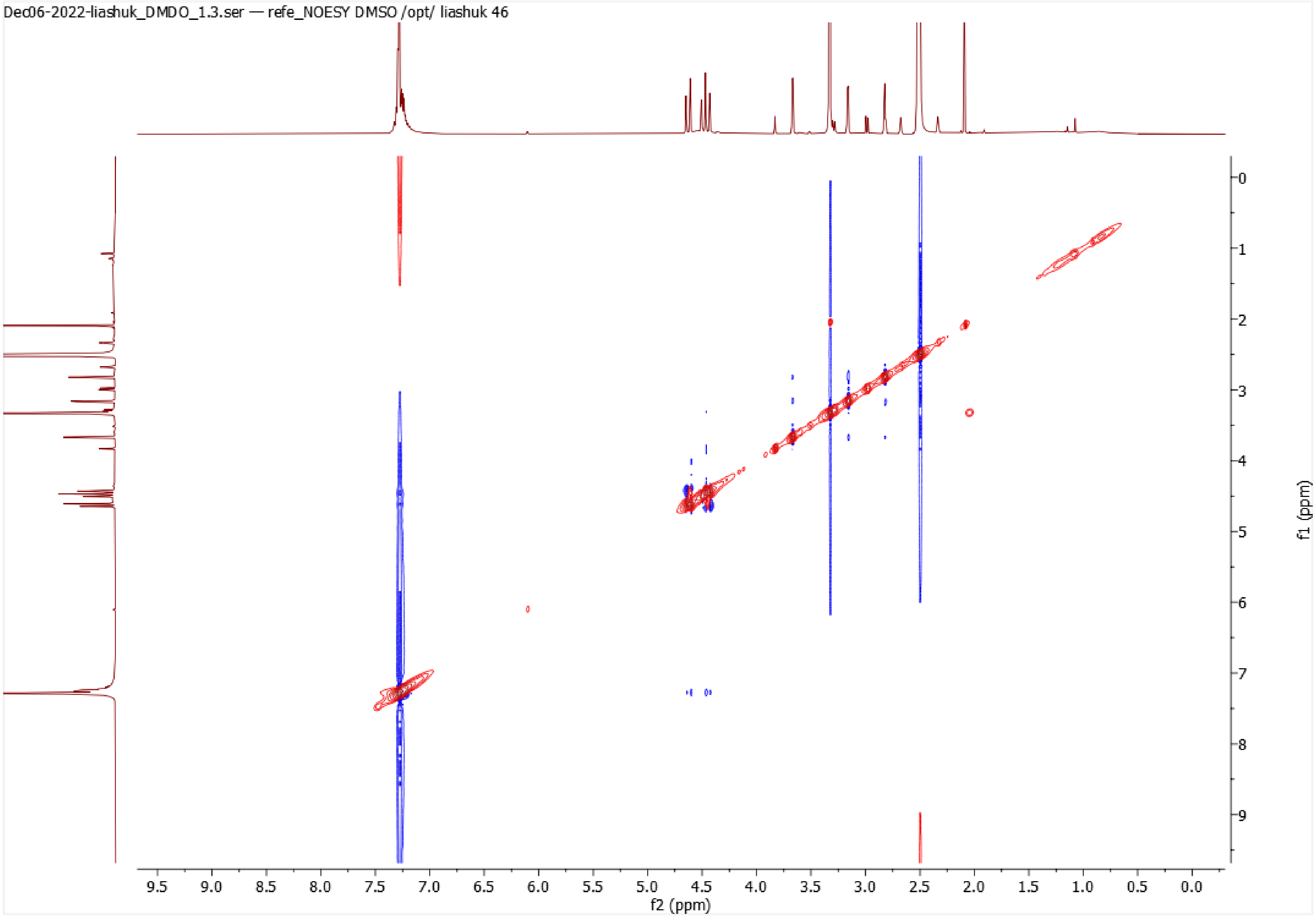

*Spectrum 171. Potassium rac-((1R,2S,4R,5S)-7-benzyl-6,8-dioxo-3-oxa-7-azatricyclo[3.3.0.02,4]octan-2-yl)trifluoroborate and potassium rac-((1R,2R,4S,5S)-7-benzyl-6,8-dioxo-3-oxa-7-azatricyclo[3.3.0.02,4]octan-2-yl)trifluoroborate **19** and **19'**, NOESY (400 MHz, DMSO-d_6)*

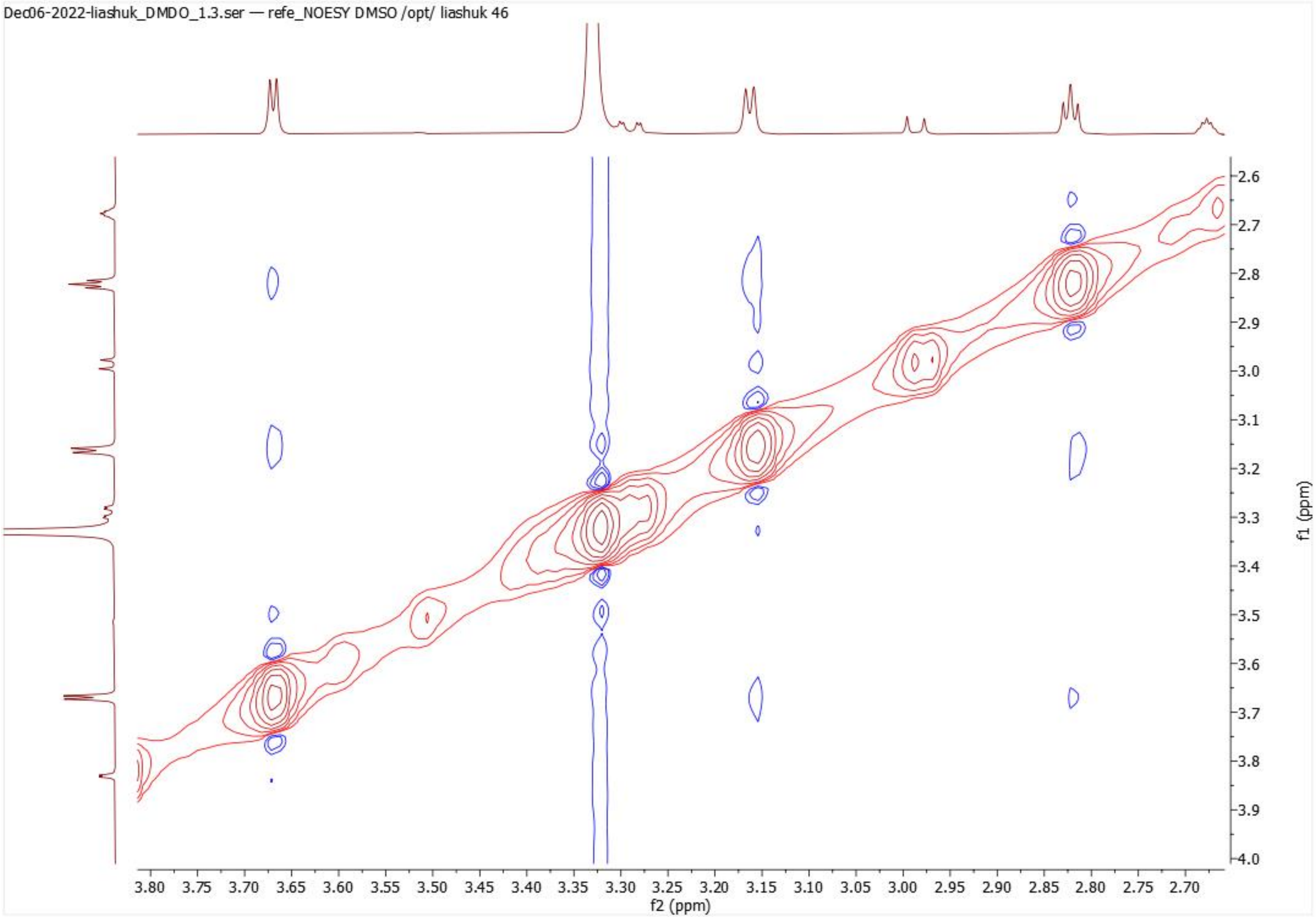

*Spectrum 172. Potassium rac-((1R,2S,4R,5S)-7-benzyl-6,8-dioxo-3-oxa-7-azatricyclo[3.3.0.02,4]octan-2-yl)trifluoroborate and potassium rac-((1R,2R,4S,5S)-7-benzyl-6,8-dioxo-3-oxa-7-azatricyclo[3.3.0.02,4]octan-2-yl)trifluoroborate **19** and **19'**, NOESY (400 MHz, DMSO-d_6), aliphatic region*

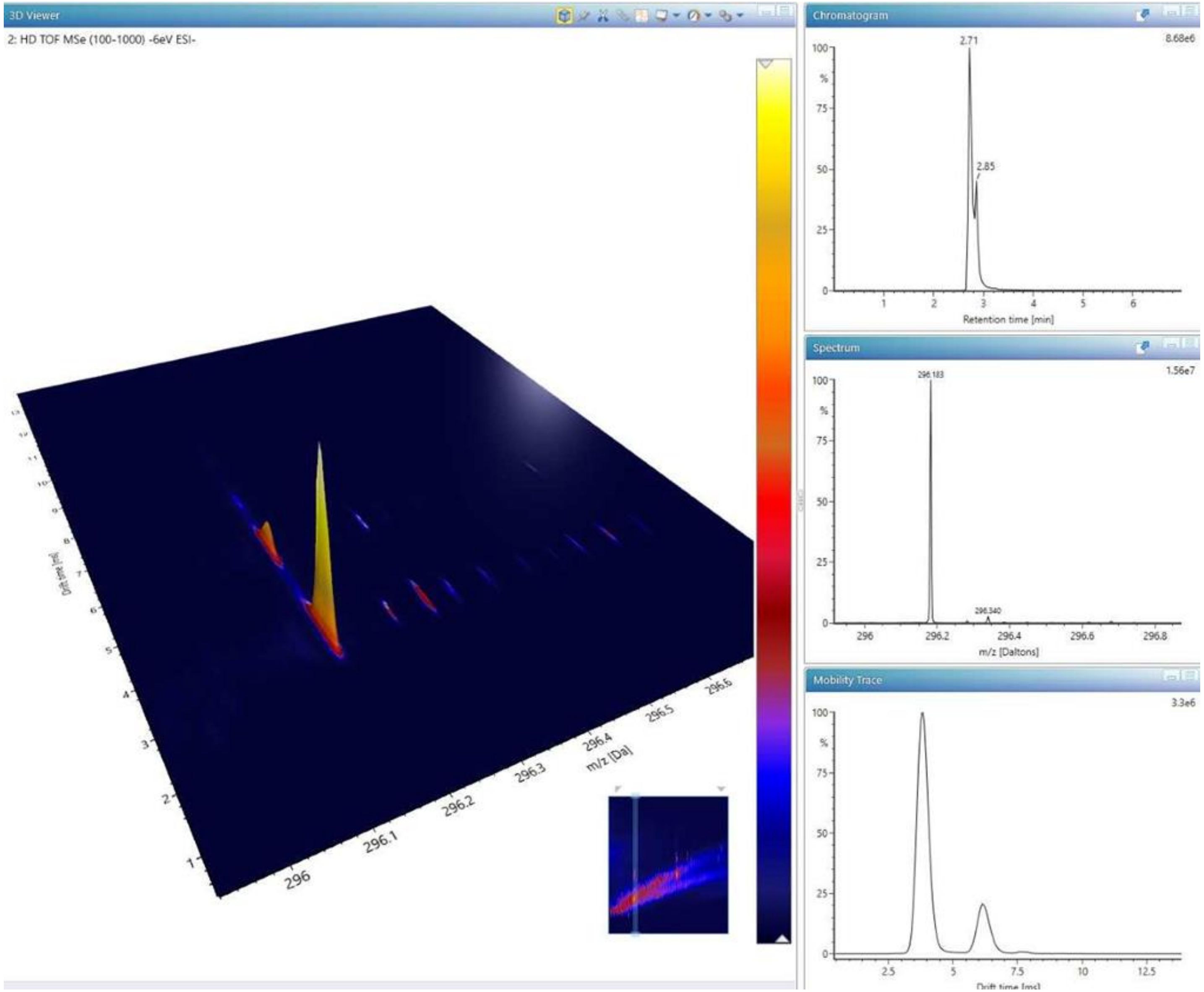

MS-analysis of diastereomers mixture 19 and 19'.

Sample was analyzed using Waters Acquity-I-UPLC Classsystem (Waters Corporation, Milford, MA, USA) coupled with a Waters Vion IMS-QTof Mass Spectrometer equipped with LockSpray (Leucine-enkephalin (200 pg/µL). The instrument was controlled by Waters UNIFI 1.9.4 (3.1.0, Waters Corporation, Milford, MA, USA). Injection volume was 5uL. The instrument was operated in positive polarity, sensitivity mode (33,000 FWHM at 556.2766 m/z). Data was acquired in HDMSe mode with a scan time of 0.072 s. The recorded mass range was from 100 to 1000 m/z for both low and high energy spectra. The collision energy was ramped from 20 to 40 V. The cone voltage was set to 30 V, capillary voltage was set to 2 kV and source offset was set to 50 V. Source temperature was set to 120 °C and desolvation temperature set to 500 °C. Cone gas flow rate was set to 50 L/h and desolvation gas flow rate was set to 1000 L/h.

Spectrum 173. Potassium rac-((1R,2S,4R,5S)-7-benzyl-6,8-dioxo-3-oxa-7-azatricyclo[3.3.0.02,4]octan-2-yl)trifluoroborate and potassium rac-((1R,2R,4S,5S)-7-benzyl-6,8-dioxo-3-oxa-7-azatricyclo[3.3.0.02,4]octan-2-yl)trifluoroborate ***19*** *and* ***19'****, LC-Ion mobility (TWIMS)-QTOF*

Crystal Data and Experimental Information. CCDC 2235657

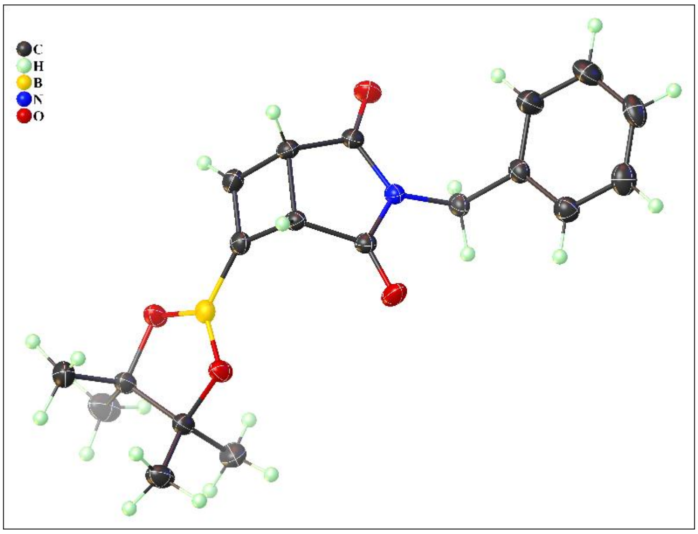

Compound	8c
Formula	$C_{19}H_{22}BNO_4$
$D_{calc.}$/ g cm^{-3}	1.278
□/mm^{-1}	0.716
Formula Weight	339.18
Colour	colourless
Shape	prism-shaped
Size/mm^3	0.38×0.12×0.07
T/K	140.00(10)
Crystal System	orthorhombic
Flack Parameter	-0.01(4)
Space Group	$Pna2_1$
a/Å	12.71258(16)
b/Å	20.8247(3)
c/Å	6.65667(7)
□/°	90
□/°	90
□/°	90
V/Å^3	1762.26(4)
Z	4
Z'	1
Wavelength/Å	1.54184
Radiation type	Cu*K*□
$□_{min}$/°	4.074
$□_{max}$/°	75.551
Measured Refl's.	33598
Indep't Refl's	3389
Refl's I≥2□(I)	3316
R_{int}	0.0205
Parameters	230
Restraints	1
Largest Peak/e Å^{-3}	0.170
Deepest Hole/e Å^{-3}	-0.174
GooF	1.054
wR_2 (all data)	0.0655
wR_2	0.0651
R_1 (all data)	0.0256
R_1	0.0250
CCDC number	2235657

Experimental. Single colourless prism-shaped crystals of **8c**were used as supplied. A suitable crystal with dimensions 0.38 × 0.12 × 0.07 mm^3 was selected and mounted on an XtaLAB Synergy R, DW system, HyPix-Arc 150 diffractometer. The crystal was kept at a steady *T* = 140.00(10) K during data collection. The structure was solved with the **ShelXT** 2018/2[21] solution program using dual methods and by using **Olex2** 1.5[22] as the graphical interface. The model was refined with **ShelXL** 2018/3[21] using full-matrix least-squares minimisation on F^2.

Crystal Data. $C_{19}H_{22}BNO_4$, M_r = 339.18, orthorhombic, $Pna2_1$ (No. 33), a = 12.71258(16) Å, b = 20.8247(3) Å, c = 6.65667(7) Å, □ = □ = □ = 90°, *V* = 1762.26(4) Å^3, *T* = 140.00(10) K, *Z* = 4, *Z'* = 1, □(Cu K□) = 0.716, 33598 reflections measured, 3389 unique (R_{int} = 0.0205) which were used in all calculations. The final wR_2 was 0.0655 (all data) and R_1 was 0.0250 (I≥2□(I)).

Structure Quality Indicators

Reflections:

d min (Cu\a) 2Θ=151.1° 0.80
I/σ(I) CIF 90.1
Rint CIF 2.05%
Full 135.4° 99% to 151.1° 100

Refinement:

Shift CIF 0.000
Max Peak CIF 0.2
Min Peak CIF -0.2
GooF CIF 1.054
Hooft CIF -.01(4)

A colourless prism-shaped crystal with dimensions 0.38 × 0.12 × 0.07 mm^3 was mounted. Data were collected using an XtaLAB Synergy R, DW system, HyPix-Arc 150 diffractometer operating at T = 140.00(10) K.

Data were measured using □ scans with Cu K$_□$ radiation. The diffraction pattern was indexed, and the total number of runs and images was based on the strategy calculation from the program CrysAlisPro 1.171.42.75a.[23] The maximum resolution achieved was □ = 75.551° (0.80 Å).

The unit cell was refined using CrysAlisPro 1.171.42.75a (Rigaku OD, 2022) on 24827 reflections, 74% of the observed reflections.

Data reduction, scaling and absorption corrections were performed using CrysAlisPro 1.171.42.75a.[23] The final completeness is 100.00 % out to 75.551° in □. A Gaussian absorption correction was performed using CrysAlisPro 1.171.42.75a.[23] Numerical absorption correction based on Gaussian integration over a multifaceted crystal model. Empirical absorption correction using spherical harmonics as implemented in SCALE3 ABSPACK scaling algorithm. The absorption coefficient □ of this material is 0.716 mm^{-1} at this wavelength (□ = 1.54184Å), and the minimum and maximum transmissions are 0.659 and 1.000.

The structure was solved in the space group $Pna2_1$ (# 33) by the ShelXT 2018/2[21] structure solution program using dual methods and refined by full-matrix least-squares minimisation on $\boldsymbol{F}^2$ using version 2018/3 of **ShelXL** 2018/3[21]. All non-hydrogen atoms were refined anisotropically. Hydrogen atom positions were calculated geometrically and refined using the riding model.

There is a single molecule in the asymmetric unit, which is represented by the reported sum formula. In other words: Z is 4 and Z' is 1.

The Flack parameter was refined to -0.01(4). Determination of absolute structure using Bayesian statistics on Bijvoet differences using the Olex2 results in None. Note: The Flack parameter is used to determine the chirality of the crystal studied, the value should be near 0, a value of 1 means that the stereochemistry is wrong and the model should be inverted. A value of 0.5 means that the crystal consists of a racemic mixture of the two enantiomers.

Citations

CrysAlis$^{\mathbf{Pro}}$ Software System, Rigaku Oxford Diffraction, (2022).

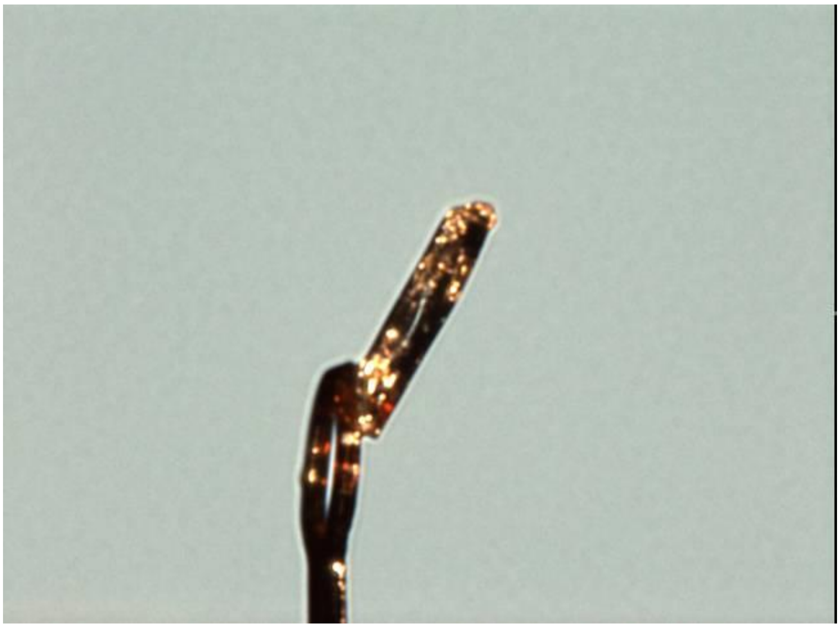

Figure S7: Image of the Crystal on the Diffractometer.

Figure S8: Image of the Crystal on the Diffractometer.

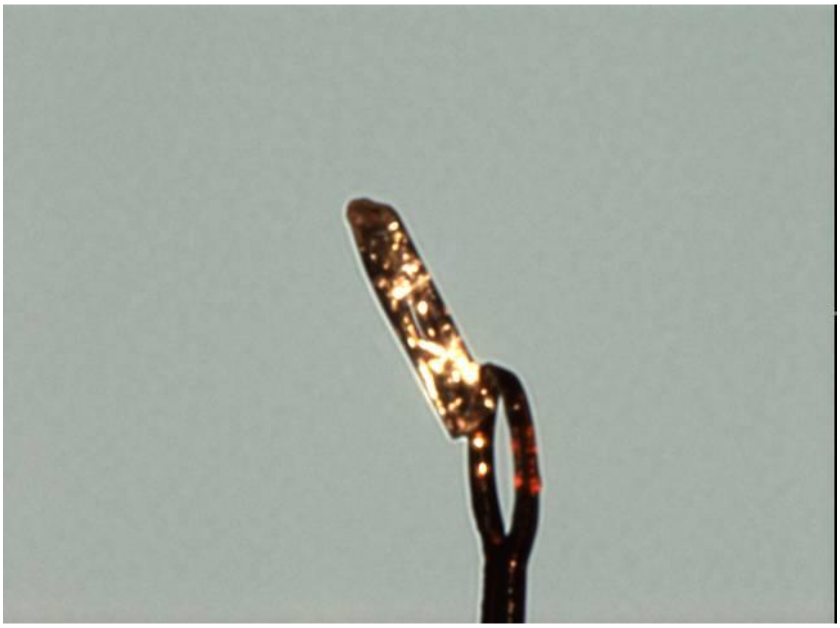

Figure S9: Image of the Crystal on the Diffractometer.

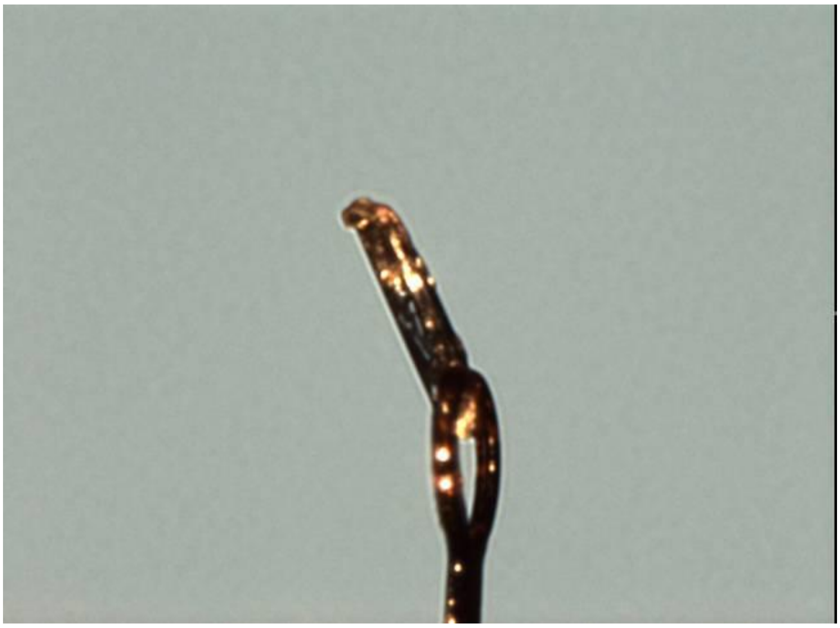

Figure S10: Image of the Crystal on the Diffractometer.

Figure S11: Image of the Crystal on the Diffractometer.

Figure S12: Image of the Crystal on the Diffractometer.

Data Plots: Diffraction Data

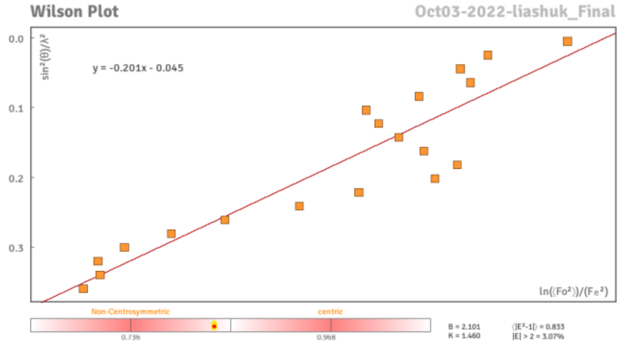

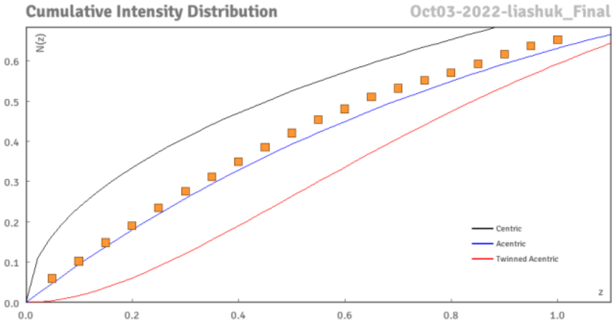

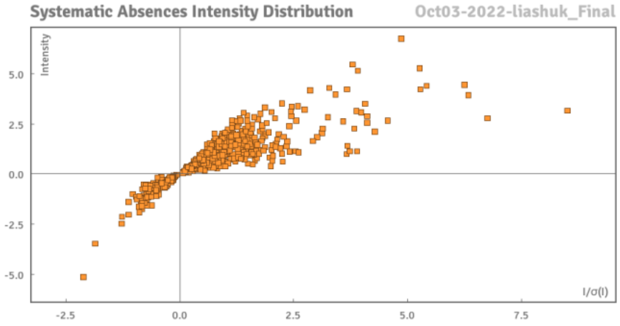

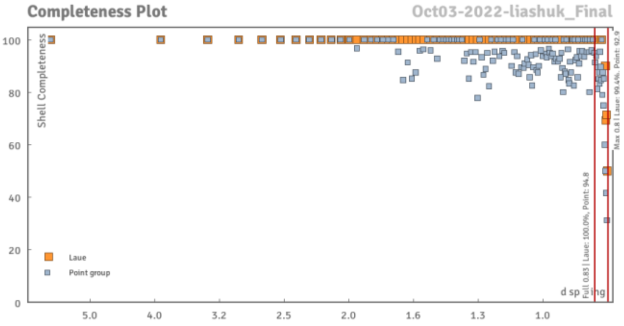

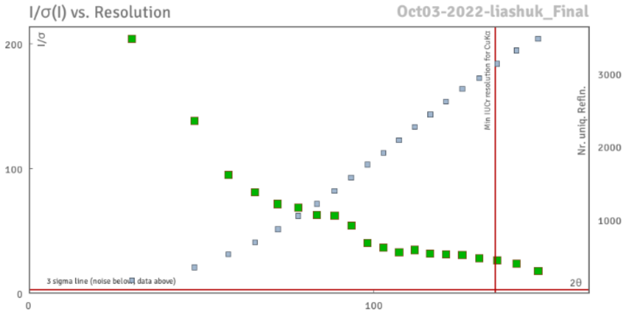

Data Plots: Refinement and Data

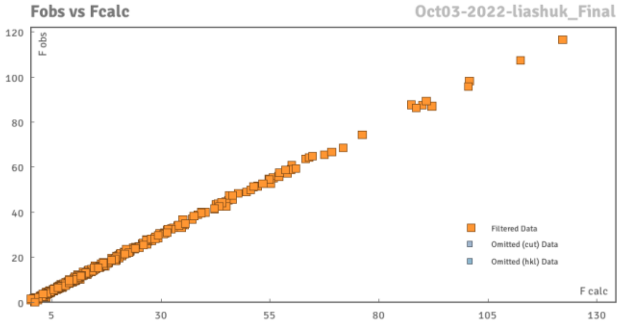

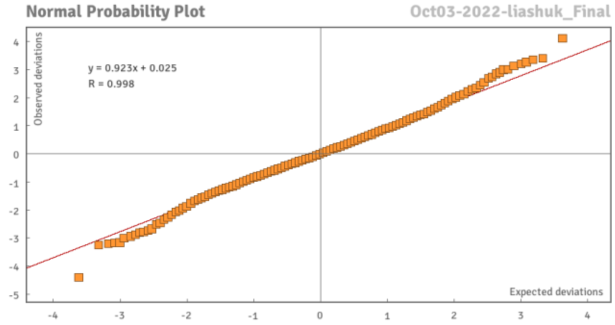

Reflection Statistics

Total reflections (after filtering)	35443	Unique reflections	3389
Completeness	0.929	Mean I/σ	60.1
hkl$_{max}$ collected	(15, 25, 7)	hkl$_{min}$ collected	(-15, -25, -8)
hkl$_{max}$ used	(15, 25, 7)	hkl$_{min}$ used	(0, 0, -8)
Lim d$_{max}$ collected	100.0	Lim d$_{min}$ collected	0.77
d$_{max}$ used	12.71	d$_{min}$ used	0.8
Friedel pairs	3941	Friedel pairs merged	0
Inconsistent equivalents	0	R$_{int}$	0.0205

R_{sigma}	0.0111	Intensity transformed	0
Omitted reflections	0	Omitted by user (OMIT hkl)	0
Multiplicity	(2606, 3022, 2169, 991, 690, 456, 266, 174, 125, 99, 74, 60, 58, 44, 28, 29, 12, 13, 11, 9, 4, 2, 0, 1)	Maximum multiplicity	66
Removed systematic absences	1845	Filtered off (Shel/OMIT)	0

Table 17: *Fractional Atomic Coordinates (×10^4) and Equivalent Isotropic Displacement Parameters (Å^2×10^3) for* ***8c***. *U_{eq} is defined as 1/3 of the trace of the orthogonalised U_{ij}.*

Atom	x	y	z	U_{eq}
O1	5843.0(9)	2787.3(5)	8190.2(19)	30.2(3)
O2	5033.6(10)	4054.9(5)	2823.9(18)	31.2(3)
O3	6853.6(8)	5468.1(5)	3912.1(18)	25.1(2)
O4	8089.2(8)	5307.0(5)	6361.3(18)	25.9(2)
N1	5423.9(9)	3309.1(6)	5255.2(19)	19.2(3)
C1	5607.1(11)	3276.1(7)	7313(2)	21.2(3)
C2	5498.8(12)	3944.7(7)	8162(2)	22.0(3)
C3	6554.1(12)	4283.5(7)	8319(2)	24.5(3)
C4	6409.9(11)	4651.8(6)	6691(2)	21.4(3)
C5	5296.0(11)	4380.9(7)	6314(2)	19.5(3)
C6	5214.9(11)	3930.2(7)	4561(2)	20.3(3)
C7	5580.3(12)	2763.8(7)	3889(3)	22.4(3)
C8	4632.5(11)	2329.7(7)	3686(2)	22.0(3)
C9	4389.1(14)	1888.3(9)	5170(3)	34.9(4)
C10	3559.1(15)	1463.6(9)	4920(3)	40.4(4)
C11	2959.8(12)	1479.6(8)	3193(3)	33.6(4)
C12	3188.7(13)	1920.3(8)	1712(3)	33.6(4)
C13	4029.8(13)	2341.7(7)	1951(3)	28.2(3)
C14	7790.5(12)	5822.5(7)	3254(2)	23.0(3)
C15	8440.9(12)	5872.1(7)	5243(2)	24.4(3)
C16	8317.2(14)	5416.0(8)	1655(3)	34.7(4)
C17	7434.0(14)	6459.9(8)	2387(3)	31.7(4)
C18	8144.6(15)	6451.7(8)	6505(3)	35.6(4)
C19	9623.1(13)	5833.8(10)	4993(3)	39.9(5)
B1	7119.2(13)	5152.8(7)	5627(3)	21.2(3)

Table 18: *Anisotropic Displacement Parameters (×10^4) for* ***8c***. *The anisotropic displacement factor exponent takes the form: $-2\pi^2[h^2a^{*2} \times U_{11} + \ldots + 2hka^* \times b^* \times U_{12}]$*

Atom	U_{11}	U_{22}	U_{33}	U_{23}	U_{13}	U_{12}
O1	40.3(6)	23.4(5)	26.8(6)	7.8(5)	-3.2(5)	0.1(5)
O2	49.9(7)	26.1(5)	17.5(6)	1.6(5)	-4.2(5)	2.3(5)
O3	23.9(5)	27.9(5)	23.5(6)	4.7(5)	-3.4(4)	-6.4(4)
O4	29.1(5)	23.2(5)	25.3(6)	5.6(4)	-6.3(4)	-4.8(4)
N1	23.1(5)	16.4(6)	18.0(6)	-0.5(5)	2.1(5)	-0.8(4)
C1	22.3(7)	21.1(7)	20.2(8)	2.6(6)	1.8(6)	-3.1(5)
C2	27.7(7)	22.3(7)	16.0(7)	0.6(6)	2.2(5)	-1.3(5)
C3	29.2(7)	23.6(7)	20.6(8)	-1.9(6)	-3.2(6)	-1.0(6)
C4	25.8(7)	17.5(6)	21.0(8)	-2.8(6)	0.1(6)	1.0(5)
C5	23.2(6)	17.9(6)	17.3(7)	0.4(6)	2.2(5)	1.4(5)
C6	21.3(7)	20.3(7)	19.2(7)	1.0(5)	1.9(5)	-0.8(5)
C7	25.1(7)	18.7(7)	23.4(8)	-3.2(6)	3.9(6)	-1.3(5)
C8	22.6(7)	18.0(6)	25.4(8)	-3.4(6)	3.8(6)	0.4(5)
C9	38.8(9)	35.2(9)	30.7(9)	5.9(8)	-3.2(7)	-11.1(7)
C10	41.5(10)	36.6(9)	43.1(12)	7.8(8)	4.6(8)	-15.4(8)
C11	23.1(7)	28.8(8)	48.8(12)	-10.6(8)	6.1(7)	-6.2(6)
C12	26.3(8)	34.6(9)	39.8(10)	-5.9(8)	-5.7(7)	0.7(6)
C13	29.4(8)	25.8(8)	29.4(9)	1.2(7)	-0.5(6)	0.4(6)

Atom	U_{11}	U_{22}	U_{33}	U_{23}	U_{13}	U_{12}
C14	24.4(7)	23.5(7)	21.2(8)	2.6(6)	-1.8(6)	-5.1(5)
C15	28.8(8)	22.2(7)	22.3(8)	4.3(6)	-4.1(6)	-5.5(6)
C16	43.4(9)	35.3(9)	25.6(9)	-2.4(7)	6.7(7)	-6.5(7)
C17	33.2(8)	31.4(8)	30.5(9)	10.1(7)	-4.1(7)	-4.8(6)
C18	52.7(10)	26.6(8)	27.4(9)	-2.3(7)	-3.8(8)	-9.9(7)
C19	27.3(8)	48.1(11)	44.2(12)	12.0(9)	-8.4(8)	-8.8(7)
B1	24.5(8)	17.3(7)	21.6(9)	-3.0(6)	-0.1(6)	1.2(6)

Table 19: Bond Lengths in Å for 8c.

Atom	Atom	Length/Å
O1	C1	1.2111(19)
O2	C6	1.2073(19)
O3	C14	1.4680(17)
O3	B1	1.359(2)
O4	C15	1.4624(18)
O4	B1	1.365(2)
N1	C1	1.3914(19)
N1	C6	1.3990(18)
N1	C7	1.4684(18)
C1	C2	1.509(2)
C2	C3	1.519(2)
C2	C5	1.551(2)
C3	C4	1.340(2)
C4	C5	1.5447(19)
C4	B1	1.550(2)
C5	C6	1.501(2)
C7	C8	1.512(2)
C8	C9	1.384(2)
C8	C13	1.386(2)
C9	C10	1.387(2)
C10	C11	1.380(3)
C11	C12	1.378(3)
C12	C13	1.392(2)
C14	C15	1.565(2)
C14	C16	1.516(2)
C14	C17	1.517(2)
C15	C18	1.518(2)
C15	C19	1.514(2)

Table 20: Bond Angles in ° for 8c.

Atom	Atom	Atom	Angle/°
B1	O3	C14	106.97(12)
B1	O4	C15	106.45(12)
C1	N1	C6	113.75(12)
C1	N1	C7	123.31(13)
C6	N1	C7	122.41(13)
O1	C1	N1	123.88(14)
O1	C1	C2	128.16(14)
N1	C1	C2	107.92(12)
C1	C2	C3	111.94(12)
C1	C2	C5	105.01(12)
C3	C2	C5	85.95(11)
C4	C3	C2	95.11(13)
C3	C4	C5	92.73(12)
C3	C4	B1	132.45(14)
C5	C4	B1	134.81(14)
C4	C5	C2	86.15(11)
C6	C5	C2	105.17(11)
C6	C5	C4	114.67(12)
O2	C6	N1	123.48(14)
O2	C6	C5	128.55(14)
N1	C6	C5	107.94(12)
N1	C7	C8	114.18(12)
C9	C8	C7	120.75(15)
C9	C8	C13	118.89(14)
C13	C8	C7	120.26(14)
C8	C9	C10	120.52(17)
C11	C10	C9	120.31(17)
C12	C11	C10	119.71(15)
C11	C12	C13	120.02(17)
C8	C13	C12	120.54(16)
O3	C14	C15	102.08(12)
O3	C14	C16	106.69(12)
O3	C14	C17	108.12(12)
C16	C14	C15	113.44(14)
C16	C14	C17	110.72(14)
C17	C14	C15	114.96(13)
O4	C15	C14	102.47(11)
O4	C15	C18	106.41(13)
O4	C15	C19	108.47(13)
C18	C15	C14	112.94(13)
C19	C15	C14	115.34(15)
C19	C15	C18	110.43(14)
O3	B1	O4	114.31(14)
O3	B1	C4	124.35(14)
O4	B1	C4	121.34(14)

Table 21: Torsion Angles in ° for 8c.

Atom	Atom	Atom	Atom	Angle/°
O1	C1	C2	C3	82.72(19)

Atom	Atom	Atom	Atom	Angle/°
O1	C1	C2	C5	174.40(14)
O3	C14	C15	O4	27.14(14)
O3	C14	C15	C18	-86.92(15)
O3	C14	C15	C19	144.77(13)
N1	C1	C2	C3	-95.05(15)
N1	C1	C2	C5	-3.37(15)
N1	C7	C8	C9	-77.59(19)
N1	C7	C8	C13	106.28(17)
C1	N1	C6	O2	-179.76(14)
C1	N1	C6	C5	2.02(16)
C1	N1	C7	C8	87.50(17)
C1	C2	C3	C4	102.79(14)
C1	C2	C5	C4	-110.11(12)
C1	C2	C5	C6	4.41(14)
C2	C3	C4	C5	1.78(12)
C2	C3	C4	B1	-177.89(16)
C2	C5	C6	O2	177.92(15)
C2	C5	C6	N1	-3.99(15)
C3	C2	C5	C4	1.53(10)
C3	C2	C5	C6	116.06(12)
C3	C4	C5	C2	-1.74(12)
C3	C4	C5	C6	-106.67(14)
C3	C4	B1	O3	177.26(16)
C3	C4	B1	O4	-2.0(3)
C4	C5	C6	O2	-89.34(19)
C4	C5	C6	N1	88.76(14)
C5	C2	C3	C4	-1.77(12)
C5	C4	B1	O3	-2.3(3)
C5	C4	B1	O4	178.46(15)
C6	N1	C1	O1	-176.94(13)
C6	N1	C1	C2	0.95(17)
C6	N1	C7	C8	-101.41(16)
C7	N1	C1	O1	-5.1(2)
C7	N1	C1	C2	172.74(12)
C7	N1	C6	O2	8.4(2)
C7	N1	C6	C5	-169.85(12)
C7	C8	C9	C10	-175.89(17)
C7	C8	C13	C12	176.69(14)
C8	C9	C10	C11	-0.5(3)
C9	C8	C13	C12	0.5(2)
C9	C10	C11	C12	0.0(3)
C10	C11	C12	C13	0.8(3)
C11	C12	C13	C8	-1.1(2)
C13	C8	C9	C10	0.3(3)
C14	O3	B1	O4	7.36(17)
C14	O3	B1	C4	-171.95(13)
C15	O4	B1	O3	11.47(17)
C15	O4	B1	C4	-169.19(13)
C16	C14	C15	O4	-87.25(15)
C16	C14	C15	C18	158.68(14)
C16	C14	C15	C19	30.38(19)
C17	C14	C15	O4	143.92(13)
C17	C14	C15	C18	29.85(19)
C17	C14	C15	C19	-98.45(17)
B1	O3	C14	C15	-21.34(15)
B1	O3	C14	C16	97.92(15)
B1	O3	C14	C17	-142.95(13)
B1	O4	C15	C14	-23.71(15)
B1	O4	C15	C18	95.06(14)
B1	O4	C15	C19	-146.13(15)
B1	C4	C5	C2	177.92(16)
B1	C4	C5	C6	73.0(2)

***Table 22**: Hydrogen Fractional Atomic Coordinates ($\times10^4$) and Equivalent Isotropic Displacement Parameters ($Å^2\times10^3$) for **8c**. U_{eq} is defined as 1/3 of the trace of the orthogonalised U_{ij}.*

Atom	**x**	**y**	**z**	U_{eq}
H2	5008.3	3996.76	9324.98	26
H3	7118.76	4246.99	9247.12	29
H5	4706.34	4695.46	6458.24	23
H7A	6182.34	2505.86	4377.27	27
H7B	5767.13	2931.16	2543.11	27
H9	4793.87	1876.34	6369.39	42
H10	3402.5	1160.17	5943.35	49
H11	2391.82	1187.98	3025.23	40
H12	2772.52	1936.61	527.73	40
H13	4191.94	2639.91	915.97	34
H16A	8509.02	4998.28	2225.75	52
H16B	8952.2	5634.41	1175.5	52
H16C	7831	5352.42	529.98	52
H17A	7054.83	6385.09	1127.17	48
H17B	8048.94	6731.32	2128.29	48
H17C	6967.74	6675.25	3347.09	48
H18A	7378.34	6469.57	6655.54	53
H18B	8391.96	6843.7	5841.57	53
H18C	8472.35	6416.01	7833.03	53
H19A	9960.27	5852.68	6316.07	60
H19B	9865.75	6194.85	4171.01	60
H19C	9808.35	5428.89	4331.67	60

Citations

[1] W. L. F. Armarego, C. L. L. Chai, *Purification of Laboratory Chemicals*, Elsevier, **2003**.

[2] Y. Nishihara, Y. Okada, J. Jiao, M. Suetsugu, M.-T. Lan, M. Kinoshita, M. Iwasaki, K. Takagi, *Angew. Chemie Int. Ed.* **2011**, *50*, 8660–8664.

[3] K. Jaiswal, K. Groutchik, D. Bawari, R. Dobrovetsky, *ChemCatChem* **2022**, *14*, e202200004.

[4] H. Kinoshita, H. Takahashi, K. Miura, *Org. Lett.* **2013**, *15*, 2962–2965.

[5] L. Wang, J. M. Lear, S. M. Rafferty, S. C. Fosu, D. A. Nagib, *Science* **2018**, *362*, 225–229.

[6] I. Gazić-Smilović, E. Casas-Arcé, S. J. Roseblade, U. Nettekoven, A. Zanotti-Gerosa, M. Kovačevič, Z. Časar, *Angew. Chemie Int. Ed.* **2012**, *51*, 1014–1018.

[7] C.-I. Lee, J. Zhou, O. V Ozerov, *J. Am. Chem. Soc.* **2013**, *135*, 3560–3566.

[8] H. E. Ho, N. Asao, Y. Yamamoto, T. Jin, *Org. Lett.* **2014**, *16*, 4670–4673.

[9] F. Possémé, M. Deligny, F. Carreaux, B. Carboni, *J. Org. Chem.* **2007**, *72*, 984–989.

[10] T. León, E. Fernández, *Chem. Commun.* **2016**, *52*, 9363–9366.

[11] A. Robertson, D. Philp, N. Spencer, *Tetrahedron* **1999**, *55*, 11365–11384.

[12] F. Feist, S. L. Walden, J. Alves, S. V Kunz, A. S. Micallef, A. J. Brock, J. C. McMurtrie, T. Weil, J. P. Blinco, C. Barner-Kowollik, *Angew. Chemie Int. Ed.* **2021**, *60*, 10402–10408.

[13] S. V Shelar, N. P. Argade, *Org. Biomol. Chem.* **2021**, *19*, 6160–6169.

[14] P. Wessig, D. Freyse, D. Schuster, A. Kelling, *Eur. J. Org. Chem.* **2020**, *2020*, 1732–

1744.

[15] G. Deng, Y. Chen, *Macromolecules* **2004**, *37*, 18–26.

[16] I. A. P. Linares, K. T. de Oliveira, J. R. Perussi, *Dye. Pigment.* **2017**, *145*, 518–527.

[17] R. M. de Figueiredo, R. Fröhlich, M. Christmann, P. Oczipka, *Synthesis (Stuttg).* **2008**, *2008*, 1316–1318.

[18] R. Shintani, W.-L. Duan, T. Hayashi, *J. Am. Chem. Soc.* **2006**, *128*, 5628–5629.

[19] K. Rix, G. H. Kelsall, K. Hellgardt, K. K. (Mimi) Hii, *ChemSusChem* **2015**, *8*, 665–671.

[20] A. Phillips, C. Nasveschuk, J. Henderson, Y. Liang, C. Chen, M. Duplessis, M. He, K. Lazarski, *AMINE-LINKED C3-GLUTARIMIDE DEGRONIMERS FOR TARGET PROTEIN DEGRADATION*, **2017**, WO/2017/197051.

[21] G. M. Sheldrick, *Acta Crystallogr. Sect. A* **2015**, *71*, 3–8.

[22] O. V Dolomanov, L. J. Bourhis, R. J. Gildea, J. A. K. Howard, H. Puschmann, *J. Appl. Crystallogr.* **2009**, *42*, 339–341.

[23] Rigaku Oxford Diffraction, **2022**.